UNIVERSIDAD AUTONOMA DE MADRID

Facultad de Ciencias

Departamento de Biología Molecular

CARACTERIZACIÓN "IN VITRO" E "IN VIVO" DE LOS VECTORES ATENUADOS DE POXVIRUS MVA Y NYVAC COMO CANDIDATOS VACUNALES FRENTE AL VIH/SIDA

Memoria presentada para optar al grado de Doctor en Ciencias por

JOSÉ LUIS NÁJERA GARCÍA

Madrid, Noviembre de 2007

El trabajo presentado en esta memoria ha sido realizado en el Departamento de Biología Molecular y Celular del Centro Nacional de Biotecnología (CNB-CSIC) de Madrid, bajo la co-dirección del Dr. Mariano Esteban y la Dra. Carmen Elena Gómez, y ha sido financiado por una beca predoctoral asociada al proyecto FIPSE.

A la memoria de mi tío Venan

A toda mi familia y amigos

A joa

ACGM: *Advisory Committee on Genetic Modifications*
Adeno: Adenovirus
ADN: ácido desoxirribonucleico
APC: célula presentadora de antígeno
ARN: ácido ribonucleico
ARNr: ácido ribonucleico ribosomal
ARNasa L: Ribonucleasa L
BCA: ácido bicincónico
BLI: Bioluminiscencia
BSA: albúmina de suero bovina
β-Gus: gen de la glucuronidasa
C3: anticuerpo monoclonal que reconoce la proteína A27 del virus vaccinia
CB: Tampón de citoesqueleto
CD4: diferenciador de grupo 4
CD8: diferenciador de grupo 8
CEF: fibroblastos embrionarios de pollo
CEV: virus extracelular asociado a la célula
CIMA: Centro de Investigación Médica Aplicada
CMV: citomegalovirus
CNB: Centro Nacional de Biotecnología
CRF: formas recombinantes circulantes
CTL: linfocitos T citotóxicos
CTRL: mezcla de péptidos control
Cys: cisteína
DAB: 3,3'-diaminobenzidina tetrahydrochloride
DAPI: 4'6'-diamidino-2-fenilindol
DIAIDS: *Division of AIDS, National Institute of Allergy and Infectious Disease*
DMEM: medio esencial mínimo de Eagle modificado por Dulbecco
DMSO: dimetilsufóxido
e.c.: escarificación en la base de la cola
EBV: virus de Epstein-Barr
EC: Efecto citopático
ELISA: *enzyme linked immunosorbent assay*
ELISPOT: *enzyme linked immunospot assay*
eIF: factor de iniciación de la traducción en eucariotas
Env: Envuelta de VIH-1
EuroVac: *European Vaccine Effort Against HIV/AIDS*
EV: virus extracelular con envuelta
FCS: suero fetal de ternera
FV: factoría viral
GPN: poliproteína Gag-Pol-Nef de VIH-1
h.p.i.: horas post-infección
HA: hemaglutinina
HAART: *highly active antiretroviral therapy*
Hr: Rango de hospedador
HVTN: *The HIV Vaccine Trials Network*
IAVI: *International AIDS Vaccine Initiative.*
i.d.: intradérmico
i.p.: intraperitoneal
IP: ioduro de propidio
i.n.: intranasal
IFN: interferón
IgG: inmunoglobulina G
IL: interleuquina
IL-1βR : receptor de la IL-1-β
IL-18R: receptor de la IL-18
IV: virión inmaduro
IRES: sitio interno de entrada al ribosoma
IRF: Factor de respuesta a IFN
ISG: genes estimulados por IFN
KDa: kilodalton
Kg: kilogramo
Kb: Kilobases
Kpb: kilo pares de bases
LB: medio Luria-Bertani
Luc: Luciferasa
Met: metionina
mg: miligramo
MHC: complejo principal de histocompatibilidad
ml: mililitro
MDA: *Melanoma diffentition –associated protein*

Mock: células sin infectar
mM: milimolar
MVs: viriones maduros
MVA: virus modificado de Ankara
MVA-B: recombinante derivado de MVA que expresa 4 antígenos (Env, Gag, Pol y Nef) del subtipo B de VIH-1
MVA-C: recombinante derivado de MVA que expresa 4 antígenos (Env, Gag, Pol y Nef) del subtipo C de VIH-1
NCS: suero de ternera recién nacida
NIH: Instituto Nacional de Salud de Estados unidos
NPLP: No progresores a largo plazo
NK: células citolíticas naturales, *Natural killer*
nm: nanómetros
NYVAC: cepa atenuada de Copenhagen
NYVAC-B: recombinante derivado de NYVAC que expresa 4 antígenos (Env, Gag, Pol y Nef) del subtipo B de VIH-1
NYVAC-C: recombinante derivado de NYVAC que expresa 4 antígenos (Env, Gag, Pol y Nef) del subtipo C de VIH-1
OMS: Organización mundial de la salud
ORFs: Pautas de lectura abierta
PARP: Poly (ADP-Ribosa) Polimerasa
PBS: tampón fosfato salino
PBS-BSA: PBS + 1% BSA
PBST: PBS + 0,05% Tween-20
PCMV: promotor de citomegalovirus
PCR: reacción en cadena de la polimerasa
Pe/l: promotor temprano/tardío
PKR: *IFN-induced protein kinase*
Pox: poxvirus
RI: región de interés
RIG: Helicasa de ARN
rpm: revoluciones por minuto
RT-PCR: reacción de la transcriptasa reversa acoplada a la amplificación de ADNc mediante PCR
SD: desviación estandar
SDS: dodecil sulfato sódico
SDS-PAGE:electroforesis en gel de poliacrilami-da con SDS
SHIV: virus de la inmunodeficiencia hibrido simio/humano
SIDA: síndrome de inmunodeficiencia adquirida
SIV: virus de la inmunodeficiencia en simios
SNE: Seronegativos expuestos
TBE: Tris- Borato + EDTA
TCA: ácido tricloroacético
T_H: linfocito T colaborador (T *helper*)
TK: timidina kinasa
TLR: *Toll like receptor*
TMB: 3,3',5,5'-tetrametilbenzidina
TNF: factor de necrosis tumoral
UE: Unión Europea
UFP: unidad formadora de placa
URL: Unidad relativa de Luciferasa
VACV: virus vaccinia
VACV-COP: Cepa Copenhagen de VACV
VACV-WR: Cepa Western Reserve de VACV
VIH: virus de la inmunodeficiencia humana
VHC: virus de la hepatitis C
WHO: *Wordl Health Organizatio*n
VHS-1: virus del herpes simplex
VRG: Virus de la rabia
WV: virus intracellular envuelto
µCi: microcurios
µg: microgramo
µM: micromolar
zVAD: Inhibidor general de caspasas

The search for a safe and effective human immunodeficiency virus (HIV) vaccine has stimulated the development of recombinant live vectors as vehicles for the induction of specific cellular immune responses. Attenuated poxvirus vectors, such as MVA and NYVAC, have a number of desirable features as HIV vaccine candidates, including promising safety profiles and the ability to incorporate substantial genetic material for the expression of foreign gene products. It has become clear that beyond these benefits and the specific physical characteristic unique to each vector, another aspect of viral vectors is critically important: the interaction between the vector and the host cell. This interaction often induces innate and acquired immune responses to the vector particle it self, and the subsequent cascade of events may significantly contribute to the success or failure of a viral-based vaccine. At present, a number of clinical trials using recombinants based on the attenuated poxvirus strains MVA or NYVAC against infectious disorders such as AIDS, malaria and human papiloma associated cancer are underway by several organizations, validating not only the safety of these strains, but also demonstrating significant antigen specific T cell immunogenicity in humans. Despite intense interest in poxvirus vectors as candidates vaccines for HIV and other infectious diseases, few direct comparisons of poxvirus-based vaccine candidates have been reported to date.

In order to understand how these vectors should best be used in regimens, it is essential to analyze both vector-specific influences on antigen expression and the effect of the vector on the host cell responses. Direct comparisons of vector elicited antigen expression and host cell effects generated by attenuated vaccinia vectors are warranted in order to choose the optimal vector to elicit a desired response and to design improved future generations of vaccines.

In this study we examined the in vitro e in vivo behabiour of NYVAC in comparison with that of MVA using cellular and biochemical approaches. Our findings revealed that In contrast with MVA, NYVAC infection triggers greater cytopathic effect in a range of permissive, and non-permissive cell lines. The yields of NYVAC cell-associated virus in permissive cells (BHK-21) were slightly reduced compared with MVA infection. During the course of infection in HeLa cells, there is a translational block induced by NYVAC late in infection, which correlated with a marked increase in phosphorylation levels of the initiation factor eIF-2α. In contrast to MVA, the synthesis of certain late viral proteins was only blocked in NYVAC infected HeLa cells. Electron microscopy (EM) analysis revealed that morphogenesis of NYVAC in HeLa cells was blocked at the stage of formation of immature viral forms (IVs). Phase-contrast microscopy, EM, flow cytometry and rRNA analyses demonstrated that contrary to MVA, NYVAC infection induces potent apoptosis, a phenomenon dependent on caspase and RNaseL activation. Apoptosis induced by NYVAC was prevented when the virus gene C7L was placed back into the NYVAC

genome, recovering the ability of NYVAC to replicate in HeLa cells and maintaining the attenuated phenotype in mice. We have also analyse the biodistribution in mice of MVA and NYVAC vectors in comparison with the replication-competent VACV strain Western Reserve (WR), when administered by different routes.In contrast to WRluc, for most of the inoculated routes, the attenuated recombinants expresed transiently the reporter gene. Our findings in mice revealed that MVA and NYVAC have restricted expression capacity, largely confined within the first 24 hpi, and that differences exist between the two virus strains in the kinetics of recombinant antigen expression. The results suggest that MVA and NYVAC vectors might stimulate differently the T cell immune response.

In order to analyse that point, here we also describe the construction and characterization of MVA and NYVAC vectors expressing multiple HIV-1 antigens (Env, Gag, Pol and Nef) from clade B in a single locus of the viral genome. The viral vectors are referred as MVA-B and NYVAC-B. In addition, we have compared in BALB/c and in transgenic HHD mice how MVA-B and NYVAC-B activate specific cellular and humoral immune responses against peptide pools spanning the heterologous antigens when they were administered using different prime/boost vaccination approaches. Our findings showed that in cultured cells both recombinants efficiently express the four HIV-1 antigens in a stable manner. In mice MVA-B and NYVAC-B were able to induce a specific immune response against peptides representing the heterologous HIV-1 antigens (Env, Gag, Pol, and Nef) independently of the immunization protocol used. Differences in the magnitude of the immune response were observed between the poxvirus vectors in the two animal models. In BALB/c, the DNA-B prime/NYVAC-B boost regime triggered an overall higher immune response than DNA-B prime/MVA-B boost whereas in HHD the magnitude of the response was similar for both recombinant viruses. When the combination of MVA-B and NYVAC-B vectors was used for prime/boost, the magnitude of the immune response was lower than in a DNA-B/poxvirus-B approach, although more peptide pools were recognized. An immunodominance of the Env peptide pools was consistently observed in HHD transgenic mice in the different protocols used. Our findings highlighted the relevance of NYVAC-B and MVA-B as potential vaccine candidates against HIV/AIDS.

1. INTRODUCCIÓN

Introducción

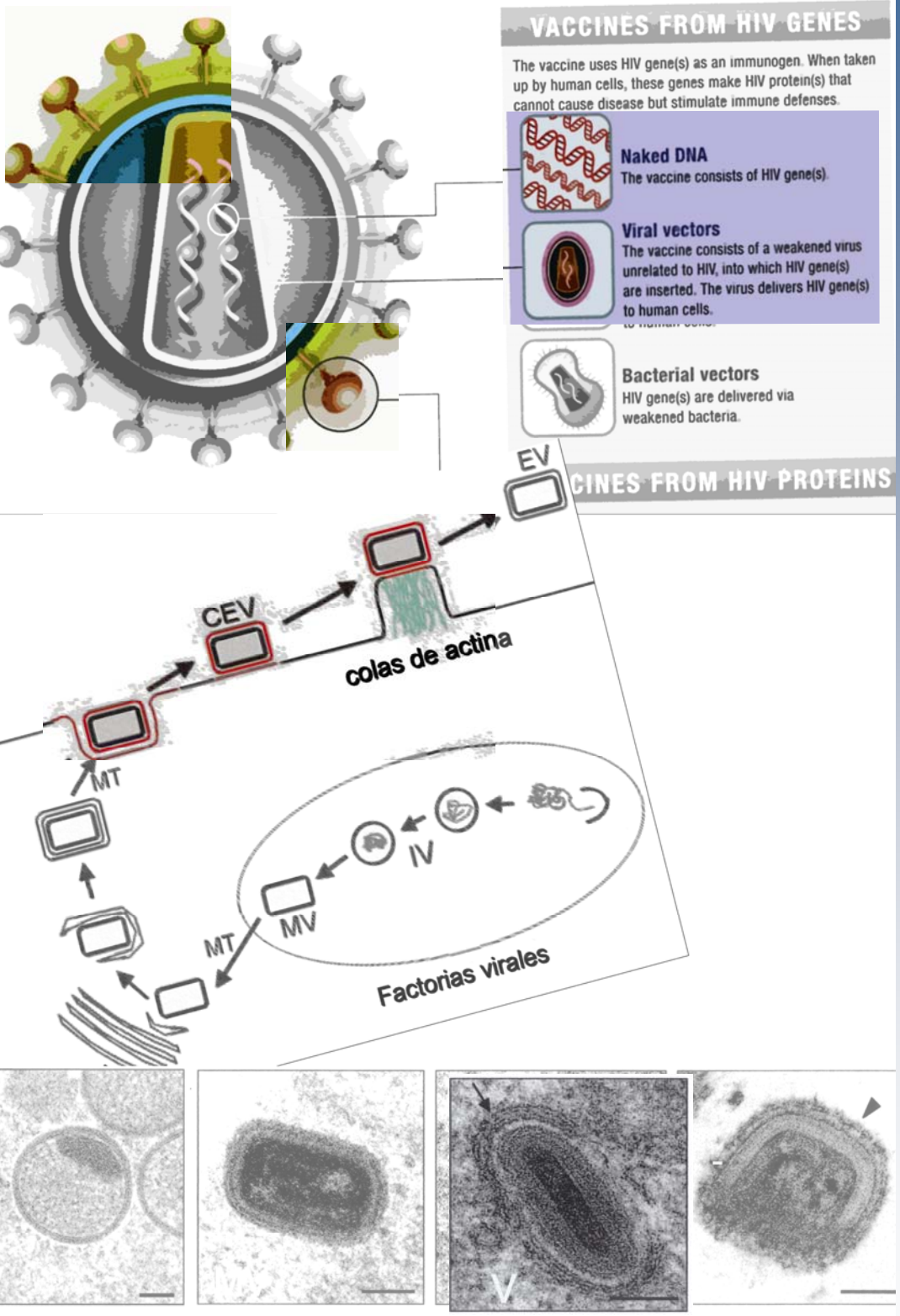

1.- POXVIRUS: Aspectos generales

Los poxvirus son una familia de virus ADN de gran tamaño y complejidad, capaces de infectar tanto vertebrados como invertebrados. El miembro más estudiado de esta familia es el virus vaccinia (Buller y Palumbo, 1991; Dales y Pogo, 1981; Moss, 2001) pero, sin duda, el más conocido es el virus de la viruela humana, causante de una de las enfermedades más devastadoras que ha conocido el hombre a lo largo de su historia.

En 1957, Fenner y Burnett publicaron una breve descripción de los poxvirus de vertebrados, que ha constituido la base de las clasificaciones posteriores en cuanto a los criterios utilizados y las subdivisiones realizadas (Fenner y Burnet, 1957).

La familia *Poxviridae* constituye el grupo más grande y complejo de los virus ADN, replican integramente en el citoplasma de la célula hospedadora, y tienen un origen evolutivo separado de los demás virus ADN (Strauss, 2002). Son virus de gran tamaño y con ADN de doble cadena que se clasifican en dos subfamilias con once géneros, ocho pertenecen a la subfamilia *Chordopoxvirinae* la cual infecta vertebrados (aves y mamíferos), y los tres géneros restantes a la subfamilia *Entomopoxvirinae* que infecta invertebrados (insectos) (Esposito y cols., 1977a, 1977b; Li y cols., 1998). En general, las especies dentro de un mismo género se diferencian por sus características biológicas, el rango de hospedador y su distribución geográfica (Esposito y cols., 1977a, 1977b). El virus vaccinia (VACV) es el prototipo de la familia *Poxviridae* y pertenece al género *Orthopoxvirus* de la familia *Chordopoxvirinae*. La infección en humanos es leve, con manifestaciones febriles y aparición de pústulas dérmicas. El VACV ha contribuido al desarrollo de una parte importante de la virología moderna, ya que fue el primer virus animal visualizado al microscopio electrónico, crecido en cultivos celulares, purificado físicamente y analizado químicamente (Moss, 2001). Como veremos más adelante, la tecnología del ADN recombinante permitió nuevas aplicaciones de los poxvirus en el campo de la inmunología ya que éstos podrían utilizarse como vectores de expresión o como vacunas vivas. Para una revisión en español sobre la familia *Poxviridae* ver el libro "Virus patógenos" (Carrasco, 2006).

2.- El VIRUS VACCINIA (VACV)

2.1.- Estructura y Morfología

La partícula viral del virus vaccinia (VACV) presenta un gran tamaño (aproximadamente 350 x 270 nm), tiene una morfología ovalada o con forma de ladrillo y es visible por microscopía óptica (Dales y cols., 1981). En secciones ultrafinas de células

infectadas con VACV, se pueden observar distintos estadíos de maduración. Las partículas infecciosas aisladas por rotura celular se denominan virus intracelular maduro (IMV) y los viriones recogidos del medio de cultivo, liberados por la célula infectada sin mediar lisis, reciben el nombre de virus extracelular envuelto (EEV) y presentan una bicapa lipídica adicional, lo que les confiere propiedades inmunológicas diferentes (Vanderplasschen y Smith, 1997). En la actualidad se ha llegado a un consenso en cuanto a la nomenclatura y los IMVs se denominan como viriones maduros (MVs) y los EEVs viriones extracelulares (EVs) (Moss, 2006).

Según imágenes obtenidas por microscopía electrónica y más recientemente por tomografía crio-electrónica, el MV está organizado en tres elementos estructurales: el core, los cuerpos laterales y la membrana externa (Figura 1).

El "core" es una zona central electrondensa con forma de disco biconcavo que contiene el ADN genómico y varias proteínas virales asociadas formando en un complejo núcleo-proteico (Jensen y cols., 1996).

Los cuerpos laterales están situados a ambos lados del core. Se ha propuesto que estos cuerpos laterales son zonas de contacto de la membrana externa con el core viral (Griffiths y cols., 2001a; Griffiths y cols., 2001b). La membrana externa rodea a ambas estructuras y presenta en su superficie una compleja red de túbulos dispuestos regularmente en forma de empalizada.

Trabajos de nuestro laboratorio en colaboración con otros grupos han determinado la estructura de la forma MV (360x270x250 nm) con una resolución de 4-6 nm mediante crio-microscopía electrónica y reconstrucción tomográfica como se indica en la figura 1 adaptada de (Cyrklaff y cols., 2005).

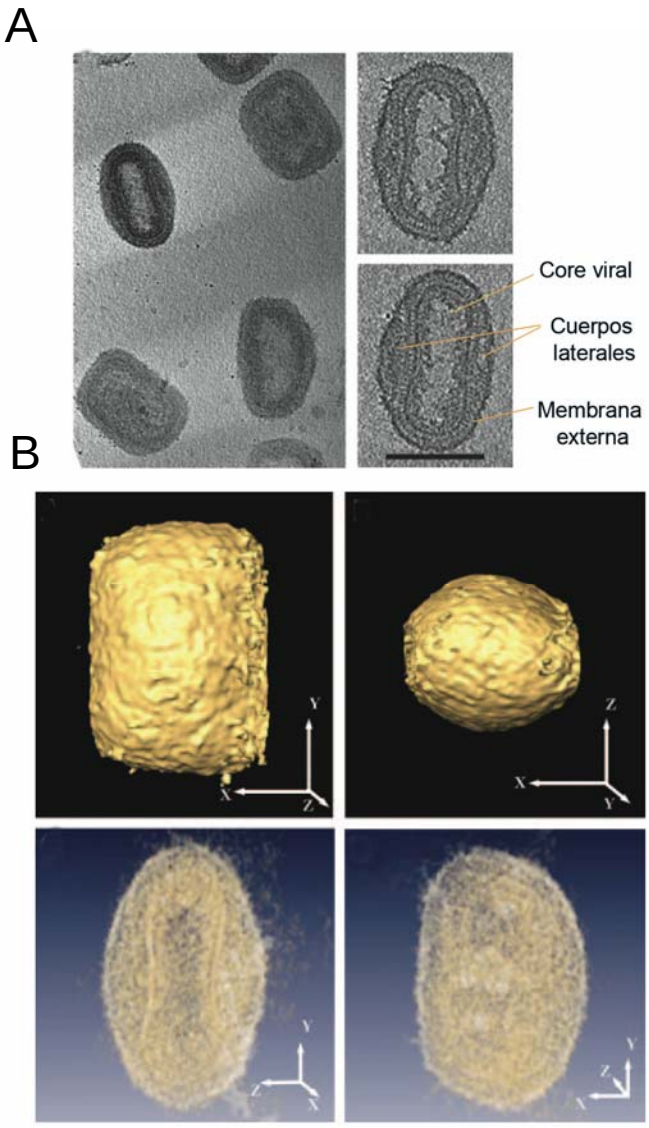

Figura 1: **Estructura del MV del virus vaccinia.** Imágenes obtenidas por microscopía electrónica **(A)** y por tomografía crioelectrónica **(B)**.

El MV se caracteriza por tener una membrana externa lipídica (5-6 nm de grosor), debajo de la cual hay dos cuerpos laterales constituidos por material heterogéneo sin estructura aparente, y más internamente un nucleoide o core rodeado por dos capas que tienen un grosor de unos 18-19 nm; la más externa con proyecciones de espículas agrupadas en forma hexagonal, y la más interna es consistente con una membrana. En el core se observan poros que pueden servir para exportar el ARNm durante el proceso de transcripción del genoma viral.

El EV presenta una envuelta lipídica adicional que envuelve al virión maduro (Essani y Dales, 1979; Oie y Ichihashi, 1981a, 1981b). Tanto la membrana externa del MV como la envuelta del EV presentan una composición lipídica diferente a la de las membranas de la célula hospedadora y están enriquecidas con proteínas virales (Anderson y Dales, 1978; Hiller y cols., 1981; Stern y Dales, 1974).

2.2.- Organización genómica

Los poxvirus poseen uno de los genomas más grandes de todos los virus ADN, pudiendo tener un tamaño aproximado de 200 Kb que codifican para unas 200 proteínas. El genoma del virus vaccinia de unos 62,3 µm (Esteban y cols., 1977) consta de una molécula lineal de ADN bicatenario con los extremos unidos covalentemente por estructuras en forma de horquilla que subyacen dentro de una región terminal invertida (ITR, de las siglas en inglés: "Inverted Terminal Repeat"). El ADN tiene un contenido muy alto en A+T y se encuentra asociado a proteínas virales adoptando una conformación superenrollada (Esteban y cols., 1977; Soloski y Holowczak, 1981). Hasta la fecha se han secuenciado varios genomas de distintas especies de poxvirus, identificándose al menos unas 100 pautas abiertas de lectura (ORFs: "Open Reading Frames") presentes en todos los *Chordopoxvirus* (Figura 2).

Convencionalmente, la nomenclatura de las pautas de lectura abierta (ORFs) de los *Orthopoxvirus* está basada en la conservación de la distribución de los sitios Hind III en la región central del genoma (Moss, 2001). Consiste en asignar la letra del fragmento de ADN digerido con Hind III, seguido por la posición que ocupa dicha pauta dentro del fragmento (de izquierda a derecha) y de la letra L (Left) o R (Right) dependiendo de la dirección de transcripción. Los genes localizados en la región central del genoma, se encuentran altamente conservados dentro de la familia *Poxviridae* y están implicados en funciones esenciales como la replicación o el ensamblaje viral. Sin embargo, en la actualidad existe un mayor interés por los genes de las zonas más variables, que se encuentran localizados en los extremos del genoma y que codifican una serie de

proteínas involucradas en la interacción con la célula huésped y en los mecanismos de evasión del sistema inmune (Moss, 2001).

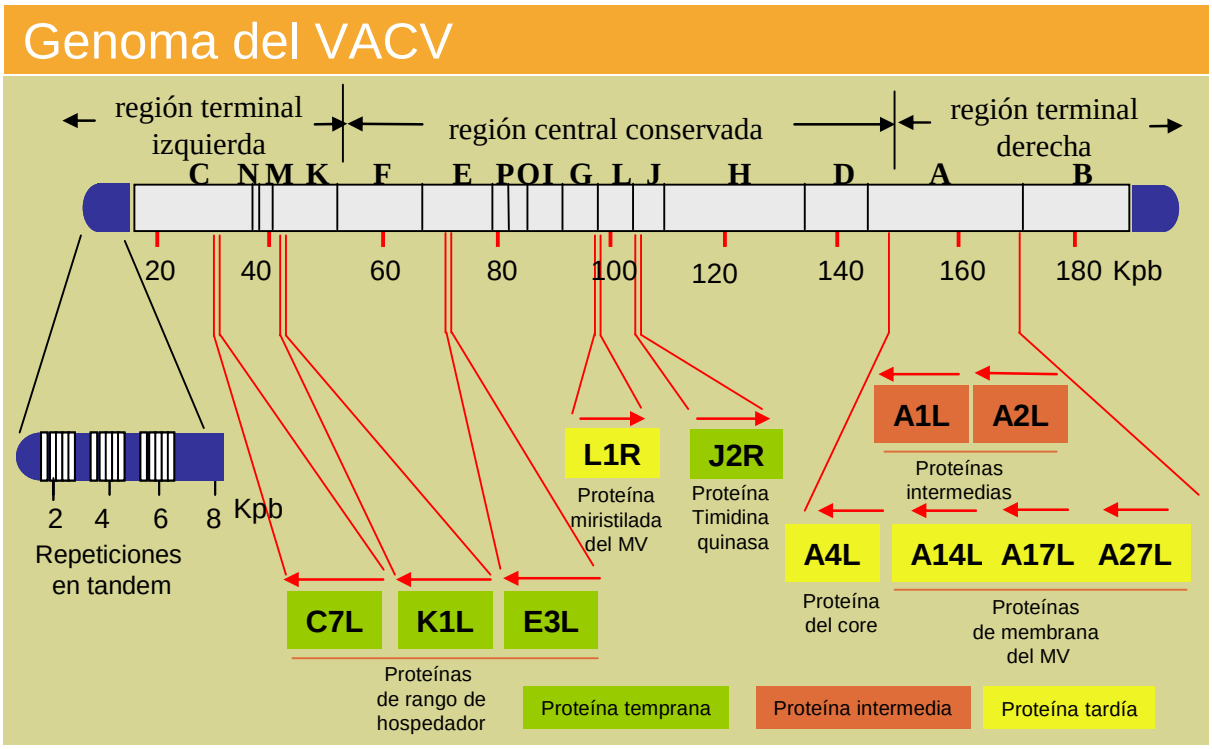

Figura 2.- Estructura y organización del genoma del virus vaccinia (VACV). En la parte superior de la figura se muestra la molécula lineal de ADN bicatenario unido covalentemente en sus extremos (formando los lazos terminales), donde existen repeticiones en tandem. En la parte inferior se muestran algunos de los genes considerados en este trabajo.

Los poxvirus expresan un extenso abanico de proteínas inmunomoduladoras que modifican el ambiente intra- y extracelular de la célula infectada. Estas proteínas modulan conjuntamente un amplio rango de respuestas celulares dirigidas a hacer frente a la infección viral entre las que se incluyen importantes procesos y rutas de señalización como la apoptosis, la inducción del interferón, las cascadas de señalización inducidas por estrés, la presentación de los antígenos por las moléculas del complejo mayor de histocompatibilidad (MHC) o la secreción de citoquinas pro-inflamatorias (Seet y cols., 2003). La respuesta específica de estos factores codificados por los poxvirus es la responsable de las diferencias de cada especie para responder a los distintos mecanismos de defensa desencadenados por el huésped, así como de la migración progresiva a los distintos tipos celulares y tejidos durante la infección (McFadden, 2005).

2.3.- Ciclo Infectivo

Una de las características que distingue a los Poxvirus de otros virus ADN es que el virus permanece en el citoplasma durante todo el ciclo infeccioso, desde su entrada en

la célula hasta que la progenie viral sale a través de la membrana plasmática, sintetizando sus propias enzimas (ADN y ARN polimerasa), lo que le confiere "cierta independencia" de la célula. El ciclo infectivo del virus vaccinia, el mejor caracterizado de los poxvirus, se divide en 4 etapas: entrada, desencapsidación, expresión génica y replicación del ADN viral y finalmente morfogénesis viral y salida de la progenie (figura 3).

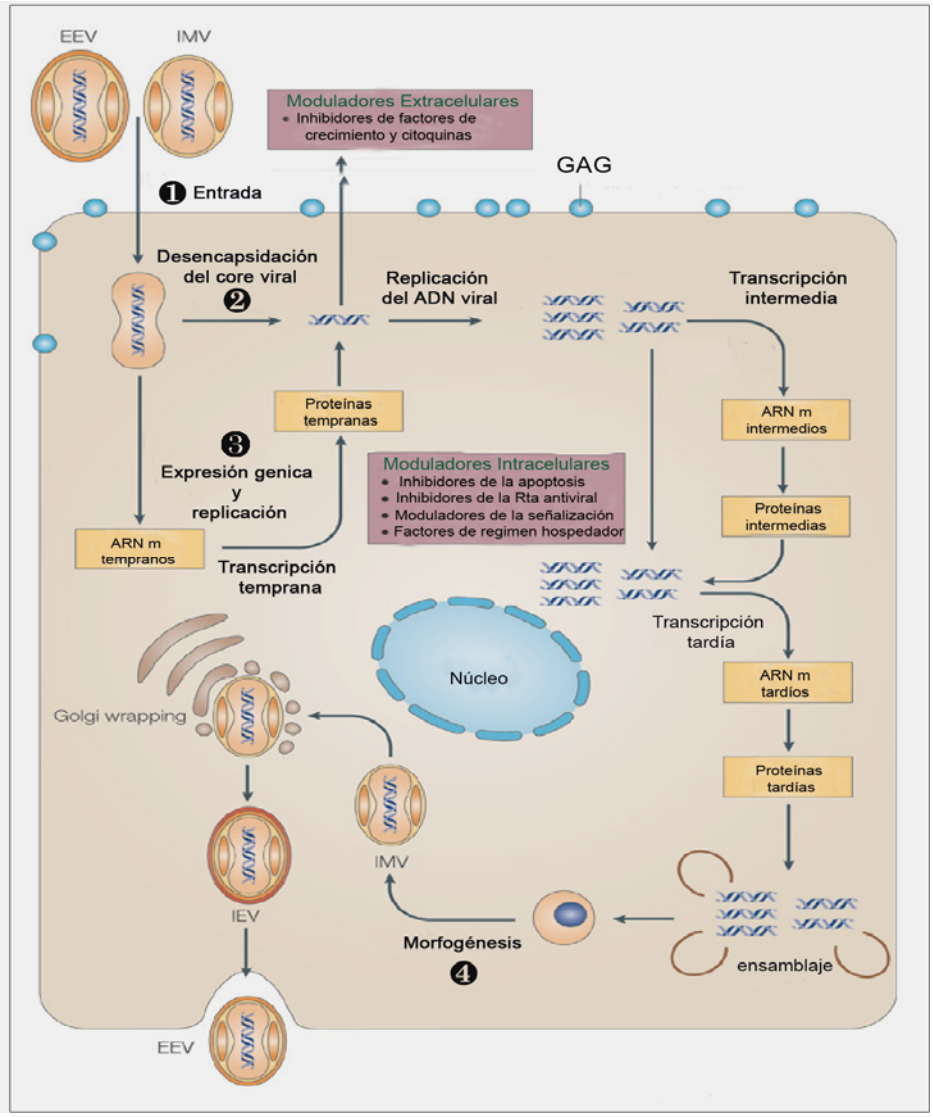

Figura 3: Ciclo infeccioso del virus vaccinia (VACV). Figura adaptada de McFadden, 2005.

1- Entrada

El proceso infectivo se inicia con la unión del virión a la membrana. El estudio de este proceso en el virus vaccinia se ha visto dificultado por la existencia de dos formas infectivas (MV y EV). Debido a la complejidad del virión, en el proceso de entrada tienen que intervenir varias proteínas cuya función aún no ha sido asignada. De hecho, el virus

vaccinia tiene un amplio tropismo y aún no se ha descrito un receptor celular específico para poxvirus (ver revisión (Moss, 2006)).

Se ha propuesto que el MV entra en la célula por un proceso de fusión entre membranas (Chang y Metz, 1976; Janeczko y cols., 1987). Este modelo de fusión directa implicaría la existencia de una o varias proteínas de fusión en la superficie del MV y la posterior liberación del core en el citoplasma tras la fusión. En este sentido se ha descrito que las proteínas D8, H3 y A27, productos de los genes D8L, H3L y A27L respectivamente, podrían estar implicadas en el proceso de adsorción viral, debido a su capacidad de unión a receptores celulares del tipo condroitín sulfato (D8) y heparán sulfato (H3 y A27) (Chang y cols., 1995; Hsiao y cols., 1999; Lai y cols., 1990; Maa y cols., 1990).

Recientemente, se ha demostrado que la proteínas A21, L5, A28, H2, G3, G9, A16 y J5 presentes en la membrana del MV, están implicadas en el proceso de entrada del virus (Ojeda y cols., 2006; Senkevich y cols., 2004a, 2004b; Townsley y cols., 2005a, 2005b). Así, partículas virales deficientes en alguna de estas proteínas son capaces de unirse a la superficie celular pero los cores no penetran en su interior, indicando un bloqueo en la fusión de membrana (Moss, 2006).

Los primeros estudios realizados sobre el mecanismo de entrada del EV (Doms y cols., 1990; Payne y Kristenson, 1979) sugerían un proceso independiente de pH, es decir, también por fusión, al romperse la membrana exterior que es muy frágil. Sin embargo, estudios posteriores utilizando drogas que inhiben la infectividad del EV, sugieren la entrada por endocitosis (Ichihashi, 1996; Townsley y Moss, 2007; Vanderplasschen y cols., 1998).

Los mecanismos moleculares de entrada del virus vaccinia en la célula no han sido elucidados, sin embargo, estudios recientes de nuestro laboratorio han identificado el complejo A17/A27 como proteínas de la membrana viral involucradas en fusión (Kochan y cols., 2007). Debido a la complejidad de los poxvirus es probable que haya varias proteínas virales necesarias para la entrada por fusión directa de la membrana viral con la celular (MV) o tras el proceso de endocitosis por fusión a pH ácido (EV).

2- Desencapsidación

El paso siguiente es la liberación del nucleoide viral en el citoplasma celular donde el virus va a replicar. Una vez en el interior, los cores experimentan un proceso de desensamblaje que no conlleva una desintegración completa de su estructura sino más bien una permeabilización. Este proceso está caracterizado, en una primera etapa, por la pérdida de lípidos y proteínas del virión (Dales, 1965) y, en una segunda etapa, por una

mayor accesibilidad del genoma a la acción de las nucleasas de ADN exógenas (Sarov y Joklik, 1972).

3- Expresión génica y replicación del ADN

La replicación viral en los poxvirus es un complejo proceso morfogenético altamente conservado. Se caracteriza por ser un proceso en cascada y en el que se distinguen 3 fases de síntesis de ARN mensajeros y de proteínas virales, que se diferencian temporalmente en tempranas, intermedias y tardías (ver revisión (Broyles, 2003)).

3.1) Expresión de genes tempranos: Los mensajeros tempranos aparecen a los pocos minutos después de la entrada del virus en la célula ya que todos las enzimas, factores de trascripción y proteínas necesarias para la síntesis de estos mensajeros se encuentran empaquetados en el core del virión. Durante esta fase se transcribe más de la mitad del genoma viral que codifica proteínas que intervienen en la modulación de los mecanismos de defensa de la célula, en la replicación del ADN y en la transcripción de genes intermedios.

Los estudios transcripcionales han demostrado que los promotores de los genes tempranos se caracterizan por tener secuencias ricas en A+T localizadas inmediatamente delante del sitio de inicio de la transcripción (Ink y Pickup, 1989; Moss, 2001). La ARN polimerasa termina de transcribir los ARN mensajeros tempranos entre 20 y 50 pb después de reconocer la señal de terminación temprana TTTTTNT (Davison y Moss, 1989a; Yuen y Moss, 1987). Estas secuencias de terminación suelen encontrarse en los extremos de los genes virales tempranos y muy raramente se localizan en la región codificante.

3.2) Replicación del ADN viral: La replicación viral tiene lugar en áreas del citoplasma denominadas factorías virales y ocurre durante las dos primeras horas después de la entrada del virus. Se generan unas 10000 copias del genoma por célula de las que sólo la mitad llegan a empaquetarse. Todas las evidencias sugieren que no existe un origen específico de replicación viral y que las moléculas de ADN de la progenie proceden de la generación y posterior resolución de largos concatémeros (Moss, 2001). El proceso de replicación se inicia por la introducción de un corte en una de las cadenas, dejando así un extremo 3´ libre para iniciar la incorporación de desoxirribonucleótidos. La molécula replicada de ADN se vuelve sobre sí misma para copiar el genoma restante. De este modo, se forman concatémeros por replicación a través del bucle terminal, pudiéndose formar grandes concatémeros ramificados antes de

su separación. Después de la transcripción de los genes tardíos, se generan moléculas lineales de ADN viral con los extremos sellados y con secuencias invertidas y complementarias (Traktman, 1991). El ADN así producido se acumula en las factorías para luego ser empaquetado y dar lugar a la formación de las partículas virales.

3.3) Expresión de genes intermedios: Después de la replicación del ADN y antes de que se expresen los genes más abundantes, es decir, los tardíos, tiene lugar la transcripción de una serie de genes llamados intermedios. Estos genes codifican los factores necesarios para la transcripción de los genes tardíos. Hasta la fecha, sólo se conocen siete genes pertenecientes a este grupo y por mutagénesis se ha identificado el tetranucleótido TAAA como elemento iniciador de promotores intermedios.

3.4) Expresión de genes tardíos: La transcripción de los genes tardíos, localizados mayoritariamente en la región central del genoma, se inicia después de la expresión de los genes intermedios, entre las 2-3 horas después del inicio de la infección, y continúa a lo largo del proceso infectivo. El elemento iniciador de la transcripción es la secuencia TAAATG/A y la secuencia de terminación temprana TTTTTNT se encuentra en la región codificante de muchos genes tardíos (Davison y Moss, 1989b). Los transcritos presentan los extremos 5´ poliadenilados y son heterogéneos en su extremo 3´ debido a la ausencia de señales de terminación específicas de transcripción tardía (Moss, 2001). Los genes tardíos codifican proteínas estructurales del virión así como las enzimas necesarias para la trascripción de genes tempranos que también se incorporan al virión.

Además, también a tiempos tardíos se produce transcripción opuesta de ambas cadenas del ADN, lo que da lugar a la formación de moléculas de ARN bicatenario. A pesar de que éstas son potentes inductores de proteínas celulares causantes de muerte celular (PKR o ARNasa L), el virus reduce sus efectos mediante la producción de proteínas tempranas que participan en la inhibición de los mecanismos de defensa antiviral, como es el caso de las proteínas E3 y K3 que se unen a ARN bicatenario.

4- Morfogénesis y salida de la progenie

Una vez replicado el ADN y sintetizadas todas las proteínas virales, comienza el proceso de morfogénesis. Como hemos descrito previamente, existen dos formas infectivas del virus vaccinia que se diferencian en el número de membranas que adquieren de la célula infectada. Así, en el proceso de formación de las partículas infecciosas hay una serie de estadíos intermedios que incluyen la adquisición de estas membranas (Figura 4). A diferencia de otros virus ADN, el VACV replica y se ensambla

en unos compartimentos perinucleares localizados en el citoplasma denominados factorías virales o virosomas.

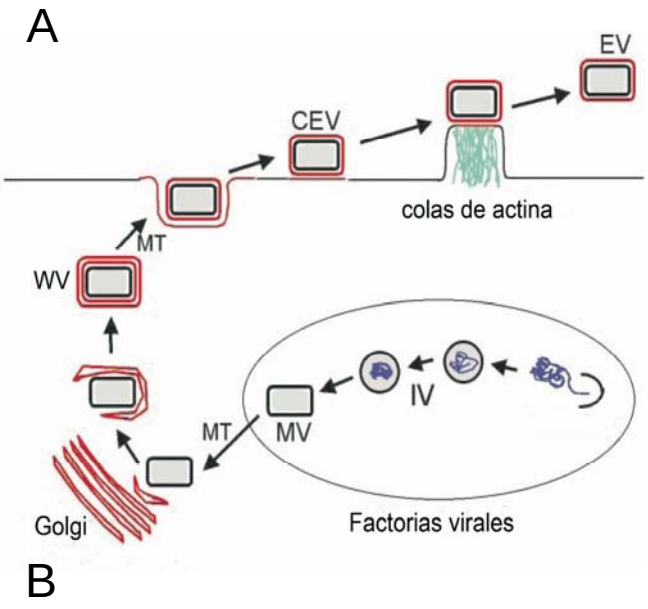

Figura 4: Morfogénesis del virus vaccinia. **(A)** Esquema de los distintos estadíos de la morfogénesis del virus vaccinia (adaptado de Smith y cols. 2002). IV: virus inmaduros; MV: virus intracelulares maduros; WV: virus intracelulares con envuelta; CEV: virus asociado a la célula; EV: virus extracelulares MT: microtúbulos. **(B)** Microscopía electrónica de las distintas formas virales que se producen en células HeLa durante el ciclo infeccioso de la cepa Western Reserve (VACV-WR) del virus vaccinia**.** Figura adaptada de Gallego-Gómez y cols., 2003)

La morfogénesis es un proceso muy complejo que ocurre en varias etapas. Comienza con la formación de crestas membranosas alrededor de un material electrondenso que contiene el ADN viral y las proteínas del core, dando lugar a la formación de formas esféricas denominadas virus inmaduros (IVs, "Inmature Virus"). A continuación tiene lugar la proteólisis y condensación del core viral, transformando los IVs en viriones intracelulares maduros (MVs, "Mature Virus"). Éstos tienen una estructura ovalada en forma de ladrillo y son las primeras formas infectivas del VACV. Los MVs representan la gran mayoría de los viriones producidos durante el ciclo infeccioso y permanecen atrapados dentro de la célula infectada hasta su lisis. Una parte de los MVs se mueven a través de microtúbulos desde las factorías virales hasta el trans-golgi, donde adquieren una segunda membrana transformándose en virus intracelulares con envuelta (WVs, "Wrapped Virus"). Los WVs son también transportados a través de la red de microtúbulos hasta la membrana plasmática, fusionándose con esta última y liberando al exterior virus envueltos que pueden permanecer retenidos en la superficie originando los virus con envuelta asociados a la célula (CEVs, "Cell-associated Enveloped Virus) o liberarse al medio que se denominan virus extracelulares con envuelta (EVs, "Enveloped

Virus"). Los CEVs inducen la formación de colas de actina que proyectan las partículas virales fuera de la célula, permitiendo la infección célula a célula, mientras que los EVs facilitan la diseminación del virus a larga distancia.

3.- APLICACIONES DE LOS POXVIRUS

La viruela ha sido una de las enfermedades más devastadoras que ha conocido el hombre a lo largo de toda su historia y, hasta el momento, es la única enfermedad que ha conseguido ser completamente erradicada.

En el año 1776, Edward Jenner, un médico inglés, inoculó a un niño de ocho años con el virus Cowpox procedente de la llaga de la mano infectada de una ordeñadora (Jenner, 1798), tras lo cual el niño quedó protegido frente a la viruela. Este procedimiento recibió el nombre de vacunación y se extendió rápidamente por Europa y el resto del mundo (Miller, 1957). Hacia finales de la década de los 60, se emprendió una campaña de erradicación de la viruela a nivel mundial que culminó en 1977 con el último caso de viruela natural detectado en Somalia (Fenner y Nakano, 1988b). De este modo, en 1980, la Organización Mundial de la Salud (OMS) declara erradicada la viruela, recomendando el cese de la vacunación con el virus vaccinia (W.H.O., 1980).

Hasta entonces, el virus vaccinia se había utilizado como modelo para los primeros estudios biológicos y bioquímicos en virología (Smadel y Hoagland, 1942). En este sentido, fue el primer virus animal en ser crecido y titulado en cultivo celular, fue analizado químicamente (Fenner, 1989) y purificado en cantidades suficientes como para demostrar que contenía ADN pero no ARN (Smadel y cols., 1942) y además, fue el primero en ser visualizado bajo un microscopio electrónico (Ruska y Kausche, 1943).

Sin embargo, fue precisamente en el año 1980, cuando los poxvirus recobran nuevamente un gran interés científico, debido al desarrollo de la manipulación genética y a la aplicación de la tecnología del ADN recombinante al virus vaccinia.

Dos años más tarde, los grupos dirigidos por los doctores Bernie Moss y Enzo Paoletti demostraron que el virus vaccinia tenía la capacidad de incorporar en su genoma de forma estable una gran variedad de genes procedentes de otras especies. Esto supuso una revolución en el campo de las vacunas, ya que estos virus recombinantes podrían conferir protección frente a un determinado agente infeccioso cuando se les inoculase a animales de laboratorio (Moss, 1996; Paoletti, 1996). Por primera vez, un poxvirus era considerado como candidato vacunal contra otros patógenos, siempre y cuando, no produjera efectos secundarios y se demostrara su eficacia.

En la actualidad, las aplicaciones de los poxvirus pueden dividirse en tres áreas:

A) Para el estudio de la propia biología molecular de los poxvirus. Todavía se desconocen muchos aspectos del ciclo infectivo como, por ejemplo, la entrada del virus, los mecanismos de interacción entre el virus y la célula hospedadora o los determinantes de la virulencia y la patogénesis de la enfermedad. Por lo tanto, el estudio de las diferentes cepas y mutantes de los poxvirus podrían ayudarnos a esclarecer alguno de estos aspectos.

B) Para la expresión y caracterización funcional de proteínas en eucariotas. Los recombinantes del virus vaccinia son un potente sistema de expresión de proteínas heterólogas en células eucariotas.

C) Como vacuna viva o como vector vacunal para la profilaxis de enfermedades infecciosas.

La experiencia obtenida durante la campaña de erradicación de la viruela sirvió para definir al virus vaccinia como un potente inmunógeno. De este modo, los recombinantes del virus vaccinia son un atractivo sistema de expresión, capaz de inducir una fuerte respuesta inmune, tanto celular como humoral, frente al antígeno heterólogo. Además de incorporar fácilmente grandes cantidades de material genético exógeno, la generación de recombinantes basados en los poxvirus tiene un bajo coste de producción y una gran estabilidad, permitiendo altos niveles de expresión del antígeno heterólogo. En la tabla I se muestran las ventajas pricipales de los poxvirus como vector vacunal.

Ventajas de los Poxvirus como vectores
• Gran capacidad de inserción de ADN exógeno (hasta 25 Kb)
• Bajo coste de producción
• Facilidad de generación de recombinantes altamente estables
• Altos niveles de expresión del antígeno heterólogo
• Fácil distribución mundial
• Inducción de una potente respuesta inmune tanto humoral como celular
• Disponibilidad de cepas altamente atenuadas (MVA, NYVAC, ALVAC)

Tabla I: Ventajas de los Poxvirus como vectores de expresión y/o vacunas vivas

El éxito de la utilización de vacunas basadas en poxvirus se demostró en los estudios de campo llevados a cabo con un virus recombinante de vaccinia que expresaba la proteína G de la envuelta del virus de la rabia (VRG). El vector se construyó

mediante la inserción del ADN bicatenario que codifica para dicha proteína G en el gen de la timidina-quinasa (TK) de la cepa Copenhagen del virus vaccinia (VACV-COP) (Kieny y cols., 1984). La eliminación del gen TK permitió una selección bioquímica del recombinante así como la obtención de un fenotipo atenuado del vector. Se observó que la administración de esta vacuna en cápsulas comestibles inducía una respuesta inmunológica contra la rabia en animales capaces de transmitir la enfermedad. Así, este recombinante ha sido utilizado como vacuna antirrábica para zorros en distintas regiones geográficas de Europa y Estados Unidos, obteniendo buenos resultados tanto de seguridad como de eficacia. Del mismo modo, se han generado una gran variedad de poxvirus recombinantes contra enfermedades virales (gripe, encefalitis, enteritis, hepatitis o SIDA), bacterianas (neumonías), parasitarias (malaria o lehismaniasis) y tumorales (melanoma, adenocarcinoma o cáncer de próstata), que se encuentran en fase de experimentación. Sin embargo, los efectos secundarios no deseados asociados al uso de las cepas convencionales del virus vaccinia, pueden comprometer la salud de individuos inmunodeprimidos, ya que en estos pacientes, el virus es capaz de diseminarse. La frecuencia de aparición de efectos adversos tras la inmunización con el virus vaccinia es de 1 en 50000 (Fenner y cols., 1988a; Fenner y cols., 1988b). Esta problemática volvió a ser evidente durante la última campaña de vacunación frente a viruela en la población militar de Estados Unidos, en el año 2003, donde aparecieron varios casos de miocarditis aguda en individuos jóvenes sanos (Halsell y cols., 2003).

Estos problemas han llevado a la comunidad científica a la búsqueda de nuevas vacunas más seguras pero todavía eficaces. Son numerosas las estrategias que se han diseñado para aumentar la seguridad de los poxvirus. En este sentido, se han generado numerosas cepas atenuadas incapaces de replicar en células humanas. Entre ellas podemos incluir: la generación de virus defectivos en genes esenciales que no llegan a completar el ciclo infeccioso (Holzer y Falkner, 1997; Ober y cols., 2002), los vectores con restricciones en el rango de hospedador como es el caso de los avipoxvirus atenuados (ALVAC, TROVAC), o aquellos vectores con mutaciones en genes no esenciales como son las cepas atenuadas del virus vaccinia MVA, NYVAC o los mutantes generados por nuestro grupo, M47, M65 y M101 (Dallo y Esteban, 1987; Paez y cols., 1985).

Las cepas atenuadas de avipoxvirus como ALVAC (canarypox) o TROVAC (fowlpox) han sido ampliamente utilizadas como vacunas en pollos para protegerlos frente a la enfermedad de Newcastle y la gripe aviar H5. Estas cepas han demostrado ser unos vectores extremadamente seguros y eficaces en mamíferos. De hecho, durante la última década, se han generado un gran número de recombinantes que utilizan la

cepa ALVAC como vector parental y son numerosos los ensayos, tanto en animales como en humanos, que demuestran la seguridad y eficacia protectora de este vector (Poulet y cols., 2007).

4.- CEPAS ATENUADAS DEL VIRUS VACCINIA

Como hemos visto en el apartado anterior, la seguridad del virus vaccinia también puede incrementarse introduciendo mutaciones en el genoma, ya sea por medio de la atenuación clásica o a través de la eliminación selectiva de genes. De esta forma, se han generado los que a día de hoy, son considerados como los candidatos vacunales de elección frente a numerosas enfermedades infecciosas y en cáncer: MVA y NYVAC.

4.1 Virus Modificado de Ankara (MVA)

La atenuación clásica, una de las estrategias seguidas para mejorar la seguridad de los vectores, consiste en someter al virus a pases sucesivos en un huésped no natural y aislar las variantes virales que tengan las características más apropiadas.

El ejemplo más significativo lo encontramos en el virus modificado de Ankara (MVA, de sus siglas en inglés). MVA fue clásicamente atenuado tras ser sometido a más de 500 pases sucesivos en fibroblastos embrionarios de pollo. Durante el curso de su generación, perdió un 15 % del genoma parental, así como su capacidad para replicar en células humanas y en la mayoría de células de mamífero.

Esta cepa se generó para ser utilizada como vacuna profiláctica durante las últimas décadas de la campaña de erradicación de la viruela en Alemania, donde más de 120000 individuos fueron vacunados sin presentar ninguna complicación, incluso en aquellos pacientes inmunodeprimidos.

En 1998, Antoine y cols., publicaron la secuencia completa de MVA. Su genoma contiene 178 Kb frente a las 208 Kb de su cepa parental. Se han mapeado 193 ORFs (fases de lectura abierta), que corresponden a 177 genes, 25 de los cuales están parcialmente delecionados y/o han sufrido mutaciones dando lugar a proteínas truncadas (Antoine y cols., 1998).

Su fenotipo atenuado es resultado de las numerosas fragmentaciones y mutaciones que presenta en su genoma viral (figura 5), particularmente de aquellas que afectan a las proteínas de interacción con el hospedador, entre las que se encuentra el producto del gen *K1L*, necesario para la replicación de VACV en células humanas, así como determinadas proteínas estructurales que controlan la morfogénesis viral (ver tabla II).

A diferencia de la cepa Copenhagen (VAC-COP), en el genoma de MVA podemos observar en la región terminal izquierda, 4 grandes deleciones y varios ORFs fagmentados. De hecho, tan sólo 8 de los 27 genes de esta zona aparecen intactos, entre los que destaca el gen de rango de hospedador *C7L*. La región terminal derecha contiene 3 deleciones más que afectan a genes cuyos productos están involucrados en la evasión de la respuesta inmune del hospedador, tales como los homólogos del receptor de los interferones α, β, γ , el homólogo del receptor de TNF o el de quimioquinas. Sin embargo, en esta región se mantiene intacto el gen que codifica el factor homólogo al IL-1βR. Finalmente, en la región central, el MVA también presenta genes fragmentados que codifican proteínas estructurales, como son *F5L, F11L* y *O1L*.

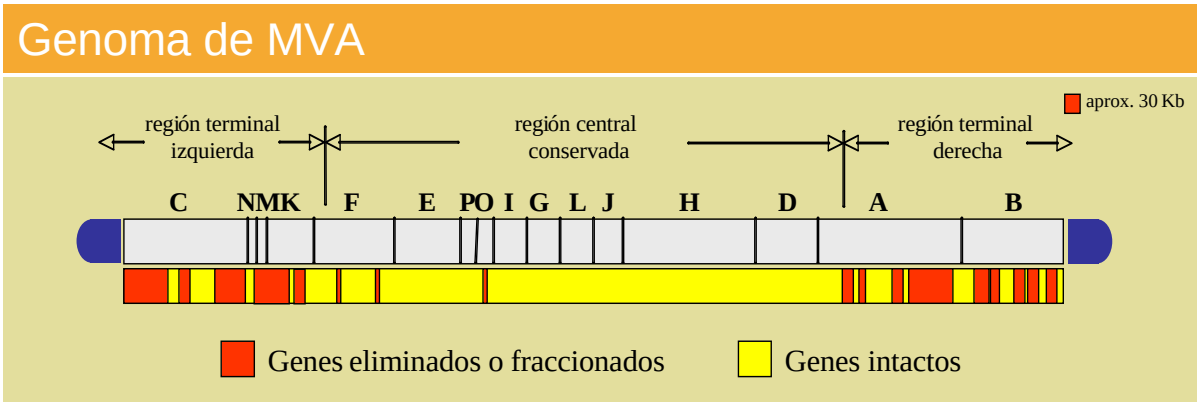

Figura 5: Organización genómica de la cepa MVA. En la parte superior de la figura se muestra la molécula lineal de ADN bicatenario. En la parte inferior se muestra en rojo las delecciones que se introdujeron en el genoma de MVA durante el curso de su atenuación.

Si comparamos la restricción de hospedador (hr, “host range”) de MVA con la de otros mutantes del virus vaccinia (Chang y cols., 1995; Hsiao y cols., 2004; Ramsey-Ewing y Moss, 1998; Ramsey-Ewing y Moss, 1996), el fenotipo de MVA es único en varios aspectos. Primero, la restricción es más amplia que la de otros mutantes, siendo sólo capaz de replicar en células CEF y BHK-21. Además, el bloqueo en las líneas celulares no permisivas ocurre en estadíos tardíos, afectando al ensamblaje de ciertas proteínas estructurales, sin alterar la expresión de genes tempranos, intermedios o tardíos. En otros mutantes, por el contrario, si que existe una inhibición en la síntesis de proteínas virales y por lo que el bloqueo en el ciclo infeccioso ocurre en estadíos más tempranos. Trabajos de microscopía electrónica entre los que se encuentran algunos realizados en el laboratorio, han identificado los estadíos donde se produce el bloqueo en el proceso de morfogénesis de MVA en células humanas, en el que sólo se forman partículas inmaduras (IVs) y no se produce diseminación del virus dentro del huésped (Sancho y cols., 2002; Sutter y Moss, 1992); (Gallego-Gomez y cols., 2003).

Son muchos los trabajos realizados para demostrar la seguridad de MVA tanto “in vitro” como “in vivo”(Belyakov y cols., 2003; Blanchard y cols., 1998; Drexler y cols., 2004). Experimentos llevados a cabo por Wyatt y cols. en 1998, indican que las deleciones tienen un efecto aditivo, ya que para la correcta replicación del virus en células de mamífero es necesaria la reinserción de varias de las mutaciones que presenta MVA (Wyatt y cols., 1998). Por otro lado, varios estudios han demostrado que la inoculación intracraneal de MVA no provoca ningún signo de enfermedad en el animal, de hecho, previene la neurovirulencia inducida tras un desafío letal con la cepa competente en replicación por ruta intracerebral. Además, la seguridad de MVA también se ha demostrado en distintos modelos de animales inmunosuprimidos (Mayr y cols., 1978; Stittelaar y cols., 2001; Werner y cols., 1980). Todos estos datos sugieren que la atenuación de MVA y la consecuente pérdida de genes del rango hospedador reduce su virulencia y patogénesis en el animal. Por todas estas razones, MVA es considerado como un virus seguro y puede ser manipulado bajo condiciones de seguridad de laboratorio de nivel 1, dado que la posibilidad de que se generen revertientes espontáneos resulta muy improbable.

A pesar de que los recombinantes basados en MVA son seguros y capaces de expresar la proteína de interés de igual manera que las cepas silvestres del VACV (Blanchard y cols., 1998), su utilización como vector requiere la demostración de su inmunogenicidad y eficacia clínica. Se han realizado numerosos esfuerzos para caracterizar las bases moleculares de la respuesta inmune estimulada por las vacunas basadas en esta cepa. Entre los logros más importantes podemos destacar los ya mencionados como la caracterización molecular del ciclo viral en líneas celulares no susceptibles a la infección (Gallego-Gómez y cols., 2003) o la secuenciación de su genoma completo (Antoine y cols., 1998), que reveló que MVA ha perdido genes importantes de evasión del sistema inmune que modulan la respuesta innata basándose en las funciones de citoquinas y quimioquinas. Consecuentemente, la ausencia de estos genes parece ser la responsable de la respuesta específica de citoquinas inducida tras la infección con MVA (Ramírez y cols., 2000). Apoyando esta hipótesis, estudios realizados en el laboratorio utilizando la técnica de microarrays (Guerra y cols., 2004; Guerra y cols., 2006), han revelado un patrón diferencial de expresión génica en células humanas tras la infección con la cepa competente en replicación WR respecto a las cepas atenuadas MVA o NYVAC. Estos estudios realizados en células HeLa indican que existen similitudes pero también diferencias claras, en genes inmunomoduladores como IL-7, IL-1α, IL-8 o IL-15 entre las distintas cepas. Las diferencias encontradas entre las

cepas MVA y NYVAC se han hecho más evidentes en un estudio reciente llevado a cabo en células dendríticas humanas ((Guerra y cols., 2007), anexo 1)

Todas estas características atribuidas a MVA hacen que, a pesar de su atenuación, los recombinantes basados en esta cepa sean altamente inmunogénicos siendo capaces de generar linfocitos T citotóxicos (CTLs) específicos y anticuerpos neutralizantes frente a antígenos recombinantes (Excler y Plotkin, 1997). Distintos estudios llevados a cabo en modelos de ratón y en primates no humanos han demostrado su eficacia en la producción de anticuerpos y en la respuesta CTL específica frente a antígenos de gripe, malaria o VIH (Sutter y Staib, 2003). Además, su restricción en rango de hospedador así como su inmunogenicidad, demostrada también en humanos, hacen del MVA un vector de expresión seguro, y convierte a los recombinantes de MVA en prometedores candidatos vacunales frente a un amplio espectro de enfermedades infecciosas y en cáncer (Amara y cols., 2001; Amara y cols., 2002; Brave y cols., 2007; Earl y cols., 2007; Gherardi y Esteban, 2005; Graham, 2002; Kreijtz y cols., 2007; Liu y cols., 2007; Ramírez y cols., 2000; Vuola y cols., 2005; Webster y cols., 2005).

4.2.- Virus atenuado de la cepa Copenhagen: NYVAC

NYVAC es una cepa altamente atenuada derivada de la cepa Copenhagen (VACV-COP) de la que fueron eliminados por ingeniería genética 18 genes no esenciales entre los que se encuentran: genes implicados en virulencia, patogenicidad y genes que interaccionan con la célula huésped (Tartaglia y cols., 1992b), dando como resultado un virus con una reducida capacidad de replicación en un amplio rango de células de mamífero entre las que se incluyen las de origen humano (Figura 6).

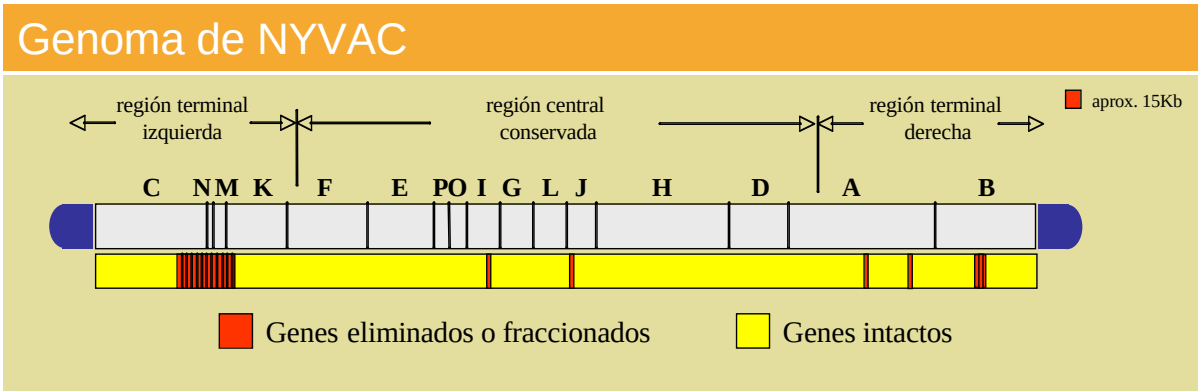

Figura 6: Organización genómica de la cepa NYVAC. En la parte superior de la figura se muestra la molécula lineal de ADN bicatenario. En la parte inferior se muestra en rojo las 18 deleciones que se introdujeron para su generación.

Entre los genes delecionados se encuentra el gen *J2R* que codifica la timidina quinasa (TK). La inactivación o deleción completa de este gen no afecta al crecimiento del virus, sin embargo, mutantes del virus vaccinia en el gen TK han mostrado un fenotipo atenuado en ratones inoculados por ruta intracerebral o intraperitoneal (Buller, 1985; Buller y cols., 1985). Lo mismo ocurre con la inactivación del gen *I4L*, que codifica la subunidad grande de la enzima ribonucleótido reductasa implicada en el metabolismo de nucleótidos (Child y cols., 1990), y con la inactivación del gen de la hemaglutinina (*A56R*), que produce una neurovirulencia reducida en conejos inoculados por ruta intracraneal (Shida y cols., 1987). Los genes *B13R/B14R* tienen homología con los inhibidores de la serina proteasa I e inhiben la respuesta inflamatoria del hospedador. El gen ATI (*A26L*), cuya función es la protección de los viriones del virus cowpox durante la diseminación entre animales (Bergoin y cols., 1971), también fue delecionado. Finalmente, se han descrito diversas deleciones espontáneas cerca del extremo izquierdo del genoma del virus vaccinia. Se demostró que la cepa WR con una deleción de 10 kb mostraba un fenotipo atenuado después de la inoculación intracraneal (Buller y cols., 1991; Buller y cols., 1985; Moss y cols., 1981). Más tarde se demostró que esta deleción incluía 17 ORFs potenciales, entre los que se incluyen los genes *N1L* o *C3L*, cuya función parece estar implicada en la evasión de los mecanismos de defensa del hospedador. El extremo izquierdo también incluye dos ORFs identificados como genes de ámbito del hospedador, *K1L* (Gillard y cols., 1986) y *C7L* (Perkus y cols., 1990). Su ausencia en el genoma de NYVAC está asociada con la reducida capacidad del virus para replicar en un amplio rango de líneas celulares de origen humano, así como en células de conejo o de cerdo (RK-13, PK15) (Oguiura y cols., 1993; Tartaglia y cols., 1992a). Sin embargo, NYVAC es capaz de replicar con la eficiencia de una cepa silvestre en células Vero y en cultivos primarios de fibroblastos embrionarios de pollo (CEF) (Tartaglia y cols., 1994; Tartaglia y cols., 1992a).

Hasta la fecha existe muy poca literatura sobre la biología molecular o el comportamiento de este virus en células en cultivo. Sin embargo, son numerosos los ejemplos en los que se utiliza NYVAC como vacuna recombinante, demostrando su eficacia y seguridad en varios modelos animales (Tartaglia y cols., 1994; Tine y cols., 1996). Así, NYVAC no es capaz de diseminarse en ratones inmunodeprimidos y muestra una reducida capacidad para replicar en una gran variedad de tejidos humanos sin llegar a producir partículas infecciosas(Tartaglia y cols., 1992b).

Por todas estas razones, NYVAC es considerado como un vector seguro y puede usarse en condiciones ACGM de nivel 1 (“Advisory Committee on Genetic

Modifications"), siempre que la naturaleza del inserto no afecte a la seguridad del vector. En este sentido, distintos ensayos clínicos en humanos han demostrado la seguridad de los vectores derivados de esta cepa frente a enfermedades como malaria, SIDA o encefalitis japonesa (Benson y cols., 1998; Franchini y cols., 2004; Ockenhouse y cols., 1998; Precopio y cols., 2007; Sheppard y cols., 2007).

En la siguiente tabla se detallan los genes delecionados en MVA y NYVAC con sus respectivas funciones.

VACV-COP	MVA	NYVAC	Función
C22L	-	C22L	Modulador de la respuesta antiviral. Codifica una proteína homóloga al receptor de TNF
C21L	-	C21L	Modulador de la respuesta antiviral. Inhibe las rutas clásica y alternativa del sistema del complemento
C20L	-	C20L	Codifica una proteína con dominios de anquirina
C18L	-	C18L	Posible gen de rango de hospedador. Codifica una proteína con dominios de anquirina.
C17L	003L 004L	C17L	Posible gen de rango de hospedador. Codifica una proteína con dominios de anquirina.
C16L	-	C16L	Función desconocida
C15L	-	C15L	Función desconocida
C12L*	008L	-	Modulador de la respuesta antiviral. Se une a la IL18 e inhibe IL18 inducida por IFN-gamma
C9L	014L 015L 016L	C9L	Posible gen de rango de hospedador. Codifica una proteína con dominios de anquirina.
C7L	018L	C7L	Rango de hospedador (hr). Necesario para la replicación del virus en células humanas
C6L	019L	C6L	Función desconocida
C5L	-	C5L	Función desconocida
C4L	-	C4L	Función desconocida
C3L	-	C3L	Modulador de la respuesta antiviral. Inhibe la ruta clásica del sistema del complemento
C2L	-	C2L	Modulador de la respuesta antiviral. De la familia de las proteínas tipo Kelch. Implicado en respuesta inflamatoria
C1L	-	C1L	Función desconocida
N1L	020L	N1L	Modulador de la respuesta antiviral. Interviene en la señalización de NFkB
N2L	021L	N2L	Codifica una proteína que tiene como diana la alpha-amianitina
M1L	-	M1L	Codifica para una proteína con dominios de anquirina
M2L	-	M2L	Función desconocida
K1L	022L	K1L	Rango de hospedador (hr). Necesario para la replicación del virus en células de conejo. Es capaz de complementar a *C7L* en células humanas
K6L	027L	K6L	Función desconocida. Posible fosfolipasa
F5L	033L 034L	F5L	Posible proteína principal de membrana

VACV-COP	MVA	NYVAC	Función
F11L	041L	F11L	Serin/threonin quinasa. Implicado en el control de la eleongación de la transcripción
O1L	059L 060L	O1L	Función desconocida
I4L	065L	I4L	Interviene en metabolismo de ácidos nucleicos. Subunidad grande de la ribonucleotido reductasa
J2R	086R	J2R	Timidina quinasa. Implicado en virulencia
A26L*	137L	A26L	Proteína tipo A que forma cuerpos de inclusión. Diseminación del virus de animal a animal
A39R	150R 151R	A39R	Modulador de la respuesta antiviral. De la familia de las semaforinas
A52R	-	A52R	Modulador de la respuesta antiviral. Homologo a TLR. Tiene como diana a IRAK-2 y TRAF-6
A53R	-	A53R	Modulador de la respuesta antiviral. Homologo al receptor de TNF
A55R	-	A55R	Modulador de la respuesta antivira. De la familia de las proteínas tipo Kelch. Implicado en respuesta inflamatoria
A56R	165R	A56R	Hemaglutinina. Proteína de membrana de los EVs. Inhibe fusión
B2R	168R 169R	B2R	Función desconocida
B4R	171R 172R	B4R	Codifica una proteína con dominios de anquirina
B8R	176R*	B8R	Modulador de la respuesta antiviral. Se une e inhibe al IFN-α/β de varias especies. * En MVA no es funcional
B13R	181R	B13R	Modulador de la respuesta antiviral. Inhibe la apoptosis mediada por TNF y FasL
B14R	182R	B14R	
B16R*	184R	-	Modulador de la respuesta antiviral. Codifica una proteína homóloga al receptor de IL-1β
B20R	-	B20R	Codifica para una proteína con dominios de anquirina
B21R	-	B21R	Homólogo a C15L
B23R	190R 191R	B23R	Homólogo a C17L
B24R	-	B24R	Homólogo a C18L
B26R	-	B26R	Homólogo a C20L
B27R	-	B27R	Homólogo a C21L
B28R	-	B28R	Homólogo a C22L

Tabla II: Función de los genes delecionados en las cepas MVA y NYVAC. En rojo se muestran los genes ausentes o parcialmente delecionados dentro del genoma de capa cepa viral y en verde los genes intactos. VACV-COP: cepa Copenhagen del virus vaccinia; El asterisco indica que el gen se encuentra inactivo o ausente en la cepa parental.

5.- Protocolo de inmunización de Prime-boost

A pesar de que los poxvirus son unos potentes inmunógenos, la experiencia obtenida tanto en los modelos preclínicos (en ratones y monos) como en los clínicos (en humanos), nos indica que para inducir una potente respuesta inmune celular es necesaria la utilización de sistemas combinados de inmunización.

En este sentido, nuestro laboratorio ha sido pionero en el desarrollo de un protocolo de inmunización heterólogo denominado “Prime-Boost” (inmunización-refuerzo) que permite combinar distintas estrategias vacunales para lograr una potenciación de la respuesta inmune que se correlacione con protección (Li y cols., 1993; Zavala y cols., 2001). Debido a su aceptación general, en este estudio utlizaremos la denominación en inglés de “prime/boost”.

Resultados de varios estudios en el modelo de malaria demuestran que la respuesta inmune aumenta considerablemente cuando se combinan dos vectores heterólogos expresando el mismo antígeno siguiendo éste protocolo de inmunización.

A partir de éstos trabajos, se han ensayado diversas combinaciones en modelos animales y humanos frente a diferentes patógenos; Así, por ejemplo, el protocolo de inmunización basado en la administración de un virus Influenza que expresa la proteína CS de *Plasmodium yoelii,* seguido de una segunda dosis con un virus vaccinia que expresa el mismo antígeno, fue capaz de incrementar más de 20 veces el número de células T CD8+ específicas secretoras de IFN-γ respecto al número obtenido tras una única inmunización. La secuencia de administración de los vectores también resultó ser esencial, ya que el protocolo de inmunización inverso no mejoró la respuesta inmunológica (Reyes-Sandoval y cols., 2007).

En la actualidad, existe un consenso generalizado de que una primera dosis con ADN recombinante, seguido de una segunda inmunización con un vector viral que exprese el mismo antígeno, genera los mayores niveles de inmunidad específica, que en algunas ocasiones, permite la protección frente a distintos enfermedades infecciosas como SIDA, leishmaniasis o malaria entre otras. De hecho, en el modelo de malaria, son numerosos los trabajos en los que emplean múltiples combinaciones de distintos vectores plasmídicos y virales (vaccinia y adenovirus). En todos ellos, la potenciación de la respuesta inmune se correlacionó con una inmunidad esterilizante frente a malaria en el 100 % de los animales vacunados (ver revisión, (Reyes-Sandoval y cols., 2007)).

Varios estudios realizados en otros campos como por ejemplo, el SIDA, han confirmado la capacidad de los poxvirus para potenciar la respuesta primaria inducida por otros vectores virales o plasmídicos. Por ejemplo, trabajos realizados en el laboratorio han demostrado que la administración del virus vaccinia que expresa la

envuelta (env) del VIH-1 es capaz de incrementar en 5 ó 6 veces la respuesta celular inducida por un recombinante basado en el virus influenza que expresa un epítopo de células T CD8+ presente en la región V3 de esta proteína, siendo incluso mayo la respuesta cuando el virus utilizado en la segunda inmunización fue MVA (Gherardi y cols., 2003).

En la actualidad se están ensayando en fase clínica varios protocolos de inmunización que utilizan éstos recombinantes contra enfermedades como SIDA, malaria, encefalitis japonesa o cáncer, validando no sólo la seguridad de estos vectores sino también demostrando su capacidad para inducir respuestas inmunológicas antígeno-específicas potentes en humanos.

6.- Vacunas frente al VIH/SIDA

Desde la identificación del virus de la inmunodeficiencia humana (VIH) como agente causal del **S**índrome de la **I**nmuno**D**eficiencia **A**dquirida (SIDA), hace ahora más de 20 años, la pandemia del VIH no ha mostrado ningún signo de desaceleración o abatimiento, y su impacto ha superado todas las expectativas. La Organización Mundial de la Salud (OMS) estima que sólo en el año 2006 más de 5 millones de personas contrajeron la infección por el VIH, lo que supone la mayor cifra registrada de nuevas infecciones en un solo año desde el principio de la epidemia. Hasta la fecha, al menos 60 millones de personas han contraído la infección, y se calcula que cada día se producen unas 14.000 nuevas infecciones (Figura 7) (www.unaids.com).

Figura 7: Prevalencia y distribución geográfica de la infección por VIH-1 en el año 2006

El 95% de las nuevas infecciones se produce en los países en vías de desarrollo, siendo el África subsahariana y Asia central las áreas de mayor impacto, lo que supone casi dos tercios del total global de personas que viven con VIH/SIDA pero sólo un 10% de la población mundial. Las diferencias geográficas y económicas de esta enfermedad son evidentes, ya que más del 95% de los casos y el 95% de las muertes por SIDA ocurren en el tercer mundo (70% en África), sobre todo entre jóvenes adultos, con un incremento progresivo entre las mujeres (OMS, 2005). España continúa siendo el país con mayor número de personas infectadas por el VIH de la Unión Europea (UE).

Una de las peculiaridades del VIH-1 es su elevada variabilidad. Las cepas de VIH-1 pueden clasificarse en 3 grupos: M ("Mayor"), O ("Outlier") y N ("New") que pueden representar tres introducciones independientes del virus de la inmunodeficiencia de simio (SIV) en el humano. El grupo O parece estar restringido al centro-oeste de África y el grupo N, descubierto en 1998, es extremadamente raro. Más del 90% de las infecciones por VIH-1 pertenecen al grupo M. Dentro del grupo M se conocen al menos 9 subtipos genéticamente distintos y se han descrito más de 30 formas recombinantes circulantes (CRFs). Los subtipos y CRFs de VIH-1 están distribuidos de un modo dispar a nivel mundial, siendo los más diseminados los subtipos B y C. Históricamente el subtipo B ha sido el genotipo más común en América, Europa, Japón y Australia, y es el que más se ha utilizado en el desarrollo de vacunas. Por otro lado, el subtipo C es el más abundante globalmente, representando más del 50% de las infecciones, especialmente en el África subsahariana, India y Nepal.

Los programas de prevención existentes han ralentizado la extensión de nuevas infecciones en algunos lugares, pero son incapaces de frenar la expansión de la pandemia. El tratamiento con antiretrovirales ha constituido una terapia importante contra el SIDA, pero estos fármacos no suponen una cura, y su coste y complejidad de utilización los sitúan fuera del alcance de la inmensa mayoría de las personas que los necesitan, especialmente en el mundo en desarrollo. Por lo tanto, el desarrollo de una vacuna eficaz frente al VIH/SIDA se ha convertido en uno de los mayores retos de este siglo para la comunidad científica mundial y una de las prioridades para la salud pública. En este sentido, la historia de las enfermedades infecciosas nos ha enseñado que sólo una vacuna preventiva segura y eficaz será capaz de romper el ciclo de nuevas infecciones, y en última instancia, hacer que revierta y acabe la pandemia. La viruela se declaró erradicada en 1980 gracias a una vacuna eficaz; la polio ya ha desaparecido del continente americano y se espera que esté completamente controlada hacia finales del 2007; el sarampión y la fiebre amarilla se han controlado gracias a las vacunas. La vacuna contra el SIDA debe añadirse cuanto antes a esta lista (Alcami y cols., 2005; Hokey y Weiner, 2006; Kegeles y cols., 2006; Letvin, 2006).

6.1 ¿Es posible el desarrollo de una vacuna efectiva frente al VIH/SIDA?

Aunque el desafío es grande y son muchos los obstáculos a superar, los científicos piensan que sí es posible. Esta convicción se basa en las observaciones realizadas hasta ahora en este campo:

1º.- Existe un pequeño grupo de individuos que, a pesar de estar expuestos repetidamente al virus, no llegan a infectarse. Se están analizando las respuestas inmunológicas frente al VIH en estas personas conocidas como seronegativos expuestos (SNE), así como cualquier característica genética que tengan en común, para averiguar qué es lo que permite a sus sistemas inmunológicos rechazar la infección.

2º.- En el curso de la infección natural por el VIH, la inmunidad celular generada durante la primoinfección suprime la carga viral por un tiempo considerable que a menudo llegan a ser años, incluso décadas. A este grupo de pacientes se les conoce como no progresores a largo plazo (NPLP) y son capaces de regular la replicación del virus retardando la progresión de la enfermedad e inhibiendo la transmisión del VIH. Se ha demostrado que ciertos tipos de HLA como B57 y B27 están asociados con una progresión lenta hacia SIDA (Gao y cols., 2005; Goulder y Watkins, 2004).

3º.- Estudios realizados en primates no humanos demostraron que la inmunización con virus vivo atenuado proporciona una protección completa frente a una posterior infección con el virus de la inmunodeficiencia de simio (SIV), que causa SIDA en monos.

4º.- La inmunización pasiva con anticuerpos ampliamente neutralizantes frente al VIH confiere una protección completa a los monos después de desafiarlos con una dosis letal del virus de la inmunodeficiencia del hibrido simio/humano (SHIV)(Mascola y cols., 2000).

De este modo, basándonos en estas observaciones, una vacuna eficaz sería aquella capaz de generar anticuerpos neutralizantes frente a un amplio espectro de los subtipos de VIH circulantes, capaz de inducir una potente respuesta inmune celular que lograse disminuir la carga viral hasta niveles indetectables y que fuese efectiva en la prevención de la infección.

6.2 ¿Por qué es tan difícil desarrollar una vacuna frente al VIH/SIDA?

Aunque son muchos los candidatos estudiados, todavía estamos lejos de lograr una vacuna eficaz, ya que su desarrollo está dificultado por las características propias de replicación y transmisión del virus.

Estas dificultades, que se resumen el la tabla III, deben tenerse en cuenta a la hora de desarrollar las estrategias de vacunación para prevenir la infección.

	Dificultades en el desarrollo de una vacuna frente al VIH/SIDA
Virus	• Hipervariabilidad del VIH • Los antígenos requeridos para conferir protección aún no se han definido • El VIH infecta, suprime y destruye las células clave del sistema inmune • Existen limitaciones en los modelos animales para estudiar el VIH/SIDA
Respuesta Inmune	• La inmunidad natural no erradica al virus • Los determinantes inmunológicos de protección aún no se han identificado • El papel de la inmunidad innata está poco estudiado • Es posible la re-infección por un segundo aislado del VIH
Transmisión y Patogénesis	• El VIH se transmite como partícula libre o asociado a las células • El VIH se transmite por contacto sexual o por ruta intravenosa • El ciclo de replicación del VIH incluye su integración en el genoma del huésped • Puede permanecen durante largos periodos de tiempo en estado de latencia • Preparación, producción y escalado a fase clínica de los candidatos vacunales

Tabla III: Dificultades en el desarrollo de una vacuna frente al VIH/SIDA.

6.3 Diseño de Vacunas frente al VIH/SIDA

En la actualidad, el diseño de vacunas frente al VIH/SIDA puede dividirse en dos grandes grupos: vacunas dirigidas hacia la producción de anticuerpos neutralizantes y vacunas encargadas de generar una potente respuesta inmune celular frente a los distintos antígenos.

A) Vacunas que generan anticuerpos neutralizantes

La producción de anticuerpos neutralizantes ampliamente específicos frente a todas las variantes del VIH sería, sin lugar a dudas, la respuesta más eficaz para prevenir la infección. Existen evidencias claras en el modelo de macaco de que la presencia de anticuerpos neutralizantes antes de la infección protege (Gauduin y cols., 1997; Mascola y cols., 2000); Sin embargo, la producción de anticuerpos neutralizantes a través de la vacunación es muy difícil de lograr.

Las primeras vacunas frente al VIH se basaron en el modelo de inmunización frente a Hepatitis B que consiste en la inmunización con una proteína recombinante. Las vacunas iniciales frente al VIH estaban compuestas por las proteínas de la envuelta gp120 y gp160 recombinantes producidas por ingeniería genética o utilizando vectores como el virus vaccinia (Mascola y cols., 1996). A pesar de que hasta el momento este tipo de vacunas han fallado a la hora de generar anticuerpos neutralizantes, la gp120 se sigue utilizando en combinación con virus recombinantes o ADN desnudo en vacunas que estimulan la respuesta inmune celular. Al mismo tiempo, se están haciendo grandes esfuerzos en el diseño de nuevas preparaciones e inmunógenos que representen distintas variantes conformacionales de la proteína gp120 y gp140 (derivada de la gp160 sin el dominio de anclaje), ya que la producción de anticuerpos ampliamente neutralizantes sigue siendo una asignatura pendiente en el desarrollo de vacunas frente al VIH.

B) Vacunas que estimulan la respuesta inmune celular

Las dificultades encontradas a la hora de generar una respuesta humoral eficaz durante la infección por VIH, han dirigido el diseño de vacunas hacia la búsqueda de nuevas estrategias e inmunógenos que estimulen una potente respuesta inmune celular, capaz de controlar la infección temprana por VIH y prevenir la progresión de la enfermedad.

Los datos experimentales apoyan a que es la respuesta celular la que controla la infección viral, tanto durante la infección primaria como en la cronicidad de la infección. Así pues, durante la fase aguda de la infección, se genera una vigorosa actividad celular virus-específica mediada por linfocitos T citotóxicos (CTLs). El pico máximo de esta respuesta coincide con el comienzo de la disminución de la carga viral (Borrow y cols., 1995; Gallimore y cols., 1995; Schmitz y cols., 1999). Esta afirmación surgió inicialmente de trabajos realizados *in vitro* donde se demostró que los linfocitos T CD8+ específicos anti-VIH producen factores solubles que inhiben la replicación viral (MIP-1 β, MIP-1 α y RANTES) y lisan (granzimas y perforinas) las células infectadas (Eccleston, 1997). De forma similar, estudios llevados a cabo en monos *reshus* infectados con el virus de la inmunodeficiencia de simio (SIV), han demostrado que la depleción de los linfocitos T CD8+ impide a los animales controlar la viremia, acelerando su progresión a SIDA (Amara y cols., 2002; Barouch y cols., 2003; Schmitz y cols., 1999) y que la estimulación de esta respuesta mediante vacunas logra disminuir la carga viral y retardar la enfermedad (Barouch y cols., 2000).

La respuesta celular también está implicada en el control de la infección en enfermos crónicos infectados por VIH. De esta manera, en los pacientes no progresores a largo plazo (NPLP) se ha observado una respuesta de CTLs potente y sostenida (Cao y cols., 1995). En estos individuos, existe una correlación inversa entre los niveles de ARN viral en sangre y la frecuencia de CTLs específicos. Estudios recientes realizados en monos demuestran que existe una correlación entre la preservación de la población de linfocitos T CD4+ memoria y la progresión a SIDA.

Sin embargo, a pesar de la amplia expansión de la población de células T CD8+ virus-específicas que ocurre durante la primoinfección, hasta la fecha no se ha documentado que dicha respuesta logre erradicar al virus, lo que demuestra que el VIH es capaz de evadirla. Se han propuesto varios mecanismos de escape (tabla III). Como se mencionó anteriormente, uno de los grandes problemas en el desarrollo de una vacuna frente al VIH es la diversidad genética de las poblaciones virales que se producen durante la infección. Las mutaciones virales se acumulan rápidamente mientras el VIH replica de tal forma que pueden variar entre si. Esta diversidad antigénica también puede afectar a la especificidad de la respuesta celular CD8+, por lo que es importante utilizar como inmunógeno varios antígenos virales, pues una mutación puntual puede eliminar un epítopo inmunodominante.

De los datos obtenidos hasta el momento podemos concluir que una vacuna eficaz necesitaría inducir cifras elevadas de células T CD8+ de memoria, capaces de secretar rápidamente citoquinas y quimioquinas al entrar en contacto con el antígeno. La respuesta también debería ser altamente reactiva frente a las diferentes cepas del VIH y ser genética y cualitativamente mejor que la respuesta que se produce durante la infección natural (Garber y Feinberg, 2003). Además, debería ser capaz de estimular una potente respuesta especifica de células T CD8+ y CD4+, ya que la ausencia de células T CD4+ ayudadoras constituiría un deterioro funcional de los CTLs y consecuentemente un fracaso del control inmune de la viremia.

6.4 Candidatos vacunales

La investigación en vacunas frente a VIH ha llevado a explorar diferentes tipos de conceptos vacunales: vectores vivos recombinantes; moléculas de ADN desnudo; proteínas recombinantes o péptidos sintéticos entre otros (figura 8).

De todos ellos, los adenovirus y poxvirus recombinantes son probablemente los sistemas más utilizados y hasta el momento la combinación de ambos o junto con ADN son los únicos candidatos que han dado resultados positivos en fase clínica con inducción de respuesta inmune celular.

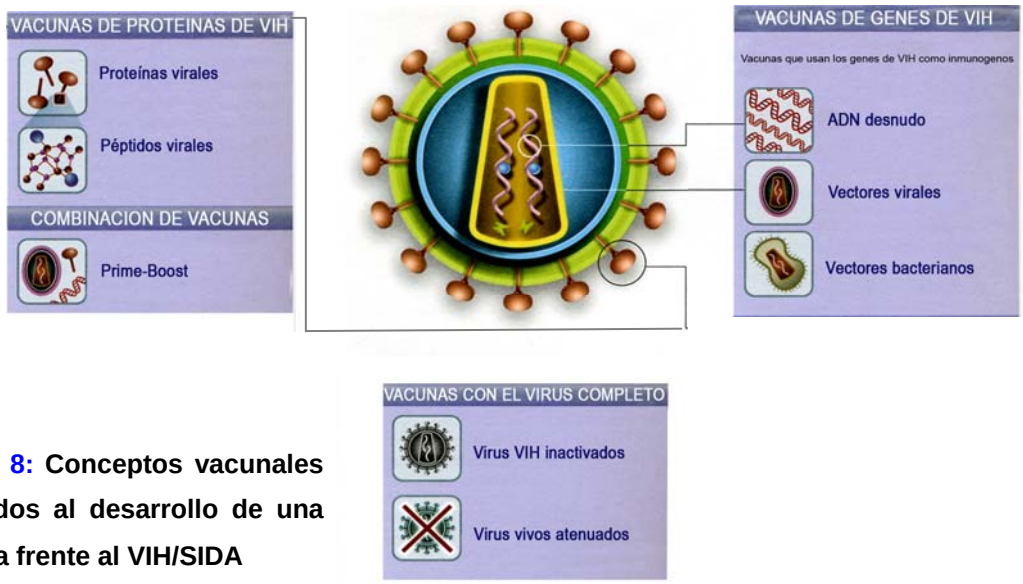

Figura 8: Conceptos vacunales aplicados al desarrollo de una vacuna frente al VIH/SIDA

El primer ensayo en fase I de una vacuna frente al VIH se realizó en Estados Unidos en 1987. Desde entonces, más de 30 candidatos vacunales han sido testados en unos 65 ensayos clínicos en fase I/II, interviniendo más de 10000 voluntarios sanos en más de 10 países (Girard y cols., 2006; Hanke y cols., 1999; Sauter y cols., 2005). Hasta la fecha se han completado dos ensayos en Fase III (Kegeles y cols., 2006) y un tercero está en proceso (Letvin, 2006).

En la tabla IV se muestran los candidatos vacunales que en la actualidad se encuentran en fase clínica de investigación. Estas pruebas han demostrado: 1) la factibilidad de realizar los ensayos clínicos, incluso en países en desarrollo; 2) que los candidatos vacunales son seguros y no producen efectos secundarios importantes; y 3) que al menos algunas de las vacunas experimentales inducen respuestas inmunológicas específicas frente al VIH.

Aunque los resultados de los primeros ensayos clínicos no han sido muy prometedores, induciendo respuestas inmunológicas muy variables e inferiores respecto a las obtenidas en el modelo de macacos (menos del 60%, en el mejor de los casos), en los últimos años un número prometedor de nuevos antígenos ha mostrado buenos resultados en los estudios de fase I. En este sentido, los datos de estudios recientes en fase clínica, aun sin publicar presentados en el últimos congresos internacionales de vacunas frente a VIH celebrados en Ámsterdam y Seattle en 2006 y 2007, muestran que los protocolos de inmunización en humanos donde se combina ADN/pox ó ADN/adeno expresando distintos antígenos de VIH (Env, Gag, Pol y Nef) son capaces de inducir la activación de linfocitos T CD4+ y CD8+ específicos en la mayoría de los voluntarios inmunizados, aunque mayoritariamente frente a la proteína Env. Estos resultados junto con los que se produzcan en los ensayos en fase II utilizando estas vacunas, alimentan

el optimismo actual para obtener una vacuna contra el VIH en los próximos años que sea segura y parcialmente eficaz.

Tabla IV: Ensayos clínicos frente a VIH/SIDA actualmente en curso.

Nombre	Fecha de inicio	Organizador	Paises	Tipo de la vacuna	Antígeno (subtipo)
FASE III	**Ensayos grandes con poblaciones de alto riesgo para probar la eficacia de la vacuna**				
RV 144	Oct-03	USMHRP, MoPH Thailand, Aventis, Vaxgen	Tailandia	Prime: ALVAC Boost: gp120	Env (B/E);gag/pol Env (B/E)
TEST-OF-CONCEPT					
HVTN 503	Feb-07	SAAVI, HVTN	Suráfrica	Adenovirus	gag/pol/nef (B)
HVTN 502	Dic-04	DAIDS, HVTN, Merk	USA,Canada,Peru, R. Dominicana, Haiti, Puerto Rico, Australia, Brasil	Adenovirus	gag/pol/nef (B)
FASE II	**Ensayos de tamaño medio para probar seguridad y capacidad inmunogénica de la vacuna**				
IAVI 002	Nov-05	IAVI, Targered Genetics	Suráfrica, Uganda, Zambia	Adenoasociados tipo2	gag/pol/ΔRT (C)
HVTN 204	Sep-05	DAIDS, HVTN, VRC, Vical, GenVec	USA, Brasil, Suráfrica, Haiti, Jamaica	Prime:ADN Boost:Adeno	gag/pol(B) Nef/Env (A) gag/pol/Env(B,C)
ANRS VAC 18	Sep-04	ANRS, Aventis	Francia	5 lipopeptidos de CTLs	gag/pol/nef (B)
FASE I/II	**Ensayos de tamaño pequeño para probar seguridad y capacidad inmunogénica de la vacuna**				
EV 03	Jun-07	Eurovac, ANRS	Inglaterra, Alemania, Suiza, Francia	Prime: ADN-C Boost: NYVAC-C	Env + gag-pol-nef (C) Env, gag-pol-nef (C)
HIVIS 03	Dic-06	MUCHS, instituto Karolisnka, SMI, Vecura, USMHRP	Tanzania	Prime: ADN Boost: MVA-CMDR	Env,gag,rev, RT (A,B) env,gag,pol (A,C,E)
RV 172	May-06	NIH, USMHRP, VCR	Kenia, Uganda, Tanzania	Prime: ADN Boost: Adenovirus	gag-pol-nef + Env (B) gag-pol + Env (A,B,C)
FASE I	**Ensayos de tamaño pequeño para probar seguridad y capacidad inmunogénica de la vacuna**				
DVP-1	May-07	St. Jude´s Children´s Research Hospital	USA	Prime-Boost: polyEnv, EnvPro, EnvDNA	Env (A,B,C,D,E)
VCR 012	May-07	NIAID, VCR	USA	Adenovirus	C
DHO-0586	Oct-06	ADARC, IAVI	USA	ADMVA	env, gag-pol, nef-tat (C)
HPTN 027	Oct-06	Makerere University, Johns Hopkins University	Uganda	ALVAC	Env, gag-pol (B)
C86P1	Sep-06	SGUL, Richmond Pharmacology, Novartis	Inglaterra	Prime: gp140+LTK63 Boost: gp140+MF59	Env (B)

Nombre	Fecha de inicio	Organizador	Paises	Tipo de la vacuna	Antígeno (subtipo)
FASE I	**Ensayos de tamaño pequeño para probar seguridad y capacidad inmunogénica de la vacuna**				
VCR 011	Abr-06	NIAID, VCR	USA	Prime: ADN Boost: Adenovirus	gag-pol-nef + Env (A,B,C) gag-pol + Env (A,B,C)
HVTN 065	Abr-06	DAIDS, HVTN, VRC, GeoVax	USA	Prime: ADN Boost: MVA	Env,gag,pro,RT,tat,Rev,vpu Env, gag,pol (B)
HVRF-380	Mar-06	Moscow Institute of immunology	Rusia	VICHREPOL + polyoxidonium	(B)
IAVI D001	Feb-06	IAVI, Therion	India	MVA	Env, gag, Tat-rev, nef-RT (C)
HVTN 064	Ene-06	DAIDS, HVTN, Pharmexa-Epimmune	USA, Peru	EP-1043 (prot) + ADN	gag, pol, vpr, nef, env, vpu (B)
HVTN 068	Feb-06	DAIDS, HVTN, VRC	USA	Prime: ADN Boost: Adenovirus	gag-pol-nef + Env (A,B,C) gag-pol + Env (A,B,C)
HIVIS 02	Ene-06	Instituti Karolinska, USMHRP	Suecia	MVA	Env, gag, pol (A,E)
RV 158	Nov-05	USMHRP, NIH	USA, Tailandia	MVA	Env-gp160, gag, pol (A,E)
HVTN 063	Sep-05	DAIDS, HVTN, Wyeth	USA, Brasil	P: Genevax +/- IL12 B: ADN GM-SCF	Gag (B) Env, gag, nef (B)
HVTN 060	Ago-05	DAIDS, HVTN, Wyeth	USA, Tailandia	P: Genevax +/- IL15 B: Genevax +/- IL12	Gag (B)
EnvDNA	May-05	St. Jude´s Children´s Hosp	USA	ADN multi-env	Env (A,B,C,D,E)
VCR 008	Abr-05	NIAID, VCR	USA	Prime: ADN Boost: Adenovirus	gag-pol-nef + Env (B) gag-pol + Env (A,B,C)
N/A	Mar-05	Changchun BCHT	China	Prime: ADN Boost: Adenovirus	C
HIVIS 01	Feb-05	I. Karolinska, USMHRP	USA	ADMVA	env, gag-pol, nef-tat (C)
EuroVacc02	Feb-05	EuroVacc	Inglaterra, Suiza	NYVAC-C	Env, gag-pol-nef (C)
IAVI C002	Ene-05	IAVI, ADARC	USA	MVA	Env, gag/pol, nef-tat (C)
RV 156A	Nov-04	NIAID, HVTN, VCR	Uganda	Adenovirus	A, B, C
HVTN 055	Sep-04	DAIDS, HVTN, Theiron	USA, Brasil	Prime: MVA Boost: FPV	Env, gag, tat, nef rev, pol (B)
HVTN 050	Ene-04	DAIDS, HVTN, Merk	USA, Surafrica, Tailandia	Adenovirus	gag (B)
HVTN 049	Dic-03	DAIDS, HVTN, Chiron	USA	Prime: ADN Boost: gp140+MF5	gag, Env (B) Env (B)
PolyEnv1	Oct-97	St. Jude´s Children´s Hosp	USA	Proteína Env	Env (B, D)

Objetivos

La búsqueda de una vacuna segura y eficaz frente al VIH/SIDA ha impulsado el desarrollo de nuevos vectores virales recombinantes capaces de inducir respuestas inmunes celulares específicas frente al patógeno externo. En este sentido, los vectores atenuados de poxvirus como MVA y NYVAC, poseen una serie de características, entre las que se incluyen su excelente perfil de seguridad así como la capacidad de incorporar grandes cantidades de ADN exógeno, que los convierten en excelentes candidatos vacunales frente al VIH/SIDA y otras enfermedades. En la actualidad, existen varios ensayos clínicos utilizando recombinantes de MVA y NYVAC frente a enfermedades infecciosas como SIDA o malaria y ciertos tipos de cáncer.

A pesar de que la seguridad y e inmunogenicidad de ambos vectores han sido ampliamente demostradas, hasta la fecha no existen estudios "*in vitro*" e "*in vivo*" donde se comparen directamente estos dos candidatos vacunales. La comparación de los niveles de expresión del antígeno ejercidos por los vectores así como los efectos generados sobre la célula huésped tras la infección con MVA y NYVAC ayudaría a mejorar el diseño de próximas generaciones de vacunas y a la elección de uno u otro vector como candidato vacunal ya que las diferencias que se observen podrían afectar a la generación de la respuesta inmunológica deseada.

Ante la relevancia que están adquiriendo estos dos vectores en este trabajo nos propusimos los siguientes objetivos:

1. **Realizar un estudio morfológico, bioquímico y genético del comportamiento de las cepas atenuadas MVA y NYVAC en células en cultivo**

2. **Definir y comparar la distribución viral y los niveles de expresión del antígeno heterólogo en ratones BALB/c inmunizados con recombinantes basados en las cepas MVA y NYVAC por rutas sistémicas y de mucosas.**

3. **Caracterizar la respuesta inmune celular y humoral inducida por recombinantes basados en MVA y NYVAC que expresan diferentes antígenos de VIH-1 (Env, Gag, Pol y Nef) empleando distintos protocolos de inmunización.**

Materiales y Métodos

3.1. MATERIALES BIOLÓGICOS

3.1.1 Líneas celulares y medios de cultivo

3.1.1.1 Líneas celulares

Las líneas celulares utilizadas en este estudio fueron las siguientes:

BSC40: Células epiteliales de riñón de mono verde africano (*Cercopithecus aethiops*).

BHK-21: Línea fibroblastoide de riñón de hámster dorado (*Mesocricetus auratus*).

CEF (Chicken embryo fibroblasts): cultivos primarios de fibroblastos embrionarios de pollo (*Gallus gallus*). Su obtención se describe más adelante.

HeLa: Línea celular procedente de un carcinoma epitelial humano de cuello uterino.

NIH-3T3: Células embrionarias murinas estables mediante el protocolo 3T3.

TK-143: Línea celular derivada de un ostesarcoma humano.

En la tabla V se muestran las líneas celulares utilizadas en este estudio clasificadas según su susceptibilidad a la infección por las distintas cepas y recombinantes virales. En el trabajo las células, BHK-21 y HeLa, han sido elegidas para representar respectivamente a una línea celular susceptible y no susceptible a la infección tanto para la cepa MVA como para NYVAC.

	WR	MVA	NYVAC	NY-C7L
CEF	+	+	+	+
BHK-21	+	+	+	+
BSC-40	+	+/-	+	+
NIH-3T3	+	-	-	+
HeLa	+	-	-	+
TK -143	+	-	-	+

Tabla V: Líneas celulares susceptibles (+) o no susceptibles (-) a la infección por las estirpes virales derivadas del virus vaccinia (VACV): Western Reserve (WR), Modified Virus Ankara (MVA) y NYVAC o el recombinante NYVAC-C7L.

3.1.1.2 Medios de cultivo

Las líneas celulares BHK21, TK-143, NIH-3T3 y CEF se cultivaron en medio esencial mínimo de Eagle modificado por Dulbecco (DMEM) (Dulbecco *y* Freeman, 1959; Gibco BRL), suplementado con 10% (v/v) de suero fetal de ternera (FCS; Sigma), penicilina (100 U/ml; Sigma), estreptomicina (100 μg/ml; Sigma), fungizona (0,5 U/ml; Gibco), glutamina (2 mM; Merck) y aminoácidos no esenciales (Sigma) (DMEM completo). Las líneas celulares BSC40 y HeLa se cultivaron en el mismo medio pero suplementado con 10% de suero de ternera recién nacida (NCS; Sigma).

Para los cultivos primarios de células del peritoneo o del bazo de ratón se empleó el medio RPMI-1640 (Gibco BRL), suplementado con 10% de FCS, penicilina, estreptomicina, β-mercaptoetanol (10 μM; Sigma), HEPES pH 7,4 (10 mM) y L-glutamina (2 mM).

Para la transfección transitoria de cultivos celulares se utilizó OPTIMEM I (Gibco).

Para las infecciones, se empleó DMEM completo para la hora de adsorción, tras la cual se retiró el inóculo y se adicionó DMEM completo suplementado con 2% de suero.

Todas las líneas celulares se mantuvieron en un incubador a una temperatura de 37ºC y un porcentaje de CO_2 del 5%.

3.1.1.3 Obtención de fibroblastos embrionarios de pollo (CEF)

Los cultivos primarios de fibroblastos embrionarios de pollo se obtuvieron a partir de embriones de 9 a 10 días de incubación, cedidos por Intervet (Salamanca). La cáscara se lavó con etanol y se colocó sobre un soporte con el polo más ancho hacia arriba. Con pinzas estériles se abrió el cascarón y se rompió la membrana corioalantoidea para penetrar en la cavidad amniótica. El embrión extraído del huevo se decapitó y eviscerό. El tejido resultante se lavó tres veces con tampón fosfato salino (PBS) precalentado a 37 ºC y se troceó mecánicamente con ayuda de unas tijeras. La papilla resultante se digirió con tripsina (10 ml de tripsina al 0,25% en PBS/embrión; Sigma) a 37 ºC durante 1 h, tras lo cual se filtró a través de una rejilla metálica, se le añadió un volumen igual de medio DMEM completo y se centrifugó a 1500 rpm durante 25 min. El precipitado de células resultante se resuspendió en un volumen adecuado de medio DMEM suplementado con 5% FCS, penicilina, estreptomicina y fungizona.

3.1.2 Bacterias

La cepa de *Escherichia coli* utilizada para las transformaciones y crecimiento de los plásmidos fue DH5α. Las bacterias se cultivaron en medio LB (Luria-Bertani) (1% bacto-

triptona, 1% NaCl, 0,5% extracto de levadura) (Sambrook *y cols.*, 1989) suplementado con 100 μg/ml de ampicilina (Boehringer Mannhein).

3.1.3 Virus

Los virus recombinantes utilizados y los generados en este trabajo se basaron en la cepa salvaje VACV-WR (*Western Reserve*), en las cepas atenuadas del virus vaccinia (VACV), MVA (*Modified Vaccinia Ankara*) y NYVAC. La cepa VACV-WR fue proporcionada por el Dr. Rostom Bablanian de la Universidad Estatal de Nueva York, la cepa MVA fue cedida por el Dr. Gerd Sutter del Instituto de Virología Molecular de Munich (Alemania) y la cepa NYVAC fue facilitada por la empresa Sanofi-Pasteur (Francia). Los virus recombinantes empleados en este estudio se describen en la siguiente tabla VI.

Tabla VI: Virus recombinantes utilizados en este estudio.

Virus	Proteína recombinante	Promotor	Locus	Referencia
WRluc	Luciferasa	pE/L	TK	Rodriguez y cols., 1998
MVAluc	Luciferasa	pE/L	TK	Ramirez y cols., 2000
NYVACluc	Luciferasa	pE/L	TK	Gómez y cols., 2007c
NYVAC-C7L	C7L	pE/L	HA	Nájera y cols., 2006
NYVAC-B	gp120 aislado Bx08 Gag-Pol-Nef aislado IIIB	pE/L	TK	Gómez y cols., 2007a
MVA-B	gp120 aislado Bx08 Gag-Pol-Nef aislado IIIB	pE/L	TK	Gomez y cols., 2007c

3.1.4 Plásmidos

Los plásmidos utilizados en este estudio se describen a continuación:

pJR101: plásmido utilizado para la inserción de genes en el genoma de VACV mediante recombinación homóloga en el locus hemaglutinina (HA) de VACV. La expresión del gen exógeno está controlada por el promotor viral sintético temprano-tardío (pE/L). Como gen marcador para la selección de virus recombinantes contiene el gen de

la *β-glucuronidasa* bajo el control del promotor viral p7.5. Toda esta construcción está delimitada por las regiones flanqueantes del gen viral de la hemaglutinina (HA) (Gherardi *y cols.*, 1999). Como marcador para la clonación en bacterias contiene el gen de resistencia a ampicilina.

pJR101-C7L: plásmido de inserción en el locus HA de NYVAC derivado del pJR101 (Vazquez *y cols.*, 1998). Este plásmido fue generado para este estudio. Contiene el gen C7L bajo el promotor sintético viral temprano/tardío. Como gen marcador para la selección de virus recombinantes contiene el gen de la *β-glucuronidasa* bajo el control del promotor viral p7.5. Para su generación se siguió la estrategia esquematizada en la siguiente figura 9.

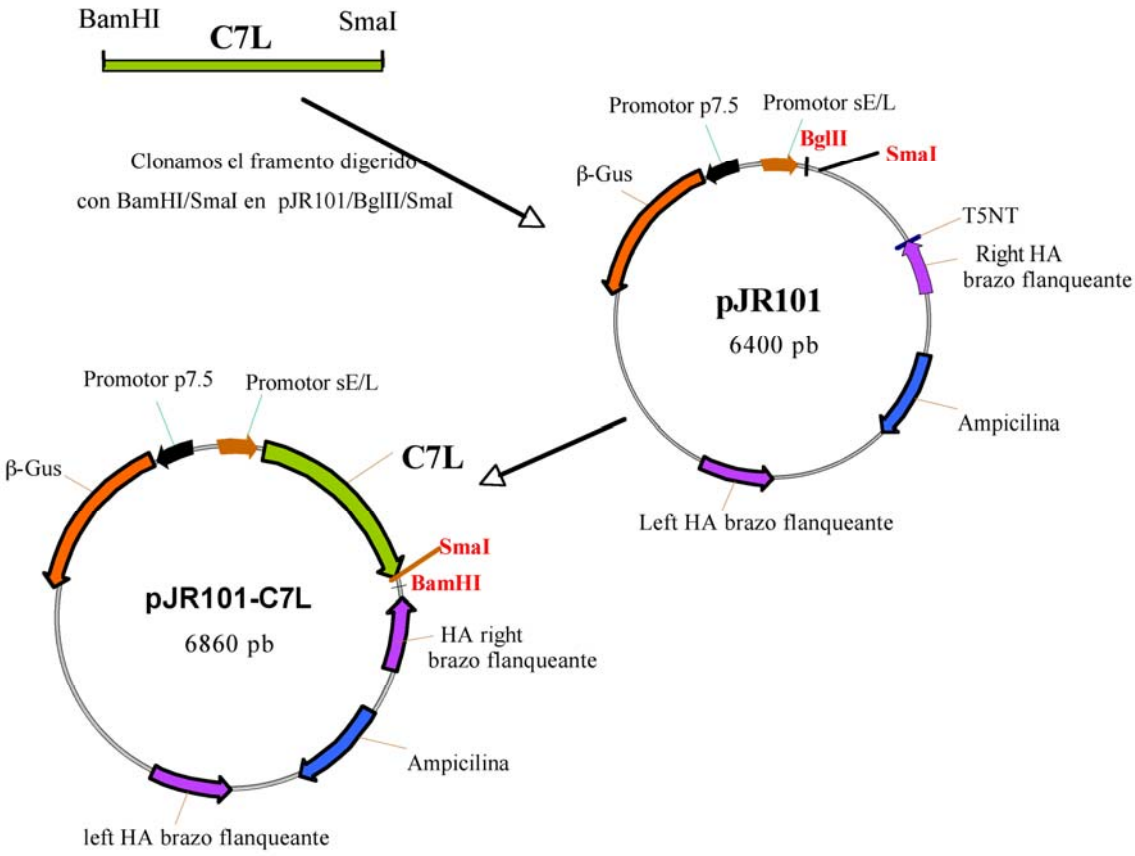

Figura 9: Generación del vector de inserción pJR101-C7L. La secuencia de ADN que codifica la proteína C7 se obtuvo a partir del producto de PCR que amplifica para dicho gen en el genoma de MVA, mediante digestión con el enzima *EcoRI*. El fragmento obtenido fue tratado con la polimerasa *Klenow* para eliminar los extremos protuberantes y clonado en el vector de inserción de vaccinia pJR-101 previamente digerido con *SmaI* y tratado con fosfatasa alcalina de gamba. El plásmido resultante, pJR-C7L, contiene el gen *C7L* bajo el control del promotor viral sintético temprano/tardío (pE/L) y el gen marcador *LacZ* bajo el control del promotor viral temprano/tardío p7.5 en la orientación opuesta. Ambos genes están flanqueados por las regiones HA del virus vaccinia.

pSC11-Luc: plásmido de inserción en el locus de la timidina quinasa (TK) del genoma de VACV derivado del pSC11. Contiene el gen codificante de la proteína de la luciferasa bajo el control del promotor viral p7.5 y el gen de la *β-galactosidasa* como marcador de selección de virus recombinantes.

pCDNA3.1-ϕ: plásmido de expresión en eucariotas suministrado por Invitrogen. Como marcadores de selección contiene el gen de resistencia a ampicilina para la clonación en bacterias y el gen de resistencia a neomicina para la selección en células eucariotas. Se utilizó junto con el pCMV-ϕ como plásmido control en los experimentos de inmunización de animales.

pCMV-ϕ: vector de expresión en células de mamífero. Como marcador de selección contiene el gen de resistencia a kanamicina para la clonación en bacterias. Se utilizó junto con el pCDNA3.1-ϕ como plásmido control en los experimentos de inmunización de animales.

pcDNA3.1-GPN (B): vector de expresión en células de mamífero derivado del vector pcDNA3.1(-) (Invitrogen). Contiene el gen que codifica la poliproteína Gag-Pol-Nef del aislado IIIB del virus VIH-1 bajo el promotor de citomegalovirus (pCMV) y la región de poliadenilación de la hormona de crecimiento bovina (pA BGH) adyacente al gen exógeno. Como marcadores de selección contiene el gen de resistencia a kanamicina para la clonación en bacterias y el gen de resistencia a neomicina para la selección en células eucariotas. Este vector fue sintetizado y suministrado por la empresa GENEART (Alemania) como se ha descrito en trabajos anteriores (Didierlaurent *y cols.,* 2004).

pCMV-Bx08gp120: vector de expresión en células de mamífero derivado del vector pCMV. Contiene el gen que codifica la proteína gp120 del aislado primario Bx08 del virus VIH-1 bajo el promotor de citomegalovirus (pCMV). Este vector fue proporcionado por la empresa Sanofi-Pasteur.

3.2 REACTIVOS

3.2.1 Anticuerpos

Los anticuerpos utilizados en este estudio se resumen en la tabla VII.

Tabla VII: Anticuerpos utilizados en este trabajo

ANTICUERPO	CARACTERISTICAS	PROCEDENCIA
Anticuerpos Primarios frente a proteínas del virus vaccinia		
Conejo α WR	Anticuerpo policlonal generado en conejo contra las proteínas de la cepa WR del virus vaccinia	Demkowicz y cols., 1992
Ratón α A27 de vaccinia (C3)	Anticuerpo monoclonal generado en ratón contra la proteína de 14 KDa del virus vaccinia A27	Centro Nacional de Biotenología,-CSIC, Madrid
Conejo α A27 de vaccinia (A27L)	Anticuerpo policlonal generado en conejo contra la proteína de 14 KDa del virus vaccinia A27	Dallo y Esteban, 1987
Conejo α p16 de vaccinia (A14L)	Anticuerpo policlonal generado en conejo contra la proteína de 16 KDa del virus vaccinia A14	Rodríguez y cols., 1998
Conejo α A4 de vaccinia (A4L)	Anticuerpo policlonal generado en conejo contra la proteína de 39 KDa del virus vaccinia A4	Centro Nacional de Biotecnología-CSIC, Madrid
Conejo αE3 de vaccinia (E3L)	Anticuerpo policlonal generado en conejo contra la proteína de 28 KDa del virus vaccinia E3	Cedido por el Dr. B. Jacobs y el Dr. B. Moss
Conejo αL1 de vaccinia (L1R)	Anticuerpo policlonal generado en conejo contra la proteína de 27,5 KDa del virus vaccinia L1	Cedido por el Dr. Y. Ichihashi
Conejo αA17 de vaccinia (A17L)	Anticuerpo policlonal generado en conejo contra la proteína de 21 KDa del virus vaccinia A17	Rodríguez y cols., 1995
Anticuerpos primarios frente a proteínas celulares		
Conejo α eIF-2 α	Anticuerpo policlonal generado en conejo que reconoce el factor eIF-2 α	Santa Cruz, CA
Conejo α fosfo-eIF-2 α	Anticuerpo policlonal generado en conejo que reconoce la forma fosforilada del factor eIF-2 α	BIOSOURCE
Ratón α β̃actina	Anticuerpo monoclonal generado en ratón que reconoce la proteína actina	SIGMA
Conejo α PARP Humano	Anticuerpo policlonal generado en conejo que reconoce la forma nativa y procesada de la proteína PARP	Cell signaling

ANTICUERPO	CARACTERISTICAS	PROCEDENCIA
Anticuerpos primarios frente a proteínas de VIH		
Conejo α gp120	Anticuerpo policlonal generado en conejo que reconoce la proteína gp-120 del aislado IIIB clade B	Centro Nacional de Biotecnología-CSIC, Madrid
Ratón α p24 Gag ARP 432	Anticuerpo monoclonal generado en ratón que reconoce la proteína de 24 KDa de Gag del subtipo B del VIH	Programa EVA
Anticuerpos conjugados (Western-blot)		
Cabra α IgG de conejo-HRP	Anticuerpo policlonal generado en cabra conjugado con peroxidasa	SIGMA
Conejo α IgG de ratón-HRP	Anticuerpo policlonal generado en conejo conjugado con peroxidasa	SIGMA
Anticuerpos conjugados (inmunofluorescencia)		
Cabra αIgG de conejo-alexa 488	Anticuerpo policlonal generado en cabra frente a IgG de conejo conjugado con alexa 488	Invitrogen
Cabra αIgG de ratón-alexa 594	Anticuerpo policlonal generado en cabra frente a IgG de ratón conjugado con alexa 594	Invitrogen
Anticuerpos (ELISPOT)		
Rata α IFN-γ de ratón	Anticuerpo monoclonal de isotipo IgG1 que reconoce el IFN-γ murino; clon R4-6 A2	BD Pharmingen, San Diego, CA
Rata α IFN-γ de ratón-biotina	Anticuerpo monoclonal de isotipo IgG1 que reconoce el IFN-γ murino conjugado con biotina; clon XMG1.2	BD Pharmingen, San Diego, CA

3.2.2 Oligonucleótidos

Los oligonucleótidos utilizados para el análisis por PCR aparecen detallados en la siguiente tabla VIII.

Tabla VIII: Oligonucleótidos utilizados en este trabajo

OLIGONUCLEÓTIDO	SECUENCIA (5' → 3')	MOLDE	PRODUCTO AMPLIFICADO
HA1	GTCACGTGTTACCACGCA	WR MVA NYVAC	*A56R*
HA2	GATCCGCATCATCGGTGG	WR	*A56R*
HAMVA	TGACACGATTACCAATAC	MVA NYVAC	*A56R*
TK1	AACGGCGGACATATTCAG	WR MVA NYVAC	*J2R*
TK2	ATGAGTCGATGTAACACT	WR MVA NYVAC	*J2R*
E3L forward*	GAGATTGTGTGTGAGGCT	WR MVA NYVAC	*E3L*
E3L reverse*	AAAAGACCAATCTCTTCT	WR MVA NYVAC	*E3L*
A27L forward*	GCGCTCGAGGATGCATCATC ATCATCACATGACGGAACTC TTTTCCCC	WR MVA NYVAC	*A27L*
A27L reverse*	CGCGGTACCTTACTCATATG GGCGCCGTCCAGTC	WR MVA NYVAC	*A27L*
C7L upper	CGGGATCCCATGGGTATACA GCACGAATTCG	WR MVA	*C7L*
C7L lower	TCCCCCGGGTAATCCATGGA CTCATAATCTCTATACG	WR MVA	*C7L*
A27L-VIC**	❖CCTCATTGTCGTCTTCATC GGC	WR MVA NYVAC	*A27L*

* oligonucleótidos usados para RT-PCR

** oligonucleótido utilizado para el ensayo de extensión del cebador

3.2.3 Enzimas de manipulación del ADN

Las enzimas de restricción empleadas en la construcción de los diferentes plásmidos fueron suministradas por Roche.

Como enzimas modificadoras del ADN se utilizaron: ADN polimerasa I (fragmento *klenow*, Roche), T4 ADN ligasa (Roche) y fosfatasa alcalina de gamba (SAP; USB). En las reacciones de PCR se utilizó la enzima Platinum Taq ADN polimerasa (Invitrogen).

Todas las enzimas se utilizaron según las indicaciones del fabricante.

3.2.4 Péptidos

Las mezclas de péptidos ("pooles") de VIH-1 específicos usados en este estudio fueron suministrados por la Fundación Eurovacc. Dentro de cada "pool", los péptidos se encuentran a una concentración de 25 μg por vial como secuencias de 15 mers que solapan en 11 aminoácidos (aa) y que cubren todas la regiones antigénicas correspondientes a las proteínas Env, Gag, Pol y Nef del subtipo B incluidas en los vectores usados en este estudio como candidatos vacunales. La proteína $gp120_{Bx08}$ de 494 aa está representada por los "pooles" Env-1 (aa:1-252; 60 péptidos) y Env-2 (aa:241-494; 61 péptidos). La poliproteína de fusión Gag-Pol-Nef de 1326 animoácidos está representada por los "pooles": Gag-1 (aa: 1-231; 55 péptidos), Gag-2 (aa: 221-431; 50 péptidos), GPN-1 (aa: 421-655; 56 péptidos), GPN-2 (aa: 645-879; 56 péptidos), GPN-3 (aa: 869-1103; 56 pétidos) y GPN-4 (aa.1093-1326; 56 péptidos). Como control (CTRL) se utilizó una mezcla de epítopos no relacionados que contiene 23 péptidos de proteínas de Citomegalovirus (CMV), virus de la gripe (Influenza) y del virus de Epstein-Barr (EBV).

3.2.5 Tampones

PBS: NaCl 137 mM, KCl 2,7 mM, Na_2PO_4 8 mM y KH_2PO_4 1,5 mM.

Tampón de carga (Laemmli): Tris-HCl 50 mM pH 6,8, SDS 2%, β-mercaptoetanol 5%, glicerol 10% y azul de bromofenol 0,012%.

Tampón de electroforesis para SDS-PAGE (Tris-glicina SDS): Tris 25 mM, glicina 192 mM y SDS 0,1%.

Tampón de citoesqueleto, CB (Cytoskeletal Buffer): 10 mM MES, 150 mM NaCl, 5 mM EGTA, 5 mM glucosa, pH: 6,1.

Tampón citrato-fosfato: Na_2HPO_4 0,2 M y citrato sódico 0,1 M.

Tampón carbonato (0,1 M pH 9,6): Na_2CO_3 0,2 M y $NaHCO_3$ 0,2 M.

Tampón Proteinasa K: Tris-HCl 50 mM pH 8,0, EDTA 100 mM, NaCl 100 mM y SDS 1%.

TBE: Tris-Borato pH 8,3 90 mM y EDTA 2 mM.

Tampón de carga de ADN: xylen-cyanol 0,25%, glicerol 30% y azul de bromofenol 0,25%.

Tampón HEPES: 10 mM, pH: 7,5.

3.3 METODOLOGÍA

3.3.1 Manipulación del ADN

Para la preparación y transformación de células competentes, la purificación de plásmidos, el aislamiento de fragmentos de ADN y las clonaciones, se ha seguido la metodología descrita en el libro *Molecular Cloning: a laboratory manual* (Sambrook *y cols.*, 1989).

3.3.1.1 Transfección transitoria de cultivos celulares

Para la transfección transitoria de cultivos celulares se utilizó lipofectamina (Invitrogen) en monocapas subconfluentes (80%) de células. Tanto el ADN plasmídico como la lipofectamina se diluyeron en medio OPTIMEM (10 μg ADN / 8 × 10^6 células; 2 μl lipofectamina/μg ADN). La solución de lipofectamina se mezcló con la solución que contiene el ADN, y se incubó durante 20 min. a temperatura ambiente, tras lo cual se añadió a las células. Tras 5-8 horas, las células se lavaron y se añadió medio DMEM suplementado con 2% de suero. Las células se recogieron en tampón de carga a distintos tiempos post-transfección según el experimento.

3.3.1.2 Análisis por PCR (Reacción en cadena de la polimerasa)

Las reacciones de PCR para el análisis de la pureza de los virus recombinantes se llevaron a cabo en un volumen final de 25 μl por reacción y contenían 10 ng de molde de ADN viral, 0,2 μM de cada oligonucleótido, 1,25 unidades de Platinum Taq ADN polimerasa y 0,2 mM de cada deoxinucleótido en el tampón suministrado por la casa comercial (Invitrogen), suplementado con 1,5 mM de $MgCl_2$. Se empleó un termociclador PTC-100™ (MJ Research, Inc.). El programa de PCR utilizado para amplificar la región contenida entre las secuencias flanqueantes de la HA y de la TK fue el siguiente: un ciclo de 7 min. a 95 ºC; 35 ciclos de 1 min. a 95 ºC, 30 segundos a 50 ºC y 7 min. a 68 ºC; seguido de una extensión final de 7 min. a 68 ºC. El programa de PCR utilizado para amplificar la región contenida entre las secuencias flanqueantes del gen C7L fue el siguiente: un ciclo de 2 min. a 95 ºC; 35 ciclos de 1 min. a 95 ºC, 1 min. a 57 ºC y 1 min. A 72 ºC; seguido de una extensión final de 7 min. a 72 ºC.

3.3.1.3 Purificación de ácidos nucléicos

Purificación de fragmentos de ADN

El aislamiento y purificación de fragmentos de ADN se realizó a partir de geles de agarosa utilizando el Kit de extracción de gel QIAquick (Qiagen).

Purificación de ADN plasmídico

Para el análisis de transformantes se realizó la purificación de pequeñas cantidades de ADN de un cultivo de bacterias crecido en un volumen de 3 ml de LB suplementado con ampicilina o kanamicina, siguiendo el método de lisis alcalina descrito por Sambrook y cols. (1989).

Para la producción de grandes cantidades de ADN de plásmidos se utilizaron las columnas QIAGEN-tip 500 (QIAGEN) siguiendo el protocolo suministrado por el fabricante. Estas preparaciones de plásmidos se emplearon para secuenciación y transfección de células de mamífero.

Para la purificación del ADN destinado a las inmunizaciones de los animales se utilizaron columnas libres de pirógenos (JetStar, Genomed), diluyéndose el ADN en agua estéril igualmente libre de pirógenos.

Purificación de ADN viral

El ADN viral destinado al análisis por PCR de la pureza de los virus recombinantes se obtuvo a partir de monocapas de células infectadas. Cuando se observó efecto citopático, la monocapa se recogió y, tras dos lavados con PBS centrifugando a baja velocidad, el precipitado se conservó a -20 ºC hasta su utilización. Para la extracción del ADN, se resuspendieron las células en Tris-HCl 50 mM pH 8,0, y se añadió Proteinasa K (200 μg/ml, Roche) en su tampón correspondiente. Se incubó a 55 ºC durante 1-2 horas, tras lo cual se añadió RNAsa (40 μg/ml, Roche) y se incubó a temperatura ambiente durante 30 min. Una vez finalizada la incubación, se añadió NaCl saturado y se mezcló cuidadosamente. A continuación se centrifugó a 13000 rpm durante 10 min. a temperatura ambiente. Se recogió el sobrenadante y se mezcló con isopropanol (proporción 1:0,7). La mezcla se centrifugó a 10000 rpm durante 10 min., el precipitado se lavó con etanol al 75% y de nuevo se centrifugó 10 min. Finalmente, el ADN precipitado se secó a temperatura ambiente y se resuspendió en 50 μl de agua estéril durante toda la noche a temperatura ambiente.

3.3.2 Manipulación de ARN

Para el aislamiento del ARN, se ha seguido la metodología descrita en el libro *Molecular Cloning: a laboratory manual* (Sambrook *y cols.*, 1989).

3.3.2.1 Purificación de ARN celular y viral

El ARN total de células infectadas y sin infectar fue aislado utilizando el sistema de purificación Ultraspect-II-resin (Biotecx). Todo el protocolo se llevó a cabo en hielo y con material especialmente limpiado de posibles contaminaciones con RNasas.

Brevemente, las células se rasparon en el tampón de extracción de ARN que contiene fenol y sales de guanilato entre otros componentes. Se añadieron 0,5 volúmenes de cloroformo y se agitó con vortex enérgicamente para después incubarlo en hielo durante 5 minutos. Se centrifugaron 15 minutos a 13 000 rpm y se recogió la fase acuosa que contiene los ácidos nucleicos. El ARN se precipitó con 0,2 volúmenes de 2-propanol en presencia de 0,02 volúmenes de la resina subministrada por el kit. Se centrifugó varias veces la mezcla de la resina con el ARN y se lavó con etanol 70 %, posteriormente se dejó secar 7 minutos y se eluyó en un volumen de agua-DEPC 2 veces el volumen de resina. Se mezcló el agua con la resina para centrifugar y fluir el ARN junto con el agua. El ARN purificado se desnaturalizó y analizó en geles desnaturalizantes de agarosa al 1% previamente teñidos con bromuro de etidio.

3.3.2.2 Limpieza del ARN de posibles restos contaminantes de ADN genómico

Se utilizó la DNasa I del kit Turbo-DNA-free de Ambion. 1,5 mg de ARN total se digirieron con 2U enzima/reacción en el tampón de incubación suministrado y después de 1 hora a 37 ºC, se inactivó la endonucleasa con el tampón de inactivacion y se centrifugó dos veces a 10 000 rpm 1 minuto para evitar restos del tampón de inactivación.

3.3.2.3 Reacción de la Transcriptasa reversa acoplada a la amplificación de cDNA mediante la Reacción en Cadena de la Polimerasa (RT-PCR)

Para las reacciones de RT-PCR, el ARN total (1,5 μg) aislado de células HeLa sin infectar o infectadas con VACV-WR, MVA, NYVAC o NYVAC-C7L (5 UFP/célula, 24 hpi) fue tratado con DNasa I para reducir el ADN genómico contaminante hasta niveles indetectables por PCR (Ambion Turbo Kit) según lo descrito en los apartados anteriores. La retrotranscripción del ARN total a cDNA se llevó a cabo utilizando el enzima SuperScript II Reverse Transcriptase (Invitrogen) siguiendo las instrucciones descritas. Brevemente, 150 ng de ARN total se mezclaron con hexámeros random 2.5 mM durante 10 minutos a temperatura ambiente en un volumen final de 8 ml. Posteriormente, se añadió al ARN con los hexámeros una mezcla que contenía: 0.5 mM de una mezcla de deoxinucleótidos (dATP, dGTP, dCTP, dTTP), 0.01 M de DTT, el tampón de reacción 1x (50mM Tris-HCl pH; 8.3, 75mM KCl, 3mM $MgCl_2$) y agua tratada con (DEPC) hasta un volumen final de 12 ml. La mezcla se incubó 2 minutos a temperatura ambiente, se le añadió la enzima retrotranscriptasa (200 unidades/ reacción) y se llevó a cabo el siguiente programa de RT-PCR en el termociclador:1) 10 minutos a 25 ºC 2) 50 minutos a 42 ºC 3) 15 minutos 70 ºC 4) 4 ºC. Los oligonucleótidos específicos para los genes

virales *E3L* y *A27L* utilizados en este ensayo se describen en la tabla VIII. Los productos de amplificación se separaron según su tamaño y se analizaron tras someterlas a electroforesis en gel desnaturalizante de agarosa al 1% coloreado con bromuro de etidio sumergido en tampón TBE sometida a un campo eléctrico de 7 V/cm de gel.

3.3.2.4 Ensayo de extensión de cebadores

El ensayo de extensión del cebador se llevó a cabo de acuerdo con Lagrandeur y cols., 1994 y se utilizó como cebador un oligolucleótido marcado con VIC en su extremo 5´ específico para el gen viral A27L cuya secuencia se encuentra a 263 pares de bases del sitio de iniciación de la traducción de dicho gen (Applied Biosystems). La mezcla de reacción con 2 μg de ARN total, contenía 2 pmol del oligonucleótido marcado, 0,5 mM de la mezcla de desoxirribonucleótidos trifosfato (dNTPs), 10 U/μl de la retrotranscriptasa SuperScript II RT (Invitrogen) y el tampón suministrado con el enzima a una concentración 1X (tampón RNX) en un volumen final de 50 μl. Las muestras se incubaron durante 5 minutos a 65 ºC para desnaturalizar el ARN y tras 5 minutos en hielo, la mezcla se mantuvo a 42 ºC durante otros 50 minutos para permitir el apareamiento del cebador con el ARN. Posteriormente, la reacción de extensión se llevo a cabo incubando las muestras durante 15 minutos a 70 ºC tras lo cual se mantuvieron en hielo hasta su precipitación. El ADN monocatenario marcado se precipitó incubándolo durante 30 minutos a 40 ºC y añadiendo 0,7 volúmenes de isopropanol, se lavó con etanol al 70% (v/v) y el pelet resultante se guardó a -20ºC hasta su análisis. Cada muestra se disolvió en una solución que contenía 2,5 μl de formamida (Promega), 0,5 μl de un control interno estándar (GeneScan -500 ROX, Applied Biosystems) y 2 μl de tampón de carga (Applied Biosystems). El tamaño de los productos del ensayo se evaluó con el programa de análisis del GeneScan en su versión 3.7 (Applied Biosystems).

3.3.3 Manipulación de *E. coli*

Para la transformación del ADN se utilizó la técnica de transformación por choque térmico a 42 ºC durante 90 segundos (Inoue *y cols.*, 1990), para lo cual las células fueron preparadas con cloruro cálcico (Sambrook *y cols.*, 1989).

3.3.4 Manipulación de proteínas

3.3.4.1 Análisis de las proteínas en SDS-PAGE

Las muestras de proteínas fueron analizadas mediante electroforesis monodimensional en geles de poliacrilamida en presencia de SDS (SDS-PAGE

desnaturalizantes) según el protocolo de Sambrook y cols (1989). El porcentaje de acrilamida varió dependiendo del peso molecular de la proteína de interés.

3.3.4.2 Transferencia de SDS-PAGE e inmunodetección en membrana (Western blot)

Para la transferencia de geles SDS-PAGE a membranas de nitrocelulosa se empleó el sistema semi-seco (Gelman Sciences) siguiendo el protocolo descrito por Towbin (Towbin *y cols.*, 1979). Se empleó un sistema discontinuo de tres soluciones tamponadas de transferencia: Tampón A (300 mM Tris y 20% metanol), Tampón B (25 mM Tris y 20% metanol) y Tampón C (25 mM Tris, 40 mM ácido 6 ε-amino-n-hexanoico y 20% metanol). El gel y la membrana de nitrocelulosa (Schleicher & Schuell) prehidratada en agua destilada, se colocaron entre papeles Whattman-3MM® empapados en estos tampones. La transferencia se efectuó a una intensidad de corriente constante de 200 mM durante 45 min. Se verificó la transferencia mediante tinción reversible con el colorante rojo Ponceau (0,2% Ponceau en 3% TCA; Sigma).

La membrana de nitrocelulosa se saturó con una solución de leche en polvo desnatada disuelta al 5% en PBS a temperatura ambiente con agitación suave durante 20 min. La incubación con los anticuerpos se efectuó en esa misma solución de saturación. El anticuerpo primario se incubó a 4 ºC durante 16 horas, mientras que la incubación con el anticuerpo secundario se realizó durante 90 min. a temperatura ambiente. Los lavados intermedios se realizaron en PBS con agitación a temperatura ambiente durante 15 min.

El revelado de las bandas de proteína reconocidas por los anticuerpos correspondientes se efectuó mediante el sistema luminol ECL® (Amersham) exponiendo una película autoradiográfica X-OMAT (kodak).

2.3.4.3 Marcaje metabólico de proteínas celulares y virales

Para el seguimiento de la síntesis *de novo* de proteínas virales y celulares se realizó el mismo protocolo que el descrito por Rodríguez y cols., 1993 empleando [^{35}S] metionina-cisteína (Amersham). Monocapas de células HeLa y BHK-21 fueron infectadas a una multiplicidad de 5 UFP/célula con MVA y con NYVAC, a distintos tiempos postinfección (4, 6 y 8 horas) las células se lavaron abundantemente y antes del marcaje se incubaron durante 30 minutos con DMEM deficiente en metionina y cisteína. Tras esta incubación se retiró el medio y se añadieron 50 μCi/ml de una mezcla de isótopos radiactivos (Promix) diluidos en DMEM deficiente en metionina y cisteína dejándose incubar durante otros 30 minutos. Tras lo cual se realizaron tres lavados con PBS y finalmente las células se resuspendieron en tampón de carga. El patrón de

síntesis de proteínas se analizó mediante electroforesis monodimensional en geles de poliacrilamida en presencia de SDS seguido de autorradiografía de cantidades equivalentes de proteínas de cada muestra.

3.3.5 Manipulación de virus

3.3.5.1 Generación de virus vaccinia recombinantes

Para la generación de los virus recombinantes se utilizó la metodología descrita en *Current protocols in Molecular Biology* (actualización de Earl y Moss, 1991). Para la construcción de recombinantes basados en la estirpe NYVAC se infectaron monocapas subconfluentes de células BSC40 a una multiplicidad de infección de 0,05 UFP/célula. Tras una hora de adsorción, se retiró el inóculo y se llevó a cabo la transfección del plásmido de inserción correspondiente en forma de complejos de ADN-liposomas formados durante 20 min. a temperatura ambiente con 10 μg de ADN y 20 μl de lipofectamina en medio OPTIMEM (Gibco). La mezcla se retiró 5-8 horas después de la transfección, añadiéndose medio DMEM completo suplementado con 2% NCS. 48 horas después de la infección-transfección se recogieron las células y se rompieron mediante tres ciclos de congelación/descongelación y sonicación. Con los extractos obtenidos se infectaron nuevamente monocapas de células BSC40 a diferentes diluciones y tras la adsorción se añadieron 4 ml de una mezcla 1:1 de agar (1,4%) y DMEM 2X, suplementado con 2% NCS. 72 horas después, o cuando las placas de lisis fueron visibles al microscopio, se añadió el sustrato correspondiente al gen de selección del plásmido de inserción (X-gal 0,03% o X-gluc 0,03%) en 1 ml de agar (1,4%) y DMEM 2X (1:1) (Carrolly Moss, 1995). Las placas de lisis que desarrollaron color azul correspondientes a los virus recombinantes fueron aisladas, y sirvieron como inóculo para infectar nuevos cultivos en monocapa de BSC40. El proceso de selección se repitió al menos cinco veces (plaqueos). Para confirmar la pureza de los virus recombinantes se llevó a cabo un análisis por PCR con oligonucleótidos de las regiones flanqueantes de los locus HA y TK.

En el caso de los recombinantes basados en la cepa atenuada MVA, la infección-transfección y los posteriores plaqueos se realizaron en cultivos de células CEF, añadiéndose el sustrato 3 días después de las infecciones. El número de plaqueos necesarios para obtener un recombinante puro de MVA por PCR fue de seis a ocho.

3.3.5.2 Purificación de virus

La purificación de los virus se realizó por gradiente de sacarosa de acuerdo con el método descrito inicialmente por Joklik (Joklik, 1962) y modificado por Esteban

(Esteban, 1984). Células CEF fueron infectadas a una multiplicidad de infección de 0,01 UFP/célula con los virus basados en las cepas NYVAC o MVA. Cuando el efecto citopático fue evidente en el 100% de la monocapa celular, se recogieron las células y se centrifugaron durante 15 min. a 2000 rpm, resuspendiéndose el precipitado en tampón Tris-HCl 10 mM pH 9,0. A continuación se realizaron dos ciclos de sonicación/centrifugación (dos pulsos de 10 segundos/1500 rpm durante 15 minutos). Los sobrenadantes recogidos en cada ciclo se centrifugaron (1 hora a 20000 rpm a 4 ºC, en rotor SW28, Beckman) sobre un colchón de sacarosa al 45% en Tris-HCl 10 mM pH 9,0. El precipitado se recogió y se centrifugó de nuevo sobre otro colchón de sacarosa al 45 % en las mismas condiciones. El precitado resultante se resuspendió en pequeños volúmenes de Tris-HCl 10mM pH 9,0. y se congelaron a -80 ºC hasta su utilización. Los virus purificados se titularon por inmunotinción en monocapas de células CEF.

3.3.5.3 Titulación de los virus recombinantes

Para la infección de los cultivos celulares y la titulación de virus se han empleado las técnicas habituales detalladas en el libro de protocolos *Current protocols in molecular biology* (Earl y Moss, 1991).

Los virus recombinantes basados en la cepa VACV-WR fueron seleccionados y crecidos en células BSC40. Su titulación se realizó en la misma línea celular, bien en medio líquido o en medio sólido (agar 1,4%:DMEM 2X, 1:1). A los dos o tres días después de la infección (en el caso de utilizar medio líquido o medio sólido, respectivamente), se tiñeron las células con cristal violeta (0,5% en metanol al 20%), revelándose las placas de lisis.

Los recombinantes basados en las cepas MVA y NYVAC se seleccionaron y crecieron en cultivos de fibroblastos embrionarios de pollo (CEF), y su titulación se llevó a cabo por inmunotinción en la misma línea celular. Monocapas de células CEF se infectaron con distintas diluciones del virus y 24-36 horas post-infección las monocapas infectadas se lavaron con PBS y se fijaron con metanol:acetona (1:1) durante dos minutos a temperatura ambiente. Una vez fijadas, se lavaron con PBS y se incubaron con una dilución 1:1000 de un anticuerpo policlonal de conejo frente a proteínas de vaccinia en PBS + 3% FCS durante 90 minutos en agitación suave a temperatura ambiente. A continuación se realizaron dos lavados con PBS y se incubó con el anticuerpo secundario anti-conejo generado en cabra conjugado con peroxidasa (diluído 1:1000 en PBS + 3% FCS) durante 90 minutos a temperatura ambiente. Posteriormente se lavó con PBS dos veces y se reveló con una solución de 3,3'-diaminobenzidina tetrahydrochloride (DAB, 0,83 mg/ml, Sigma) en PBS, suplementada con $NiSO_4$ 3%

(0,01%) y H_2O_2 30% (0,001%). Tras la aparición de señal en las células infectadas la reacción se detuvo con PBS.

3.3.5.4 Evaluación del efecto citopático (EC)

Las células fueron cultivadas en placas de 12 pocillos y crecidas hasta confluencia. Las monocapas celulares fueron infectadas a una multiplicidad de 5 UFP/célula con las diferentes cepas virales (VACV-WR, MVA y NYVAC) o con el virus recombinante NYVAC-C7L. El efecto citopático inducido por el virus en el cultivo celular fue visualizado bajo un microscopio de contraste de fase, tomándose fotografías de los cultivos celulares a los distintos tiempos postinfección. Características como redondeamiento celular, contracción citoplasmática o pérdida de adherencia de las células infectadas al sustrato fueron analizadas.

3.3.5.5 Curvas de Crecimiento. Rendimiento viral

Para analizar la eficiencia de replicación de las distintas cepas virales o los virus recombinantes utilizados en este estudio, monocapas de líneas celulares (permisivas y no a la infección) fueron infectadas a una multiplicidad de 0.01 UFP/célula con cada virus. Tras una adsorción de 60 minutos a 37 ºC, se retiró el inoculo y las células fueron lavadas abundantemente con medio DMEM sin suero. A continuación las células se incubaron a 37 ºC y en atmósfera de CO_2 con medio DMEM fresco enriquecido al 2% con suero FCS. A distintos tiempos postinfección, las células se recogieron por pipeteo y se centrifugaron a 1500 rpm durante 5 minutos recogiéndose finalmente tanto el pelet como el sobrenadante. Los distintos sobrenadantes fueron mantenidos a 4 ºC hasta su titulación durante un tiempo nunca superior a 48 horas. Los precipitados se resuspendieron en medio DMEM libre de suero a una concentración final de 20 x 10^6 cels/ml, las partículas virales se liberaron tras romper las células mediante tres ciclos de congelación descongelación y sonicación. Después de centrifugar durante 5 minutos a 1500 rpm el sobrenadante fue recogido y referido como virus asociado a la célula. El número de partículas virales infecciosas que permanecen asociadas a la célula o aquellas que son liberadas al sobrenadante durante el curso de la infección fueron contabilizadas por la técnica de inmunotinción descrita en el apartado 3.3.5.3.

3.3.5.6 Inmunofluorescencia

Células HeLa o BHK-21 sembradas sobre cubreojetos se infectaron a una multiplicidad de 0,1 UFP/célula con las diferentes cepas virales. Tras 16 horas de infección, las células se lavaron con PBS y se fijaron con paraformaldehído al 4% durante 30 min. Después de varios lavados, las células se trataron con NH_4Cl 50 mM

durante 10 min. y se permeabilizaron con 0,5% Tritón X-100 durante 10 min. a temperatura ambiente. Tras varios lavados con PBS, se bloqueó con una solución de 0,5% Tween y 20% FCS en PBS durante 1 hora. Los cubreobjetos fueron lavados con PBS e incubados durante 1 hora a 37 ºC con un anticuerpo policlonal dirigido frente a la proteína A27 (A27L) del virus vaccinia (generado en conejo) y con un anticuerpo monoclonal dirigido frente a la proteína celular actina (generado en ratón). Después de lavar los cubreobjetos, se incubaron con los anticuerpos secundarios: anti-conejo conjugado con Alexa-488 (Invitrogen) y anti-ratón conjugado con Alexa-594 (Invitrogen), durante una hora a 37 ºC. A continuación se llevó a cabo una incubación adicional con el reactivo To-Pro (Invitrogen) para teñir el ADN, durante 20 min. a 37 ºC. El exceso de anticuerpo no unido fue eliminado mediante frecuentes lavados, tras lo cual los cubreobjetos se montaron en portaobjetos con Mowiol (Calbiochem). Para la obtención de imágenes se utilizó un microscopio confocal (Bio-Rad Radiance 2100). El mismo procedimiento y condiciones se utilizaron para analizar la expresión de otras proteínas virales como A17 (*A17L*) o L1 (*L1R*) aunque estos resultados no se muestran en este trabajo.

3.3.5.7 Microscopía Electrónica

Esta técnica fue desarrollada por el servicio de Microscopía Electrónica del Centro Nacional de Biotecnología (CNB) en Madrid, bajo la supervisión de la Dra. Cristina Patiño.

Monocapas de células HeLa fueron infectadas con MVA o con NYVAC a una multiplicidad de infección de 5 UFP/célula, a las 16 hpi las células fueron fijadas *in situ* con una mezcla de glutaraldheído al 2 % y ácido tánico al 1 % en 0,4 M de tampón HEPES (pH: 7,5) durante una hora a temperatura ambiente.

Las monocapas fijadas fueron levantadas de las placas de cultivo en el fijador y se transfirieron a tubos eppendorf. Después de centrifugar y lavar con tampón HEPES, fueron guardadas a 4 ºC hasta su uso. Las células fijadas fueron procesadas por inclusión en epoxi-resinas EML-812 (TAAB Laboratorios Ltd., Berkshire, United Kingdom), como está descrito previamente (Risco y cols., 1998). La postfijación de las células infectadas fue hecha con una mezcla de tetróxido de osmio al 1% y ferricianuro de potasio al 0,8% en agua destilada por 1 hora a 4ºC. Después de 4 lavados en tampón HEPES, las muestras fueron tratadas con acetato de uranilo al 2%, y deshidratadas siguiendo concentraciones crecientes de acetona (50, 70, 90 y 100%), cada una de 100 minutos a 4 ºC. La infiltración en la resina fue hecha durante 1 día a temperatura ambiente. La polimerización de las muestras incluidas se hizo a 60 ºC durante 3 días. Después de esto se hicieron las secciones ultrafinas que se tiñeron con acetato de

uranilo saturado y citrato de plomo según procedimiento estándar. Las imágenes se tomaron en un microscopio electrónico Jeol 1200-EX II operado a 100 kV.

3.3.6 Mediada de apoptosis

Para la medición de apoptosis se realizaron distintas técnicas que se describen a continuación.

3.3.6.1 Cambios morfológicos presentes en la muerte celular por apoptosis

Una de las primeras manifestaciones morfológicas de la presencia de muerte celular por apoptosis es la pérdida de la unión celular. Así como cambios en la presencia de estructuras especializadas, como son las microvellosidades. Al mismo tiempo se observan cambios en la organización del citoplasma y la aparición de condensación de la cromatina. Por medio de la microscopía de luz pudimos apreciar cambios en la organización celular, tales como la condensación de la cromatina o la aparición de cuerpos apoptóticos.

Para apreciar alteraciones celulares como cambios en las microvellosidades, así como alteraciones mitocondriales se recurrió a la observación por microscopía electrónica, en la cual se hicieron evidentes características morfológicas de apoptosis como condensación de cromatina en patrón de media luna, reducción del volumen celular o la fragmentación nuclear. Estas técnicas se aplicaron en cultivos celulares sometidos a la infección por las distintas cepas virales como se han descrito anteriormente.

3.3.6.2 Tinción con fluorescencia (DAPI)

La observación de células teñidas con el colorante DAPI (4´6´-diamidino-2-fenilindol) nos permitió identificar fácilmente características como la condensación de cromatina y la fragmentación nuclear, así mismo pudimos evaluar y cuantificar un número considerable de células. Esta técnica se llevo a cabo siguiendo el siguiente protocolo. Células HeLa sembradas sobre cubreojetos se infectaron a una multiplicidad de 5 UFP/célula con las diferentes cepas virales. A distintos tiempos post-infección, las células se lavaron con PBS y se fijaron con paraformaldehído al 4% durante 30 min. Tras varios lavados, las células se trataron con el colorante DAPI durante 30 min. a temperatura ambiente. La fragmentación nuclear se evaluó analizando las muestras en un microscopio de fluorescencia.

3.3.6.3 Degradación de ARN ribosomal

Se examinó la degradación del ARN ribosomal en células HeLa sin infectar o infectadas con VACV-WR, MVA, NYVAC o NYVAC-C7L a una multiplicidad de 5 UFP/ml. El ARN total de células infectadas y sin infectar fue aislado utilizando el sistema de purificación Ultraspect-II-resin (Biotecx). Todo el protocolo se llevó a cabo en hielo y con material específicamente limpiado de posibles contaminaciones con ARNasas. Brevemente, las células se recogieron en el tampón de extracción de RNA que contiene fenol y sales de guanilato entre otros componentes. Se añadieron 0,5 volúmenes de cloroformo y se agitó enérgicamente con vortex para después incubarlo en hielo durante 5 minutos. Se centrifugaron 15 minutos a 13000 rpm y se recogió la fase acuosa que contiene los ácidos nucleicos. El ARN se precipitó con 0,2 volúmenes de 2-propanol en presencia de 0,02 volúmenes de la resina suministrada con el kit. Se centrifugó la mezcla de la resina con el RNA a 13000 rpm 2 minutos y se lavó dos veces con etanol frío al 70%, posteriormente se dejó secar 7 minutos y se eluyó en un volumen de agua DEPC correspondiente a 2 veces el volumen de resina utilizada. Se mezcló el agua con la resina para centrifugar y eluir el ARN en el agua. Se hicieron distintas alícuotas de ARN y se guardaron a -70ºC hasta su análisis. Para el análisis se emplearon 2 microgramos de ARN total de cada muestra que fueron fraccionados mediante electroforesis en un gel de formaldehído agarosa al 1%. La degradación del ARNr se visualizó tras teñir el gel con bromuro de etidio.

3.3.6.4 Análisis del ciclo celular por citometría de flujo

Esta técnica se usó para cuantificar la apoptosis inducida en las células infectadas con los distintos virus. Este ensayo se basa en la detección del contenido de ADN en la célula. Durante el proceso apoptótico, al haber degradación y fragmentación nuclear, las células presentan un menor contenido de ADN, lo cual aparece reflejado en el histograma de la citometría como una población sub-G_0 por debajo de la región en la que se encuentran las células en el proceso anterior al de la replicación del ADN (G_0-G_1), lo que indicaría que podrían estar en apoptosis (Martín y cols., 2002). EL número de células apoptóticas en las células infectadas se cuantificó siguiendo este criterio.

Para ello, células HeLa fueron infectadas a una multiplicidad de 5 UFP/célula con las cepas VACV-WR, MVA o NYVAC o con el virus recombinante NYVAC-C7L en presencia o ausencia de zVAD-fmk, un inhibidor general de caspasas (40 μM, Calbiochem). Las células sin infectar se usaron como control negativo. A las 24, las células fueron recogidas mediante pipeteo, y tras un lavado con PBS frío se permeabilizaron durante toda la noche a 4 ºC, con una mezcla de etanol y PBS al 70 %.

A continuación, se realizaron tres nuevos lavados con PBS y las células fueron tratadas con RNasa A durante 45 min. a 37 ºC, tras lo cual, fueron teñidas con ioduro de propidio (IP, 10 mg/ml). El porcentaje de células marcadas de este modo se analizó mediante citometría de flujo (FACSscan, Becton Dickinson, Mountain View, CA) utilizando el software Expo32. El número de eventos captados fue de 30 000.

3.3.7 Manipulación de animales

En la realización de este trabajo se han utilizado dos modelos distintos de ratón. En los ensayos de caracterización de la respuesta inmune especifica frente a antígenos de VIH-1 en los animales inmunizados, se utilizaron ratones trasgénicos HHD II cedidos por el Dr. Lemonnier del Instituto Pasteur en Francia, estos ratones son doble Knockout para el haplotipo H2-D^b y $\beta_2$microglobulina y transgénicos para la molécula quimera HLA-A2 Humana. Para el resto de los ensayos se utilizaron ratones de la cepa BALB/c (haplotipo H-2^d) de 6 a 8 semanas de edad obtenidos de Harlan Inc.

3.3.7.1 Protocolos de inmunización

Para la realización de los distintos experimentos se han empleado las siguientes rutas de inmunización: Intraperitoneal (i.p.), Intramuscular (i.m.), Escarificación en la base de la cola (e.c.), intranasal (i.n.) e intrarrectal (i.r.).

Ruta de inoculación	vol (µl)	Inóculo	dosis/ratón	Ensayo
Intraperitoneal (i.p.)	200	WRluc MVAluc NYVACluc	1 x 10^7 UFP	Bioluminiscencia
	200	WRluc MVAluc NYVACluc	1 x 10^7 UFP	Luciferasa "ex vivo"
	200	MVA-B NYVAC-B	2 x 107 UFP	ELISPOT
	200	NYVAC NYVAC-C7L VACV-WR	2 x 107 UFP	Luciferasa "ex vivo"
	200	WRluc MVAluc NYVACluc	1 x 10^7 UFP	Bioluminiscencia
Intramuscular (i.m.)	50	WRluc MVAluc NYVACluc	1 x 10^7 UFP	Bioluminiscencia
	100	ADN-B	100 µg	ELISPOT
intranasal (i.n.)	50	WRluc MVAluc NYVACluc	1 x 10^7 UFP	Bioluminiscencia
	50	NYVAC NYVAC-C7L VACV-WR	10^6-10^8 UFP	Virulencia

Ruta de inoculación	vol (µl)	Inóculo	dosis/ratón	Ensayo
Escarificación en la base de la cola (e.c.)	10	WRluc	1 x 10^6 UFP	Bioluminiscencia
		MVAluc	1 x 10^7 UFP	
		NYVACluc	1 x 10^7 UFP	
Intrarrectal (i.r.)	50	WRluc MVAluc NYVACluc	1 x 10^7 UFP	Bioluminiscencia

Tabla IX. Rutas de inoculación, inóculos y dosis utilizadas en los distintos ensayos realizados en este trabajo.

3.3.7.2 Obtención de muestras de los animales inmunizados

Para la obtención de los sueros, a diferentes tiempos post-inoculación según el experimento, se recogió la sangre del plexus reto orbital con un capilar heparinizado, se incubó 1 hora a 37 ºC y posteriormente toda la noche a 4ºC. La sangre se centrifugó durante 20 min. a 3500 rpm, obteniéndose de este modo el suero, que fue almacenado a -80 ºC hasta su utilización.

Los tejidos recogidos variaron en función del experimento. El bazo fue el órgano elegido para determinar los parámetros inmunológicos mediante la técnica de ELISPOT inducidos en los animales tras los diferentes protocolos de inmunización. Este fue recogido de los animales 10-12 días después de la última inmunización.

El grado de diseminación viral tras la inmunización por ruta intraperitoneal se analizó en órganos como los lavados peritoneales y los ovarios como sitios próximos al lugar de inoculación, mientras que bazo e hígado fueron seleccionados como órganos más distantes.

3.3.7.3 Ensayo de virulencia del recombinante NYVAC-C7L

Para la realización de este ensayo se utilizaron ratones BALB/c de 6 a 8 semanas de edad a los que se les inoculó por ruta intranasal una dosis letal de la cepa competente en replicación WR (1 x 10^6 UFP/ratón en 50 µl de PBS) o una dosis hasta 100 veces superior de la cepa NYVAC o del recombinante NYVAC-C7L (1 x 10^8 UFP/ratón en 50 µl de PBS). El aspecto y peso de los ratones fue monitorizado diariamente con el objetivo de determinar signos de enfermedad. Aquellos animales que sufrieron una pérdida de peso superior al 25 % de su peso inicial fueron sacrificados por razones éticas.

3.3.7.4 Ensayo de Bioluminiscencia (BLI)

Este ensayo ha sido realizado por el departamento de Hepatología y terapia génica del Centro de Investigación Médica Aplicada (CIMA) de Pamplona bajo la supervisión de la Dra. Gloria González-Aseguinolaza.

La técnica de bioluminiscencia está basada en la detección de luz visible emitida tras la descarboxilización oxidativa de la luciferina, una reacción que es catalizada por la enzima luciferasa en presencia de ATP y oxígeno (Sandikot y Blackwell, 2005). Esta técnica nos permite cuantificar en un mismo animal la progresión de la infección viral en el espacio y en el tiempo, identificando las variaciones en replicación y diseminación del virus.

Ratones Balb/c de 6 a 8 semanas de edad (Harlan OLAC, NL) fueron inoculados con los distintos virus recombinantes que expresan el gen de la luciferasa bajo el control trascripcional del promotor viral sintético temprano tardío pE/L. A distintos tiempos postinoculación, los animales fueron anestesiados y se le administró por ruta intraperitoneal 100 μl de D-luciferina (Xelogen, Alameda, CA) a una concentración de 30 mg/ml diluído en una solución de NaCl 150 mM. Los animales se colocaron en una cámara de análisis IVIS de Xenogen y se tomaron fotografías en escala de grises de los animales seguido de una adquisición con luminiscencia empezando 10 minutos después de la inyección de luciferina. Las imágenes fueron recogidas cada tres minutos en posición dorsal y ventral de los animales. La intensidad de luz se cuantificó mediante una escala de colores siendo el rojo la mayor intensidad y el azul el flujo de fotones más bajo. La medida de bioluminiscencia se llevó a cabo diariamente y la progresión de la infección se monitorizó hasta la desaparición de la señal.

3.3.7.5 Determinación de los niveles de luciferasa *"ex vivo"*

La expresión génica de lso virus recombinantes en los diferentes tejidos se evaluó mediante el ensayo de luciferasa descrito previamente por Rodríguez y colaboradores en 1988.

Diferentes grupos de animales recibieron una inyección intraperitoneal (1×10^7 UFP por animal) de MVAluc, NYVACluc o WRluc. A distintos tiempos postinoculación los animales fueron sacrificados, se realizaron lavados peritoneales con 10 ml de PBS y se recogieron los nódulos linfáticos, el bazo y los ovarios que fueron diseccionados en condiciones estériles y almacenados a -70 ºC hasta su análisis.

Los diferentes tejidos de los ratones individualizados fueron homogenizados en un tampón de extracción de luciferasa (promega) con la utilización de un homogenizador Ultraturrax T8 (Janke & Kunkel). La actividad luciferasa se midió en presencia de luciferina y ATP mediante la utilización de un luminómetro Lumat LB 9501 (Berthold Technologies) siguiendo las indicaciones del fabricante. La señal de luciferasa se expresó como Unidades relativas de luciferasa (URL) por mg de proteína. El contenido proteíco de los diferentes tejidos se determinó utilizando el kit comercial BCA (Pierce Biotechnology).

2.3.7.6 Inmunización mediante protocolos de Prime-Boost

Para los ensayos de inmunización de activación y refuerzo (prime/boost) con los candidatos vacunales MVA-B y NYVAC-B, el calendario de inmunización y toma de muestras fue el siguiente (Figura 10):

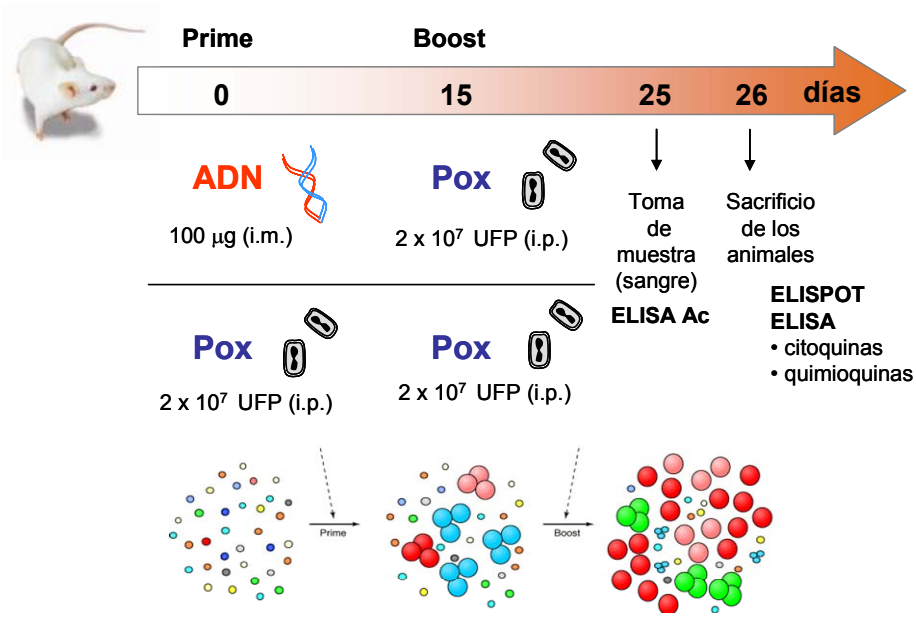

- **Día 0:** Primera dosis de inmunización (Priming): inmunización con ADN
- **Día 15:** Segunda dosis de inmunización (Boost): Día 15, inmunización con poxvirus
- **Día 25:** Toma de muestras (sangre)
- **Día 26:** Sacrificio de los animales y análisis por ELISPOT de la respuesta inmune

Figura 10: Esquema de inmunización mediante protocolos de prime-Boost empleados para el análisis de la respuesta inmunológica inducida por los distintos vectores.

La inoculación del ADN se realizó por vía intramuscular, inoculándose 100 µg de ADN-B en 100 µl de agua estéril libre de pirógenos (50 µg de pcDNA-GPN y 50 µg de pCMVgp120). Los virus recombinantes se inocularon en la cavidad intraperitoneal en un volumen total de 200 µl de PBS estéril con una dosis viral de 2 x 10^7 UFP/ratón. Los virus empleados en todas las inmunizaciones fueron purificados por gradiente (VACV-WR) o doble colchón (MVA y NYVAC) de sacarosa para asegurar su pureza.

3.3.7.7 Determinación de las células T secretoras de IFN-γ mediante el ensayo de ELISPOT

Para evaluar la inmunogenicidad de las células T específicas de antígeno se utilizó el ensayo de ELISPOT, que cuantifica la respuesta inmune celular mediada por un protocolo de inmunización detectando las células que secretan determinadas citoquinas

al ser reestimuladas por un antígeno o péptido específico (Miyahira *y cols.*, 1995). En resumen, placas de 96 pocillos con fondo de nitrocelulosa (Millipore) se cubrieron con 75 μl/pocillo de una solución del anticuerpo monoclonal de rata anti-IFN-γ murino (clon R4-6A2, Pharmingen, San Diego, CA) a una concentración de 6 μg/ml en PBS. Tras incubarlo toda la noche a temperatura ambiente, se lavaron los pocillos tres veces con medio RPMI y finalmente se incubó con medio suplementado con 10% FCS, durante al menos una hora a 37 ºC en atmósfera de CO_2 al 5%. Los bazos y/o ganglios de los animales inmunizados se recogieron en medio RPMI + 10% FCS y se homogeneizaron en un separador celular (Falcon). Las células disgregadas se centrifugaron durante 5 min. a 1500 rpm a 4 ºC, y se lavaron dos veces con RPMI + 10% FCS. En el caso de los bazos, se lisaron los eritrocitos añadiendo NH_4Cl 0,1M (2 ml/bazo) durante 3-5 min. en hielo. Transcurrido este tiempo se añadió RPMI + 10% FCS y se centrifugó, se lavó dos veces más con RPMI + 10% FCS y finalmente las células se resuspendieron en un pequeño volumen de RPMI + 10% FCS. Se contó el número de esplenocitos mediante tinción con azul tripan (4% en agua; SIGMA).

En el caso de evaluar la respuesta específica frente a los antígenos de VIH, se usaron pooles de péptidos que abarcan todos los antígenos de VIH presentes en las construcciones. Después de realizar tres lavados, las células presentadoras, a las que se adicionó IL-2 (60 U/ml), se añadieron a una concentración de 10^5 células/pocillo. Asimismo, se añadieron 100 μl/pocillo de una suspensión de 10^7 esplenocitos/ml y de diluciones 1/4 y 1/16. Las placas se incubaron durante 48 horas a 37 ºC en atmósfera de CO_2, se lavaron 5 veces con PBS + 0,05% Tween-20 (PBST), y se incubaron con 2 μg/ml del anticuerpo monoclonal de rata anti-IFN-γ biotinilado XMG1.2 (Pharmingen) diluido en PBST, durante 2 horas a temperatura ambiente. Posteriormente se lavaron las placas 5 veces con PBST y se añadió una dilución 1/800 de avidina-peroxidasa (0,5 mg/ml; Sigma). Tras 1 hora a temperatura ambiente se lavó 3 veces con PBST y dos con PBS, añadiéndose finalmente la mezcla de revelado: 1 μg/ml del sustrato DAB (Sigma), resuspendido en Tris-Cl 50 mM pH 7,5, 0,015% de H_2O_2. La reacción se detuvo lavando la placa con abundante agua, y una vez seca se realizó el recuento de los spots con la ayuda del software AID ELISPOT *reader system* (Vitro).

3.3.7.8 Evaluación de los niveles de citoquinas y β-quimioquinas por ELISA

Los niveles de citoquinas y b-quimioquinas presentes en las sobrenadantes de cultivos celulares de los esplenocitos reestimulados *in vitro* se determinaron mediante ELISA utilizando kits comerciales de Pharmingen. Siguiendo las instrucciones del fabricante, placas de 96 pocillos de fondo plano (Maxisorp, Nunc) se tapizaron con el

anticuerpo anti-citoquina o anti-quimioquina, diluido en su correspondiente tampón (Carbonato sódico 0,1M pH 9,5 para IFN-γ, Fosfato sódico 0,2M pH 6,5 para INF-γ e IL-10), y se incubaron toda la noche a 4 ºC. Los pocillos se lavaron con PBST, y se bloquearon durante 1 hora a temperatura ambiente con PBS + 10% FCS. Tras el bloqueo se añadieron diluciones seriadas de las muestras y de los estándares de citoquinas o quimioquinas en PBS + 10% FCS. La placa se incubó durante dos horas a temperatura ambiente o durante toda la noche a 4 ºC. Después se lavó con PBST y se incubó a temperatura ambiente durante una hora con el anticuerpo anti-citoquina o anti-quimioquina biotinilado, junto con la estreptavidina conjugada con peroxidasa, diluido en PBS + 10% FCS. Se lavaron los pocillos y se añadió el sustrato TMB (Sigma). Se incubó a temperatura ambiente y en oscuridad durante 30 min. tras lo cual la reacción se detuvo con H_2SO_4 2N. La absorbancia se leyó a 450 nm en un lector de placas Labsystems Multiskan Plus (Chicago, IL.) y los valores obtenidos fueron extrapolados en la curva estándar (pg/ml).

3.3.7.9 Determinación de anticuerpos por ELISA

La presencia de anticuerpos en el suero de los ratones inmunizados, tanto frente a *vaccinia* como frente a los antígenos específicos de VIH-1, se determinó mediante ELISA. Se tapizaron placas Maxisorp (Nunc) de 96 pocillos con 50 µl/pocillo del antígeno correspondiente (gp160 LAV o Extracto celular de vaccinia) a una concentración de 2 µg/ml en PBS y se incubó toda la noche a 4 ºC. Posteriormente, se lavó con PBST dos veces y se bloqueó con PBST + 10% FCS durante 1 hora a 37 ºC. Después del bloqueo se añadieron 100 µl/pocillo de los sueros diluidos en PBST + 10% FCS y se incubó durante 1-2 horas a 37 ºC. Se lavó tres veces con PBST y se añadieron los anticuerpos de cabra anti-inmunoglobulinas de ratón conjugados con peroxidasa diluidos en PBST (IgG total, dilución 1/1 000; Southern Biotechnology Associates, Birmingham, AL.). Tras 1 hora a 37 ºC se lavó tres veces con PBST y se añadieron 50 ml/pocillo del sustrato TMB (Sigma). Tras 10-15 min. en oscuridad, la reacción se detuvo con 50 µl de H_2SO_4 2N. Se midió la absorbancia a 450 nm en un lector de placas Labsystems Multiskan Plus (Chicago, IL.).

3.3.7.10 Análisis estadístico

El análisis estadístico de los datos para determinar la significancia de las diferencias encontradas entre los distintos grupos se realizó mediante el test de análisis de la varianza (ANOVA). Para analizar las diferencias entre dos grupos se realizó un test *t* de Student. Se consideraron significativos valores de p menores de 0,05: *, $p<0,05$, **, $p<0,01$, ***, $p<0,005$.

Resultados

Resultados

4.1- ESTUDIO COMPARATIVO DEL COMPORTAMIENTO EN CÉLULAS EN CULTIVO DE LAS CEPAS MVA Y NYVAC.

4.1.1- Caracterización del Efecto Citopático (EC) inducido en la célula tras la infección con las cepas MVA y NYVAC.

La infección por el virus vaccinia (VACV) induce importantes cambios bioquímicos y morfológicos en la célula infectada que conjuntamente se denominan efecto citopático o EC (Bablanian *y cols.*, 1978a; Bablanian *y cols.*, 1981a; Bablanian *y cols.*, 1981b; Bablanian *y cols.*, 1978b).

En primer lugar, nos propusimos caracterizar el efecto citopático inducido en diferentes líneas celulares tras la infección con las cepas atenuadas MVA y NYVAC. Para ello, se realizó un seguimiento a lo largo del tiempo de los cambios producidos en las células infectadas según se describe en el apartado 2.3.5.4 de materiales y métodos. De este modo, fueron analizadas una serie de características como el redondeamiento celular, la aparición de cuerpos de inclusión o la pérdida de adherencia al sustrato mediante microscopía de contraste de fase.

En la figura 11 se muestra un ejemplo representativo del EC inducido por las cepas MVA y NYVAC en una línea celular no susceptible a la infección productiva como las células HeLa. Casi la totalidad de las células infectadas con NYVAC mostraron un pronunciado redondeamiento celular a tiempos tan tempranos como 2 horas postinfección. Este efecto citopático fue aumentando progresivamente a medida que avanzó la infección, observándose a tiempos tardíos, 24 horas, una gran pérdida de adhesión celular. Este fenotipo fue bastante similar al que encontramos en las células infectadas con la cepa competente en replicación WR. Sin embargo, el redondeamiento celular inducido por éste a tiempos tempranos fue menos pronunciado.

Por el contrario, el EC fue menor o estaba más retrasado cuando las células fueron infectadas con la cepa atenuada MVA, donde a tiempos tardíos toda la monocapa celular se mantenía todavía adherida al sustrato (Figura 11). El mismo efecto se observó en líneas celulares permisivas (BHK-21 y CEF), e incluso cuando las células infectadas fueron pretratadas con la droga Ara C que bloquea la replicación del ADN viral (dato no mostrado), lo que nos sugiere que el EC depende de la expresión de genes virales tempranos.

Otro de los efectos que pudimos observar en las fotografías fue que a partir de las 16 horas en aquellas células infectadas con NYVAC, y a diferencia de las infecciones con MVA o con WR, un gran número de células presentaban cambios morfológicos característicos de un proceso de muerte celular por apoptosis. En este sentido, observando las imágenes a mayor aumento se detectó la formación de vesículas unidas a la membrana plasmática adquiriendo una forma característica de "burbujas" (zeiosis) y la posterior fragmentación celular dando lugar a estructuras esféricas que corresponden a fragmentos citoplasmáticos denominados cuerpos apoptóticos, imágenes compatibles con la fase de ejecución del proceso apoptótico.

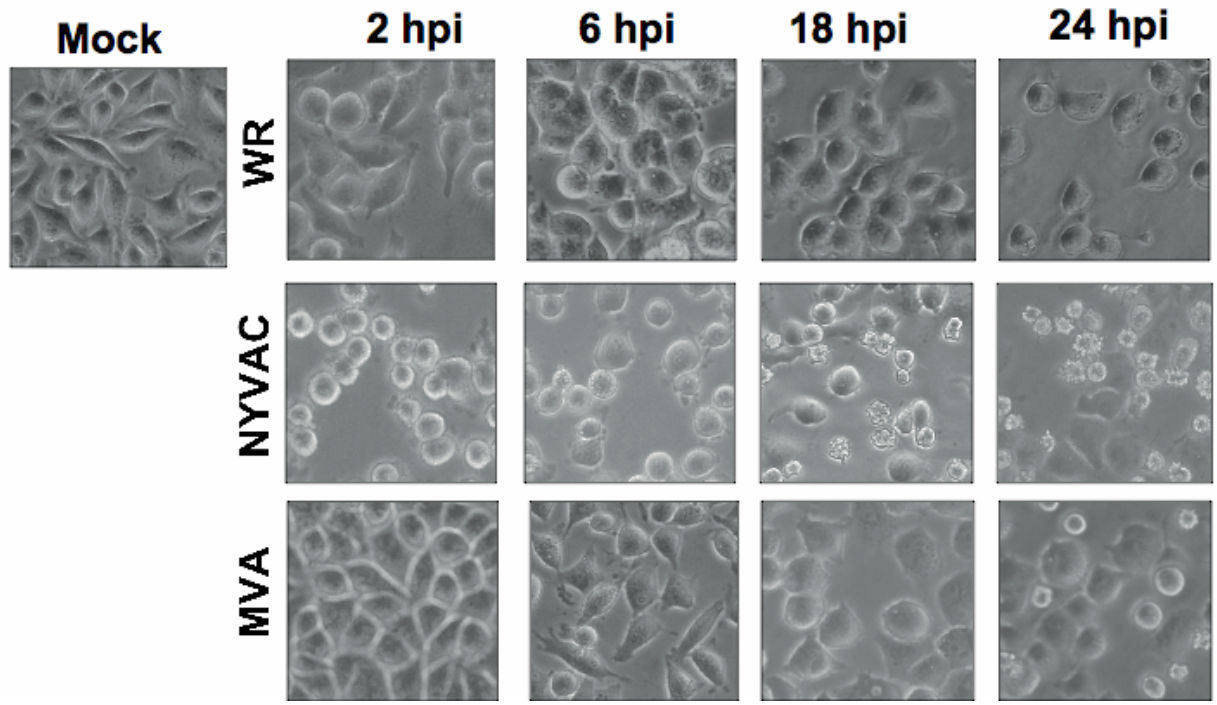

Figura 11: Efecto Citopático de MVA y NYVAC en células de origen humano HeLa. Los cambios morfológicos inducidos a los distintos tiempos postinfección fueron analizados mediante microscopía de contraste de fase en células HeLa sin infectar (mock) o tras la infección con las cepas virales WR, MVA o NYVAC a una multiplicidad de 5 UFP/célula.

4.1.2- Análisis del rendimiento de MVA y NYVAC en células permisivas y no permisivas.

Para analizar las propiedades de restricción de hospedador de cada cepa, decidimos comparar y cuantificar la capacidad de replicación y propagación de MVA y NYVAC bajo condiciones permisivas y no permisivas de producción viral. De este modo, infectamos monocapas de células BHK-21(línea celular permisiva) o HeLa (línea celular no permisiva) a una multiplicidad de infección de 0,01 UFP/célula con cada virus. A

distintos tiempos postinfección las partículas virales infecciosas que permanecen asociadas a la célula o aquellas que se han liberado al sobrenadante durante el curso de la infección, fueron contabilizadas por inmunotinción. El rendimiento viral de las cepas atenuadas fue comparado con el de la cepa competente en replicación WR también incluido en este análisis.

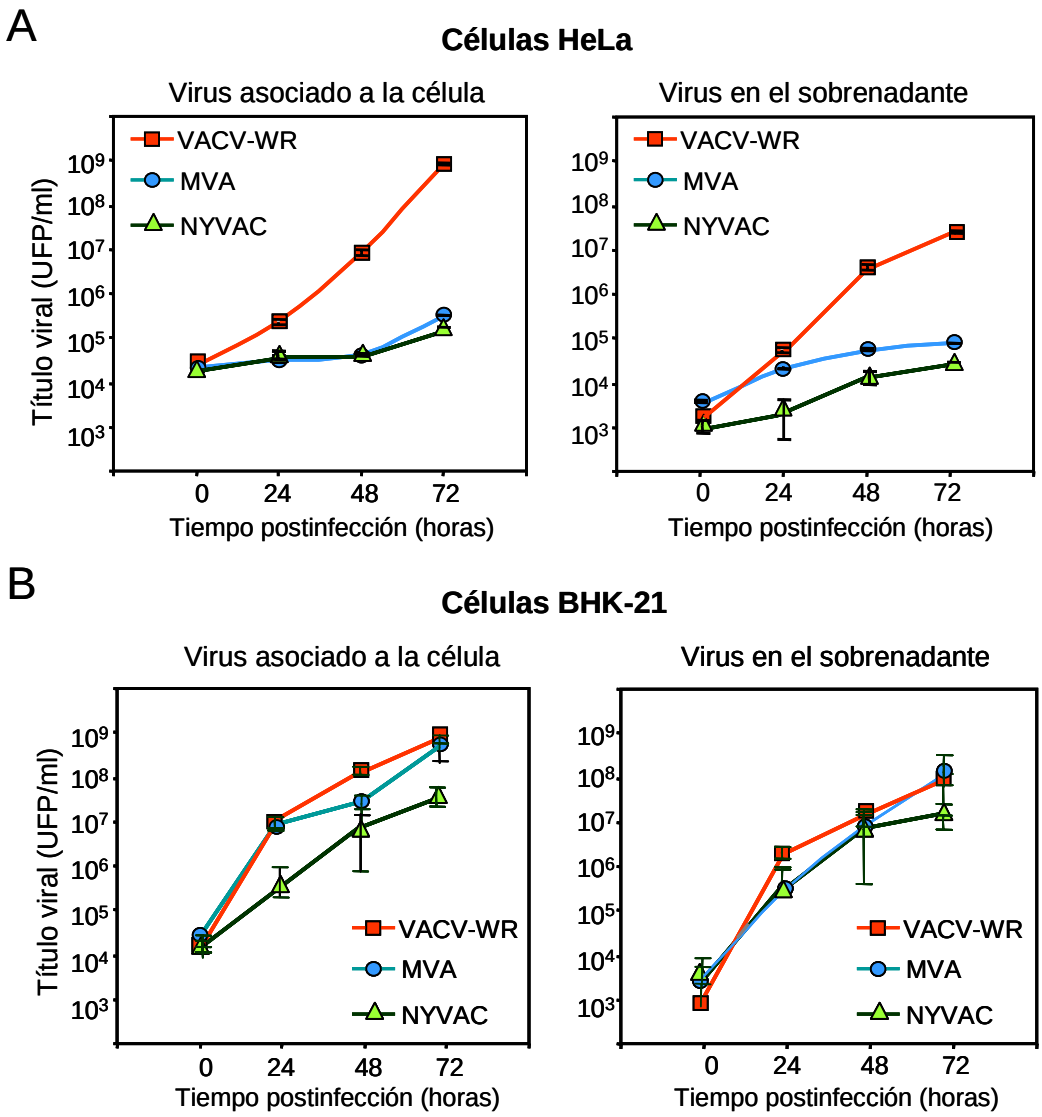

Figura 12: Rendimiento de MVA y NYVAC en líneas celulares permisivas y no permisivas. Células HeLa (A) y BHK-21 (B) fueron infectadas a una multiplicidad de infección de 0,01 UFP/célula con los virus WR, MVA o NYVAC. A los tiempos indicados las células infectadas fueron recogidas por centrifugación y las partículas infecciosas asociadas a las células, o liberadas al sobrenadante durante en curso de la infección, se cuantificaron por inmunotinción.

Como podemos observar en la figura 12-A, en las células de origen humano HeLa infectadas con la cepa WR, el título viral se incrementó a lo largo del tiempo en más de 10000 veces, mientras que no se observó ningún incremento significativo ni con MVA ni

con NYVAC. Por el contrario, bajo condiciones permisivas la cinética de crecimiento de las tres estirpes fue muy similar (Figura 12-B). Aunque si analizamos los títulos obtenidos con NYVAC, podemos observar que a tiempos tardíos hay una reducción en la producción de partículas infecciosas de casi un logaritmo respecto a los títulos obtenidos con la cepas WR o MVA.

En conjunto, los resultados de la figura 12 demuestran que las dos cepas atenuadas tienen un comportamiento bastante similar en cuanto a la eficiencia de replicación. Así, bajo condiciones no permisivas (HeLa), ninguna de las cepas es capaz de replicar de forma productiva. Mientras que en condiciones permisivas (BHK-21), ambos virus siguen la misma cinética de crecimiento viral, aunque la eficiencia de replicación de NYVAC fue casi un logaritmo menor que la de MVA. Esta reducción podría estar relacionada con el marcado EC que se induce en la célula tras la infección con NYVAC (Figura 11).

4.1.3- Análisis de la síntesis de proteínas durante la infección con MVA y NYVAC.

A continuación, quisimos analizar el proceso de síntesis de proteínas, tanto celulares como virales, en líneas susceptibles y no susceptibles a la infección productiva de MVA o NYVAC.

Para comparar la síntesis *de novo* en ambas infecciones, cultivos celulares de BHK-21 y HeLa fueron infectados con MVA o NYVAC a una multiplicidad de 5 UFP/célula. A las 2, 4, 8 y 16 horas tras la adsorción del virus, las células infectadas fueron marcadas metabólicamente durante 30 minutos. Tras dicho marcaje, las muestras se recogieron y el patrón de proteínas en los distintos lisados celulares fue analizado por SDS-PAGE y autorradiografía. Como podemos observar en la figura 13, en ambas líneas celulares infectadas tanto con MVA como con NYVAC, el comienzo de la síntesis de proteínas virales y la inhibición de la síntesis de las proteínas celulares ocurre entre las 4 y 8 primeras horas de infección como demuestra la aparición de nuevas bandas (marcadas con puntos). A dichos tiempos no se observaron diferencias entre ambos virus ni en la cinética de síntesis ni en el patrón de proteínas virales. Sin embargo, a tiempos más tardíos (16 hpi) los niveles en la síntesis de proteínas virales fueron más reducidos en la infección por NYVAC respecto a la de MVA.

Estas diferencias en la cantidad de proteínas virales fueron confirmadas por un ensayo de western-blot, analizando los mismos lisados con un anticuerpo policlonal que reconoce proteínas virales del virus vaccinia (Figura 14).

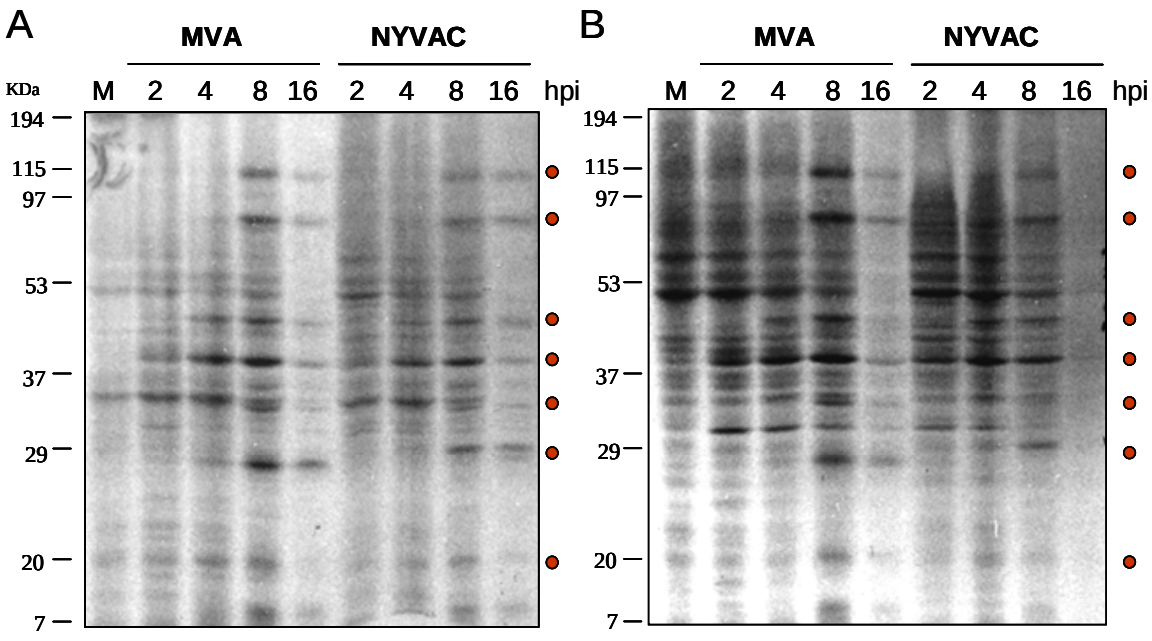

Figura 13: Síntesis *de novo* de proteínas durante la infección con MVA o NYVAC. Monocapas de células BHK-21 **(A)** o HeLa **(B)** sin infectar (Mock: M) o infectadas con MVA o NYVAC a una multiplicidad de 5 UFP/célula fueron marcadas metabólicamente durante 30 minutos con [S^{35}] Met-Cys (Promix, 50 μCi/ml) a distintos tiempos postinfección. Tras el marcaje, las muestras fueron recogidas y cantidades equivalentes de proteínas fueron analizadas por SDS-PAGE (10 %) y autorradiografía. Los puntos a la derecha indican proteínas virales. El tiempo está indicado en horas postinfección.

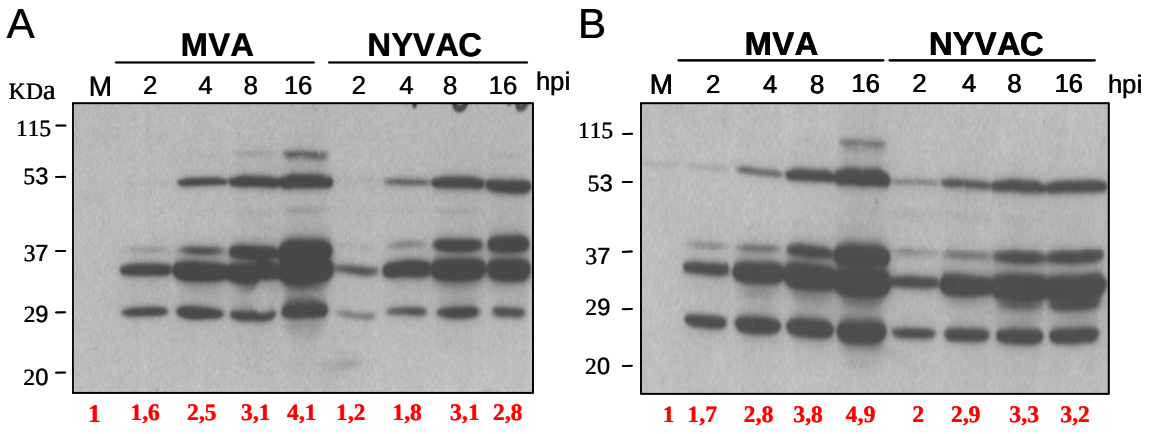

Figura 14: Acumulación de proteínas virales durante la infección con MVA o NYVAC. Análisis por western-blot de la expresión de antígenos virales durante la infección con MVA o con NYVAC en células BHK-21 **(A)** y HeLa **(B)**. Los números que aparecen en la parte inferior de cada carril representan el ratio determinado por densitometría, correspondiente a la intensidad de las bandas en las células infectadas respecto a los niveles obtenidos en las células sin infectar. M: células sin infectar.

Cuando una célula es infectada, se activan los mecanismos de acción antiviral con el objetivo de bloquear eficientemente la producción de proteínas virales y así evitar la formación de nuevas partículas infecciosas (Opferman, 2007). La expresión génica en células eucarióticas está regulada a nivel de la traducción de sus ARN mensajeros (ARNm). La fosforilación del factor de iniciación eIF2 representa uno de los mecanismos de regulación de la síntesis de proteínas mejor caracterizado en células de mamífero ya que impide la traducción de proteínas. En dicho proceso participa una familia de proteínas que fosforilan específicamente la subunidad alfa de dicho factor en respuesta a varias condiciones de estrés, como por ejemplo, la falta de nutrientes, la deficiencia en hierro, el choque térmico o la infección viral (de Haro *y cols.*, 1996). Por ello, nuestro siguiente objetivo fue examinar los niveles de fosforilación de eIF2α en el contexto de la infección viral. Así, determinamos los niveles de eIF2α fosforilado en células BHK-21 y HeLa infectadas con MVA o NYVAC mediante un ensayo de western-blot empleando anticuerpos específicos frente a eIF2α y frente a su forma fosforilada. Como muestra la figura 15, en ambas líneas celulares se observó un nivel basal de fosforilación de eIF2α similar al de las células sin infectar a tiempos tempranos postinfección. Sin embargo, hubo un incremento en dicho nivel en las células infectadas con NYVAC y no en aquellas infectadas con MVA a medida que la infección fue avanzando. Comparando estos resultados con los de la figura 14, dicha fosforilación de eIF2α se produjo después del comienzo de la inhibición en la síntesis de proteínas celulares, coincidiendo con la disminución en la síntesis de proteínas virales.

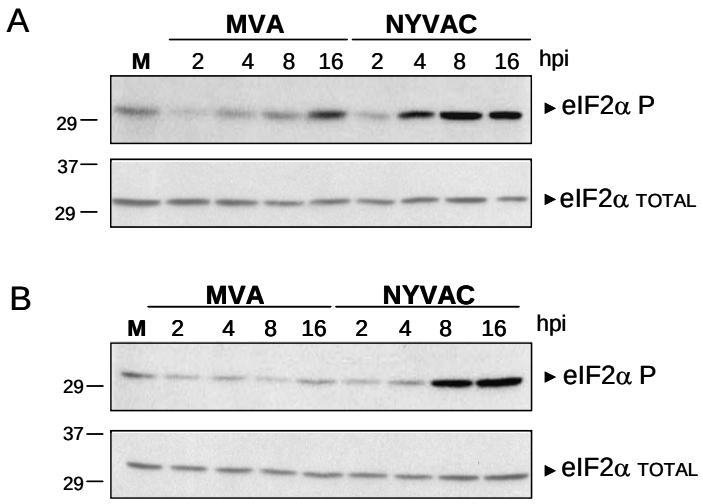

Figura 15: Fosforilación de eIF2α durante el curso de la infección con MVA y NYVAC. Análisis por western-blot de los niveles de fosforilación de eIF2α a lo largo del tiempo en células BHK-21 **(A)** y HeLa **(B)** sin infectar (M) o infectadas por MVA o NYVAC a una multiplicidad de 5 UFP/célula.

Como hemos descrito previamente en la introducción, la expresión génica de los poxvirus está regulada en forma de cascada, donde primero se sintetizan las proteínas tempranas mientras que la síntesis de proteínas intermedias y tardías sólo ocurre después de la replicación del ADN viral (Broyles, 2003). Ante el posible control traduccional de las proteínas virales debido a la fosforilación del factor eIF2 durante la infección con NYVAC, nos propusimos analizar si dicho bloqueo en la síntesis de proteínas virales podría ser específico de un determinado grupo de genes.

Para ello, analizamos la expresión de proteínas virales tempranas y tardías mediante western-blot en lisados de células HeLa y BHK-21 infectadas con MVA o NYVAC empleando anticuerpos que reconocen específicamente la proteína viral temprana E3 (producto del gen *E3L)* y las proteínas virales tardías A27, A14, A17, L1 y A4 (productos de los genes *A27L*, *A14L*, *A17L, L1R* y *A4L,* respectivamente).

Como podemos observar en la figura 16, la expresión de las proteínas virales tempranas y tardías analizadas fue similar tras la infección con WR, MVA o NYVAC bajo condiciones permisivas (BHK-21). Sin embargo, en condiciones no susceptibles a la infección productiva (HeLa), el patrón de síntesis de proteínas virales en la infección con NYVAC fue distinto respecto al de MVA o WR. Concretamente, las bandas pertenecientes a las proteínas virales tardías A27, A17 y L1, no se detectaron en los extractos de células infectadas con NYVAC, mientras que sí estaban presentes en los lisados celulares procedentes de las infecciones con MVA o WR. Por el contrario, las bandas correspondientes a la proteína temprana E3 o a las proteínas tardías A4 y A14 fueron detectadas eficientemente en los lisados de células infectadas con cualquiera de las tres cepas.

Estos resultados nos indican que durante la infección con NYVAC en condiciones no permisivas existe un bloqueo específico que afecta a la síntesis de ciertas proteínas virales tardías.

Para confirmar estos resultados, analizamos mediante inmunofluorescencia la expresión de la proteína A27, que no pudimos detectar por western-blot. En la figura 17 se muestra localización de la proteína A27 en condiciones permisivas (BHK-21) y no permisivas (HeLa) tras la infección con WR, MVA o NYVAC.

La proteína viral A27, es una proteína estructural localizada en la membrana del virus intracelular maduro (MV). Como puede observarse en la figura 17, en condiciones permisivas (BHK-21), donde el virus puede replicar, la distribución de esta proteína es similar en las tres infecciones, mostrando un marcaje punteado distribuido por todo el citoplasma que correspondería a la formación de los viriones intracelulares maduros (MVs). Sin embargo, en la línea no permisiva (HeLa), el marcaje de la proteína A27 es diferente para cada una de las cepas virales. En las células infectadas con WR el

marcaje es similar al descrito en células BHK-21 ya que ambas líneas celulares son susceptibles a la infección por WR. En las células infectadas por NYVAC no se observa ningún tipo de marca para la proteína A27, lo que confirma el resultado obtenido por western-blot (Figura 16). En las células infectadas por MVA se observa una acumulación citoplasmática de la proteína A27 lo que se correlaciona con lo descrito previamente para la infección con MVA en líneas celulares no permisivas, donde existe un bloqueo en el ensamblaje de las proteínas estructurales sin afectar a la síntesis de proteínas virales. Resultados similares se obtuvieron para las proteínas virales tardías A17 y L1 (datos no mostrados).

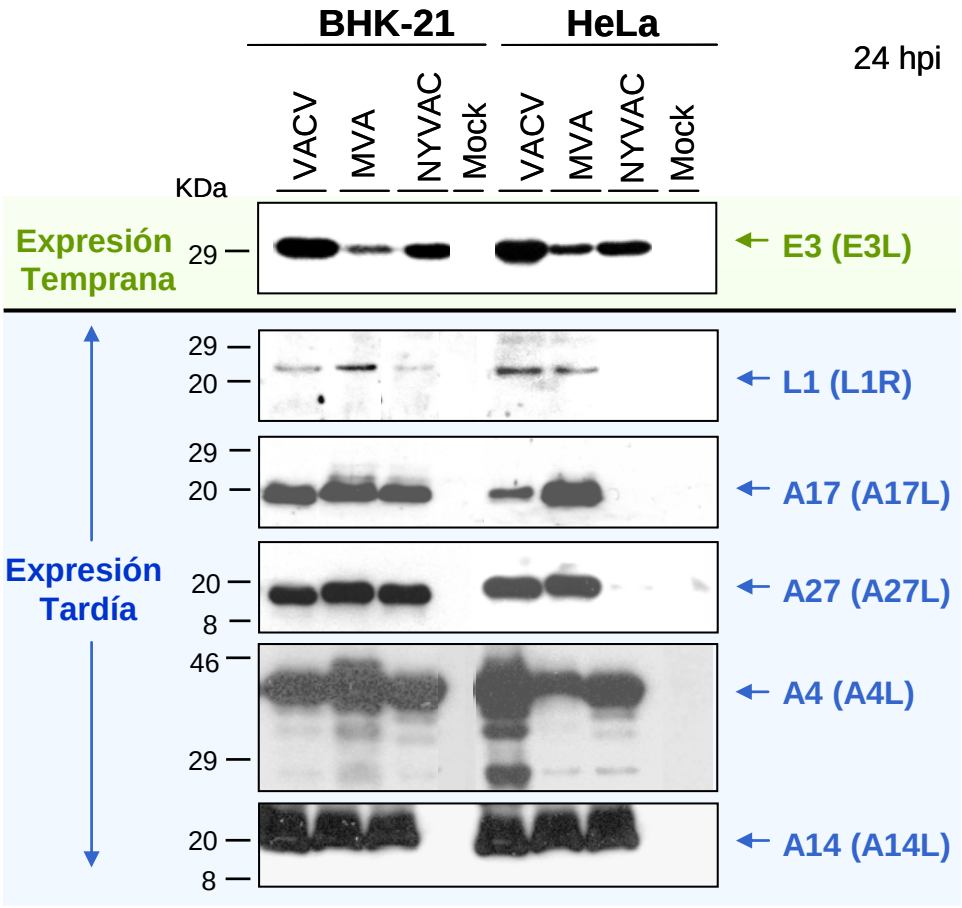

Figura 16: Expresión de proteínas virales específicas bajo condiciones susceptibles y no susceptibles a la infección. La expresión de las proteínas virales tempranas (E3) y tardías (L1, A17, A27, A4 y A14) en células BHK-21 y HeLa sin infectar (Mock) o infectadas con las cepas WR, MVA o NYVAC a una multiplicidad de 5 UFP/célula fue analizada por western-blot. Los extractos celulares se recogieron a las 24 hpi y cantidades equivalentes de proteína fueron resueltas por SDS-PAGE y transferidas a una membrana de nitrocelulosa que fue incubada con distintos anticuerpos específicos que reconocen las distintas proteínas virales.

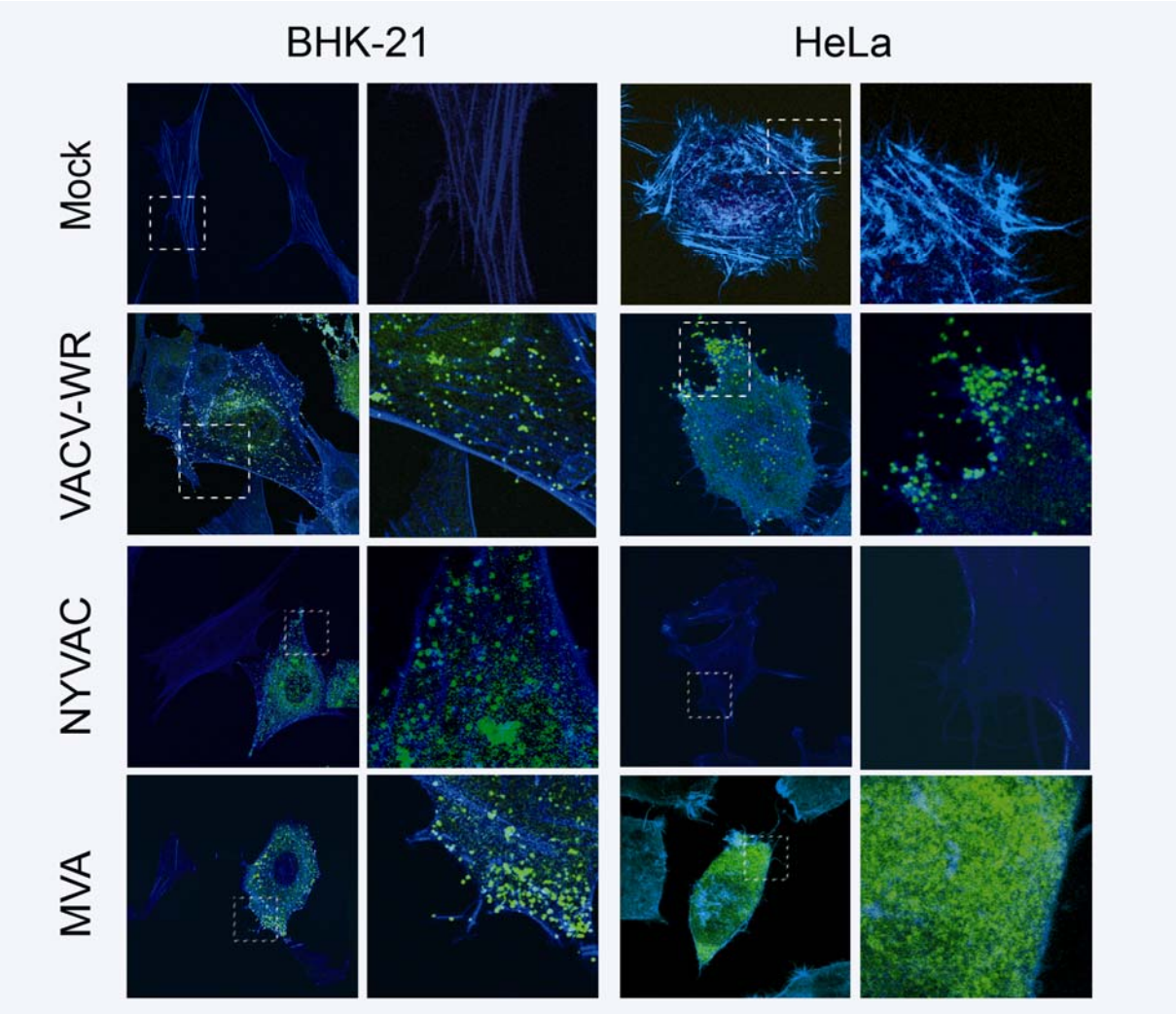

Figura 17: Análisis de la expresión de la proteína A27 por inmunofluorescencia. Células BHK-21 y HeLa fueron infectadas con las cepas WR, MVA o NYVAC a una multiplicidad de 5 PFU/célula. A las 16 horas postinfección las células fueron fijadas, permeabilizadas y marcadas con el anticuerpo monoclonal C3, que reconoce la proteína viral A27 **(•)** y con faloidina para detectar la actina celular **(•)** Como control negativo se utilizaron las células sin infectar. Los paneles de la derecha muestran una mayor magnificación de las áreas indicadas.

Ante estos resultados quisimos determinar si la ausencia de las proteínas A27, A17 y L1 podría ser debida a un defecto a nivel transcripcional. Para ello, analizamos la transcripción de los genes virales *E3L* y *A27L* en células HeLa infectadas con WR, MVA o NYVAC. A las 24 hpi el ARN total de las células infectadas fue aislado y los niveles de ARNm específicos fueron analizados por RT-PCR. Como muestra la figura 18, hubo amplificación en todas las infecciones y no se apreciaron diferencias en los tamaños de los productos amplificados, lo que nos podría indicar una correcta transcripción de ambos genes.

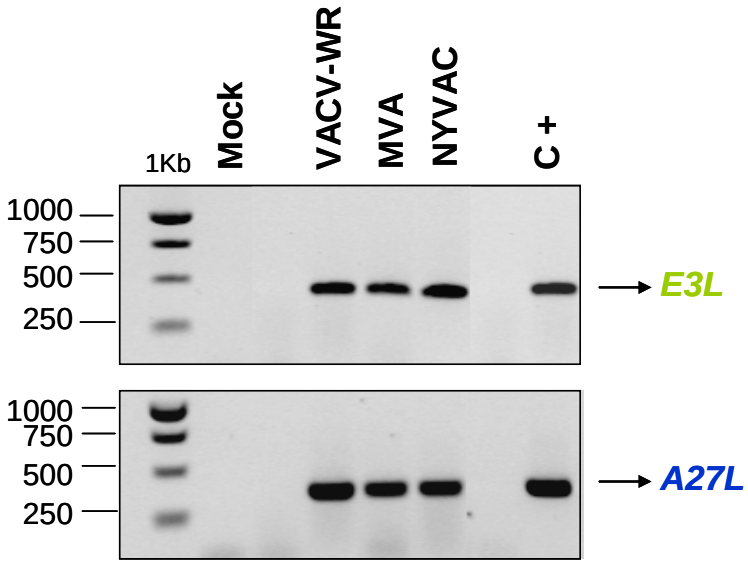

Figura 18: Transcripción viral de los genes *E3L* y *A27L*. La transcripción de los genes *E3L* y *A27L* fue determinada por RT-PCR como se describe en el apartado 2.3.2.3 de materiales y métodos. El ARN total procedente de células sin infectar y el ADN extraído de células infectadas con MVA fueron utilizados como control negativo (mock) y positivo (C+) respectivamente.

A continuación, decidimos analizar en mayor profundidad la integridad del ARNm del gen *A27L* realizando un análisis de extensión del cebador como se describe en el apartado 2.3.2.4 de materiales y métodos.

Como se observa en la figura 19, tanto en las muestras procedentes de la infección de células HeLa con NYVAC como con WR se obtuvo un mismo producto de ADNc de 263 pares de bases. Estos resultados nos indican que el extremo 5´ del gen *A27L* se encuentra intacto y confirma su correcta transcripción durante la infección por NYVAC.

Por lo tanto, podemos concluir que la inhibición en la síntesis de ciertas proteínas virales tardías durante la infección de líneas no permisivas con NYVAC parece ser una consecuencia de un bloqueo en la traducción y no de una inhibición específica en la transcripción de genes tardíos.

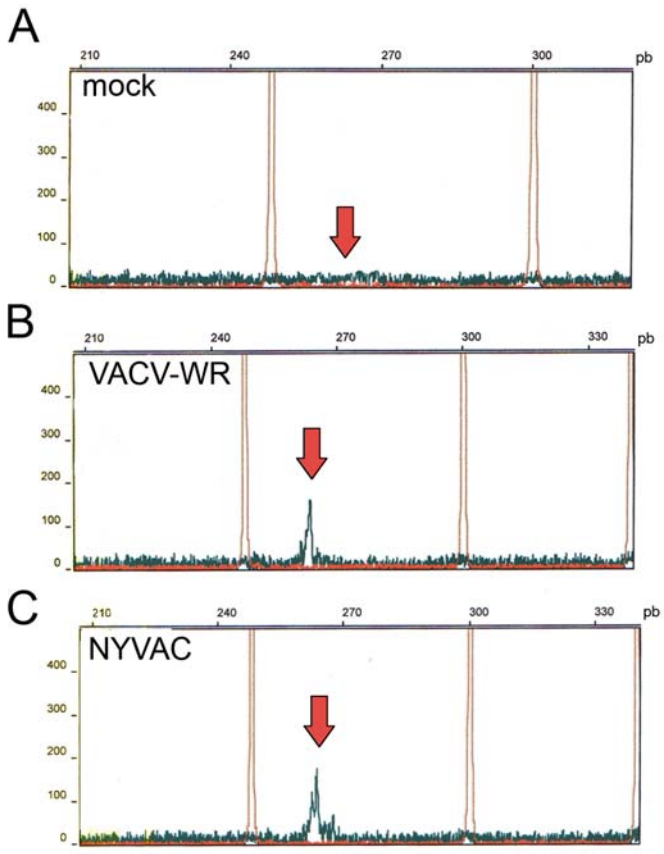

Figura 19: Ensayo de extensión del cebador del gen A27L. Producto de extensión del cebador obtenido utilizando 2 μg de ARN total aislado de células HeLa sin infectar **(A)** o infectadas con VACV-WR **(B)** o NYVAC **(C)** a 5 UFP/célula durante 16 horas. En el gráfico se muestran los tamaños de los picos (en pares de bases) y los controles estándar internos obtenidos con GeneScan 500 ROX. Las flechas indican los productos (ADNc marcado con VIC) obtenidos para el gen *A27L*. El área del pico es una medida de la intensidad de fluorescencia de la señal de VIC. Las áreas de pico para cada muestra fueron: 177 para NYVAC, 164 para WR, y 55 para las células sin infectar (mock) (datos no mostrados).

4.1.4- Estudio comparativo del proceso de morfogénesis de MVA y NYVAC en células HeLa.

Trabajos previos de microscopía electrónica entre los que se incluyen algunos realizados en el laboratorio del Dr. Esteban, han descrito que mutantes de deleción del virus vaccinia en alguno de los genes que codifican para proteínas virales tardías como A17, A27 o L1, presentan un bloqueo en distintas etapas de la morfogénesis viral (Rodriguez *y cols.*, 1995; Smith *y cols.*, 2002).

En la figura 20, se muestra un esquema de la morfogénesis del virus vaccinia (VACV) donde se indica en qué etapas intervienen algunas de las proteínas virales cuya síntesis se encuentra inhibida durante la infección con NYVAC de células HeLa.

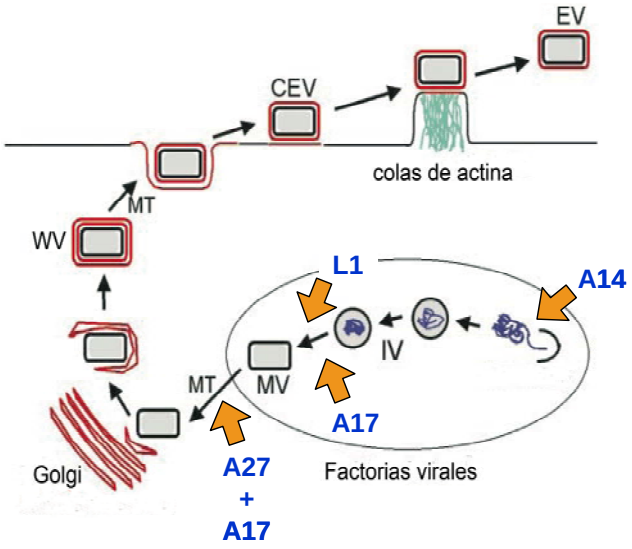

Figura 20: Esquema de los estadíos de la morfogénesis viral del virus vaccinia. En la figura se indican los estadíos en los que están implicadas algunas de las proteínas que participan en el proceso de morfogénesis. Figura adaptada de Smith y cols., 2002.

La ausencia de varias proteínas como A27, L1 o A17 en células HeLa infectadas con NYVAC nos sugería por lo tanto, que podría existir un bloqueo a nivel de morfogénesis en dichas células. Por ello, decidimos realizar un estudio comparativo del proceso de morfogénesis en células HeLa infectadas con MVA o NYVAC.

La morfogénesis de MVA bajo condiciones permisivas y no permisivas ha sido ampliamente estudiada (Carroll *y cols.*, 1997; Gallego-Gomez *y cols.*, 2003; Meiser *y cols.*, 2003; Sancho *y cols.*, 2002; Suttery Moss, 1992). El estadío en el que se produce el bloqueo depende del tipo celular. En células HeLa, el bloqueo en el programa morfogenético de MVA ocurre en los pasos siguientes a la formación de los viriones inmaduros (IVs), sin alterar la expresión de genes tempranos, intermedios ni tardíos (Sancho *y cols.*, 2002; Sutter *y cols.*, 1992).

Por el contrario, no hay estudios disponibles sobre la morfogénesis de NYVAC. Por lo tanto decidimos caracterizar este proceso en condiciones no permisivas. Para ello, se infectaron células HeLa con las cepas MVA o NYVAC a una multiplicidad de infección de 5 UFP/célula. A las 16 hpi las células infectadas fueron examinadas por microscopía electrónica para detectar la presencia de intermediarios en la morfogénesis.

Como muestra la figura 21, en las células infectadas con NYVAC (B) se detectaron muy pocos IVs en comparación con los presentes en las células infectadas con MVA (A). Además, no se detectó ninguna forma viral madura tras la infección con

NYVAC, sugiriendo que el bloqueo en el programa morfogenético de esta cepa ocurre en un paso anterior a la maduración o la formación de los viriones (IVs).

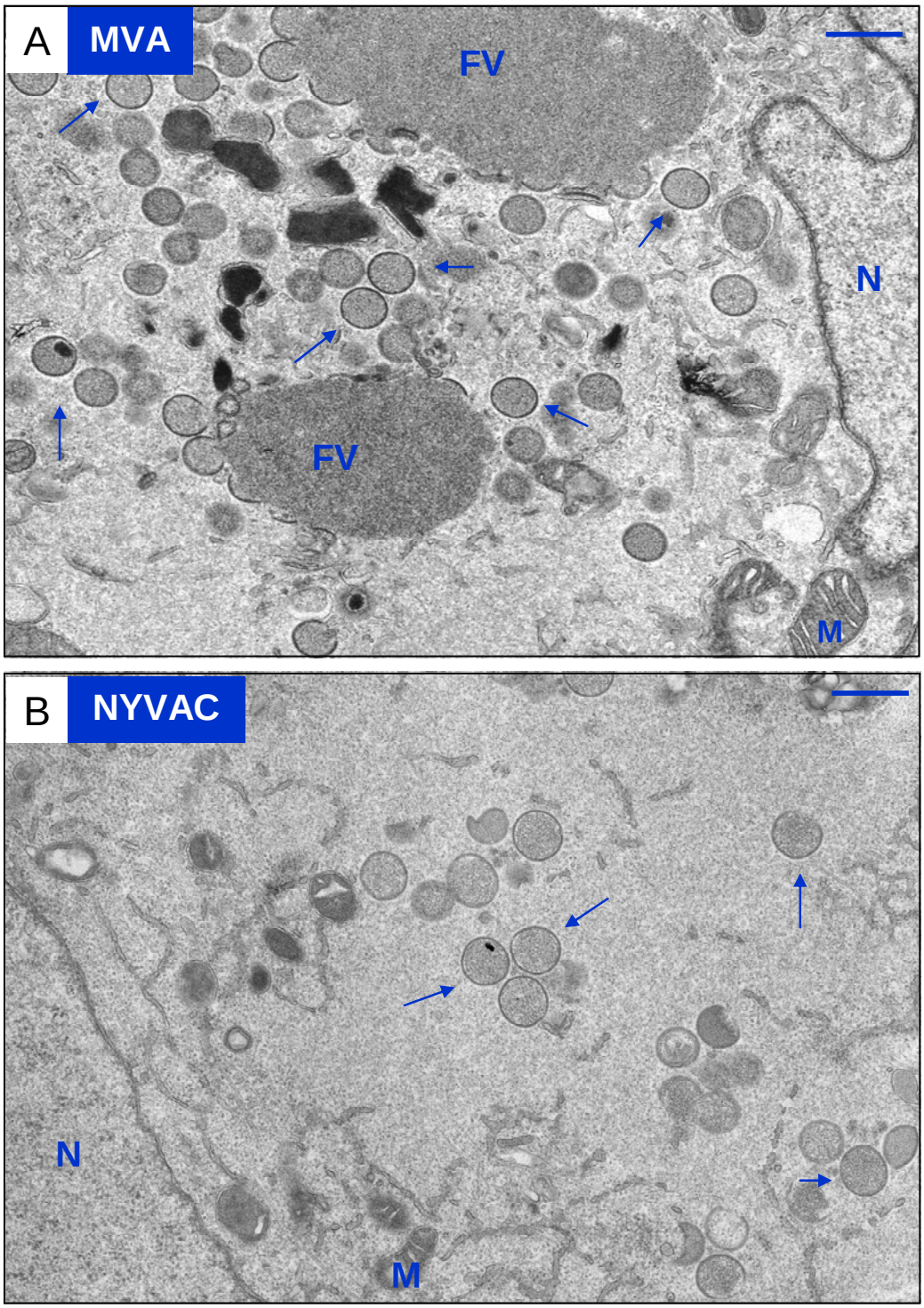

Figura 21: Microscopía Electrónica de células HeLa infectadas con MVA o NYVAC. Micrografías electrónicas de células HeLa infectadas con MVA **(A)** o NYVAC **(B)** a una multiplicidad de 5 UFP/célula durante 16 horas. La barra situada en la esquina superior derecha de cada panel indica la magnificación de cada fotografía (500nm). N: núcleo; M: mitocondria; FV: Factoría viral. Las flechas indican los viriones inmaduros (IVs).

Las imágenes tomadas con el microscopio electrónico de las células infectadas con NYVAC también revelaron la severidad de la infección. En dichas células fueron evidentes características propias de la inducción de apoptosis como la condensación de cromatina en patrón de media luna (Figura 22-A) o la formación de vacuolas translúcidas a nivel citoplasmático asociadas a la reducción del volumen celular (Figura 22-B). Como se había descrito previamente (Gallego-Gomez *y cols.*, 2003), ninguna de estas alteraciones se observaron en las células infectadas con MVA (imágenes no mostradas).

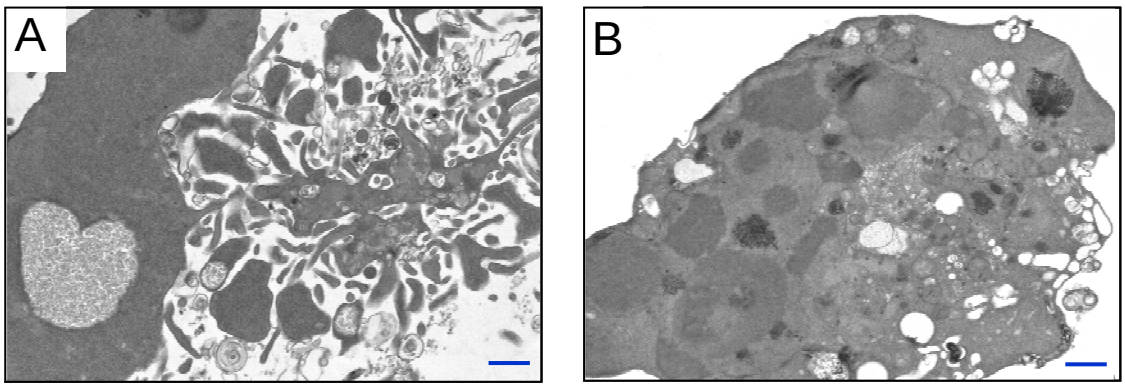

Figura 3.12: Características morfológicas propias de un proceso de muerte celular programada detectadas en las células infectadas con NYVAC. (A) Condensación de cromatina. **(B)** Formación de vacuolas translúcidas. La barra situada en la esquina superior izquierda de cada panel indica la magnificación de cada fotografía (500 nm).

4.1.5- Estudio del proceso de apoptosis en células humanas infectadas con MVA o NYVAC.

Los resultados descritos en los apartados 3.1.1 y 3.1.4 sugerían que la infección por NYVAC era responsable del fenotipo apoptótico observado por lo que quisimos analizar más detalladamente este proceso.

La apoptosis comprende un complejo sistema de señalización molecular que tiene lugar en la célula como respuesta a una serie de estímulos concretos y que concluyen con su muerte de una manera ordenada, programada y silenciosa. Es un proceso que se caracteriza por una serie de cambios bioquímicos y morfológicos como son la condensación del citoplasma y la compactación de la cromatina dando lugar a la formación de agregados densos que se deslocalizan para situarse junto a la membrana nuclear. Posteriormente, sobre la cromatina actúan una serie de endonucleasas que cortan el ADN en una serie de fragmentos oligonucleosomales (180 pb ó múltiplos de éstos) (Leisty Jaattela, 2001). Durante las últimas fases de la apoptosis se originan unas

vesículas que tienden a unirse a la membrana plasmática adquiriendo una forma característica en burbujas (zeonesis). Finalmente, la célula se fragmenta en los llamados cuerpos apoptóticos (Wyllie, 1980).

La gran mayoría de los cambios morfológicos observados anteriormente en las células infectadas por NYVAC podrían ser causados por un grupo de cisteín-proteasas denominadas caspasas que son activadas específicamente en las células apoptóticas. Todas las caspasas contienen un dominio activo cisteína-proteasa, y degradan proteínas cuya función es proteger a la célula de la muerte por apoptosis. Uno de estos sustratos es la proteína celular PARP (Poly (ADP-Ribosa) Polimerasa) (Riedly Shi, 2004).

Por esta razón decidimos analizar el procesamiento de dicha proteína en células HeLa infectadas con MVA o NYVAC mediante western-blot empleando un anticuerpo que reconoce tanto la forma completa así como la forma procesada de PARP.

Como se muestra en la figura 23, a tiempos tempranos de la infección con NYVAC, la proteína PARP se encuentra en su forma completa, detectándose una banda de 116 KDa. Esta banda fue perdiendo intensidad a medida que avanzó la infección apareciendo un producto mayoritario de 89 KDa correspondiente a la forma procesada de PARP. Por el contrario, el procesamiento de PARP fue menor en la infección por MVA, donde tras 16 horas de infección, la banda mayoritaria de PARP fue la de 116 KDa, correspondiente a su forma nativa.

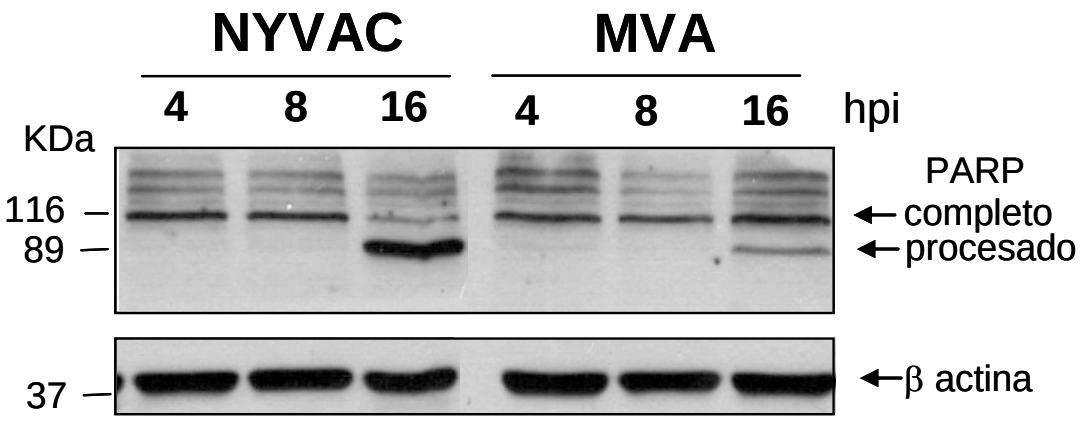

Figura 23: **Procesamiento de la proteína PARP durante la infección con MVA y NYVAC.** El procesamiento de la proteína celular PARP fue analizado en células HeLa infectadas con MVA o NYVAC a una multiplicidad de 5 UFP/célula por western-blot. Los extractos celulares se recogieron a los tiempos postinfección indicados (horas) y se resolvieron por SDS-PAGE y transferidas a una membrana de nitrocelulosa que fue incubada con un anticuerpo específico que reconoce la forma completa y procesada de PARP. La expresión de actina en los distintos extactos celulares se utilizó como control de carga.

Otro de los procesos que se asocia generalmente con la inducción de apoptosis es la degradación del ADN de forma específica entre nucleosomas. Se han desarrollado diferentes métodos que permiten analizar individualmente cada célula en busca de esta degradación. Entre ellos destaca la utilización de colorantes fluorescentes con afinidad por los ácidos nucleicos como el Hoechst o el DAPI (4´6´-diamino-2-fenilindol), que permite identificar fácilmente alteraciones del núcleo como la condensación de la cromatina o la fragmentación nuclear. La figura 24 muestra una tinción con DAPI de células HeLa infectadas con MVA o NYVAC. La fragmentación nuclear fue evidente en las células infectadas con NYVAC, donde se observaron fragmentos de ADN formando "esferas densas nucleares"; Sin embargo esta fragmentación no se apreció durante la infección por MVA.

Figura 24: Morfología de los núcleos de células infectadas con MVA o NYVAC. Células HeLa sin infectar (Mock) o infectadas con MVA o NYVAC a una multiplicidad de 5 UFP/célula durante 24 horas fueron fijadas y teñidas con el colorante DAPI y analizadas en un microscopio de fluorescencia. Las flechas indican las células que presentan fragmentación nuclear.

En conjunto, los resultados anteriores indican que durante la infección por NYVAC se induce apoptosis contrariamente a lo que ocurre en las células infectadas por MVA. Nuestro siguiente objetivo fue determinar de forma cuantitativa la magnitud de dicha apoptosis. Para ello recurrimos a la citometría de flujo analizando el ciclo celular de las células infectadas con las distintas cepas virales en presencia o ausencia de zVAD, un inhibidor general de caspasas (Figura 25). Cuando las células son teñidas con ioduro de propidio, los niveles de fluorescencia en las células apoptóticas son menores respecto a las células normales y aparecen como una subpoblación denominada sub G_0. Atendiendo a este criterio, observamos que aproximadamente un 42% de las células infectadas con NYVAC se localizaban en la población SubG_0, lo que representa un incremento significativo en el número de células apoptóticas comparado con el 17,6%

observado en las células infectadas con MVA o con el 9,3% observado en las células infectadas con WR. Este porcentaje (42%) fue hasta 7 veces superior respecto al obtenido en las células sin infectar (mock), utilizadas como control negativo. Además, en presencia del inhibidor zVAD, el porcentaje de células apoptóticas se redujo significativamente a los niveles basales (3,67%), lo que demuestra que la apoptosis inducida tras la infección con NYVAC es dependiente de la activación de caspasas.

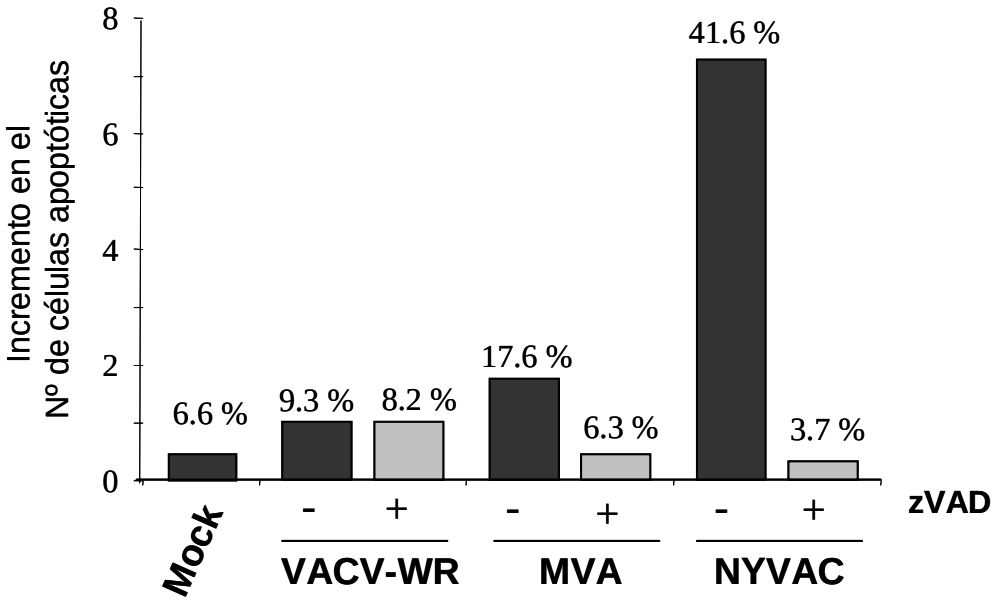

Figura 25: Cuantificación de la apoptosis inducida por NYVAC por citometría de flujo. Monocapas de células HeLa fueron infectadas con 5 UFP/célula de WR, MVA o NYVAC en presencia o ausencia de zVAD (40 μM). Tras 24 horas de infección, las células fueron marcadas con ioduro de propidio para realizar un ensayo de ciclo celular. Como control negativo se utilizaron células sin infectar (Mock). Las barras representan el incremento en el número de células apoptóticas respecto del Mock. El porcentaje de células apoptóticas para cada condición se muestra en la parte superior de cada barra.

Como hemos descrito anteriormente, la activación de endonucleasas es un evento tardío en el proceso apoptótico. Por esta razón, decidimos analizar el efecto de las nucleasas sobre la integridad del ARN ribosomal en la infección con NYVAC.

Como se muestra en la figura 26, las bandas correspondientes a las subunidades 28S y 18S del ARN ribosómico se encontraban intactas en las muestras correspondientes a las células sin infectar (mock) o a las células infectadas con WR o MVA. Por el contrario, si se observó degradación del ARN ribosómico en las muestras correspondientes a la infección por NYVAC. Los fragmentos generados en dicha

degradación son similares al patrón de degradación observado tras la activación de la enzima ARNasa L (dato no mostrado).

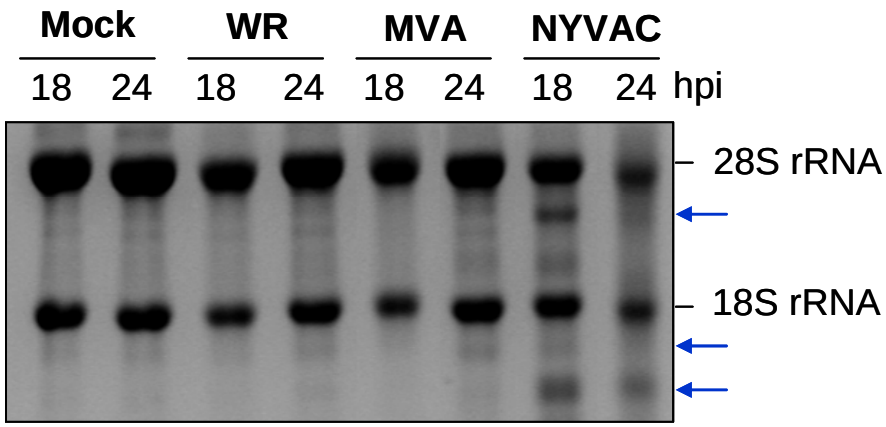

Figura 26: Degradación del ARN ribosomal. El ARN total de células HeLa sin infectar (Mock) o infectadas con WR, MVA o NYVAC a 5 UFP/célula fue aislado a 18 y 24 hpi, y 2 μg de ARN se fraccionó por electroforesis en geles de formaldehído-agarosa según se describe en materiales y métodos. Las flechas indican los productos de degradación de las subunidades 28S y 18S del ARN ribosómico.

En conjunto, todas estas observaciones confirman que durante la infección de células HeLa por NYVAC se induce una potente apoptosis.

4.1.6- Determinación del gen o los genes implicados en el comportamiento diferencial entre las cepas MVA y NYVAC.

Todos los resultados descritos hasta el momento muestran la existencia de claras diferencias en el comportamiento entre las cepas virales MVA y NYVAC en células en cultivo. Estas diferencias podrían ser debidas a las múltiples deleciones que se introdujeron en ambos genomas durante el curso de su atenuación. Por esta razón, quisimos comparar los dos genomas virales y analizar los posibles genes responsables del comportamiento diferencial. En la figura 27 se representan los genomas de ambos vectores con sus correspondientes deleciones.

Como podemos observar, existen 5 genes ausentes en el genoma de NYVAC que están intactos en el de MVA: *C6L*, *C7L*, *N2L*, *I4L* y *J2R*. Estos genes podrían ser por lo tanto, los responsables del comportamiento diferencial entre las cepas MVA y NYVAC.

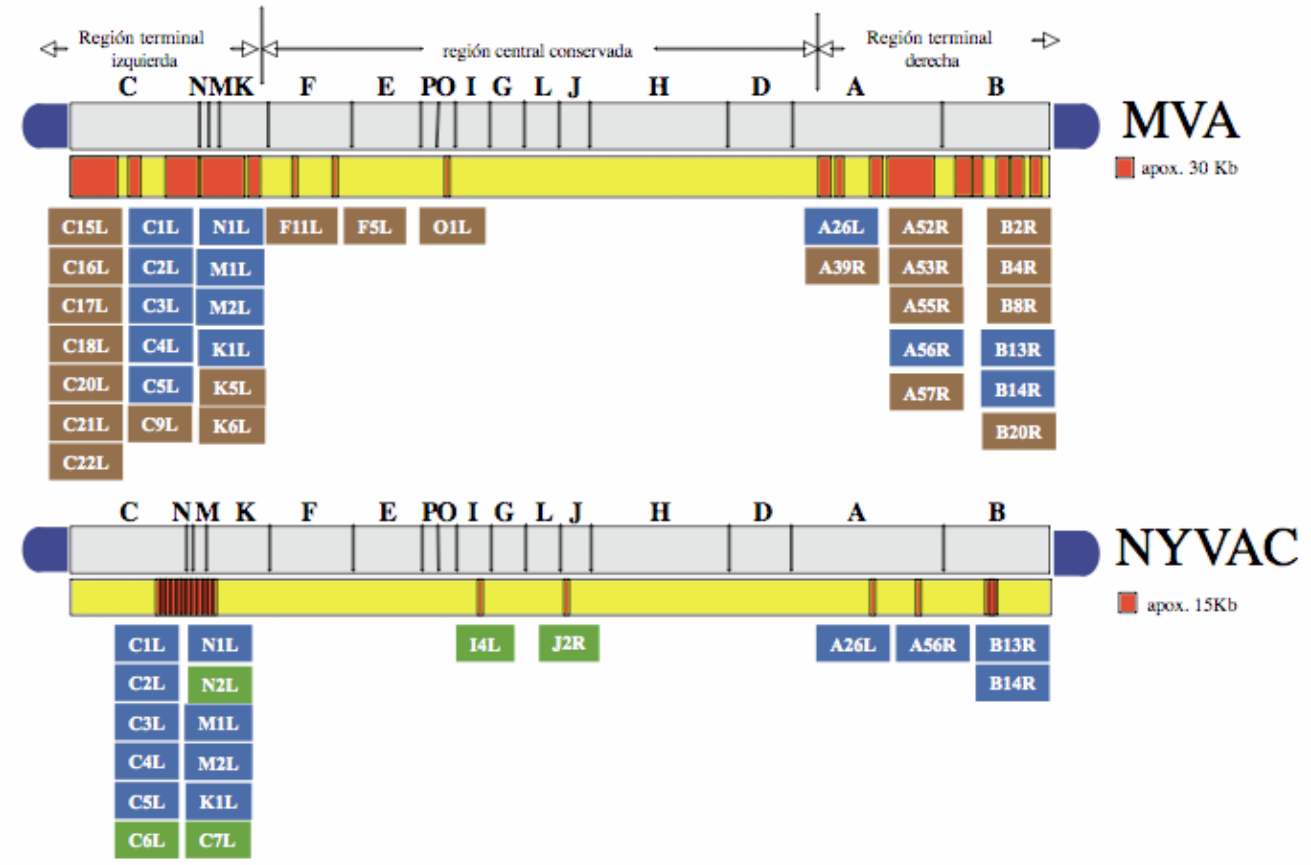

Figura 27: Análisis comparativo de los genomas de MVA y de NYVAC. En marrón se muestran los genes delecionados en MVA e intactos en el genoma de NYVAC, en azul las deleciones comunes en ambos genomas y en verde los genes inactivados en NYVAC e intactos en MVA. Los genes han sido nombrados según la nomenclatura correspondiente a la cepa Copenhagen propuesta por Goebel y cols., 1990.

Entre ellos, se encuentra el gen *C7L*, un gen del rango de hospedador, de expresión temprano-tardía y necesario para la replicación del virus en células humanas.

Dicho gen se encuentra altamente conservado dentro del genero *Orthopoxvirus* lo que refleja la importancia de éste gen para el virus (Figura 28) por lo que fue elegido para ser analizado como responsable del comportamiento diferencial entre MVA y NYVAC.

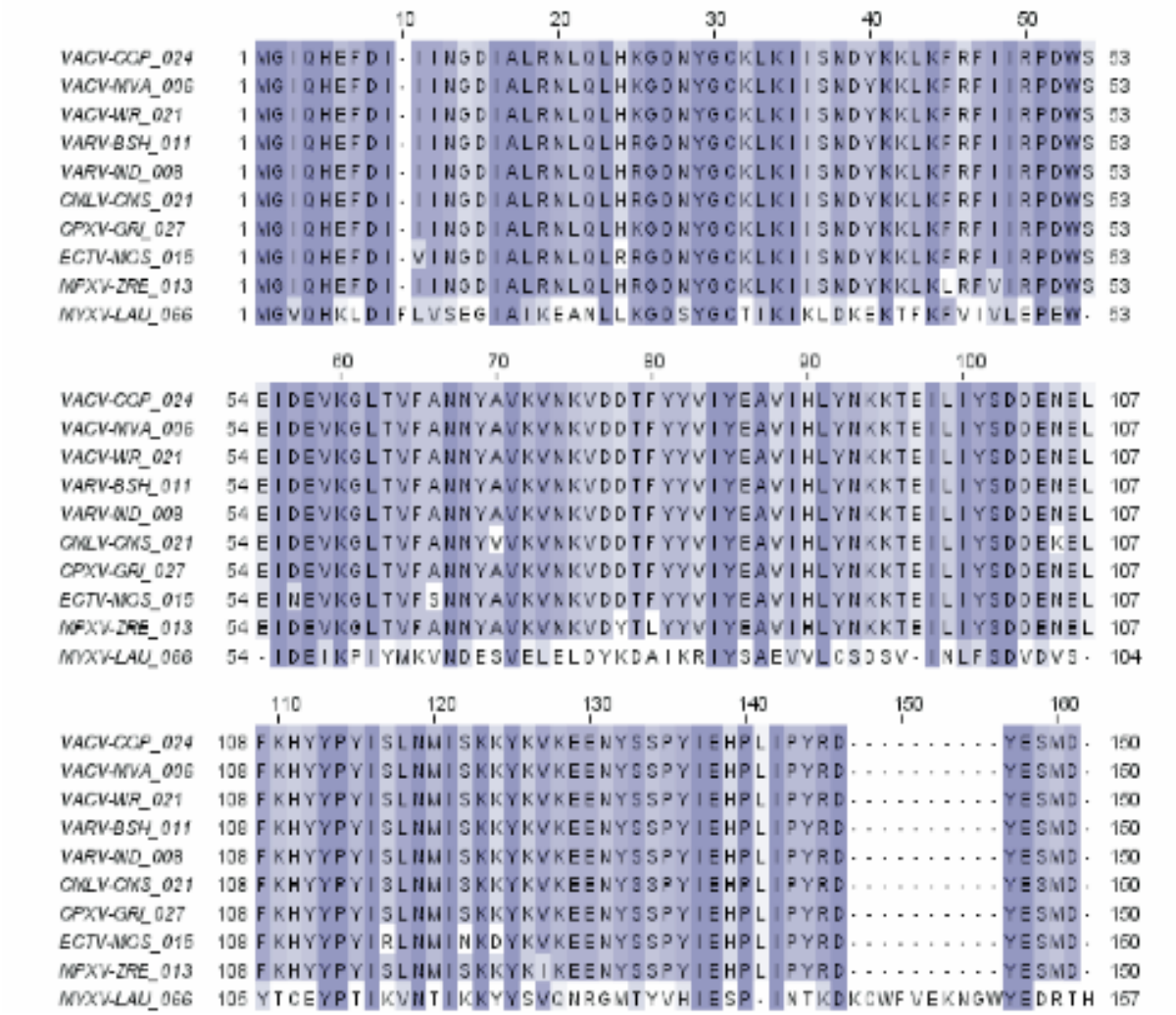

Figura 28: Secuencia de aminoácidos del gen *C7L* y homología con distintas especies del género *Orthopoxvirus*.

4.1.6.1 Generación del recombinante NYVAC-C7L

Para determinar el papel que podría desempeñar el gen *C7L* en el comportamiento de NYVAC, decidimos reintroducir dicho gen en su genoma. En primer lugar, generamos el plásmido de inserción pJR101-C7L como se describe en materiales y métodos. Este plásmido tiene clonado, entre los flancos del gen de la hemaglutinina (HA), el gen *C7L* del virus vaccinia bajo el control transcripcional del promotor viral sintético temprano/tardío y el gen marcador *LacZ* bajo el control del promotor viral p7.5 en orientación opuesta. Este vector fue utilizado para generar el recombinante NYVAC-C7L que contiene el gen *C7L* en el locus HA y así poder comparar el efecto que produce

su expresión en el comportamiento de NYVAC. La presencia del gen *C7L* y la pureza del recombinante se verificó por PCR como se muestra en la figura 29.

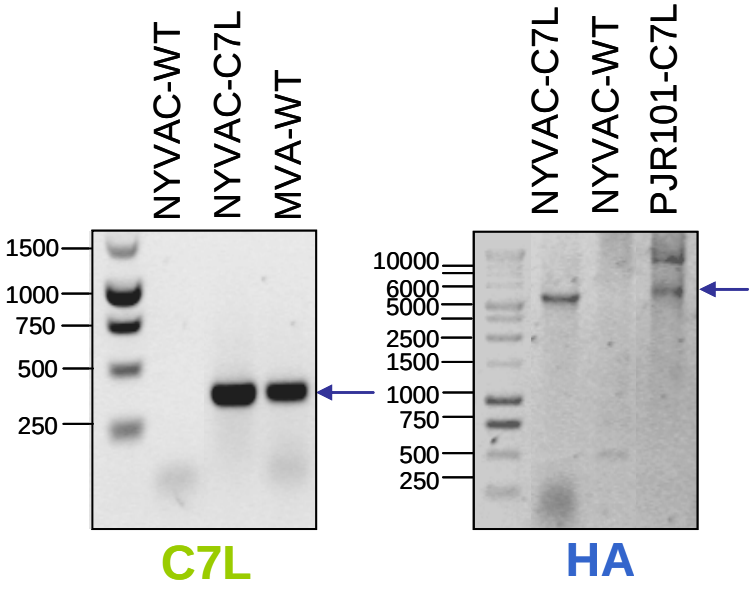

Figura 29: **Análisis por PCR del gen *C7L* y del locus de inserción en el recombinante NYVAC-C7L**. La presencia del gen *C7L* y la pureza del recombinante se analizaron por PCR utilizando oligonucleótidos específicos descritos en materiales y métodos.

4.1.6.2.- Efecto del gen *C7L* sobre la traducción y replicación viral

Una de las características descritas para el gen *C7L* es que su expresión es necesaria para la replicación del virus en células humanas (Perkus *y cols.*, 1990). Por ello, lo primero que quisimos comprobar era si la re-introducción del gen *C7L* en el genoma de NYVAC permitía al virus replicar en células HeLa. Como vemos en la figura 30, a diferencia de lo que ocurre en las células infectadas con NYVAC, en las células infectadas con NYVAC-C7L se obtuvieron altos títulos virales a lo largo del tiempo, lo que nos indica que el gen *C7L* se está expresando y es funcional.

Con anterioridad habíamos descrito que durante la infección por NYVAC en condiciones no permisivas, se inducen altos niveles de fosforilación del factor de iniciación de la traducción eIF2α que podrían asociarse con la inhibición en la síntesis de determinadas proteínas tardías implicadas en la morfogénesis viral. Por lo que quisimos analizar la fosforilación de este factor en células infectadas con NYVAC-C7L. Como vemos en la figura 30, la introducción del gen *C7L* en el genoma de NYVAC fue capaz de prevenir la fosforilación de eIF2α y consecuentemente, se rescató la expresión de las

proteínas tardías A17 y A27, lo que estaría relacionado con la capacidad del virus recombinante para producir partículas infecciosas en células humanas. Resultados similares fueron observados en otras líneas celulares no susceptibles a la infección por NYVAC como las células de origen murino 3T3 o las células humanas TK -143 (datos no mostrados).

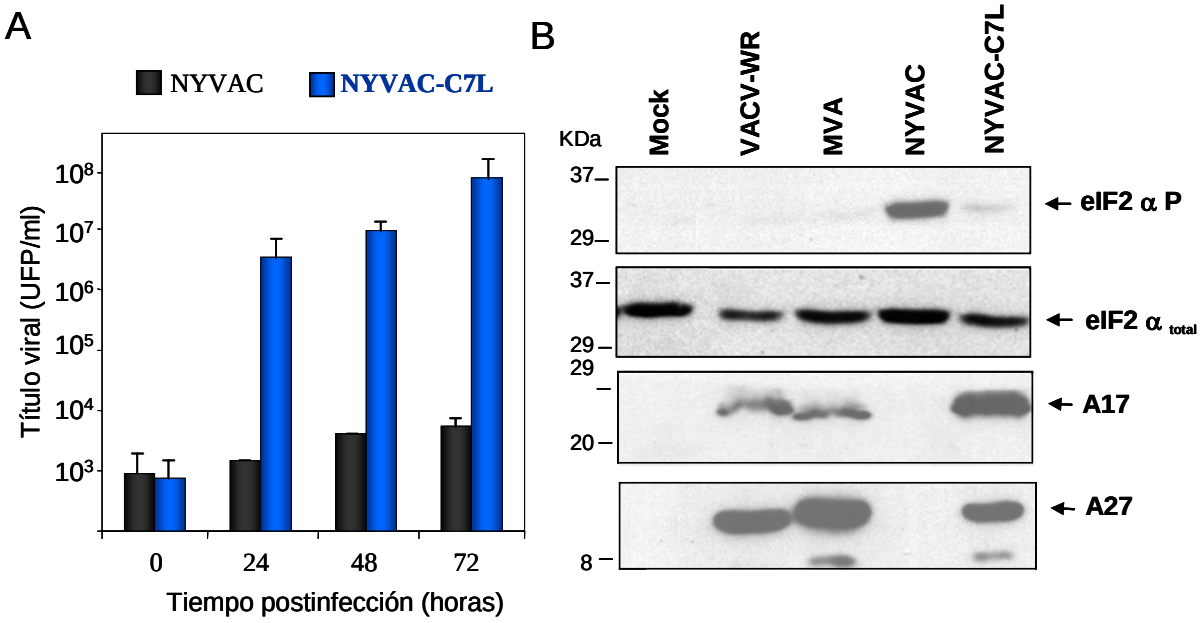

Figura 30: Efecto del gen *C7L* sobre la traducción y replicación viral. (A) Curva de crecimiento de NYVAC y NYVAC-C7L en células HeLa infectadas a una MOI de 0,01 UFP/célula. **(B)** Análisis por western blot de la fosforilación de eIF2α y de la expresión de las proteínas virales tardías A17 y A27 en células HeLa sin infectar (mock) o infectadas con WR, MVA, NYVAC o NYVAC-C7L a una MOI de 5 UFP/célula.

En líneas celulares permisivas a la infección por NYVAC como son las células BHK-21, la introducción del gen *C7L* aumentó la capacidad replicativa del virus, alcanzando títulos virales similares incluso superiores a los obtenidos tras la infección por MVA (Figura 31).

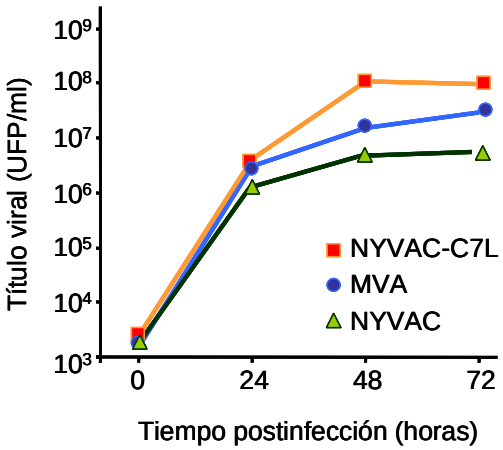

Figura 31: Curva de crecimiento de MVA, NYVAC y NYVAC-C7L en células BHK-21. Células BHK-21 fueron infectadas a una multiplicidad de infección de 0,01 UFP/célula con los virus MVA, NYVAC o el recombinante NYVAC-C7L. A distintos tiempos se cuantificó el número de partículas infecciosas asociadas a las células por inmunotinción.

Estos resultados, por lo tanto, nos sugieren que el gen *C7L* juega un importante papel en el control de la traducción y la replicación viral.

4.1.6.3 Efecto del gen C7L sobre la apoptosis durante la infección con NYVAC

Otra de las características que hemos atribuido con anterioridad a la infección por NYVAC en células HeLa es la inducción de apoptosis. Por lo que quisimos determinar el efecto del gen *C7L* en este proceso. Como puede observarse claramente en la figura 32 el fenotipo apoptótico observado en una gran parte de las células infectadas con NYVAC, estaba totalmente ausente en aquellas células infectadas con NYVAC-C7L.

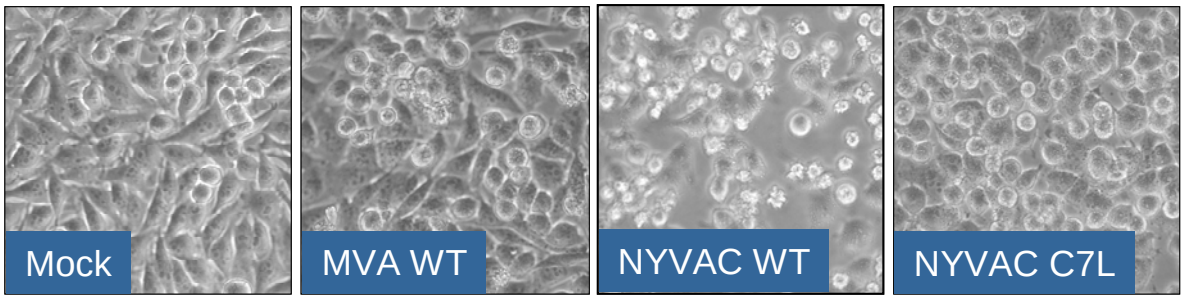

Figura 32: Efecto del gen *C7L* sobre la apoptosis inducida en células HeLa tras la infección por NYVAC. Efecto citopático de células HeLa infectadas con MVA, NYVAC o NYVAC-C7L a una multiplicidad de 5 UFP/célula a las 24 horas postinfección.

Por otro lado, observamos que la expresión de la proteína C7 era capaz de prevenir el procesamiento de PARP (Figura 33-A) lo que se correlaciona con un número significativamente menor de células apoptóticas (Figura 33-B).

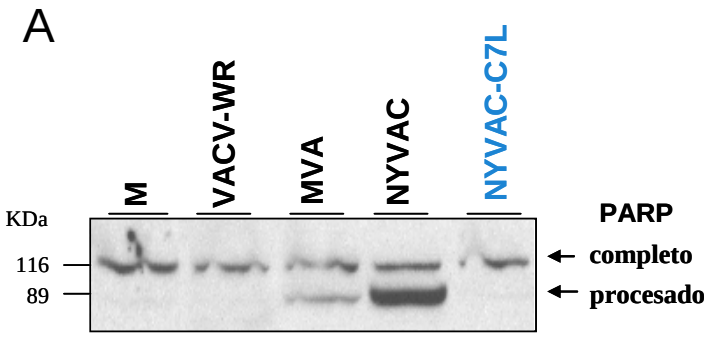

Figura 33-A: Efecto del gen *C7L* sobre la apoptosis inducida en células HeLa tras la infección por NYVAC.
(A) El procesamiento de la proteína celular PARP fue analizado en células HeLa infectadas con NYVAC o NYVAC-C7L a una multiplicidad de 5 UFP/célula por western-blot. Los extractos celulares se recogieron a los tiempos postinfección indicados (horas) y se resolvieron por SDS-PAGE y transferidas a una membrana de nitrocelulosa que fue incubada con un anticuerpo específico que reconoce la forma completa y procesada de PARP.

Figura 33-B: Efecto del gen *C7L* sobre la apoptosis inducida en células HeLa tras la infección por NYVAC.

(B) Cuantificación de la apoptosis por citometría de flujo. Monocapas de células HeLa fueron infectadas con 5 UFP/célula con NYVAC o NYVAC-C7L. Tras 24 horas de infección, las células fueron marcadas con ioduro de propidio para realizar un ensayo de ciclo celular. Como control negativo se utilizaron células sin infectar (Mock). Las barras representan el incremento en el número de células apoptóticas respecto del Mock.

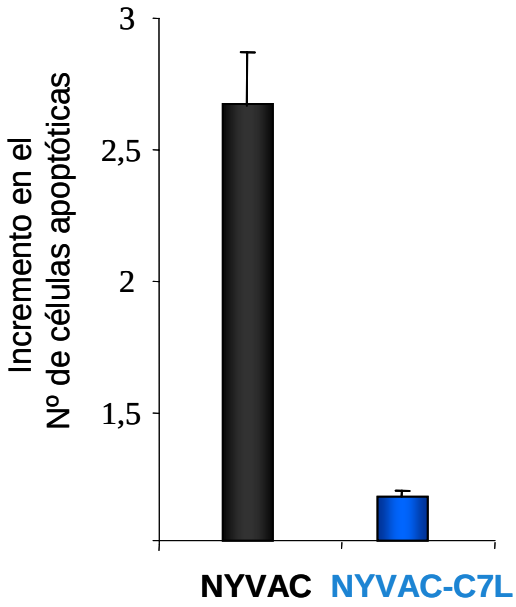

Finalmente, el patrón de degradación del ARN ribosomal que observábamos durante la infección con NYVAC no se detectó en las células infectadas con NYVAC-C7L (Figura 34).

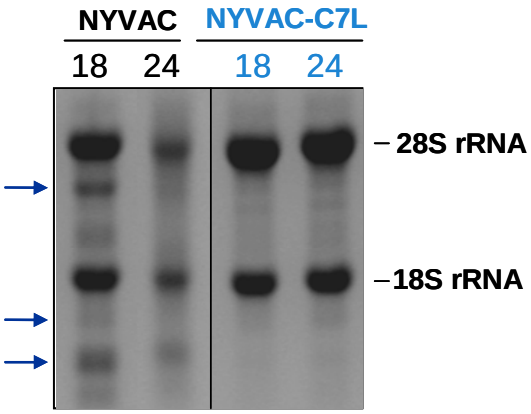

Figura 34: Degradación del ARN ribosomal en células HeLa tras la infección con NYVAC o NYVAC-C7L. El ARN total de células HeLa infectadas con NYVAC o NYVAC-C7L a 5 UFP/célula fue aislado a 18 y 24 hpi. 2 μg de ARN fueron fraccionados por electroforesis en geles de formaldehído-agarosa según se describe en materiales y métodos. Las flechas indican los productos de degradación de las subunidades 28S y 18S del ARN ribosómico.

Todos estos resultados nos indican que la proteína C7 tiene propiedades antiapoptóticas.

4.1.6.4 Comportamiento "*in vivo*" del recombinante NYVAC-C7L

Una vez confirmado que el recombinante NYVAC-C7L recupera la capacidad replicativa en células en cultivo de origen humano y murino. Nuestro siguiente objetivo fue comprobar si este virus era también capaz de replicar "*in vivo*". Para ello, inoculamos por ruta intraperitoneal ratones BALB/c con una dosis de 2×10^7 UFP/ratón de NYVAC o NYVAC-C7L. A distintos tiempos postinoculación (18, 24 y 48 horas) los animales fueron

sacrificados y se extrajeron distintos órganos en los que se cuantificó la cantidad de virus presente como un parámetro indicativo de la capacidad de replicación y diseminación viral.

Como vemos en la figura 35, no fuimos capaces de detectar partículas infecciosas en ningún órgano procedente de los animales inmunizados con NYVAC lo que se correlaciona con un aclaramiento total de la infección a los tiempos analizados. Sin embargo, tras la inoculación de NYVAC-C7L sí se detectó un incremento en el número de partículas infecciosas a lo largo del tiempo en ovarios e hígado, lo que nos indica que la introducción del gen *C7L* en el genoma de NYVAC incrementa también la eficiencia de replicación "*in vivo*". No obstante, hay que destacar que los títulos virales fueron menores a los obtenidos con la cepa competente en replicación VACV-WR.

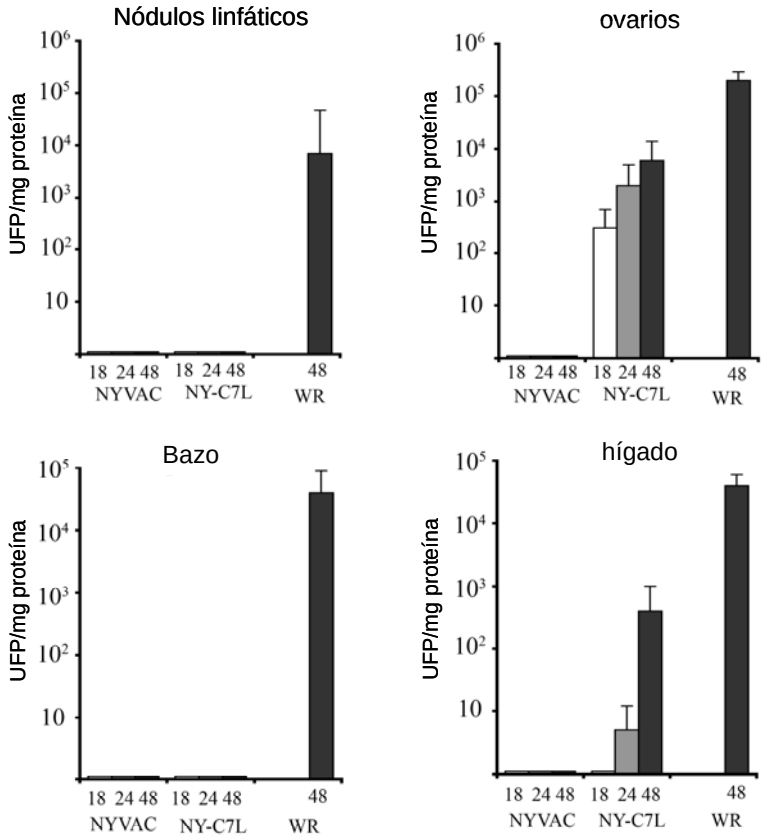

Figura 35: Replicación "*in vivo*" de NYVAC y NYVAC-C7L en diferentes tejidos de ratón. Ratones BALB/c fueron inoculados con una dosis de 2 x 10^7 PFU/ratón de NYVAC o NYVAC-C7L. A distintos tiempos postinoculación, se analizó el número de partículas infecciosas presentes en los distintos tejidos (nódulos linfáticos, ovarios, bazo e hígado). Como control positivo se utilizó la cepa competente en replicación VACV-WR. En las gráficas se muestran los valores obtenidos en cada tejido representados como el número de partículas infecciosas por mg de proteína junto con la desviación estándar.

Ante estos últimos resultados nos planteamos determinar qué efecto podría tener la inserción del gen *C7L* sobre la patogenicidad del virus en el modelo de ratón. Para ello, se inocularon ratones BALB/c por ruta intranasal con una dosis letal (10^6 UFP/ratón) del virus competente en replicación VACV-WR o con una dosis hasta 100 veces superior de NYVAC o NYVAC-C7L, realizándose un seguimiento diario del aspecto y la pérdida de peso de los ratones con el fin de determinar signos visibles de enfermedad.

Como se observa en la figura 36, todos los ratones inoculados con la cepa VACV-WR experimentaron una progresiva pérdida de peso y claros signos de enfermedad (dato no mostrado) a partir del cuarto día, teniendo que ser sacrificados a día 7 por razones éticas. Sin embargo, ninguno de los ratones vacunados con NYVAC o NYVAC-C7L presentaron ni pérdida de peso ni signos de enfermedad a lo largo del tiempo.

Este resultado nos sugiere que a pesar de su capacidad para replicar en el ratón, NYVAC-C7L mantiene el fenotipo atenuado "*in vivo",* lo que le convierte en un posible candidato a vector vacunal con mayor capacidad replicativa que el vector parental NYVAC.

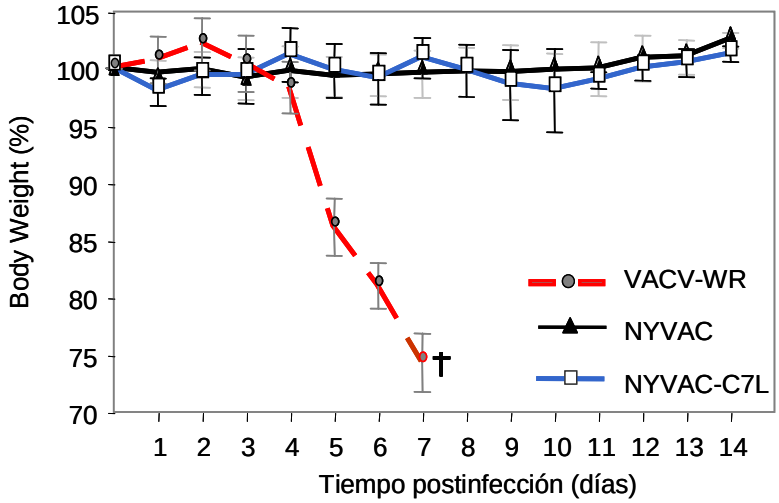

Figura 36: Patogenicidad de NYVAC-C7L en ratones BALB/c. Ratones BALB/c fueron inoculados por ruta intranasal con una dosis de 10^8 UFP/ratón de NYVAC o NYVAC-C7L o con una dosis de 10^6 UFP/ratón de WR. El peso de los ratones fue monitorizado diariamente representándose la media de la pérdida de peso obtenida en cada grupo.

En conjunto, todos estos resultados demuestran que el gen *C7L* posee propiedades antiapoptóticas y desempeña un papel importante en el control de la síntesis de proteínas virales ya que su reintroducción en el genoma de NYVAC recupera la capacidad para replicar tanto *"in vitro"* como *"in vivo"* sin afectar a la virulencia del vector. Debido a estas propiedades descritas para el gen *C7L*, se ha solicitado una patente.

4.2- ESTUDIO COMPARATIVO DEL COMPORTAMIENTO *"IN VIVO"* DE RECOMBINANTES BASADOS EN LAS CEPAS MVA Y NYVAC

Tanto MVA como NYVAC han demostrado ser vectores vacunales seguros y altamente inmunogénicos en ensayos preclínicos y clínicos. Sin embargo, poco se sabe todavía sobre su comportamiento diferencial "*in vivo*". Por esta razón, y teniendo en cuenta las diferencias observadas entre ambas cepas en células en cultivo, decidimos realizar un estudio comparativo de la distribución de MVA y NYVAC en el modelo murino empleando diferentes rutas de inoculación.

Para cumplimentar este objetivo hemos recurrido a la técnica de bioluminiscencia (BLI) que ofrece la posibilidad de estudiar procesos biológicos en organismos vivos. Esta técnica está basada en la detección de luz visible emitida tras la descarboxilación oxidativa de la luciferina, una reacción que es catalizada por la enzima luciferasa en presencia de ATP y oxígeno (Sadikoty Blackwell, 2005). Esta tecnología se ha aplicado en numerosos estudios para monitorizar la expresión de un determinado gen utilizado en terapia génica o para analizar el crecimiento tumoral y la producción de metástasis (Doyle *y cols.*, 2004; Edinger *y cols.*, 1999; Ray *y cols.*, 2004). Además, nos permite cuantificar en un mismo animal la progresión de la infección viral en el espacio y en el tiempo, identificando las variaciones en replicación y diseminación del virus (Hutchensy Luker, 2007).

En este estudio hemos utilizado poxvirus recombinantes basados en las cepas WR, MVA y NYVAC que expresan la proteína luciferasa como gen reportero. Los virus WRluc y MVAluc ya habían sido generados y caracterizados previamente en el laboratorio (Ramirez *y cols.*, 2000; Rodriguez *y cols.*, 1988) mientras que NYVACluc fue generado para la realización de este trabajo según se describe en materiales y métodos. El gen de la luciferasa en los tres virus se encuentra insertado en el locus de la timidina quinasa (TK) y su expresión está bajo el control transcripcional del promotor viral sintético temprano-tardío (pE/L).

4.2.1- Biodistribución de MVA y NYVAC por ruta sistémica

Para visualizar la diseminación "*in vivo*" de MVA y NYVAC por ruta sistémica, ratones BALB/c fueron inoculados con una dosis de 1 x 10^7 UFP/animal de los virus atenuados MVAluc o NYVACluc o con una dosis 10 veces inferior del virus competente en replicación (WRluc) por las siguientes rutas: Intraperitoneal (i.p.), intramuscular (i.m.)

y mediante escarificación en la base de la cola (e.c.). La medida de bioluminiscencia se analizó diariamente según se describe en materiales y métodos y la progresión de la infección se monitorizó hasta la desaparición de la señal. La distribución y la intensidad relativa de la emisión de luz se utilizaron para determinar los sitios de infección y cuantificar las cantidades relativas del gen reportero (ya que la luciferasa sólo se detectará si hay expresión de genes virales). De esta forma, se obtuvieron imágenes seriadas de los animales y se determinó la media del flujo de fotones correspondiente al pico de la señal. En los animales sin infectar, utilizados como control negativo, la señal de bioluminiscencia se mantuvo por debajo de los niveles basales. Además, también se cuantificaron los incrementos relativos en la cantidad de bioluminiscencia en la región de interés producidos en respuesta a la infección por las distintas cepas del virus vaccinia.

4.2.1.1. Ruta intraperitoneal

En aquellos animales inoculados por ruta intraperitoneal con MVAluc o NYVACluc, la emisión de luz se restringió a la región abdominal (Figura 37-A), demostrando que la diseminación de estos virus va más allá del sitio de inoculación. Esta diseminación fue más evidente en aquellos animales inoculados con WRluc, donde el virus se propagó extensivamente por todo el ratón y la expresión de luciferasa se mantuvo por un tiempo superior a los 4 días. Los mayores niveles de expresión de luciferasa en los animales que recibieron los virus atenuados se detectaron un día después de su inoculación. Sin embargo, mientras que en los animales inmunizados con MVAluc la señal disminuyó drásticamente a día 2 y no se detectó actividad luciferasa a tiempos posteriores, en los animales infectados con NYVACluc la señal se mantuvo a niveles detectables hasta día 3.

Estos resultados fueron confirmados cuantificando el flujo de fotones en la región de interés (Figura 37-B). Para WRluc los niveles de luciferasa se incrementaron en 5 logaritmos respecto al mock en los distintos tiempos ensayados mientras que para NYVACluc o MVAluc, los niveles se incrementaron 74 y 16 veces, respectivamente a día 1 y 15 y 2,5 veces, respectivamente a día 2.

Figura 3.27-A: Distribución de WRluc, MVAluc y NYVACluc en ratones inoculados por ruta intraperitoneal. (A) Localización de la señal de luciferasa en ratones BALB/c inoculados por ruta intraperitoneal con WRluc, MVAluc o NYVACluc a distintos tiempos postinfección. En la esquina superior derecha se muestra la señal procedente de los ratones inoculados con PBS (CTRL) **(B)** Cuantificación de la emisión de fotones a lo largo del tiempo en la región de interés (RI) tras la inoculación por ruta intraperitoneal con WRluc, MVAluc o NYVACluc. En la gráfica se representan

los valores obtenidos a lo largo del tiempo (días) junto con la desviación estándar. La línea horizontal representa el nivel basal de luminiscencia.

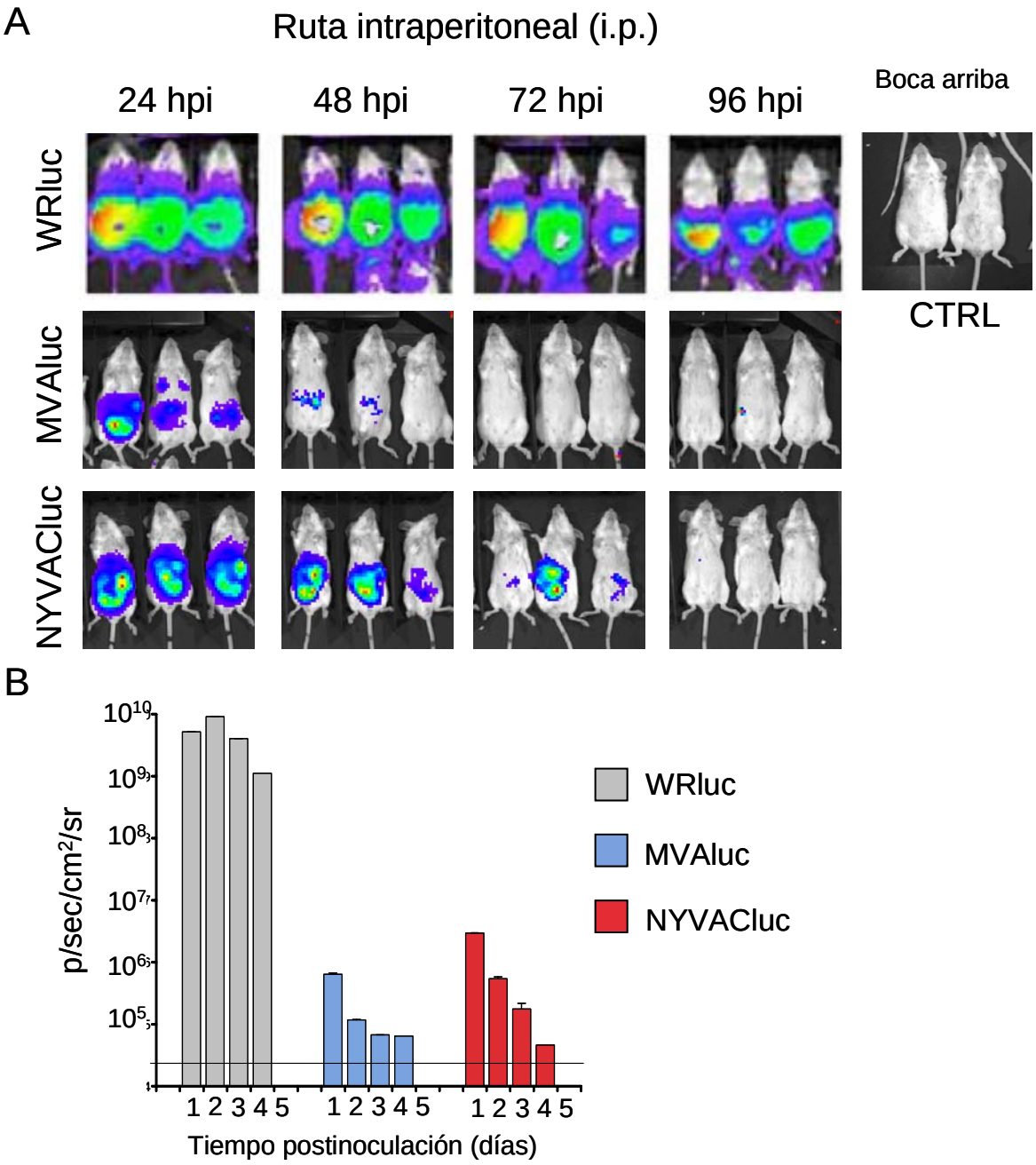

4.2.1.2. Ruta intramuscular

Para la inmunización de candidatos vacunales basados en poxvirus y ADN desnudo en ensayos clínicos, la ruta utilizada por excelencia es la intramuscular (i.m.) ya que por esta ruta se minimizan las reacciones secundarias asociadas a la inyección. Por esta razón es una vía de elección frente a otras como la ruta subcutánea o intradérmica.

Cuando inoculamos los animales intramuscularmente con los diferentes virus observamos que la señal de luciferasa se restringe principalmente al sitio de inoculación

(Figura 38-A). La cuantificación de la emisión de fotones de luz en la región de interés muestra que los niveles de luciferasa en el sitio de inoculación disminuyeron a lo largo del tiempo con los vectores MVAluc y NYVACluc al contrario de lo que ocurría en los animales inmunizados con WRluc en los que se mantenía a lo largo del tiempo (Figura 38-B). Además, mientras que a día 1 las dos cepas atenuadas indujeron niveles similares de luciferasa, a día 2 se observaron diferencias entre ambos vectores. NYVACluc indujo valores 100 veces superiores al valor basal detectado en los ratones inoculados con PBS, mientras que con MVAluc los niveles sólo aumentaron 4 veces.

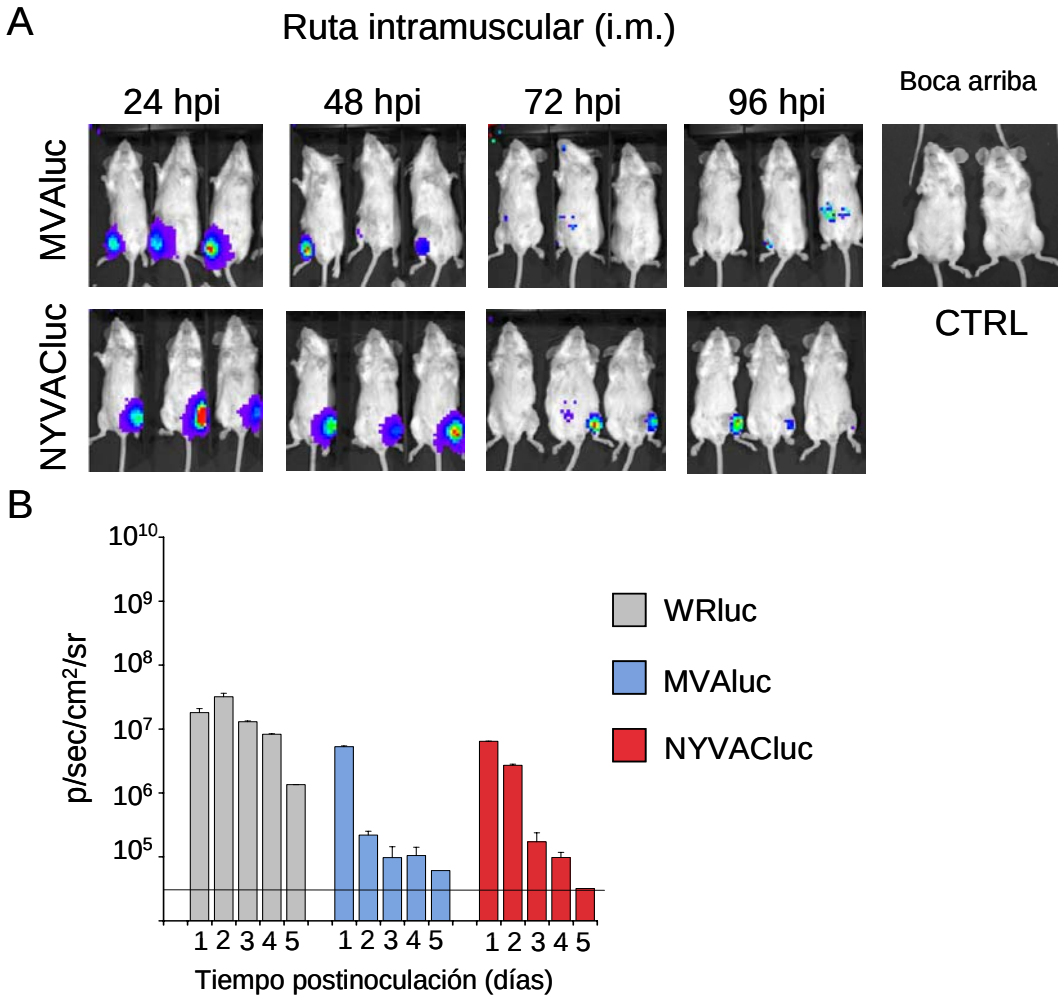

Figura 38: Distribución de MVAluc y NYVACluc en ratones inoculados por ruta intramuscular. (A) Localización de la señal de luciferasa en ratones BALB/c inoculados por ruta intramuscular con MVAluc o NYVACluc a distintos tiempos postinfección. En la esquina superior derecha se muestra la señal procedente de los ratones inoculados con PBS (CTRL) **(B)** Cuantificación de la emisión de fotones a lo largo del tiempo en la región de interés (RI) tras la inoculación por ruta intramuscular con WRluc, MVAluc o NYVACluc. En la gráfica se representan los valores obtenidos a lo largo del tiempo (días) junto con la desviación estándar. La línea horizontal representa el nivel basal de luminiscencia.

4.2.1.3. Ruta de escarificación en la base de la cola

La ruta de escarificación fue una de las vías más utilizadas para la vacunación frente a viruela durante la campaña de erradicación. Por esta ruta, la expresión de luciferasa en los animales inoculados con los recombinantes atenuados fue muy baja y restringida al sitio de inoculación. Por el contrario, en los animales que recibieron WRluc, la señal incrementó gradualmente durante la infección extendiéndose por todo el animal, un claro indicador de la diseminación del virus (Figura 39-A). En la figura 39-B podemos ver la cuantificación de la emisión de fotones a través de dicha ruta. En aquellos animales animales inoculados con WRluc los valores aumentaron en más de 5 logaritmos los niveles basales obtenidos en los ratones inoculados con PBS. Por el contrario, sólo en los ratones inoculados con NYVACluc se obtuvieron valores por encima del control aunque estos no fueron significativamente superiores a los obtenidos con MVAluc.

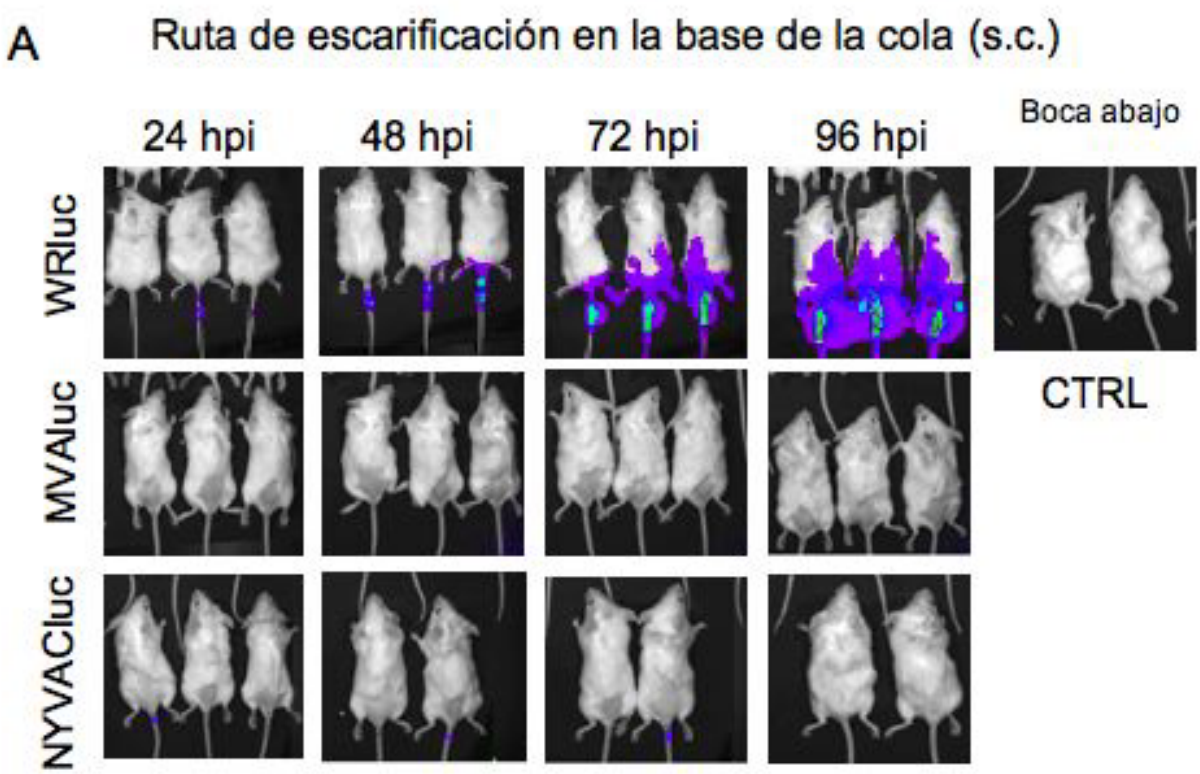

Figura 39-A: Distribución de WRluc, MVAluc y NYVACluc en ratones inoculados por escarificación en la base de la cola.

A) Localización de la señal de luciferasa en ratones BALB/c inoculados mediante escarificación en la base de la cola con WRluc, MVAluc o NYVACluc a distintos tiempos postinfección. En la esquina superior derecha se muestra la señal procedente de los ratones inoculados con PBS (CTRL)

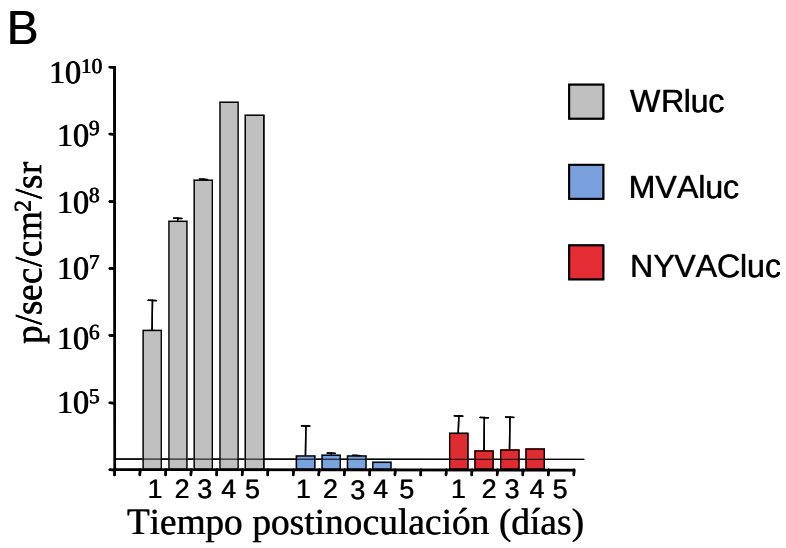

Figura 39-B: Distribución de WRluc, MVAluc y NYVACluc en ratones inoculados mediante escarificación en la base de la cola. **(B)** Cuantificación de la emisión de fotones a lo largo del tiempo en la región de interés (RI) tras la inoculación por escarificación en la base de la cola con WRluc, MVAluc o NYVACluc. En la gráfica se representan los valores obtenidos a lo largo del tiempo (días) junto con la desviación estándar. La línea horizontal representa el nivel basal de luminiscencia.

Los resultados anteriores nos indican que existen diferencias en los niveles de emisión de luciferasa a partir de las 24 horas postinfección entre MVAluc y NYVACluc. Sin embargo, nos propusimos definir la cinética de expresión de luciferasa a tiempos más tempranos. Para ello, cuantificamos la actividad enzimática en extractos de tejidos de ratones inoculados por ruta intraperitoneal, ya que fue la ruta más efectiva en cuanto a la diseminación de los virus atenuados. Diferentes grupos de animales fueron inoculados con una dosis de 1 x 10^7 UFP por ratón de los tres virus recombinantes. A distintos tiempos postinoculación (4, 6, 18, 24 y 48 hpi) se recogieron las células del peritoneo, el bazo, los ganglios y los ovarios de los ratones inmunizados tal y como se describe en materiales y métodos. Los tejidos de cada ratón fueron homogeneizados y se midió la actividad luciferasa, expresada como unidades relativas de luciferasa (URL) por mg de proteína.

Como muestra la figura 40, los niveles de luciferasa en los extractos celulares del peritoneo, de los ovarios y los nódulos linfáticos de los animales inoculados con MVAluc fueron entre 5 y 10 veces mayores respecto a los detectados en los tejidos de los ratones inmunizados con NYVACluc a las 4 horas postinfección; sin embargo, en el bazo, los niveles fueron similares. Estos niveles fueron comparables a las 6 horas, y disminuyeron a lo largo del tiempo, alcanzando los niveles basales a las 48 horas. Por el contrario, a este tiempo, los niveles de luciferasa en los tejidos de ratones inoculados con WRluc fueron entre 2 y 4 logaritmos mayores que en aquellos que recibieron MVAluc o NYVACluc. Estos resultados coinciden con los descritos previamente (Ramirez *y cols.*,

2000) e indican una mayor eficiencia de expresión génica "*in vivo*" de MVA respecto a NYVAC a tiempos tempranos.

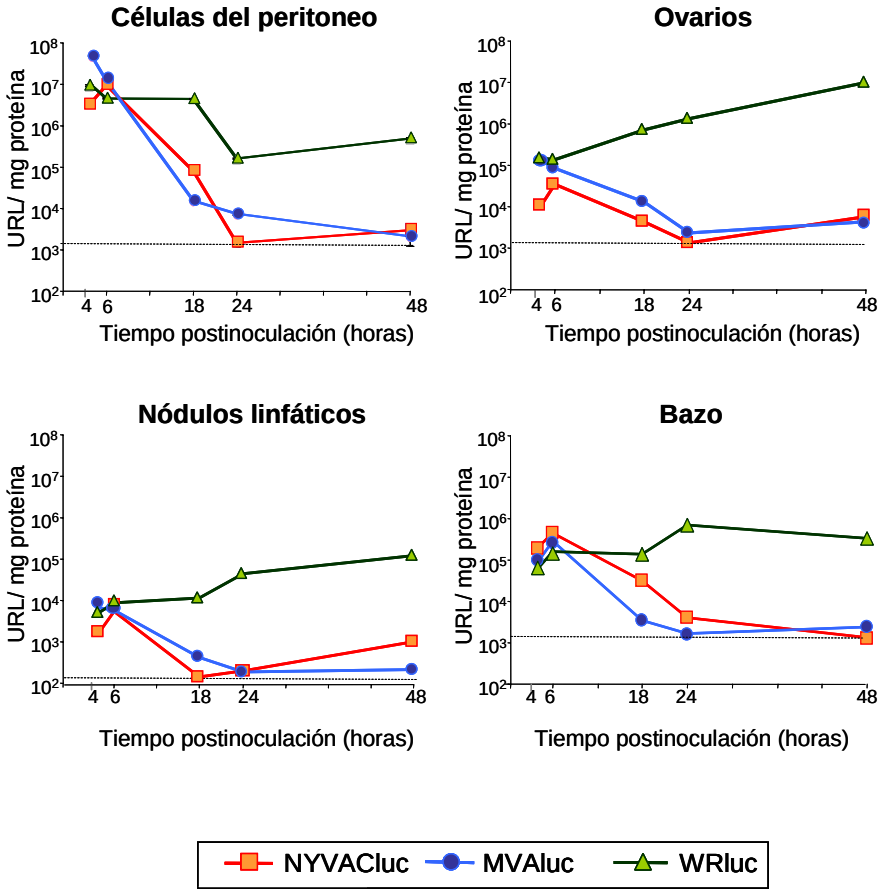

Figura 40: Determinación de los niveles de luciferasa a lo largo del tiempo en distintos tejidos de animales inoculados con WRluc, MVAluc o NYVACluc por ruta intraperitoneal. En las gráficas se muestran los valores obtenidos junto con las desviaciones estándar. La región sombreada representa los valores de actividad luciferasa en los tejidos de animales inoculados con PBS.

Para confirmar que la ausencia de bioluminiscencia a tiempos tardíos se debía a un aclaramiento del virus, cuantificamos los títulos virales a las 24 y 48 horas postinfección en los distintos órganos de los animales inmunizados. Al contrario de lo que ocurre durante la infección con WRluc, no se encontraron partículas infecciosas en las muestras procedentes de los ratones inmunizados con MVAluc o NYVACluc (datos no mostrados).

4.2.2- Biodistribución de MVA y NYVAC por ruta de mucosas

A continuación, analizamos el patrón de expresión de luciferasa en ratones BALB/c inoculados con los distintos recombinantes por las siguientes rutas de mucosas: intrarrectal (i.r.) e intranasal (i.n.). Por ruta intrarrectal apenas se detectó señal de

bioluminiscencia tras la inoculación de las cepas atenuadas MVAluc y NYVACluc a los tiempos estudiados (datos no mostrados).

4.2.2.1 Ruta intranasal

Por ruta intranasal la expresión de luciferasa en los animales inmunizados con MVAluc o NYVACluc fue transitoria y restringida a los pulmones, mientras que en los ratones inoculados con WRluc la bioluminiscencia se detectó en la nariz y pecho de los animales y se incrementó con el tiempo. Esto sugiere una distribución del virus dentro del tracto respiratorio que afecta a tráquea y pulmones y que su diseminación llega incluso hasta cerebro. A ninguno de los tiempos analizados no se detectó diseminación del virus hacia órganos sistémicos (Figura 41-A). La cuantificación del flujo de fotones en la región de interés reveló que la expresión de luciferasa por los dos vectores atenuados fue baja y más duradera en los animales inoculados con NYVACluc respecto a los inoculados con MVAluc (figura 41-B).

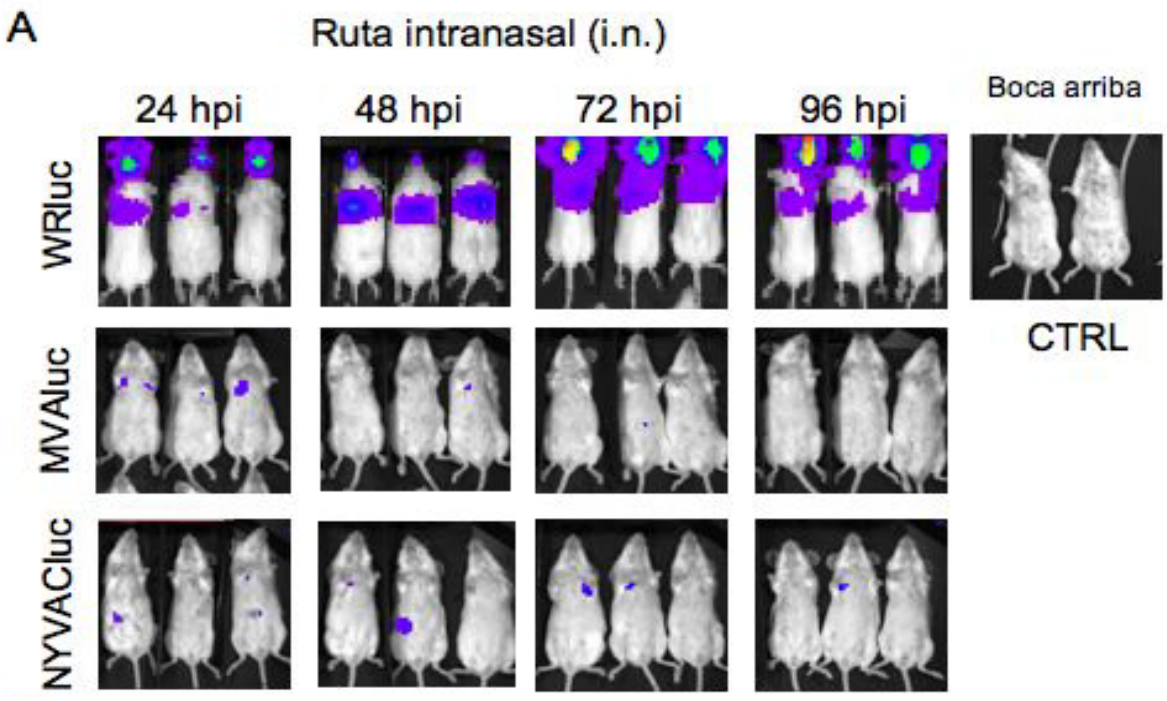

Figura 41-A: Distribución de WRluc, MVAluc y NYVACluc en ratones inoculados por ruta intranasal.

(A) Localización de la señal de luciferasa en ratones BALB/c inoculados por ruta intranasal con WRluc, MVAluc o NYVACluc a distintos tiempos postinfección. En la esquina superior derecha se muestra la señal procedente de los ratones inoculados con PBS (CTRL) representa el nivel basal de luminiscencia.

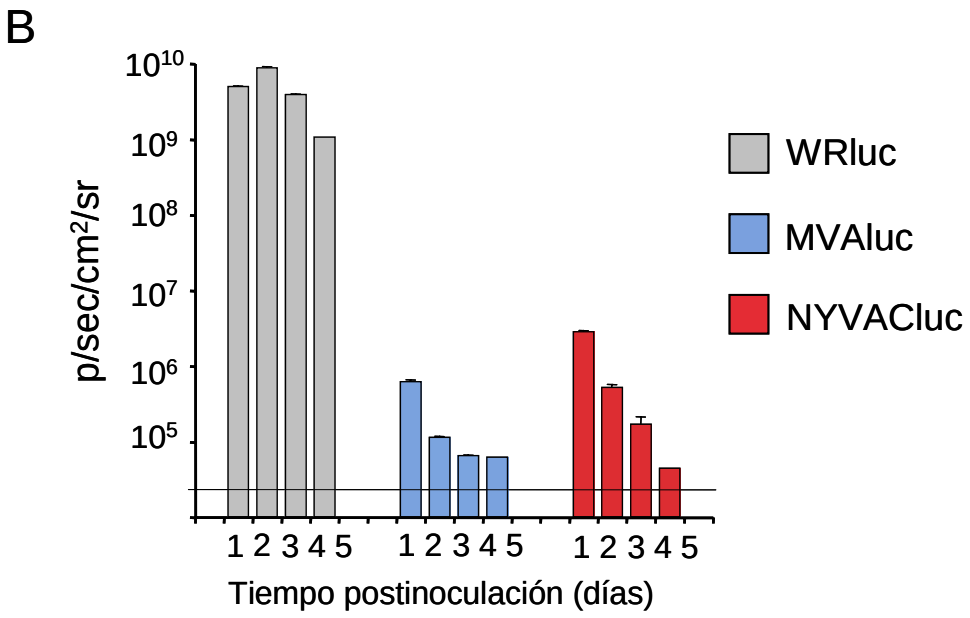

Figura 41-B: Distribución de WRluc, MVAluc y NYVACluc en ratones inoculados por ruta intranasal.

(B) Cuantificación de la emisión de fotones a lo largo del tiempo en la región de interés (RI) tras la inoculación por ruta intranasal con WRluc, MVAluc o NYVACluc. En la gráfica se representan los valores obtenidos a lo largo del tiempo (días) junto con la desviación estándar. La línea horizontal representa el nivel basal de bioluminiscencia.

Todos estos resultados nos indican que existen diferencias en el comportamiento "*in vivo*" entre las cepas MVA y NYVAC y que dichas diferencias afectan tanto a los niveles de expresión del gen reportero como a su permanencia dentro del animal. En la mayoría de las rutas analizadas, en los ratones inoculados con MVAluc la expresión de luciferasa se limita a las 24 primeras horas mientras que con NYVAC la señal permanece hasta las 72 horas postinoculación. Estos resultados podrían tener una gran relevancia cuando estos vectores se utilicen como vacunas recombinantes.

3.3- CARACTERIZACIÓN DE LA INMUNOGENICIDAD INDUCIDA POR RECOMBINANTES BASADOS EN LAS CEPAS ATENUADAS MVA Y NYVAC QUE EXPRESAN ANTÍGENOS DE VIH-1 EN EL MODELO MURINO.

Como hemos descrito anteriormente, la principal aplicación de las cepas MVA y NYVAC es su utilización como vectores vacunales. En este sentido, nuestro laboratorio participa en un proyecto europeo denominado Eurovac (European Vaccine Effort Against HIV/AIDS) cuyo objetivo principal es desarrollar y analizar la seguridad y eficacia de varios candidatos vacunales frente a VIH-1 basados en cepas atenuadas de poxvirus (www.eurovacc.org). Este proyecto se basa en las propiedades que presentan los poxvirus como candidatos vacunales y más específicamente las cepas atenuadas MVA y NYVAC.

En el laboratorio se han generado dos virus recombinantes derivados de la cepa MVA. Uno de ellos, al que se denominó MVA-B, expresa 4 genes de VIH-1 (env, gag, pol y nef) procedentes de dos aislados europeos, Bx08 y IIIB (subtipo B). El otro, denominado MVA-C, contiene los mismos 4 antígenos pero procedentes del aislado asiático CN54 (subtipo C). Estos dos vectores son homólogos a los generados por la empresa Sanofi-Aventis sobre la cepa NYVAC y que han sido referidos como NYVAC-B y NYVAC-C.

Todos los virus recombinantes tienen insertados dentro de un mismo locus viral (timidina quinasa, TK) los genes de VIH-1 que codifican para la proteína gp120 y para la poliproteína de fusión Gag-Pol-Nef. Ambos antígenos se encuentran bajo el control transcripcional del promotor viral sintético temprano-tardío pE/L y han sido optimizados con el objetivo de eliminar regiones antigénicas no deseadas, así como para mejorar su expresión en células humanas. Por razones de seguridad y con el fin de ensayar estos vectores en fase clínica, los recombinantes se han generado de tal forma que el marcador de selección se pierde después de los primeros pases de purificación, mediante un proceso de recombinación homóloga entre el flanco izquierdo del gen viral TK y una repetición del mismo.

La expresión y estabilidad del inserto y la pureza de los diferentes virus recombinantes han sido analizadas en varios experimentos llevados a cabo en células en cultivo, verificándose que los cuatro vectores (MVA-B, NYVAC-B, MVA-C y NYVAC-C) son genéticamente estables y expresan correctamente los cuatro antígenos del VIH-1, la gp120 como un producto que se libera al sobrenadante y Gag-Pol-Nef (GPN) como

una poliproteína intracelular. Además, también hemos demostrado que todos ellos mantienen las características propias de la cepa parental a partir de la cual fueron generados y que han sido descritas en apartados anteriores (Gomez *y cols.*, 2007a; Gomez *y cols.*, 2007b; Nájera *y cols.*, 2006) ver anexo).

Para facilitar la lectura de este trabajo, sólo se mostrarán algunos de los resultados obtenidos con los recombinantes MVA-B y NYVAC-B. El resto de los datos, incluidos aquellos correspondientes a los recombinantes del subtipo C, pueden ser consultados en el anexo 1 (Gómez y cols., 2007a, 2007b).

Una vez generados los recombinantes, nos propusimos comparar la respuesta inmunológica inducida por estos nuevos candidatos vacunales tras su inoculación en animales.

4.3.1- Caracterización de la inmunogenicidad de MVA-B y NYVAC-B en ratones BALB/c

Como se ha explicado en la introducción, trabajos previos, entre los que se encuentran algunos de nuestro laboratorio, indican que el protocolo de inmunización denominado "prime-boost" es una de las estrategias más efectivas para inducir una potente respuesta inmune frente a antígenos de VIH (Amara *y cols.*, 2001; del Real *y cols.*, 1998; Gherardi *y cols.*, 2003; Hanke *y cols.*, 1998; Kenty Lewis, 1998). Este protocolo consiste en una primera inmunización con ADN recombinante ("priming"), seguido de una segunda inoculación con una dosis de un poxvirus recombinante que expresa el mismo antígeno ("booster").

En primer lugar, diseñamos un experimento para comparar la respuesta inmune generada en ratones inoculados con ADN-B, seguido de una segunda dosis con MVA-B o NYVAC-B, respecto a otro grupo de animales que recibieron dos dosis del vector de ADN. Para ello, grupos de ratones BALB/c fueron inmunizados con 100 μg de ADN-B por vía intramuscular (i.m.). Dos semanas más tarde los animales recibieron una segunda inyección con la misma dosis de ADN-B por ruta i.m. o con una dosis de 2×10^7 UFP/ratón de MVA-B o NYVAC-B por vía intraperitoneal (i.p.). Como controles se utilizaron grupos de ratones inmunizados con el mismo protocolo pero utilizando los vectores parentales, que no expresan los antígenos de VIH (ADN-ϕ , MVA-WT o NYVAC-WT). Diez días después de la última inmunización, se determinó el número de células secretoras de IFN-γ en los cultivos de esplenocitos mediante el ensayo de ELISPOT empleando mezclas ("pooles") de péptidos solapantes que cubren todas las regiones antigénicas de las proteínas de VIH-1 expresadas desde los distintos vectores. Para simplificar utilizaremos el nombre inglés "pool" para referirnos a la mezcla de péptidos. El

número de spots obtenidos frente al pool de péptidos control (CTRL) se sustrajo en todos los casos.

Como se observa en la figura 42 los animales que recibieron MVA-B o NYVAC-B en la segunda inmunización (grupos 1 y 2) desarrollaron una mayor respuesta inmune celular frente a los antígenos de VIH que el grupo que recibió dos dosis de ADN-B (grupo 3) o los grupos control (grupos 4 y 5). La magnitud total de la respuesta frente a VIH respecto del grupo ADN-B/ADN-B, fue casi 10 veces superior en el grupo ADN-B/NYVAC-B y más de 5 veces en los animales inmunizados con ADN-B/MVA-B, lo que demuestra la eficacia de los poxvirus como potenciadores de la respuesta primaria.

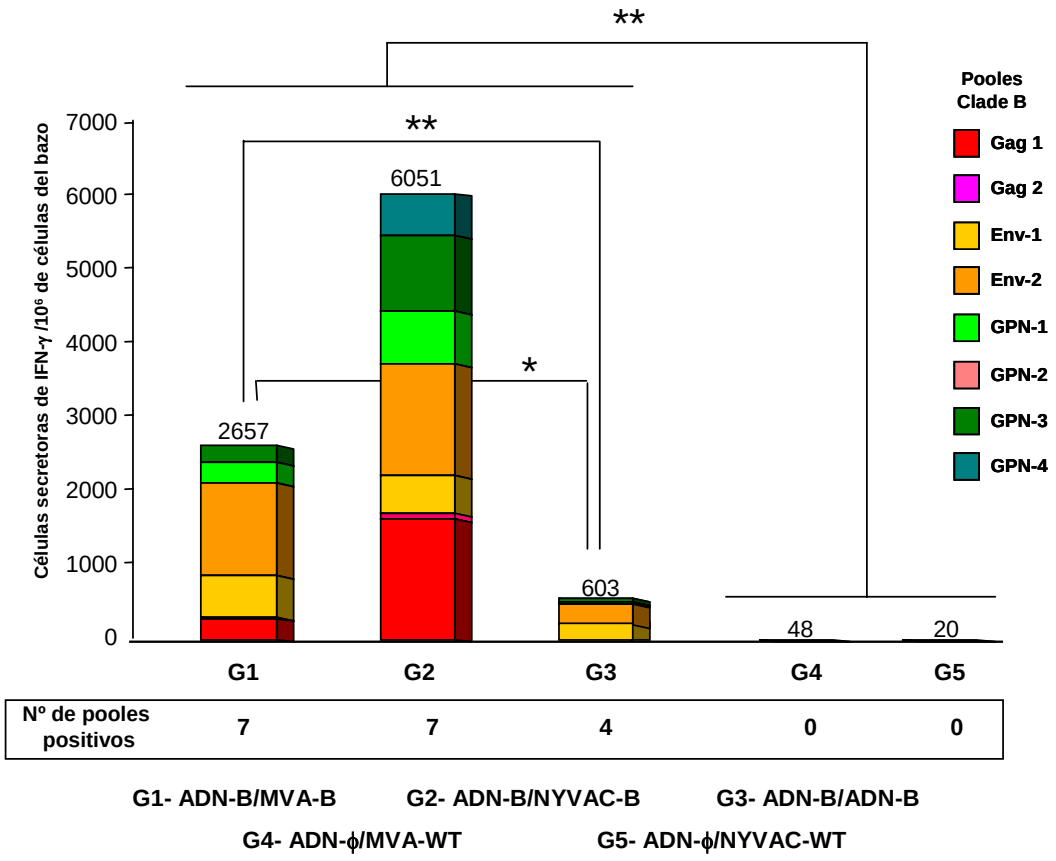

Figura 42: Inmunogenicidad de MVA-B y NYVAC-B después del protocolo de inmunización de prime-boost (ADN/Pox) en ratones BALB/c. La respuesta inmune celular específica frente a los antígenos de VIH en los animales inmunizados se determinó mediante la técnica de ELISPOT según se describe en materiales y métodos. En la figura se muestra el número de células secretoras de IFN-γ específicas frente a todos los antígenos de VIH-1 incluidos en los vectores así como la respuesta específica para cada péptido y el número de pooles positivos respecto al péptido control dentro de cada grupo. En la parte superior de cada barra se muestra la magnitud total de la respuesta anti-VIH. * representa diferencias significativas entre los diferentes grupos (*p<0,05; **p<0.005).

Si analizamos en detalle la respuesta específica frente a cada mezcla de péptidos, podemos observar que los pooles de péptidos Gag-1, Env-1, Env-2, GPN-1, GPN-3 y GPN-4 fueron los más inmunogénicos. Por el contrario, el pool Gag-2 apenas fue reconocido, y el pool GPN-2 no estimuló una respuesta celular específica. Estos resultados nos indican una gran dispersión de la respuesta hacia todos los antígenos de VIH-1 en los animales inmunizados con los poxvirus recombinantes. Si definimos la amplitud de la respuesta antígeno-específica como el número de pooles de péptidos positivos para cada grupo, observamos que en los grupos que recibieron una segunda dosis de MVA-B o NYVAC-B (grupos 1 y 2) la amplitud de la respuesta es idéntica (7 pooles positivos). Sin embargo, en el grupo de animales que recibió dos dosis de ADN-B (grupo 3) sólo fueron reconocidos 4 de los 8 pooles.

Debido a que la proteína gp120 expresada por nuestros vectores se secreta al medio extracelular, quisimos analizar la respuesta humoral anti-gp120 generada en los diferentes grupos de animales inmunizados mediante ELISA. Como puede observarse en la figura 43, sólo los animales que recibieron una segunda dosis de MVA-B o NYVAC-B (grupos 1 y 2) fueron capaces de producir anticuerpos específicos frente a la proteína gp160 del aislado LAV del subtipo B del VIH-1.Con estos resultados, por lo tanto, podemos concluir que MVA-B y NYVAC-B, además de generar una potente respuesta inmune celular, son capaces de producir una respuesta de anticuerpos específicos frente al antígeno de la envuelta del VIH.

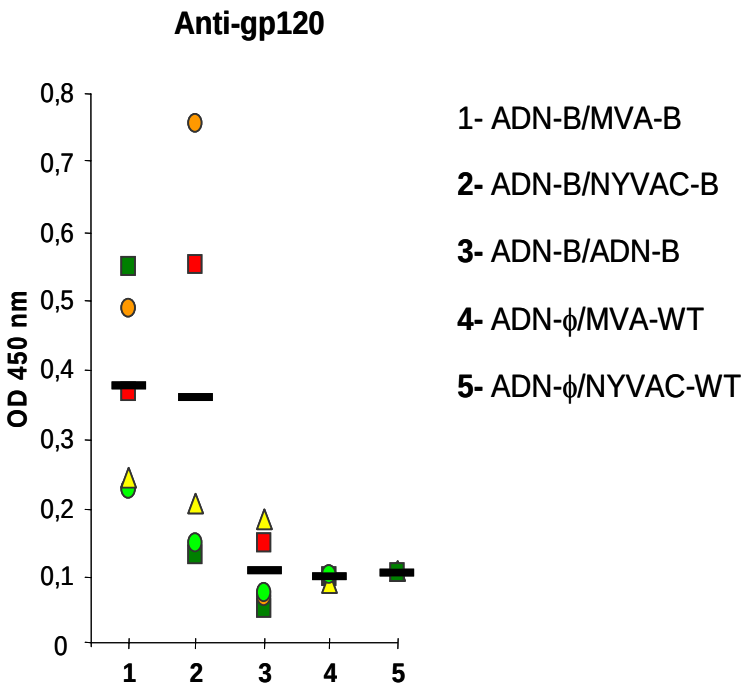

Figura 43: Respuesta humoral frente a la envuelta de VIH-1. Los niveles específicos de IgG total frente a la proteína gp160 de VIH (LAV) presentes en los sueros de los ratones inmunizados se determinaron mediante ELISA como se describe en materiales y métodos. Cada símbolo corresponde a los valores de absorbancia (medidos a 450 nm) de una dilucción 1:50 de los sueros individualizados. La barra (-) representa la media de los valores obtenidos en cada grupo.

4.3.2- Caracterización de la inmunogenicidad de MVA-B y NYVAC-B en ratones humanizados HHD.

Como hemos descrito anteriormente, los antígenos env, gag, pol y nef, incluidos en nuestros vectores (plasmídicos y virales), han sido optimizados en sus codones para mejorar la presentación por moléculas de HLA de clase I humanas. Por esta razón, decidimos analizar la respuesta inmunológica que inducen los recombinantes MVA-B y NYVAC-B en ratones transgénicos HHD, que solamente disponen de la quimera humana HLA-A2.1 como molécula de histocompatibilidad de clase I (Pascolo y cols., 1997).

De este modo, tres grupos de ratones HHD fueron inmunizados con 100 μg de ADN-B o ADN-ϕ por ruta intramuscular. Dos semanas más tarde los animales recibieron una segunda inmunización con una dosis de 2 x 10^7 UFP/ratón de MVA-B, NYVAC-B o MVA-WT por ruta intraperitoneal. La respuesta inmune celular antígeno-específica se determinó 10 días después de la última inmunización mediante el ensayo de ELISPOT empleando los pooles de péptidos de VIH del subtipo B. El número de spots obtenidos frente al grupo de péptidos control (CTRL) se sustrajo en todos los casos.

Como muestra la figura 44, los animales que recibieron MVA-B o NYVAC-B en la segunda inmunización desarrollaron una respuesta inmune específica frente a los antígenos de VIH-1 en comparación con el grupo control (ADN-ϕ/MVA-WT) siendo la magnitud total y la amplitud de la respuesta similar en ambos grupos. Curiosamente, en este modelo de ratón se observó una inmunodominancia hacia los pooles que cubren la envuelta de VIH-1, siendo Env-1 y Env-2 más inmunogénicos que Gag1, Gag2 o GPN-1 ($p<0.05$). Sin embargo, los pooles GPN-2, GPN-3 y GPN-4 no fueron capaces de estimular una respuesta específica en ninguno de los dos grupos.

En numerosos trabajos se ha descrito que la utilización de poxvirus recombinantes frente a diferentes patógenos induce mayoritariamente una polarización de la respuesta hacia un subtipo Th1 (Gherardi *y cols.*, 2003; Gomez *y cols.*, 2001; Perez-Jimenez *y cols.*, 2006). Debido a que el balance Th1-Th2 de la respuesta inmune puede ser crítico a la hora de controlar la infección por VIH decidimos determinar el perfil de citoquinas secretadas en los animales inmunizados. Para ello, estimulamos *"in vitro"* los esplenocitos de los animales inoculados con los distintos pooles de péptidos de los antígenos de VIH del subtipo B. Tres días después de esta estimulación, recogimos los sobrenadantes del cultivo y cuantificamos los niveles de IFN-γ (Th1) e IL-10 (Th2) secretados mediante ELISA.

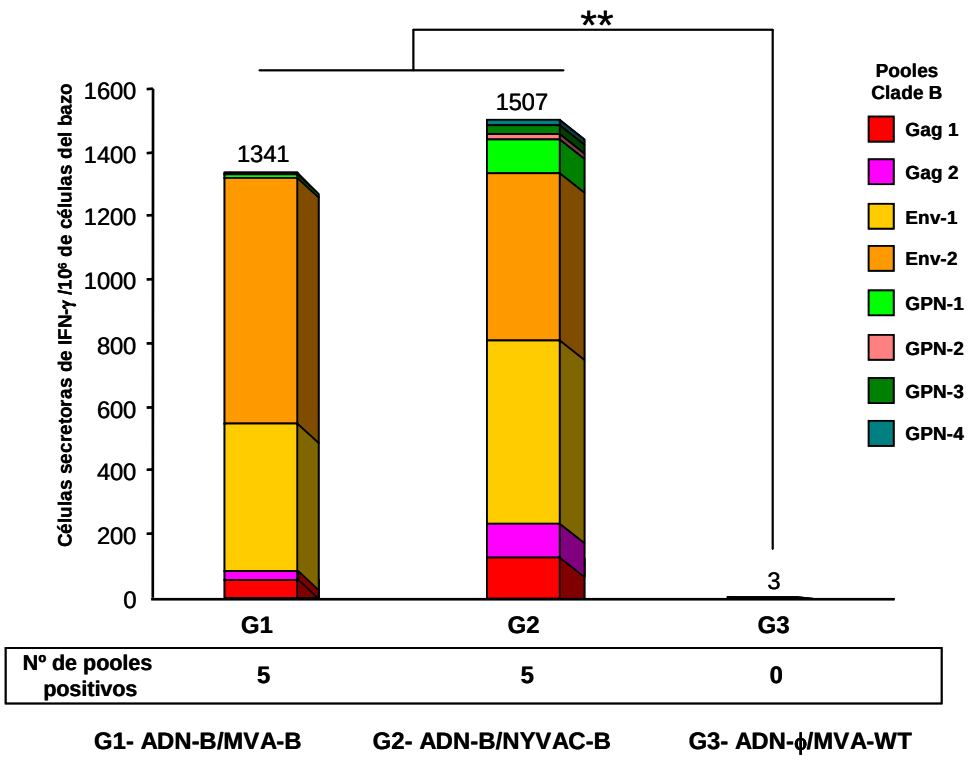

Figura 44: Respuesta inmune específica de células T productoras de IFN-γ frente a pooles de péptidos del clade B en ratones humanizados HHD. La respuesta inmune celular específica frente a los antígenos de VIH-1 en los animales inmunizados se determinó mediante la técnica de ELISPOT según se describe en materiales y métodos. En la figura se muestra el número de células secretoras de IFN-γ específicas frente a todos los antígenos de VIH-1 incluidos en los vectores así como la respuesta específica para cada péptido y el número de pooles positivos respecto al péptido control dentro de cada grupo. En la parte superior de cada barra se muestra la magnitud total de la respuesta anti-VIH. * representa diferencias significativas entre los diferentes grupos (**p<0.005).

Como muestra la tabla IX, los esplenocitos de los animales inmunizados con ADN-B seguido de los vectores virales recombinantes (MVA-B o NYVAC-B) mostraron unos niveles altos de IFN-γ frente a los diferentes pooles de VIH. Por el contrario, los niveles de IL-10 fueron significativamente más bajos. Estos resultados coinciden con la respuesta observada en el ensayo de ELISPOT y sugieren que la respuesta inmune inducida como una medida del ratio IFN-γ/IL-10 es del tipo Th1.

	ADN-B/ MVA-B		ADN-B/NYVAC-B		ADN-ϕ/NYVAC-WT	
	IFN-γ	IL-10	IFN-γ	IL-10	IFN-γ	IL-10
Gag-1	908	406	142	204	<20	254
Gag-2	314	120	605	200	<20	<10
Env-1	16194	1206	14178	372	<20	<10
Env-2	18203	1583	11680	444	<20	<10
GPN-1	157	<10	203	<10	<20	<10
Total	35776	3315	26808	1220	<20	254
IFN-γ/IL-10	10,8		21,9		<1	

Tabla IX: Producción de citoquinas (pg/ml) por los esplenocitos de ratones inmunizados en régimen combinado ADN/pox. Ratones HHD fueron inmunizados como se describe en materiales y métodos, 10 días después de la última dosis, las células del bazo fueron extraídas y estimuladas "in vitro" con los pooles de péptidos que cubren los antígenos de VIH e incubados durante 72 horas a 37 ºC. Pasado este tiempo, se recogieron los sobrenadantes y se determinaron los niveles de citoquinas mediante ELISA.

Se ha descrito que las β-quimioquinas como MIP-1β o RANTES pueden suprimir la replicación del VIH *in vitro* impidiendo la entrada del virus a través de su interacción con el co-receptor CCR5 (Eccleston, 1997). Por este motivo, nos pareció interesante cuantificar los niveles de estas dos quimioquinas en los sobrenadantes de cultivos celulares descritos anteriormente. Los niveles totales de RANTES y MIP-1β fueron más altos en aquellos animales que recibieron una segunda dosis de MVA-B (grupo 1) respecto a los que recibieron NYVAC-B (grupo 2). Los niveles más altos de β-quimioquinas fueron secretados frente a los pooles de péptidos que cubren la proteína de la envuelta gp120 de VIH (Env-1 y Env-2) coincidiendo con los resultados obtenidos en el ELISPOT (tabla X).

	ADN-B/ MVA-B		ADN-B/NYVAC-B		ADN-ϕ/NYVAC-WT	
	RANTES	MIP1-β	RANTES	MIP1-β	RANTES	MIP1-β
Gag-1	908	406	<20	<20	<20	<20
Gag-2	314	120	<20	<20	<20	<20
Env-1	16194	1206	266	1103	<20	422
Env-2	18203	1583	380	1231	<20	<20
GPN-1	157	<10	<20	<20	<20	<20
Total	792	3364	646	2334	<20	422

Tabla X: Producción de β-quimioquinas (pg/ml) por los esplenocitos de ratones inmunizados en régimen combinado ADN/pox. Se analizó los niveles de β-quimioquinas mediante ELISA en sobrenadantes de las células del bazo estimuladas "in vitro" con los pooles de péptidos que cubren los antígenos de VIH e incubados durante 72 horas a 37 ºC.

Por último, determinamos los niveles de anticuerpos en el suero de los ratones inmunizados frente a la proteína gp160 de VIH-1 LAV (Subtipo B). Se observó un incremento de hasta 5 veces en la producción de anticuerpos anti-gp160 cuando se utilizó NYVAC-B en el booster respecto al grupo control. Por el contrario, los niveles observados tras la inmunización con MVA-B tan sólo fueron 2,5 veces superiores (datos no mostrados).

4.3.3- Caracterización de la inmunogenicidad de MVA-B y NYVAC-B en un protocolo de inmunización de prime/boost heterólogo en ratones humanizados HHD.

En los experimentos anteriores hemos demostrado que el protocolo de inmunización ADN/pox es capaz de estimular una potente respuesta inmune celular frente a determinados grupos de péptidos de VIH, siendo aquellos "pooles" que cubren la proteína gp120 (Env-1 y Env-2) los más inmunodominantes.

Para determinar si era posible mejorar la amplitud de la respuesta antígeno-específica, desarrollamos un protocolo de inmunización donde combinamos los dos vectores virales recombinantes. De esta forma, ratones transgénicos HHD fueron inoculados con una dosis de 2 x 10^7 UFP/ratón de MVA-B o NYVAC-B por ruta intraperitoneal. A los 15 días se les administró una segunda dosis (2 x 10^7 UFP/ratón) con el virus recombinante homólogo o heterólogo. La respuesta inmune fue evaluada 10 días después de la última inoculación mediante un ensayo de ELISPOT empleando los pooles de péptidos de VIH-1 del subtipo B.

Como muestra la figura 45, los protocolos de inmunización donde se combinan los recombinantes MVA-B y NYVAC-B de forma heteróloga (grupos 1 y 2) u homóloga (grupos 3 y 4) indujeron una estimulación significativa ($p<0,05$) de las células T del bazo en respuesta específica a determinados antígenos de VIH (Gag-1, Env-1, Env-2 y GPN-2) en comparación con los animales inmunizados con la combinación de los vectores parentales (grupo 5). Sin embargo, se observaron algunas diferencias entre los distintos grupos. En los ratones inmunizados con el protocolo MVA-B/NYVAC-B (grupo 1) no hubo reconocimiento de los pooles Gag-2 y GPN-3, mientras que en el resto de grupos estos pooles si activaron la secreción de IFN-γ. Por otro lado, la combinación NYVAC-B/MVA-B (grupo 2), indujo una respuesta específica frente a los pooles GPN-1 y GPN-4 que no fue observada en ninguna otra combinación.

La amplitud y la magnitud total de la respuesta frente a VIH fue muy similar en aquellos animales que recibieron dos inmunizaciones con el mismo vector (grupos 3 y 4).

Ambos parámetros se incrementaron, aunque no significativamente (p>0.05), cuando los ratones fueron inmunizados con NYVAC-B seguido de una dosis de MVA-B (grupo 2). Este grupo, a diferencia de los grupos 3 y 4 que reconocieron 6 de los 8 pooles de péptidos frente a los antígenos de VIH, fue capaz de estimular una respuesta frente a todos los péptidos ensayados. Por el contrario, el grupo de ratones vacunados con el protocolo de inmunización inverso MVA-B/NYVAC-B (grupo 1), fue el que indujo menor número total de células secretoras de IFN-γ y dicha respuesta se dirigió solamente frente a 4 de los pooles.

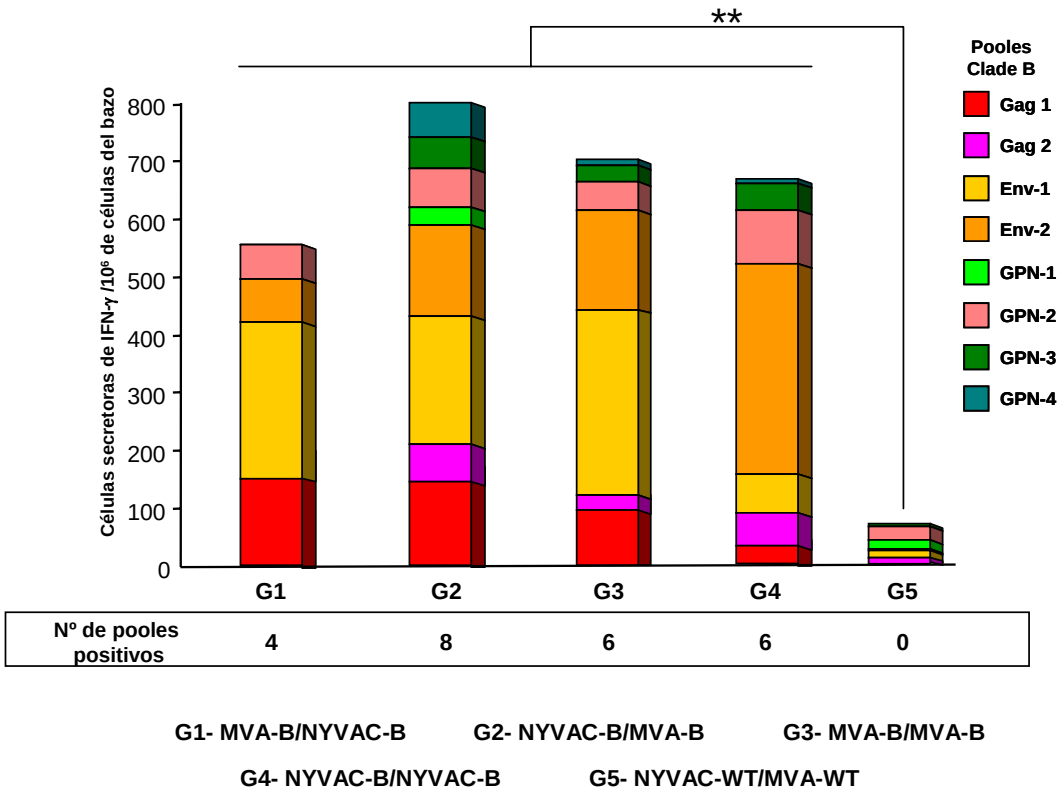

Figura 45: Respuesta inmune específica de células T productoras de IFN-γ frente a pooles de péptidos del clade B en ratones humanizados HHD con diferentes combinaciones de MVA-B y NYVAC-B. La respuesta inmune celular específica frente a los antígenos de VIH-1 en los animales inmunizados se determinó mediante la técnica de ELISPOT según se describe en materiales y métodos. En la figura se muestra la magnitud total de la respuesta anti-VIH en los distintos grupos así como el número de células específicas para cada péptido secretoras de IFN-γ y el número de pooles positivos respecto al péptido control dentro de cada grupo. * representa diferencias significativas entre los diferentes grupos (**p<0.005).

También analizamos el perfil de citoquinas y quimioquinas producidas por los esplenocitos de los animales inmunizados. La tabla XI muestra que todas las combinaciones ensayadas inducen una respuesta inmune del tipo Th1, caracterizada por niveles elevados de IFN-γ y niveles bajos e incluso indetectables de IL-10. Los grupos que recibieron MVA-B en el booster (grupos 2 y 3), indujeron los niveles más altos de IFN-γ en comparación con los grupos inmunizados con dos dosis de NYVAC-B (grupo 4) o la combinación MVA-B/NYVAC-B (grupo 1) siendo esta observación coherente con los resultados obtenidos mediante ELISPOT. Los resultados obtenidos para la secreción de β-quimioquinas fueron similares, con niveles de RANTES y MIP-1β significativamente más altos en los grupos 2 y 3 (NYVAC-B/MVA-B y MVA-B/MVA-B respectivamente).

		Gag-1	Gag-2	Env-1	Env-2	GPN-1	GPN-2	GPN-3	GPN-4	total
MVA-B/NYVAC-B	IFN-γ	1428	<20	9874	2711	<20	<20	<20	<20	14013
	IL-10	<10	<10	568	302	<10	<10	<10	<10	870
NYVAC-B/MVA-B	IFN-γ	3397	2089	2671	2775	3815	1729	2071	3157	21704
	IL-10	399	302	444	456	380	452	468	376	3277
MVA-B/MVA-B	IFN-γ	9951	535	14729	7806	348	<20	132	271	33772
	IL-10	<10	<10	332	206	<10	<10	<10	<10	538
NYVAC-B/NYVAC-B	IFN-γ	2585	<20	3148	2948	<20	<20	<20	145	8826
	IL-10	<10	<10	<10	<10	<10	<10	<10	<10	<10
NYVAC-WT/MVA-WT	IFN-γ	738	<20	<20	157	<20	<20	<20	<20	895
	IL-10	<10	<10	162	<10	<10	<10	<10	<10	162

		Gag-1	Gag-2	Env-1	Env-2	GPN-1	GPN-2	GPN-3	GPN-4	total
MVA-B/NYVAC-B	RANTES	<20	<20	112	<20	<20	<20	<20	<20	112
	MIP-1β	<20	<20	<20	<20	<20	<20	<20	<20	<20
NYVAC-B/MVA-B	RANTES	453	<20	<20	<20	120	<20	<20	134	707
	MIP-1β	237	209	<20	<20	220	<20	1149	109	1924
MVA-B/MVA-B	RANTES	431	251	143	<20	<20	<20	<20	<20	825
	MIP-1β	<20	1986	<20	1263	1157	726	363	<20	5495
NYVAC-B/NYVAC-B	RANTES	105	<20	<20	<20	<20	<20	<20	<20	105
	MIP-1β	<20	<20	<20	<20	<20	<20	<20	<20	<20
NYVAC-WT/MVA-WT	RANTES	<20	<20	<20	<20	<20	<20	<20	<20	<20
	MIP-1β	<20	<20	<20	<20	<20	<20	<20	<20	<20

Tabla XI: Producción de citoquinas y β-quimioquinas (pg/ml) por los esplenocitos de ratones inmunizados en régimen combinado pox/pox. Los niveles de β-quimioquinas se determinaron por ELISA en los sobrenadantes de esplenocitos de los animales inoculados estimulamos "*in vitro*" con los distintos pooles de péptidos de los antígenos de VIH del subtipo B.

Finalmente, decidimos determinar los niveles de anticuerpos específicos frente a la envuelta de VIH-1 en el suero de los ratones inmunizados mediante ELISA. Los

animales que recibieron dos dosis del recombinante NYVAC-B (grupo 1) no produjeron anticuerpos frente a la proteína gp160 del VIH clon LAV. Sin embargo, el resto de las combinaciones de vectores, estimularon niveles similares de anticuerpos que fueron significativamente mayores que los del grupo control (datos no mostrados).

Los resultados demuestran un comportamiento distinto de los vectores “in vivo”. Ambos, tanto MVA-B como NYVAC-C, son unos inmunógenos eficientes capaces de inducir una potente respuesta inmune celular frente a los cuatro antígenos de VIH-1 y por lo tanto, cumplen los criterios necesarios para ser considerados como posibles candidatos vacunales frente a VIH/SIDA. Además, también se ha demostrado que la calidad de la respuesta depende del protocolo de inmunización empleado, pudiendo modularse utilizando diferentes combinaciones de los vectores.

Discusión

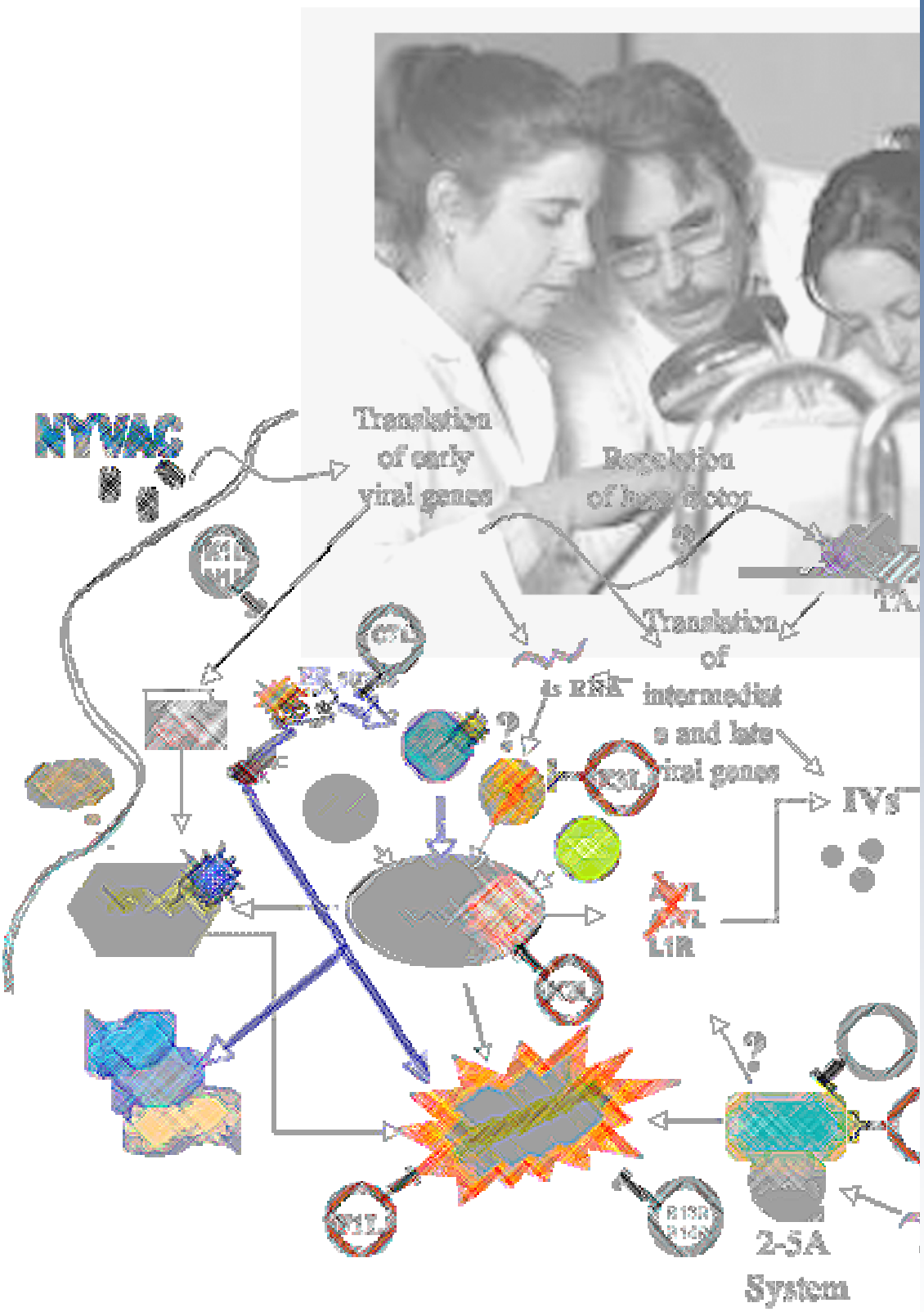
NYVAC
Translation of early viral genes
Translation of
ds RNA
IVs
2-5A System

En la actualidad, las cepas atenuadas del virus vaccinia MVA y NYVAC son consideradas dos de los vectores de elección en el desarrollo de vacunas frente a un gran número de enfermedades infecciosas, e incluso para el tratamiento y prevención de ciertos tipos de cáncer (Pincus y cols., 1995; Franchini y cols., 1996; Ockenhouse y cols., 1998; Raengsakulrach y cols., 1999; Belyakov y cols., 2003; Sutter y Staib, 2003; Franchini y cols., 2004; Drexler y cols., 2004; Sauter y cols., 2005; Gherardi y Esteban, 2005; Precopio y cols, 2007; Amato, 2007). Entre las cualidades que han convertido a estas dos cepas atenuadas en excelentes candidatos vacunales destacan su capacidad para modular la respuesta inmune del hospedador y su capacidad de expresar eficientemente los antígenos recombinantes dentro de la célula diana, de la misma forma que lo haría la infección natural pero sin riesgos para la salud.

A pesar de su atenuación, los recombinantes basados en MVA y NYVAC, han demostrado ser altamente eficaces en la inducción de una respuesta inmune antígeno específica potente y duradera (Sutter y Moss, 1992; Tartaglia y cols., 1992). De hecho, en numerosos casos, su utilización en animales de experimentación da lugar a protección contra distintas enfermedades (Patterson y cols., 2000; Kazanji y cols., 2001; Belyakov y cols., 2003). Estos resultados han hecho que varios candidatos vacunales basados en MVA y NYVAC se encuentren ya en fase clínica de experimentación, validando no sólo la seguridad de estos vectores sino también demostrando su inmunogenicidad en humanos (Ockenhouse y cols., 1998; Sutter y Staib, 2003; Bayes y cols., 2005; Precopio y cols, 2007).

A parte de las características propias de cada cepa, otro aspecto clave a la hora de la elección de un determinado vector viral para su empleo como vacuna es su interacción con el hospedador. Esta interacción va a inducir una respuesta innata y adquirida frente a la partícula viral que desencadenará una serie de eventos en cascada que pueden contribuir al éxito o al fracaso de la vacuna. De este modo, el estudio de las interacciones virus-célula así como el comportamiento *"in vivo"* del vector, podrían ayudarnos a definir los mecanismos que confieren protección frente a un determinado patógeno. Sin embargo, a pesar de su importancia, hasta la fecha existen muy pocos trabajos en los que se analice y compare la biología molecular de MVA y NYVAC o su interacción con la célula diana hospedadora.

Ante la relevancia que están adquiriendo estas dos cepas por su aplicación como vectores vacunales, en este trabajo nos propusimos caracterizar el comportamiento de MVA y NYVAC tanto "*in vitro*" como *"in vivo"* así como, determinar el impacto que podría

tener dicho comportamiento en la respuesta inmune generada por recombinantes basados en estas dos cepas que expresan cuatro antígenos de VIH-1 (Env, Gag, Pol y Nef).

1) Características de los vectores atenuados MVA y NYVAC en células en cultivo

En primer lugar decidimos caracterizar la biología de estos dos vectores en células en cultivo. Para ello, hemos analizado morfológica, bioquímica y genéticamente las alteraciones que se producen en las células tras la infección con uno u otro vector.

En cuanto a su comportamiento *"in vitro",* MVA y NYVAC comparten características comunes. Sin embargo, en este trabajo hemos definido algunas diferencias significativas entre las dos cepas que podrían afectar a su capacidad inmunogénica.

El estudio morfológico de las células infectadas reveló que NYVAC produce un efecto citopático (EC) más severo que el producido por las cepas MVA o VACV-WR. Este efecto se observó desde tiempos muy tempranos y en un amplio rango de células permisivas y no permisivas, lo que nos indica que es independiente de la restricción del hospedador. El mismo efecto fue también evidente cuando añadimos a las células infectadas la droga Ara C, que bloquea la replicación del ADN viral. Previamente se había descrito que la inducción del redondeamiento celular es un proceso que depende de la síntesis de proteínas virales tempranas (Bablanian y cols., 1978a; 1978b; 1981). De acuerdo con estos resultados, Tsung y colaboradores describieron la ausencia de EC en células infectadas con cepas del virus vaccinia (VACV) inactivadas con psoralen o luz ultravioleta, dos tratamientos que afectan a la transcripción de genes virales tempranos (Tsung y cols., 1996). Teniendo en cuenta estos datos y como ya ha sido postulado con anterioridad (Carroll y Moss, 1997), nuestros resultados sugieren que el menor efecto citopático observado durante la infección con MVA respecto a VACV-WR o NYVAC podría ser debido a la ausencia en su genoma de alguno de los genes de expresión temprana implicados en la inducción de este proceso. En este sentido, se ha descrito una familia de proteínas virales similares a las proteínas tipo Kelch que regulan el efecto citopático interviniendo en la adhesión de las células a la matriz extracelular (ECM) de una forma independiente del Ca^{+2}. Hasta el momento, se han identificado tres genes virales que codifican estas proteínas: *C2L, F3L* y *A55R*, e interesantemente, los genes *C2L* y *A55R* se encuentran ausentes en el genoma de MVA (Pires de Miranda y cols., 2003). Por otro lado, también hemos observado que existe un redondeamiento más pronunciado en las células infectadas con NYVAC a tiempos tempranos postinfección que el observado tras la infección con la cepa VACV-WR, lo que nos sugiere que entre

las deleciones realizadas a NYVAC se encuentra algún gen que regula y compensa el EC inducido tras la infección, aunque hasta la fecha no se han descrito ningún gen que desempeñe dicha función.

Otra de las diferencias que encontramos entre las cepas MVA y NYVAC se refiere a la restricción de hospedador. Los poxvirus codifican distintas moléculas virales que modulan la respuesta celular para así cubrir sus necesidades. Sin embargo, en algunos tipos celulares, los poxvirus no logran completar su ciclo infeccioso, un fenómeno denominado restricción de hospedador (Tagaya y cols., 1961; McClain, 1965; Hruby y cols., 1980; Drillien y cols., 1981; Somogyi y cols., 1993; Fenner y Sambrook, 1996; Wyatt y cols., 1998). En este sentido, nuestros datos ponen de manifiesto que los mecanismos de restricción de hospedador para MVA y NYVAC en líneas celulares no susceptibles a la infección (humanas y murinas) son distintos.

El estudio bioquímico realizado en células humanas indica que durante la infección con NYVAC se produce una reducción en la cinética de síntesis de proteínas y en la acumulación de proteínas virales respecto a la infección con MVA. Dicha inhibición está asociada a un incremento en los niveles de fosforilación de la subunidad alfa del factor eIF2. Este factor juega un papel clave en la respuesta antiviral en células eucariotas controlando la traducción y síntesis de proteínas (De Haro y cols., 1996). Coincidiendo con la fosforilación de eIF2α, durante la infección por NYVAC no se detectó la expresión de ciertas proteínas estructurales tardías como A27, A17 o L1. Esta inhibición en la síntesis afecta específicamente al proceso de traducción, ya que la presencia e integridad de los mensajeros ha quedado demostrada.

La posibilidad de que durante la infección por NYVAC el factor eIF2 pudiese estar involucrado directamente en el bloqueo de la síntesis de las proteínas virales resulta atractiva. Este hecho ha sido demostrado para otras infecciones como por ejemplo el virus del herpes simple (VHS-1) o durante la expresión de la poliproteína del virus de la hepatitis C (VHC) (Gómez y cols., 2005). Sin embargo, en el caso de NYVAC, en líneas permisivas (BHK-21) también observamos un incremento en los niveles de fosforilación de dicho factor, incluso durante la infección por MVA, y en estas condiciones no existe restricción en la síntesis de proteínas como A27, A17 o L1.

Como mostramos en este trabajo, durante la infección por NYVAC no sólo se induce un incremento en los niveles de fosforilación del factor eIF2 sino que también se produce una degradación del ARN ribosómico (ARNr) a tiempos tardíos postinfección. El patrón de degradación del ARNr es similar al producido tras la activación de la ribonucleasa celular ARNasa L, indicando una posible activación de dicha enzima. Por lo tanto, la inhibición en la síntesis de las proteínas tanto virales como celulares podría producirse a estos dos niveles. Está establecido que ambos mecanismos juegan un

papel clave en la respuesta antiviral de los interferones (IFN) y son activados por ARN de doble cadena (Sutter y Moss, 1992; Yang y cols., 1995; Seet y cols., 2003). Como la activación de la enzima ARNasa L no debería discriminar entre los diferentes ARNm presentes en el citoplasma de la célula, la fosforilación de eIF2 podría ser responsable de la selectividad de los transcritos. Recientemente se ha descrito la resistencia a la inhibición traduccional de mensajeros virales tardíos de alfavirus a pesar de la fosforilación de eIF2α como una nueva estrategia para escapar del efecto antiviral de la proteína PKR (Ventoso y cols., 2006). Estos mensajeros poseen una estructura secundaria que permite su traducción en presencia de altos niveles de fosforilación del factor eIF2α. De acuerdo con estos datos, una posible explicación para nuestros resultados podría ser que algunos mensajeros virales tardíos sean capaces de traducirse en presencia de altos niveles de fosforilación de eIF2α por un mecanismo similar al descrito para los alfavirus. La predicción de la estructura secundaria de los mensajeros de genes tardíos como *A4L* o *A14L* podría confirmar este planteamiento.

Por otro lado, tampoco podemos descartar que este efecto sea mediado a través de la inhibición de ciertas proteínas celulares. Como hemos descrito en la introducción, estudios previos han demostrado que para la correcta expresión de los genes virales intermedios y tardíos, además de la ARN polimerasa viral, es necesaria la presencia de ciertos factores celulares (Broyles, 2003). En este sentido, varios grupos han identificado proteínas celulares como VITF-2, VITF-X o RBM3 que actúan como factores de la transcripción viral (Rosales y cols., 1994; Wright y cols., 1998; Wright y cols., 2001). Sin embargo, el papel exacto de dichas proteínas, así como los niveles de éstas en las distintas líneas celulares, están todavía por determinar. Otros autores sugieren que ciertos genes virales, entre los que se incluyen aquellos de rango de hospedador, podrían modular la actividad de esas proteínas y de esta forma conferir al virus la capacidad para replicar en determinadas líneas celulares (Hsiao y cols., 2004). No obstante, hasta la fecha no se ha descrito que estos factores celulares afecten selectivamente a la expresión de determinadas proteínas virales tardías.

A pesar de que no hayamos definido los mecanismos de la inhibición selectiva en la síntesis de determinadas proteínas tardías, dicha inhibición puede ser la causa del bloqueo en la morfogénesis viral observado por microscopía electrónica en células HeLa infectadas por NYVAC. Estudios previos realizados en el laboratorio con mutantes de deleción del virus vaccinia han demostrado la implicación de las proteínas A27, A17 y L1 en la formación de los distintos estadíos de la morfogénesis viral, concretamente en el proceso de maduración de los viriones (Rodríguez y cols., 1995; Smith y cols., 2002). Como revelan las micrografías, el bloqueo en la morfogénesis viral inducido tras la infección por NYVAC se produce en un estadío anterior al de la formación y maduración

de los viriones. Sin embargo, en el caso de MVA está descrito que el bloqueo es debido a un defecto en el ensamblaje de las proteínas estructurales ya que la síntesis de las proteínas virales no se encuentra alterada (Sutter y Moss, 1992). Este bloqueo en MVA se traduce en una baja producción de virus intracelulares maduros (MVs), inferior al 4%, y la producción de una gran cantidad de viriones atípicos que no son infectivos (Sancho y cols., 2002; Gallego-Gómez y cols., 2003). Estos resultados reflejan la seguridad de estos dos vectores para su utilización en ensayos clínicos.

Otra diferencia importante que hemos observado en las células infectadas con ambos vectores es que, contrariamente a lo que ocurre con MVA, en las células infectadas con NYVAC se producen una serie de cambios morfológicos y bioquímicos característicos de la inducción de muerte celular por apoptosis. Entre los cambios bioquímicos observados en las células infectadas con NYVAC podemos destacar el procesamiento de la proteína celular PARP o la degradación del ADN nuclear. También se detectaron por microscopía electrónica distintas alteraciones morfológicas propias de una muerte celular programada como la condensación de la cromatina o la formación de vacuolas. El análisis por citometría de flujo reveló que un 42 % de las células presentan un fenotipo apoptótico tras 24 horas de infección con NYVAC, mientras que dicho porcentaje se limitaba a un 17 % tras la infección por MVA. Ambos valores se redujeron a los niveles basales cuando las células infectadas fueron tratadas con zVAD, un inhibidor general de las caspasas, lo que nos indica que el proceso apoptótico inducido tras la infección es dependiente de la activación de caspasas.

Corroborando estos resultados, varios estudios desarrollados en el laboratorio utilizando la técnica de los microarrays han demostrando diferencias claras en el perfil de genes celulares que se inducen a nivel del ARNm tras la infección con MVA respecto a NYVAC (Guerra y cols., 2004; Guerra y cols., 2006). Concretamente, MVA es capaz de inducir la expresión de una gran cantidad de mensajeros de genes inmunomoduladores como IL-7, IL1A, IL-8 o IL-15, mientras que la ruta de señalización apoptótica sólo se encuentra activada tras la infección por NYVAC.

Hasta el momento desconocemos por qué a diferencia de MVA o VACV-WR, NYVAC induce apoptosis. La explicación más sencilla podría referirse a la ausencia en su genoma de genes reguladores de este proceso. En este sentido, entre las 18 deleciones de NYVAC se ha descrito que las proteínas codificadas por los genes *B13R/B14R* o *N1L* tienen una función antiapoptótica (Kettle y cols., 1997); Sin embargo, estos genes tampoco están presentes o se encuentran mutados en el genoma de MVA (*MVA182R/ 181R, MVA020L,* respectivamente), lo que nos sugiere la existencia de algún otro gen antiapoptótico todavía sin identificar. Recientemente Chahroudi y colaboradores han realizado un estudio en células dendríticas humanas donde proponen que la

apoptosis inducida en estas células por VACV-WR y MVA puede ser consecuencia de la ausencia de alguna o algunas proteínas virales tardías que regulen este proceso (Chahroudi y cols., 2006). Estos autores se basan en la observación de que la apoptosis ocurre en infecciones abortivas, donde se produce una inhibición en la síntesis de proteínas virales tardías. De esta forma, podría ser que durante la infección, el virus sintetizase factores tempranos y tardíos que modulasen la respuesta pro-apoptótica mediada por la célula con el objetivo de ganar tiempo para replicar. En nuestro caso, donde existe un bloqueo en la síntesis de ciertas proteínas virales tardías, la ausencia de estos posibles factores virales tardíos de protección frente a la apoptosis desencadenaría el proceso de muerte celular.

Todos estos resultados revelan que existen diferencias claras en el comportamiento de MVA y NYVAC en células en cultivo. Estas diferencias son debidas a las numerosas deleciones y mutaciones generadas en sus genomas durante el curso de su atenuación. Por ello, decidimos realizar un estudio comparativo de los genes delecionados en MVA y NYVAC (tabla II) con la finalidad de tratar de identificar algún factor viral que pudiera ser el responsable de los diferentes fenotipos observados entre ambos vectores. Hasta la fecha, se han secuenciado más de 100 genomas de distintas especies de poxvirus, entre los que se encuentran las cepas del virus vaccinia Copenhagen VACV-COP (de la cual deriva NYVAC) y MVA (Antoine y cols., 1998; Goebel y cols., 1990; Johnson y cols., 1993). De la comparación de los dos genomas hemos idntificado al gen *C7L*, presente en MVA (*021L*) y ausente en NYVAC, como uno de los posibles genes responsables del comportamiento diferencial entre ambas cepas. El gen *C7L* se encuentra altamente conservado dentro del género *orthopoxvirus* lo que refleja su importancia para la biología del virus modulando la respuesta celular. Se ha definido como un gen de rango de hospedador necesario para la replicación del virus en células humanas (Perkus y cols., 1990; Oguiura y cols., 1993).

Para determinar la función que podría desempeñar el gen *C7L* en el comportamiento de NYVAC, decidimos reintroducirlo en su genoma, generando para ello el recombinante NYVAC-C7L. La caracterización de este recombinante demostró que la reinserción de este gen juega un papel crítico en el control de la apoptosis y revierte muchas de las características bioquímicas y biológicas que hemos atribuido a NYVAC en este trabajo.

De acuerdo con nuestros resultados, la presencia de la proteína C7 es capaz de prevenir la fosforilación del factor eIF2 y la degradación del ARN ribosomal, lo que se traduce en un rescate de la expresión de las proteínas virales tardías cuya síntesis se encontraba inhibida en la infección por NYVAC (A17, A27 o L1). Como consecuencia de esto, el nuevo vector recupera la capacidad para crecer en células humanas y murinas.

Estos datos definen un posible mecanismo de restricción celular para NYVAC en líneas celulares de origen humano y murino y un papel importante del gen *C7L* en el control de la traducción de las proteínas virales.

En este estudio también hemos observado que la reinserción del gen *C7L* en NYVAC es capaz de inhibir la apoptosis que se induce tras la infección con la cepa parental. Existe una gran controversia en cuanto a los mecanismos celulares que dan lugar a la restricción del virus en determinados tipos celulares. Algunos estudios sugieren que los genes de rango de hospedador poseen propiedades antiapoptóticas que antagonizan la restricción celular, asociando este proceso a la reducción del crecimiento viral y a la inhibición en la síntesis de proteínas virales (Lee y Esteban, 1994; Brooks y cols., 1995; Ink y cols., 1995). Por el contrario, otros estudios definen la inducción de apoptosis durante la infección viral como una última señal de estrés asociada con la restricción celular (Chang y cols., 1995; Ray y Pickup, 1996, Blair y cols., 1996; Hsiao y cols., 2004) y de hecho, como hemos comentado anteriormente, algunos de estos autores sugieren la presencia de proteínas virales tardías con una función antiapoptótica (Chaoroudi y cols., 2006). Nuestros resultados indican que el gen *C7L* interviene directa o indirectamente en la regulación del proceso de muerte celular aunque su función antiapoptótica así como su mecanismo de acción debería examinarse fuera del contexto viral ya que no podemos descartar que otras deleciones también pudiesen estar implicadas en la apoptosis inducida tras la infección por NYVAC. En este sentido, se ha descrito que en algunos tipos celulares los genes de rango de hospedador del virus vaccinia como *C7L, K1L* y el gen de cowpox *CP77* podrían comportar como genes equivalentes, donde unos compensen la ausencia de otros (Turner y Moyer, 1998; Hsiao y cols., 2004).

Además de recuperar la capacidad para crecer en células en cultivo de origen humano y murino, la reinserción del gen *C7L* en el genoma de NYVAC incrementó su eficiencia de replicación *"in vivo"* en ratones BALB/c. Sin embargo, NYVAC-C7L mantuvo el fenotipo atenuado en ratón. Este resultado podría ser relevante desde el punto de vista del desarrollo de vacunas ya que un vector atenuado eficiente en replicación permitiría una mayor expresión del antígeno heterólogo antes de que el virus sea clarificado por el organismo y por consiguiente podría potenciar su inmunogenicidad (Harari y Pantaleo, 2005; Sauter y cols., 2005).

2) Comportamiento diferencial de los vectores atenuados MVA y NYVAC *"in vivo"* en ratones BALB/c

Una vez definidas las caraterísticas de MVA y NYVAC en células en cultivo, decidimos analizar el comportamiento de estas cepas atenuadas *"in vivo".* Para ello,

generamos vectores recombinantes que expresan como gen reportero la proteína luciferasa y llevamos a cabo un estudio comparativo de la distribución del virus y de la diseminación del antígeno empleando distintas rutas de inmunización tanto sistémicas como de mucosas.

Como revela el análisis por bioluminiscencia, las vías más eficientes en cuanto a la obtención de altos niveles de expresión del antígeno heterólogo son las rutas intraperitoneal e intramuscular. Además, como ya había sido descrito previamente para MVAluc (Ramírez y cols., 2000), NYVACluc también muestra una expresión transitoria del gen reportero, cuya distribución y diseminación depende de la ruta de administración a diferencia de lo que ocurre con la cepa competente en replicación WRluc. Por lo tanto, ambos recombinantes atenuados muestran una reducida capacidad de replicación *"in vivo*", evidenciando de nuevo su seguridad como vectores vacunales.

Interesantemente, en los ratones infectados con NYVACluc el análisis por bioluminiscencia reveló que la expresión del antígeno permanece durante un tiempo más prolongado que en los animales inoculados con MVAluc, observándose diferencias en los niveles de expresión de luciferasa a partir de las 24 horas y de ahí en adelante. Sin embargo, los resultados obtenidos tras el análisis de la cinética de expresión de luciferasa en los distintos órganos mediante ensayos bioquímicos nos indican que MVA muestra una eficiencia de expresión mayor que NYVAC a tiempos tempranos postinfección. Estas diferencias podrían estar relacionadas con la susceptibilidad de determinados tipos de células a la infección con MVA o NYVAC. En este sentido, trabajos previos han descrito que MVA exhibe un tropismo celular diferente respecto a la cepa competente en replicación VACV en células primarias humanas (Sánchez-Puig y cols., 2004; Chahroudi y cols., 2005). Por lo tanto, se deberían realizar distintos estudios para identificar los tipos celulares infectados por las dos cepas virales atenuadas tanto en animales como en humanos.

En conjunto, los resultados mostrados hasta el momento sobre la biología de MVA y NYVAC, junto con otros trabajos realizados en el laboratorio sobre el impacto en la expresión génica tras la infección de células HeLa con ambas cepas atenuadas (Guerra y cols., 2005; 2006) y células dendríticas humanas (Guerra y cols., 2007), sugieren que MVA y NYVAC estimulan de forma diferencial la respuesta inmune celular.

Se han propuesto varios factores que podrían influir en la inmunogenicidad y en el tipo de respuesta inducida por distintos vectores vacunales (Estcourt y cols., 2005). Entre ellos se incluyen: a) la ruta de administración que, como hemos mostrado, determina la localización anatómica inicial y la subsiguiente distribución del antígeno en el organismo, lo que podría tener un efecto en la respuesta inmune inducida en tejidos linfoides más distantes; b) la dosis que, como una medida de la carga antigénica inicial,

podría mediar en la magnitud de la respuesta primaria; c) la persistencia del antígeno, que podría influir en el desarrollo de la respuesta de memoria; y d) el tipo de procesamiento del antígeno y su presentación, que podría determinar en el tipo de respuesta celular activando de forma diferente las células T CD4+ o T CD8+.

Recientemente, se ha propuesto que la cross-presentación es el mecanismo prioritario para inducir una respuesta citotóxica (CTLs) frente a antígenos derivados de las cepas WR y MVA *"in vivo"* (Chahroudi y cols., 2006; Gasteiger y cols., 2007). En este sentido, la apoptosis inducida por NYVAC podría contribuir a estimular su inmunogenicidad ya que células dendríticas sin infectar podrían cross-presentar a los linfocitos T los antígenos virales exógenos adquiridos de las células apoptóticas (Albert y cols., 1998; Larsson y cols., 2001).

Con todos estos antecedentes, decidimos analizar la inmunogenicidad de recombinantes de MVA y NYVAC en el modelo murino y valorar su aplicación como vectores vacunales frente al VIH/SIDA.

3) Generación de candidatos vacunales basados en MVA y NYVAC que expresan cuatro antígenos de VIH-1 subtipos B y C

Durante los últimos 20 años se han desarrollado una gran variedad de candidatos vacunales frente al VIH/SIDA entre los que se incluyen proteínas recombinantes, péptidos sintéticos, vectores de ADN desnudo o vectores virales incapaces de completar su ciclo infeccioso en células humanas (Girard y cols., 2006). A pesar de que hasta el momento siguen sin identificarse el ó los parámetros inmunológicos que correlacionan con protección, los estudios realizados tanto en animales de experimentación como en fase clínica en humanos, han demostrado que la respuesta inmune celular específica frente al VIH, y particularmente la respuesta de linfocitos T citotóxicos (CTLs), puede controlar la infección viral, retrasando o previniendo la progresión hacia SIDA. De este modo, prototipos de vacunas que estimulen el brazo celular de la respuesta inmune pueden controlar la replicación viral y reducir los niveles de carga viral en individuos vacunados, lo que conlleva a una menor probabilidad de transmisión del virus a individuos seronegativos. En los últimos años se ha producido un auge en el desarrollo de vacunas frente al VIH/SIDA que potencian la respuesta inmune celular (Koup y cols., 1994; Kuroda y cols., 1999; Schmitz y cols., 1999; Lifson y cols., 2001; Amara y cols., 2005). Entre ellas destacan los candidatos basados en adenovirus o en las cepas atenuadas de poxvirus MVA y NYVAC.

Como hemos comentado con anterioridad, MVA y NYVAC han demostrado ser dos vectores seguros y altamente inmunogénicos por lo que hoy en día son considerados candidatos de elección en el diseño de vacunas, no sólo frente al SIDA

sino también frente a un amplio abanico de enfermedades, como malaria, lehismaniasis e incluso frente a cáncer.

En este trabajo se describe la generación y caracterización de la respuesta inmune inducida frente al VIH/SIDA basados por MVA y NYVAC en dos modelos de ratones, BALB/c y transgénicos humanizados HHD. Los recombinantes generados MVA-B y MVA-C han sido objeto de una solicitud de patente.

En el caso del VIH/SIDA, se ha descrito que para la inducción de una respuesta celular amplia y eficaz es necesario, la inclusión de antígenos virales tanto estructurales como reguladores (Shiver y cols., 2002; Berzofsky y cols 2003; Mooji y cols., 2004). Este es un aspecto extremadamente importante en el desarrollo de vacunas dirigidas a potenciar una respuesta celular, ya que una respuesta inmunológica frente a un solo antígeno podría llevar a la selección de mutantes que escapen a dicha respuesta, especialmente si la protección no es completa (Barouch y cols., 2002; Shiver y cols., 2004). Por este motivo, se seleccionaron los antígenos Env, Gag, Pol y Nef de VIH-1 para la generación de nuestros candidatos vacunales. Los 4 antígenos (Env/Gag-Pol-Nef) del subtipo B o C de VIH-1 fueron insertados en el genoma de MVA y NYVAC en el locus del gen que codifica para la timidina quinasa (TK). En MVA-B y NYVAC-B, el gen de la envuelta (Env) codifica para la proteína gp120 del aislado primario Bx08, tiene un tropismo celular CCR5, que se trasmite más frecuentemente que las cepas tipo CXCR4 (Berger y cols., 1999) y por lo tanto constituye una posible diana para inhibir la diseminación del VIH. Por otro lado, el gen sintético gag-pol-nef proviene del aislado IIIB y en su secuencia se incluyen los principales determinantes antigénicos que han sido descritos para las proteínas Gag, Pol y Nef. En MVA-C y NYVAC-C tanto la envuelta (Env), como el gen sintético gag-pol-nef, derivan del aislado primario asiático CN54. Estas construcciones han sido optimizadas en sus codones y diseñadas para obtener los máximos niveles de expresión en células humanas. Además, se han eliminado aquellas secuencias que podrían comprometer su seguridad o eficacia. Estos antígenos representan las proteínas más inmunogénicas de VIH-1 expresadas durante la infección viral y se encuentran actualmente en fase de experimentación expresados desde los distintos candidatos vacunales que se están ensayando en fase clínica (Tabla IV).

Nuestros resultados demuestran que tanto los vectores del subtipo B: MVA-B y NYVAC-B, como los del subtipo C: MVA-C y NYVAC-C, cumplen los criterios deseables a la hora de generar una vacuna (ver anexo 1): 1) capacidad de obtención de títulos virales altos de replicación en células CEF; 2) niveles altos de expresión génica de los productos recombinantes; 3) elevada estabilidad del inserto tras someter al vector a pases sucesivos en cultivos celulares y 4) generación de una respuesta inmune específica frente a los antígenos heterólogos. Además, hemos observado que la

inserción de los antígenos de VIH no modifica las características propias de cada vector, como la inducción de apoptosis o la síntesis de proteínas, descritas en este trabajo y que podrían afectar de alguna manera a su inmunogenicidad.

Para la simplificación de la lectura de este trabajo, se han detallado solamente los datos correspondientes al estudio de la inmunogenicidad de MVA-B y NYVAC-B en ratones BALB/c y transgénicos humanizados HHD. Los resultados del estudio de inmunogenicidad correspondientes a los recombinantes MVA-C y NYVAC-C se adjuntan en el anexo 1 (Gómez y cols., 2007a).

4) Ensayos preclínicos frente al VIH/SIDA con los vectores atenuados MVA y NYVAC

Una vez generados y caracterizados los vectores, decidimos evaluar el potencial inmunogénico de MVA-B y NYVAC-B en ratones BALB/c y transgénicos humanizados HHD.

Actualmente, el modo más efectivo para inducir una inmunidad celular es mediante protocolos de inmunización de "prime-boost" donde se combinan la inmunización con un vector de ADN seguido de una dosis de refuerzo con un vector viral recombinante, ambos codificando los mismos antígenos (Zavala y cols., 2001; Harari y Pantaleo, 2005).

Debido a esto, analizamos la respuesta inmune inducida tras la administración de una dosis de ADN seguido de una segunda dosis con un poxvirus recombinante, ambos expresando los antígenos Env, Gag, Pol y Nef de VIH-1 en dos modelos de ratones. Nuestros resultados demuestran que los vectores MVA-B y NYVAC-B son unos inmunógenos eficientes, capaces de inducir una potente respuesta inmune celular específica frente a los antígenos Env, Gag, Pol y Nef de VIH-1 tanto en ratones BALB/c como en ratones humanizados HHD. Sin embargo, hemos observado diferencias entre los recombinantes en cuanto a la magnitud y amplitud de la respuesta frente a los distintos epítopos de VIH-1 que depende del protocolo de inmunización utilizado en cada modelo animal.

En ratones BALB/c, el protocolo ADN-B/NYVAC-B indujo una respuesta significativamente mayor que la inmunización con ADN-B/MVA-B. Sin embargo, la magnitud de la respuesta en los ratones transgénicos HHD con ambos protocolos de inmunización fue similar. Los niveles de células secretoras de IFN-γ fueron más bajos en los animales transgénicos que en los BALB/c, lo que se correlaciona con la menor proporción de células T CD8+ en los ratones HHD (una media de un 3% sobre el total de las células del bazo). Cuando analizamos intrínsecamente frente a qué péptidos se

dirigió la respuesta celular también observamos diferencias entre los dos modelos animales. Mientras que en BALB/c la respuesta se encuentra ampliamente distribuida entre los 4 antígenos de VIH-1 (7 mezclas de péptidos solapantes, referidos en denominación inglesa como “pooles” positivos), en los ratones transgénicos, los “pooles” de péptidos que cubren la envuelta (Env-1 y Env-2) fueron los más inmunogénicos. Varios estudios han descrito que la competición o inmunodominancia de varios epítopos de CTLs puede reducir la amplitud de la respuesta inducida tras la vacunación (Rodríguez y cols., 2002; Palmowsky y cols., 2002). En nuestro caso, la inmunodominancia en la respuesta observada frente al grupo de péptidos que cubren la envuelta (Env) podría afectar al reconocimiento del “pool” de péptidos que cubren el resto de los antígenos incluidos en los candidatos vacunales. Se ha propuesto que la rapidez con la que una célula produce IFN-γ constituye uno de los principales criterios que determinan la supervivencia de la célula y su posterior expansión clonal (Liu y cols., 2004). De este modo, las células T CD8+ podrían producir rápidamente la secreción de IFN-γ como respuesta a la expresión y secreción temprana de la proteína de la envuelta de VIH y así permitir la supervivencia y expansión de los clones de células específicas frente a Env. Sin embargo, existen otros factores que podrían contribuir a la inmunodominancia de la envuelta frente al resto de los antígenos en el modelo HHD: la afinidad para unirse al MHC, la eficiencia de procesamiento de los epítopos o la competición entre células T para acceder a la célula presentadora del antigéno (APC).

Con la intención de mejorar la amplitud de la respuesta en los ratones transgénicos HHD, decidimos evaluar la respuesta tras la administración de distintos protocolos de inmunización donde se combinen los dos vectores virales.

El protocolo de inmunización NYVAC-B/MVA-B indujo la respuesta inmune celular más amplia, seguido del grupo que recibió dos dosis de MVA-B. De esta forma, con este tipo de combinaciones conseguimos evitar la inmunodominacia de la respuesta frente a la envuelta generando una respuesta más homogénea frente a todos los grupos de péptidos que cubren los cuatro antígenos incluidos en nuestras construcciones. Este resultado podría ser relevante en el diseño de un protocolo de inmunización eficaz, ya que se ha demostrado que vacunas que generan una respuesta inmune celular potente frente a uno o dos epítopos específicos pueden, con el tiempo, perder su eficacia protectora debido a la generación por parte del agente infeccioso de mutantes que escapan de la respuesta inmunológica (Pantaleo y cols., 1995; Barouch y cols., 2002). Además, se ha descrito que los individuos no progresores a largo plazo presentan una respuesta ampliamente reactiva de CTLs, lo que nos indica la importancia de la amplitud de la respuesta en el control de la infección viral (Pantaleo y cols., 1995; Gea-Banachone y cols., 2000).

Por otro lado, la secuencia de administración de los vectores resultó ser esencial ya que el protocolo de inmunización inverso, MVA-B/NYVAC-B, no mejoró la amplitud de la respuesta inmunológica. MVA-B demostró su eficacia como potenciador de la respuesta inmune cuando se administra tras una primera dosis de MVA-B o NYVAC-B. Sin embargo, NYVAC-B fue menos eficaz. Como ya ha sido postulado anteriormente, esto podría explicarse por el tipo de respuesta generada por cada recombinante frente al propio vector (Webster y cols., 2005). Estudios realizados en el laboratorio demuestran que la respuesta inmune, tanto celular como humoral, generada frente al propio vector es mayor en NYVAC que en MVA (Gómez y cols., 2007a; 2007b). MVA tiene un genoma de 186 Kb que codifica 193 fases de lectura abiertas, "ORFs", de las cuales tan sólo 152 permanecen intactas (Antoine y cols., 1998), mientras que NYVAC sólo tiene 18 genes delecionados respecto a su cepa parental (Tartaglia y cols., 1992). Debido a que el genoma de MVA presenta un menor tamaño, la respuesta inmune generada frente al vector tras la inmunización con MVA podría dirigirse frente a antígenos comunes presentes en las regiones altamente conservadas dentro del género *Orthopoxvirus* y de esta manera atenuar o inhibir la posterior infección con NYVAC. Por el contrario, la respuesta inducida frente a NYVAC podría estar dirigida frente a antígenos que no se expresasen durante la infección con MVA y de este modo no influirían o influirían en menor medida en la posterior inmunización con MVA. En este sentido, Oseroff y colaboradores han identificado en PBMCs de pacientes vacunados con Dryvax, 48 epítopos derivados de distintos antígenos del virus vaccinia como B8R, D1R, D5R, C10L, C19L, C7L, F12L y O1L. Estos antígenos fueros reconocidos eficientemente por distintos donantes en el contexto de diferentes tipos de HLA (Oseroff y cols., 2005). Alguno de estos genes se encuentran mutados o ausentes en el genoma de MVA. Estas observaciones ayudan a explicar las diferencias inmunológicas que hemos encontrado entre los dos vectores y deberían tenerse en consideración cuando se utilicen recombinantes basados en MVA o NYVAC en diferentes protocolos de inmunización.

En la mayoría de las infecciones virales, y en el caso de VIH en particular, la protección y el control de la infección se ha correlacionado preferentemente con la inducción de una respuesta inmunológica de tipo Th1. Esta respuesta se caracteriza por la producción de citoquinas como IL-12, IL-2 e IFN-γ mientras que la secreción de IL-10, IL-4, IL-5 o IL-13 determina un tipo de respuesta Th2 (Graham, 2002). En nuestro caso, el patrón de citoquinas detectado en los sobrenadantes de los cultivos celulares de linfocitos del bazo tras la reestimulación con las diferentes mezclas de péptidos, es claramente el de una respuesta del tipo Th1. Además, en estos sobrenadantes también hemos detectado altos niveles de β-quimioquinas como MIP-1β o RANTES cuya actividad antiviral ha sido descrita en varios trabajos (Eccleston y cols., 1997). De hecho,

se han detectado niveles elevados de RANTES en un grupo de prostitutas en Kenia, quienes a pesar de estar continuamente expuestas al virus, no llegan a infectarse (Isqal y cols., 2005) por lo que este resultado podría ser de gran importancia en el control de la infección.

En las distintas estrategias de inmunización ensayadas en este trabajo hemos sido capaces de detectar una inducción moderada de la respuesta humoral producida por los distintos recombinantes, aunque la capacidad neutralizante de los anticuerpos generados no ha sido analizada.

Nuestros resultados demuestran que tanto MVA-B como NYVAC-B son unos inmunógenos eficientes capaces de inducir una potente respuesta inmune celular frente a los cuatro antígenos de VIH-1. Además, hemos observado que la calidad de la respuesta va a depender del protocolo de inmunización utilizado, pudiendo modularse utilizando diferentes combinaciones de vectores.

A pesar de que en el modelo murino no hemos podido evaluar la eficacia de MVA y NYVAC para conferir protección frente a la infección por VIH, los resultados obtenidos en este trabajo son prometedores. De hecho, en colaboración con el grupo del Dr. Heeney, del Centro de Primates de Holanda, se ha llevado a cabo un estudio en macacos para evaluar la inmunogenicidad y la eficacia de MVA y NYVAC en sistemas de inmunización combinado, ADN/pox.

Nuestro grupo ha contribuido en la generación de los recombinantes híbridos simio/humanos (SHIV) utilizados para este modelo. Dichos recombinantes expresan el gen de la envuelta del VIH-1 humano Env89.6p y el gen sintético gag-pol-nef procedente del virus de simio SIVmac239. Los datos mostrados en esta tesis han servido para corroborar y explicar algunos de los resultados obtenidos en los ensayos de macacos.

Lo más relevante que se observó en el estudio desarrollado en primates fue que tanto MVA como NYVAC fueron capaces de conferir una protección similar frente a un desafío con un virus altamente patogénico (SHIV89.6p). En los monos inmunizados con MVA y NYVAC los niveles de células CD4+ se mantuvieron constantes durante un periodo de tiempo superior a un año y la carga viral permaneció por debajo de los límites de detección durante todo el periodo de análisis. Interesantemente, esta protección se correlacionó con una inducción de una respuesta celular específica frente a los cuatro antígenos, aunque existe una predominancia hacia Env al igual que ocurre en los ratones transgénicos HHD, y con una activación diferencial de células T CD4+ o T CD8+. El análisis detallado de la respuesta inmune inducida por MVA frente a los distintos antígenos reveló una activación mayoritaria de células T CD8+ mientras que NYVAC activó preferentemente células T CD4+ (Mooij y cols., manuscrito en revisión). Estos

resultados demuestran que tal y como habíamos planteado, MVA y NYVAC inducen respuestas inmunológicas diferentes.

Existen varios factores que podrían explicar los diferentes mecanismos de inducción de la respuesta inmune. Evidencias recientes indican que tanto para la expansión clonal de las células T CD8+ como para el desarrollo de sus funciones efectoras o el establecimiento de una población de memoria, es necesario la presencia de una señal de citoquinas, denominada "tercera señal" (Mescher y cols., 2006; Mescher y cols., 2007). Esta tercera señal proviene de la secreción por parte de la célula dendrítica madura de citoquinas como IL-12 y/o IFN del tipo I (IFNα/β), cuya activación es mediada por una cascada de señalización distinta a la activada por el TCR y la molécula coestimuladora CD28. Si analizamos el perfil de genes activados tras la infección con MVA de células dendríticas humanas (Guerra y cols., 2007) podemos observar que existe un aumento significativo en la expresión a nivel de ARN mensajero de genes como IL-12, IFN-α e IFN-β, así como un incremento del factor regulador del IFN IRF-7 y de proteínas implicadas en la producción de IFN tipo I como RIG-I o MDA5. Consecuentemente, se observa una mayor regulación de genes estimulados por IFN (ISGs) como ISG56, ISG60 o SCYB10. Además, el programa de diferenciación activado por la secreción de IL-12 junto con IFNα/β incrementa la expresión de un gran número de genes implicados en otras funciones como el gen GADD45B (Lu, 2006) o el factor de transcripción NFAT5 (Sundrud y Rao, 2007) que intervienen en la regulación de las células efectoras; o genes implicados en la señal de transducción (MAP2K5) y en la regulación del ciclo celular (Ciclina B1); o miembros de la familia de los TNF (Anel y cols., 2007). Todos ellos se encuentran consistentemente aumentados durante la infección por MVA. Además, otros genes implicados en la modulación de la respuesta inmune como los de las citoquinas pro-inflamatorias o las β-quimioquinas también se expresaron diferencialmente en las células infectadas con MVA o NYVAC. Todos estos datos apoyan la preferencia de MVA en la estimulación de células T CD8+.

Está descrito que una exposición relativamente corta del antígeno es suficiente para la correcta expansión clonal y diferenciación de los linfocitos T CD8+, pero contrariamente, para las células T CD4+ es necesario una mayor persistencia del antígeno para superar su fase de expansión (Obst y cols., 2005). La mayor persistencia del antígeno *"in vivo"* durante la infección por NYVAC respecto a MVA demostrada en este trabajo puede ser el determinante de que en los macacos vacunados con NYVAC se potencie preferentemente una respuesta de células T CD4+. Además, no podemos descartar que la apoptosis inducida tras la infección por NYVAC pueda contribuir de forma diferencial a la respuesta inmune generada por ambos vectores (Albert, 2004).

En conjunto, todos estos datos demuestran claramente cómo la interacción entre el virus y el huésped puede determinar el tipo de respuesta inmunológica inducida por un determinado vector y cómo las deleciones introducidas en uno u otro vector influyen sobre su capacidad inmunogénica. Estos resultados ponen de manifiesto la necesidad de estudios comparativos con diferentes vectores virales que expresen el mismo antígeno ya que, de esta forma, podremos identificar el papel que juega la respuesta inmunológica generada por el propio vector en la generación de una respuesta eficaz frente a un determinado patógeno.

En la actualidad, algunos de los vectores descritos en este trabajo ya se encuentran en fase clínica de experimentación dentro del proyecto EuroVac. Hasta la fecha se han llevado a cabo dos ensayos clínicos en fase I con NYVAC-C obteniéndose resultados muy prometedores. El primero, realizado sólo con NYVAC-C, sirvió para demostrar la seguridad e inmunogenicidad de este vector. En el segundo, iniciado en el año 2005, se evaluó la seguridad e inmunogenicidad del protocolo de inmunización que combina el vector ADN-C seguido de una dosis con el poxvirus NYVAC-C (Harari y cols.,J. Exp. Med, en revisión). Los resultados de este ensayo demuestran que la combinación es segura y que se produce un incremento considerable de la respuesta inmune frente a los antígenos del VIH en los voluntarios inmunizados. Los resultados de este ensayo son relevantes ya que con este protocolo de inmunización se consigue que el 90% de los individuos vacunados respondan frente a al menos uno de los antígenos incluidos en los inmunógenos, algo que no se había conseguido con otros protocolos de inmunización y que había frustrado las aspiraciones de muchos grupos que intentaban desarrollar una vacuna frente al VIH/SIDA. En este ensayo, la respuesta inmune también fue dirigida mayoritariamente frente a la proteína de la envuelta. El siguiente ensayo clínico en fase II se iniciará a finales del año 2007 con el mismo protocolo ADN/NYVAC pero con un mayor número de voluntarios y se está planificando un ensayo de eficacia en fase IIb para realizarlo con unos 2000 voluntarios en África.

En relación al vector MVA-B, en el año 2007 se ha iniciado en Holanda un ensayo terapéutico con pacientes seropositivos con niveles de CD4 en sangre por encima de 200/mL. El objetivo del estudio será demostrar si se puede aumentar la respuesta inmune celular, especialmente de linfocitos T CD8+ y mantener la población de linfocitos T CD4+ en los individuos infectados. Por otro lado, nuestro laboratorio en colaboración con los hospitales Clinic de Barcelona y Gregorio Marañón de Madrid, ha iniciado los trámites para realizar un ensayo profiláctico en fase I en España con el vector MVA-B. El objetivo es demostrar su inmunogenicidad en voluntarios sanos y se espera iniciar el ensayo a principio de 2008.

En los próximos años veremos los resultados procedentes de éstos y otros ensayos que sin duda nos ayudaran a mejorar el diseño de futuros nuevos candidatos vacunales frente al VIH/SIDA que logren controlar la pandemia.

Conclusiones

Con los datos obtenidos en este estudio podemos establecer las siguientes conclusiones:

1. El estudio morfológico por microscopía de contraste de fase revela que NYVAC induce un efecto citopático más severo que MVA en células en cultivo.

2. El estudio a nivel bioquímico en líneas celulares no permisivas de origen humano y murino reveló que, a diferencia de MVA, la infección por NYVAC produce una inhibición a nivel traducional de la síntesis de ciertas proteínas estructurales tardías (A17, A27 y L1) y altos niveles de apoptosis dependiente de la activación de las caspasas.

3. El análisis por microscopía electronica de células HeLa infectadas con NYVAC demuestra que existe un bloqueo en la morfogénesis que afecta a la formación y maduración de los viriones, además se obserban signos característicos de una muerte celular por apoptosis.

4. La reinserción del gen *C7L* en el genoma de NYVAC es suficiente para recuperar la capacidad del virus para replicar en células de origen humano e inhibir la apoptosis. El nuevo recombinante NYVAC-C7L, a pesar de replicar “in vivo” mantiene un fenotipo atenuado en ratón.

5. Experimentos en ratones BALB/c demuestran que la expresión del gen marcador luciferasa es transitoria para ambos vectores. En MVA se limita a las primeras 24 horas, mientras que con NYVAC la señal se mantiene por un periodo de tiempo superior a las 72 horas después de su inoculación.

6. Las rutas de administración intraperitoneal e intramuscular son muy eficaces para la expresión de antígenos virales desde recombinantes basados en las cepas MVA y NYVAC. Por el contrario, su utilización por ruta de mucosas la expresión del antígeno es más limitada (intranasal e intrarrectal).

7. Recombinantes basados en las cepas atenuadas MVA y NYVAC que expresan cuatro antígenos del VIH-1 (Env, Gag, Pol y Nef) han demostrado su estabilidad durante pases sucesivos.

8. En modelo experimental de ratón (BALB/c y HHD) se han desarrollado procedimientos de inmunización combinada de vectores de ADN y poxvirus ("*prime-booster*") que inducen una respuesta inmune específica frente a los antígenos del VIH-1.

9. Se ha demostrado a nivel preclínico que la amplitud y magnitud de la respuesta inmune antígeno-específica frente al VIH-1 puede modularse utilizando distintas estrategias de inmunización.

10. Este estudio demuestra la utilidad de MVA y NYVAC como vectores vacunales frente al VIH-1

Bibliografía

Albert, M. L. (2004). Death-defying immunity: do apoptotic cells influence antigen processing and presentation? *Nat Rev Immunol* **4**(3)**,** 223-31.

Albert, M. L., Sauter, B., and Bhardwaj, N. (1998). Dendritic cells acquire antigen from apoptotic cells and induce class I-restricted CTLs. *Nature* **392**(6671)**,** 86-9.

Alcami, J., Joseph Munne, J., Munoz-Fernandez, M. A., and Esteban, M. (2005). Current situation in the development of a preventive HIV vaccine. *Enferm Infecc Microbiol Clin* **23**(Supl.2)**,** 15-24.

Amara, R. R., Ibegbu, C., Villinger, F., Montefiori, D. C., Sharma, S., Nigam, P., Xu, Y., McClure, H. M., and Robinson, H. L. (2005). Studies using a viral challenge and CD8 T cell depletions on the roles of cellular and humoral immunity in the control of an SHIV-89.6P challenge in DNA/MVA-vaccinated macaques. *Virology* **343**(2)**,** 246-55.

Amara, R. R., Villinger, F., Altman, J. D., Lydy, S. L., O'Neil, S. P., Staprans, S. I., Montefiori, D. C., Xu, Y., Herndon, J. G., Wyatt, L. S., Candido, M. A., Kozyr, N. L., Earl, P. L., Smith, J. M., Ma, H. L., Grimm, B. D., Hulsey, M. L., Miller, J., McClure, H. M., McNicholl, J. M., Moss, B., and Robinson, H. L. (2001). Control of a mucosal challenge and prevention of AIDS by a multiprotein DNA/MVA vaccine. *Science* **292**(5514)**,** 69-74.

Amara, R. R., Villinger, F., Staprans, S. I., Altman, J. D., Montefiori, D. C., Kozyr, N. L., Xu, Y., Wyatt, L. S., Earl, P. L., Herndon, J. G., McClure, H. M., Moss, B., and Robinson, H. L. (2002). Different patterns of immune responses but similar control of a simian-human immunodeficiency virus 89.6P mucosal challenge by modified vaccinia virus Ankara (MVA) and DNA/MVA vaccines. *J Virol* **76**(15)**,** 7625-31.

Amato, R. J. (2007). 5T4-modified vaccinia ankara: progress in tumor-associated antigen-based immunotherapy. *Expert Opin Biol Ther* **7**(9)**,** 1463-9.

Anderson, R., and Dales, S. (1978). Biogenesis of poxviruses: glycolipid metabolism in vaccinia-infected cells. *Virology* **84**(1)**,** 108-17.

Anel, A., Bosque, A., Naval, J., Pineiro, A., Larrad, L., Alava, M. A., and Martinez-Lorenzo, M. J. (2007). Apo2L/TRAIL and immune regulation. *Front Biosci* **12,** 2074-84.

Antoine, G., Scheiflinger, F., Dorner, F., and Falkner, F. G. (1998). The complete genomic sequence of the modified vaccinia Ankara strain: comparison with other orthopoxviruses. *Virology* **244**(2)**,** 365-96.

Bablanian, R., Baxt, B., Sonnabend, J. A., and Esteban, M. (1978a). Studies on the mechanisms of vaccinia virus cytopathic effects. II. Early cell rounding is associated with virus polypeptide synthesis. *J Gen Virol* **39**(3)**,** 403-13.

Bablanian, R., Coppola, G., Scribani, S., and Esteban, M. (1981a). Inhibition of protein synthesis by vaccinia virus. III. The effect of ultraviolet-irradiated virus on the inhibition of protein synthesis. *Virology* **112**(1)**,** 1-12.

Bablanian, R., Coppola, G., Scribani, S., and Esteban, M. (1981b). Inhibition of protein synthesis by vaccinia virus. IV. The role of low-molecular-weight viral RNA in the inhibition of protein synthesis. *Virology* **112**(1)**,** 13-24.

Bablanian, R., Esteban, M., Baxt, B., and Sonnabend, J. A. (1978b). Studies on the mechanisms of vaccina virus cytopathic effects. I. Inhibition of protein synthesis in infected cells is associated with virus-induced RNA synthesis. *J Gen Virol* **39**(3)**,** 391-402.

Bair, C. H., Chung, C. S., Vasilevskaya, I. A., and Chang, W. (1996). Isolation and characterization of a Chinese hamster ovary mutant cell line with altered sensitivity to vaccinia virus killing. *J Virol* **70**(7)**,** 4655-66.

Barouch, D. H., Kunstman, J., Glowczwskie, J., Kunstman, K. J., Egan, M. A., Peyerl, F. W., Santra, S., Kuroda, M. J., Schmitz, J. E., Beaudry, K., Krivulka, G. R., Lifton, M. A., Gorgone, D. A., Wolinsky, S. M., and Letvin, N. L. (2003). Viral escape from dominant simian immunodeficiency virus epitope-specific cytotoxic T lymphocytes in DNA-vaccinated rhesus monkeys. *J Virol* **77**(13)**,** 7367-75.

Barouch, D. H., Kunstman, J., Kuroda, M. J., Schmitz, J. E., Santra, S., Peyerl, F. W., Krivulka, G. R., Beaudry, K., Lifton, M. A., Gorgone, D. A., Montefiori, D. C., Lewis, M. G., Wolinsky, S. M., and Letvin, N. L. (2002). Eventual AIDS vaccine failure in a rhesus monkey by viral escape from cytotoxic T lymphocytes. *Nature* **415**(6869)**,** 335-9.

Barouch, D. H., Santra, S., Schmitz, J. E., Kuroda, M. J., Fu, T. M., Wagner, W., Bilska, M., Craiu, A., Zheng, X. X., Krivulka, G. R., Beaudry, K., Lifton, M. A., Nickerson, C. E., Trigona, W. L., Punt, K., Freed, D. C., Guan, L., Dubey, S., Casimiro, D., Simon, A., Davies, M. E., Chastain, M., Strom, T. B., Gelman, R. S., Montefiori, D. C., Lewis, M. G., Emini, E. A., Shiver, J. W., and Letvin, N. L. (2000). Control of viremia and prevention of clinical AIDS in rhesus monkeys by cytokine-augmented DNA vaccination. *Science* **290**(5491)**,** 486-92.

Bayes, M., Rabasseda, X., and Prous, J. R. (2005). Gateways to clinical trials. *Methods Find Exp Clin Pharmacol* **27**(1)**,** 49-77.

Belyakov, I. M., Earl, P., Dzutsev, A., Kuznetsov, V. A., Lemon, M., Wyatt, L. S., Snyder, J. T., Ahlers, J. D., Franchini, G., Moss, B., and Berzofsky, J. A. (2003). Shared modes of protection against poxvirus infection by attenuated and conventional smallpox vaccine viruses. *Proc Natl Acad Sci U S A* **100**(16)**,** 9458-63.

Benson, J., Chougnet, C., Robert-Guroff, M., Montefiori, D., Markham, P., Shearer, G., Gallo, R. C., Cranage, M., Paoletti, E., Limbach, K., Venzon, D., Tartaglia, J., and Franchini, G. (1998). Recombinant vaccine-induced protection against the highly pathogenic simian immunodeficiency virus SIV(mac251): dependence on route of challenge exposure. *J Virol* **72**(5)**,** 4170-82.

Berger, E. A., Murphy, P. M., and Farber, J. M. (1999). Chemokine receptors as HIV-1 coreceptors: roles in viral entry, tropism, and disease. *Annu Rev Immunol* **17,** 657-700.

Bergoin, M., Devauchelle, G., and Vago, C. (1971). Electron microscopy study of Melolontha poxvirus: the fine structure of occluded virions. *Virology* **43**(2)**,** 453-67.

Blanchard, T. J., Alcami, A., Andrea, P., and Smith, G. L. (1998). Modified vaccinia virus Ankara undergoes limited replication in human cells and lacks several immunomodulatory proteins: implications for use as a human vaccine. *J Gen Virol* **79 (Pt 5),** 1159-67.

Borrow, P., Evans, C. F., and Oldstone, M. B. (1995). Virus-induced immunosuppression: immune system-mediated destruction of virus-infected dendritic cells results in generalized immune suppression. *J Virol* **69**(2)**,** 1059-70.

Brave, A., Boberg, A., Gudmundsdotter, L., Rollman, E., Hallermalm, K., Ljungberg, K., Blomberg, P., Stout, R., Paulie, S., Sandstrom, E., Biberfeld, G., Earl, P., Moss, B., Cox, J. H., and Wahren, B. (2007). A New Multi-clade DNA Prime/Recombinant MVA Boost Vaccine Induces Broad and High Levels of HIV-1-specific CD8(+) T-cell and Humoral Responses in Mice. *Mol Ther* **15**(9)**,** 1724-33.

Brooks, M. A., Ali, A. N., Turner, P. C., and Moyer, R. W. (1995). A rabbitpox virus serpin gene controls host range by inhibiting apoptosis in restrictive cells. *J Virol* **69**(12)**,** 7688-98.

Broyles, S. S. (2003). Vaccinia virus transcription. *J Gen Virol* **84**(Pt 9)**,** 2293-303.

Buller, R. M. (1985). The BALB/c mouse as a model to study orthopoxviruses. *Curr Top Microbiol Immunol* **122,** 148-53.

Buller, R. M., and Palumbo, G. J. (1991). Poxvirus pathogenesis. *Microbiol Rev* **55**(1)**,** 80-122.

Buller, R. M., Smith, G. L., Cremer, K., Notkins, A. L., and Moss, B. (1985). Decreased virulence of recombinant vaccinia virus expression vectors is associated with a thymidine kinase-negative phenotype. *Nature* **317**(6040)**,** 813-5.

Cao, Y., Qin, L., Zhang, L., Safrit, J., and Ho, D. D. (1995). Virologic and immunologic characterization of long-term survivors of human immunodeficiency virus type 1 infection. *N Engl J Med* **332**(4)**,** 201-8.

Carrasco, L. A., JM (2006). "Virus Patógenos." Helice.

Carroll, M. W., and Moss, B. (1997a). Host range and cytopathogenicity of the highly attenuated MVA strain of vaccinia virus: propagation and generation of recombinant viruses in a nonhuman mammalian cell line. *Virology* **238**(2)**,** 198-211.

Carroll, M. W., Overwijk, W. W., Chamberlain, R. S., Rosenberg, S. A., Moss, B., and Restifo, N. P. (1997b). Highly attenuated modified vaccinia virus Ankara (MVA) as an effective recombinant vector: a murine tumor model. *Vaccine* **15**(4)**,** 387-94.

Chahroudi, A., Chavan, R., Kozyr, N., Waller, E. K., Silvestri, G., and Feinberg, M. B. (2005). Vaccinia virus tropism for primary hematolymphoid cells is determined by restricted expression of a unique virus receptor. *J Virol* **79**(16)**,** 10397-407.

Chahroudi, A., Garber, D. A., Reeves, P., Liu, L., Kalman, D., and Feinberg, M. B. (2006). Differences and similarities in viral life cycle progression and host cell physiology after infection of human dendritic cells with modified vaccinia virus Ankara and vaccinia virus. *J Virol* **80**(17)**,** 8469-81.

Chang, A., and Metz, D. H. (1976). Further investigations on the mode of entry of vaccinia virus into cells. *J Gen Virol* **32**(2)**,** 275-82.

Chang, W., Hsiao, J. C., Chung, C. S., and Bair, C. H. (1995). Isolation of a monoclonal antibody which blocks vaccinia virus infection. *J Virol* **69**(1)**,** 517-22.

Child, S. J., Palumbo, G. J., Buller, R. M., and Hruby, D. E. (1990). Insertional inactivation of the large subunit of ribonucleotide reductase encoded by vaccinia virus is associated with reduced virulence in vivo. *Virology* **174**(2)**,** 625-9.

Cyrklaff, M., Risco, C., Fernandez, J. J., Jimenez, M. V., Esteban, M., Baumeister, W., and Carrascosa, J. L. (2005). Cryo-electron tomography of vaccinia virus. *Proc Natl Acad Sci U S A* **102**(8)**,** 2772-7.

Dales, S. (1965). Replication Of Animal Viruses As Studied By Electron Microscopy. *Am J Med* **38,** 699-715.

Dales, S., and Pogo, B. G. (1981). Biology of poxviruses. *Virol Monogr* **18,** 1-109.

Dallo, S., and Esteban, M. (1987). Isolation and characterization of attenuated mutants of vaccinia virus. *Virology* **159**(2)**,** 408-22.

Davison, A. J., and Moss, B. (1989a). Structure of vaccinia virus early promoters. *J Mol Biol* **210**(4)**,** 749-69.

Davison, A. J., and Moss, B. (1989b). Structure of vaccinia virus late promoters. *J Mol Biol* **210**(4)**,** 771-84.

de Haro, C., Mendez, R., and Santoyo, J. (1996). The eIF-2alpha kinases and the control of protein synthesis. *Faseb J* **10**(12)**,** 1378-87.

del Real, G., Llorente, M., Bosca, L., Hortelano, S., Serrano, A., Lucas, P., Gomez, L., Toran, J. L., Redondo, C., and Martinez, C. (1998). Suppression of HIV-1 infection in linomide-treated SCID-hu-PBL mice. *Aids* **12**(8)**,** 865-72.

Doms, R. W., Blumenthal, R., and Moss, B. (1990). Fusion of intra- and extracellular forms of vaccinia virus with the cell membrane. *J Virol* **64**(10)**,** 4884-92.

Doyle, T. C., Burns, S. M., and Contag, C. H. (2004). In vivo bioluminescence imaging for integrated studies of infection. *Cell Microbiol* **6**(4)**,** 303-17.

Drexler, I., Staib, C., and Sutter, G. (2004). Modified vaccinia virus Ankara as antigen delivery system: how can we best use its potential? *Curr Opin Biotechnol* **15**(6)**,** 506-12.

Drillien, R., Koehren, F., and Kirn, A. (1981). Host range deletion mutant of vaccinia virus defective in human cells. *Virology* **111**(2)**,** 488-99.

Dulbecco, R., and Freeman, G. (1959). Plaque production by the polyoma virus. *Virology* **8**(3)**,** 396-7.

Earl, P. L., Americo, J. L., Wyatt, L. S., Anne Eller, L., Montefiori, D. C., Byrum, R., Piatak, M., Lifson, J. D., Rao Amara, R., Robinson, H. L., Huggins, J. W., and Moss, B. (2007). Recombinant modified vaccinia virus Ankara provides durable protection against disease caused by an immunodeficiency virus as well as long-term immunity to an orthopoxvirus in a non-human primate. *Virology* **366**(1)**,** 84-97.

Eccleston, A. (1997). Chemokine inhibitors for HIV. *Nat Biotechnol* **15**(8)**,** 709, 710.

Edinger, M., Sweeney, T. J., Tucker, A. A., Olomu, A. B., Negrin, R. S., and Contag, C. H. (1999). Noninvasive assessment of tumor cell proliferation in animal models. *Neoplasia* **1**(4)**,** 303-10.

Esposito, J. J., Obijeski, J. F., and Nakano, J. H. (1977a). Serological relatedness of monkeypox, variola, and vaccinia viruses. *J Med Virol* **1**(1)**,** 35-47.

Esposito, J. J., Obijeski, J. F., and Nakano, J. H. (1977b). The virion and soluble antigen proteins of variola, monkeypox, and vaccinia viruses. *J Med Virol* **1**(2)**,** 95-110.

Essani, K., and Dales, S. (1979). Biogenesis of vaccinia: evidence for more than 100 polypeptides in the virion. *Virology* **95**(2)**,** 385-94.

Estcourt, M. J., Letourneau, S., McMichael, A. J., and Hanke, T. (2005). Vaccine route, dose and type of delivery vector determine patterns of primary CD8+ T cell responses. *Eur J Immunol* **35**(9)**,** 2532-40.

Esteban, M., Flores, L., and Holowczak, J. A. (1977). Model for vaccinia virus DNA replication. *Virology* **83**(2)**,** 467-73.

Excler, J. L., and Plotkin, S. (1997). The prime-boost concept applied to HIV preventive vaccines. *Aids* **11 Suppl A,** S127-37.

Fenner, F. (1989). Risks and benefits of vaccinia vaccine use in the worldwide smallpox eradication campaign. *Res Virol* **140**(5)**,** 465-6; discussion 487-91.

Fenner, F., and Burnet, F. M. (1957). A short description of the poxvirus group (vaccinia and related viruses). *Virology* **4**(2)**,** 305-14.

Fenner, F., Henderson, D. A., Arita, I., Jezek, A., and ladnyi, I. D. (1988a). "Smallpox and its erradication." World Health Organization, Geneva.

Fenner, F., and Nakano, J. H. (1988b). "Poxviridae." Laboratory diagnosis of infectious diseases: principles and practise (Springer-Verlag, Ed.), 2, New York.

Franchini, G., Benson, J., Gallo, R., Paoletti, E., and Tartaglia, J. (1996). Attenuated poxvirus vectors as carriers in vaccines against human T cell leukemia-lymphoma virus type I. *AIDS Res Hum Retroviruses* **12**(5)**,** 407-8.

Franchini, G., Gurunathan, S., Baglyos, L., Plotkin, S., and Tartaglia, J. (2004). Poxvirus-based vaccine candidates for HIV: two decades of experience with special emphasis on canarypox vectors. *Expert Rev Vaccines* **3**(4 Suppl)**,** S75-88.

Gallego-Gomez, J. C., Risco, C., Rodriguez, D., Cabezas, P., Guerra, S., Carrascosa, J. L., and Esteban, M. (2003). Differences in virus-induced cell morphology and in virus maturation between MVA and other strains (WR, Ankara, and NYCBH) of vaccinia virus in infected human cells. *J Virol* **77**(19)**,** 10606-22.

Gallimore, A., Cranage, M., Cook, N., Almond, N., Bootman, J., Rud, E., Silvera, P., Dennis, M., Corcoran, T., Stott, J., and et al. (1995). Early suppression of SIV replication by CD8+ nef-specific cytotoxic T cells in vaccinated macaques. *Nat Med* **1**(11)**,** 1167-73.

Gao, X., Bashirova, A., Iversen, A. K., Phair, J., Goedert, J. J., Buchbinder, S., Hoots, K., Vlahov, D., Altfeld, M., O'Brien, S. J., and Carrington, M. (2005). AIDS restriction HLA allotypes target distinct intervals of HIV-1 pathogenesis. *Nat Med* **11**(12)**,** 1290-2.

Garber, D. A., and Feinberg, M. B. (2003). AIDS vaccine development: the long and winding road. *AIDS Rev* **5**(3)**,** 131-9.

Gasteiger, G., Kastenmuller, W., Ljapoci, R., Sutter, G., and Drexler, I. (2007). Crosspriming of Cytotoxic T-cells Dictates Antigen Requisites for MVA Vector Vaccines. *J Virol*.

Gauduin, M. C., Parren, P. W., Weir, R., Barbas, C. F., Burton, D. R., and Koup, R. A. (1997). Passive immunization with a human monoclonal antibody protects hu-PBL-SCID mice against challenge by primary isolates of HIV-1. *Nat Med* **3**(12)**,** 1389-93.

Gea-Banacloche, J. C., Migueles, S. A., Martino, L., Shupert, W. L., McNeil, A. C., Sabbaghian, M. S., Ehler, L., Prussin, C., Stevens, R., Lambert, L., Altman, J.,

Hallahan, C. W., de Quiros, J. C., and Connors, M. (2000). Maintenance of large numbers of virus-specific CD8+ T cells in HIV-infected progressors and long-term nonprogressors. *J Immunol* **165**(2)**,** 1082-92.

Gherardi, M. M., and Esteban, M. (2005). Recombinant poxviruses as mucosal vaccine vectors. *J Gen Virol* **86**(Pt 11)**,** 2925-36.

Gherardi, M. M., Najera, J. L., Perez-Jimenez, E., Guerra, S., Garcia-Sastre, A., and Esteban, M. (2003). Prime-boost immunization schedules based on influenza virus and vaccinia virus vectors potentiate cellular immune responses against human immunodeficiency virus Env protein systemically and in the genitorectal draining lymph nodes. *J Virol* **77**(12)**,** 7048-57.

Gillard, S., Spehner, D., Drillien, R., and Kirn, A. (1986). Localization and sequence of a vaccinia virus gene required for multiplication in human cells. *Proc Natl Acad Sci U S A* **83**(15)**,** 5573-7.

Girard, M. P., Osmanov, S. K., and Kieny, M. P. (2006). A review of vaccine research and development: the human immunodeficiency virus (HIV). *Vaccine* **24**(19)**,** 4062-81.

Goebel, S. J., Johnson, G. P., Perkus, M. E., Davis, S. W., Winslow, J. P., and Paoletti, E. (1990). The complete DNA sequence of vaccinia virus. *Virology* **179**(1)**,** 247-66, 517-63.

Gomez, C. E., Najera, J. L., Jimenez, E. P., Jimenez, V., Wagner, R., Graf, M., Frachette, M. J., Liljestrom, P., Pantaleo, G., and Esteban, M. (2007a). Head-to-head comparison on the immunogenicity of two HIV/AIDS vaccine candidates based on the attenuated poxvirus strains MVA and NYVAC co-expressing in a single locus the HIV-1BX08 gp120 and HIV-1(IIIB) Gag-Pol-Nef proteins of clade B. *Vaccine* **25**(15)**,** 2863-85.

Gomez, C. E., Najera, J. L., Jimenez, V., Bieler, K., Wild, J., Kostic, L., Heidari, S., Chen, M., Frachette, M. J., Pantaleo, G., Wolf, H., Liljestrom, P., Wagner, R., and Esteban, M. (2007b). Generation and immunogenicity of novel HIV/AIDS vaccine candidates targeting HIV-1 Env/Gag-Pol-Nef antigens of clade C. *Vaccine* **25**(11)**,** 1969-92.

Gomez, C. E., Rodriguez, D., Rodriguez, J. R., Abaitua, F., Duarte, C., and Esteban, M. (2001). Enhanced CD8+ T cell immune response against a V3 loop multi-epitope polypeptide (TAB13) of HIV-1 Env after priming with purified fusion protein and booster with modified vaccinia virus Ankara (MVA-TAB) recombinant: a comparison of humoral and cellular immune responses with the vaccinia virus Western Reserve (WR) vector. *Vaccine* **20**(5-6)**,** 961-71.

Gomez, C. E., Vandermeeren, A. M., Garcia, M. A., Domingo-Gil, E., and Esteban, M. (2005). Involvement of PKR and RNase L in translational control and induction of

apoptosis after Hepatitis C polyprotein expression from a vaccinia virus recombinant. *Virol J* **2,** 81.

Goulder, P. J., and Watkins, D. I. (2004). HIV and SIV CTL escape: implications for vaccine design. *Nat Rev Immunol* **4**(8)**,** 630-40.

Graham, B. S. (2002). Clinical trials of HIV vaccines. *Annu Rev Med* **53,** 207-21.

Griffiths, G., Roos, N., Schleich, S., and Locker, J. K. (2001a). Structure and assembly of intracellular mature vaccinia virus: thin-section analyses. *J Virol* **75**(22)**,** 11056-70.

Griffiths, G., Wepf, R., Wendt, T., Locker, J. K., Cyrklaff, M., and Roos, N. (2001b). Structure and assembly of intracellular mature vaccinia virus: isolated-particle analysis. *J Virol* **75**(22)**,** 11034-55.

Guerra, S., Lopez-Fernandez, L. A., Conde, R., Pascual-Montano, A., Harshman, K., and Esteban, M. (2004). Microarray analysis reveals characteristic changes of host cell gene expression in response to attenuated modified vaccinia virus Ankara infection of human HeLa cells. *J Virol* **78**(11)**,** 5820-34.

Guerra, S., Lopez-Fernandez, L. A., Pascual-Montano, A., Najera, J. L., Zaballos, A., and Esteban, M. (2006). Host response to the attenuated poxvirus vector NYVAC: upregulation of apoptotic genes and NF-kappaB-responsive genes in infected HeLa cells. *J Virol* **80**(2)**,** 985-98.

Guerra, S., Najera, J. L., Gonzalez, J. M., Lopez-Fernandez, L. A., Climent, N., Gatell, J. M., Gallart, T., and Esteban, M. (2007). Distinct gene expression profiling after infection of immature human monocyte-derived dendritic cells by the attenuated poxvirus vectors MVA and NYVAC. *J Virol* **81**(16)**,** 8707-21.

Halsell, J. S., Riddle, J. R., Atwood, J. E., Gardner, P., Shope, R., Poland, G. A., Gray, G. C., Ostroff, S., Eckart, R. E., Hospenthal, D. R., Gibson, R. L., Grabenstein, J. D., Arness, M. K., and Tornberg, D. N. (2003). Myopericarditis following smallpox vaccination among vaccinia-naive US military personnel. *Jama* **289**(24)**,** 3283-9.

Hanke, T., Blanchard, T. J., Schneider, J., Hannan, C. M., Becker, M., Gilbert, S. C., Hill, A. V., Smith, G. L., and McMichael, A. (1998). Enhancement of MHC class I-restricted peptide-specific T cell induction by a DNA prime/MVA boost vaccination regime. *Vaccine* **16**(5)**,** 439-45.

Hanke, T., Neumann, V. C., Blanchard, T. J., Sweeney, P., Hill, A. V., Smith, G. L., and McMichael, A. (1999). Effective induction of HIV-specific CTL by multi-epitope using gene gun in a combined vaccination regime. *Vaccine* **17**(6)**,** 589-96.

Harari, A., and Pantaleo, G. (2005). Understanding what makes a good versus a bad vaccine. *Eur J Immunol* **35**(9)**,** 2528-31.

Hiller, G., Eibl, H., and Weber, K. (1981). Characterization of intracellular and extracellular vaccinia virus variants: N1-isonicotinoyl-N2-3-methyl-4-

chlorobenzoylhydrazine interferes with cytoplasmic virus dissemination and release. *J Virol* **39**(3)**,** 903-13.

Hokey, D. A., and Weiner, D. B. (2006). DNA vaccines for HIV: challenges and opportunities. *Springer Semin Immunopathol* **28**(3)**,** 267-79.

Holzer, G. W., and Falkner, F. G. (1997). Construction of a vaccinia virus deficient in the essential DNA repair enzyme uracil DNA glycosylase by a complementing cell line. *J Virol* **71**(7)**,** 4997-5002.

Hruby, D. E., Lynn, D. L., Condit, R. C., and Kates, J. R. (1980). Cellular differences in the molecular mechanisms of vaccinia virus host range restriction. *J Gen Virol* **47**(2)**,** 485-8.

Hsiao, J. C., Chung, C. S., and Chang, W. (1999). Vaccinia virus envelope D8L protein binds to cell surface chondroitin sulfate and mediates the adsorption of intracellular mature virions to cells. *J Virol* **73**(10)**,** 8750-61.

Hsiao, J. C., Chung, C. S., Drillien, R., and Chang, W. (2004). The cowpox virus host range gene, CP77, affects phosphorylation of eIF2 alpha and vaccinia viral translation in apoptotic HeLa cells. *Virology* **329**(1)**,** 199-212.

Hutchens, M., and Luker, G. D. (2007). Applications of bioluminescence imaging to the study of infectious diseases. *Cell Microbiol* **9**(10)**,** 2315-22.

Ichihashi, Y. (1996). Extracellular enveloped vaccinia virus escapes neutralization. *Virology* **217**(2)**,** 478-85.

Ink, B. S., Gilbert, C. S., and Evan, G. I. (1995). Delay of vaccinia virus-induced apoptosis in nonpermissive Chinese hamster ovary cells by the cowpox virus CHOhr and adenovirus E1B 19K genes. *J Virol* **69**(2)**,** 661-8.

Ink, B. S., and Pickup, D. J. (1989). Transcription of a poxvirus early gene is regulated both by a short promoter element and by a transcriptional termination signal controlling transcriptional interference. *J Virol* **63**(11)**,** 4632-44.

Iqbal, S. M., Ball, T. B., Kimani, J., Kiama, P., Thottingal, P., Embree, J. E., Fowke, K. R., and Plummer, F. A. (2005). Elevated T cell counts and RANTES expression in the genital mucosa of HIV-1-resistant Kenyan commercial sex workers. *J Infect Dis* **192**(5)**,** 728-38.

Janeczko, R. A., Rodriguez, J. F., and Esteban, M. (1987). Studies on the mechanism of entry of vaccinia virus in animal cells. *Arch Virol* **92**(1-2)**,** 135-50.

Jenner, E. (1798). "An inquiry into the causes and effects of the variolae vaccinae, a disease discovered in some of the western contries of England, particularly Gloucestershire, and known by the name of cowpox." Camac (L.N.B., Ed.), London.

Jensen, O. N., Houthaeve, T., Shevchenko, A., Cudmore, S., Ashford, T., Mann, M., Griffiths, G., and Krijnse Locker, J. (1996). Identification of the major membrane and core proteins of vaccinia virus by two-dimensional electrophoresis. *J Virol* **70**(11)**,** 7485-97.

Johnson, G. P., Goebel, S. J., and Paoletti, E. (1993). An update on the vaccinia virus genome. *Virology* **196**(2)**,** 381-401.

Kazanji, M., Tartaglia, J., Franchini, G., de Thoisy, B., Talarmin, A., Contamin, H., Gessain, A., and de The, G. (2001). Immunogenicity and protective efficacy of recombinant human T-cell leukemia/lymphoma virus type 1 NYVAC and naked DNA vaccine candidates in squirrel monkeys (Saimiri sciureus). *J Virol* **75**(13)**,** 5939-48.

Kegeles, S. M., Johnson, M. O., Strauss, R. P., Ralston, B., Hays, R. B., Metzger, D. S., McLellan-Lemal, E., and MacQueen, K. M. (2006). How should HIV vaccine efficacy trials be conducted? Diverse U.S. communities speak out. *AIDS Educ Prev* **18**(6)**,** 560-72.

Kent, S. J., and Lewis, I. M. (1998). Genetically identical primate modelling systems for HIV vaccines. *Reprod Fertil Dev* **10**(7-8)**,** 651-7.

Kettle, S., Alcami, A., Khanna, A., Ehret, R., Jassoy, C., and Smith, G. L. (1997). Vaccinia virus serpin B13R (SPI-2) inhibits interleukin-1beta-converting enzyme and protects virus-infected cells from TNF- and Fas-mediated apoptosis, but does not prevent IL-1beta-induced fever. *J Gen Virol* **78 (Pt 3),** 677-85.

Kieny, M. P., Lathe, R., Drillien, R., Spehner, D., Skory, S., Schmitt, D., Wiktor, T., Koprowski, H., and Lecocq, J. P. (1984). Expression of rabies virus glycoprotein from a recombinant vaccinia virus. *Nature* **312**(5990)**,** 163-6.

Kochan, G., Escors, D., Gonzalez, J. M., Casasnovas, J. M., and Esteban, M. (2007). Membrane cell fusion activity of the vaccinia virus A17-A27 protein complex. *Cell Microbiol*.

Koup, R. A., Safrit, J. T., Cao, Y., Andrews, C. A., McLeod, G., Borkowsky, W., Farthing, C., and Ho, D. D. (1994). Temporal association of cellular immune responses with the initial control of viremia in primary human immunodeficiency virus type 1 syndrome. *J Virol* **68**(7)**,** 4650-5.

Kreijtz, J. H., Suezer, Y., van Amerongen, G., de Mutsert, G., Schnierle, B. S., Wood, J. M., Kuiken, T., Fouchier, R. A., Lower, J., Osterhaus, A. D., Sutter, G., and Rimmelzwaan, G. F. (2007). Recombinant modified vaccinia virus Ankara-based vaccine induces protective immunity in mice against infection with influenza virus H5N1. *J Infect Dis* **195**(11)**,** 1598-606.

Kuroda, M. J., Schmitz, J. E., Charini, W. A., Nickerson, C. E., Lifton, M. A., Lord, C. I., Forman, M. A., and Letvin, N. L. (1999). Emergence of CTL coincides with clearance of virus during primary simian immunodeficiency virus infection in rhesus monkeys. *J Immunol* **162**(9)**,** 5127-33.

Lai, C. F., Gong, S. C., and Esteban, M. (1990). Structural and functional properties of the 14-kDa envelope protein of vaccinia virus synthesized in Escherichia coli. *J Biol Chem* **265**(36)**,** 22174-80.

Larsson, M., Fonteneau, J. F., Somersan, S., Sanders, C., Bickham, K., Thomas, E. K., Mahnke, K., and Bhardwaj, N. (2001). Efficiency of cross presentation of vaccinia virus-derived antigens by human dendritic cells. *Eur J Immunol* **31**(12)**,** 3432-42.

Lee, S. B., and Esteban, M. (1994). The interferon-induced double-stranded RNA-activated protein kinase induces apoptosis. *Virology* **199**(2)**,** 491-6.

Leist, M., and Jaattela, M. (2001). Four deaths and a funeral: from caspases to alternative mechanisms. *Nat Rev Mol Cell Biol* **2**(8)**,** 589-98.

Letvin, N. L. (2006). Progress and obstacles in the development of an AIDS vaccine. *Nat Rev Immunol* **6**(12)**,** 930-9.

Li, S., Rodrigues, M., Rodriguez, D., Rodriguez, J. R., Esteban, M., Palese, P., Nussenzweig, R. S., and Zavala, F. (1993). Priming with recombinant influenza virus followed by administration of recombinant vaccinia virus induces CD8+ T-cell-mediated protective immunity against malaria. *Proc Natl Acad Sci U S A* **90**(11)**,** 5214-8.

Li, Y., Yuan, S., and Moyer, R. W. (1998). The non-permissive infection of insect (gypsy moth) LD-652 cells by Vaccinia virus. *Virology* **248**(1)**,** 74-82.

Lifson, J. D., Rossio, J. L., Piatak, M., Jr., Parks, T., Li, L., Kiser, R., Coalter, V., Fisher, B., Flynn, B. M., Czajak, S., Hirsch, V. M., Reimann, K. A., Schmitz, J. E., Ghrayeb, J., Bischofberger, N., Nowak, M. A., Desrosiers, R. C., and Wodarz, D. (2001). Role of CD8(+) lymphocytes in control of simian immunodeficiency virus infection and resistance to rechallenge after transient early antiretroviral treatment. *J Virol* **75**(21)**,** 10187-99.

Liu, F., Whitton, J. L., and Slifka, M. K. (2004). The rapidity with which virus-specific CD8+ T cells initiate IFN-gamma synthesis increases markedly over the course of infection and correlates with immunodominance. *J Immunol* **173**(1)**,** 456-62.

Liu, J., Hellerstein, M., McDonnel, M., Amara, R. R., Wyatt, L. S., Moss, B., and Robinson, H. L. (2007). Dose-response studies for the elicitation of CD8 T cells by a DNA vaccine, used alone or as the prime for a modified vaccinia Ankara boost. *Vaccine* **25**(15)**,** 2951-8.

Lu, B. (2006). The molecular mechanisms that control function and death of effector CD4+ T cells. *Immunol Res* **36**(1-3)**,** 275-82.

Maa, J. S., Rodriguez, J. F., and Esteban, M. (1990). Structural and functional characterization of a cell surface binding protein of vaccinia virus. *J Biol Chem* **265**(3)**,** 1569-77.

Mascola, J. R., Snyder, S. W., Weislow, O. S., Belay, S. M., Belshe, R. B., Schwartz, D. H., Clements, M. L., Dolin, R., Graham, B. S., Gorse, G. J., Keefer, M. C., McElrath, M. J., Walker, M. C., Wagner, K. F., McNeil, J. G., McCutchan, F. E., and Burke, D. S. (1996). Immunization with envelope subunit vaccine products elicits neutralizing antibodies against laboratory-adapted but not primary isolates of human immunodeficiency virus type 1. The National Institute of Allergy and Infectious Diseases AIDS Vaccine Evaluation Group. *J Infect Dis* **173**(2)**,** 340-8.

Mascola, J. R., Stiegler, G., VanCott, T. C., Katinger, H., Carpenter, C. B., Hanson, C. E., Beary, H., Hayes, D., Frankel, S. S., Birx, D. L., and Lewis, M. G. (2000). Protection of macaques against vaginal transmission of a pathogenic HIV-1/SIV chimeric virus by passive infusion of neutralizing antibodies. *Nat Med* **6**(2)**,** 207-10.

Mayr, A., Stickl, H., Muller, H. K., Danner, K., and Singer, H. (1978). [The smallpox vaccination strain MVA: marker, genetic structure, experience gained with the parenteral vaccination and behavior in organisms with a debilitated defence mechanism (author's transl)]. *Zentralbl Bakteriol [B]* **167**(5-6)**,** 375-90.

McClain, M. E. (1965). The Host Range And Plaque Morphology Of Rabbitpox Virus (Rpu+) And Its U Mutants On Chick Fibroblast, Pk-2a, And L929 Cells. *Aust J Exp Biol Med Sci* **43,** 31-44.

McFadden, G. (2005). Poxvirus tropism. *Nat Rev Microbiol* **3**(3)**,** 201-13.

Meiser, A., Boulanger, D., Sutter, G., and Krijnse Locker, J. (2003). Comparison of virus production in chicken embryo fibroblasts infected with the WR, IHD-J and MVA strains of vaccinia virus: IHD-J is most efficient in trans-Golgi network wrapping and extracellular enveloped virus release. *J Gen Virol* **84**(Pt 6)**,** 1383-92.

Mescher, A. L., Wolf, W. L., Moseman, E. A., Hartman, B., Harrison, C., Nguyen, E., and Neff, A. W. (2007). Cells of cutaneous immunity in Xenopus: studies during larval development and limb regeneration. *Dev Comp Immunol* **31**(4)**,** 383-93.

Mescher, M. F., Curtsinger, J. M., Agarwal, P., Casey, K. A., Gerner, M., Hammerbeck, C. D., Popescu, F., and Xiao, Z. (2006). Signals required for programming effector and memory development by CD8+ T cells. *Immunol Rev* **211,** 81-92.

Miller, G. (1957). "The adoption of inoculation for smallpox in England and France." Univer. of Pennsylvania Press, 137, Philadelphia.

Mooij, P., Nieuwenhuis, I. G., Knoop, C. J., Doms, R. W., Bogers, W. M., Ten Haaft, P. J., Niphuis, H., Koornstra, W., Bieler, K., Kostler, J., Morein, B., Cafaro, A., Ensoli, B., Wagner, R., and Heeney, J. L. (2004). Qualitative T-helper responses to multiple viral antigens correlate with vaccine-induced immunity to simian/human immunodeficiency virus infection. *J Virol* **78**(7)**,** 3333-42.

Moss, B. (1996). Genetically engineered poxviruses for recombinant gene expression, vaccination, and safety. *Proc Natl Acad Sci U S A* **93**(21)**,** 11341-8.

Moss, B. (2001). "Poxviridae: the viruses and their replication." 4ª ed. Fundamental Virology. Fields, p. 1249-1283 Knipe, D. M.; Howley, P. M., Philadelphia, PA 19106 USA.

Moss, B. (2006). Poxvirus entry and membrane fusion. *Virology* **344**(1)**,** 48-54.

Moss, B., Winters, E., and Cooper, J. A. (1981). Deletion of a 9,000-base-pair segment of the vaccinia virus genome that encodes nonessential polypeptides. *J Virol* **40**(2)**,** 387-95.

Najera, J. L., Gomez, C. E., Domingo-Gil, E., Gherardi, M. M., and Esteban, M. (2006). Cellular and biochemical differences between two attenuated poxvirus vaccine candidates (MVA and NYVAC) and role of the C7L gene. *J Virol* **80**(12)**,** 6033-47.

Ober, B. T., Bruhl, P., Schmidt, M., Wieser, V., Gritschenberger, W., Coulibaly, S., Savidis-Dacho, H., Gerencer, M., and Falkner, F. G. (2002). Immunogenicity and safety of defective vaccinia virus lister: comparison with modified vaccinia virus Ankara. *J Virol* **76**(15)**,** 7713-23.

Obst, R., van Santen, H. M., Mathis, D., and Benoist, C. (2005). Antigen persistence is required throughout the expansion phase of a CD4(+) T cell response. *J Exp Med* **201**(10)**,** 1555-65.

Ockenhouse, C. F., Sun, P. F., Lanar, D. E., Wellde, B. T., Hall, B. T., Kester, K., Stoute, J. A., Magill, A., Krzych, U., Farley, L., Wirtz, R. A., Sadoff, J. C., Kaslow, D. C., Kumar, S., Church, L. W., Crutcher, J. M., Wizel, B., Hoffman, S., Lalvani, A., Hill, A. V., Tine, J. A., Guito, K. P., de Taisne, C., Anders, R., Ballou, W. R., and et al. (1998). Phase I/IIa safety, immunogenicity, and efficacy trial of NYVAC-Pf7, a pox-vectored, multiantigen, multistage vaccine candidate for Plasmodium falciparum malaria. *J Infect Dis* **177**(6)**,** 1664-73.

Oguiura, N., Spehner, D., and Drillien, R. (1993). Detection of a protein encoded by the vaccinia virus C7L open reading frame and study of its effect on virus multiplication in different cell lines. *J Gen Virol* **74 (Pt 7),** 1409-13.

Oie, M., and Ichihashi, Y. (1981a). Characterization of vaccinia polypeptides. *Virology* **113**(1)**,** 263-76.

Oie, M., and Ichihashi, Y. (1981b). Target antigen of vaccinia-infected cells recognized by virus-specific cytotoxic T lymphocytes. *Microbiol Immunol* **25**(4)**,** 361-75.

Ojeda, S., Domi, A., and Moss, B. (2006). Vaccinia virus G9 protein is an essential component of the poxvirus entry-fusion complex. *J Virol* **80**(19)**,** 9822-30.

Opferman, J. T. (2007). Apoptosis in the development of the immune system. *Cell Death Differ*.

Oseroff, C., Kos, F., Bui, H. H., Peters, B., Pasquetto, V., Glenn, J., Palmore, T., Sidney, J., Tscharke, D. C., Bennink, J. R., Southwood, S., Grey, H. M., Yewdell, J. W., and Sette, A. (2005). HLA class I-restricted responses to vaccinia recognize a broad array of proteins mainly involved in virulence and viral gene regulation. *Proc Natl Acad Sci U S A* **102**(39)**,** 13980-5.

Paez, E., Dallo, S., and Esteban, M. (1985). Generation of a dominant 8-MDa deletion at the left terminus of vaccinia virus DNA. *Proc Natl Acad Sci U S A* **82**(10)**,** 3365-9.

Palmowski, M. J., Choi, E. M., Hermans, I. F., Gilbert, S. C., Chen, J. L., Gileadi, U., Salio, M., Van Pel, A., Man, S., Bonin, E., Liljestrom, P., Dunbar, P. R., and Cerundolo, V. (2002). Competition between CTL narrows the immune response induced by prime-boost vaccination protocols. *J Immunol* **168**(9)**,** 4391-8.

Pantaleo, G., Menzo, S., Vaccarezza, M., Graziosi, C., Cohen, O. J., Demarest, J. F., Montefiori, D., Orenstein, J. M., Fox, C., Schrager, L. K., and et al. (1995). Studies in subjects with long-term nonprogressive human immunodeficiency virus infection. *N Engl J Med* **332**(4)**,** 209-16.

Paoletti, E. (1996). Applications of pox virus vectors to vaccination: an update. *Proc Natl Acad Sci U S A* **93**(21)**,** 11349-53.

Patterson, L. J., Peng, B., Abimiku, A. G., Aldrich, K., Murty, L., Markham, P. D., Kalyanaraman, V. S., Alvord, W. G., Tartaglia, J., Franchini, G., and Robert-Guroff, M. (2000). Cross-protection in NYVAC-HIV-1-immunized/HIV-2-challenged but not in NYVAC-HIV-2-immunized/SHIV-challenged rhesus macaques. *Aids* **14**(16)**,** 2445-55.

Payne, L. G., and Kristenson, K. (1979). Mechanism of vaccinia virus release and its specific inhibition by N1-isonicotinoyl-N2-3-methyl-4-chlorobenzoylhydrazine. *J Virol* **32**(2)**,** 614-22.

Perez-Jimenez, E., Kochan, G., Gherardi, M. M., and Esteban, M. (2006). MVA-LACK as a safe and efficient vector for vaccination against leishmaniasis. *Microbes Infect* **8**(3)**,** 810-22.

Perkus, M. E., Goebel, S. J., Davis, S. W., Johnson, G. P., Limbach, K., Norton, E. K., and Paoletti, E. (1990). Vaccinia virus host range genes. *Virology* **179**(1)**,** 276-86.

Pincus, S., Tartaglia, J., and Paoletti, E. (1995). Poxvirus-based vectors as vaccine candidates. *Biologicals* **23**(2)**,** 159-64.

Pires de Miranda, M., Reading, P. C., Tscharke, D. C., Murphy, B. J., and Smith, G. L. (2003). The vaccinia virus kelch-like protein C2L affects calcium-independent adhesion to the extracellular matrix and inflammation in a murine intradermal model. *J Gen Virol* **84**(Pt 9)**,** 2459-71.

Poulet, H., Minke, J., Pardo, M. C., Juillard, V., Nordgren, B., and Audonnet, J. C. (2007). Development and registration of recombinant veterinary vaccines. The example of the canarypox vector platform. *Vaccine* **25**(30)**,** 5606-12.

Precopio, M. L., Betts, M. R., Parrino, J., Price, D. A., Gostick, E., Ambrozak, D. R., Asher, T. E., Douek, D. C., Harari, A., Pantaleo, G., Bailer, R., Graham, B. S., Roederer, M., and Koup, R. A. (2007). Immunization with vaccinia virus induces polyfunctional and phenotypically distinctive CD8(+) T cell responses. *J Exp Med* **204**(6)**,** 1405-16.

Raengsakulrach, B., Nisalak, A., Gettayacamin, M., Thirawuth, V., Young, G. D., Myint, K. S., Ferguson, L. M., Hoke, C. H., Jr., Innis, B. L., and Vaughn, D. W. (1999). Safety, immunogenicity, and protective efficacy of NYVAC-JEV and ALVAC-JEV recombinant Japanese encephalitis vaccines in rhesus monkeys. *Am J Trop Med Hyg* **60**(3)**,** 343-9.

Ramirez, J. C., Gherardi, M. M., and Esteban, M. (2000). Biology of attenuated modified vaccinia virus Ankara recombinant vector in mice: virus fate and activation of B- and T-cell immune responses in comparison with the Western Reserve strain and advantages as a vaccine. *J Virol* **74**(2)**,** 923-33.

Ramsey-Ewing, A., and Moss, B. (1998). Apoptosis induced by a postbinding step of vaccinia virus entry into Chinese hamster ovary cells. *Virology* **242**(1)**,** 138-49.

Ramsey-Ewing, A. L., and Moss, B. (1996). Complementation of a vaccinia virus host-range K1L gene deletion by the nonhomologous CP77 gene. *Virology* **222**(1)**,** 75-86.

Ray, C. A., and Pickup, D. J. (1996). The mode of death of pig kidney cells infected with cowpox virus is governed by the expression of the crmA gene. *Virology* **217**(1)**,** 384-91.

Ray, P., De, A., Min, J. J., Tsien, R. Y., and Gambhir, S. S. (2004). Imaging tri-fusion multimodality reporter gene expression in living subjects. *Cancer Res* **64**(4)**,** 1323-30.

Reyes-Sandoval, A., Harty, J. T., and Todryk, S. M. (2007). Viral vector vaccines make memory T cells against malaria. *Immunology* **121**(2)**,** 158-65.

Riedl, S. J., and Shi, Y. (2004). Molecular mechanisms of caspase regulation during apoptosis. *Nat Rev Mol Cell Biol* **5**(11)**,** 897-907.

Rodriguez, D., Esteban, M., and Rodriguez, J. R. (1995). Vaccinia virus A17L gene product is essential for an early step in virion morphogenesis. *J Virol* **69**(8)**,** 4640-8.

Rodriguez, F., Harkins, S., Slifka, M. K., and Whitton, J. L. (2002). Immunodominance in virus-induced CD8(+) T-cell responses is dramatically modified by DNA immunization and is regulated by gamma interferon. *J Virol* **76**(9)**,** 4251-9.

Rodriguez, J. F., Rodriguez, D., Rodriguez, J. R., McGowan, E. B., and Esteban, M. (1988). Expression of the firefly luciferase gene in vaccinia virus: a highly sensitive gene marker to follow virus dissemination in tissues of infected animals. *Proc Natl Acad Sci U S A* **85**(5)**,** 1667-71.

Rosales, R., Sutter, G., and Moss, B. (1994). A cellular factor is required for transcription of vaccinia viral intermediate-stage genes. *Proc Natl Acad Sci U S A* **91**(9)**,** 3794-8.

Ruska, H., and Kausche, G. A. (1943). Über Form, Grössenverteilung und Struktur einiger Virus-Elementarköper. *Zbl. Bakteriol. Parasitenkd. Infektionskr. Hyg.Abt. 1 Orig.* **150,** 311-318.

Sadikot, R. T., and Blackwell, T. S. (2005). Bioluminescence imaging. *Proc Am Thorac Soc* **2**(6)**,** 537-40, 511-2.

Sancho, M. C., Schleich, S., Griffiths, G., and Krijnse-Locker, J. (2002). The block in assembly of modified vaccinia virus Ankara in HeLa cells reveals new insights into vaccinia virus morphogenesis. *J Virol* **76**(16)**,** 8318-34.

Sarov, I., and Joklik, W. K. (1972). Characterization of intermediates in the uncoating of vaccinia virus DNA. *Virology* **50**(2)**,** 593-602.

Sauter, S. L., Rahman, A., and Muralidhar, G. (2005). Non-replicating viral vector-based AIDS vaccines: interplay between viral vectors and the immune system. *Curr HIV Res* **3**(2)**,** 157-81.

Schmitz, J. E., Kuroda, M. J., Santra, S., Sasseville, V. G., Simon, M. A., Lifton, M. A., Racz, P., Tenner-Racz, K., Dalesandro, M., Scallon, B. J., Ghrayeb, J., Forman, M. A., Montefiori, D. C., Rieber, E. P., Letvin, N. L., and Reimann, K. A. (1999). Control of viremia in simian immunodeficiency virus infection by CD8+ lymphocytes. *Science* **283**(5403)**,** 857-60.

Seet, B. T., Johnston, J. B., Brunetti, C. R., Barrett, J. W., Everett, H., Cameron, C., Sypula, J., Nazarian, S. H., Lucas, A., and McFadden, G. (2003). Poxviruses and immune evasion. *Annu Rev Immunol* **21,** 377-423.

Senkevich, T. G., Ward, B. M., and Moss, B. (2004a). Vaccinia virus A28L gene encodes an essential protein component of the virion membrane with intramolecular disulfide bonds formed by the viral cytoplasmic redox pathway. *J Virol* **78**(5)**,** 2348-56.

Senkevich, T. G., Ward, B. M., and Moss, B. (2004b). Vaccinia virus entry into cells is dependent on a virion surface protein encoded by the A28L gene. *J Virol* **78**(5)**,** 2357-66.

Sheppard, N. C., Bates, A. C., and Sattentau, Q. J. (2007). A functional human IgM response to HIV-1 Env after immunization with NYVAC HIV C. *Aids* **21**(4)**,** 524-7.

Shida, H., Tochikura, T., Sato, T., Konno, T., Hirayoshi, K., Seki, M., Ito, Y., Hatanaka, M., Hinuma, Y., Sugimoto, M., and et al. (1987). Effect of the recombinant vaccinia viruses that express HTLV-I envelope gene on HTLV-I infection. *Embo J* **6**(11)**,** 3379-84.

Shiver, J. W., and Emini, E. A. (2004). Recent advances in the development of HIV-1 vaccines using replication-incompetent adenovirus vectors. *Annu Rev Med* **55,** 355-72.

Shiver, J. W., Fu, T. M., Chen, L., Casimiro, D. R., Davies, M. E., Evans, R. K., Zhang, Z. Q., Simon, A. J., Trigona, W. L., Dubey, S. A., Huang, L., Harris, V. A., Long, R. S., Liang, X., Handt, L., Schleif, W. A., Zhu, L., Freed, D. C., Persaud, N. V., Guan, L., Punt, K. S., Tang, A., Chen, M., Wilson, K. A., Collins, K. B., Heidecker, G. J., Fernandez, V. R., Perry, H. C., Joyce, J. G., Grimm, K. M., Cook, J. C., Keller, P. M., Kresock, D. S., Mach, H., Troutman, R. D., Isopi, L. A., Williams, D. M., Xu, Z., Bohannon, K. E., Volkin, D. B., Montefiori, D. C., Miura, A., Krivulka, G. R., Lifton, M. A., Kuroda, M. J., Schmitz, J. E., Letvin, N. L., Caulfield, M. J., Bett, A. J., Youil, R., Kaslow, D. C., and Emini, E. A. (2002). Replication-incompetent adenoviral vaccine vector elicits effective anti-immunodeficiency-virus immunity. *Nature* **415**(6869)**,** 331-5.

Smadel, J. E., and Hoagland, C. L. (1942). Elementary Bodies Of Vaccinia. *Bacteriol Rev* **6**(2)**,** 79-110.

Smith, G. L., Vanderplasschen, A., and Law, M. (2002). The formation and function of extracellular enveloped vaccinia virus. *J Gen Virol* **83**(Pt 12)**,** 2915-31.

Soloski, M. J., and Holowczak, J. A. (1981). Characterization of supercoiled nucleoprotein complexes released from detergent-treated vaccinia virions. *J Virol* **37**(2)**,** 770-83.

Somogyi, P., Frazier, J., and Skinner, M. A. (1993). Fowlpox virus host range restriction: gene expression, DNA replication, and morphogenesis in nonpermissive mammalian cells. *Virology* **197**(1)**,** 439-44.

Stern, W., and Dales, S. (1974). Biogenesis of vaccinia: concerning the origin of the envelope phospholipids. *Virology* **62**(2)**,** 293-306.

Stittelaar, K. J., Kuiken, T., de Swart, R. L., van Amerongen, G., Vos, H. W., Niesters, H. G., van Schalkwijk, P., van der Kwast, T., Wyatt, L. S., Moss, B., and Osterhaus, A. D. (2001). Safety of modified vaccinia virus Ankara (MVA) in immune-suppressed macaques. *Vaccine* **19**(27)**,** 3700-9.

Strauss, J. H., Strauss, E. G. (2002). "Overview of viruses and virus infection." Viruses and Human Disease (A. Press, Ed.), 383p Academic Press, San Diego.

Sundrud, M. S., and Rao, A. (2007). Regulatory T-cell gene expression: ChIP'ing away at Foxp3. *Immunol Cell Biol* **85**(3)**,** 177-8.

Sutter, G., and Moss, B. (1992). Nonreplicating vaccinia vector efficiently expresses recombinant genes. *Proc Natl Acad Sci U S A* **89**(22)**,** 10847-51.

Sutter, G., and Staib, C. (2003). Vaccinia vectors as candidate vaccines: the development of modified vaccinia virus Ankara for antigen delivery. *Curr Drug Targets Infect Disord* **3**(3)**,** 263-71.

Tagaya, I., Kitamura, T., and Sano, Y. (1961). A new mutant of dermovaccinia virus. *Nature* **192,** 381-2.

Tartaglia, J., Cox, W. I., Pincus, S., and Paoletti, E. (1994). Safety and immunogenicity of recombinants based on the genetically-engineered vaccinia strain, NYVAC. *Dev Biol Stand* **82,** 125-9.

Tartaglia, J., Cox, W. I., Taylor, J., Perkus, M., Riviere, M., Meignier, B., and Paoletti, E. (1992a). Highly attenuated poxvirus vectors. *AIDS Res Hum Retroviruses* **8**(8)**,** 1445-7.

Tartaglia, J., Perkus, M. E., Taylor, J., Norton, E. K., Audonnet, J. C., Cox, W. I., Davis, S. W., van der Hoeven, J., Meignier, B., Riviere, M., and et al. (1992b). NYVAC: a highly attenuated strain of vaccinia virus. *Virology* **188**(1)**,** 217-32.

Tine, J. A., Lanar, D. E., Smith, D. M., Wellde, B. T., Schultheiss, P., Ware, L. A., Kauffman, E. B., Wirtz, R. A., De Taisne, C., Hui, G. S., Chang, S. P., Church, P., Hollingdale, M. R., Kaslow, D. C., Hoffman, S., Guito, K. P., Ballou, W. R., Sadoff, J. C., and Paoletti, E. (1996). NYVAC-Pf7: a poxvirus-vectored, multiantigen, multistage vaccine candidate for Plasmodium falciparum malaria. *Infect Immun* **64**(9)**,** 3833-44.

Townsley, A. C., and Moss, B. (2007). Two distinct low-pH steps promote entry of vaccinia virus. *J Virol* **81**(16)**,** 8613-20.

Townsley, A. C., Senkevich, T. G., and Moss, B. (2005a). The product of the vaccinia virus L5R gene is a fourth membrane protein encoded by all poxviruses that is required for cell entry and cell-cell fusion. *J Virol* **79**(17)**,** 10988-98.

Townsley, A. C., Senkevich, T. G., and Moss, B. (2005b). Vaccinia virus A21 virion membrane protein is required for cell entry and fusion. *J Virol* **79**(15)**,** 9458-69.

Traktman, P. (1991). Molecular genetic and bochemical analysis of poxvirus DNA replication. *Semin. Virol* **2,** 291-304.

Tsung, K., Yim, J. H., Marti, W., Buller, R. M., and Norton, J. A. (1996). Gene expression and cytopathic effect of vaccinia virus inactivated by psoralen and long-wave UV light. *J Virol* **70**(1)**,** 165-71.

Turner, P. a. M., RW (1998). Poxviruses and apoptosis. *Semin Virology* **8,** 453-469.

Vanderplasschen, A., Hollinshead, M., and Smith, G. L. (1998). Intracellular and extracellular vaccinia virions enter cells by different mechanisms. *J Gen Virol* **79 (Pt 4),** 877-87.

Vanderplasschen, A., and Smith, G. L. (1997). A novel virus binding assay using confocal microscopy: demonstration that the intracellular and extracellular vaccinia virions bind to different cellular receptors. *J Virol* **71**(5)**,** 4032-41.

Ventoso, I., Sanz, M. A., Molina, S., Berlanga, J. J., Carrasco, L., and Esteban, M. (2006). Translational resistance of late alphavirus mRNA to eIF2alpha phosphorylation: a strategy to overcome the antiviral effect of protein kinase PKR. *Genes Dev* **20**(1)**,** 87-100.

Vuola, J. M., Keating, S., Webster, D. P., Berthoud, T., Dunachie, S., Gilbert, S. C., and Hill, A. V. (2005). Differential immunogenicity of various heterologous prime-boost vaccine regimens using DNA and viral vectors in healthy volunteers. *J Immunol* **174**(1)**,** 449-55.

W.H.O. (1980). "The global erradication of smallpox. Final report of the global commision for the certification of smallpox erradication, Geneva, December 1979." World Health Organization, Geneva.

Webster, D. P., Dunachie, S., Vuola, J. M., Berthoud, T., Keating, S., Laidlaw, S. M., McConkey, S. J., Poulton, I., Andrews, L., Andersen, R. F., Bejon, P., Butcher, G., Sinden, R., Skinner, M. A., Gilbert, S. C., and Hill, A. V. (2005). Enhanced T cell-mediated protection against malaria in human challenges by using the recombinant poxviruses FP9 and modified vaccinia virus Ankara. *Proc Natl Acad Sci U S A* **102**(13)**,** 4836-41.

Werner, G. T., Jentzsch, U., Metzger, E., and Simon, J. (1980). Studies on poxvirus infections in irradiated animals. *Arch Virol* **64**(3)**,** 247-56.

Wright, C. F., Hubbs, A. E., Gunasinghe, S. K., and Oswald, B. W. (1998). A vaccinia virus late transcription factor copurifies with a factor that binds to a viral late promoter and is complemented by extracts from uninfected HeLa cells. *J Virol* **72**(2)**,** 1446-51.

Wright, C. F., Oswald, B. W., and Dellis, S. (2001). Vaccinia virus late transcription is activated in vitro by cellular heterogeneous nuclear ribonucleoproteins. *J Biol Chem* **276**(44)**,** 40680-6.

Wyatt, L. S., Carroll, M. W., Czerny, C. P., Merchlinsky, M., Sisler, J. R., and Moss, B. (1998). Marker rescue of the host range restriction defects of modified vaccinia virus Ankara. *Virology* **251**(2)**,** 334-42.

Wyllie, A. H. (1980). Glucocorticoid-induced thymocyte apoptosis is associated with endogenous endonuclease activation. *Nature* **284**(5756)**,** 555-6.

Yang, Y. L., Reis, L. F., Pavlovic, J., Aguzzi, A., Schafer, R., Kumar, A., Williams, B. R., Aguet, M., and Weissmann, C. (1995). Deficient signaling in mice devoid of double-stranded RNA-dependent protein kinase. *Embo J* **14**(24)**,** 6095-106.

Yuen, L., and Moss, B. (1987). Oligonucleotide sequence signaling transcriptional termination of vaccinia virus early genes. *Proc Natl Acad Sci U S A* **84**(18)**,** 6417-21.

Zavala, F., Rodrigues, M., Rodriguez, D., Rodriguez, J. R., Nussenzweig, R. S., and Esteban, M. (2001). A striking property of recombinant poxviruses: efficient inducers of in vivo expansion of primed CD8(+) T cells. *Virology* **280**(2)**,** 155-9.

Anexo

CARACTERIZACIÓN "IN VITRO" E "IN VIVO" DE LOS VECTORES ATENUADOS DE POXVIRUS MVA Y NYVAC COMO CANDIDATOS VACUNALES FRENTE AL VIH/SIDA

Memoria presentada para optar al grado de Doctor en Ciencias por

JOSÉ LUIS NÁJERA GARCÍA

Madrid, Noviembre de 2007

El Trabajo realizado por el autor en el laboratorio del Dr. Mariano Esteban en el Centro Nacional de Biotecnología ha servido para publicar los siguientes artículos, de los cuales directamente relacionados con la tesis se señalan en negrita y se incluyen en el anexo:

1. Gherardi, M.M., **Nájera, J.L.,** Pérez-Jiménez, E., Guerra, S., García-Sastre, A, and Esteban, M (2003). Prime/boost immunization schedules based on influenza and vaccinia virus (VV) vectors (MVA and WR) potentiate cellular immune responses against HIV-env protein systemically and in the genito-rectal draining lymph nodes. J. Virol 77, 7048-7057

2. Gherardi, M. M., Perez-Jimenez, E., **Nájera, J.L** and Esteban, M (2004). Induction of HIV immunity in the genital tract after intranasal delivery of a MVA vector: enhanced immunogenicity after DNA prime-modified vaccinia virus Ankara boost immunization schedule." J Immunol **172**(10): 6209-20.

3. **Guerra, S., López-Fernández, L.A., Pascual-Montano, A., Nájera, J.L., Zaballos., A, and Esteban, M (2006). Host response to the attenuated poxvirus vector NYVAC: upregulation of apoptotic genes and NF-kB-responsive genes in infected HeLa cells. J. Virol 80, 985-998**

4. **Nájera, J.L., Gómez, C.E., Domingo, E., Gherardi, M.M, and Esteban, M (2006). Cellular and biochemical differences between two attenuated poxvirus vaccine candidates (MVA and NYVAC) and role of C7L gene. J. Virol 80, 6033-6047**

5. **Gómez, C.E., Nájera, J.L., Pérez-Jiménez, E., Jiménez, V., Wagner, R., Graf, M., Franchette, M.J., Liljeström, P., Pantaleo, G., and Esteban, M (2007). Head-to-head comparison on the immunogenicity of two HIV/AIDS vaccine candidates based on the poxvirus strains MVA and NYVAC coexpressing in a single locus the HIV-1BX08 and HIV-1 Gag-Pol-Nef proteins of clade B. Vaccine 25, 2863-2885**

6. **Gómez, C.E., Nájera, J.L., Jiménez, V., Goranson, E., Liljestöm, P., Bieler, K., Wild, J., Franchette, M.J., Pantaleo, G., Wolf, H., Wagner, R, and Esteban, M. Immunogenicity of HIV/AIDS vaccine candidates targetting HIV-1 Env/Gag-Pol-Nef antigens of clade C (2007). Vaccine 25, 1969-1992**

7. **Gómez, C.E., Nájera, J.L., Domingo-Gil, E., Ochoa-Callejero, L., Gloria González-Aseguinolaza, and Esteban M, (2007). Virus distribution of the attenuated MVA and NYVAC poxvirus strains in mice. J. Gen. Virol 88, 2473-2478**

8. **Guerra, S., Nájera, J.L., González, J.M., López, L., Climent, N., Gallart, T., Gatell, J.M, and Esteban, M (2007). Distinct gene expression profiling after infection of immature human monocyte-derived dendritic cells by the attenuated poxvirus vectors MVA and NYVAC. J.Virol 81, 8707-8721**

9. **Mooij, P., Balla-Jaghjoorsingh, S.S., Koopman, G., Beenhakker, N., van Haaften, P., Baak, I., Nieuwenhuis, I., Kondova, I., Wagner ,R., Wolf, H., Gómez, C.E., Nájera,J.L., Jiménez,V., Esteban,M, and Heeney, J.L (2007). MVA versus NYVAC vectors expressing HIV-1 Env and SIV Gag/Pol/Nef induce preferential boosting of CD8+ versus CD4+T-cell responses but provide similar efficacy against SHIV89.6p challenge in Indian rhesus machaques. J. Exp. Med (submitted).**

El trabajo de Tesis también ha dado lugar a dos solicitudes de patentes, una sobre los vectores de MVA que expresan cuatro antígenos del VIH para los subtipos B y C, y otra sobre el gen C7L y su uso en vacunas y terapia génica.

- VECTORES RECOMBINANTES BASADOS EN EL VIRUS MODIFICADO DE ANKARA (MVA) COMO VACUNAS PREVENTIVAS Y TERAPEUTICAS CONTRA EL SIDA. Solicitud de invención Nº 200501841, 27 Julio, 2005. Carmen E. Gómez, **José L. Nájera**, Victoria Jiménez y Mariano Esteban

-MEJORAS INTRODUCIDAS EN EL OBJETO DE LA PATENTE PRINCIPAL Nº ES200501841 PARA VECTORES RECOMBINANTES BASADOS EN EL VIRUS MODIFICADO DE ANKARA (MVA) COMO VACUNAS PREVENTIVAS Y TERAPÉUTICAS CONTRA EL SIDA. Solicitud P200600762. 24 Marzo, 2006; PCT/ES2006/070114. Carmen E. Gómez, **José L. Nájera**, Victoria Jiménez y Mariano Esteban

- VECTORES EN LOS QUE SE INSERTA EL GEN C7L Y USO DE LOS MISMOS EN LA FABRICACION DE VACUNAS Y DE COMPOSICIONES PARA TERAPIA GÉNICA. Solicitud de Invención Nº200601240, 18 Mayo, 2006; PCT/ES2007/070091. **José Luis Nájera**, Carmen E. Gómez y Mariano Esteban.

JOURNAL OF VIROLOGY, June 2006, p. 6033–6047 Vol. 80, No. 12
0022-538X/06/$08.00+0 doi:10.1128/JVI.02108-05
Copyright © 2006, American Society for Microbiology. All Rights Reserved.

Cellular and Biochemical Differences between Two Attenuated Poxvirus Vaccine Candidates (MVA and NYVAC) and Role of the C7L Gene

José Luis Nájera, Carmen Elena Gómez, Elena Domingo-Gil, María Magdalena Gherardi,† and Mariano Esteban*

Department of Molecular and Cellular Biology, Centro Nacional de Biotecnología, CSIC, Ciudad Universitaria Cantoblanco, 28049, Madrid, Spain

Received 6 November 2005/Accepted 13 February 2006

The poxvirus strains NYVAC and MVA are two candidate vectors for the development of vaccines against a broad spectrum of diseases. Although these attenuated virus strains have proven to be safe in animals and humans, little is known about their comparative behavior in vitro. In contrast with MVA, NYVAC infection triggers greater cytopathic effect in a range of permissive and nonpermissive cell lines. The yields of NYVAC cell-associated virus in permissive cells (BHK-21) were slightly reduced compared with those of MVA infection. During the course of infection in HeLa cells, there is a translational block induced by NYVAC late in infection, which correlated with a marked increase in phosphorylation levels of the initiation factor eIF-2α. In contrast to MVA, the synthesis of certain late viral proteins was only blocked in NYVAC-infected HeLa cells. Electron microscopy (EM) analysis revealed that morphogenesis of NYVAC in HeLa cells was blocked at the stage of formation of immature viral forms. Phase-contrast microscopy, EM, flow cytometry, and rRNA analyses demonstrated that contrary to MVA, NYVAC infection induces potent apoptosis, a phenomenon dependent on activation of caspases and RNase L. Apoptosis induced by NYVAC was prevented when the virus gene C7L was placed back into the NYVAC genome, recovering the ability of NYVAC to replicate in HeLa cells and maintaining the attenuated phenotype in mice. Overall, our findings demonstrate distinct behavior between NYVAC and MVA strains in cultured cells, as well as a new role for the C7L viral gene as an inhibitor of apoptosis in NYVAC infection.

Poxvirus vectors are considered to be prime candidates for use as recombinant vaccines due to their efficient expression of the foreign antigen and unique immunological properties in eliciting long-term protective humoral and cell-mediated immune responses (44). Increased immunosuppression as a result of human immunodeficiency virus (HIV) infection, cancer treatments, and organ transplantation, in addition to the possible vaccination of the general public due to the emerging threat of smallpox bioterrorism, requires the need for the development of safe and efficacious vectors (46). Numerous approaches have been taken to enhance the safety of poxviruses. These include the replication-deficient modified vaccinia virus Ankara (MVA) (21), nonreplicating defective vaccinia virus (VV) (46), host cell-restricted vectors such as avipoxviruses (ALVAC) (72), fowlpox virus (44), and poxvirus vectors with deletions in nonessential genes (60), such as those coding for serpins (37), or host range genes, such as the NYVAC strain (71). In this regard, recombinants based on MVA or NYVAC strains are emerging as important candidates to be used as live vaccines against numerous infectious diseases and in cancer therapy.

The current widely used MVA strain was classically attenuated by growing the virus after more than 500 passages in chicken embryo fibroblasts (CEF) (40). During the course of attenuation, 15% of the parental viral genome was lost (1) as was the ability to grow in human cells and a majority of mammalian cells (15, 20, 43). MVA has been shown to be safe in humans, with no adverse side effects, as demonstrated when over 120,000 individuals were vaccinated during the smallpox eradication campaign (40). At present, first-generation recombinant MVA vaccines inducing relevant recombinant antigen-specific T-cell immunogenicity in humans have been clinically tested against infectious disorders such as AIDS, malaria, and human papillomavirus-associated cancer (for review, see reference 68).

The NYVAC vector was derived from the Copenhagen strain of VV. It was genetically attenuated by the deletion of 18 nonessential genes implicated in virulence, host range, or pathogenicity, resulting in a strain with a highly debilitated in vitro replicative capacity on cells derived from humans, mice, and equid origin, but with the ability to replicate with wild-type efficiency in CEFs and Vero cells (69–71). A number of examples employing the NYVAC vector as a recombinant vaccine delivery system have been provided in various animal models and humans with promising results (50, 52, 69). Although NYVAC is a highly attenuated virus, it retained the ability to induce a protective immune response to foreign antigens in a similar way to the thymidine kinase mutant of the parental strain (49). To date, all of the data obtained from human clinical trials using NYVAC-based vectors illustrate a positive safety profile and the induction of high levels of immunity against the expressed heterologous antigens (10, 12, 19, 23, 32, 47, 50, 53).

* Corresponding author. Mailing address: Department of Molecular and Cellular Biology, Centro Nacional de Biotecnología, CSIC, Ciudad Universitaria Cantoblanco, 28049, Madrid, Spain. Phone: 34-91-585-4553. Fax: 34-91-585-4506. E-mail: mesteban@cnb.uam.es.

† Present address: National Reference Center for AIDS, Department of Microbiology, School of Medicine, University of Buenos Aires, Buenos Aires, Argentina.

Downloaded from jvi.asm.org at Centro Nacional de Biotecnología - Biblioteca on October 15, 2007

Even though the attenuated poxvirus vectors MVA and NYVAC have been widely characterized in terms of safety and immunogenicity, a careful evaluation of the differences in MVA and NYVAC biology remains to be established. A comparative analysis of expression profiles obtained by cDNA microarray screening of over 15,000 human genes in NYVAC- or MVA-infected HeLa cells revealed that both virus strains induced common and distinct proinflammatory cytokine profiles (30, 31).

In this study, we examined the in vitro behavior of NYVAC in comparison with that of MVA using cellular and biochemical approaches. Our findings revealed distinct biological characteristics of MVA and NYVAC strains, which are likely to influence the immunogenicity of these recombinant vectors when used as vaccines. Among the candidate genes deleted in NYVAC and intact in the MVA genome (1), we found the C7L gene responsible for the distinct biological differences between both attenuated strains.

MATERIALS AND METHODS

Cells and viruses. Cells were maintained in a humidified air–5% CO_2 atmosphere at 37°C. African green monkey kidney cells (BSC-40) and human cells (HeLa) were grown in Dulbecco's modified Eagle's medium (DMEM) supplemented with 10% newborn calf serum. Mouse 3T3-like fibroblast cells (3T3), baby hamster kidney cells (BHK-21), CEF, and human cells (TK-143) were grown in DMEM supplemented with 10% fetal calf serum (FCS). The VV strains used in this work include Western Reserve (WR), MVA obtained after 586 passages in CEFs (passage 585 of MVA was kindly provided by G. Sutter, Munich, Germany), and NYVAC (provided by J. Tartaglia from Aventis-Pasteur). These strains were grown and titrated in BSC-40 cells (WR) or in CEFs (MVA or NYVAC). All viruses were purified by two sucrose cushions and titrated by immunostaining (25). The particle/PFU ratio in the different virus preparations was determined by measurements of optical density at 260 nm (OD_{260}) and virus titration (1 OD_{260} unit represents 1.2×10^{10} particles per ml) (22).

Generation of NYVAC-C7L. The C7L gene was obtained by PCR of genomic MVA DNA using the following set of primers: 5′-CGGGATCCCATGGGTAT ACAGCACGAATTCG (BamHI site underlined) and 5′-TCCCCCGGGTAAT CCATGGACTCATAATCTCTATACG (SmaI site underlined). The amplified DNA fragments were digested with restriction endonucleases BamHI and SmaI and cloned into pJR101 vector (27) previously digested with BglII and SmaI. The resulting plasmid, pJR101-C7L, directs the insertion of the C7L gene into the hemagglutinin locus of the NYVAC genome under the transcriptional control of the synthetic early/late (E/L) promoter. BSC-40 cells were infected with the attenuated NYVAC strain at a multiplicity of 0.01 PFU/cell and then transfected with 10 μg of DNA from plasmid pJR101-C7L using Lipofectamine reagent according to the manufacturer's instructions (Invitrogen). Recombinant NYVAC viruses containing the C7L gene were selected by consecutive rounds of plaque purification in BSC-40 cells stained with X-Gluc (5-bromo-4-chloro-3-indoxyl-β-D-glucuronidase acid). Purity of the recombinant NYVAC-C7L virus was confirmed by PCR and by DNA sequence analysis.

Evaluation of CPE by phase-contrast microscopy. In the evaluation of cytopathic effects (CPE) under permissive and nonpermissive conditions, the indicated cell lines were seeded into 12-well tissue culture plates and grown to confluence. The cells (duplicate wells) were infected at 5 PFU/cell with WR, MVA, NYVAC, or NYVAC-C7L and visualized under a phase-contrast microscope at various times postinfection (p.i.) for CPE (such as cell rounding, cytoplasmic contraction, and slow detachment). In addition, we analyzed this effect in infected HeLa cells treated with a DNA synthesis inhibitor, Ara C, at a concentration of 50 μg/ml. A total of three independent experiments were performed.

Analysis of virus growth. To determine virus growth profiles, monolayers of HeLa or BHK-21 cells grown in 12-well tissue culture plates were infected at 0.01 PFU/cell with WR, MVA, or NYVAC strains. Following virus adsorption for 60 min at 37°C, the inoculum was removed. The infected cells were washed twice with DMEM without serum and incubated with fresh DMEM containing 2% of FCS at 37°C in a 5% CO_2 atmosphere. At different times postinfection, cell supernatants were removed by scraping with a pipette and cells in the monolayer were independently collected in serum-free medium. The supernatants were stored at 4°C for no more than 48 h before virus titration, and cell-associated virus in the collected monolayer was released from cells by freeze-thawing and brief sonication. Serial dilutions of the resulting cell lysates and of supernatants were plated on confluent BHK-21 monolayers grown in six-well plates in duplicate. Following virus adsorption for 60 min at 37°C, the inoculum was removed. The infected cells were washed twice with DMEM without serum and incubated with fresh DMEM containing 2% of FCS at 37°C in a 5% CO_2 atmosphere. Following 24 h postinfection, the virus titers were determined by immunostaining assay with anti-VV antibodies as previously described (33). At least three independent virus titrations were performed with the samples containing the virus released to the medium during infection (supernatant) and the virus that remained cell associated (monolayer cells).

Metabolic labeling of proteins. HeLa and BHK-21 cells grown in 12-well plates were infected at 5 PFU/cell with MVA or NYVAC. At different times postinfection (4, 8, and 16 h), cells were rinsed three times and incubated with Met-Cys-free DMEM 30 min prior to labeling. After incubation, the medium was removed and 50 μCi of [^{35}S]Met-Cys Promix per ml in Met-Cys-free DMEM was added for an additional 30 min. After three washes with phosphate-buffered saline (PBS), cells were resuspended in Laemmli sample buffer, and equal amounts of proteins (20 μg) were analyzed by sodium-dodecyl sulfate-polyacrylamide gel electrophoresis (SDS-PAGE) followed by autoradiography.

Western blot analysis. Antibodies that specifically recognize the products of viral early and late genes, such as E3L (p25), A14L (p16), A4L (p39), A17L (p21), A27L (p14), and L1R (p27.5), were used in the identification of viral proteins. Anti-E3L was kindly provided by B. Moss and B. Jacobs and anti-L1R by Y. Ichihashi. The remaining antibodies were generated in our laboratory and have been described previously (17, 57, 59, 61). The rabbit polyclonal antiserum raised against live VV was previously described (57). The rabbit polyclonal anti-eIF2α phospho-specific antibody was supplied by BIOSOURCE. The monoclonal antibody against β-actin was supplied by Sigma. Rabbit polyclonal anti-eIF2α antibody was supplied by Santa Cruz Biotechnology, Santa Cruz, CA. Rabbit polyclonal anti-human poly(ADP)-ribose polymerase (PARP) was supplied by Cell Signaling.

For Western blot analyses, total cell extracts were boiled in Laemmli sample buffer, and proteins were fractionated by 10% SDS-PAGE. Following electrophoresis, proteins were transferred to nitrocellulose membranes using a semidry blotting apparatus (Gelman Sciences). The filters were incubated for 30 min with PBS containing nonfat dry milk at 5% (BLOTTO) at room temperature, mixed with antisera in BLOTTO, incubated overnight at 4°C, washed three times with PBS, and further incubated with secondary antibodies coupled to horseradish peroxidase in BLOTTO. After the PBS wash, the immunocomplexes were detected by enhanced chemiluminescence (ECL) Western blotting reagents (Amersham).

RT-PCR. HeLa cells cultured in six-well plates were mock infected or infected with WR, MVA, NYVAC, or NYVAC-C7L at 5 PFU/cell. Total RNA was isolated at 24 h p.i. using the Ultraspec-II RNA resin purification system (Biotecx) following the manufacturer's instructions. Total RNA (1.5 μg) was digested with DNases to avoid genomic DNA contamination (Ambion Turbo kit). PCR with *Taq* Platinum DNA polymerase (Invitrogen) and primers for a control viral gene was performed to ensure there was no DNA contamination (data not shown). Reverse transcription-PCR (RT-PCR) was carried out with 150 ng of total RNA (free of DNA contaminant) using the Invitrogen ONE-STEP kit. Primers for amplification of E3L were 5′-GAGATTGTGTGTGAGGCT and 3′-AAAAGACCAATCTCTTCT. Primers for A27L were (forward) 5′GCGCT CGAGATGCATCATCATCATCATCATGACGGAACTCTTTTCCCC and (reverse) 5′-CGCGGTACCTTACTCATATGGGCGCCGTCCAGTC.

Primer extension. Primer extension was carried out under the following conditions: 2 pmol of VIC-labeled primer from Applied Biosystems (specific for the viral A27L gene), 2 μg of total RNA, and 0.5 mM of deoxynucleoside triphosphate (dNTP) mix in a 0.5-ml microcentrifuge tube. Samples were heated at 65°C for 5 min before quenching in ice for at least 5 min. First-strand cDNA synthesis was performed using SuperScript II RT and 5× RNX buffer (Invitrogen) according to the manufacturer's instructions for 50 min at 42°C. Samples were next incubated for 15 min at 70°C and quenched in ice before precipitation. VIC-labeled cDNAs were allowed to precipitate for 30 min at 40°C following the addition of 0.7 volume of isopropanol. cDNAs were pelleted by centrifugation at 15,000 rpm for 10 min and washed with 70% ethanol before being air dried and stored at −20°C. Each cDNA sample was dissolved in a solution consisting of 2.5 μl formamide (Promega), 0.5 μl GeneScan −500 ROX internal lane standard (Applied Biosystems), and 2 μl of loading buffer (Applied Biosystems) per sample. The primer extension products were sized using the GeneScan analysis software version 3.7 (Applied Biosystems).

Downloaded from jvi.asm.org at Centro Nacional de Biotecnología - Biblioteca on October 15, 2007

Electron microscopy. Monolayers of HeLa cells were infected at 5 PFU/cell with MVA or NYVAC. At 16 h p.i., cells were fixed in situ with a mixture of 2% glutaraldehyde and 1% tannic acid in 0.4 M HEPES buffer (pH 7.5) for 1 h at room temperature. Fixed monolayers were removed from culture dishes in a fixative and transferred to Eppendorf tubes. After centrifugation and a wash with HEPES buffer, the cells were stored at 4°C until used. For ultrastructural studies, fixed cells were processed for embedding in epoxy resin EML-812 (TAAB Laboratories, Ltd., Berkshire, United Kingdom) as previously described (57). Postfixation of cells was completed with a mixture of 1% osmium tetroxide and 0.8% potassium ferricyanide in distillate water for 1 h at 4°C. After two washes with HEPES buffer, samples were treated with 2% uranyl acetate, washed again, and dehydrated in increased concentrations of acetone for 10 min each time at 4°C. Infiltration in resin was done at room temperature for 1 day. Polymerization of infiltrated samples was done at 60°C for 3 days. Ultrathin sections (20 to 30 nm thick) of the samples were stained with saturated uranyl acetate and lead citrate by standard procedures. Collection of images from negative staining and ultrathin sections was done in a JEOL 1200-EX II electron microscope operating at 100 kV (25, 57).

DAPI staining. HeLa cells were grown to confluence in 12-well plates containing 12-mm-diameter glass coverlips were either uninfected or infected with WR, MVA, or NYVAC at 5 PFU/cell. Cells were stained at 24 h p.i. with 4′,6′-diamidino-2-phenylindole (DAPI; 10 μg/ml) for 30 min at room temperature and photographed under a fluorescence microscope.

rRNA breakdown. HeLa cells cultured in six-well plates were mock infected or infected with WR, MVA, NYVAC, or NYVAC-C7L at 5 PFU/cell. Total RNA was isolated at 18 and 24 h p.i. using the Ultraspec-II RNA resin purification system (Biotecx) following the manufacturer's instructions. Fractionation of rRNA was performed by electrophoresis in 1% agarose formaldehyde gel containing 2 μg of total RNA per lane. Breakdown of rRNA was visualized after staining the gel with ethidium bromide.

Measurement of apoptotic cell death by cell cycle analysis. The different stages of the cell cycle and the percentage of cells with sub-G_0 DNA content were analyzed by propidium iodide (PI) staining (38). Briefly, HeLa cells were infected at 5 PFU/cell with WR, MVA, NYVAC, or NYVAC-C7L in the presence or absence of the general caspase inhibitor zVAD-fmk (40 μM; Calbiochem). Mock-infected cells were used as a negative control. At 24 h p.i., cells were removed by pipetting, washed once with cold PBS, and permeabilized with 70% ethanol in PBS at 4°C overnight. After three washes with PBS, the cells were incubated for 45 min at 37°C with RNase A and stained with PI (10 μg/ml). The percentage of cells with hypodiploid DNA content was determined by flow cytometry. Data were acquired for 15,000 cells per sample and analyzed as described above, and the results are expressed as fold increase in apoptotic cells with respect to uninfected cells.

Virus pathogenicity. Groups of 10-week-old female BALB/c mice ($n = 4$ per group) were inoculated intranasally (i.n.) with different challenge doses of NYVAC or NYVAC-C7L (10^6 to 10^8 PFU/mouse) or with 10^6 PFU/mouse of WR (diluted in 50 μl of PBS). The mortality and body weight loss were monitored for at least 2 weeks, with daily measurements of individual animals. Animals suffering from severe systemic infection and having lost >25% body weight were sacrificed. The mean change in body weight was calculated as the percentage of the mean weight for each group on the day of challenge.

RESULTS

NYVAC infection triggered more severe CPE than MVA in permissive and nonpermissive cell lines. Infection with VV induces dramatic changes in cell functions, metabolism, and morphology, all of which are collectively termed the CPE (2, 4, 6). In order to characterize the CPE produced by the VV strains WR, NYVAC, and MVA, monolayers of different cell lines (permissive and nonpermissive) were infected at 5 PFU/cell with each virus and the extent of CPE was analyzed by phase-contrast microscopy at different times postinfection. The particle/PFU ratios determined in the different viral preparations were 302 for MVA, 272 for NYVAC, and 310 for WR, demonstrating the same infectivity of the purified viruses. Characteristics such as cytoplasmic contraction, cell rounding, and cell detachment were monitored. The cell lines infected with NYVAC (HeLa, BHK-21, BSC-40, and 3T3), independently of the host restriction, exhibited evident cell rounding as early as 2 h p.i. Representative findings are shown for HeLa cells (Fig. 1). During the course of NYVAC infection, the CPE increased with time, and by 24 h p.i, a high level of cell detachment was noted. The same effects were observed in NYVAC-infected cells treated with Ara C, a drug that blocks DNA replication (not shown). In contrast, the CPE was delayed and significantly reduced in cells infected with MVA (Fig. 1). The morphology of the CPE in NYVAC-infected cells, but not in WR or MVA infections, at late times was reminiscent of apoptosis.

Virus growth of MVA and NYVAC in permissive and nonpermissive cell lines. Deletion of two of the host range genes K1L and C7L in the NYVAC genome is associated with a reduced ability of the virus to replicate within a broad range of cell lines of human origin, as well as rabbit kidney and pig kidney cells (48, 71). Nonetheless, NYVAC can replicate with wild-type efficiency in Vero cells and primary CEF (69, 70). The host range phenotype observed with MVA includes a characteristic late block upon nonproductive infection of many mammalian cells, with unimpaired viral DNA replication and late gene expression (67, 76). As previously described, the restriction exhibited by MVA in nonpermissive cell lines is a consequence of a defect in virus morphogenesis (11, 17, 39). The restriction observed in NYVAC may also be due to a defect in virus morphogenesis or virus spread. To analyze the viral growth characteristics of MVA and NYVAC under permissive and nonpermissive conditions, monolayers of BHK-21 and HeLa cells were infected at 0.01 PFU/cell with each virus for 0, 24, 48, and 72 h. Infectious viruses that remained cell-associated and were released to the medium during the course of the infection were measured by an immunostaining assay. For comparative purposes, we used the replication-competent WR strain. In HeLa cells infected with WR, the virus titer increased with time more than 10,000-fold, while there was no increase in virus titer with either MVA nor NYVAC infection (Fig. 2A and B). In contrast, under permissive conditions, the growth kinetics of the three virus strains were similar (Fig. 2C and D). Interestingly, the titers of cell-associated virus in BHK-21 cells infected with NYVAC were lower than the titers obtained in cells infected with WR or MVA (Fig. 2C). This finding was consistent in three independent experiments. The results of Fig. 2 demonstrate that under nonpermissive conditions, there is a similarly restricted production of infectious viral particles in NYVAC- and MVA-infected cells, while under permissive conditions, the total viral yields are not affected. Nonetheless, the virus that remains cell associated late in infection is reduced in NYVAC-infected cells compared to that in MVA- or WR-infected cells. This reduction is probably the consequence of the severe cell destruction that followed NYVAC infection (see Fig. 1).

Protein synthesis during NYVAC and MVA infection. In order to compare the shutoff and kinetics of synthesis of viral proteins in permissive and nonpermissive cell lines infected with MVA and NYVAC, BHK-21 and HeLa cells were infected at 5 PFU/cell with each virus, and at 2, 4, 8, and 16 h p.i., the infected cells were metabolically labeled for 30 min with [^{35}S]Met-Cys Promix. Cell lysates were fractionated by SDS-PAGE, and the protein pattern examined by autoradiography. As shown in Fig. 3A, in BHK-21 cells infected with MVA and

Downloaded from jvi.asm.org at Centro Nacional de Biotecnología - Biblioteca on October 15, 2007

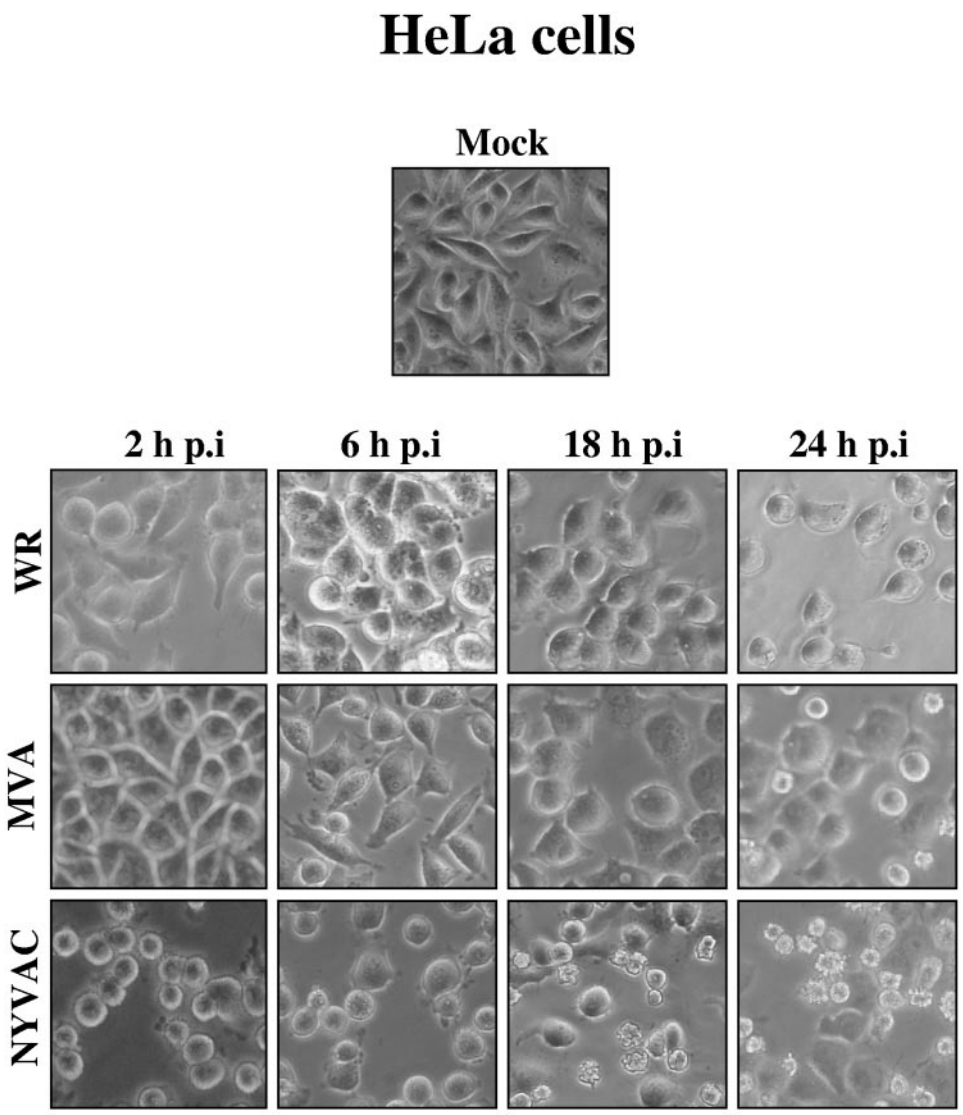

FIG. 1. CPE of MVA and NYVAC in human cells. Monolayers of HeLa cells were mock infected or infected at 5 PFU/cell with WR, MVA, or NYVAC. At different times postinfection, as indicated in the figure, the morphological changes in the cells were examined by phase-contrast microscopy. Mock, uninfected cells.

NYVAC, the pattern of viral proteins and the shutoff of cellular proteins occur with similar kinetics between the two viruses, although some differences were noted in protein abundance. This was confirmed by Western blot analysis from the same cell homogenates. Accumulation of viral proteins during infection was reduced in NYVAC-infected cells compared with MVA-infected BHK-21 cells (Fig. 3C). In HeLa cells infected with NYVAC or MVA, a similar pattern of viral proteins was observed between the two viruses, while the shutoff was more pronounced in cells infected with NYVAC late in infection (Fig. 3B). Some differences were also noted in protein abundance between NYVAC and MVA, a finding confirmed by Western blot analysis (Fig. 3D). The accumulation of viral proteins in NYVAC-infected permissive and nonpermissive cells was reduced compared with that in MVA-infected cells, which could be due to a defect in translation or transcription or a cell lysis effect. It is well established that phosphorylation of the α subunit of the eukaryotic translation initiation factor 2 (eIF-2) on serine 51 leads to the downregulation of translation initiation (62). As such, we determined whether NYVAC infection alters this initiation step. Thus, the levels of phospho-eIF-2α-S51 in BHK-21 and HeLa cells infected with MVA or NYVAC were determined by immunoblot analysis with specific anti-eIF-2α-S51 antibody. As shown in both cell lines (Fig. 3E and F), a low level of phosphorylated eIF2-α was detectable in mock-infected cells and at early times after NYVAC or MVA infection. However, with time of infection there was an increase in eIF2-α phosphorylation in cells infected with NYVAC but not in cells infected with MVA. The increase in eIF2-α phosphorylation correlates with the shutoff of host protein synthesis, suggesting that levels of viral proteins in NYVAC-infected cells could be compromised by the extent of eIF2-α phosphorylation induced by the virus.

Downloaded from jvi.asm.org at Centro Nacional de Biotecnología - Biblioteca on October 15, 2007

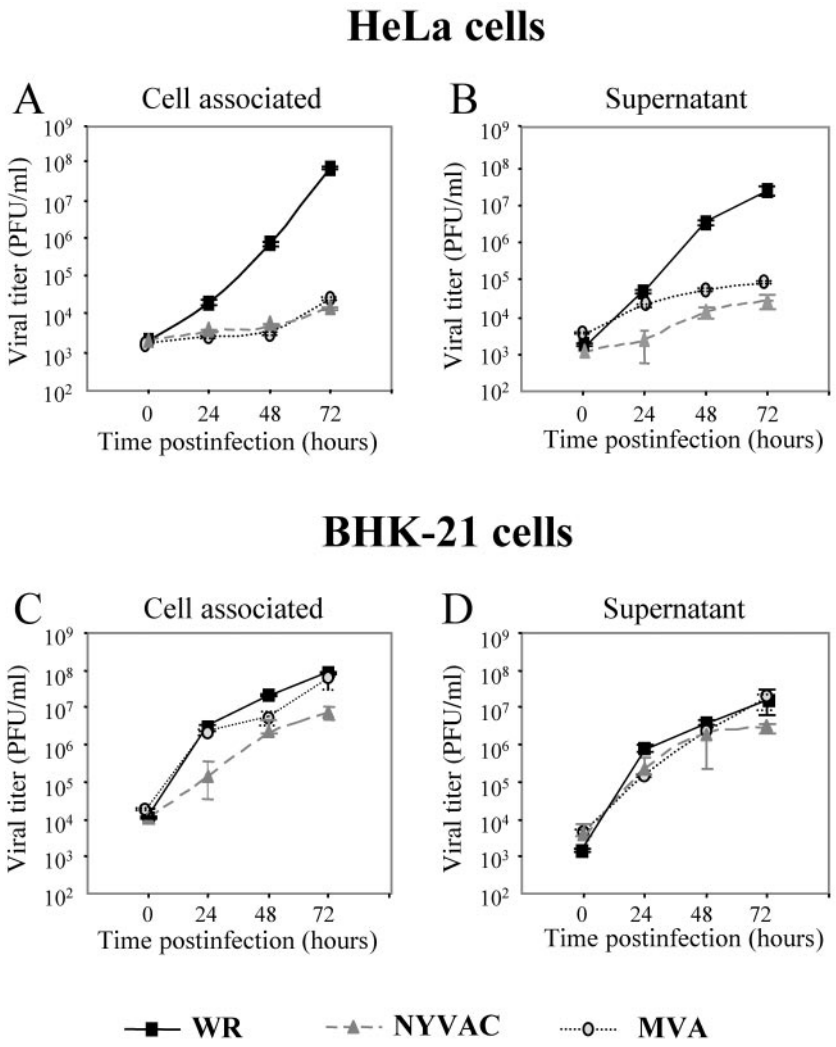

FIG. 2. Virus growth of MVA and NYVAC in permissive and nonpermissive cell lines. Monolayers of HeLa and BHK-21 cells were infected at 0.01 PFU/cell with WR, MVA, or NYVAC for 0, 24, 48, and 72 h. Cells were collected by centrifugation, and infectious virus associated with the cells (A and C) and released to the supernatant (B and D) during the course of the infection was quantified by immunostaining assay. For comparative purposes, we used the replication-competent WR strain. Averages of three independent experiments are shown with standard error bars.

Differences in late viral proteins between MVA and NYVAC infection in nonpermissive cells. Poxvirus gene expression is regulated in a cascade manner. As such, early genes are transcribed immediately following infection by enzymes and transcription factors contained within the infecting virion, while late and intermediate genes are transcribed after the start of viral DNA replication (13, 41, 45). Consequently, in view of the translational control exerted by phosphorylation of eIF-2α during NYVAC infection, we next determined if the translation of specific early and late viral genes was blocked. This was analyzed by Western blotting in cell lysates of BHK-21 and HeLa cells infected with WR, MVA, or NYVAC, using different antibodies that specifically recognized the early viral protein p25 (E3L) and the late viral proteins p14 (A27L), p21 (A17L), p16 (A14L), p39 (A4L), and p27.5 (L1R). As shown in Fig. 4A, under permissive conditions, early and late viral proteins were efficiently detected in lysates of cells infected with WR, MVA, or NYVAC. However, under nonpermissive conditions, apparent differences in specific proteins were observed between NYVAC and MVA. Early viral proteins were efficiently detected in lysates of cells infected with the three viruses. In contrast, late viral proteins that corresponded to the gene products of A27L, A17L, and L1R were not detected in the lysates of cells infected with NYVAC, while in lysates from cells infected with MVA or WR, all proteins were produced. Interestingly, other late proteins such as p16 (A14L) and p39 (A4L) were efficiently detected in NYVAC-infected cells. Similar results were confirmed by confocal immunofluorescence analysis (data not shown).

To determine a possible defect at the transcriptional level, we analyzed early and late transcription of viral genes in WR-, MVA-, and NYVAC-infected HeLa cells. For this purpose, total RNA was isolated at 24 h p.i. and mRNA levels of a specific viral early gene (E3L) and a late viral gene (A27L)

Downloaded from jvi.asm.org at Centro Nacional de Biotecnología - Biblioteca on October 15, 2007

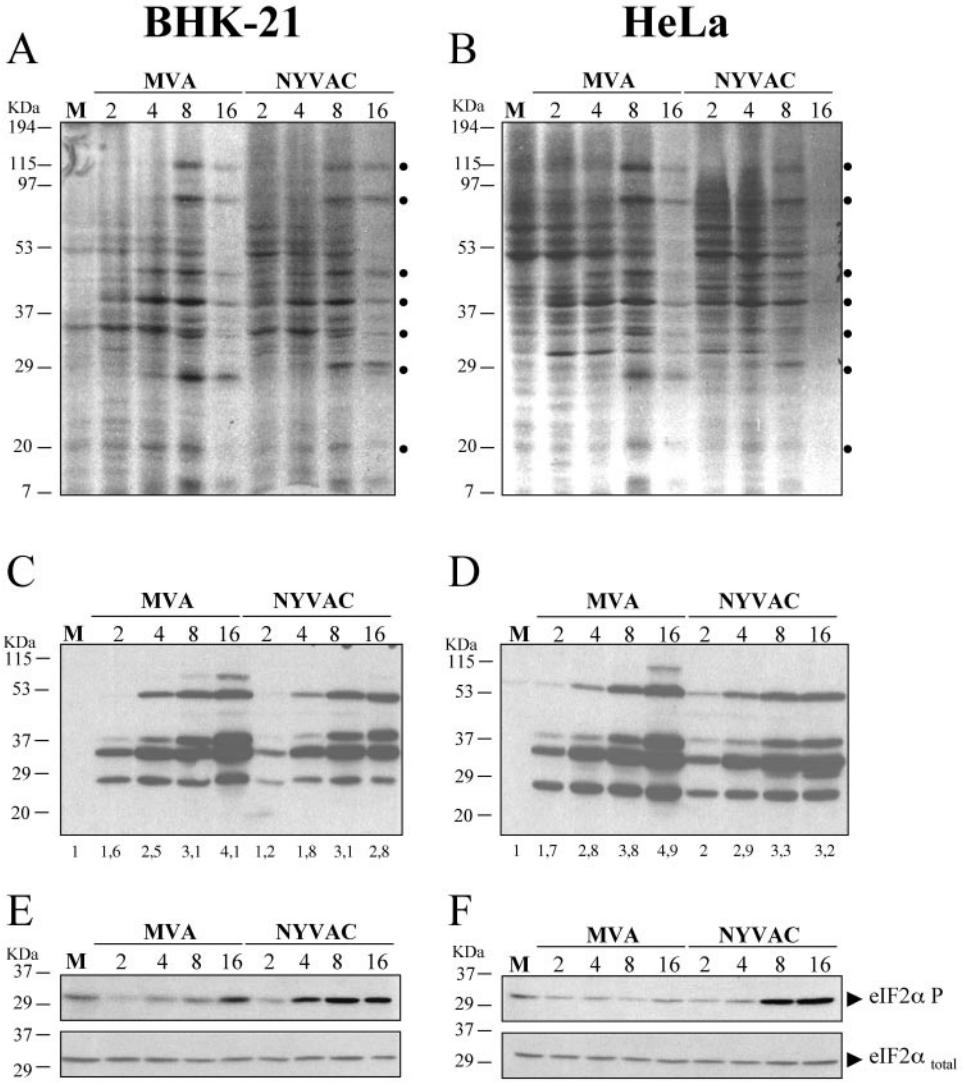

FIG. 3. Protein synthesis during NYVAC and MVA infection. Monolayers of BHK-21 (A) and HeLa (B) cells were mock infected (M) or infected at 5 PFU/cell with MVA or NYVAC. At the indicated times (h p.i.), cells were metabolically labeled for 30 min with [^{35}S]Met-Cys Promix (50 μCi/ml) and equal amounts of proteins were analyzed by SDS-PAGE (10%) and autoradiography. The dots on the right indicate prominent viral proteins. (C and D) Western blot showing expression of VV antigens during the time course of MVA and NYVAC infection in infected BHK-21 (C) and HeLa (D) cells. The blot was probed with a rabbit polyclonal antiserum (1:500 dilution) raised against live VV. Numbers appearing under each lane represent the ratio of intensity of the bands in infected cells to levels in uninfected cells, as determined by densitometric analyses. (E and F) Western blot analysis of total eIF2-α and phospho-eIF-2α-S51 protein levels during the time course of MVA and NYVAC infection in infected BHK-21 (E) and HeLa (F) cells.

were monitored by RT-PCR. As shown in Fig. 4B, the transcription of both early and late viral genes occurred similarly in all infections.

Due to the extensive read-through that characterized transcription of late viral mRNAs, we analyzed in more detail the integrity of the A27L mRNA using primer extension analysis. As shown in Fig. 4C, the same cDNA product of 263 bp was identified using total RNAs isolated from NYVAC- and WR-infected HeLa cells. Thus, failure to produce some of the NYVAC late proteins appeared to be a consequence of a block in translation and was not due to a specific inhibition of late viral transcription.

Since it has been established that mutants of VV lacking one of the late proteins p21 (A17L), p14 (A27L), or p27.5 (L1R) are blocked at different stages in viral morphogenesis (59, 66), the absence of these proteins in NYVAC-infected cells is likely to lead to a blockade in viral morphogenesis. Thus, we next analyzed the morphogenetic process during NYVAC and MVA infection in nonpermissive cells.

Morphogenesis of NYVAC is blocked at the IV formation in HeLa-infected cells. The morphogenesis of MVA under permissive and nonpermissive conditions has been widely studied (14, 25, 42, 63, 67). The stage at which this process is blocked is dependent on the cell type. In HeLa cells, the blockade of the morphogenetic program of MVA occurs in steps following the formation of immature viral forms (IVs), without an alter-

Downloaded from jvi.asm.org at Centro Nacional de Biotecnología - Biblioteca on October 15, 2007

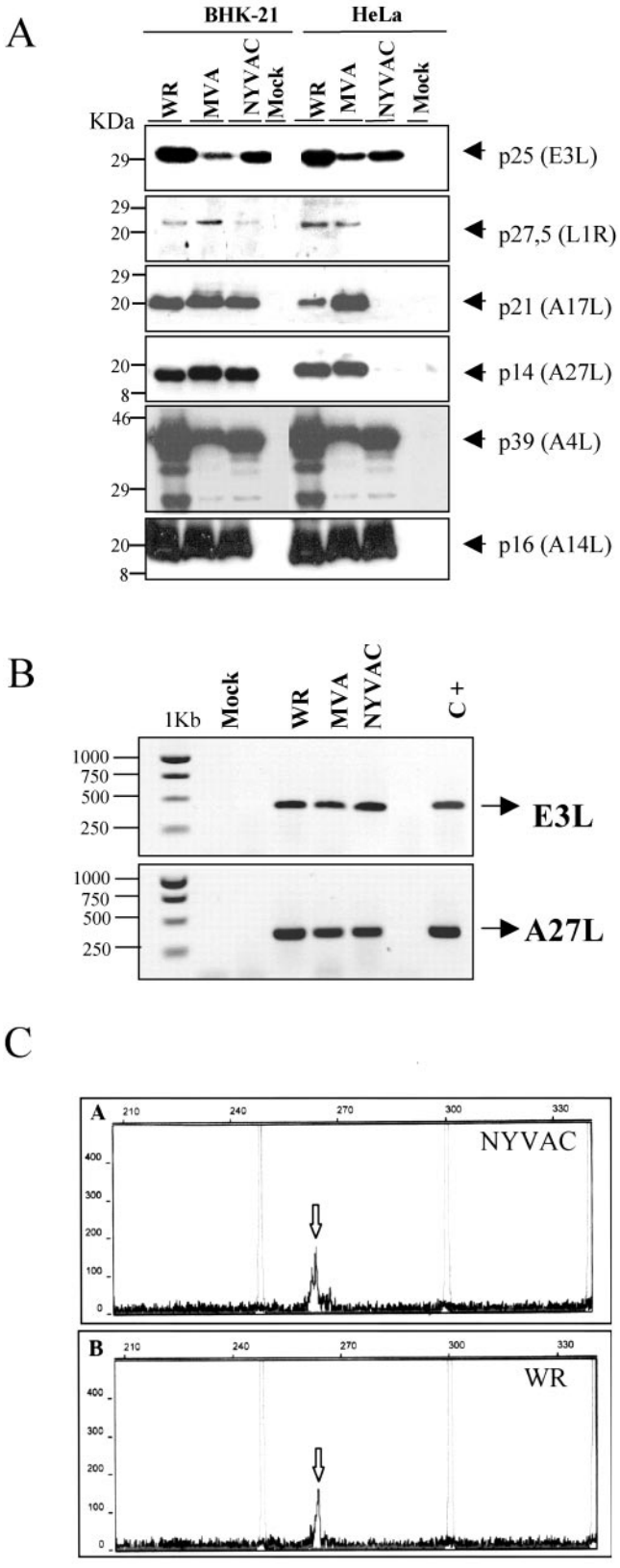

FIG. 4. Expression of specific viral proteins under permissive and nonpermissive conditions. (A) Monolayers of BHK-21 and HeLa cells were mock infected (M) or infected at 5 PFU/cell with WR, MVA, or NYVAC, and cell extracts were analyzed by Western blotting. Cell lysates were harvested at 24 h p.i., and equal amounts of proteins were fractionated by SDS-PAGE, transferred to nitrocellulose paper, and reacted with different antibodies recognizing specific viral early proteins, such as p25, and viral late proteins, such as p27.5, p21, p14, p39, or p16. (B) Transcription of early and late viral genes. The transcription of E3L and A27L genes was determined by RT-PCR from total RNAs as described in Materials and Methods. Total RNA from uninfected cells and DNA extracted from MVA-infected cells were used as the negative (Mock) and positive (C+) control, respectively. (C) Primer extension product obtained using 2 μg of total RNA isolated from HeLa cells either uninfected (Mock) or infected at 5 PFU/cell with WR or NYVAC for 16 h. The sizes of the peaks from the GeneScan-500 ROX internal lane standards are shown (in base pairs). The arrows indicate the primer extension products (VIC-labeled cDNA) for the A27L gene. Peak height is a measure of fluorescence intensity and indicates the strength of the VIC signal. The peak heights for each sample were 177 for NYVAC (A), 164 for WR (B), and 55 for mock infected (not shown).

ation in early or late viral gene expression (25, 63). In contrast, studies based on NYVAC morphogenesis are unavailable. To characterize this process under nonpermissive conditions, HeLa cells were infected at 5 PFU/cell with NYVAC or MVA. At 16 h p.i., the infected cells were examined by transmission electron microscopy for the presence of intermediates in viral morphogenesis. As shown in Fig. 5A, fewer IVs were detected in the cytoplasm of NYVAC-infected cells than in MVA-infected cells (Fig. 5B). Intracellular mature viruses were minimally detected in NYVAC-infected HeLa cells, suggesting that the blockade of the morphogenetic program of this virus occurs in steps at or prior to the formation of IVs.

Transmission electron micrographs of HeLa cells infected with NYVAC also revealed the severity of virus infection in the cell ultrastructure. As shown in Fig. 5 (panels C, D and E), morphological hallmarks of apoptosis, including chromatin condensation and margination, marked nuclear invagination, and cytoplasmic vacuolization, were observed. None of these characteristics was seen in cells infected with MVA or WR, as previously noted (25).

Infection with NYVAC induces apoptosis in human cells with activation of caspases and breakdown of rRNA. The results shown in Fig. 1 and 5 prompted us to question the extent to which NYVAC infection was responsible for an apoptotic phenotype. The cleavage of PARP commonly occurs in apoptotic cells by the activation of caspases (56). Therefore, PARP cleavage was analyzed by Western blotting of HeLa cells infected with MVA or NYVAC at different times postinfection. As shown in Fig. 6A, the 116-kDa PARP present at early times postinfection was almost completely cleaved (89 kDa) in cells infected with NYVAC at 16 h p.i. In contrast, the cleavage of PARP did not take place or was minor in MVA-infected cells. Apoptotic cells are also characterized by the presence of fragmented DNA in their nuclei. Thus, infected HeLa cells were further stained with DAPI reagent and analyzed by fluorescence microscopy. As shown in Fig. 6B, numerous HeLa nuclei displayed apoptotic morphology (chromatin condensation and disintegration) at 24 h p.i. in cells infected with NYVAC. In contrast, a very low percentage of all the cells infected with MVA presented this phenotype. These results were further supported by an enzyme-linked immunosorbent assay-based

Downloaded from jvi.asm.org at Centro Nacional de Biotecnología - Biblioteca on October 15, 2007

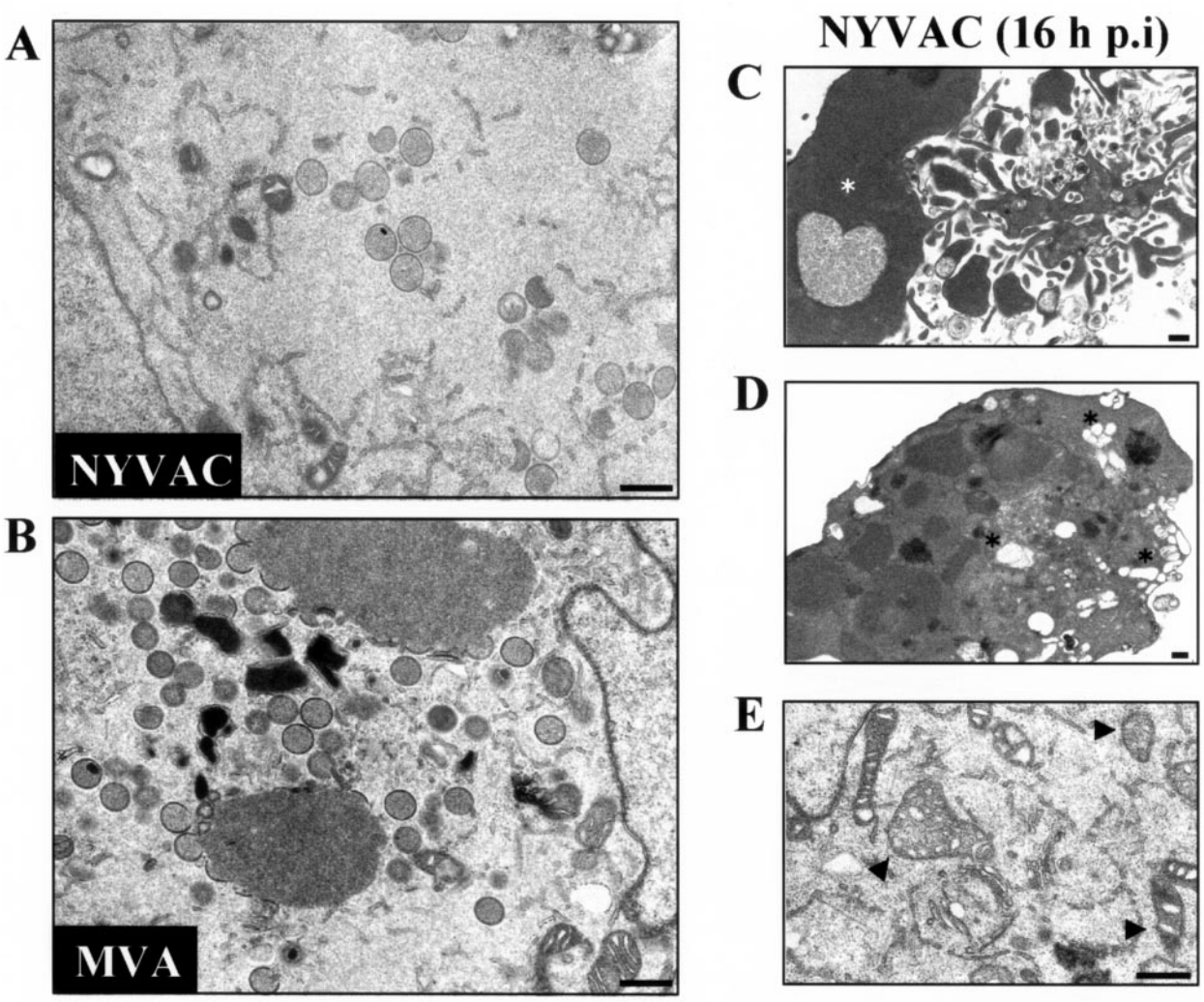

FIG. 5. Electron microscopy of NYVAC morphogenesis in HeLa cells. (A and B) Electron micrographs of HeLa cells infected with 5 PFU/cell of NYVAC (A) or with 5 PFU/cell of MVA (B) at 16 h p.i. The magnification of each panel is indicated by bars in the upper right corner. Characteristics of apoptosis in NYVAC-infected cells are shown in panels C to E. (C) An infected cell with nuclear condensation (white asterisk). (D) Cytoplasm of an infected cell with extensive vacuolation (black asterisks). (E) Cytoplasm of an infected cell with dense mitochondria (arrowheads). Bars = 500 nm.

assay that detects the amount of cytoplasmic histone-associated DNA fragments (data not shown).

To quantify the percentage of cell death following infection, we used flow cytometry. When these cells are stained with propidium iodide, apoptotic cells show reduced levels of fluorescence compared to normal cells and appear in the sub-G_0/G_1 peak (18). Thus, HeLa cells were infected at 5 PFU/cell with WR, MVA, or NYVAC in the presence or absence of zVAD (a general caspase inhibitor). At 24 h p.i., the infected cells were stained with propidium iodide followed by cell cycle analysis using flow cytometry. Mock-infected HeLa cells were used as a negative control. As shown in Fig. 6C, approximately 42% of cells infected with NYVAC were present in the sub-G_0/G_1 peak, which represents an increase of nearly sevenfold with respect to uninfected cells, in comparison with the 17.6% and 9.3% obtained in MVA- or WR-infected cells, respectively. In the presence of zVAD, the percentage of apoptotic cells was significantly reduced (3.67%), demonstrating that the apoptosis induced by NYVAC infection is caspase dependent.

The activation of nucleases appears to be a final commitment step in the apoptotic process. Thus, we next examined the effect of nuclease activation on rRNA integrity. Total RNA was isolated from infected and mock-infected cells and fractionated by formaldehyde-agarose gel electrophoresis. As shown in Fig. 6D, the bands corresponding to 28S and 18S rRNA were intact in those samples from mock-, WR-, or MVA-infected cells. In contrast, in NYVAC-infected cells there was breakdown of rRNA. The rRNA fragments generated by NYVAC infection were similar to those produced after activation of the enzyme RNase L (not shown). Clearly, by 24 h p.i. NYVAC induces severe rRNA cleavage. These biochemical findings indicate a remarkable apoptotic process during NYVAC infection.

Downloaded from jvi.asm.org at Centro Nacional de Biotecnología - Biblioteca on October 15, 2007

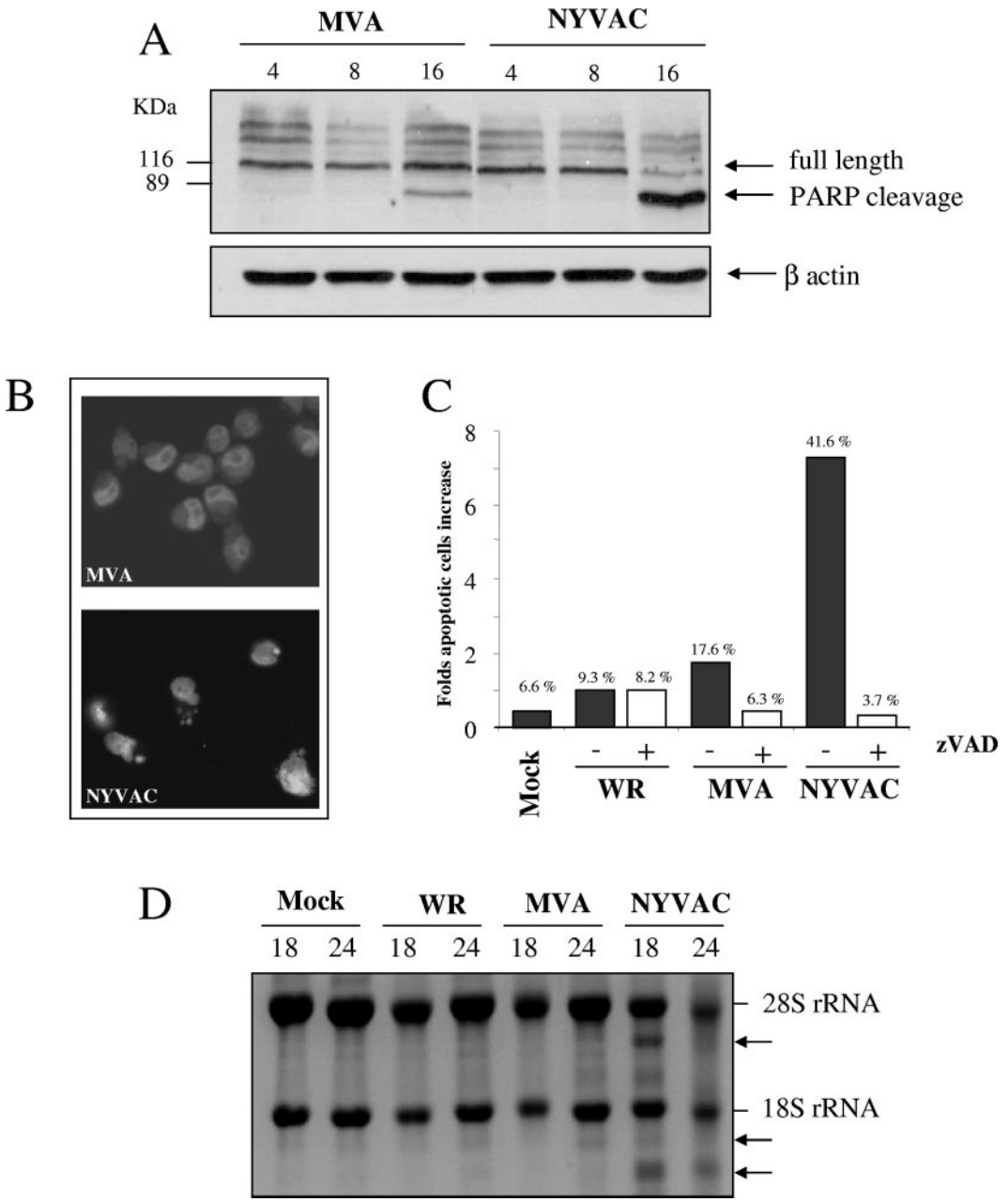

FIG. 6. Infection with NYVAC induces apoptosis in nonpermissive HeLa cells. (A) Western blot analysis of PARP cleavage in HeLa cells infected with 5 PFU/cell of MVA or NYVAC at different times postinfection. (B) DAPI staining of HeLa cells infected with 5 PFU/cell of MVA and NYVAC at 24 h p.i. (C) Monolayers of HeLa cells were infected at 5 PFU/cell with WR, MVA, or NYVAC in the presence or absence of zVAD (40 μM). At 24 h p.i., the infected cells were stained with propidium iodide followed by cell cycle analysis using a flow cytometer to detect cells with hypodiploid DNA content. Untreated HeLa cells were used as a negative control (Mock). Bars represent the fold increase in apoptotic cells with respect to mock infected. The percentage of apoptotic cells is indicated over the bars. Similar results were obtained in two independent experiments. (D) rRNA breakdown. HeLa cells were mock infected or infected with WR, MVA, or NYVAC at 5 PFU/cell. Total RNA was isolated at 18 and 24 h p.i., and 2 μg of each was applied for electrophoresis. The arrows indicate bands corresponding to characteristic degradation products of rRNA.

The viral C7L gene blocked apoptosis induced by NYVAC infection and rescued the biological and biochemical properties assigned to NYVAC. Critical parts of the cellular antiviral response range from the induction of apoptosis and the global inhibition of translation to effectively dampening virus production (64). Since NYVAC was generated by target deletion of 18 genes, including the host range (Hr) gene C7L, and Hr genes have been implicated in apoptosis (74), it was of interest to know whether reintroduction of C7L in the NYVAC genome could rescue some of the biological properties of NYVAC assigned in this study. To this aim, the C7L gene from MVA was used for the generation of the recombinant virus NYVAC-C7L. Because our data demonstrated that NYVAC infection triggered programmed cell death in HeLa cells, we asked

Downloaded from jvi.asm.org at Centro Nacional de Biotecnología - Biblioteca on October 15, 2007

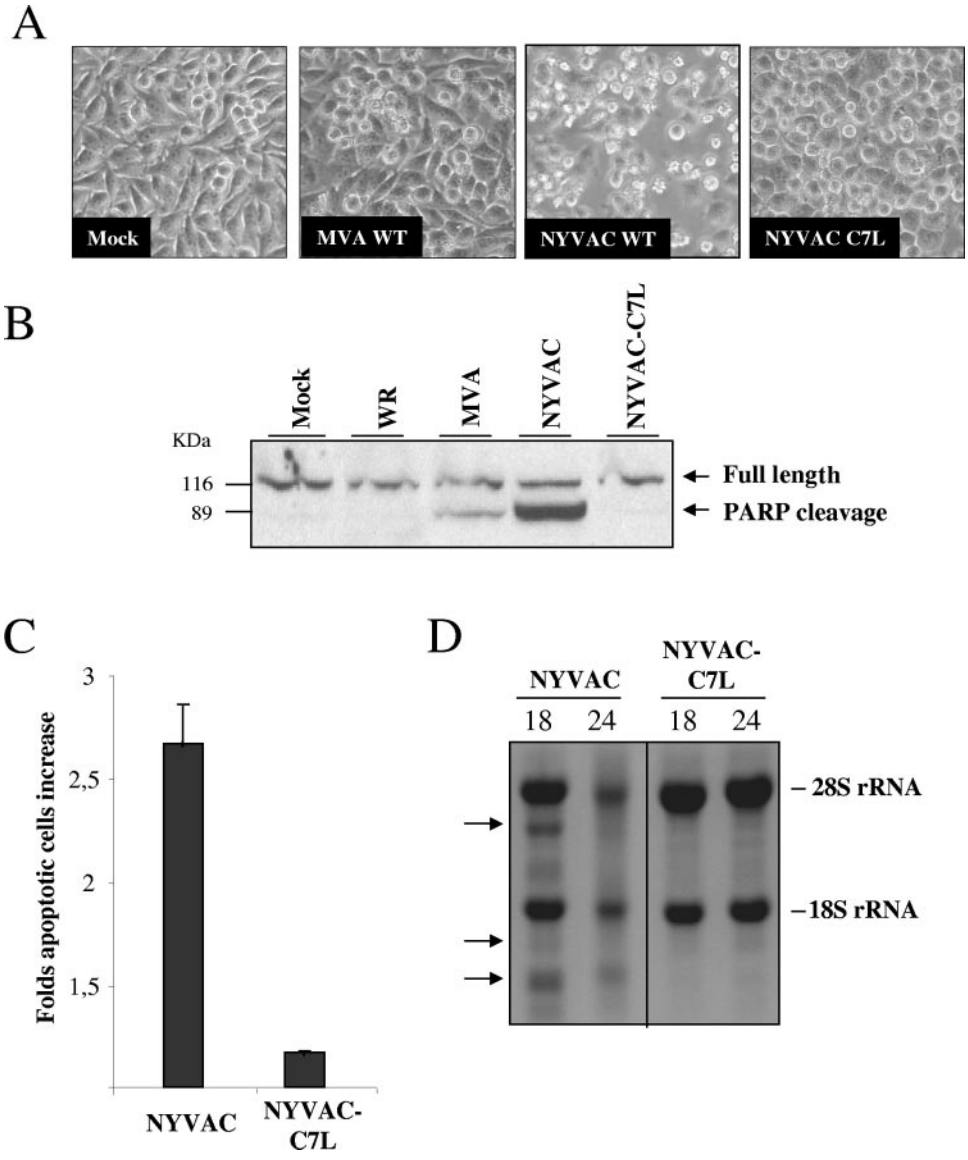

FIG. 7. The apoptotic phenotype of NYVAC is inhibited by the expression of the virus C7L host range gene. Monolayers of HeLa cells were infected with recombinant NYVAC-C7L or with MVA or the NYVAC wild type (WT) at 5 PFU/cell. (A) The morphology of cells in apoptosis was observed by phase-contrast microscopy. (B) Western blot analysis of PARP cleavage in HeLa cells infected with WR, MVA, NYVAC, or NYVAC-C7L at 24 h p.i. (C) Monolayers of HeLa cells were infected at 5 PFU/cell with NYVAC or NYVAC-C7L. At 24 h p.i., the infected cells were stained with propidium iodide followed by cell cycle analysis using a flow cytometer to detect cells with hypodiploid DNA. Uninfected HeLa cells (Mock) were used as a negative control. Bars represent the fold increase in apoptotic cells with respect to mock infected. (D) rRNA breakdown. HeLa cells were infected with NYVAC or NYVAC-C7L at 5 PFU/cell. Total RNA was isolated at 18 and 24 h p.i., and 2 μg of each was applied for electrophoresis. The arrows indicate bands corresponding to characteristic degradation products of rRNA.

whether NYVAC-C7L was capable of inhibiting apoptosis. We monitored apoptosis by assessing morphological changes, cleavage of PARP, rRNA degradation, and cell cycle assays. The morphological signs of apoptosis observed in NYVAC-infected HeLa cells were not evident after infection with NYVAC-C7L (Fig. 7A). In addition, the recombinant virus was able to prevent cleavage of PARP (Fig. 7B), reduced the percentage of cells in apoptosis (Fig. 7C), and inhibited the breakdown of rRNA (Fig. 7D). These observations clearly revealed that the C7L gene is involved in the control of apoptosis induced by NYVAC infection. Since during NYVAC infection the enhanced shutoff correlated with eIF2-α phosphorylation, we next investigated the role of C7L in translational control by measuring phosphorylation of eIF2-α and expression of p14 (A27L) and p21 (A17L) late viral proteins. As shown in Fig. 8A, in NYVAC-C7L-infected HeLa cells there was rescue in the synthesis of late viral proteins (p14 and p21) at 24 h p.i. compared with parental NYVAC infection and the levels of phosphorylated eIF2-α were similar to those in MVA-infected cells. This rescue in the synthesis of late viral proteins is likely to favor virus replication in the human cells. Thus, the viral growth efficiency of NYVAC-C7L in HeLa cells was measured. Monolayers of HeLa cells were infected at 0.01 PFU/cell with NYVAC or NYVAC-C7L, and at times 0, 24,

Downloaded from jvi.asm.org at Centro Nacional de Biotecnología - Biblioteca on October 15, 2007

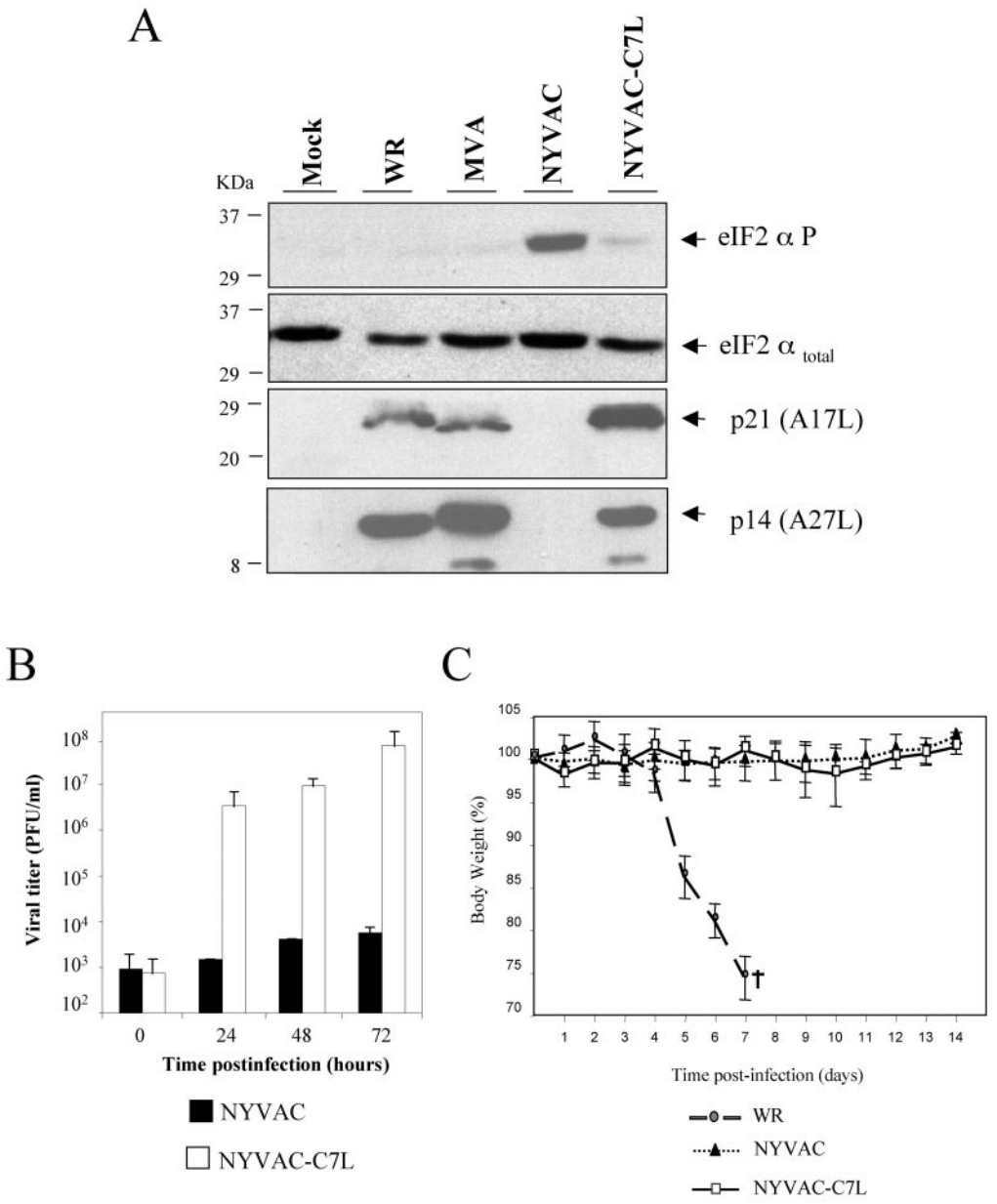

FIG. 8. The VV C7L gene rescued NYVAC translation capacity and virus growth in human cells but retained the attenuated phenotype in vivo. (A) Expression of total and phospho-eIF2-α and late viral proteins (p21 and p14) in HeLa cells uninfected (Mock) or infected with 5 PFU/cell of WR, MVA, NYVAC, or NYVAC-C7L at 24 h p.i. was analyzed by Western blotting. (B) Monolayers of HeLa cells were infected at 0.01 PFU/cell with NYVAC or NYVAC-C7L virus for 0, 24, 48, and 72 h. Cells were collected by centrifugation, and infectious virus associated with the cells during the course of the infection was quantified by immunostaining assay. Two independent experiments are shown with standard error bars. (C) BALB/c mice ($n = 4$) were inoculated by the i.n. route with different challenge doses of either NYVAC or NYVAC-C7L (from 10^6 to 10^8 PFU/mouse) or with 10^6 PFU/mouse of WR. Body weight was monitored daily and is expressed as the mean for each group. Animals suffering from severe systemic infection and having lost >25% body weight were sacrificed (black cross). The graph represents the values obtained using the highest dose of NYVAC and NYVAC-C7L (10^8 PFU/mouse) and the low dose (10^6 PFU/mouse) of WR.

48, and 72 h, cells were collected in the media and virus titers in cell homogenates were determined by immunostaining assay. As shown in Fig. 8B, reintroduction of the C7L gene in the NYVAC genome rescues the ability of this virus to replicate in HeLa cells. To define if the introduction of the C7L gene in NYVAC alters the attenuated phenotype of the virus, BALB/c mice were infected by the i.n. route with different challenge doses of NYVAC or NYVAC-C7L (from 10^6 to 10^8 PFU/mouse) or with 10^6 PFU of WR as a control. Animals were monitored for lethality and weight loss over a period of 2 weeks. In contrast to WR infection, which caused drastic body weight loss and severe signs of illness, infection of mice with NYVAC or with the recombinant NYVAC-C7L did not lead to any obvious disease, even at the highest dose used (Fig. 8C). These results revealed that reintroduction of the C7L gene into the backbone of NYVAC maintains an attenuated phenotype of the recombinant virus. Thus, the findings of Fig. 7 and 8 demonstrate that most, if not all, of the biological and bio-

Downloaded from jvi.asm.org at Centro Nacional de Biotecnología - Biblioteca on October 15, 2007

chemical features of NYVAC infection that we have observed in this study are largely due to the lack of the C7L gene.

DISCUSSION

There is major interest in the use of poxviruses as vaccine vectors and as oncolytic agents against a broad spectrum of diseases, due to their ability to trigger specific immune responses leading to protection in animal models and their capacity to destroy tumor cells (24, 41). Live attenuated strains, such as MVA, NYVAC, ALVAC, and fowlpox virus, which have been modified to be less virulent and to exhibit a specific phenotype, are the most extensively studied vectors. The rational design of such vaccines requires detailed information on vector-host cell interactions and how viral genomic modifications impact the biology and immunogenicity of the poxvirus vectors (35). Currently, a number of clinical trials are under way by EuroVacc (www.eurovacc.org) as well as other organizations with the two attenuated poxvirus vectors NYVAC and MVA (8, 9). As such, it is crucial to understand the behavior of the two vectors in both in vitro and in vivo systems. In this work, we carried out an in vitro head-to-head comparison of the cellular and biochemical properties between NYVAC and MVA in nonpermissive and permissive cultured cells.

Several biological differences between both strains in vitro were evident. The first significant difference involves the CPE produced by NYVAC compared with WR and MVA strains. This CPE was observed early in NYVAC infection in a range of permissive and nonpermissive cell lines, indicating that CPE is independent of the host range restriction and was maintained even when DNA replication was blocked by the drug Ara C. As reported by previous authors, the induction of early cell rounding is dependent on early viral protein synthesis (2, 3, 5). Consequently, Tsung and coworkers demonstrated the absence of CPE in cells infected with a VV strain inactivated by psoralen and long-wave UV light, a treatment that affects the transcription of early viral genes (73). Although WR and NYVAC induced a similar CPE at early times postinfection from 2 to 6 h p.i., NYVAC-infected cells displayed a more pronounced cell rounding than WR-infected cells. The CPE induced by MVA was minor compared to those induced by WR and NYVAC. The reduced CPE by MVA may be attributed to the fact that MVA has lost 15% of its parental genome and could be related to the absence of some early viral proteins encoded by the deleted genes. We discard the possibility that these effects could be due to differences in the number of virus particles used to infect cells, since the particle/PFU ratios for the three virus preparations were similar.

The second significant difference between NYVAC and MVA includes the amount of virus that remains cell associated late in infection. As has been shown by other studies, the growth of MVA (14, 20) and NYVAC (69) is restricted in HeLa cells; however, both strains can be grown in BHK-21 cells. Interestingly, as shown here, the titers of cell-associated virus in BHK-21 cells infected with NYVAC were consistently lower than the titers obtained in cells infected with WR or MVA. This result might be linked with the pronounced CPE induced in NYVAC-infected cells, as the structures of some organelles involved in virus morphogenesis, such as the Golgi apparatus, were altered at early times postinfection. The lower cell-associated viral yields obtained in NYVAC-infected cells under permissive conditions could explain the difficulties encountered by Gonin and coworkers in producing high titers of a NYVAC recombinant (28).

A third significant difference observed between NYVAC and MVA infection was in the synthesis of viral proteins and the extent of phosphorylation of the translational initiation factor eIF-2α. In permissive and nonpermissive cell lines, NYVAC infection produces a reduction in the kinetics of synthesis and accumulation of viral proteins with time. Inhibition of protein synthesis during NYVAC infection was associated with an increase in the phospho-eIF-2α-S51 levels. Since eIF-2α is a key regulator of translation, our observations imply that protein synthesis is more compromised during NYVAC than MVA infection. Consequently, certain late viral proteins such as p14 (A27L), p21 (A17L), or the L1R gene product (p27.5) were not detected in nonpermissive cells infected with NYVAC, while other late viral proteins required for early steps in morphogenesis (59), such as p16 (A14L) or p39 (A4L), were synthesized. The lack of synthesis of some late viral proteins was not due to inhibition of transcription of these genes but rather to a block at the translational level, as revealed by the integrity of mRNAs for these genes in NYVAC-infected cells determined by RT-PCR and primer extension (Fig. 4). The fact that such proteins were not detected in cell lines in which NYVAC growth was restricted (mouse 3T3 and human TK-143 cells; data not shown), indicates that it is a feature of the host restriction of this attenuated strain. Nonetheless, we cannot exclude the possibility that trace amounts of these proteins may be synthesized but are not detected by Western blotting or by immunofluorescence analysis. These findings could be considered promising with regards to the safety of NYVAC, since the virus is unable to synthesize the late viral proteins needed for the correct assembly and formation of infectious viral particles under nonpermissive conditions.

A fourth variation obtained between MVA and NYVAC infection is based on morphogenesis. The stage of infection in which the block in the viral life cycle of both strains occurs is dependent on the cell type. In cell lines of human origin such as HeLa, MVA infection is blocked at late times postinfection, while early and late viral protein syntheses are produced like in permissive cells; MVA assembly is inhibited after IV formation (25, 63, 67). In the case of NYVAC-infected HeLa cells, the block in morphogenesis occurs at or prior to the formation of IVs. This block could be related to the absence of certain late structural proteins required for morphogenesis. Although this study examined a limited number of late proteins, it is important to note that some of the late proteins required for virus assembly (59, 66), including p21 (A17L) and p27.5 (L1R), are not produced or are produced minimally in NYVAC-infected cells. Translational inhibition in the synthesis of some of the late viral proteins in NYVAC-infected human cells could occur at two levels. As shown here, NYVAC infection was associated with an increase in the phospho-eIF-2α-S51 levels and with rRNA breakdown. The rRNA cleavage fragments were similar in size to those produced after activation of the cellular RNase L enzyme (not shown), indicating that NYVAC infection triggered RNase L function. It is well established that eIF-2 phosphorylation and rRNA cleavage are two pathways that play a critical role in the antiviral response of interferons and are

Downloaded from jvi.asm.org at Centro Nacional de Biotecnología - Biblioteca on October 15, 2007

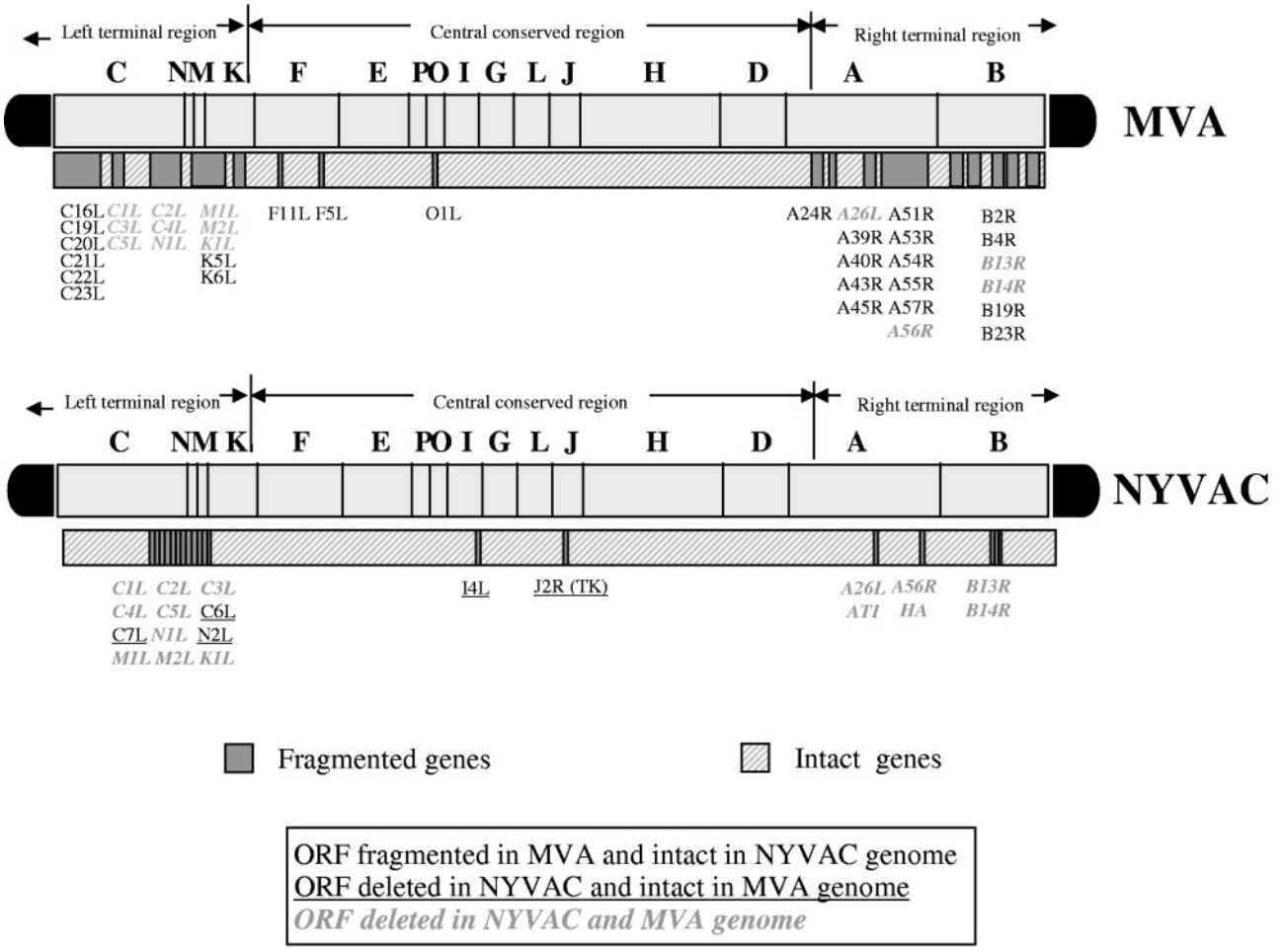

FIG. 9. Scheme of deleted genes in MVA and NYVAC genomes. Genome maps of MVA and NYVAC strains adapted from Antoine et al. (1) are represented. The deleted or fragmented genes in each genome are indicated. The right and left terminal regions are shown.

activated by double-stranded RNA (dsRNA) (64, 77). Since RNA breakdown should not discriminate between different mRNAs in the cytoplasm of the cell, local activation of eIF-2 phosphorylation could, in turn, be responsible for the apparent selective block in translation of some late viral proteins. As yet, it has not been explored whether there is specificity in translation of late viral mRNAs at focal sites in the cell cytoplasm, and the NYVAC-infected cell system could provide the means to unravel translational selectivity.

A fifth important difference observed between MVA and NYVAC was related to apoptosis. Upon infection with NYVAC, HeLa cells display morphological and biochemical features typical of apoptosis. In addition to the characteristic morphological hallmarks of programmed cell death observed by electron and light microscopy in NYVAC infection, and not in MVA, biochemical parameters such us PARP cleavage or DNA fragmentation were also evident. Flow cytometry analysis of cells infected with MVA and NYVAC that had been stained with propidium iodide revealed that the percentage of apoptotic cells in MVA infection was significantly lower than in NYVAC infection. Nearly 42% of NYVAC-infected cells demonstrated an apoptotic phenotype by 24 h p.i. Furthermore, these percentages were reduced to background levels when infected cells were treated with zVAD, a general caspase inhibitor, indicating that the apoptosis induced by NYVAC infection is caspase dependent.

Since apoptosis is an important mechanism for limiting virus infection, it is not surprising that poxviruses encode certain proteins to counteract the cell death phenomenon (7, 41, 65, 74). Some of the genes coding for these proteins critical for the control of apoptosis, such as the serpin homologs encoded by the gene B14R or B13R (the corresponding homologs of the Copenhagen VV strain referred as MVA182R and 181R), are deleted in both MVA and NYVAC (1, 36, 76). Other gene products known to block apoptosis are encoded by E3L (MVA050L) (acting through sequestration of dsRNA and prevention of activation of PKR and the 2-5A system) (16, 26, 58) and by F1L (MVA029L), an inhibitor of the mitochondrial caspase 9-induced apoptosis (75). Both genes E3L and F1L are present in NYVAC and MVA. Antoine and coworkers (1) compared the genomes of MVA and NYVAC and their respective deleted genes, which is detailed in Fig. 9. A comparison between MVA and NYVAC revealed that both viruses share common deleted or nonfunctional open reading frames (ORFs), including the six ORFs within the deletion d4817 (C5L-N1L), ORFs B13R and B14R encoding the ICE inhibi-

Downloaded from jvi.asm.org at Centro Nacional de Biotecnología - Biblioteca on October 15, 2007

tor, the ATI remnant ORF A26L, and the K1L (MVA022L) host range gene. In contrast to NYVAC, the MVA strain has a functional thymidine kinase gene (TK), an intact C7L (MVA018L) host range gene, and intact C6L (MVA019L), A56R (MVA165R), N2L (MVA021L), and I4L (MVA065L) ORFs. This suggests that some of these genes might be involved in the differential NYVAC in vitro behavior with respect to MVA. As has been reported by others, the host range genes for VV C7L, K1L, and cowpox virus CP77 in some cell lines (including HeLa cells) behaved as equivalent genes, even in the absence of amino acid similarity. Thus, deletion of one host gene could be compensated for by the presence of another, suggesting that these host range genes act in common pathways (34, 51, 54, 55). As shown here, the viral C7L gene plays a critical role in apoptosis induced by NYVAC infection as well as in many of the biological and biochemical features described in this work for NYVAC. When the C7L gene was reintroduced into the NYVAC genome, the recombinant NYVAC-C7L virus lost the ability to trigger apoptosis, to induce eIF-2α phosphorylation, and to activate rRNA breakdown, and in turn it rescued the translation capacity of late viral mRNAs and of virus multiplication in human cells. Significantly, the recombinant NYVAC-C7L virus maintains an in vivo attenuated phenotype. The fact that the C7L gene is well conserved in all of the orthopoxvirus genomes that have been sequenced highlights the importance of this gene in virus biology by counteracting host responses (29).

The head-to-head comparative analysis performed in this study between MVA and NYVAC not only will be a crucial basis for eventual prioritization of the most promising vaccine candidates based on these vectors, but also will be of great significance to vaccine research for the development of new innovative poxvirus vectors for clinical testing, providing enhanced immune responses to the foreign antigen by deletions and/or additions of immunomodulators. This approach must be applied and extended to the comparative analysis of the different immune responses produced by recombinants based on MVA or NYVAC strains. Mouse, monkey, and clinical studies of head-to-head comparison between NYVAC and MVA expressing the same cassette of HIV genes are under way by EuroVacc (www.eurovacc.org). Undoubtedly, the differential behavior observed in this study between NYVAC and MVA could play a role in the magnitude and extent of immune responses triggered by these vectors when applied for vaccination purposes.

ACKNOWLEDGMENTS

This investigation was supported by research grants from the Spanish Ministry of Education and Science BIO2004-03954, the Spanish Foundation for AIDS Research (FIPSE 36344/02), Fundación Marcelino Botín, and the EU (EuroVac QLRT-PL-1999-01321 and QLK2-CT-2002-01867). C. E. Gómez was the recipient of a Fundación Carolina fellowship, and J. L. Nájera was supported by FIPSE.

We thank Victoria Jiménez, C. Patiño, and Sylvia Gutiérrez for expert technical assistance and Patricia Martínez for editorial assistance. We are grateful to J. Tartaglia (Aventis-Pasteur) for generously providing the NYVAC strain.

REFERENCES

1. **Antoine, G., F. Scheiflinger, F. Dorner, and F. G. Falkner.** 1998. The complete genomic sequence of the modified vaccinia Ankara strain: comparison with other orthopoxviruses. Virology **244:**365–396.
2. **Bablanian, R., B. Baxt, J. A. Sonnabend, and M. Esteban.** 1978. Studies on the mechanisms of vaccinia virus cytopathic effects. II. Early cell rounding is associated with virus polypeptide synthesis. J. Gen. Virol. **39:**403–413.
3. **Bablanian, R., G. Coppola, S. Scribani, and M. Esteban.** 1981. Inhibition of protein synthesis by vaccinia virus. III. The effect of ultraviolet-irradiated virus on the inhibition of protein synthesis. Virology **112:**1–12.
4. **Bablanian, R., G. Coppola, S. Scribani, and M. Esteban.** 1981. Inhibition of protein synthesis by vaccinia virus. IV. The role of low-molecular-weight viral RNA in the inhibition of protein synthesis. Virology **112:**13–24.
5. **Bablanian, R., M. Esteban, B. Baxt, and J. A. Sonnabend.** 1978. Studies on the mechanisms of vaccinia virus cytopathic effects. I. Inhibition of protein synthesis in infected cells is associated with virus-induced RNA synthesis. J. Gen. Virol. **39:**391–402.
6. **Bablanian, R., S. K. Goswami, M. Esteban, and A. K. Banerjee.** 1987. Selective inhibition of protein synthesis by synthetic and vaccinia virus core synthesized poly(riboadenylic acids). Virology **161:**366–373.
7. **Barry, M., S. T. Wasilenko, T. L. Stewart, and J. M. Taylor.** 2004. Apoptosis regulator genes encoded by poxviruses. Prog. Mol. Subcell. Biol. **36:**19–37.
8. **Bayes, M., X. Rabasseda, and J. R. Prous.** 2005. Gateways to clinical trials. Methods Find. Exp. Clin. Pharmacol. **27:**193–219.
9. **Bayes, M., X. Rabasseda, and J. R. Prous.** 2005. Gateways to clinical trials. Methods Find. Exp. Clin. Pharmacol. **27:**49–77.
10. **Belyakov, I. M., P. Earl, A. Dzutsev, V. A. Kuznetsov, M. Lemon, L. S. Wyatt, J. T. Snyder, J. D. Ahlers, G. Franchini, B. Moss, and J. A. Berzofsky.** 2003. Shared modes of protection against poxvirus infection by attenuated and conventional smallpox vaccine viruses. Proc. Natl. Acad. Sci. USA **100:**9458–9463.
11. **Blasco, R., and B. Moss.** 1991. Extracellular vaccinia virus formation and cell-to-cell virus transmission are prevented by deletion of the gene encoding the 37,000-dalton outer envelope protein. J. Virol. **65:**5910–5920.
12. **Brockmeier, S. L., and W. L. Mengeling.** 1996. Comparison of the protective response induced by NYVAC vaccinia recombinants expressing either gp50 or gII and gp50 of pseudorabies virus. Can. J. Vet. Res. **60:**315–317.
13. **Broyles, S. S.** 2003. Vaccinia virus transcription. J. Gen. Virol. **84:**2293–2303.
14. **Carroll, M. W., and B. Moss.** 1997. Host range and cytopathogenicity of the highly attenuated MVA strain of vaccinia virus: propagation and generation of recombinant viruses in a nonhuman mammalian cell line. Virology **238:**198–211.
15. **Carroll, M. W., W. W. Overwijk, R. S. Chamberlain, S. A. Rosenberg, B. Moss, and N. P. Restifo.** 1997. Highly attenuated modified vaccinia virus Ankara (MVA) as an effective recombinant vector: a murine tumor model. Vaccine **15:**387–394.
16. **Chang, H. W., J. C. Watson, and B. L. Jacobs.** 1992. The E3L gene of vaccinia virus encodes an inhibitor of the interferon-induced, double-stranded RNA-dependent protein kinase. Proc. Natl. Acad. Sci. USA **89:**4825–4829.
17. **Dallo, S., J. F. Rodriguez, and M. Esteban.** 1987. A 14K envelope protein of vaccinia virus with an important role in virus-host cell interactions is altered during virus persistence and determines the plaque size phenotype of the virus. Virology **159:**423–432.
18. **Darzynkiewicz, Z., S. Bruno, G. Del Bino, W. Gorczyca, M. A. Hotz, P. Lassota, and F. Traganos.** 1992. Features of apoptotic cells measured by flow cytometry. Cytometry **13:**795–808.
19. **Didierlaurent, A., J. C. Ramirez, M. Gherardi, S. C. Zimmerli, M. Graf, H. A. Orbea, G. Pantaleo, R. Wagner, M. Esteban, J. P. Kraehenbuhl, and J. C. Sirard.** 2004. Attenuated poxviruses expressing a synthetic HIV protein stimulate HLA-A2-restricted cytotoxic T-cell responses. Vaccine **22:**3395–3403.
20. **Drexler, I., K. Heller, B. Wahren, V. Erfle, and G. Sutter.** 1998. Highly attenuated modified vaccinia virus Ankara replicates in baby hamster kidney cells, a potential host for virus propagation, but not in various human transformed and primary cells. J. Gen. Virol. **79:**347–352.
21. **Drexler, I., C. Staib, and G. Sutter.** 2004. Modified vaccinia virus Ankara as antigen delivery system: how can we best use its potential? Curr. Opin. Biotechnol. **15:**506–512.
22. **Esteban, M.** 1984. Defective vaccinia virus particles in interferon-treated infected cells. Virology **133:**220–227.
23. **Franchini, G., J. Benson, R. Gallo, E. Paoletti, and J. Tartaglia.** 1996. Attenuated poxvirus vectors as carriers in vaccines against human T cell leukemia-lymphoma virus type I. AIDS Res. Hum. Retrovir. **12:**407–408.
24. **Franchini, G., S. Gurunathan, L. Baglyos, S. Plotkin, and J. Tartaglia.** 2004. Poxvirus-based vaccine candidates for HIV: two decades of experience with special emphasis on canarypox vectors. Expert Rev. Vaccines **3:**S75–S88.
25. **Gallego-Gómez, J. C., C. Risco, D. Rodriguez, P. Cabezas, S. Guerra, J. L. Carrascosa, and M. Esteban.** 2003. Differences in virus-induced cell morphology and in virus maturation between MVA and other strains (WR, Ankara, and NYCBH) of vaccinia virus in infected human cells. J. Virol. **77:**10606–10622.
26. **Garcia, M. A., S. Guerra, J. Gil, V. Jimenez, and M. Esteban.** 2002. Anti-apoptotic and oncogenic properties of the dsRNA-binding protein of vaccinia virus, E3L. Oncogene **21:**8379–8387.
27. **Gherardi, M. M., J. C. Ramirez, D. Rodriguez, J. R. Rodriguez, G. Sano, F. Zavala, and M. Esteban.** 1999. IL-12 delivery from recombinant vaccinia virus

Downloaded from jvi.asm.org at Centro Nacional de Biotecnología - Biblioteca on October 15, 2007

attenuates the vector and enhances the cellular immune response against HIV-1 Env in a dose-dependent manner. J. Immunol. **162:**6724–6733.
28. **Gonin, P., W. Oualikene, A. Fournier, and M. Eloit.** 1996. Comparison of the efficacy of replication-defective adenovirus and Nyvac poxvirus as vaccine vectors in mice. Vaccine **14:**1083–1087.
29. **Gubser, C., S. Hue, P. Kellam, and G. L. Smith.** 2004. Poxvirus genomes: a phylogenetic analysis. J. Gen. Virol. **85:**105–117.
30. **Guerra, S., L. A. López-Fernández, R. Conde, A. Pascual-Montano, K. Harshman, and M. Esteban.** 2004. Microarray analysis reveals characteristic changes of host cell gene expression in response to attenuated modified vaccinia virus Ankara infection of human HeLa cells. J. Virol. **78:**5820–5834.
31. **Guerra, S., L. A. López-Fernández, A. Pascual-Montano, J. L. Nájera, A. Zaballos, and M. Esteban.** 2006. Host response to the attenuated poxvirus vector NYVAC: upregulation of apoptotic genes and NF-κB-responsive genes in infected HeLa cells. J. Virol. **80:**985–998.
32. **Hel, Z., J. Nacsa, W. P. Tsai, A. Thornton, L. Giuliani, J. Tartaglia, and G. Franchini.** 2002. Equivalent immunogenicity of the highly attenuated poxvirus-based ALVAC-SIV and NYVAC-SIV vaccine candidates in SIVmac251-infected macaques. Virology **304:**125–134.
33. **Hornemann, S., O. Harlin, C. Staib, S. Kisling, V. Erfle, B. Kaspers, G. Hacker, and G. Sutter.** 2003. Replication of modified vaccinia virus Ankara in primary chicken embryo fibroblasts requires expression of the interferon resistance gene E3L. J. Virol. **77:**8394–8407.
34. **Hsiao, J. C., C. S. Chung, R. Drillien, and W. Chang.** 2004. The cowpox virus host range gene, CP77, affects phosphorylation of eIF2 alpha and vaccinia viral translation in apoptotic HeLa cells. Virology **329:**199–212.
35. **Johnston, J. B., and G. McFadden.** 2004. Technical knockout: understanding poxvirus pathogenesis by selectively deleting viral immunomodulatory genes. Cell Microbiol. **6:**695–705.
36. **Kettle, S., A. Alcami, A. Khanna, R. Ehret, C. Jassoy, and G. L. Smith.** 1997. Vaccinia virus serpin B13R (SPI-2) inhibits interleukin-1beta-converting enzyme and protects virus-infected cells from TNF- and Fas-mediated apoptosis, but does not prevent IL-1beta-induced fever. J. Gen. Virol. **78:**677–685.
37. **Legrand, F. A., P. H. Verardi, L. A. Jones, K. S. Chan, Y. Peng, and T. D. Yilma.** 2004. Induction of potent humoral and cell-mediated immune responses by attenuated vaccinia virus vectors with deleted serpin genes. J. Virol. **78:**2770–2779.
38. **Martin, A. G., and H. O. Fearnhead.** 2002. Apocytochrome c blocks caspase-9 activation and Bax-induced apoptosis. J. Biol. Chem. **277:**50834–50841.
39. **Martinez-Pomares, L., R. J. Stern, and R. W. Moyer.** 1993. The ps/hr gene (B5R open reading frame homolog) of rabbitpox virus controls pock color, is a component of extracellular enveloped virus, and is secreted into the medium. J. Virol. **67:**5450–5462.
40. **Mayr, A., H. Stickl, H. K. Muller, K. Danner, and H. Singer.** 1978. The smallpox vaccination strain MVA: marker, genetic structure, experience gained with the parenteral vaccination and behavior in organisms with a debilitated defence mechanism. Zentbl. Bakteriol. B **167:**375–390. (Author's translation.)
41. **McFadden, G.** 2005. Poxvirus tropism. Nat. Rev. Microbiol. **3:**201–213.
42. **Meiser, A., D. Boulanger, G. Sutter, and J. Krijnse Locker.** 2003. Comparison of virus production in chicken embryo fibroblasts infected with the WR, IHD-J and MVA strains of vaccinia virus: IHD-J is most efficient in trans-Golgi network wrapping and extracellular enveloped virus release. J. Gen. Virol. **84:**1383–1392.
43. **Meyer, H., G. Sutter, and A. Mayr.** 1991. Mapping of deletions in the genome of the highly attenuated vaccinia virus MVA and their influence on virulence. J. Gen. Virol. **72:**1031–1038.
44. **Moss, B.** 1996. Genetically engineered poxviruses for recombinant gene expression, vaccination, and safety. Proc. Natl. Acad. Sci. USA **93:**11341–11348.
45. **Moss, B., and J. L. Shisler.** 2001. Immunology 101 at poxvirus U: immune evasion genes. Semin. Immunol. **13:**59–66.
46. **Ober, B. T., P. Bruhl, M. Schmidt, V. Wieser, W. Gritschenberger, S. Coulibaly, H. Savidis-Dacho, M. Gerencer, and F. G. Falkner.** 2002. Immunogenicity and safety of defective vaccinia virus Lister: comparison with modified vaccinia virus Ankara. J. Virol. **76:**7713–7723.
47. **Ockenhouse, C. F., P. F. Sun, D. E. Lanar, B. T. Wellde, B. T. Hall, K. Kester, J. A. Stoute, A. Magill, U. Krzych, L. Farley, R. A. Wirtz, J. C. Sadoff, D. C. Kaslow, S. Kumar, L. W. Church, J. M. Crutcher, B. Wizel, S. Hoffman, A. Lalvani, A. V. Hill, J. A. Tine, K. P. Guito, C. de Taisne, R. Anders, W. R. Ballou, et al.** 1998. Phase I/IIa safety, immunogenicity, and efficacy trial of NYVAC-Pf7, a pox-vectored, multiantigen, multistage vaccine candidate for Plasmodium falciparum malaria. J. Infect. Dis. **177:**1664–1673.
48. **Oguiura, N., D. Spehner, and R. Drillien.** 1993. Detection of a protein encoded by the vaccinia virus C7L open reading frame and study of its effect on virus multiplication in different cell lines. J. Gen. Virol. **74:**1409–1413.
49. **Paoletti, E.** 1996. Applications of pox virus vectors to vaccination: an update. Proc. Natl. Acad. Sci. USA **93:**11349–11353.
50. **Paoletti, E., J. Tartaglia, and J. Taylor.** 1994. Safe and effective poxvirus vectors—NYVAC and ALVAC. Dev. Biol. Stand. **82:**65–69.
51. **Perkus, M. E., S. J. Goebel, S. W. Davis, G. P. Johnson, K. Limbach, E. K. Norton, and E. Paoletti.** 1990. Vaccinia virus host range genes. Virology **179:**276–286.
52. **Pincus, S., J. Tartaglia, and E. Paoletti.** 1995. Poxvirus-based vectors as vaccine candidates. Biologicals **23:**159–164.
53. **Raengsakulrach, B., A. Nisalak, M. Gettayacamin, V. Thirawuth, G. D. Young, K. S. Myint, L. M. Ferguson, C. H. Hoke, Jr., B. L. Innis, and D. W. Vaughn.** 1999. Safety, immunogenicity, and protective efficacy of NYVAC-JEV and ALVAC-JEV recombinant Japanese encephalitis vaccines in rhesus monkeys. Am. J. Trop. Med. Hyg. **60:**343–349.
54. **Ramsey-Ewing, A., and B. Moss.** 1996. Recombinant protein synthesis in Chinese hamster ovary cells using a vaccinia virus/bacteriophage T7 hybrid expression system. J. Biol. Chem. **271:**16962–16966.
55. **Ramsey-Ewing, A., and B. Moss.** 1995. Restriction of vaccinia virus replication in CHO cells occurs at the stage of viral intermediate protein synthesis. Virology **206:**984–993.
56. **Riedl, S. J., and Y. Shi.** 2004. Molecular mechanisms of caspase regulation during apoptosis. Nat. Rev. Mol. Cell Biol. **5:**897–907.
57. **Risco, C., J. R. Rodriguez, W. Demkowicz, R. Heljasvaara, J. L. Carrascosa, M. Esteban, and D. Rodriguez.** 1999. The vaccinia virus 39-kDa protein forms a stable complex with the p4a/4a major core protein early in morphogenesis. Virology **265:**375–386.
58. **Rivas, C., J. Gil, Z. Melkova, M. Esteban, and M. Diaz-Guerra.** 1998. Vaccinia virus E3L protein is an inhibitor of the interferon (i.f.n.)-induced 2-5A synthetase enzyme. Virology **243:**406–414.
59. **Rodriguez, D., M. Esteban, and J. R. Rodriguez.** 1995. Vaccinia virus A17L gene product is essential for an early step in virion morphogenesis. J. Virol. **69:**4640–4648.
60. **Rodriguez, D., J. R. Rodriguez, J. F. Rodriguez, D. Trauber, and M. Esteban.** 1989. Highly attenuated vaccinia virus mutants for the generation of safe recombinant viruses. Proc. Natl. Acad. Sci. USA **86:**1287–1291.
61. **Rodriguez, J. R., C. Risco, J. L. Carrascosa, M. Esteban, and D. Rodriguez.** 1998. Vaccinia virus 15-kilodalton (A14L) protein is essential for assembly and attachment of viral crescents to virosomes. J. Virol. **72:**1287–1296.
62. **Rowlands, A. G., R. Panniers, and E. C. Henshaw.** 1988. The catalytic mechanism of guanine nucleotide exchange factor action and competitive inhibition by phosphorylated eukaryotic initiation factor 2. J. Biol. Chem. **263:**5526–5533.
63. **Sancho, M. C., S. Schleich, G. Griffiths, and J. Krijnse-Locker.** 2002. The block in assembly of modified vaccinia virus Ankara in HeLa cells reveals new insights into vaccinia virus morphogenesis. J. Virol. **76:**8318–8334.
64. **Sen, G. C.** 2001. Viruses and interferons. Annu. Rev. Microbiol. **55:**255–281.
65. **Shisler, J. L., and B. Moss.** 2001. Immunology 102 at poxvirus U: avoiding apoptosis. Semin. Immunol. **13:**67–72.
66. **Smith, G. L., A. Vanderplasschen, and M. Law.** 2002. The formation and function of extracellular enveloped vaccinia virus. J. Gen. Virol. **83:**2915–2931.
67. **Sutter, G., and B. Moss.** 1992. Nonreplicating vaccinia vector efficiently expresses recombinant genes. Proc. Natl. Acad. Sci. USA **89:**10847–10851.
68. **Sutter, G., and C. Staib.** 2003. Vaccinia vectors as candidate vaccines: the development of modified vaccinia virus Ankara for antigen delivery. Curr. Drug Targets Infect. Disord. **3:**263–271.
69. **Tartaglia, J., W. I. Cox, S. Pincus, and E. Paoletti.** 1994. Safety and immunogenicity of recombinants based on the genetically-engineered vaccinia strain, NYVAC. Dev. Biol. Stand. **82:**125–129.
70. **Tartaglia, J., W. I. Cox, J. Taylor, M. Perkus, M. Riviere, B. Meignier, and E. Paoletti.** 1992. Highly attenuated poxvirus vectors. AIDS Res. Hum. Retrovir. **8:**1445–1447.
71. **Tartaglia, J., M. E. Perkus, J. Taylor, E. K. Norton, J. C. Audonnet, W. I. Cox, S. W. Davis, J. van der Hoeven, B. Meignier, M. Riviere, et al.** 1992. NYVAC: a highly attenuated strain of vaccinia virus. Virology **188:**217–232.
72. **Taylor, J., R. Weinberg, J. Tartaglia, C. Richardson, G. Alkhatib, D. Briedis, M. Appel, E. Norton, and E. Paoletti.** 1992. Nonreplicating viral vectors as potential vaccines: recombinant canarypox virus expressing measles virus fusion (F) and hemagglutinin (HA) glycoproteins. Virology **187:**321–328.
73. **Tsung, K., J. H. Yim, W. Marti, R. M. L. Buller, and J. A. Norton.** 1996. Gene expression and cytopathic effect of vaccinia virus inactivated by psoralen and long-wave UV light. J. Virol. **70:**165–171.
74. **Turner, P., and R. W. Moyer.** 1998. Control of apoptosis by poxviruses. Semin. Virol. **8:**453–469.
75. **Wasilenko, S. T., T. L. Stewart, A. F. Meyers, and M. Barry.** 2003. Vaccinia virus encodes a previously uncharacterized mitochondrial-associated inhibitor of apoptosis. Proc. Natl. Acad. Sci. USA **100:**14345–14350.
76. **Wyatt, L. S., M. W. Carroll, C. P. Czerny, M. Merchlinsky, J. R. Sisler, and B. Moss.** 1998. Marker rescue of the host range restriction defects of modified vaccinia virus Ankara. Virology **251:**334–342.
77. **Yang, Y. L., L. F. Reis, J. Pavlovic, A. Aguzzi, R. Schafer, A. Kumar, B. R. Williams, M. Aguet, and C. Weissmann.** 1995. Deficient signaling in mice devoid of double-stranded RNA-dependent protein kinase. EMBO J. **14:**6095–6106.

Downloaded from jvi.asm.org at Centro Nacional de Biotecnología - Biblioteca on October 15, 2007

JOURNAL OF VIROLOGY, Jan. 2006, p. 985–998 Vol. 80, No. 2
0022-538X/06/$08.00+0 doi:10.1128/JVI.80.2.985–998.2006
Copyright © 2006, American Society for Microbiology. All Rights Reserved.

Host Response to the Attenuated Poxvirus Vector NYVAC: Upregulation of Apoptotic Genes and NF-κB-Responsive Genes in Infected HeLa Cells

Susana Guerra,[1] Luis A. López-Fernández,[2] Alberto Pascual-Montano,[3] José Luis Nájera,[1] Angel Zaballos,[2] and Mariano Esteban[1]*

Department of Molecular and Cellular Biology,[1] Department of Immunology and Oncology,[2] and Biocomputing Unit,[3] Centro Nacional de Biotecnología, CSIC, Ciudad Universitaria Cantoblanco, E-28049 Madrid, Spain

Received 19 August 2005/Accepted 10 October 2005

NYVAC has been engineered as a safe, attenuated vaccinia virus (VV) vector for use in vaccination against a broad spectrum of pathogens and tumors. Due to the interest in NYVAC-based vectors as vaccines and current phase I/II clinical trials with this vector, there is a need to analyze the human host response to NYVAC infection. Using high-density cDNA microarrays, we found 368 differentially regulated genes after NYVAC infection of HeLa cells. Clustering of the regulated genes identified six discrete gene clusters with altered expression patterns. Clusters 1 to 3 represented 47.5% of the regulated genes, with three patterns of gene activation kinetics, whereas clusters 4 to 6 showed distinct repression kinetics. Quantitative real-time reverse transcription-PCR analysis of selected genes validated the array data. Upregulated transcripts correlated with genes implicated in immune responses, including those encoding interleukin-1 receptor 2 (IL-1R2), IL-6, ISG-15, CD-80, and TNFSF7. NYVAC upregulated several intermediates of apoptotic cascades, including caspase-9, correlating with its ability to induce apoptosis. NYVAC infection also stimulated the expression of NF-κB1 and NF-κB2 as well as that of NF-κB target genes. Expression of the VV host range K1L gene during NYVAC infection prevented NF-κB activation, but not the induction of apoptosis. This study is the first overall analysis of the transcriptional response of human cells to NYVAC infection and provides a framework for future functional studies to evaluate this vector and its derivatives as human vaccines.

Attenuated strains of vaccinia virus (VV) were developed in response to the need for safer vaccines (37). NYVAC is a derivative of the VV Copenhagen strain in which 18 open reading frames were specifically deleted from the parental viral genome; genes involved in host range, virulence, and pathogenesis were thus lost (49). NYVAC-derived vectors are able to express antigens from a wide range of species (50). A number of examples have been reported, using NYVAC as a recombinant vaccine delivery system against pathogens and tumors (5, 10, 31, 46). Clinical trials using NYVAC-based vectors show a good safety profile, with induction of high levels of immunity against heterologous antigens (24, 34).

Since phase I/II clinical trials using this vector are currently under way, particularly for human immunodeficiency virus type 1 (HIV-1) (www.eurovacc.org), it is essential to obtain a comprehensive understanding of the effect of NYVAC infection on human host gene expression (34). DNA microarray technology allows monitoring of the expression of several thousand individual genes (22) and has been used to identify the differential expression of cellular genes in response to infection by several animal viruses, including VV strains WR (Western Reserve) and MVA (modified vaccinia Ankara) (15, 16, 29, 55).

Host genes that govern vital cell processes such as replication, transcription, and translation are downregulated during the course of WR infection. The expression of genes involved in apoptosis or the proteasome-ubiquitin degradation pathway is also repressed; few genes are upregulated after WR infection (15). A larger number of genes than that seen with WR is upregulated during strain MVA infection; most encode immune modulator proteins, some of which may be involved in host resistance and immune modulation during MVA infection (16). Wiskott-Aldrich syndrome protein (WASP) family members are upregulated after MVA or WR infection (15, 16). This family includes the gene that codes for the N-WASP protein, implicated in the actin-mediated motility of VV as a mechanism for intercellular viral spreading (8, 11). Additional studies show that WASP is required for VV pathogenesis (17). The results of microarray analysis have implicated cell signaling events and cell proteins as important regulators of VV infection.

For this study, we used cDNA microarray technology to analyze host gene expression changes in HeLa cell cultures following NYVAC infection. This is the first large-scale analysis of the transcriptional response of HeLa cells to NYVAC infection. It provides a better understanding of the mechanisms of vaccine protection against VV infection and will aid in the development of NYVAC recombinant-based vaccines against pathogens and tumors.

MATERIALS AND METHODS

Cells, viruses, and infection conditions. HeLa cells (ATCC) were cultured in Dulbecco's medium supplemented with 10% newborn bovine serum and antibiotics. The VV WR strain was cultured in monkey BSC-40 cells, purified by sucrose gradient banding, and titrated on BSC-40 cells by a plaque assay. The NYVAC and MVA strains were cultured in BHK-21 cells, purified by sucrose gradient banding, and titrated on BHK-21 cells by immunostaining of fixed infected cultures with a polyclonal anti-VV protein antibody (12).

* Corresponding author. Mailing address: Centro Nacional de Biotecnología/CSIC, Ciudad Universitaria Cantoblanco, 28049 Madrid, Spain. Phone: (34) 91/585-4553. Fax: (34) 91/585-4506. E-mail: mesteban@cnb.uam.es.

Downloaded from jvi.asm.org at Centro Nacional de Biotecnología - Biblioteca on October 15, 2007

Microarray production. The Research Genetics 40K sequence-verified human cDNA clone library (http://www.resgen.com/products/SVHcDNA.php3) was used to generate cDNA arrays as described previously (15). Slides contained 15,360 cDNAs, of which 13,295 correspond to known genes and 2,065 correspond to control genes. The cDNAs were printed on CMT-GAPS II slides (Corning) with a Microgrid II apparatus (BioRobotics).

Microarray hybridization. Total RNA was isolated from purified NYVAC-infected (5 PFU/cell) or mock-infected HeLa cells cultured in 10-cm plates, using Ultraspect-II RNA (Biotecx). RNAs were then purified with Megaclear (Ambion), and their integrity was confirmed using an Agilent 2100 bioanalyzer (Agilent). Uninfected samples were isolated at each infection time point and processed in parallel with infected cells. Two independent replicates were processed for analysis. Total RNA (1.5 μg for each replicate) was amplified using an amino allyl MessageAmp aRNA kit (Ambion), and approximately 25 to 40 μg of amplified RNA (aRNA) was obtained. The mean aRNA size was 1,500 nucleotides. For each sample, 5 μg aRNA was labeled with Cy3 or Cy5 (CyDye postlabeling reactive dye pack; Amersham) and purified. We measured Cy3 and Cy5 incorporation using 1 μl of probe in a Nanodrop spectrophotometer (Nanodrop Technologies Inc.). For each hybridization, Cy3 and Cy5 probes (150 pmol each) were mixed, dried in a Speed-Vac machine, and resuspended in 9 μl of RNase-free water. Two dye-swapped hybridizations were performed; in one, the mock-infected sample was Cy3 labeled and the NYVAC-infected sample was Cy5 labeled; in the second, the labeling was reversed. Double labeling was used to abolish dye-specific labeling and hybridization differences. Slides were prehybridized and hybridized as described previously (15, 16), dried by centrifugation, and scanned on an Axon 4000B instrument (Axon). Images and raw data were obtained using GenePix 5.0 software (Axon) and were processed using SOLAR software (Bioalma, Spain). Briefly, the background was subtracted from the signal, $\log_{10}$ (signal) values were plotted versus $\log_2$ (ratio) values, and Lowess normalization was used to adjust most spots to a log ratio of 0. This was calculated for all four replicates, and a table was obtained with mean signals, degrees of change, log ratios, standard deviations of the log ratios, and *z* scores (40).

Gene expression analysis. The original data set, containing 13,295 clones per slide, was prepared for clustering. Genes with an interreplicate standard deviation of >1 were removed from the analysis. The resulting data set was reduced to 8,722 transcripts that showed consistent expression values among the four replicates. The *z* score (a measure of the proximity of one value [log ratio] to other values with similar signals) was used to eliminate genes that did not show significant expression under at least one experimental condition (40). Only genes with a *z* score of >2 were thus selected for clustering. A new data set was created with the 368 transcripts that passed the filter. After data preprocessing, genes were clustered using Kohonen's self-organizing map (25). The resulting seven-by-five map was analyzed using the Engene software package (13) at http://www.engene.cnb.uam.es.

Quantitative real-time RT-PCR. RNAs (1 μg) were reverse transcribed using the Superscript first-strand synthesis system for reverse transcription-PCR (RT-PCR) (Invitrogen). A 1:40 dilution of the RT reaction mixture was used for quantitative PCR. The primer and probe sets used to amplify the genes for PCNT2, WASL, NF-κB2, interleukin-7 (IL-7), IL-6, gamma interferon (IFN-γ), CASP-9, ATF-3, GADD34, and APEXL2 were purchased from Applied Biosystems. RT-PCRs were performed according to Assay-on-Demand, optimized for TaqMan Universal PCR master mix with no AmpErase UNG (15, 16). All samples were assayed in duplicate. Threshold cycle (C_T) values were used to plot a standard curve in which the C_T decreased in linear proportion to the log of the template copy number. Correlation values of standard curves were always >99%.

Gel retardation assay. Nuclear extracts (3 μg) from HeLa cells grown in 6-cm-well plates, either uninfected or infected with WR, MVA, or NYVAC at 5 PFU/cell, were analyzed using the synthetic [α-^{32}P]dCTP-labeled double-stranded wild-type HIV enhancer oligonucleotide 5′-AGCTTACAAGGGACTTTCCGCTGGGGACTTTCCAGGGA-3′, containing two κB consensus motifs, as described previously (3). For supershift assays, anti-p50 antibody (1 μl; Santa Cruz) was added 15 min before the labeled probe.

ELISA. IL-6 secreted into the medium of NYVAC-, MVA-, or WR-infected HeLa cells (5 PFU/cell) in 12-well plates was measured with a quantitative human IL-6 kit (BD Biosciences). Supernatants (100 μl) from uninfected or infected HeLa cells at 2, 6, and 16 h postinfection (hpi) were used for enzyme-linked immunosorbent assays (ELISAs). Captured IL-6 was quantified at 450 nm in a spectrophotometer. Duplicate samples were measured in two independent experiments.

Apoptosis assay. HeLa cells cultured in 12-well plates were infected (5 PFU/cell) with the indicated viruses and harvested at 24 hpi for determination of the absorbance (405 nm). Cell death was detected with an ELISA kit (Roche) which uses mouse anti-DNA and -histone monoclonal antibodies to estimate the amount of cytoplasmic histone-associated DNA.

Western blotting. HeLa cells grown in six-well plates were infected (5 PFU/cell) with WR, MVA, or NYVAC and collected, and cell extracts were prepared at 2, 6, and 16 hpi by lysis in buffer (50 mM Tris-HCl, pH 8.0, 0.5 M NaCl, 10% NP-40, 1% sodium dodecyl sulfate [SDS]) on ice for 5 min. Protein lysates (100 μg) were separated by SDS-polyacrylamide gel electrophoresis (SDS-PAGE) on 14% or 8% gels, transferred to nitrocellulose membranes, and incubated with the following antibodies: anti-caspase-9 (Oncogene), -PARP (Cell Signaling), -actin (Santa Cruz), -E3L (a gift from B. L. Jacobs), -A14L (43), -NF-κB1, which recognizes p105 and p50 (Santa Cruz), -IκBα (Santa Cruz), -ATF-3 (Santa Cruz), -initiation factor 2α-P (IF-2α-P; Biosource), and -eIF-2α (Santa Cruz), followed by secondary antibodies (mouse and rabbit peroxidase conjugates). Protein expression was detected using ECL reagents (Amersham).

Immunofluorescence. HeLa cells cultured on coverslips were infected with NYVAC or WR (5 PFU/cell). At 6 and 16 hpi, cells were washed with phosphate-buffered saline, fixed with 4% paraformaldehyde, and permeabilized with 0.1% Triton X-100 in phosphate-buffered saline (room temperature, 10 min). Cells were incubated with the primary antibody anti-ATF-3, -caspase-9 (Calbiochem), -T7-tag (Novagen), or -E3L, followed by fluorescein- or Texas red-conjugated isotype-specific secondary antibodies and the DNA staining reagent ToPro (Molecular Probes). Images were obtained using a Bio-Rad Radiance 2100 confocal laser microscope.

Transfection assay. HeLa cells cultured on coverslips were infected (0.1 PFU/cell) with NYVAC, and after 1 h, were transfected with the expression plasmid pK1L (3 μg DNA) using JetPEI (Q-Biogene). At 40 h posttransfection, cells were fixed and analyzed by immunofluorescence. The pK1L expression plasmid was derived from pMJ601 by insertion of the VV (WR strain) *K1L* gene, containing the code for T7-Tag at the N terminus, under the transcriptional control of the VV early-late promoter p7.5 (kindly provided by A. Alcamí). The transfection efficiency was approximately 80%, with ≤5% interexperiment variation.

RESULTS

Cellular gene expression pattern after NYVAC infection. cDNA microarray technology was used to analyze the overall changes in human cellular gene expression following NYVAC infection. Due to the interest in NYVAC as a live recombinant vaccine vector, it is important to define the effects of NYVAC infection on human host gene expression. We thus used human HeLa cells, as many fundamental studies in poxvirus biology are based on this cell line.

We used chips carrying cDNAs from 13,295 human genes to profile gene expression in HeLa cells which were mock infected or infected for 2, 6, and 16 h. We analyzed mRNA duplicates isolated at 2, 6, and 16 hpi in two independent experiments and identified 368 genes that were differentially expressed after NYVAC infection, which represent 2.8% of the genes in the array. Following detailed analysis of their profiles, we grouped these genes into six main clusters according to their behavior at three time points during NYVAC infection. The expression clusters of genes that were up- or downregulated after infection and that passed the filtering conditions are depicted in Supplementary Fig. 1 on our website (http://www.cnb.uam.es/~sguerra/JVirol/supplementary.pdf). The clusters appear to represent specific regulation patterns; the average profile for each cluster is shown in Fig. 1.

Clusters 1 to 3 correspond to three patterns of gene activation kinetics, whereas clusters 4 to 6 show distinct repression kinetics. Cluster 1 contains 73 transcripts (20.16%) that are upregulated during infection; this is the only cluster that shows generalized induction from 2 to 16 hpi. Cluster 2 contains 58 transcripts (16.02%), including genes with induction maintained from 6 to 16 hpi that are unaffected at 2 hpi. Cluster 3 contains 41 transcripts (11.32%) that are upregulated at 6 hpi but return to basal levels by 16 hpi. Cluster 4 contains 79 transcripts (21.82%) that are downregulated at 6 hpi and are

Downloaded from jvi.asm.org at Centro Nacional de Biotecnología - Biblioteca on October 15, 2007

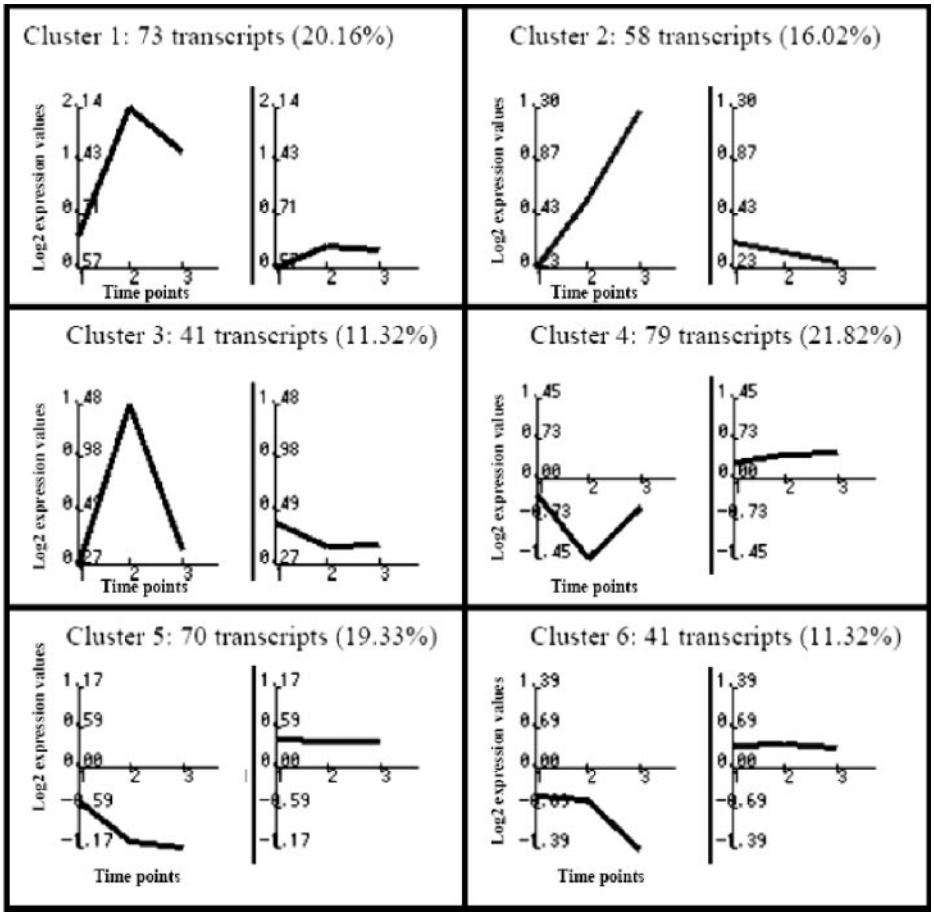

FIG. 1. Characteristic expression patterns represented in clusters 1 to 6. Mean values (left) and standard deviations (right) of the expression profiles of genes assigned to each cluster are shown. Experimental points on the *x* axis are indicated as follows: 1 for 2 h, 2 for 6 h, and 3 for 16 hpi. The *y* axis shows normalized expression values. Each value in parentheses shows the percentage of genes in each cluster with reference to the total of 368 differentially expressed genes.

unaltered at the other times studied. Clusters 5 and 6 contain 111 transcripts (30.7%); both show downregulation throughout infection, with distinct profiles.

Representative human genes that are upregulated in NYVAC infection (clusters 1 to 3) are classified according to their biological functions in Table 1. Genes whose expression was repressed after NYVAC infection represented 52.5% of the 368 genes; examples of human genes downregulated by NYVAC in clusters 5 and 6 are detailed in supplementary Table 1 on our website (http://www.cnb.uam.es/~sguerra/JVirol/supplementary.pdf).

Confirmation of microarray data by quantitative real-time RT-PCR. We used real-time RT-PCR to verify the transcriptional changes in selected genes, as detected by microarray analysis. We analyzed 10 genes, 6 of which were upregulated (*WASL*, *NF-κB-2*, *CASP-9*, *ATF-3*, *GADD-34*, and *IL-6*), 2 of which were downregulated (*IL-7* and *IFNγ*), and 2 of which were unaltered (*PCNT2* and *APEXL*); *HPRT* was used as an internal control (Table 2). The assay was performed with the same RNA samples from infected and uninfected HeLa cells used in microarray experiments. The expression patterns and relative mRNA abundances of the genes selected concurred with the microarray data in all cases, with only slight variations, validating the microarray results.

Target verification and activation of representative cell proteins after NYVAC infection. Although changes in mRNA levels do not necessarily represent changes in protein expression, we used various approaches to analyze whether the gene expression changes detected by microarray analysis correlated with protein levels and the activities of selected gene products.

(i) Caspase-9 activation. The caspase-9 gene was differentially expressed following NYVAC infection (Tables 1 and 2); thus, we analyzed the effect of the mRNA increase on the protein level. Immunofluorescence experiments indicated that transcriptional upregulation of caspase-9 after NYVAC infection corresponded with an increase in active caspase-9 protein levels, confirming the microarray data. Whereas no active caspase-9 signal was found in control or WR-infected HeLa cells, a distinct punctate pattern was observed in NYVAC-infected cells at 6 and 16 hpi (Fig. 2A). In addition, we used Western blotting to measure the levels of procaspase cleavage to activated caspase-9 in HeLa cells infected with NYVAC compared to those in cells infected with other VV strains. Caspase-9 activation was detected, with a 10-kDa cleavage product from the 46-kDa procaspase. We observed a clear increment in procaspase-9 and a notable increase in active caspase-9 after NYVAC infection. In MVA-infected cells,

Downloaded from jvi.asm.org at Centro Nacional de Biotecnología - Biblioteca on October 15, 2007

TABLE 1. Representative human genes in clusters 1 to 3 (upregulated by NYVAC)

Cluster, function, and gene name	Accession no.	Gene symbol[a]	Change (fold) at indicated time (hpi)		
			2.00	6.00	16.00
Cluster 1					
Cell cycle, apoptosis					
V-Jun avian sarcoma virus 17 oncogene homolog	W96155	JUN	2.14	13.75	8.01
Activating transcription factor 3	H21042	ATF3	2.42	8.36	6.10
Caspase-9, apoptosis-related cysteine protease	AA281152	CASP9	2.59	2.37	1.98
Dual-specificity phosphatase 2	AA759046	DUSP2	2.43	5.25	1.56
JunB proto-oncogene	T99236	JUNB	1.96	2.64	1.65
Cytochrome P450, subfamily I (dioxin-inducible)	N21019	CYP1B1	1.89	2.73	2.15
Cytoskeleton					
Connective tissue growth factor	AA598794	CTGF	4.24	11.45	5.14
Pleckstrin homology-like domain, family A, member 1	AA258396	PHLDA1	4.19	8.24	5.28
Pleckstrin homology-like domain, family A, member 1	AA258396	PHLDA1	3.85	5.22	4.11
Calcineurin-binding protein calsarcin-1	AA065090	CS-1	1.70	2.30	2.55
Kinesin family member 5A	AA984728	KIF5A	1.89	5.45	4.64
Immune system					
Tumor necrosis factor (ligand) superfamily, member 7	AI347622	TNFSF7	1.79	3.08	3.41
Coagulation factor III (thromboplastin, tissue factor)	AI313387	F3	1.58	2.04	1.53
Interleukin-6 (interferon beta 2)	N98591	IL6	2.02	5.85	2.68
Signaling					
Early growth response 1	AA488533	EGR1	4.74	10.38	6.83
Nuclear factor kappa light polypeptide gene enhancer in B cells 2 (p49/p100)	AA952897	NFKB2	1.53	2.02	1.79
Serum-inducible kinase	AA460152	SNK	1.57	6.49	2.44
Tissue factor pathway inhibitor 2	AA399473	TFPI2	1.62	1.77	2.60
Brain-derived neurotrophic factor	AA262988	BDNF	1.78	4.35	2.12
Small inducible cytokine subfamily A, member B	AI268937	SCYA8	1.76	3.04	2.89
Miscellaneous					
Nucleoporin, 88 kDa	AA488609	NUP88	3.52	6.49	4.23
DHHC1 protein	W80739	LOC51304	1.96	8.09	4.32
Ubiquitin-conjugating enzyme E2M	AA449119	UBE2M	1.52	3.06	2.91
Prostagtandin-endoperoxide synthase 2	AA644211	PTGS2	1.80	2.90	2.68
Small nuclear ribonucleoprotein polypeptides B and B1	AA279662	SNRPB	1.66	2.85	2.87
Hypothetical protein A-211C6.1	N39229	LOC57149	1.55	2.74	2.54
Cluster 2					
Adhesion and cytoskeleton					
Collagen, type VII, alpha 1	AA598507	COL7A1	1.46	2.82	2.26
Tight junction protein 1 (zona occludens 1)	H50344	TJP1	1.18	1.93	2.96
Protocadherin alpha 9	AA437139	PCDHA9	1.21	1.31	2.04
Cell cycle, apoptosis					
Myeloid cell leukemia sequence 1 (BCL2-related)	AA488674	MCL1	1.31	3.61	2.18
Growth arrest and DNA-damage-inducible 34	AA460168	GADD34	1.21	2.48	1.93
SRC homology three (SH3) and cysteine-rich domain	AA031284	STAC	1.11	2.41	2.84
Growth arrest and DNA-damage-inducible 135	AA404666	GADD135	1.32	2.98	2.06
Mitochondrial translational release factor 1	AI347695	MTRF1	1.19	2.06	2.21
DnaJ (Hsp40) homolog, subfamily B, member 2	AA455298	DNAJB2	1.22	2.69	2.39
Ras homolog gene family, member E	W86282	ARHE	1.08	2.68	2.35
GRO3 oncogene	AA935273	GRO3	1.20	2.62	2.38
v-Myc avian myelocytomatosis viral oncogene homolog	AA464600	MYC	1.05	2.93	1.65
v-Myc avian myelocytomatosis viral oncogene homolog	W87741	MYC	1.08	2.93	1.59
v-Akt murine thymoma viral oncogene homolog 2;	AA457097	AKT2	1.22	2.15	1.57
Murine leukemia viral (Bmi-1) oncogene homolog	AA478036	BMI1	1.15	1.36	3.18
Immune system					
CD80 antigen (CD28 antigen ligand 1, B7-1 antigen)	AA983817	CD80	1.25	2.02	2.70
Interleukin-1 receptor, type II	H78386	IL1R2	1.29	1.58	4.02
Interferon stimulated protein					
Interferon-stimulated protein, 15 kDa	AA406020	ISG15	1.21	1.14	3.39
Metabolism					
Fatty acid desaturase 3	AI123992	FADS3	1.45	2.94	2.41
Carboxypeptidase A2 (pancreatic)	AA844831	CPA2	1.48	2.83	3.45
Miscellaneous					
Discs, large (*Drosophila*) homolog 1	AA521155	DLG1	1.24	2.16	2.80
CGI-20 protein	R02578	LOC51608	1.22	2.11	2.94
Bromodomain, testis specific	AA454222	BRDT	1.37	1.56	2.17
RNA binding motif protein 5	AA456007	RBM5	1.18	3.20	2.42

Continued on facing page

Downloaded from jvi.asm.org at Centro Nacional de Biotecnología - Biblioteca on October 15, 2007

TABLE 1—*Continued*

Cluster, function, and gene name	Accession no.	Gene symbol[a]	Change (fold) at indicated time (hpi)		
			2.00	6.00	16.00
Spermidine/spermine *N*1-acetyltransferase	AA598631	SAT	1.20	2.51	2.62
Spermidine/spermine *N*1-acetyltransferase	AA011215	SAT	1.20	2.47	2.25
Splicing factor, arginine/serine-rich 10	AI583623	SFRS10	1.19	4.41	3.21
CBP/p300-interacting transactivator 2	AA115078	CITED2	1.19	4.86	1.87
Solute carrier family 2, member 3	AA406552	SLC2A3	1.43	2.12	1.77
RAE1 (RNA export 1, from *Schizosaccharomyces pombe*) homolog	AA504128	RAE1	1.39	2.07	1.82
Apg12 (autophagy 12, *S. cerevisiae*)-like	AA251737	APG12L	1.17	2.70	2.07
Discs, large (Drosophila) homolog 1	H24708	DLG1	1.35	1.89	3.15
Signaling					
Nuclear factor kappa light polypeptide gene enhancer	AA451716	NFKB1	1.19	2.13	1.92
A kinase (PRKA) anchor protein (gravin) 12	AA478543	AKAP12	1.43	4.55	2.86
Phorbol-12-myristate-13-acetate-induced protein 1	AA458838	PMAIP1	1.10	2.46	2.93
Glutamate receptor, ionotropic, *N*-methyl D-aspartate 2D	AI565972	GRIN2D	1.30	2.36	2.24
Receptor tyrosine kinase-like orphan receptor 2	N94921	ROR2	1.26	1.68	2.46
Immediate-early response 3	AA457705	IER3	1.44	1.38	2.99
Prostaglandin E receptor 3 (subtype EP3)	AA406362	PTGER3	1.29	1.22	4.32
Solute carrier family 17 (sodium phosphate)	H60423	SLC17A2	1.29	1.60	2.14
Adaptor-related protein complex 3, delta 1 subunit	AA630776	AP3D1	1.18	2.05	2.34
Translation and transcription					
Splicing factor (CC1.3)	H47069	CC1.3	1.24	2.36	2.40
Splicing factor (CC1.3)	AA171948	CC1.3	1.04	1.89	2.26
Splicing factor, proline/glutamine-rich	AA425853	SFPQ	1.09	1.69	2.55
Wiskott-Aldrich family					
Wiskott-Aldrich syndrome-like protein	AI261600	WASL	1.22	1.62	2.60
Cluster 3					
Adhesion and cytoskeleton					
Claudin 1	AA194833	CLDN1	1.48	2.29	1.30
Catenin (cadherin-associated protein), alpha 1 (102 kDa)	AA676957	CTNNA1	1.76	2.20	1.48
Collagen, type III, alpha 1	COL3A1	COL3A1	1.19	2.03	1.09
Cadherin 18, type 2	AA865745	CDH18	0.27	2.17	1.24
Cell cycle, apoptosis					
BCL2-associated athanogene	AI017240	BAG1	1.06	2.05	1.32
FOS-like antigen 1	T89996	FOSL1	1.19	2.08	−1.10
CDC10 (cell division cycle 10, *S. cerevisiae*), homolog	AA633993	CDC10	1.07	3.76	1.45
Transforming growth factor beta-stimulated protein TSC-22	AA664389	TSC22	1.20	3.16	1.41
Transformer-2 alpha (hTra-2 alpha)	AA701944	HSU53209	1.25	2.05	1.46
Signaling					
Delodinase, iodothyronine, type II	AA864322	DIO2	1.17	3.86	1.40
Mitogen-activated protein kinase kinase 3	H08749	MAP2K3	1.73	2.15	1.47
Phosphatidylinositol-4-phosphate 5-kinase, type I, gamma	AA482251	PIP5K1C	1.25	2.17	1.36
Phosphatidylinositol-4-phosphate 5-kinase, type I, alpha	AA255881	PIP5K1A	1.08	2.31	1.44
Immune system					
Insulin-like growth factor binding protein 3	AA598601	IGFBP3	1.14	4.58	1.56
Chemokine (C-X-C motif), receptor 4 (fusin)	T62636	CXCR4	1.47	2.40	1.41
Inhibitor of growth 1 family, member 1	N33574	ING1	1.49	2.24	1.76
Coagulation factor III (thromboplastin, tissue factor)	AI313387	F3	1.31	2.23	1.39
Miscellaneous					
Serum/glucocorticoid-regulated kinase	AI375353	SGK	1.12	2.89	1.41
Cofactor required for Sp1 transcriptional activation	N92735	CRSP6	1.19	2.11	1.49
Tryptophan 2,3-dioxygenase	T72398	TDO2	1.26	2.12	1.44
Transiation and transcription					
Slug (chicken homolog), zinc finger protein	H57310	SLUG	1.07	3.29	1.47
Eukaryotic translation initiation factor 5A	H99842	EIF5A	1.10	2.78	1.14
Zinc finger protein 274	AI085519	ZNF274	1.07	2.08	1.33

[a] Representative human gene targets of NF-κB are underlined.

weakly active caspase-9 was observed at 16 hpi, whereas there was no evidence of active caspase-9 in WR-infected HeLa cells at any time postinfection (Fig. 2B).

This apparent caspase activation in NYVAC-infected cells prompted us to compare apoptosis in HeLa cells infected with different VV strains. To measure apoptosis, we determined the amount of cytoplasmic histone-associated DNA in mock-, WR-, MVA-, or NYVAC-infected cells (Fig. 2C). As a positive control, we infected HeLa cells with an inducible VV recombinant expressing protein kinase R (PKR) in an isopropyl-β-D-thiogalactopyranoside (IPTG)-dependent manner, which produces apoptosis (27). Apoptosis levels in NYVAC-infected

Downloaded from jvi.asm.org at Centro Nacional de Biotecnología - Biblioteca on October 15, 2007

TABLE 2. Confirmation of microarray data by real-time RT-PCR

Gene product	Fold change at indicated time (hpi)					
	Microarray			RT-PCR		
	2	6	16	2	6	16
IL-6	2.02	5.85	2.68	3.2	4.65	3.25
WASL	1.22	1.62	2.6	2.6	2.03	4.3
NF-κB2	1.53	2.02	1.79	1.68	2.87	2.06
IL-7	0.80	0.55	0.88	0.95	0.63	0.79
IFN-γ	1.08	0.95	0.74	1.20	0.96	0.85
APEXL2	1.18	1.0	1.45	1.01	0.98	1.25
PCNT2	1.01	1.30	1.07	1.10	1.28	1.20
CASP-9	2.59	2.37	1.98	2.98	3.02	2.10
GADD-34	1.21	2.48	1.93	1.90	2.82	1.80
ATF-3	2.42	8.36	6.10	2.31	9.21	5.69

cells at 24 hpi were similar to those in VV-PKR-infected cells. Apoptosis was not detected in mock- or WR-infected cells, whereas low apoptosis levels were found after MVA infection. Altogether, these results indicated that NYVAC upregulates several intermediates of apoptotic cascades, in correlation with the ability of this virus to induce apoptosis.

(ii) Activation of effector caspases. Apoptosis is mediated by the activation of caspase-8 or -9, leading to the activation of effector caspases-3 and -7, which cleave specific substrates, including PARP-1. This enzyme catalyzes the formation of poly(ADP-ribose) polymers on acceptor proteins involved in the maintenance of chromatin structure, which indicates activation of the apoptotic cascade (47). To study apoptosis induction after NYVAC infection, we measured the kinetics of apoptosis in Western blot analysis by the detection of PARP-1, using an antibody that recognizes both the full-length and the cleaved protein. As shown in Fig. 3A, the 89-kDa cleaved PARP-1 fragment became evident at 16 hpi. As a control of infection, we measured the virus gene expression patterns of representative early (E3L) and late (A14L) VV proteins (Fig. 3A).

By phase-contrast microscopy, we monitored apoptosis induction in WR-, MVA-, or NYVAC-infected HeLa cells (5 PFU/cell). A characteristic apoptotic phenotype was manifested at 16 hpi in NYVAC-infected cells, defined by the rounded, floating, phase-bright, and wrinkled shape of the cells (Fig. 3B). At 16 hpi, a nonapoptotic phenotype was observed in WR- and MVA-infected cells (Fig. 3B). WR produced a pronounced cytopathic effect, including a change in cell morphology from an elongated spindle-shaped form to a rounded form. Compared to WR, MVA produced a minor cytopathic effect, with a characteristic bipolar phenotype as described previously (12).

(iii) Enhanced NF-κB expression and activation. To further validate the microarray data, we measured NF-κB1 by Western blotting of NYVAC- compared to mock-, WR-, or MVA-infected HeLa cells, using an antibody that recognizes both the p105 and p50 subunits of NF-κB1 (Fig. 4A). In WR-infected cells, NF-κB1 protein levels (p105 and p50) were similar to those in mock-infected cells. In MVA- and NYVAC-infected cells, the NF-κB1 signal was higher than that in mock- or WR-infected cells due to enhanced NF-κB1 expression, as shown by microarray analysis (Table 1). To evaluate whether the NYVAC-induced increase in NF-κB component mRNA and protein expression corresponded to NF-κB activation, nuclear extracts from mock-, NYVAC-, MVA-, or WR-infected HeLa cells were incubated with radiolabeled oligonucleotides containing a consensus NF-κB binding site sequence and analyzed by electrophoretic mobility shift assays (EMSAs). The MVA and NYVAC strains activated NF-κB at 6 and 16 hpi, whereas NF-κB activation was not observed in WR-infected nuclear extracts at 6 and 16 hpi (Fig. 4B). NYVAC-infected HeLa cells at 16 hpi produced a specific complex that showed a supershift when a specific anti-NF-κB p50 antibody was added to nuclear extracts. NYVAC produced an increase in NF-κB protein levels and transcription factor activity (Fig. 4A and B). NF-κB translocation from the cytoplasm to the nucleus is governed by IκBα degradation; we thus evaluated IκBα levels by Western blotting of cytoplasmic extracts from mock-, WR-, MVA-, or NYVAC-infected cells at 4 hpi. IκBα was localized in the cytoplasm in mock- and WR-infected cells (Fig. 4C), whereas cytoplasmic IκBα was greatly reduced in MVA- and NYVAC-infected cells, concurring with NF-κB activation in the nucleus (Fig. 4B).

NF-κB plays an important role in the expression of inflammatory cytokines, including IL-6 (21). To correlate NF-κB activation with IL-6 expression, we used ELISA to quantify the levels of secreted IL-6 in WR-, MVA-, or NYVAC-infected HeLa cells at 2, 6, and 16 hpi. We observed a strong IL-6 increase over time after MVA or NYVAC infection. The increase in IL-6 protein levels following NYVAC infection is in complete agreement with the upregulation of IL-6 mRNA levels detected by microarray analysis and real-time RT-PCR (Tables 1 and 2). IL-6 synthesis is augmented due to the increase in transcription, which results in higher levels of protein translation and secretion. When HeLa cells were infected with WR, we did not observe NF-κB activation, and IL-6 was not detected by ELISA in cell-free supernatants (Fig. 4B and D). NF-κB activation by NYVAC infection occurs by 2 hpi (observed by IL-6 secretion in Fig. 4D) and before apoptosis induction (observed at 16 hpi by PARP-1 cleavage in Fig. 3).

(iv) Enhanced expression of ATF-3 transcription factor. NF-κB pathway activation contributes to the transcription of NF-κB-dependent genes, such as *ATF-3* (activating transcription factor 3), which is specifically upregulated after NYVAC or MVA infection and unaltered by WR infection. ATF-3 protein levels increased after NYVAC infection compared to those in mock-, WR-, or MVA-infected HeLa cells (Fig. 5A, upper panel). More-than-fourfold increases in ATF-3 protein levels were evident at 6 and 16 hpi in NYVAC-infected cells compared to controls, as determined by densitometric analyses (data not shown). These data concur with microarray and real-time RT-PCR results. In an immunofluorescence assay, whereas ATF-3 was nearly undetectable in uninfected and WR-infected cells, there was a clear increase in ATF-3 staining intensity after NYVAC infection, with a mainly nuclear and perinuclear localization (Fig. 5B).

Phosphorylation of the α subunit of eukaryotic initiation factor 2 (eIF-2α) enhances the transcription of genes involved in stress-sensing pathways, such as the genes for ATF-4, GADD34, and GADD153 (57). NYVAC infection induced mRNA expression of the GADD34 (Tables 1 and 2) and GADD153 (Table 1) genes, suggesting that eIF-2α may be phosphorylated after NYVAC infection. To determine the effect of NYVAC infection on eIF-2α phosphorylation, we mea-

Downloaded from jvi.asm.org at Centro Nacional de Biotecnología - Biblioteca on October 15, 2007

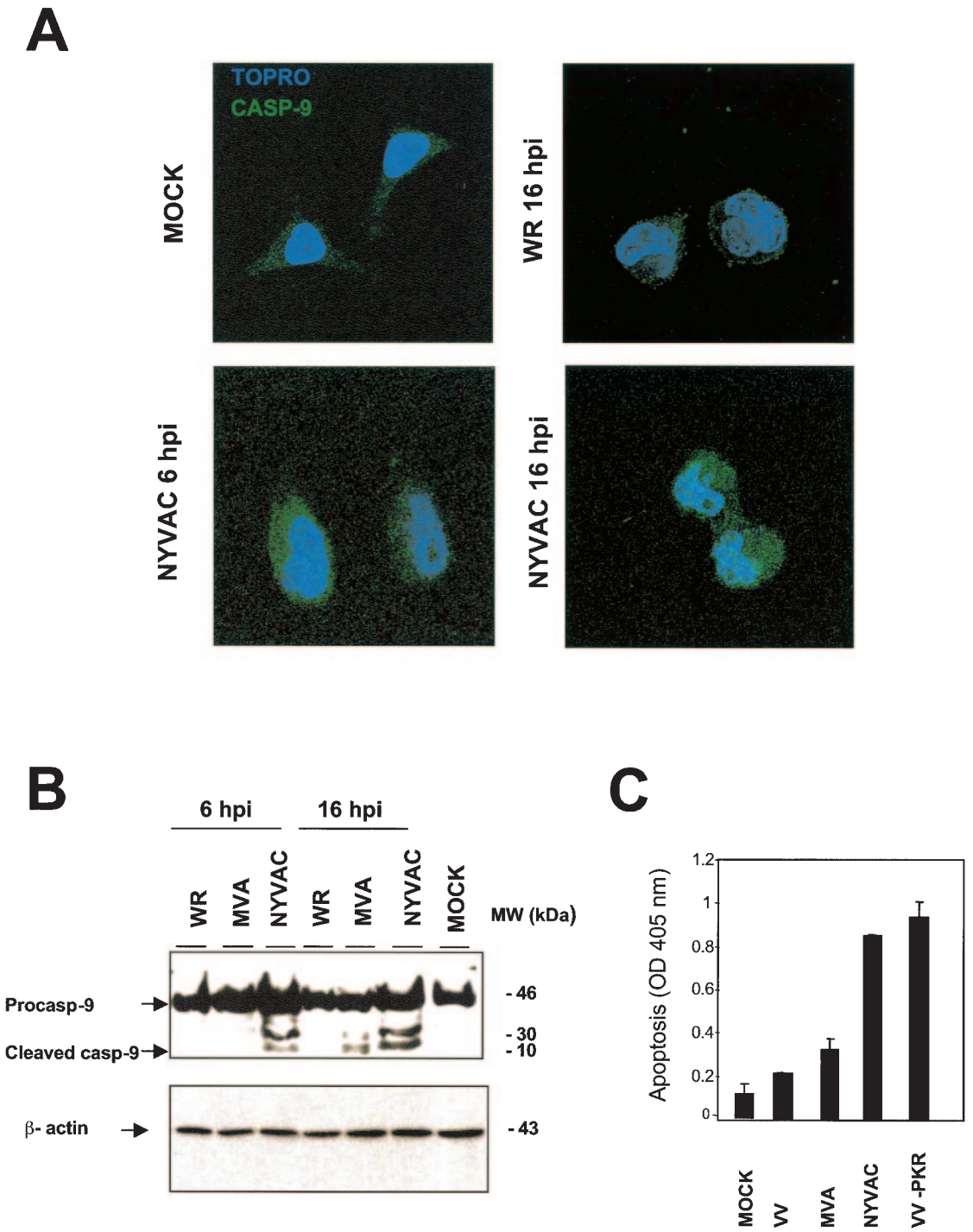

FIG. 2. NYVAC-induced apoptosis in HeLa cells. (A) Protein validation of microarray data by immunofluorescence analysis of the effect of NYVAC infection on caspase-9 distribution in HeLa cells. Mock-, WR-, or NYVAC-infected cells were incubated at the indicated times with an anti-caspase-9 antibody (Calbiochem) that recognizes the active form of caspase-9, followed by the appropriate conjugated secondary antibody and the ToPro reagent. The samples were analyzed by confocal immunofluorescence microscopy. (B) Activation of caspase-9 after WR, MVA, or NYVAC infection. Total proteins (100 μg) were separated by SDS-PAGE, transferred to nitrocellulose, and immunoblotted at various times (6 and 16 hpi) with an anti-caspase-9 antibody (Oncogene) that recognizes the procaspase and the cleaved active form of caspase-9. Caspase-9 presented a proform (46 kDa) that it is cleaved into a heterodimer of 35-kDa and 10-kDa chains. The molecular sizes (in kilodaltons) of the proteins are indicated on the right. Actin levels revealed that the same amount of protein was loaded into each lane. (C) Apoptosis assays after WR, MVA, or NYVAC infection determined the amount of cytoplasmic histone-associated DNA by ELISA. HeLa cells grown in 12-well plates were infected (5 PFU/cell) with the viruses indicated and harvested at 24 hpi for determinations with an ELISA kit of the absorbance at 405 nm. As a positive control for apoptosis, we used VV-PKR-infected HeLa cells. Duplicate samples were measured in two independent experiments.

Downloaded from jvi.asm.org at Centro Nacional de Biotecnología - Biblioteca on October 15, 2007

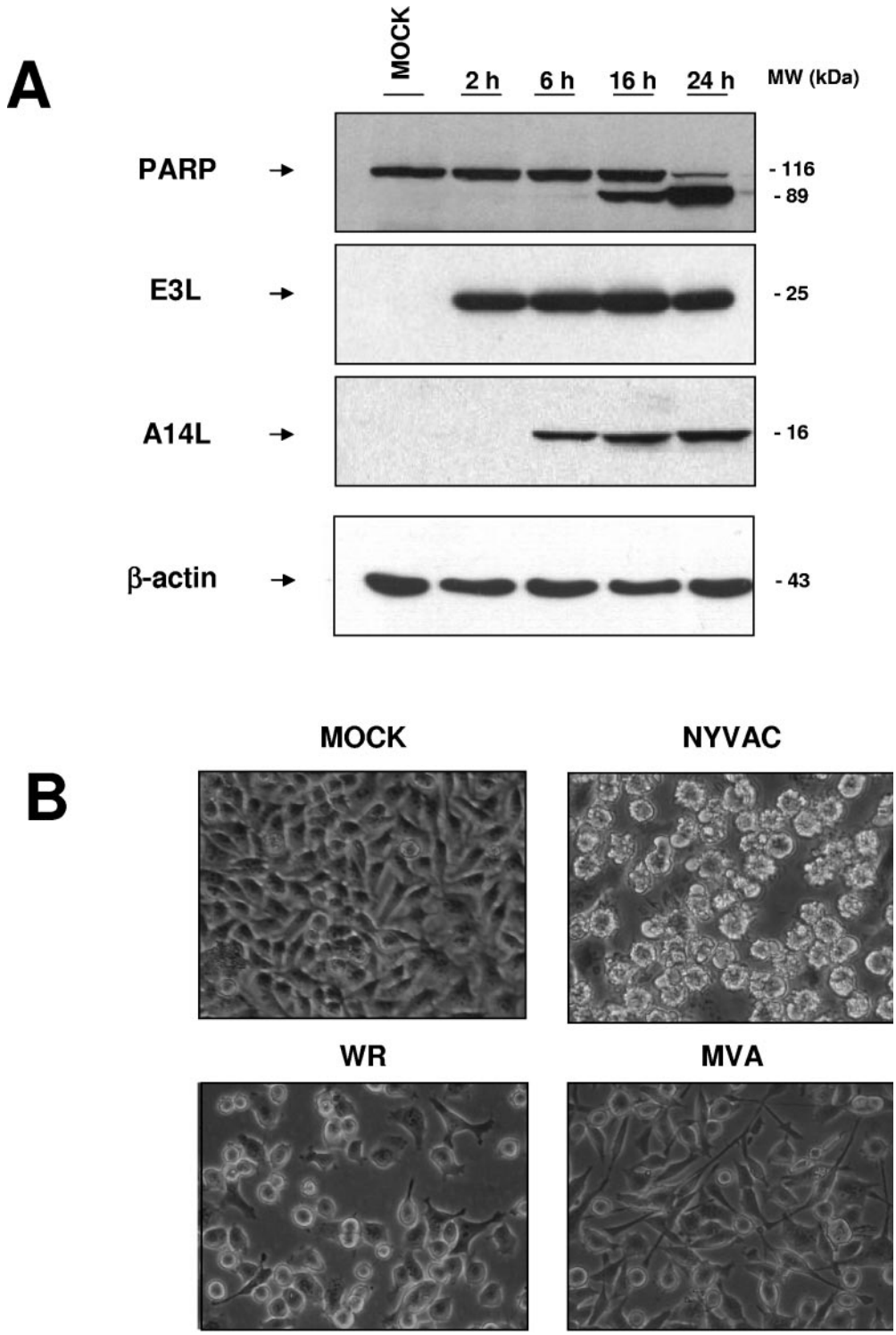

FIG. 3. Apoptosis induction kinetics during NYVAC infection. (A) Time course of PARP-1 cleavage during NYVAC infection. HeLa cells were infected with NYVAC, and at the indicated times, total proteins (100 μg) were separated by SDS-PAGE, transferred to nitrocellulose, and immunoblotted with anti-PARP-1, which recognizes both the full-length and the cleaved protein. An 89-kDa cleavage product of PARP-1 was observed at 16 hpi. As a measure of infection, we used immunoblotting to visualize the viral proteins E3L and A14L. The molecular sizes (in kilodaltons) of the proteins are indicated on the right. Actin levels showed that the same amount of protein was loaded in each lane. (B) Apoptotic phenotype of NYVAC-infected HeLa cells. Monolayer cultures of HeLa cells were left uninfected or infected (5 PFU/cell) with the different VV strains for 16 h, and the apoptotic phenotype was visualized by phase-contrast microscopy. NYVAC-infected cells showed characteristic apoptosis, defined by a rounded, floating, phase-bright, wrinkled shape.

Downloaded from jvi.asm.org at Centro Nacional de Biotecnología - Biblioteca on October 15, 2007

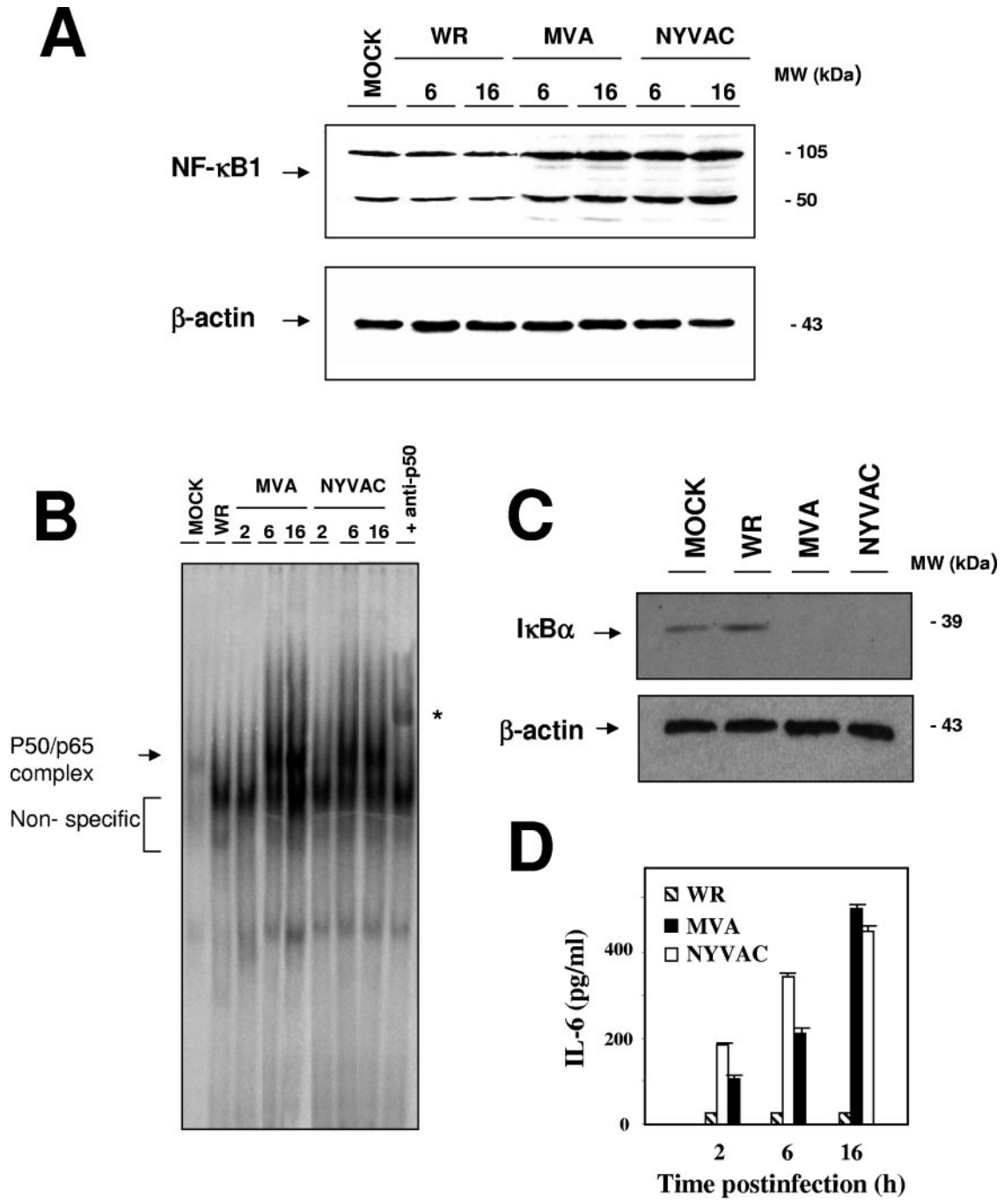

FIG. 4. NYVAC-induced NF-κB signaling. (A) Validation of microarray data by NF-κB protein levels and comparison between WR, MVA, and NYVAC infections. Total proteins (100 μg) were separated by SDS-PAGE, transferred to nitrocellulose, and immunoblotted with anti-NF-κB1 antibody at various times (6 and 16 hpi). Actin levels indicated that the same amount of protein was loaded into each lane. The molecular sizes (in kilodaltons) of the proteins are indicated on the right. (B) Autoradiogram of NF-κB activity, determined by EMSA performed with nuclear extracts of mock-, MVA-, and NYVAC-infected HeLa cells at the indicated times. WR, nuclear extract from WR-infected HeLa cells at 16 hpi. The arrow indicates the ^{32}P-labeled NF-κB/DNA complex and the nonspecific signal, and the asterisk indicates the supershift of NF-κB after incubation of the nuclear extracts with the ^{32}P-labeled probe and anti-p50 antibody. (C) IκBα degradation kinetics of WR-, MVA-, and NYVAC-infected HeLa cells. Cytoplasmic extracts were prepared, as previously described (45), from uninfected and poxvirus-infected (5 PFU/cell) HeLa cells. IκBα levels were detected by immunoblotting at 4 hpi. The molecular sizes (in kilodaltons) of the proteins are indicated on the right. Actin levels indicated that the same amount of protein was loaded into each lane of the gel. (D) Levels of IL-6 secreted from WR-, MVA-, and NYVAC-infected HeLa cells (5 PFU/cell), as determined by ELISA. Protein levels of IL-6 in supernatants of infected cells were measured at 2, 6, and 16 hpi. Duplicate samples were measured in two independent experiments.

Downloaded from jvi.asm.org at Centro Nacional de Biotecnología - Biblioteca on October 15, 2007

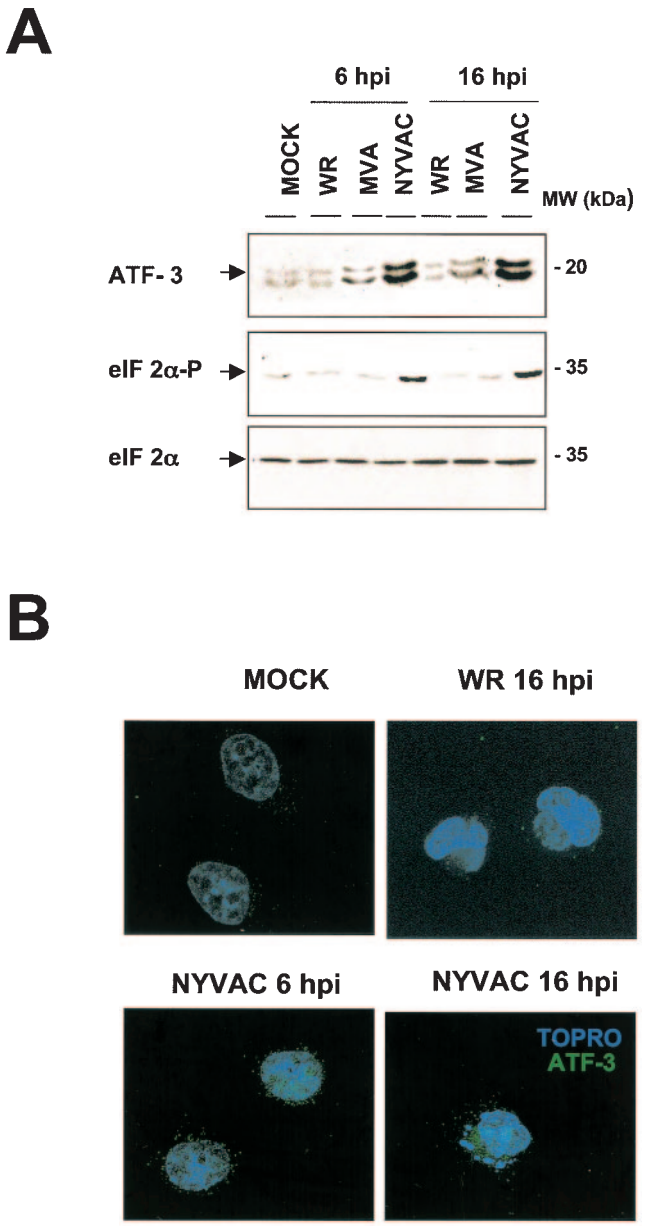

FIG. 5. ATF-3 protein expression is induced by NYVAC infection. (A) Levels of ATF-3, phosphorylated eIF2α at Ser-51, and total eIF2α were measured by immunoblot analysis of extracts of HeLa cells after WR, MVA, and NYVAC infection. Total proteins (100 μg) were separated by SDS-PAGE, transferred to nitrocellulose, and immunoblotted with anti-ATF-3, anti-phosphorylated-eIF2α, or anti-eIF2α antibody at various times (6 and 16 hpi). The molecular sizes (in kilodaltons) of the proteins are indicated on the right. The antibody against ATF-3 recognizes two or three bands, depending on the running conditions, perhaps as a result of posttranslational modifications of the transcription factor, which can be cell dependent. (B) Immunofluorescence analysis of the effect of NYVAC infection on ATF-3 distribution in HeLa cells. Mock-, WR-, and NYVAC-infected cells were labeled with anti-ATF-3 (Santacruz) at the indicated times, followed by the appropriate conjugated secondary antibody and ToPro reagent. The samples were analyzed by confocal immunofluorescence microscopy.

sured specific eIF-2α phosphorylation at Ser-51 by Western blotting of mock-, WR-, MVA-, or NYVAC-infected HeLa cells. Clear eIF-2α phosphorylation was observed at 6 and 16 hpi in NYVAC-infected cells but not in WR- or MVA-infected cells (Fig. 5A, lower panels). Thus, we found a correlation of enhanced ATF-3 expression at the mRNA and protein levels and enhanced GADD34 and GADD153 expression at the RNA level with eIF-2α phosphorylation, suggesting that these stress pathways could be involved in apoptosis induction by NYVAC infection.

VV *K1L* gene prevents NF-κB activation but not apoptosis induction after NYVAC infection. The VV *K1L* host range gene acts as an NF-κB inhibitor (45). Since NYVAC lacks the *K1L* gene, we analyzed whether apoptosis induction and NF-κB activation by NYVAC can be inhibited by the *K1L* gene. NYVAC-infected HeLa cells were transfected with a plasmid containing the *K1L* gene with a T7-Tag tag or with a control empty plasmid (pC), and apoptosis was measured by immunofluorescence. The *K1L* gene is necessary for VV replication in RK13 cells (38, 41), and after infection-transfection, we confirmed that the transfected *K1L* gene rescued the host range by producing plaques in RK13 cells (data not shown). Apoptotic cells were counted based on the characteristic increase in nucleus granularity and the appearance of apoptotic bodies. Cells were costained with E3L antibody to detect VV, ToPro for DNA detection, and anti-T7-Tag to detect transfected cells. The apoptotic phenotype of *K1L*-transfected NYVAC-infected cells was comparable to that found in the absence of *K1L* (not shown). We observed similar numbers of apoptotic cells after *K1L* expression as for pC-transfected cells (Fig. 6A), indicating that the *K1L* gene was not responsible for the apoptotic phenotype after NYVAC infection. To analyze the ability of *K1L* to repress NF-κB activation after NYVAC infection, we used ELISA to quantify secreted IL-6, an indicator of NF-κB activity, in supernatants from NYVAC-infected HeLa cells that were untransfected or transfected with pC or pK1L. We observed a marked decrease in secreted IL-6 in NYVAC-infected HeLa cells after pK1L transfection (Fig. 6B). This result indicated that *K1L* expression inhibits NF-κB activity in NYVAC-infected cells.

DISCUSSION

Poxvirus vector technology has provided reagents for high-level expression of proteins for vaccine use. Due to their infection efficiencies, high gene product expression levels, and safety, attenuated poxvirus vectors are useful for gene delivery in immunotherapy (10, 35). NYVAC is a highly attenuated VV strain, generated by the specific deletion of 18 open reading frames from the viral genome, which affects host range, virulence, and pathogenesis genes (32, 49, 50). This vector has been applied as a recombinant vaccine delivery system in animal models and target species, including humans (34, 37). NYVAC-based vectors have been analyzed as vaccines for several tumors (23, 46) and are protective against pathogens such as retroviruses (5, 10, 31), Japanese encephalitis virus (24), and *Plasmodium falciparum* (34). The potential use of variola virus as a biological weapon requires the development of safer smallpox vaccines, using attenuated VV strains such as MVA and NYVAC (4, 9).

Downloaded from jvi.asm.org at Centro Nacional de Biotecnología - Biblioteca on October 15, 2007

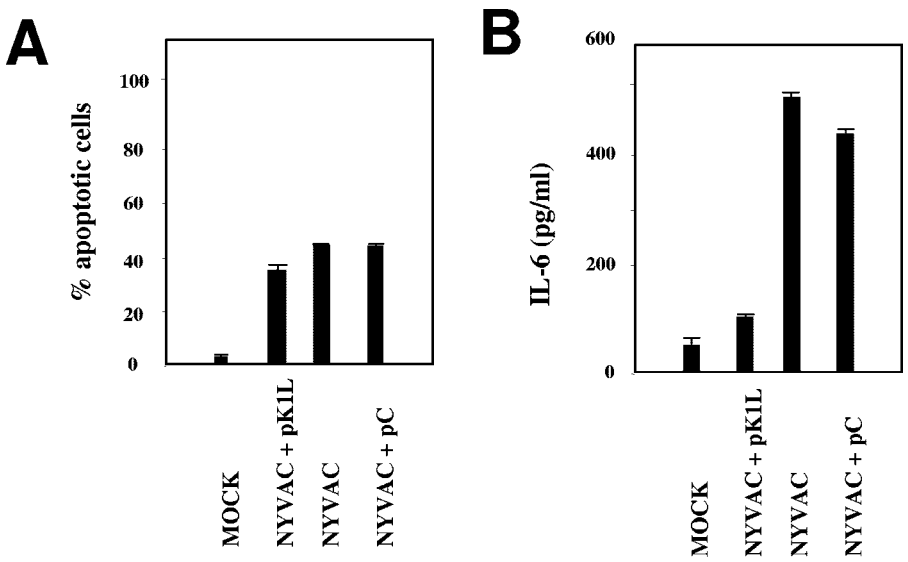

FIG. 6. *K1L* is necessary for NF-κB inhibition but not for apoptotic induction in NYVAC infection. (A) Ectopic *K1L* expression in NYVAC-infected HeLa cells does not inhibit apoptosis during NYVAC infection. HeLa cells grown on coverslips were infected with NYVAC at 0.1 PFU/cell, and at 1 hpi, cells were transfected (3 μg) with an expression plasmid containing the *K1L* gene with T7-Tag (pK1L) or with an empty control plasmid (pC). At 40 h posttransfection, cells were fixed and processed to measure apoptosis by immunofluorescence, using antibodies directed against the E3L protein (red), T7-Tag (green), and ToPro for DNA staining (blue). The ratios of infected apoptotic cells to infected nonapoptotic cells were determined by counting (about 2,000 cells per experiment); each point represents the average of two independent experiments. (B) Ectopic *K1L* expression inhibits NF-κB activation in NYVAC infection. Levels of IL-6 secreted from cells infected and transfected as described above were quantified by ELISA. Duplicate samples were measured in two independent experiments.

The use of these vectors as vaccines requires a better understanding of the impact of NYVAC infection in the human host, including the identification of differentially regulated genes and their functions. Using high-throughput cDNA microarray screening of over 15,000 genes in NYVAC-infected HeLa cells, we identified transcriptional alterations in a defined subset of human genes. When grouped into functional categories, a large proportion of altered transcripts were from genes involved in apoptosis, adhesion, cytoskeletal architecture, cell cycling, and immune modulation.

Apoptosis is regarded as an innate cellular response that limits virus propagation. The importance of apoptosis as an antiviral defense against poxvirus infection is suggested by the finding that a number of poxvirus genes encode proteins that interfere with apoptosis in specific cell types (30, 39). During NYVAC infection, we found an upregulation of the caspase-9 gene, an apoptosis-linked gene. Increased caspase-9 protein levels reflected an increase in caspase-9 activity and effector caspases, as determined by the appearance of a cleavage product from the target 89-kDa PARP-1 protein. Although we detected caspase-9 activation at 6 hpi, as shown by cleavage of the 46-kDa procaspase, apoptosis and PARP-1 cleavage were not evident until 16 hpi. These temporal differences in NYVAC-induced apoptosis may be due to distinct target specificities and the sequence of biochemical events. The role of apoptosis in poxvirus biology is not well understood; previous studies of *K1L* gene-defective viruses found no correlation between apoptosis suppression and virus growth (7), and similar results were obtained by inactivation of the cowpox virus *crmA* gene (42). CrmA/SPI-2 is the best-characterized apoptosis modulator encoded by poxvirus family members; it inhibits apoptosis by preventing caspase-8 activity (51, 56). An antiapoptotic function was previously described for the VV *E3L* gene product that blocks PKR activity (27, 29) and was recently shown for the viral protein F1L, which inhibits mitochondrial release of cytochrome *c*, which is essential for apoptosis induction (48, 52). *B13R* and *B14R*, encoding the interleukin-1β-converting enzyme inhibitor, are also involved in antiapoptotic functions (39, 49). Since the antiapoptotic genes *F1L* and *E3L* are present in the NYVAC genome, other genes with antiapoptotic functions, such as *B13R* and *B14R* or others with unknown functions that are absent in NYVAC, may be the cause for apoptotic induction of this virus. Our results indicate that the *K1L* gene does not act as an inhibitor of apoptosis during NYVAC infection, as we did not observe a blockade of apoptosis by ectopic expression of this gene (Fig. 6).

With regard to immune modulators, our microarray experiments showed NF-κB upregulation, which induces the transcription of several genes that encode cytokines or are essential for immune response activation (14, 21). NF-κB forms a heterodimer composed of 50- and 65-kDa subunits (p50 and p65) which is retained in the cytoplasm by its inhibitor, IκBα. Specific stimuli cause proteolytic degradation of IκBα in the cytoplasm and subsequent NF-κB protein translocation to the nucleus, where it transactivates certain genes (14, 21). Our microarray data indicated upregulated expression for both NF-κB1 and NF-κB2 messengers during NYVAC infection (Table 1). NF-κB2 upregulation was confirmed by real-time RT-PCR. The increase in NF-κB1 mRNA corresponded to increased levels of the p105 and p50 proteins (Fig. 4A). NYVAC infection also upregulated NF-κB transcriptional activity (Fig. 4B). NF-κB was activated early in infection, although EMSA did not detect activation at 2 hpi, when upregulation of IL-6, an indicator of NF-κB activation, was observed by real-time

Downloaded from jvi.asm.org at Centro Nacional de Biotecnología - Biblioteca on October 15, 2007

TABLE 3. Representative gene expression profiling of MVA and NYVAC infections of human HeLa cells[a]

Expression profile and gene product name	Gene symbol	Fold change with MVA			Fold change with NYVAC		
		2 hpi	6 hpi	16 hpi	2 hpi	6 hpi	16 hpi
Increased in MVA and NYVAC infections							
Early growth response 1	EGR1	4.17	4.60	1.94	4.74	10.38	6.83
Nuclear factor (erythroid-derived 2)-like 3	NFE2L3	2.36	2.36	2.52	1.19	2.13	1.32
Nuclear factor kappa light polypeptide 2	NFKB2	2.03	2.22	2.34	1.53	2.02	1.79
Interleukin-6	IL6	2.65	2.14	1.56	2.02	5.85	2.68
Interferon-stimulated protein, 15 kDa	ISG15	2.57	2.25	1.61	1.21	1.14	3.39
CD80 antigen	CD80	1.75	2.58	2.06	1.25	2.02	2.7
Dual-specificity phosphatase 5	DUSP5	3.01	2.91	1.87	1.98	4.16	2.18
JunB proto-oncogene	JUNB	2.93	3.92	1.06	2.16	2.14	1.32
v-Jun avian sarcoma virus 17 oncogene homolog	JUN	2.17	2.02	1.31	2.14	13.75	8.01
v-Myc avian myelocytomatosis viral oncogene homolog	MYC	2.22	1.53	1.05	1.05	2.93	1.65
Activating transcription factor 3	ATF3	1.78	1.98	0.99	2.42	8.36	6.10
Dual-specificity phosphatase 2	DUSP2	3.93	3.59	1.85	2.43	5.25	1.56
Connective tissue growth factor	CTGF	5.77	4.51	1.12	4.24	11.45	5.14
Kinesin family member 5A	KIF5A	2.05	1.88	1.73	1.89	5.45	4.64
Increased in MVA infection							
Interleukin-7	IL7	6.1	5.3	3.2	0.80	0.55	0.88
B7 protein	B7	1.97	1.75	3.53	1.58	1.58	1.78
CD47 antigen	CD47	5.35	4.08	3.16	1.02	0.76	1.03
Mitogen-activated protein kinase kinase 5	MAP2K5	2.37	2.74	1.69	1.02	0.76	1.03
Nuclear factor kappa light polypeptide epsilon	NFKBIE	2.41	1.61	1.12	1.18	1.27	1.42
Nuclear factor of activated T cells, cytoplasmic 3	NFATC3	3.46	2.97	1.30	1.01	1.34	1.34
Increased in NYVAC infection							
Caspase-9, apoptosis-related cysteine protease	CASP9	1.1	0.82	0.32	2.59	2.37	1.98
Nucleoporin (88 kDa)	NUP88	0.87	0.93	0.92	3.52	6.49	4.23
Pleckstrin homology-like domain, family A, member 1	PHLDA1	1.01	0.95	0.99	4.19	8.24	5.28

[a] MVA data are from a previous report (16).

RT-PCR and microarray analysis. The NF-κB activation pathway contributes to the transcription of κB-dependent genes. Many transcripts upregulated by NYVAC are known NF-κB target genes (Table 1), although other κB-dependent genes such as *TNF*, *A20*, *CCL2*, *CXCL1*, and *IL-8* were not upregulated during NYVAC infection. In view of the dual NF-κB-activating effect and apoptotic phenotype triggered by NYVAC infection, it is not surprising to find that not all of the NF-κB-dependent genes are upregulated by virus infection. One of the NF-κB-dependent genes that is upregulated is *ATF-3*, a stress-inducible gene that encodes an ATF/CREB transcription factor (18, 19, 28). Recent reports describe the effect of ATF-3 in apoptosis induction (20, 53); ATF-3, considered a proapoptotic factor, might be involved in apoptosis activation in NYVAC-infected cells, although its physiological relevance in this system remains to be established. NYVAC infection also induced mRNAs such as those encoding GADD34 and GADD153, whose activation is eIF-2α phosphorylation dependent; eIF-2α phosphorylation in NYVAC infection was confirmed by Western blotting (Fig. 5A).

MVA, another attenuated VV strain, also activates NF-κB (16, 36). NF-κB activation mediated by NYVAC and MVA may reflect the loss of a specific viral gene from the parental viral genome, deleted during the generation of MVA and NYVAC. Indeed, the *K1L* gene was deleted in NYVAC (49), and the viral K1L protein inhibits NF-κB activation by preventing IκBα degradation (45). Since both the MVA and NYVAC genomes lack *K1L*, which is present in VV, we studied the effect of the absence of *K1L* on NF-κB activation by measuring IL-6 levels in NYVAC-infected HeLa cells transfected with an expression plasmid bearing the *K1L* gene. IL-6 levels were considerably lower in *K1L*-expressing cells than in control-transfected cells, indicating that *K1L* inhibits NF-κB activity during NYVAC infection (Fig. 6B). *K1L* inhibition of NF-κB activity was independent of NYVAC-induced apoptosis, as indicated by counting NYVAC-infected apoptotic cells expressing *K1L* (Fig. 6A).

Although NF-κB activation and apoptosis induction might be negative factors in the NYVAC cycle, the triggering of these mechanisms may favor a better immune response to a recombinant vector. NF-κB activation from a recombinant NYVAC infection should stimulate and amplify the immune response against recombinant products and facilitate clearance of the vector. The role of apoptosis in the immune response is still unclear, but antigens produced by apoptotic cells are reported to increase antigen immunogenicity (54). Dendritic cells that phagocytose apoptotic bodies from virus-infected cells can present viral antigens to cytotoxic T cells, inducing a cytotoxic response (1). It remains to be defined whether apoptosis induced by a NYVAC-based vector increases antigen immunogenicity in comparison with that induced by MVA vectors or NYVAC vectors unable to induce apoptosis by gene targeting.

We compared expression profiles of representative genes obtained in this study with those obtained from MVA infections (16) (Table 3). In infected HeLa cells, one group of genes is upregulated by both MVA and NYVAC, whereas others are

Downloaded from jvi.asm.org at Centro Nacional de Biotecnología - Biblioteca on October 15, 2007

upregulated selectively by MVA or NYVAC. Both viruses trigger cellular transcription factors, including NF-κB, Myc, c-Jun, ATF-3, DUSP2, and CTGF, and cell adhesion molecules such as the kinesin KIF5C. *EGR1* (early gene response 1) was also upregulated by MVA and NYVAC, as also reported for MVA-ΔE3L-infected HeLa cells (29), and the MEK/ERK/RSK2/Elk-1/EGR-1 signaling pathway is necessary for VV multiplication (2). The immunomodulatory molecules IL-6, ISG15, and CD80 were upregulated in NYVAC- and MVA-infected cells, whereas IL-7, IL-1A, IL-8, and IL-15 were upregulated after MVA but not NYVAC infection. This indicates that MVA and NYVAC induce distinct proinflammatory cytokine profiles in vitro. In HeLa cells, WR infection also upregulates CD80 (15), but IL-6 and ISG15 upregulation is specific to MVA and NYVAC infections. *ISG15* was first identified as an interferon-stimulated gene (6, 26) that affects IFN-α/β signal transduction; its expression increases markedly after viral infection (16, 33, 55). IFN-α/β-induced ISG15 activation suggests a role for ISG15 in the innate immune response to viral infection (44).

In view of our findings, we propose that NYVAC infection activates a sequence of survival and apoptotic responses in the injured cell. NYVAC induces NF-κB activation early in infection and will trigger the expression of several gene classes, each of which might be required at different times of infection for cell survival. The NF-κB-activated early signals will not be able to overcome the cell death process caused by the virus infection, and cells will ultimately die by apoptosis. Some of the NF-κB-induced genes, such as *ATF-3*, together with other stress signals, such as *GADD34* and *GADD153* and other unknown signals, might promote apoptosis. Since apoptosis is a late event in NYVAC infection, most of the virus cycle will be completed, and hence the contribution of apoptosis to virus replication will be minimized. While the poxvirus genome encodes several genes that antagonize apoptosis and NF-κB activation, it is likely that these virus genes have a major impact on the evasion of the immune system by the virus rather than on virus growth in culture. We demonstrated that the K1L viral protein prevented NF-κB activation but not apoptosis induction in NYVAC infection, although the viral gene(s) involved in NYVAC-induced apoptosis remains unknown.

Overall, our results provide a basis for future functional evaluations of the NYVAC vector for use in human vaccines. Gene expression profiling permits detailed analyses of the impact of poxvirus vectors on immune system target cells after vaccination and the development of more effective poxvirus vaccines against a broad spectrum of pathogens and tumors.

ACKNOWLEDGMENTS

We are indebted to R. Bablanian for critically reviewing the manuscript. We thank J. Tartaglia (Aventis-Pasteur) for the generous gift of NYVAC, and we are grateful to B. L. Jacobs for the anti-E3L antibody and A. Alcamí for the K1L expression plasmid. We thank S. Gutiérrez for confocal microscopy, V. Jiménez for expert technical assistance, and C. Mark and P. Martinez for editorial assistance.

S.G. was supported by a contract from the EU Project on Vaccinia Vectors. A.P.-M. was partially supported by the Spanish CAM grant GR/SAL/0653/2004 and the Ramón y Cajal Program. This work was supported by grants from the Spanish Ministry of Education and Science (BIO2004-03954), the Spanish Foundation for AIDS Research (FIPSE 36344/02), Fundación Botín, and the European Union (EuroVac QLRT-PL-1999-01321, Vaccinia Vectors QLK2-CT-2002-01867). The Department of Immunology and Oncology was founded and is supported by the Spanish Council for Scientific Research (CSIC) and Pfizer.

REFERENCES

1. **Albert, M. L.** 2004. Death-defying immunity: do apoptotic cells influence antigen processing and presentation? Nat. Rev. Immunol. **4:**223–231.
2. **Andrade, A. A., P. N. G. Silva, A. C. T. C. Pereira, L. P. de Sousa, P. C. P. Ferreira, R. T. Gazzinelli, E. G. Kroon, C. Ropert, and C. A. Bonjardim.** 2004. The vaccinia virus-stimulated mitogen-activated protein kinase (MAPK) pathway is required for virus multiplication. Biochem. J. **381:**437–446.
3. **Arenzana-Seisdedos, F., J. Thompson, M. S. Rodriguez, F. Bachelerie, D. Thomas, and R. T. Hay.** 1995. Inducible nuclear expression of newly synthesized I kappa B alpha negatively regulates DNA-binding and transcriptional activities of NF-kappa B. Mol. Cell. Biol. **15:**2689–2696.
4. **Belyakov, I. M., P. Earl, A. Dzutsev, V. A. Kuznetsov, M. Lemon, L. S. Wyatt, J. T. Snyder, J. D. Ahlers, G. Franchini, B. Moss, and J. A. Berzofsky.** 2003. Shared modes of protection against poxvirus infection by attenuated and conventional smallpox vaccine viruses. Proc. Natl. Acad. Sci. USA **16:**9458–9463.
5. **Benson, J., C. Chougnet, M. Robert-Guroff, D. Montefiori, P. Markham, G. Shearer, R. C. Gallo, M. Cranage, E. Paoletti, K. Limbach, D. Venzon, J. Tartaglia, and G. Franchini.** 1998. Recombinant vaccine-induced protection against the highly pathogenic simian immunodeficiency virus SIV_{mac251}: dependence on route of challenge exposure. J. Virol. **72:**4170–4182.
6. **Blomstrom, D. C., D. Fahey, R. Kutny, B. D. Korant, and E. Knight.** 1986. Molecular characterization of the interferon-induced 15-kDa protein. Molecular cloning and nucleotide and amino acid sequence. J. Biol. Chem. **261:**8811–8816.
7. **Chung, C. S., I. A. Vasilevskaya, S. C. Wang, C. H. Bair, and W. Chang.** 1997. Apoptosis and host restriction of vaccinia virus in RK13 cells. Virus Res. **52:**121–132.
8. **Cudmore, S., P. Cossart, G. Griffiths, and M. Way.** 1995. Actin-based motility of vaccinia virus. Nature **378:**636–638.
9. **Edghill-Smith, Y., D. Venzon, T. Karpova, J. McNally, J. Nacsa, W. P. Tsai, E. Tryniszewska, M. Moniuszko, J. Manischewitz, L. R. King, S. J. Snodgrass, J. Parrish, P. Markham, M. Sowers, D. Martin, M. G. Lewis, J. A. Berzofsky, I. M. Belyakov, B. Moss, J. Tartaglia, M. Bray, V. Hirsch, H. Golding, and G. Franchini.** 2003. Modelling a safer smallpox vaccination regimen, for human immunodeficiency virus type 1-infected patients in immunocompromised macaques. J. Infect. Dis. **8:**1181–1191.
10. **Franchini, G., S. Gurunathan, L. Baglyos, S. Plotkin, and J. Tartaglia.** 2004. Poxvirus-based vaccine candidates for HIV: two decades of experience with special emphasis on canarypox vectors. Exp. Rev. Vaccines **3:**75–88.
11. **Frischknecht, F., V. Moreau, S. Rottger, I. Reckmann, C. Superti-Furga, and M. Way.** 1999. Actin based motility of vaccinia virus mimics receptor tyrosine kinase signalling. Nature **404:**1007–1011.
12. **Gallego-Gómez, J. C., C. Risco, D. Rodriguez, P. Cabezas, S. Guerra, J. L. Carrascosa, and M. Esteban.** 2003. Differences in virus-induced cell morphology and virus maturation between the WR and MVA strains of vaccinia virus. J. Virol. **77:**10606–10622.
13. **García de la Nava, J., D. Franco Santaella, J. Cuenca Alba, J. M. Carazo, O. Trelles, and A. Pascual-Montano.** 2003. Engene: the processing and exploratory analysis of gene expression data. Bioinformatics **19:**657–658.
14. **Ghosh, S., and M. Karin.** 2002. Missing pieces in the NF-kappaB puzzle. Cell **109:**81–96.
15. **Guerra, S., L. A. López-Fernandez, A. Pascual-Montano, M. Muñoz, K. Harshman, and M. Esteban.** 2003. Cellular gene expression survey of vaccinia virus infection of human HeLa cells. J. Virol. **77:**6493–6506.
16. **Guerra, S., L. A. López-Fernandez, R. Conde, A. Pascual-Montano, M. Muñoz, K. Harshman, and M. Esteban.** 2004. Microarray analysis reveals characteristic changes of host cell gene expression in response to attenuated modified vaccinia virus Ankara (MVA) infection of human HeLa cells. J. Virol. **78:**5820–5835.
17. **Guerra, S., M. Aracil, R. Conde, A. Bernad, and M. Esteban.** 2005. Wiskott-Aldrich syndrome protein is needed for vaccinia virus pathogenesis. J. Virol. **79:**2133–2140.
18. **Hai, T., C. D. Wolfgang, D. K. Marsee, A. E. Allen, and U. Sivaprasad.** 1999. ATF3 and stress responses. Gene Exp. **7:**321–335.
19. **Hai, T., and M. G. Hartman.** 2001. The molecular biology and nomenclature of the activating transcription factor/cAMP responsive element binding family of transcription factors: activating transcription factor proteins and homeostasis. Gene **1:**1–11.
20. **Hartman, M. G., D. Lu, M. L. Kim, G. J. Kociba, T. Shukri, J. Buteau, X. Wang, W. L. Frankel, D. Guttridge, M. Prentki, S. T. Grey, D. Ron, and T. Hai.** 2004. Role for activating transcription factor 3 in stress-induced beta-cell apoptosis. Mol. Cell. Biol. **13:**5721–5732.
21. **Hayden, M. S., and S. Ghosh.** 2004. Signaling to NF-kappaB. Genes Dev. **18:**2195–2224.
22. **Hughes, T. R., M. J. Marton, A. R. Jones, C. J. Roberts, R. Stoughton, C. D. Armour, H. A. Bennett, E. Coffey, H. Dai, Y. D. He, M. J. Kidd, A. M. King, M. R. Meyer, D. Slade, P. Y. Lum, S. B. Stepaniants, D. D. Shoemaker,**

Downloaded from jvi.asm.org at Centro Nacional de Biotecnología - Biblioteca on October 15, 2007

D. Gachotte, K. Chakraburtty, J. Simon, M. Bard, and S. H. Friend. 2000. Functional discovery via a compendium of expression profiles. Cell **102:**109–126.

23. **Jourdier, T. M., C. Moste, M. C. Bonnet, F. Delisle, J. P. Tafani, P. Devauchelle, J. Tartaglia, and P. Moingeon.** 2003. Local immunotherapy of spontaneous feline fibrosarcomas using recombinant poxviruses expressing interleukin 2 (IL-2). Gene Ther. **26:**2126–2132.
24. **Kanesa-thasan, N., J. J. Smucny, C. H. Hoke, D. H. Marks, E. Konishi, I. Kurane, D. B. Tang, D. W. Vaughn, P. W. Mason, and R. E. Shope.** 2000. Safety and immunogenicity of NYVAC-JEV and ALVAC-JEV attenuated recombinant Japanese encephalitis virus-poxvirus vaccines in vaccinia-non-immune and vaccinia-immune humans. Vaccine **19:**483–491.
25. **Kohonen, T.** 1997. Self-organizing maps, 2nd ed. Springer-Verlag, Heidelberg, Germany.
26. **Korant, B. D., D. C. Blomstrom, G. J. Jonak, and E. Knight.** 1984. Interferon-induced proteins. Purification and characterization of a 15,000-dalton protein from human and bovine cells induced by interferon. J. Biol. Chem. **23:**14835–14839.
27. **Lee, S. B., and M. Esteban.** 1994. The interferon-induced double-stranded RNA-activated protein kinase induces apoptosis. Virology **199:**491–496.
28. **Liang, G., A. D. Wolfgang, B. P. C. Chen, T. H. Chen, and T. Hai.** 1996. ATF3 gene: genome organization, promoter and regulation. J. Biol. Chem. **271:**1695–1701.
29. **Ludwig, H., J. Mages, C. Staib, M. H. Lehmann, R. Lang, and G. Sutter.** 2005. Role of viral factor E3L in modified vaccinia virus Ankara infection of human HeLa cells: regulation of the virus life cycle and identification of differentially expressed host genes. J. Virol. **79:**2584–2596.
30. **McFadden, G.** 2005. Poxvirus tropism. Nat. Rev. Microbiol. **3:**201–213.
31. **Myagkikh, M., S. Alipanah, P. D. Markham, J. Tartaglia, E. Paoletti, R. C. Gallo, G. Franchini, and M. Robert-Guroff.** 1996. Multiple immunizations with attenuated poxvirus HIV type 2 recombinants and subunit boosts required for protection of rhesus macaques. AIDS Res. Hum. Retrovir. **12:** 985–992.
32. **Nájera, J. L., C. E. Gómez, M. M. Gherardi, E. Domingo-Gil, and M. Esteban.** Unpublished data.
33. **Nicholl, M. J., L. H. Robinson, and C. M. Preston.** 2000. Activation of cellular interferon-responsive genes after infection of human cells with herpes simplex virus type 1. J. Gen. Virol. **9:**2215–2218.
34. **Ockenhouse, C. F., P. F. Sun, D. E. Lanar, B. T. Wellde, B. T. Hall, K. Kester, J. A. Stoute, A. Magill, U. Krzych, L. Farley, R. A. Wirtz, J. C. Sadoff, D. C. Kaslow, S. Kumar, L. W. Church, J. M. Crutcher, B. Wizel, S. Hoffman, A. Lalvani, A. V. Hill, J. A. Tine, K. P. Guito, C. de Taisne, R. Anders, W. R. Ballou, et al.** 1998. Phase I/IIa safety, immunogenicity, and efficacy trial of NYVAC-Pf7, a pox-vectored, multiantigen, multistage vaccine candidate for Plasmodium falciparum malaria. J. Infect. Dis. **6:**1664–1673.
35. **Odin, L., M. Favrot, D. Poujol, J. P. Michot, P. Moingeon, J. Tartaglia, and I. Puisieux.** 2001. Canarypox virus expressing wild type p53 for gene therapy in murine tumors mutated in p53. Cancer Gene Ther. **2:**87–98.
36. **Oie, L. K., and D. Pickup.** 2001. Cowpox and other members of the orthopoxvirus genus interfere with the regulation of NF-κB activation. Virology **288:**175–187.
37. **Paoletti, E.** 1996. Applications of poxvirus vectors to vaccination: an update. Proc. Natl. Acad. Sci. USA **21:**11349–11353.
38. **Perkus, M. E., S. J. Goebel, S. W. Davis, G. P. Johnson, K. Limbach, E. K. Norton, and E. Paoleti.** 1990. Vaccinia virus host range genes. Virology **179:**276–286.
39. **Pogo, B. G., S. M. Melana, and J. Blaho.** 2004. Poxvirus infection and apoptosis. Int. Rev. Immunol. **23:**61–74.
40. **Quackenbush, J.** 2002. Microarray data normalization and transformation. Nat. Genet. **32:**496–501.
41. **Ramsey-Ewing, A. L., and B. Moss.** 1996. Complementation of a vaccinia virus host-range K1L gene deletion by the nonhomologous CP77 gene. Virology **222:**75–86.
42. **Ray, C. A., and D. J. Pickup.** 1996. The mode of death of pig kidney cells infected with cowpox virus is governed by the expression of the crmA gene. Virology **217:**384–391.
43. **Rodriguez, J. R., C. Risco, J. L. Carrascosa, M. Esteban, and D. Rodríguez.** 1998. Vaccinia virus 15-kilodalton (A14L) protein is essential for assembly and attachment of viral crescents to virosomes. J. Virol. **72:**1287–1296.
44. **Ritchie, K. J., C. S. Hahn, K. I. Kim, M. Yan, D. Rosario, L. Li, J. C. de la Torre, and D. E. Zhang.** 2004. Role of ISG15 protease UBP43 (USP18) in innate immunity to viral infection. Nat. Med. **12:**1374–1378.
45. **Shisler, J. L., and X. L. Jin.** 2004. The vaccinia virus K1L gene product inhibits host NF-kappaB activation by preventing IkappaBalpha degradation. J. Virol. **78:**3553–3560.
46. **Sivanandham, M., P. Shaw, S. F. Bernik, E. Paoletti, and M. K. Wallack.** 1998. Colon cancer cell vaccine prepared with replication-deficient vaccinia viruses encoding B7.1 and interleukin-2 induce antitumor response in syngeneic mice. Cancer Immunol. Immunother. **5:**261–267.
47. **Soldani, C., and A. I. Scovassi.** 2002. Poly(ADP-ribose) polymerase-1 cleavage during apoptosis: an update. Apoptosis **7:**321–328.
48. **Stewart, T. L., S. T. Wasilenko, and M. Barry.** 2005. Vaccinia virus F1L protein is a tail-anchored protein that functions at the mitochondria to inhibit apoptosis. J. Virol. **79:**1084–1098.
49. **Tartaglia, J., M. E. Perkus, J. Taylor, E. K. Norton, J. C. Audonnet, W. I. Cox, S. W. Davis, J. van der Hoeven, B. Meignier, and M. Riviere.** 1992. NYVAC: a highly attenuated strain of vaccinia virus. Virology **188:**217–232.
50. **Tartaglia, J., W. I. Cox, S. Pincus, and E. Paoletti.** 1994. Safety and immunogenicity of recombinants based on the genetically-engineered vaccinia strain, NYVAC. Dev. Biol. Stand. **82:**125–129.
51. **Tewari, M., W. G. Telford, R. A. Miller, and V. M. Dixit.** 1995. CrmA, a poxvirus-encoded serpin, inhibits cytotoxic T-lymphocyte-mediated apoptosis. J. Biol. Chem. **270:**22705–22708.
52. **Wasilenko, S. T., T. L. Stewart, A. F. Meyers, and M. Barry.** 2003. Vaccinia virus encodes a previously uncharacterized mitochondrial-associated inhibitor of apoptosis. Proc. Natl. Acad. Sci. USA **24:**14345–14350.
53. **Yan, C., M. S. Jamaluddin, B. Aggarwal, J. Myers, and D. D. Boyd.** 2005. Gene expression profiling identifies activating transcription factor 3 as a novel contributor to the proapoptotic effect of curcumin. Mol. Cancer Ther. **2:**233–241.
54. **Ying, H., T. Z. Zaks, R. F. Wang, K. R. Irvine, U. S. Kammula, F. M. Marincola, W. W. Leitner, and N. P. Restifo.** 1999. Cancer therapy using a self-replicating RNA vaccine. Nat. Med. **5:**823–827.
55. **Zhu, H., J. P. Cong, G. Mantora, T. Gineras, and T. Shenk.** 1998. Cellular gene expression altered by human cytomegalovirus: global monitoring with oligonucleotide arrays. Proc. Natl. Acad. Sci. USA **95:**14470–14475.
56. **Zhu, W., A. Cowie, G. W. Wasfy, L. Z. Penn, B. Leber, and D. W. Andrews.** 1996. Bcl-2 mutants with restricted subcellular location reveal spatially distinct pathways for apoptosis in different cell types. EMBO J. **15:**4130–4141.
57. **Zinszner, H., M. Kuroda, X. Z. Wang, N. Batchvarova, R. T. Lightfoot, H. Remotti, J. L. Stevens, and D. Ron.** 1998. CHOP is implicated in programmed cell death in response to impaired function of the endoplasmic reticulum. Genes Dev. **12:**982–995.

Downloaded from jvi.asm.org at Centro Nacional de Biotecnología - Biblioteca on October 15, 2007

Available online at www.sciencedirect.com
ScienceDirect
Vaccine 25 (2007) 2863–2885
Vaccine
www.elsevier.com/locate/vaccine

Head-to-head comparison on the immunogenicity of two HIV/AIDS vaccine candidates based on the attenuated poxvirus strains MVA and NYVAC co-expressing in a single locus the HIV-1_{BX08} gp120 and HIV-1_{IIIB} Gag-Pol-Nef proteins of clade B

Carmen Elena Gómez [a], Jose Luis Nájera [a], Eva Pérez Jiménez [a], Victoria Jiménez [a], Ralf Wagner [b], Marcus Graf [c], Marie-Joelle Frachette [d], Peter Liljeström [e], Giuseppe Pantaleo [f], Mariano Esteban [a,*]

[a] *Department of Molecular and Cellular Biology, Centro Nacional de Biotecnología, CSIC, Ciudad Universitaria Cantoblanco, 28049 Madrid, Spain*
[b] *Institute of Medical Microbiology and Hygiene, University of Regensburg, Germany*
[c] *Geneart GmbH, Josef-Engert-Str. 11, 93053 Regensburg, Germany*
[d] *Sanofi Pasteur, 1541 Avenue Marcel Merieux, 69280 Marcy Létoile, France*
[e] *Microbiology and Tumorbiology Centre, Karolinska Institut, Stockholm, Sweeden*
[f] *Laboratory of AIDS Immunopathogenesis, Departmen of Medicine, Centre Hospitalier Universitaire Vaudois, Av. De Beaumont 29-Hopital Beaumont, 1011 Lausanne, Switzerland*

Received 12 July 2006; received in revised form 6 September 2006; accepted 21 September 2006
Available online 16 October 2006

Abstract

In this investigation we have generated and defined the immunogenicity of two novel HIV/AIDS vaccine candidates based on the highly attenuated vaccinia virus strains, MVA and NYVAC, efficiently expressing in the same locus (TK) and under the same viral promoter the codon optimized HIV-1 genes encoding gp120 and Gag-Pol-Nef antigens of clade B (referred as MVA-B and NYVAC-B). In infected human HeLa cells, gp120 is released from cells and GPN is produced as a polyprotein; NYVAC-B induces severe apoptosis but not MVA-B. The two poxvirus vectors showed genetic stability of the inserts. In BALB/c and in transgenic HHD mice for human HLA-A2 class I, both vectors are efficient immunogens and induced broad cellular immune responses against peptides represented in the four HIV-1 antigens. Some differences were observed in the magnitude and breadth of the immune response in the mouse models. In DNA prime/poxvirus boost protocols, the strongest immune response, as measured by fresh IFN-γ and IL-2 ELISPOT, was obtained in BALB/c mice boosted with NYVAC-B, while in HHD mice there were no differences between the poxvirus vectors. When the prime/boost was performed with homologous or with combination of poxvirus vectors, the protocols MVA-B/MVA-B and NYVAC-B/NYVAC-B, or the combination NYVAC-B/MVA-B gave the most consistent broader immune response in both mouse models, although the magnitude of the overall response was higher for the DNA-B/poxvirus-B regime. All of the immunization protocols induced some humoral response against the gp160 protein from HIV-1 clone LAV. Our findings indicate that MVA-B and NYVAC-B meet the criteria to be potentially useful vaccine candidates against HIV/AIDS.
© 2006 Elsevier Ltd. All rights reserved.

Keywords: HIV/AIDS; Clade B vaccine; Poxvirus vectors; MVA; NYVAC; Immune response; Mouse models

1. Introduction

Since human immunodeficiency virus (HIV) was first identified more than 20 years ago, the AIDS epidemic has continued in severity and scale of its impact beyond all expectations. If this epidemic continues to spread at its current

* Corresponding author. Tel.: +34 91 5854553; fax: +34 91 5854506.
E-mail address: mesteban@cnb.uam.es (M. Esteban).

0264-410X/$ – see front matter © 2006 Elsevier Ltd. All rights reserved.
doi:10.1016/j.vaccine.2006.09.090

rate, there will be an additional 45 million new infections and nearly 70 million deaths from the disease by 2010 [1]. Under these circumstances, development of an effective vaccine to suppress the worldwide AIDS epidemic is a major and pressing international goal.

The development of a vaccine against AIDS has been hindered in part by inefficient stimulation of the corresponding protective humoral and cellular immune responses. The variability of the HIV envelope and inaccessibility of potentially neutralizing epitopes on primary isolates continues to hamper the development of vaccines that induce neutralizing antibodies [2,3]. This shifted the focus of many vaccinologists towards the induction of CTLs. Over recent years several studies in non human primates supported the correlation between vaccine-induced HIV-specific cellular immunity and protection against subsequent challenge with pathogenic simian/human immunodeficiency virus [4,5]. In the same way, a recent report highlighted the central role of CD8+ T cells in long-term vaccine-mediated control of SHIV-89.6P and suggest a dynamic relationship between the titer of neutralizing antibodies, antigen loads and anti-viral CD4+ T cells in the maturation of high-quality anti-viral CD8+ T cells [6].

Many HIV vaccine strategies designed to induce T cell immunity, either encode a limited number of the nine HIV-1 genes (often just Env and/or Gag) and/or encode multiple individual CD8+ T cell epitopes. However, the identification of viruses that escape from CTL and thus evade the immune system has highlighted the need to induce broad CTL responses against an array of epitopes from multiple HIV-1 antigens. Thus far, an effective HIV-1 vaccine may require strong humoral and cellular immune responses to multiple viral antigens including structural and regulatory proteins.

New vehicles for antigen delivery, immunization adjuvants and vaccinations protocols to improve the anti-HIV immune response are currently being tested in both animals and humans. Among the new vehicles for antigen delivery, some of the most promising are vaccines based on poxvirus recombinants. These are valuable tools for the expression of foreign antigens directly inside the cells of the host organism, as would happen in natural infection, inducing potent cellular immune responses against the heterologous product with long-lasting immunity after a single inoculation [7,8]. Concerns about the safety of poxviruses have been addressed by the use of viruses that are replication-defective in human cells. Among these, highly attenuated strains such as MVA or NYVAC, with multiple deletions into their viral genome, can be considered as the strains of choice for preclinical and clinical vaccine development. Their major advantage is the safety record. Despite of their limited replication in human and most mammalian cell types, both viral strains provide high level of gene expression and have been proven to be immunogenic when delivered foreign antigens in animals and humans [4,9–14].

At present, a number of clinical trials using recombinants based on the attenuated poxvirus strains MVA or NYVAC against infectious disorders such as AIDS, malaria, and human papiloma associated cancer are underway by several organizations, validating not only the safety of these strains, but also demonstrating significant antigen specific T cell immunogenicity in humans. Although the capacity of these attenuated vectors to produce similar levels of recombinant antigens as replication-competent viruses has been widely demonstrated, to date, a comparative immune response induced by recombinants based on MVA and NYVAC strains has not been done.

Here we describe the construction and characterization *in vitro* and *in vivo* of MVA and NYVAC vectors expressing multiple HIV-1 antigens (Env, Gag, Pol and Nef) from clade B in a single locus of the viral genome. The viral vectors are referred as MVA-B and NYVAC-B. The novel vectors have been generated in a way where a marker is removed by homologous recombination from the final product and express simultaneously and under the same synthetic early/late viral promoter, gp120 as a cell release product and Gag-Pol-Nef (GPN) as an intracellular polyprotein. The HIV-1 genes have been codon optimized and GPN has been engineered by the removal of immunosuppressed sequences and to prevent VLP formation. In cultured cells both recombinants efficiently express the four HIV-1 antigens in a stable manner. Using different prime/boost vaccination approaches, we have compared in BALB/c and in transgenic HHD mice inoculated with MVA-B or NYVAC-B the specific cellular and humoral immune responses elicited by the viral recombinants. Our findings showed that in mice, MVA-B and NYVAC-B were quite efficient at inducing specific immune responses against peptides representing the heterologous HIV-1 antigens (Env, Gag, Pol, and Nef) independently of the immunization protocol used. Differences in the magnitude of the immune response were observed between the poxvirus vectors in the two animal models. In BALB/c, the DNA-B prime/NYVAC-B boost regime triggered an overall higher immune response than DNA-B prime/MVA-B boost whereas in HHD the magnitude of the response was similar for both recombinant viruses. When the combination of MVA-B and NYVAC-B vectors was used for prime/boost, the magnitude of the immune response was lower than in a DNA-B/poxvirus-B approach, although more peptide pools were recognized. An immunodominance of the Env peptide pools was consistently observed in HHD transgenic mice in the different protocols used. Our findings demonstrate the efficient immunogenicity in mice of the two novel poxvirus vectors expressing four HIV-1 clade B antigens in a single locus, and suggest that NYVAC-B and MVA-B are potential vaccine candidates against HIV/AIDS.

2. Materials and methods

2.1. Cells and viruses

Cells were maintained in a humidified air 5% CO_2 atmosphere at 37 °C. Primary chicken embryo fibroblast cells

(CEF) and human cells (HeLa) were grown in Dulbecco's modified Eagle's medium (DMEM) supplemented with 10% fetal calf serum (FCS). The poxvirus strains used in this work included: modified vaccinia virus Ankara (MVA) obtained after 586 passages in CEF cells (derived from clone F6 at passage 585, kindly provided by G. Sutter, Germany), the genetically attenuated vaccinia-based vector NYVAC (generated from the vaccinia virus Copenhagen strain by selected deletion of 18 viral genes) and the recombinant NYVAC-B expressing the HIV-1_{BX08} gp120 and HIV-1_{IIIB} Gag-Pol-Nef proteins (both viruses provided by Sanofi-Pasteur). The parental and recombinant NYVAC and MVA viruses were grown in CEF cells, similarly purified through two 45% (w/v) sucrose cushions, and titrated by immunostaining plaque assay as previously described [15]. The titration of the different viruses was performed in CEF at least three times.

2.2. DNA vectors and codon optimized genes

The DNA construct expressing the HIV-1_{BX08} gp120 (pCMV-$_{BX08}$gp120) was kindly provided by Sanofi-Pasteur. The RNA- and codon-optimized HIV-IIIB *gag-pol-nef* (GPN) gene construct was synthesized by GENEART GmbH (Regensburg, Germany) as described previously [9], resulting in an artificial budding defective 1326 aa read-through Gag-Pol-Nef fusion protein. To generate the final DNA vaccine construct, the GPN gene was positioned between the EcoRI/XhoI sites of pcDNA3.1 (Invitrogen, UK). Plasmids were purified using Maxi-Prep purification kits (Qiagen, Hilden, Germany) and diluted for injection in endotoxin-free phosphate buffered saline (PBS). All DNA preparations were pyrogen free.

2.3. Construction of plasmid transfer vector

Plasmids pMA60gp120B/gagpolnefB-12,17 and pLZAW1 were provided by Sanofi-Pasteur. A 5.6 kbp DNA fragment containing the two synthetic early/late (E/L) promoters of VV [16] in a back-to-back orientation individually driving a codon optimized $_{BX08}$gp120 and $_{IIIB}$GPN genes of HIV-1 clade B was excised from plasmid pMA60gp120B/gagpolnefB-12,17 with the restriction endonuclease BamHI. The insert was modified by incubation

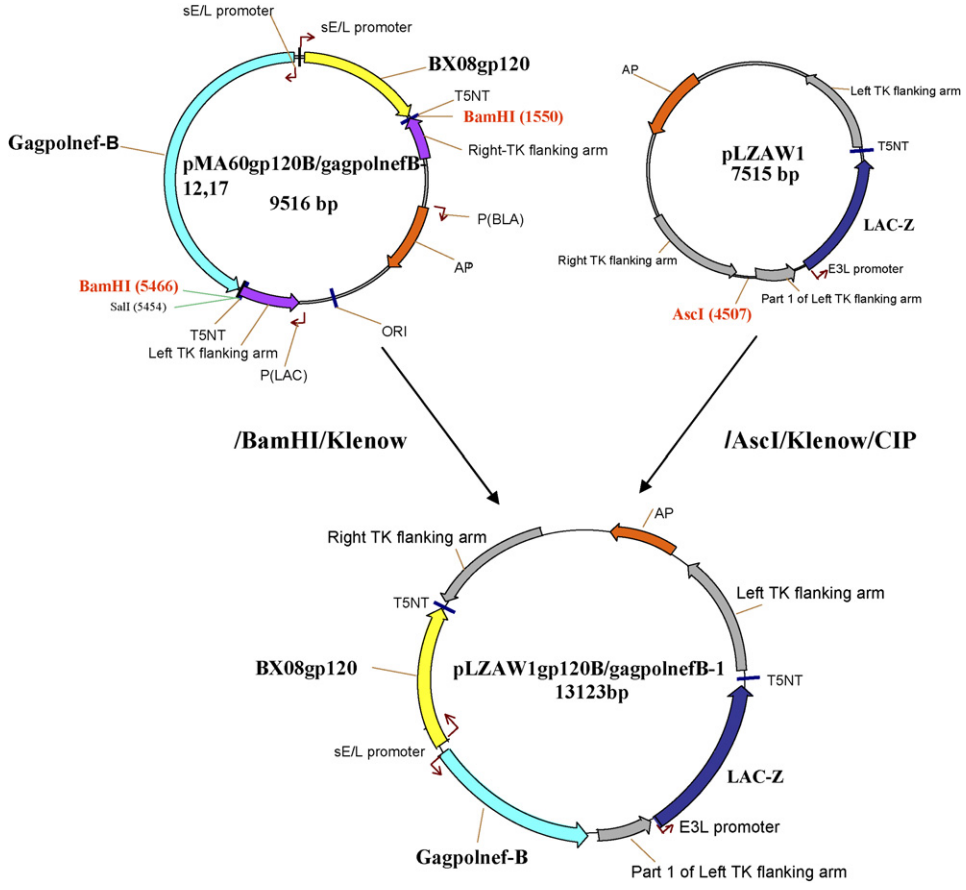

Fig. 1. Scheme for the construction of the transfer vector pLZAW1gp120B/gagpolnefB-1. A 5.6 kbp DNA containing the two synthetic early/late (E/L) promoters in a back-to-back orientation individually driving a codon optimized $_{BX08}$gp120 and $_{IIIB}$GPN genes of HIV-1 clade B was excised from plasmid pMA60gp120B/gagpolnefB-12,17 with the restriction endonuclease BamHI. The insert was modified by incubation with Klenow DNA polymerase to generate blunt ends, and inserted into pLZAW1 vector (previously digested with *Asc*I, modified by incubation with Klenow, and dephosphorylated by incubation with Alkaline Phosphatase, Calf Intestinal (CIP)) generating the plasmid transfer vector pLZAW1gp120B/gagpolnef-B-1. The resulting plasmid directs the insertion of the foreign genes into the thymidine kinase (TK) locus of MVA genome and allows the generation of a recombinant virus without the selectable marker.

with Klenow DNA polymerase to generate blunt ends, and inserted into the pLZAW1 vector (previously digested with *Asc*I, modified by incubation with Klenow, and dephosphorylated by incubation with Alkaline Phosphatase, Calf Intestinal (CIP)) generating the plasmid transfer vector pLZAW1 gp120B/gagpolnef-B-1 (Fig. 1). The new transfer vector contained a β-gal reporter gene sequence between two repetitions of the left TK flanking arm which permitted the reporter to be deleted from the final recombinant virus by homologous recombination after two–three passages. The plasmid transfer vector pLZAW1gp120B/gagpolnef-B-1 allows the insertion of the *gag-pol-nef* and *env* ORFs in the same viral locus (TK), both under the transcriptional control of the synthetic early/late viral promoter of VV and enables the elimination of the reporter gene.

2.4. Construction of the recombinant virus MVA-B

Primary chicken embryo fibroblast cells (CEF) from 11-day old SPF eggs were infected with MVA at a multiplicity of 0.05 PFU/cell and then transfected with 10 μg DNA of plasmid pLZAW1 gp120B/gagpolnef-B-1 using lipofectamine reagent according to the manufacturer's protocol (Invitrogen, San Diego, CA). After 72 h post infection the cells were harvested, sonicated and used for recombinant virus screening. Recombinant MVA viruses containing the $_{BX08}$gp120 and $_{IIIB}$Gag-Pol-Nef genes from clade B, and transiently co-expressing the β-gal marker gene (MVA-B (X-gal+)), were selected by consecutive rounds of plaque purification in CEF cells stained with 5-bromo-4-chloro-3-indolyl β-galactoside (X-Gal) (300 μg/mL). In the following plaque purification steps, recombinant MVA viruses containing the $_{BX08}$gp120 and $_{IIIB}$Gag-Pol-Nef genes and having deleted the β-gal gene (by homologous recombination between the TK left arm and the short TK left arm repeat that are flanking the marker) were isolated by two additional consecutive rounds of plaque purification screening for non-staining viral foci in CEF cells in the presence of X-Gal (300 μg/mL). In each round of purification the isolated plaques were expanded in CEF cells for 3 days, and the crude virus obtained were used for the next plaque purification round. The resulting MVA-B virus was grown in CEF, purified through two 45% (w/v) sucrose cushions and titrated by immunostaining. Purity of the recombinant virus was confirmed by PCR with primers spanning the junction and internal regions of the inserts and by DNA sequence analysis.

2.5. Construction of the recombinant virus NYVAC-B

The recombinant virus NYVAC-B containing the same cassette of HIV-1 genes in the TK locus as for MVA-B was generated by Sanofi-Pasteur using a similar approach as for MVA-B but different transfer vector (pMA60gp120B/gagpolnefB-12,17), except that plaque-lifting and ^{32}P-labeled of the inserts were used for the screening of recombinant viruses. NYVAC-B uses the same synthetic early/late promoter of VV as in the case of MVA-B for expression of HIV genes. The correct inserts in the virus genome were confirmed by PCR and DNA sequence analyses (not shown).

2.6. PCR analysis of recombinant MVA-B

Viral DNA was extracted by the method of SDS-Protease K-Phenol from CEF cells infected at 5 PFU/cell with the recombinant MVA-B virus. Different set of primers annealing in the TK flanking sequences and in internal regions of the inserted genes were used for PCR analysis (see Table 1). The amplifications were performed with Platinum Taq DNA polymerase (Invitrogen, San Diego, CA), and the conditions were optimized for each set of primers.

2.7. Time course expression of $_{BX08}$gp120 and $_{IIIB}$GPN proteins from MVA-B and NYVAC-B

CEF cells grown in 12 well-plates were infected at 5 PFU/cell with the recombinants MVA-B and NYVAC-B. At 4, 8, 16 and 24 h post infection (h p.i), cells were collected and centrifuged at 1500 rpm for 10 min. The supernatant (S) was removed and concentrated by speed-vacuum. Cellular pellets (P) were lysed in cold buffer (50 mM Tris–HCl pH 8, 0.5 M NaCl, 10% NP-40, 1% SDS). The supernatant and pellet samples, both containing equal amounts of protein (12 μg), were run on 10% SDS-PAGE. The expression of $_{BX08}$gp120 and $_{IIIB}$GPN proteins was visualized following Western blotting using rabbit polyclonal anti-gp120 antibodies and polyclonal anti-gag p24 serum (ARP 432, NIBSC, Centralised Facility for AIDS reagent, UK), respectively. Detection of cellular β-actin protein was used as an internal loading control.

Table 1
DNA sequence of primers used in the PCR analysis of MVA-B recombinant virus

Oligos	Sequences	Position
TK-L (Forward)	5′ TGATTAGTTTGATGCGATTC 3′	342–361
TK-R (Reverse)	5′ TGTCCTTGATACGGCAG 3′	6383–6399
$_{BX08}$556 (Forward)	5′TGCCCATCGACAACG 3′	5133–5147
GPN7649 (Reverse)	5′ AGCCCCATCGAGACCG 3′	2702–2717
GPN8170 (Forward)	5′ ATTAGCCTGCCTCTCGG 3′	3222–3238
E/L (Reverse)	5′ TATTTTTTTTTTTTGGAATATAAATAG 3′	4526–4552

Their positions in the DNA sequence of MVA-B within the TK viral locus are represented.

2.8. Genetic stability of recombinant viruses by expression analyses

Monolayers of CEF cells were infected at 0.05 PFU/cell with MVA-B or NYVAC-B recombinants. At 72 h p.i cells were collected by scrapping. After three freeze–thaw cycles and brief sonication, the cellular extract was centrifuged at 1500 rpm for 5 min and the supernatant was used for a new round of infection at 0.05 PFU/cell. The same procedure was repeated until passage 10. Expression of $_{BX08}$gp120 and $_{IIIB}$GPN proteins at all passages was detected by Western blot after infection of CEF cells with the virus stocks and after serial dilutions, infection of CEF and immunostaining using anti-gp120 and anti-gag p24 polyclonal antibodies, respectively. The stability of the clinical lot of MVA-B produced under GMP conditions by IDT (Germany), was also evaluated. Monolayers of CEF cells grown in 6 well tissue culture plates were infected with serial dilutions of the clinical lot of MVA-B. After 1 h of virus adsorption, the virus inoculum was removed, washed and cells overlayed with agar. At 72 h p.i cells were stained with 0.01% neutral red (SIGMA) and 46 individual plaques were pick up, resuspended in 0.5 mL of DMEM by freez–thawing and sonication, 0.1 mL used for infection of CEF in 24 well tissue culture plates for 24 h, cells collected, lysed in Laemmli buffer, cell extracts fractionated by 12% SDS-PAGE and analysed by Western blot with specific anti-Env and anti-Gag antibodies to evaluate expression of $_{BX08}$gp120 and $_{IIIB}$GPN proteins.

2.9. Analysis of virus growth

To determine virus-growth profiles, monolayers of CEF cells grown in 6 well tissue culture plates were infected at 0.01 PFU/cell with MVA-B or NYVAC-B recombinants. Following virus adsorption for 60 min at 37 °C, the inoculum was removed. The infected cells were washed twice with DMEM medium without serum, and incubated with fresh DMEM containing 2% of FCS at 37 °C in a 5% CO_2 atmosphere. At 24, 48 and 72 h p.i, cells were removed by scraping, centrifuged at 1500 rpm for 5 min and both pellet and supernatant were collected. The supernatants were stored at 4 °C for no more than 48 h before virus titration. The pellet was resuspended in serum-free medium at 20×10^6 cells/mL, freeze–thawed three times, sonicated, and centrifuged at 1500 rpm for 5 min. The supernatant was collected and referred as cell lysates. Virus titers in supernatants and cell lysates were determined by immunostaining assay in CEF cells using anti-VV antibodies.

2.10. Immunofluorescence

HeLa cells cultured on coverslips were mock-infected or infected at 5 PFU/cell with either the wild type MVA and NYVAC strains or MVA-B and NYVAC-B recombinants. At 16 h p.i, cells were washed with PBS, fixed with 4% paraformaldehyde and permeabilized with 2% Triton X-100 in PBS (room temperature (RT), 5 min). Cells were incubated with polyclonal antibodies recognizing HIV-1 $_{BX08}$gp120 and $_{IIIB}$GPN proteins together with WGA reagent (Molecular Probes). Coverslips were then extensively washed with PBS, and incubated in darkness for 1 h at 37 °C, with secondary antibody conjugated with green fluorochrome Cy2 (Jackson Immunoresearch) and with the DNA staining reagent ToPro (Molecular Probes). Images were obtained by using Bio-Rad Radiance 2100 confocal laser microscope, were collected by using Lasersharp 2000 software and were processed in LaserPix.

2.11. Measurement of apoptosis

For induction of cytopathic effects (CPE) under non-permissive conditions, HeLa cells were seeded into six-well tissue culture plates and grown to confluence. The cells (duplicate wells) were infected at 5 PFU/cell with MVA-B or NYVAC-B recombinants and visually monitored under a microscope at 24 h p.i.

The cleavage of poly ADP-ribose polymerase (PARP) was analyzed by Western blot at 4, 8 and 16 h post-infection in HeLa cells infected with MVA-B or NYVAC-B recombinants at 5 PFU/cell. Rabbit polyclonal anti-Human PARP was supplied by Cell Signaling and the monoclonal antiboby against β-actin was supplied by SIGMA.

The apoptosis levels were measured using the cell death detection enzyme-linked immunosorbent assay (ELISA) kit (Roche) according to manufacturer's instructions. This assay is based on the quantitative sandwich enzyme immunoassay principle, and uses mouse monoclonal antibodies directed against DNA and histones to estimate the amount of cytoplasmic histone-associated DNA fragments.

2.12. Peptides

The HIV-1 peptide pools, with each purified peptide at 25 μg per vial, were provided by the EuroVacc Foundation. They spanned the entire Env, Gag, Pol and Nef regions from clade B included in the virus vectors as consecutive 15-mers overlapped by 11 amino acids. The $_{BX08}$gp120 protein (494 aa) was spanned by the Env-1 (aa: 1-251; 60 peptides) and Env-2 (aa: 241–494; 61 peptides) pools. The Gag-Pol-Nef fusion protein (1326 aa) was spanned by the following pools: Gag-1 (aa: 1–231; 55 peptides), Gag-2 (aa: 221–431; 50 peptides), GPN-1 (aa: 421–655; 56 peptides), GPN-2 (aa: 645–879; 56 peptides), GPN-3 (aa: 869–1103; 56 peptides) and GPN-4 (aa: 1093–1326; 56 peptides). The CTRL peptide pool was used as negative control. It contains 23 peptides mostly from CMV, EBV and influenza, each at 50 μg.

2.13. Mice immunization

BALB/c mice were purchased from Harlan. Transgenic HHD mice were kindly provided by Dr. Lemonnier (Pasteur Institute, France). They are double-knockout for H2-D^b and β2-microglobulin and transgenic for a chimeric HLA-A2 molecule [17]. When the heterologous DNA/poxvirus prime-boost approach was assayed, animals received 100 μg of DNA-B (50 μg of pCMV-$_{BX08}$gp120 + 50 μg of pcDNA-$_{IIIB}$GPN) by intramuscular route (i.m.) and 2 weeks later received an intraperitoneal (i.p.) inoculation of 2×10^7 PFU of the corresponding recombinant vaccinia viruses (rVVs) in 200 μL of PBS. When the homologous rVV/rVV prime-boost approach was used, animals received 2×10^7 PFU of the corresponding rVVs by i.p route at day 0 and 15. Ten days after the last immunization mice were sacrificed and spleens processed for fresh ELISPOT assay. At least two independent experiments have been performed for the different immunization protocols.

2.14. Fresh IFN-γ and IL-2 ELISPOT assay

Fresh IFN-γ ELISPOT assay was performed as previously described [18]. Briefly, 10^5–10^6 splenocytes (depleted of red blood cells) were plated in triplicate in 96-well nitrocellulose-bottomed plates previously coated with 6 μg/mL of anti-mouse IFN-γ mAb R4-6A2 (Pharmingen, San Diego, CA). HIV-1 peptide pools from clade B and negative control (CTRL) pool were resuspended in RPMI 1640 supplemented with 10% FCS and added to the cells at a final concentration of 5 μg/mL for each peptide. Plates were incubated at 37 °C, 5% CO_2 for 48 h, washed extensively with PBS containing 0.05% of Tween 20 (PBS-T) and incubated 2 h at RT with a solution of 2 μg/mL of biotinylated anti-mouse IFN-γ mAb XMG1.2 (Pharmingen, San Diego, CA) in PBS-T. Afterwards, plates were washed with PBS-T and 100 μL of peroxidase-labeled avidin (Sigma, St. Louis, MO) at 1:800 dilution in PBS-T was added to each well. After 1 h of incubation at RT, wells were washed with PBS-T and PBS. The spots were developed by adding 1 μg/mL of the substrate 3,3′-diaminobenzidine tetrahydrochloride (Sigma, St. Louis, MO) in 50 mM Tris–HCl, pH 7.5 containing 0.015% hydrogen peroxide. The spots were counted with the aid of a stereomicroscope. Fresh IL-2 ELISPOT assay was carried out identically but using the anti-mouse IL-2 mAb JES6-1A12 (Pharmingen, San Diego, CA) and biotinylated anti-mouse IL-2 mAb JES6-5H4 (Pharmingen, San Diego, CA) as capture and detection antibody, respectively.

2.15. Evaluation of cytokine levels by ELISA

Splenocytes from immunized mice (5×10^5 cells) were stimulated with 2 μg/mL of each peptide pools at 37 °C, 5% CO_2 for 3 days. Culture supernatants were collected and stored at −70 °C until performing the assay. Levels of IFN-γ, IL-10, RANTES and MIP-1β were evaluated using commercial ELISA kits (Pharmingen, San Diego, CA).

2.16. Antibody measurements by Enzyme-linked immunosorbent assay (ELISA)

High binding polystyrene microtitre plates (Nunc) were coated with 100 μL of the HIV-1 gp160LAV envelope protein (Protein Sciences) diluted at 10 μg/mL in 0.05 M carbonate–bicarbonate buffer pH 9.6 overnight at 4 °C. The wells were washed twice with PBS plus 0.05% Tween 20 (PBS-T) and blocked with PBS containing 10% FCS (blocking solution) during 1 h at 37 °C. Serum samples diluted in blocking solution were added in a volume of 100 μL/well and incubated 2 h at 37 °C. Plates were washed five times with PBS-T before the detection antibody was added. Peroxidase-conjugated goat anti-mouse immunoglobulin G (IgG) antibody (Southern Biotechnology Associated, Birmingham, Ala) was diluted 1:1000 in blocking solution and incubated for 1 h at 37 °C. The plates were washed again five times with PBS-T and hydrogen peroxide and ortophenylenediamine (OPD) 0.05% were used to reveal the reaction. After 10–15 min of incubation at RT, the reaction was stopped by adding 2 N H_2SO_4, and absorbance was measured at 492 nm on a Multiskan Plus plate reader (Labsystem, Chicago, Ill).

2.17. Statistical procedures

All the data were logarithmically transformed and the means compared using ANOVA and Duncan's multiple range test.

3. Results

3.1. Characterization of recombinant MVA-B virus by PCR analysis

MVA-B, a recombinant MVA expressing HIV-1 clade B Gag-Pol-Nef and Env (gp120) antigens in the TK locus under control of the same synthetic early/late promoter of VV, was constructed by homologous recombination in CEF cells as described in Section 2. Gag-Pol-Nef is a fusion protein of 1326 amino acids composed of *gag, pol* and *nef ORFs* from HIV-1 clone IIIB, that has been modified to enhance its immunogenicity and for safety by removing undesirable domains. Gp120 Env protein comes from the HIV-1 primary isolate $_{BX08}$. In both cases, the codon usage was adapted to highly express human genes. The correct insertion of the HIV-1 genes in the recombinant MVA-B virus was confirmed by PCR and DNA sequence analysis. Viral DNA purified from CEF cells infected with MVA-B was amplified using different set of primers annealing in the TK flanking sequences and in internal regions of the inserted genes (see Table 1). The sizes

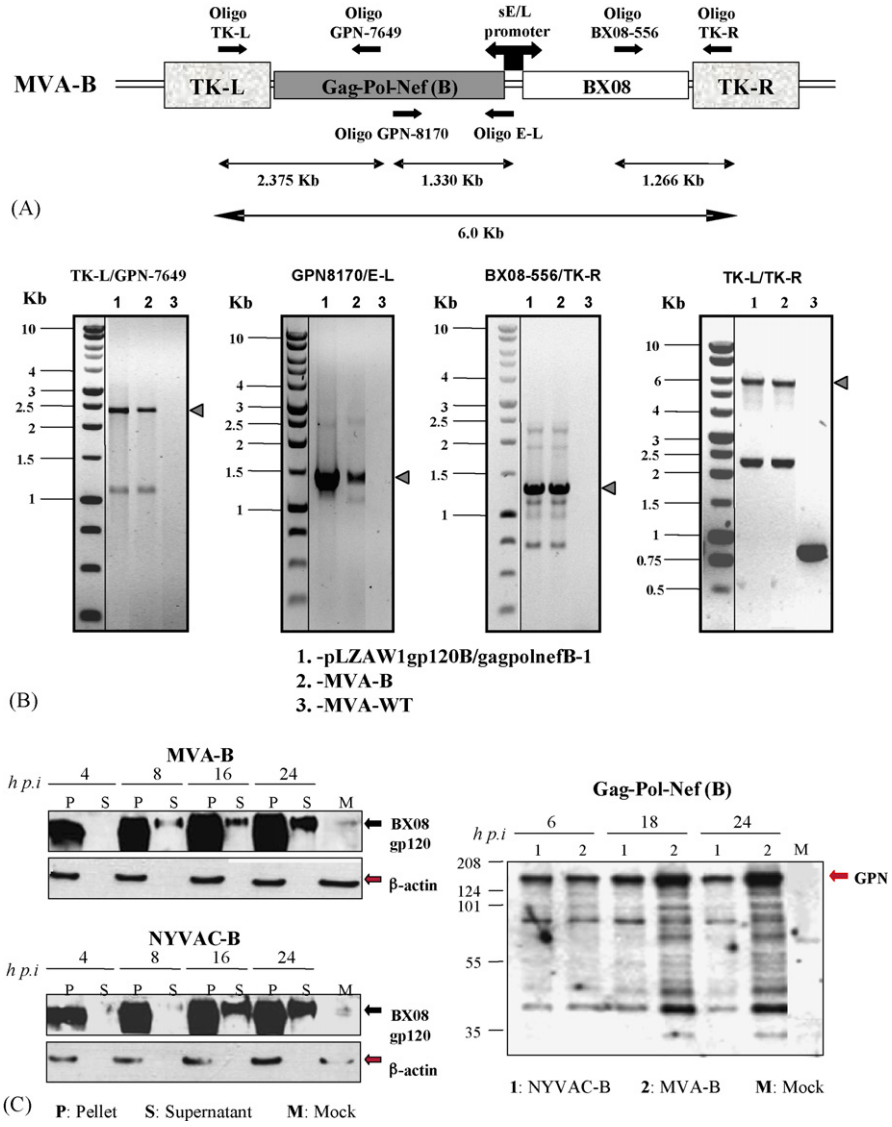

Fig. 2. Characterization of MVA-B and NYVAC-B recombinant viruses. (A) Scheme of the MVA-B insert within the TK viral locus. The positions of the different sets of primers used for PCR analysis and the expected sizes of PCR products are represented. (B) PCR analysis of the MVA-B insert in the TK viral locus. 100 ng of viral DNA extracted from CEF cells infected at 5 PFU/cell with MVA-B (line 2) or MVA-WT (line 3) were used for PCR analysis. The transfer vector pLZAW1gp120B/gagpolnef-B-1 was used as positive control (line 1). PCR conditions were optimized for each set of primers. (C) Time-course expression of $_{BX08}$gp120 and $_{IIIB}$GPN proteins in cells infected with MVA-B and NYVAC-B recombinants. The expression of $_{BX08}$gp120 and $_{IIIB}$GPN proteins at indicated times post-infection of CEF cells was visualized by Western blot in supernatants (S) and pellet (P) samples of mock (M) or infected cells at 5 PFU/cell with MVA-B or NYVAC-B recombinant viruses. The cellular β-actin protein expression was used as internal loading control. Arrows at the right indicate the position of gp120, GPN and β-actin proteins.

of the expected PCR products are represented in Fig. 2A. For comparison purpose, pLZAW1gp120B/gagpolnef-B-1 plasmid and DNA extracted from CEF cells infected with the wild type parental strain of MVA (MVA-WT) were used. As shown in Fig. 2B, the amplifications performed with the different set of primers reveals that *gag-pol-nef* and *env* ORFs were inserted successfully into the MVA TK locus, and also that no wild-type contamination was present in the rMVA preparation. These results were confirmed by DNA sequence analysis of the MVA-B TK locus (see Appendix A).

3.2. Characteristics of MVA-B and NYVAC-B recombinants in cultured cells

3.2.1. Expression of $_{BX08}$gp120 and $_{IIIB}$GPN proteins by MVA-B and NYVAC-B

NYVAC-B, a recombinant NYVAC expressing the identical HIV-1 clade B antigens as MVA-B in the TK locus and under control of the same synthetic early/late promoter of VV, was generated by Sanofi-Pasteur. In order to characterize the expression of $_{BX08}$gp120 and $_{IIIB}$GPN proteins by MVA-B and NYVAC-B recombinants, a time-course analysis was

carried out. The kinetic of synthesis of Env protein was similar in MVA-B and NYVAC-B infected cells. $_{BX08}$gp120 was efficiently released from cells by 8 h p.i (Fig. 2C, left panel). As compared to NYVAC-B, the full length $_{IIIB}$GPN fusion protein was produced in MVA-B infected cells but at different levels depending on the time point after infection (Fig. 2C, right panel). With time (18 and 24 h p.i) the $_{IIIB}$GPN expression levels decreased in NYVAC-B versus MVA-B infected cells.

Immunofluorescence analysis by confocal microscopy in infected Hela cells confirmed that both viruses (MVA-B and NYVAC-B) expressed Env and Gag-Pol-Nef antigens. $_{BX08}$gp120 was predominantly found in the Golgi of infected cells whereas $_{IIIB}$GPN localised in the cytoplasm (data not shown).

3.2.2. Genetic stability of MVA-B and NYVAC-B

To verify that MVA-B and NYVAC-B recombinants could be passage without the lost of the transgene, a stability test was performed. The recombinants were continuously passage from P2 stock to P10 in CEF cells (4 passages beyond production level). Expression of Env and Gag-Pol-Nef antigens at the different passages was determined by Western blot and immunostaining assay. MVA-B efficiently expressed $_{BX08}$gp120 and $_{IIIB}$GPN proteins after 7, 8, 9 and 10 passages in CEF cells. By counting over 100 immunoplaques stained with antibodies specific for VV antigens versus Env and Gag, we observed that 95–100% of the plaques generated in cells infected with the P10 stock stained with the antibodies for both Gag and Env proteins (data not shown). We also evaluated the stability of a clinical lot of MVA-

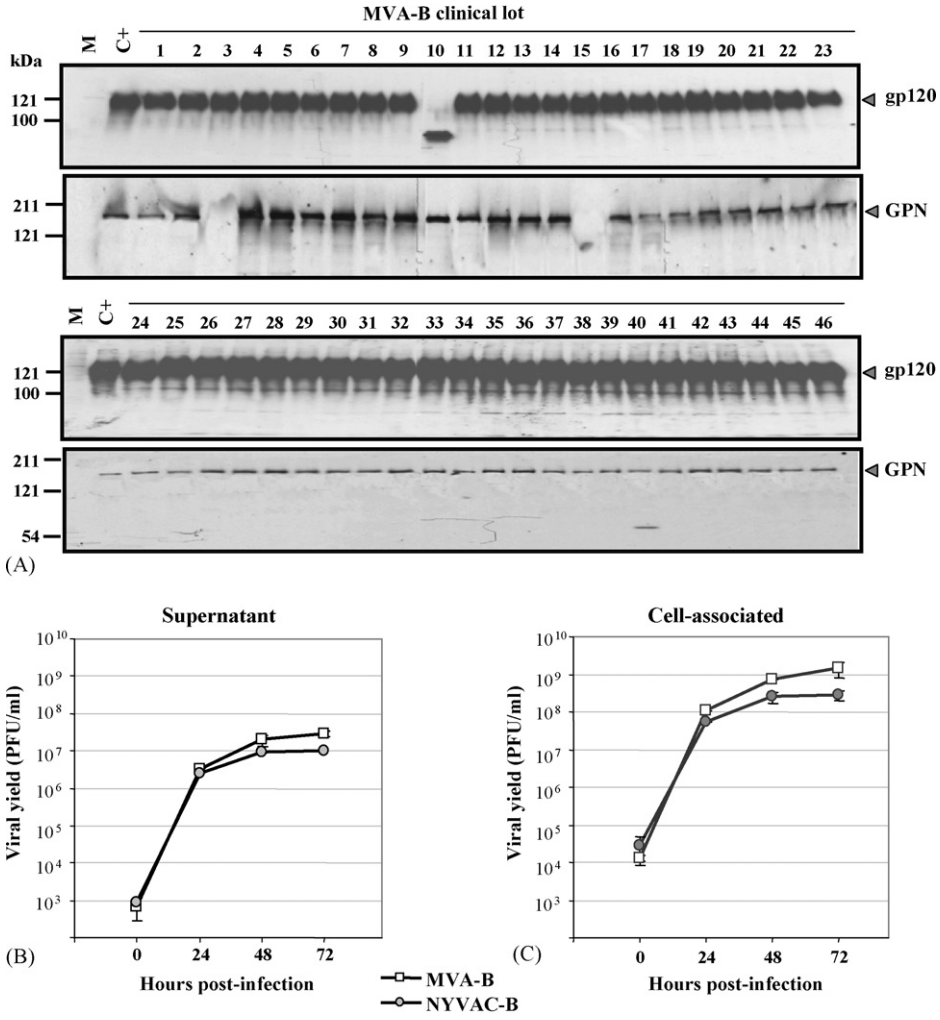

Fig. 3. Stability and growth characteristics of MVA-B and NYVAC-B. (A) Stability of MVA-B from a GMP manufactured clinical lot. Forty six individual plaques isolated from a clinical lot of MVA-B as described in Section 2 were amplified in CEF cells, cell lysates used for infection of CEF for 24 h, washed, cells collected, lysed, proteins fractionated by SDS-PAGE and analyzed by Western blot with specific antibodies. The expression of $_{BX08}$gp120 and $_{IIIB}$GPN proteins in samples of mock-infected CEF cells (M) or infected with individual plaques (1–46) is shown. A positive control (C+) were cellular extracts from CEF cells infected with the original MVA-B stock used for the generation of the clinical lot (Passage 8). Arrows to the right indicate the migration of gp120 and GPN proteins in the gels. (B and C) Virus growth of MVA-B and NYVAC-B in CEF cells. Monolayers of CEF cells were infected at 0.01 PFU/cell with MVA-B or NYVAC-B recombinants for 0, 24, 48 and 72 h. Cells were collected by centrifugation and infectious virus associated to the cells (panel C) and released to the supernatant (panel B) during the course of the infection were quantified by plaque immunostaining assay. Averages of three independent experiments are shown with standard error bars.

B produced under GMP conditions. As shown in Fig. 3A, out of 46 isolated plaques analysed by Western blot none of them represent wild type reversion. All of them (100%) expressed gp120, but 45 out of 46 plaques (97.8%) expressed correctly the $_{BX08}$gp120 protein. In the case of GPN, 43 out of 46 plaques (93.5%) expressed correctly the $_{IIIB}$GPN protein. These results revealed that MVA-B is genetically stable, even when grown and purified at large scale under GMP conditions. The genetic stability of the inserts for NYVAC-B was similarly confirmed after the tenth passage (not shown).

3.2.3. Virus growth of MVA-B and NYVAC-B

To analyze the viral growth characteristics of MVA-B in comparison with NYVAC-B under permissive conditions, monolayers of CEF cells were infected at 0.01 PFU/cell with each virus for 0, 24, 48 and 72 h. Infectious viruses that remained cell-associated and released to the medium during the course of the infection were measured by immunostaining plaque assay. The growth kinetics of MVA-B and NYVAC-B were similar (Fig. 3B and C). The titers of cell-associated virus in cells infected with NYVAC-B were by 48 h lower than the titers obtained in cells infected with MVA-B (Fig. 3C).

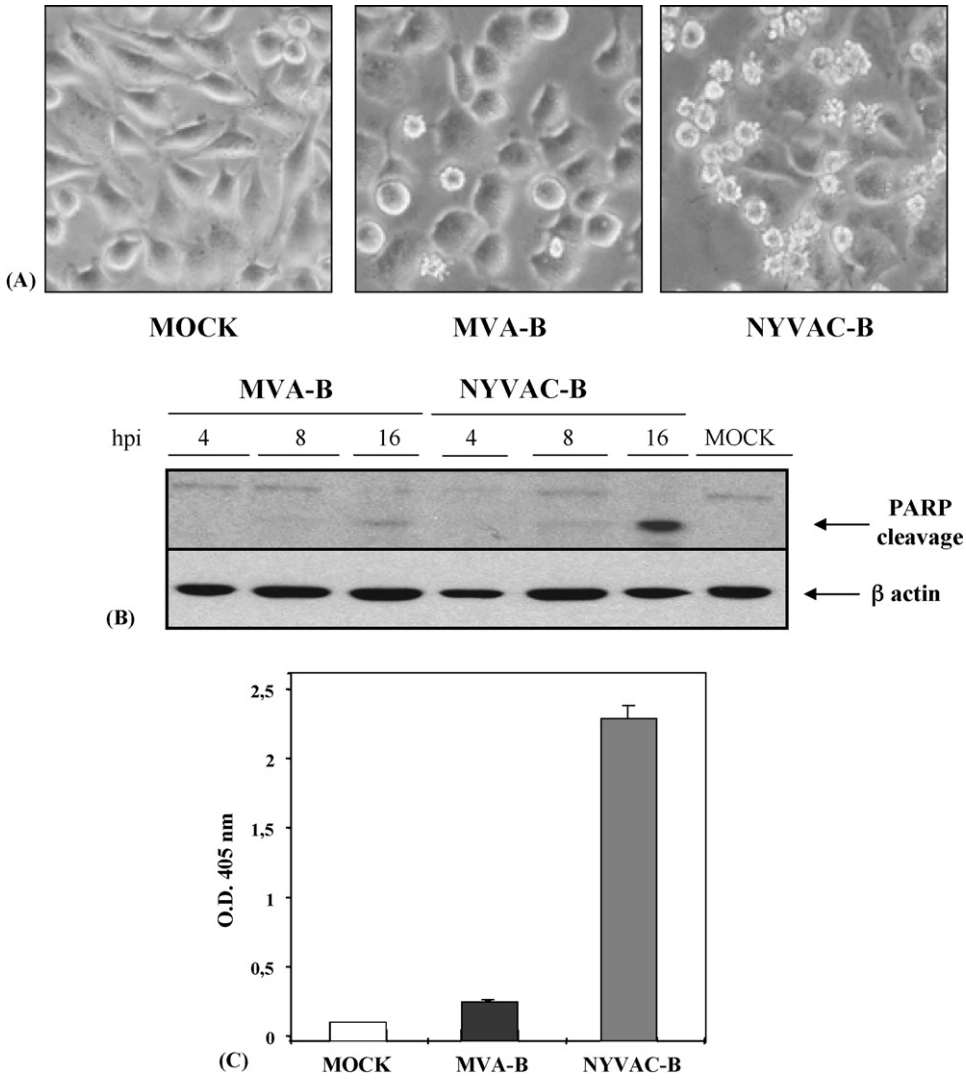

Fig. 4. Differences in apoptosis induction by MVA-B versus NYVAC-B. (A) Cytopathic effects of MVA-B and NYVAC-B in human cells. Monolayers of HeLa cells were mock-infected or infected at 5 PFU/cell with recombinant MVA-B and NYVAC-B viruses. At 24 h p.i the morphological changes characteristic of apoptosis in the cells were examined by phase-contrast microscopy. In NYVAC-B infected cells, numerous cells are in apoptosis compared to MVA-B infection. (B) Western blot analysis of PARP cleavage in HeLa cells infected with MVA-B and NYVAC-B. Monolayers of HeLa cells were mock-infected or infected at 5 PFU/cell with recombinant MVA-B and NYVAC-B viruses. At different times post-infection the cell extracts were collected and analysed by Western blot. The cellular β-actin protein expression was used as internal loading control. Extensive cleavage of PARP was observed at 16 h p.i in NYVAC-B infected cells compared to MVA-B infection. (C) Quantitation of apoptosis after infection with MVA-B or NYVAC-B. Monolayers of HeLa cells were mock-infected or infected at 5 PFU/cell with recombinant MVA-B and NYVAC-B viruses and the extent of apoptosis was determined at 24 h p.i by ELISA. Absorbance at 405 nm is represented.

3.2.4. A hallmark of NYVAC-B infection is the induction of apoptosis, but not of MVA-B

The difference in virus titers between the two recombinant viruses described above could be attributed to different degrees in apoptosis induction. We have recently described that during infection with parental NYVAC strain there is induction of apoptosis while parental MVA does not induce apoptosis [19]. To define if the recombinant NYVAC-B also induces apoptosis and to compare it with MVA-B, we performed three different assays. As shown in Fig. 4, NYVAC-B infection triggers apoptosis in infected cells as measured by phase contrast microscopy (panel A), by PARP cleavage (panel B) and by ELISA test (panel C). These effects were minimally observed in cells infected with MVA-B. These dif-

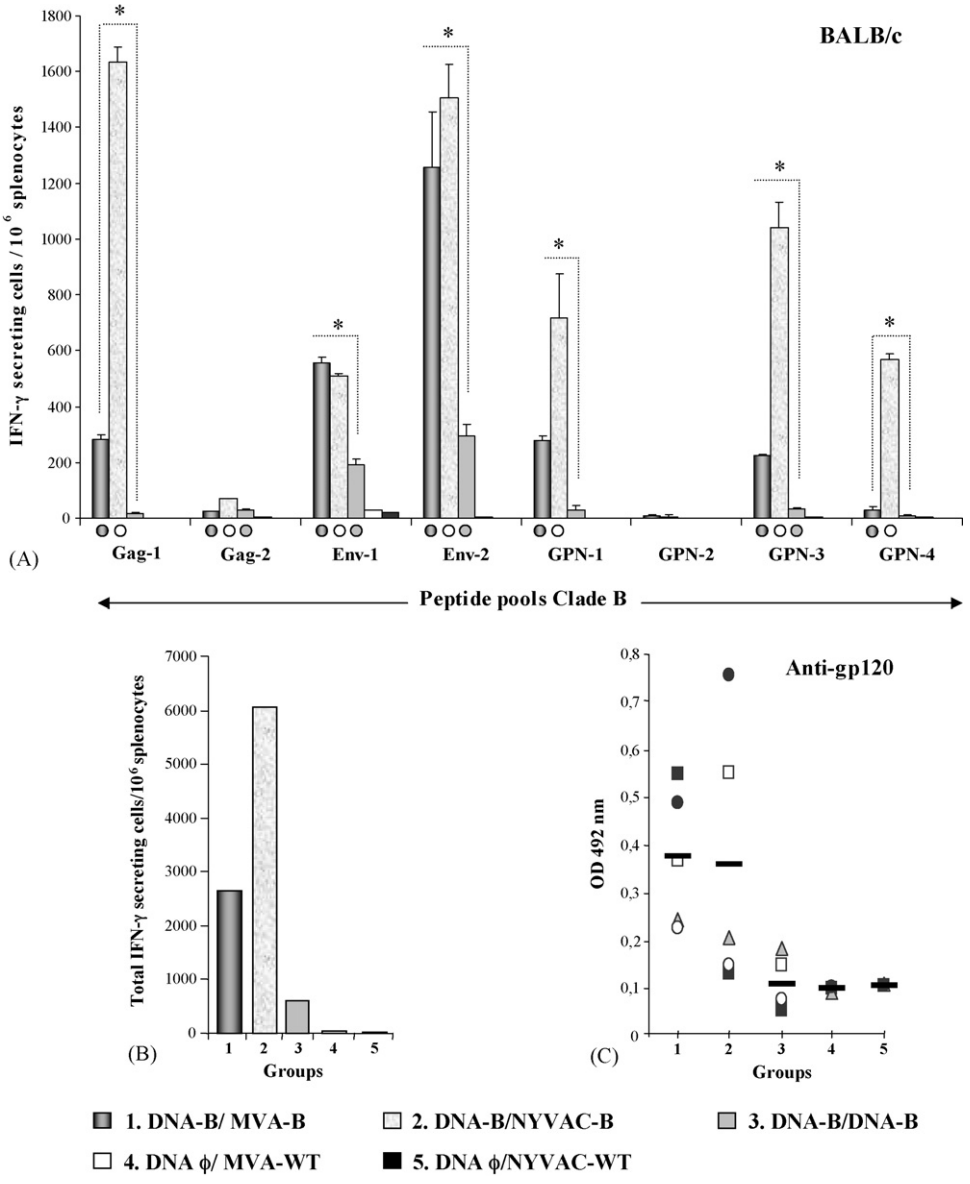

Fig. 5. Immunogenicity of MVA-B and NYVAC-B after DNA/rVV prime-boost protocols in BALB/c mice. (A) Cell-mediated immune response detected by fresh IFN-γ ELISPOT. Groups of 5 BALB/c mice were primed with 100 μg of either DNA-B or sham DNA (DNA-φ) by intramuscular route. Two weeks after priming, the mice received an intraperitoneal inoculation of 2×10^7 PFU of the corresponding rVV. Vaccine-elicited functional immune responses of splenocytes were measured 10 days after the last immunization in a fresh IFN-γ ELISPOT assay following stimulation with 5 μg/mL of pools of overlapping peptides spanning the entire HIV-1 $_{BX08}$gp120 and $_{IIIB}$GPN proteins. The number of spots obtained with the negative CTRL pool ranged between 5 and 15 and was subtracted in all cases. Peptide-specific IFN-γ secreting cells with standard deviation from triplicate cultures are shown. (●) represents statistically significant differences ($p < 0.05$) between each peptide pool and the CTRL pool. (*) represents statistically significant differences ($p < 0.05$) between groups. (B) Magnitude of the total response for clade B pools. Bars represent the total number of antigen-specific IFN-γ secreting cells detected in each group against all the peptide pools spanning the Ags included in MVA-B and NYVAC-B recombinants. (C) Humoral immune response elicited against HIV-1 gp160 protein from HIV-1 LAV clone. Serum from immunized mice was evaluated by ELISA for specific anti-gp120 antibodies in blood taken 10 days after the booster. Absorbance values (measured at 492 nm) correspond to 1/50 dilution of individual serum. (—) represents the mean value for each group.

ferences may have an impact on immune responses. Thus, we next analyzed the immune responses elicited in mice by the two recombinant poxvirus vectors.

3.3. Booster with MVA-B and NYVAC-B efficiently induces HIV-specific cellular immune responses in BALB/c mice

Since a DNA prime/rVV boost immunization regime has proven to be an effective means of activating CD8+ T cell responses to HIV antigens [11,20], we wished to evaluate the magnitude and breadth of the HIV-specific cellular immune response triggered in BALB/c mice using this strategy. For this purpose, groups of mice were first primed with two DNA vectors, one that expresses only HIV-1 Env ($_{BX08}$gp120), and the other expressing the Gag-Pol-Nef polyprotein from clade B (both vectors referred as DNA-B), and 2 weeks later the animals were boosted with the same dose of DNA-B, or with 2×10^7 PFU of either MVA-B or NYVAC-B, both expressing the same HIV antigens as DNA-B. Animals primed with sham DNA (DNA-φ) and boosted with either MVA-WT or NYVAC-WT were used as controls. Vaccine-elicited functional immune responses in splenocytes were measured 10 days after the last immunization in a fresh IFN-γ ELISPOT assay following stimulation with a pool of overlapping peptides that span the entire HIV-1 $_{BX08}$gp120 and $_{IIIB}$GPN proteins. The number of spots obtained with the negative CTRL pool was subtracted in all cases.

As shown in Fig. 5A, animals that received MVA-B or NYVAC-B in the booster (groups 1 and 2) induced a significant enhancement of splenic T-cell response against the clade B peptide pools Gag-1, Env-1, Env-2, GPN-1, GPN-3 and GPN-4, in comparison with mice that received two doses of DNA-B vector (group 3) ($p < 0.05$). However, the highest response was detected in mice boosted with NYVAC-B virus (group 2). The Gag-2 pool was poorly recognized by the three groups, and no specific cellular response was detected against the GPN-2 pool. The numbers of specific IFN-γ secreting cells in animals immunized either with DNA-φ/MVA-WT (group 4) or with DNA-φ/NYVAC-WT (group 5) were lower than 30 spots. The magnitude of the total response for clade B pools, determined by the overall number of IFN-γ secreting cells, was more than 5 times higher in group 1 (DNA-B/MVA-B) and group 2 (DNA-B/NYVAC-B) than that induced in group 3 (DNA-B/DNA-B) (Fig. 5B), demonstrating the efficiency of rVV in boosting the cellular immune response. The breadth of the B-specific response per group, as measured by the number of positive pools, was similar in mice boosted with MVA-B and NYVAC-B (7 positive pools), and lower in mice that received two doses of DNA-B (4 positive pools).

Since a balance between a Th1 and Th2 type of immune responses may be critical for the control of HIV infection [21], our next approach was to determine the profile of cytokines triggered in immunized mice. Thus, we quantified the levels of type 1 (IFN-γ) and type 2 (IL-10) cytokines in cell culture supernatants re-stimulated with specific HIV-1 peptide pools. As shown in Table 2(A), higher levels of IFN-γ were secreted against the different clade B pools by splenocytes from mice primed with DNA-B and boosted with recombinant viral vectors (MVA-B and NYVAC-B), com-

Table 2
(A) Cytokine production (pg/mL) by splenocytes from BALB/c mice immunized in DNA prime/rVV boost regime and (B) β-chemokine production (pg/mL) by splenocytes from BALB/c mice immunized in DNA prime/rVV boost regime

A

		Gag-1	Gag-2	Env-1	Env-2	GPN-1	GPN-2	GPN-3	GPN-4	Total
DNA-B/MVA-B	IFN-γ	3170	813	5187	5787	3553	173	573	830	20086
DNA-B/NYVAC-B	IFN-γ	7690	1417	6393	5300	4807	980	5087	2207	33881
DNA-B/DNA-B	IFN-γ	757	640	3213	1927	437	<20	<20	<20	6974
DNA-φ/MVA-WT	IFN-γ	877	887	573	280	247	133	360	67	3424
DNA-φ/NYVAC-WT	IFN-γ	367	287	517	123	<20	<20	<20	<20	1294

B

		Gag-1	Gag-2	Env-1	Env-2	GPN-1	GPN-2	GPN-3	GPN-4	Total
DNA-B / MVA-B	**RANTES**	678	34	591	2178	781	30	244	27	**4563**
	MIP-1β	<20	<20	<20	2047	824	<20	<20	<20	**2871**
DNA-B / NYVAC-B	**RANTES**	1758	<20	435	1713	1578	<20	1216	<20	**6700**
	MIP-1β	2960	<20	1112	3017	3227	<20	2702	752	**13770**
DNA-B / DNA-B	**RANTES**	63	1017	190	509	216	<20	45	<20	**2040**
	MIP-1β	228	1347	<20	<20	<20	424	<20	385	**2384**
DNA-ϕ / MVA-WT	**RANTES**	<20	<20	<20	18	<20	42	<20	<20	**60**
	MIP-1β	<20	<20	<20	<20	<20	<20	<20	<20	**<20**
DNA-ϕ / NYVAC-WT	**RANTES**	43	<20	<20	24	<20	106	<20	<20	**173**
	MIP-1β	<20	62	<20	<20	<20	<20	<20	<20	**62**

BALB/c mice were immunized as described in Section 2. Ten days after the last immunization the animals were sacrificed and their spleens were processed. The splenocytes from each group were stimulated *in vitro* with 2 μg/mL of different HIV-1 peptide pools from clade B and incubated for 3 days at 37 °C. Thereafter, cell supernatants were collected and stored at −70 °C. Cytokine and β-chemokine levels were measured with specific commercial kits.

pared with two doses of DNA-B, or with control groups (DNA-φ/MVA-WT and DNA-φ/NYVAC-WT). The levels of IL-10 (as index of Th2) in cell culture supernatants were low and not significant, and hence, they are not represented. These results are in agreement with the response detected by ELISPOT, and suggest induction of a Th1 type of immune response by the vaccination protocol of DNA prime/poxvirus boost.

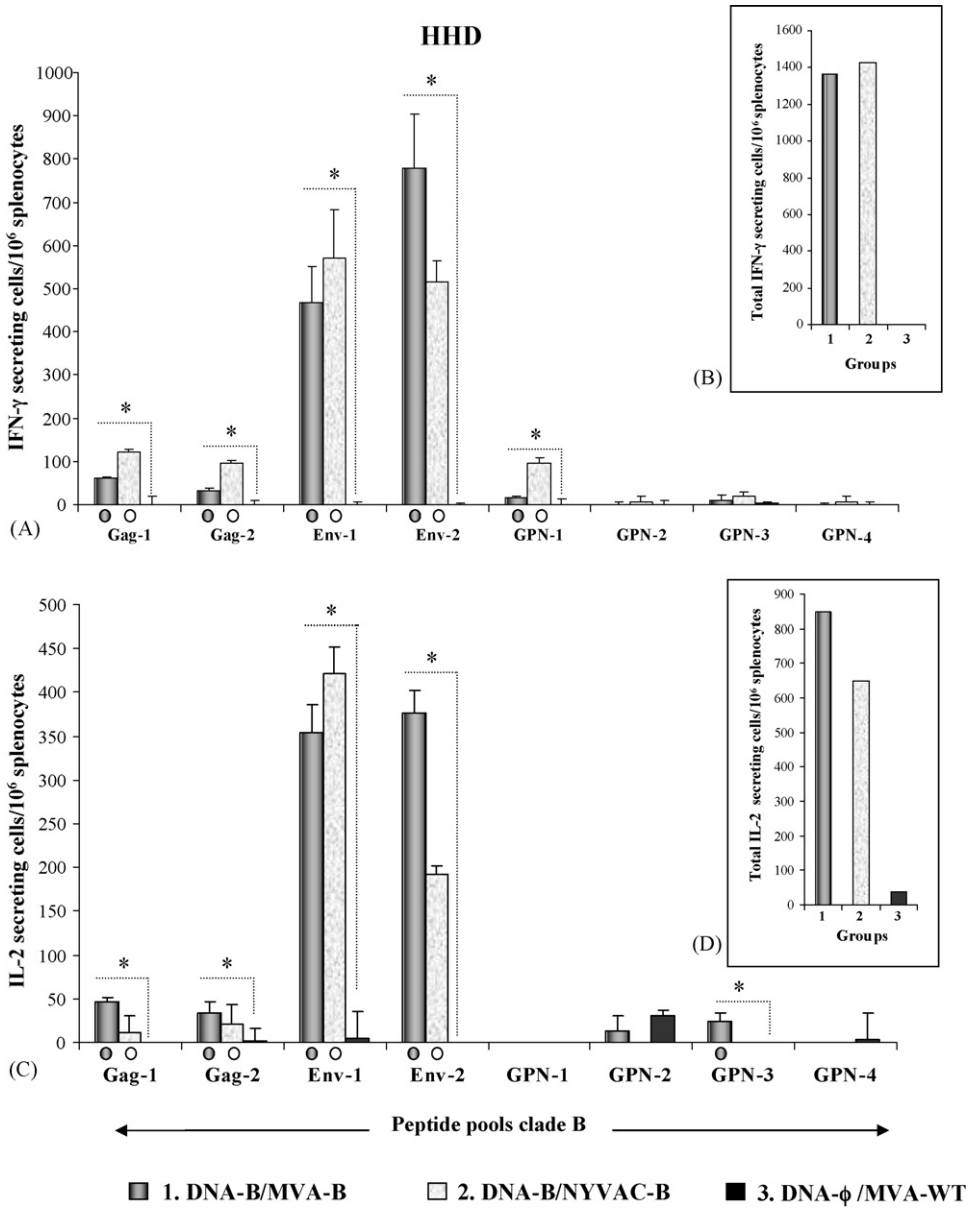

Fig. 6. Immunogenicity of MVA-B and NYVAC-B after DNA/rVV prime-boost protocol in HHD transgenic mice. (A) Cell-mediated immune response detected by fresh IFN-γ ELISPOT. Groups of 4 HHD transgenic mice were primed with 100 μg of either DNA-B or sham DNA (DNA-φ) by intramuscular route. Two weeks after priming, the mice received an intraperitoneal inoculation of 2×10^7 PFU of the corresponding rVV. Vaccine-elicited functional immune responses of splenocytes were measured 10 days after the last immunization in a fresh IFN-γ ELISPOT assay following stimulation with 5 μg/mL of pools of overlapping peptides spanning the HIV-1 $_{BX08}$gp120 and $_{IIIB}$GPN proteins. The number of spots obtained with the negative CTRL pool ranged between 32 and 38 and was subtracted in all cases. Peptide-specific IFN-γ secreting cells with standard deviation from triplicate cultures are shown. (●) represents statistically significant differences ($p < 0.05$) between each peptide pool and the CTRL pool. (*) represents statistically significant differences ($p < 0.05$) between groups. (B) Magnitude of the total response for clade B pools. Bars represent the total number of antigen-specific IFN-γ secreting cells detected in each group against all of the peptide pools spanning the Ags included in MVA-B and NYVAC-B recombinants. (C) Cell-mediated immune response detected by fresh IL-2 ELISPOT. The IL-2 response against clade B peptide pools in splenocytes from immunized animals was determined as previously described. The number of spots obtained with the negative CTRL pool was subtracted in all cases. Peptide-specific IL-2 secreting cells with standard deviation from triplicate cultures are shown. (●) represents statistically significant differences ($p < 0.05$) between each peptide pool and the CTRL pool; (*) represents statistically significant differences ($p < 0.05$) between groups. (D) Magnitude of the total response for clade B pools. Bars represent the total number of antigen-specific IL-2 secreting cells detected in each group against all the peptide pools spanning the Ags included in MVA-B and NYVAC-B recombinants.

It has been shown that β-chemokines such as MIP-1β and RANTES can suppress HIV-1 replication *in vitro* by inhibiting the entry of the virus via CCR5 co-receptor [22]. Hence, it was of interest to evaluate whether splenocytes from the different immunization groups can elicit the Ag-specific production of these chemokines. The levels of MIP-1β and RANTES were quantified in cell culture supernatants after 3 days of incubation of splenocytes in the presence of 2 μg/mL of each clade B peptide pools (Table 2(B)). The total levels of RANTES in groups boosted with MVA-B or NYVAC-B were more than 2-fold superior to those obtained with the homologous DNA-B/DNA-B scheme. The specific response was directed against the Gag-1, Env-1, Env-2, GPN-1 and GPN-3 peptide pools. When the production of MIP-1β was evaluated, the highest levels of this chemokine were found in the group immunized with DNA-B/NYVAC-B against the Gag-1, Env-1, Env-2, GPN-1, GPN-3 and GPN-4 peptide pools. The DNA-B/MVA-B and DNA-B/DNA-B groups produced similar level of MIP-1β but against different pools. While the production of MIP-1β in the group that received MVA-B in the booster was mainly triggered by Env-2 and GPN-1 pools, in the group DNA-B/DNA-B it was induced by Gag-1, Gag-2, GPN-2 and GPN-4 pools.

To assay the antibody reactivity against HIV-1 Env protein, the individual serum from each group of mice was analyzed at a dilution of 1:50 by ELISA (Fig. 5C). Only animals boosted with MVA-B or NYVAC-B elicited specific antibodies against the gp160 protein from the HIV-1 clone LAV (clade B). Thus, the two poxvirus recombinants induced, in addition to a cellular response, some humoral immune response against the HIV-1 Env antigen.

3.4. Immunization with MVA-B and NYVAC-B induces HIV-specific HLA-A2 restricted cellular response in humanized HHD mice

To analyse whether $_{BX08}$gp120 and $_{IIIB}$GPN proteins expressed by MVA-B and NYVAC-B were recognized by human MHC class I molecules, we immunized transgenic HHD mice that exclusively display a chimerical human HLA-A2.1 as MHC class I molecule [17]. Three groups of HHD mice ($n=4$) were primed with either DNA-B or sham DNA (DNA-φ) and 2 weeks later, they were boosted with 2×10^7 PFU of either MVA-B, NYVAC-B or MVA-WT. The specific cellular immune response was analysed 10 days after the last immunization by fresh IFN-γ and IL-2 ELISPOT assays using pools of overlapping peptides specific to clade B of HIV-1. The number of spots obtained with the negative CTRL pool was subtracted in all cases.

As shown in Fig. 6A, animals that received MVA-B or NYVAC-B in the booster (groups 1 and 2) induced higher number of IFN-γ secreting cells against the HIV-1 peptide pools Gag-1, Gag-2, Env-1, Env-2 and GPN-1, in comparison with the control group (DNA-φ/MVA-WT) ($p<0.05$). The magnitude of the total response, determined by the overall number of IFN-γ secreting cells (Fig. 6B), and the breadth of the B-specific response per group, as measured by the number of positive pools, were similar in animals that received DNA-B/MVA-B and DNA-B/NYVAC-B. However, the specific response in both groups varied among the peptides. Env-1 and Env-2 pools were significantly more immunogenic than Gag-1, Gag-2 and GPN-1 ($p<0.05$).

In order to characterize in more detail the cellular immune response elicited in HHD mice using DNA/rVV approach, we performed a fresh IL-2 ELISPOT. IL-2 induces proliferation and activation of both CD4+ and CD8+ T cells, potentiates the cytotoxicity of CD8+ T lymphocytes and NK cells, and stimulates B cell function, therefore, playing a major role in the containment of viral infection [23]. Therefore, it was of interest to determine the specific number of IL-2 secreting cells in splenocytes of immunized mice. As shown in Fig. 6C and by comparison with Fig. 6A, the IL-2 and IFN-γ responses behaved similarly in the three groups. Mice immunized with DNA-B/MVA-B and DNA-B/NYVAC-B developed a specific cellular immune response against the HIV-1 peptide pools Gag-1, Gag-2, Env-1 and Env-2. The total number of IL-2 secreting cells in the spleen of animals boosted with MVA-B was 1.3-fold higher than in mice boosted with NYVAC-B (Fig. 6D); however, the breadth of the B-specific response, as measured by the number of positive pools, was similar in both groups. Env-1 and Env-2 pools were once more the most immunogenic epitopes. The Th type of immune response and the Ag-specific production of β-chemokines induced in the immunized groups were also evaluated using the positive HIV-1 peptide pools recognized by ELISPOT. As shown in Table 3(A), booster with either MVA-B or NYVAC-B induced a Th1 type immune response, as measured by the IFN-γ/IL-10 ratio. The levels of IFN-γ found in supernatants from stimulated splenocytes correlated with the number of IFN-γ secreting cells detected by ELISPOT. The levels of RANTES and MIP-1β were higher in mice boosted with MVA-B with regard to animals boosted with NYVAC-B (Table 3(B)). The highest levels of cytokines and β-chemokines were induced by the peptide pools spanning the HIV-1 $_{BX08}$gp120 protein (Env-1 and Env-2).

We also measured the antibody levels against Env in sera from immunized mice. When NYVAC-B was used in the booster a 5-fold increase in anti-gp160 antibodies was observed, contrasting with the minor 2.5-fold increase detected after MVA-B boost (data not shown).

3.5. Prime/boost combination with homologous or heterologous poxvirus vectors improves the breadth of HIV-specific HLA-A2 restricted cellular immune response in HHD mice

In the previous experiments we demonstrated that DNA/rVV immunization regime was able to induce a cellular immune response against some of the HIV-1 peptide pools from clade B, the Env-1 and Env-2 pools being immunodominants in both BALB/c and HHD mouse models. To

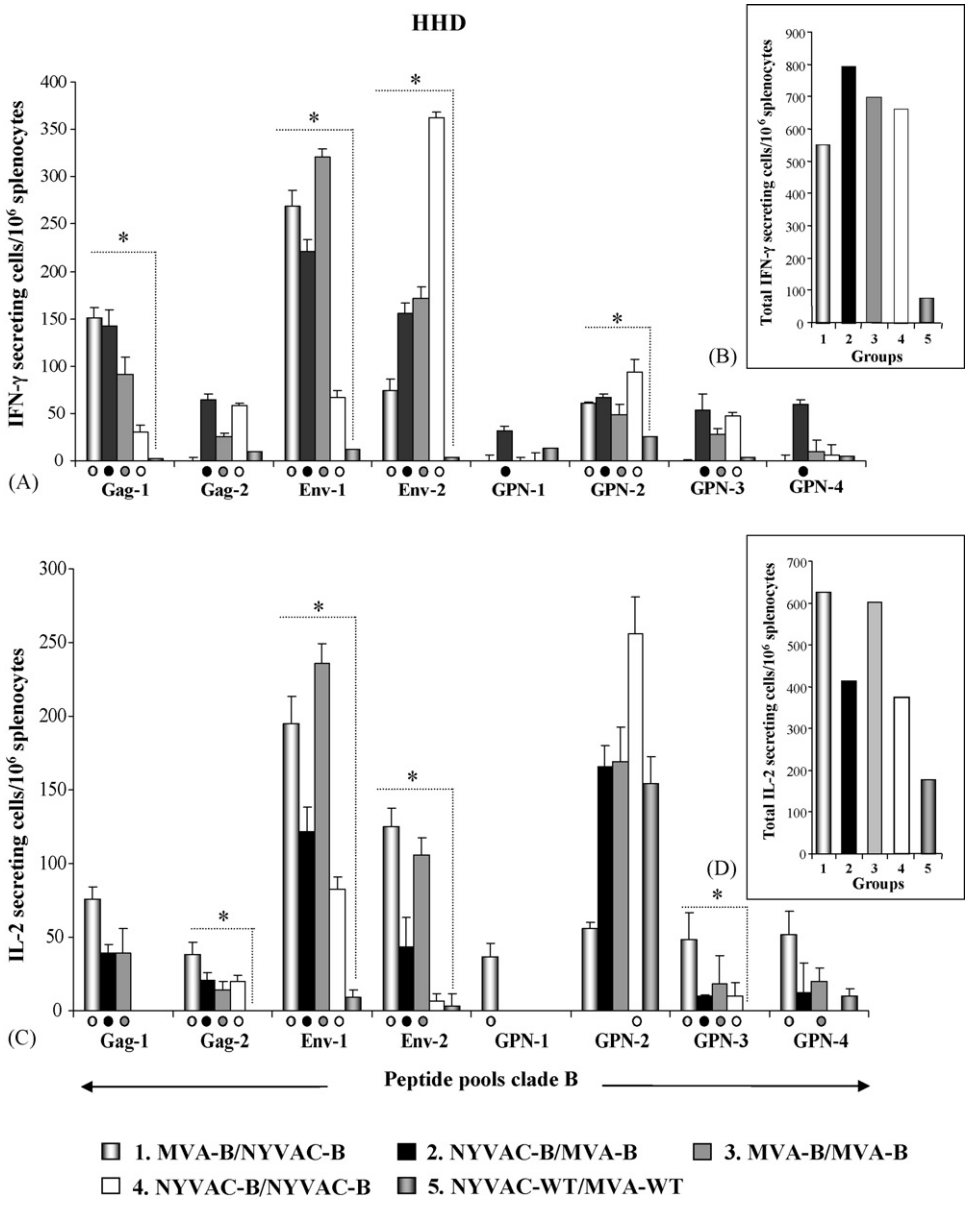

Fig. 7. Immune response elicited in transgenic HHD mice after inoculation with homologous and heterologous combinations of MVA-B and NYVAC-B recombinants. (A) Cell-mediated immune response detected by fresh IFN-γ ELISPOT. Groups of 4 HHD mice were inoculated intraperitoneally with 2×10^7 PFU of each recombinant at day 0 and 15. Vaccine-elicited functional immune responses of splenocytes were measured 10 days after the last immunization in a fresh IFN-γ ELISPOT assay following stimulation with 5 μg/mL of pools of overlapping peptides spanning the HIV-1 $_{BX08}$gp120 and $_{IIIB}$GPN proteins. The number of spots obtained with the negative CTRL pool ranged between 36 and 48 and was subtracted in all cases. Peptide-specific IFN-γ secreting cells with standard deviation from triplicate cultures are shown. (●) represents statistically significant differences ($p < 0.05$) between each peptide pool and the CTRL pool. (*) represents statistically significant differences ($p < 0.05$) between groups. (B) Magnitude of the total response for clade B pools. Bars represent the total number of antigen-specific IFN-γ secreting cells detected in each group against all the peptide pools spanning the Ags included in MVA-B and NYVAC-B recombinants. (C) Cell-mediated immune response detected by fresh IL-2 ELISPOT. The IL-2 response against clade B peptide pools in splenocytes from immunized animals was determined as previously described. The number of spots obtained with the negative CTRL pool was subtracted in all cases. Peptide-specific IL-2 secreting cells with standard deviation from triplicate cultures are shown. (●) represents statistically significant differences ($p < 0.05$) between each peptide pool and the CTRL pool; (*) represents statistically significant differences ($p < 0.05$) between groups. (D) Magnitude of the total response for clade B pools. Bars represent the total number of antigen-specific IL-2 secreting cells detected in each group against all the peptide pools spanning the Ags included in MVA-B and NYVAC-B recombinants.

determine whether it was possible to improve the breadth of the B-specific response, we performed homologous and heterologous immunizations by combination of MVA-B and NYVAC-B viruses. Thus, HHD mice ($n = 4$) were inoculated intraperitoneally with 2×10^7 PFU of each recombinant virus at days 0 and 15, and 10 days after the last immunization the cellular immune responses were evaluated.

As shown in Fig. 7A, heterologous (groups 1 and 2) and homologous (groups 3 and 4) combinations of MVA-B and NYVAC-B recombinants induced a significant enhance-

Table 3
(A) Cytokine production (pg/mL) by splenocytes from HHD mice immunized in DNA prime/rVV boost regime and (B) β-chemokine production (pg/mL) by splenocytes from HHD mice inoculated in DNA prime/rVV boost regime

A

	DNA-B/ MVA-B		DNA-B/ NYVAC-B		DNA-ϕ/ NYVAC-WT	
	IFN-γ	IL-10	IFN-γ	IL-10	IFN-γ	IL-10
Gag-1	908	406	142	204	<20	254
Gag-2	314	120	605	200	<20	<10
Env-1	16194	1206	14178	372	<20	<10
Env-2	18203	1583	11680	444	<20	<10
GPN-1	157	<10	203	<10	<20	<10
Total	**35776**	**3315**	**26808**	**1220**	**<20**	**254**
IFN-γ/IL-10	**10.8**		**21.9**		**<1**	

B

	DNA-B/ MVA-B		DNA-B/ NYVAC-B		DNA-ϕ/ NYVAC-WT	
	RANTES	MIP-1β	RANTES	MIP-1β	RANTES	MIP-1β
Gag-1	110	129	<20	<20	<20	<20
Gag-2	<20	<20	<20	<20	<20	<20
Env-1	257	669	266	1103	<20	422
Env-2	425	2257	380	1231	<20	<20
GPN-1	<20	309	<20	<20	<20	<20
Total	**792**	**3364**	**646**	**2334**	**<20**	**422**

HHD mice were immunized as described in Section 2. Ten days after the last immunization the animals were sacrificed and their spleens were processed. The splenocytes from each group were stimulated *in vitro* with 2 μg/mL of different HIV-1 peptide pools from clade B and incubated for 3 days at 37 °C. Thereafter, cell supernatants were collected and stored at −70 °C. Cytokine and β-chemokine levels were measured with specific commercial kits.

ment of splenic T-cell response against the clade B peptide pools Gag-1, Env-1, Env-2, and GPN-2, in comparison with mice immunized with NYVAC-WT/MVA-WT used as control (group 5) ($p < 0.05$). Animals from group 1 (MVA-B/NYVAC-B) failed to recognized the Gag-2 and GPN-3 pools, which were identified by the rest of the groups. Interestingly, the combination of NYVAC-B/MVA-B (group 2) also recognized the GPN-1 and GPN-4 peptide pools.

The magnitude of the total response, determined by the overall number of IFN-γ secreting cells (Fig. 7B), and the breadth of the B-specific response per group, as measured by the number of positive pools, were similar in animals receiving the homologous prime/boost regime (groups 3 and 4). Both immunological markers were improved, but not significantly ($p > 0.05$), when mice were primed with NYVAC-B and boosted with MVA-B recombinant (group 2). In contrast to groups 3 and 4, which recognized 6 out of 8 clade B peptide pools, group 2 recognized all of the pools assayed. Interestingly, the reverse order (MVA-B/NYVAC-B) gave the lower number of total IFN-γ secreting cells and only recognized 4 pools.

When the cellular response was next evaluated by fresh IL-2 ELISPOT, we observed that heterologous (groups 1 and 2) and homologous (groups 3 and 4) combinations of MVA-B and NYVAC-B recombinants developed a specific cellular immune response against the HIV-1 peptide pools Gag-2, Env-1, Env-2 and GPN-3 (Fig. 7C). Animals receiving two doses of NYVAC-B (group 4) failed to recognize the Gag-1 pool, which was efficiently identified by the rest of the groups. The total number of IL-2 secreting cells in the spleen of animals immunized with MVA-B/NYVAC-B (group 1) or MVA-B/MVA-B (group 3) were 1.5-fold higher than that found in mice immunized with NYVAC-B/MVA-B (group 2) or NYVAC-B/NYVAC-B (group 4) (Fig. 7D). However, the breadth of the B-specific response was only affected in group 4 (NYVAC-B/NYVAC-B), in which only 4 out of 8 peptide pools were recognized.

We also examined the profile of cytokines and chemokines produced by splenocytes from these mice after cultured with 2 μg/mL of each peptide pool. As shown in Table 4(A), all of the combinations assayed induced an evident Th1 type immune response characterized by elevated levels of IFN-γ and low or undetectable levels of IL-10. Interestingly, groups receiving heterologous NYVAC-B/MVA-B (group 2) or homologous MVA-B/MVA-B (group 3) combinations induced higher levels of IFN-γ and broader reactive cellular responses in comparison with groups immunized with MVA-B/NYVAC-B (group 1) or NYVAC-B/NYVAC-B (group 4). When the profile of β-chemokines was measured, we obtained similar results (Table 4(B)). The levels of RANTES and MIP-1β were significantly higher in groups 2 (NYVAC-B/MVA-B) and 3 (MVA-B/MVA-B).

We also measured the antibody levels against Env in sera from immunized mice. Serum from mice receiving two doses of NYVAC-B recombinant (group 4) did not recognize the gp160 protein from HIV-1 clone LAV by ELISA, while the other groups induced similar specific humoral response to gp120 (data not shown).

3.6. NYVAC-B prime/MVA-B boost and no the reverse combination efficiently improved the breadth and magnitude of anti-clade B cellular immune response in BALB/c mice

To confirm the results obtained by the heterologous poxvirus combination of vectors observed in HHD mice in another mouse model, we performed an experiment in which BALB/c mice were immunized with heterologous combination of MVA-B and NYVAC-B vectors. Three groups of mice ($n = 4$) were inoculated intraperitoneally with 2×10^7 PFU of each recombinant at day 0 and 15. The specific cellular immune response was analysed 10 days after the last immunization by fresh IFN-γ ELISPOT assay using pools of overlapping peptides specific to clade B of HIV-1. The number of spots obtained with the negative CTRL pool was subtracted in all cases. As shown in Fig. 8A, heterologous combinations of MVA-B and NYVAC-B recombinants induced higher number of IFN-γ secreting cells

Table 4
(A) Cytokine production (pg/mL) by splenocytes from HHD mice immunized with homologous and heterologous combination of MVA-B and NYVAC-B and (B) β-chemokine production (pg/mL) by splenocytes from HHD mice immunized with homologous and heterologous combination of MVA-B and NYVAC-B
A

	(pg/mL)	Gag-1	Gag-2	Env-1	Env-2	GPN-1	GPN-2	GPN-3	GPN-4	Total
MVA-B / NYVAC-B	**IFN-γ**	1428	<20	9874	2711	<20	<20	<20	<20	**14013**
	IL-10	<10	<10	568	302	<10	<10	<10	<10	**870**
NYVAC-B / MVA-B	**IFN-γ**	3397	2089	2671	2775	3815	1729	2071	3157	**21704**
	IL-10	399	302	444	456	380	452	468	376	**3277**
MVA-B / MVA-B	**IFN-γ**	9951	535	14729	7806	348	<20	132	271	**33772**
	IL-10	<10	<10	332	206	<10	<10	<10	<10	**538**
NYVAC-B / NYVAC-B	**IFN-γ**	2585	<20	3148	2948	<20	<20	<20	145	**8826**
	IL-10	<10	<10	<10	<10	<10	<10	<10	<10	**<10**
NYVAC-WT/MVA-WT	**IFN-γ**	738	<10	<10	157	<10	<10	<10	<10	**895**
	IL-10	<10	<10	162	<10	<10	<10	<10	<10	**162**

B

	(pg/mL)	Gag-1	Gag-2	Env-1	Env-2	GPN-1	GPN-2	GPN-3	GPN-4	Total
MVA-B / NYVAC-B	**RANTES**	<20	<20	112	<20	<20	<20	<20	<20	**112**
	MIP-1β	<20	<20	<20	<20	<20	<20	<20	<20	**<20**
NYVAC-B / MVA-B	**RANTES**	453	<20	<20	<20	120	<20	<20	134	**707**
	MIP-1β	237	209	<20	<20	220	<20	1149	109	**1924**
MVA-B / MVA-B	**RANTES**	431	251	143	<20	<20	<20	<20	<20	**825**
	MIP-1β	<20	1986	<20	1263	1157	726	363	<20	**5495**
NYVAC-B / NYVAC-B	**RANTES**	105	<20	<20	<20	<20	<20	<20	<20	**105**
	MIP-1β	<20	<20	<20	<20	<20	<20	<20	<20	**<20**
NYVAC-WT/MVA-WT	**RANTES**	<20	<20	<20	<20	<20	<20	<20	<20	**<20**
	MIP-1β	<20	<20	<20	<20	<20	<20	<20	<20	**<20**

HHD mice were immunized as described in Section 2. Ten days after the last immunization the animals were sacrificed and their spleens were processed. The splenocytes from each group were stimulated *in vitro* with 2 μg/mL of different HIV-1 peptide pools from clade B and incubated for 3 days at 37 °C. Thereafter, cell supernatants were collected and stored at −70 °C. Cytokine and β-chemokine levels were measured with specific commercial kits.

against the HIV-1 peptide pools Gag-1, Env-1, Env-2, GPN-1, GPN-3 and GPN-4, in comparison with control group (NYVAC-WT/MVA-WT) ($p < 0.05$). Animals from group 2 (MVA-B/NYVAC-B) failed to recognize the Gag-2 and GPN-2 pools, which were efficiently identified by the group receiving the reverse combination NYVAC-B/MVA-B (group 1). The magnitude of the total response, determined by the overall number of IFN-γ secreting cells (Fig. 8B), and the breadth of the B-specific response per group, as measured by the number of positive pools, were significantly higher in mice primed with NYVAC-B and boosted with MVA-B (group 1). These results correlate with the response detected in HHD mice using the same immunization approach.

The cytokine profile produced by splenocytes from these mice reveals a Th1 type of immune response characterized by high levels of IFN-γ and low or undetectable levels of IL-10 (data not shown). We also evaluated the presence of specific anti-gp160 Abs in sera from immunized mice. Animals primed with NYVAC-B and boosted with MVA-B (group 1) induced an Env specific humoral response 2.5-fold higher than that induced by the reverse combination (MVA-B/NYVAC-B) (data not shown).

4. Discussion

In this study we describe the construction and immunogenicity of two novel HIV/AIDS poxvirus vaccine candidates, one based on the modified vaccinia virus Ankara (MVA) strain and the other based on the NYVAC strain, with both attenuated vectors expressing in the same viral TK locus four HIV-1 antigens from clade B, the Env (gp120) and Gag-Pol-Nef as a polyprotein. These antigens represent the major antigenic proteins of HIV-1 expressed during virus infection. The *env* gene was derived from the HIV-1 primary isolate $_{BX08}$, a CCR5-tropic strain which is transmitted most frequently than CXCR4 strains [24], and hence, a suitable target to inhibit HIV spread. The synthetic *gag-pol-nef* polygene comes from the HIV-1 IIIB isolate and included the key antigenic determinants that have been described for each gene. The work described here is the first study in which two different attenuated

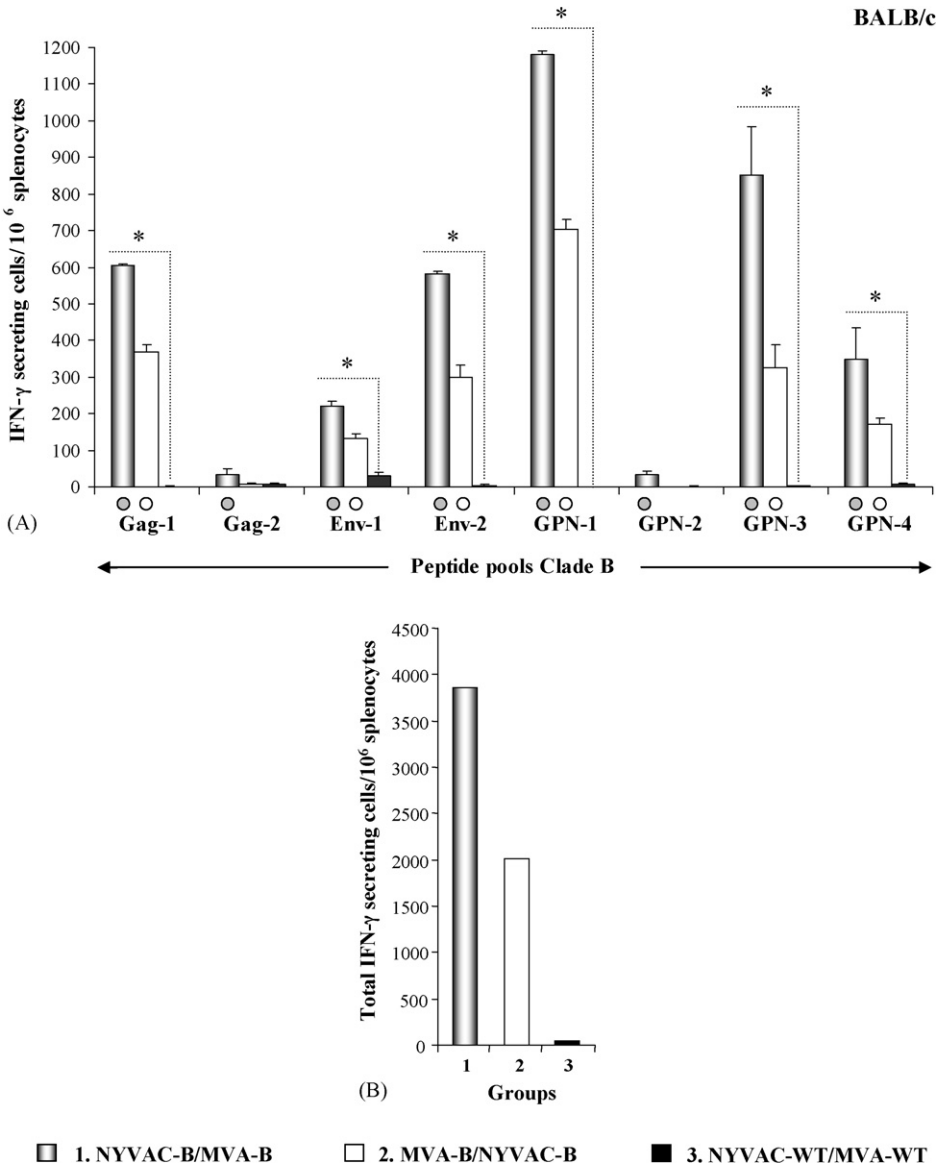

Fig. 8. Immune response elicited in BALB/c mice using heterologous combinations of MVA-B and NYVAC-B recombinants. (A) Cell-mediated immune response detected by fresh IFN-γ ELISPOT. Groups of 4 BALB/c mice were inoculated intraperitoneally with 2×10^7 PFU of each recombinant at day 0 and 15. Vaccine-elicited functional immune responses of splenocytes were measured 10 days after the last immunization in a fresh IFN-γ ELISPOT assay following stimulation with 5 μg/mL of pools of overlapping peptides spanning the HIV-1 $_{BX08}$gp120 and $_{IIIB}$GPN proteins. The number of spots obtained with the negative CTRL pool ranged between 26 and 46 and was subtracted in all cases. Peptide-specific IFN-γ secreting cells with standard deviation from triplicate cultures are shown. (●) represents statistically significant differences ($p < 0.05$) between each peptide pool and the CTRL pool. (*) represents statistically significant differences ($p < 0.05$) between groups. (B) Magnitude of the total response for clade B pools. Bars represent the total number of antigen-specific IFN-γ secreting cells detected in each group against all the peptide pools spanning the Ags included in MVA-B and NYVAC-B recombinants.

poxvirus vectors (NYVAC and MVA) expressing four HIV-1 genes in the same locus of the viral genome are compared *in vitro* and *in vivo*. We previously compared in HLA-A2 transgenic mice the immune response induced by NYVAC and MVA expressing the HIV-1 Gag-Pol-Nef polyprotein from clade B, but with a limited number of peptides [9]. The findings described here of engineering the simultaneous expression of the cassette gp120-GPN in the poxvirus vectors extend previous results and provide an in depth preclinical characterization of the immunogenicity in mice of these novel MVA-B and NYVAC-B vectors.

The *in vitro* characterization of MVA-B and NYVAC-B recombinants revealed that both viruses express to high levels the heterologous $_{BX08}$gp120 and $_{IIIB}$GPN proteins, can be passage in culture without the loss of the transgene, and grew efficiently in CEF cells. However, in contrast to MVA-B, NYVAC-B infection induces potent apoptosis. We have recently described the distinct biological and biochemical properties of the parental MVA and NYVAC strains [25].

Moreover, a comparative analysis of cellular gene expression profiling by cDNA microarrays screening over 15,000 genes revealed differences between NYVAC and MVA-infected HeLa cells in proinflammatory cytokine profiles. In fact, while MVA enhanced the expression of the cytokines IL-7, IL-1A, IL-8, IL-15, NYVAC infection did not triggered expression of these cytokines [19]. These differences might influence the immunogenic characteristics of the two recombinant vectors. Since dying cells are capable of transferring antigen to the immune system for the induction of T cell immunity [26,27], and the *in vitro* differences that we have observed between MVA and NYVAC strains could have an impact on the immune system, it was important to demonstrate the immunogenic potential of each poxvirus vector *in vivo*. In this report we have conducted a head-to-head comparison of the cellular immune response induced in BALB/c and in transgenic HHD mice by different prime-boost immunization strategies with the poxvirus vectors. We first analyzed the effect of priming with DNA vectors expressing the HIV-1 Env ($_{BX08}$gp120), and Gag-Pol-Nef antigens from clade B, followed by a booster with the poxvirus vectors. We showed that prime-boost immunization schemes employing a naked DNA-B vector at priming and recombinant poxvirus vectors (MVA-B and NYVAC-B) at booster were efficient immunization protocols to induce specific cellular immune responses against HIV-1 peptide pools spanning Env, Gag, Pol and Nef antigens in both BALB/c and HHD mice. Differences in the magnitude of the immune response were observed between the poxvirus vectors in the two animal models. In BALB/c, the DNA-B prime/NYVAC-B boost regime triggered an overall higher immune response than DNA-B prime/MVA-B boost, whereas in HHD the magnitude of the response was similar for both recombinant viruses. The levels of IFN-γ secreting cells were lower in HHD than in BALB/c mice, which correlate with the lower proportion of total splenic CD8+ T cells in HHD mice (an average 3% of total splenocytes). When we analyzed the intrinsic cellular response directed against peptides represented in each individual pool, we observed significant differences between them. Env-1 and Env-2 pools were the most immunogenic in the transgenic mice. Other studies have demonstrated that competition or immunological dominance between CTL epitopes would effectively reduce the breadth of the total response induced by vaccination [28,29]. It has been proposed that the rapidity with which a cell produces IFN-γ is a major criterion that determines the cell survival and future expansion [30]. CD8+ T cells that can produce IFN-γ most rapidly in response to early expression and secretion of Env protein will be selectively expanded; in this way, the dominant primary CD8+ T cell response will comprise fast-onset cells that are specific for Env antigen. Other factors such as MHC-binding affinity, efficiency of epitope processing, and competition between T cells for access to APCs can also contribute in the establishment of an immunodominant response. In the case of the non-recognized peptide pools, the MHC-binding affinity could have an effect on their immunogenicity. It has been demonstrated that the location of the epitope (and flanking sequences) within a peptide can affect its binding to the MHC class I molecules and/or recognition by CTLs when added exogenously, even at excess concentrations. Thus, some responses may not be detected in libraries of overlapping peptides even if the recognized epitope sequences are represented [31]. When prime/boost was carried out with a combination of the poxvirus vectors, the heterologous NYVAC-B/MVA-B approach induced the broadest cellular immune response in both mouse models, followed by the group receiving two doses of MVA-B. In contrast, the breadth of the cellular immune response in mice receiving the reverse MVA-B/NYVAC-B combination was significantly affected. This result could be relevant in the design of an effective immunization protocol with the poxvirus vectors. Vaccines with very narrow cellular immune responses directed against one or a couple of epitopes can, over time, lose protective efficacy due to escape mutants of the infectious agent, as it has been shown in the case of simian-HIV infection [32]. Moreover, a broad reactive CTL response was observed in long term non-progressors [33,34].

For HIV and most other viruses, induction of Th1 type response, characterized by the production of IL-12, IL-2 and IFN-γ is more likely to provide protection than induction of Th2 type response characterized by the production of IL-4, IL-5, IL-10, IL-13 [35]. In our case, the pattern of cytokine secretion after restimulation with the different peptide pools indicated that the different protocols used induced a Th1 type response. We also detected high levels of MIP-1β and RANTES β-chemokines in the cell culture supernatants of splenocytes stimulated with the different clade B peptide pools. This result could be immunologically relevant if we considered that elevated levels of RANTES were detected in the genital tracts of Kenyan commercial sex workers who were exposed to HIV-1, and yet uninfected [36]. The strategies employed in this study also elicited a specific humoral immune response against the gp160 protein from HIV-1 clone LAV.

The above findings demonstrate that the two poxvirus vectors MVA-B and NYVAC-B are efficient immunogens as they induced broad cellular immune responses against the four different HIV antigens. In addition, we observed some differences in the magnitude and breadth of the immune response to the HIV-1 epitopes, which depends on the vector and protocol of immunization used. Although MVA-B was a potent booster of cellular response, NYVAC-B was less efficient at inducing IFN-γ response after MVA-B or NYVAC-B priming. This result might be explained with the type of anti-vector immunity induced by these recombinants. MVA has a genome size of 186 kb with 193 ORFs but only 152 intact genes [37], while in NYVAC only 18 ORFs were deleted from the parental viral genome [38]. As it has been previously suggested [12], a plausible mechanism could be that because MVA has a smaller genome size with regions highly conserved among poxviruses, the anti-vector immune response, which is developed after priming

against MVA, might be directed against common antigens and, in turn, inhibit subsequent infection with NYVAC. In contrast, NYVAC might induce anti-vector immunity to antigens that are not expressed in MVA and thus might have little influence in the subsequent infection with MVA. This prediction was confirmed assessing comparative data on anti-vector immunity induced by the two recombinants. After priming of BALB/c mice with 2×10^7 PFU of NYVAC-B inoculated by i.p route, this vector induced a significantly higher anti-VV cellular immune response in comparison with that induced by priming with MVA-B (9074 IFN-γ secreting cells/10^6 splenocytes in NYVAC versus 5954 IFN-γ secreting cells/10^6 in MVA). Moreover, the IFN-γ secreted against viral antigens was mainly produced by the T CD8+ cells, as revealed by an Intracellular Cytokine Staining (ICS) assay. In animals primed with MVA-B, 1.9% of CD8+ T cells and 0.3% of CD4+ T cells produced IFN-γ against MVA antigens. In contrast, in animals primed with NYVAC-B, 6% of CD8+ T cells and 0.8% of CD4+ T cells produced IFN-γ against NYVAC antigens. Furthermore, NYVAC-B also induced a significantly higher anti-VV humoral immune response in comparison with that induced by MVA-B. A recent study that provided the original description of poxvirus determinants recognized by mouse CD8+ T cells, demonstrated that MVA failed to induce responses to two of the defined epitopes, probably because genes encoding the cryptic determinants may not be expressed at immunogenic levels by MVA *in vivo* [39]. In another study, Oseroff et al., had defined 48 epitopes derived from vaccinia antigens that were identified by PBMCs from humans vaccinated with Dryvax vaccine. Some of these epitopes derived from B8R, D1R, D5R, C10L, C19L, C7L, F12L and O1L ORFs were efficiently recognized by multiple donors in the context of different HLA types [40]. Interestingly, some of these ORFs are deleted in the MVA genome. These observations also help to explain the immunological differences that we have observed between the two poxvirus vectors and should be taking into consideration when MVA and NYVAC recombinants are used in heterologous prime/boost combination, as the quality of the immune response might be critical in protection.

That the quality of the immune response obtained in prime/boost protocols with poxvirus vectors is relevant in protection has been suggested by previous works using different viruses encoding the same antigen in prime/boost [10,41–44]. In a study performed in the SIV macaque model, it was shown that a systemic prime/boost immunization with Semliki Forest virus in combination with MVA, both vectors expressing the *env, gag-pol, nef, rev* and *tat* genes of SIV, was more efficient that multiple immunizations with the same vector for the induction of both humoral and cellular immune responses [45]. Significantly, other work conducted in humans showed that the substitution of plasmid DNA as the priming vector with a specific attenuated recombinant fowlpox virus (FP9) vaccine in such FP9 prime/MVA boost regimes can elicit sterile protection against malaria that can last for 20 months [12]. The IFN-γ response to the DNA/MVA vaccine regime was greater than that of the FP9/MVA regime, but only the latter could induce complete protection in some subjects. The same group demonstrated that in the DNA-primed vaccinees the IFN-γ response was mainly due to CD4+ T cells, whereas in the FP9-primed vaccinees it was mainly due to CD4-dependent CD8+ T cells [46]. These observations indicated that combinations with MVA and NYVAC vectors, that we have shown triggered a broad immune response to HIV-1 antigens, should be further explored in other animal models and humans.

A phase I clinical trial conducted by EuroVacc using NYVAC expressing the *gag, pol, nef* and *env* genes of HIV-1 Clade C (NYVAC-C) with a similar arrangement of inserts as described here for NYVAC-B, indicated that the vaccine was well tolerated by the human volunteers. Vaccine-induced anti-HIV T cell responses were observed in 5/12 of the vaccine recipients. Env-specific responses were found in all five responding subjects but additional responses against other proteins of HIV (e.g. Gag and Nef) were detected in 40% of the responders (see www.EuroVacc.org). Another phase I clinical study conducted by EuroVacc in prime/boost with DNA-C and NYVAC-C has shown promising results. Moreover, a phase I clinical trial with the MVA-B immunogen described in this report will be carried out by EU-supported TheraVac. In this respect, the mouse preclinical results obtained in this study demonstrate the efficient immunogenicity and distinct characteristics of the two novel poxvirus vectors, and highlight the relevance of MVA-B and NYVAC-B as vaccine candidates against HIV/AIDS.

Acknowledgments

This investigation was supported by research grants from the EU (EuroVac QLRT-PL-1999-01321), the Spanish Ministry of Education and Science BIO2004-03954, the Spanish Foundation for AIDS Research (FIPSE 36344/02) and Fundación Marcelino Botín. We thank the expert technical assistance of Silvia Gutiérrez for immunofluorescence analysis. C.E. Gómez was the recipient of a Fundación Carolina fellowship and J.L. Nájera was supported from FIPSE.

Appendix A. DNA sequence of MVA-B in the TK viral locus. Primers used to characterize the viral recombinants are in bold and underlined

AAGCTTTTGC GATCAATAAA TGGATCACAA CCAGTATCTC TTAACGATGT TCTTCGCAGA 60
TGATGATTCA TTTTTTAAGT ATTTGGCTAG TCAAGATGAT GAATCTTCAT TATCTGATAT 120
ATTGCAAATC ACTCAATATC TAGACTTTCT GTTATTATTA TTATTGATCC AATCAAAAAA 180
TAAATTAGAA GCCGTGGGTC ATTGTTATGA ATCTCTTTCA GAGGAATACA GACAATTGAC 240
AAAATTCACA GACTCTCAAG ATTTTAAAAA ACTGTTTAAC AAGGTCCCTA TTGTTACAGA 300
TGGAAGGGTC AAACTTAATA AAGGATATTT GTTCGACTTT G**TGATTAGTT TGATGCGATT** 360
CAAAAAAGAA TCCTCTCTAG CTACCACCGC AATAGATCCT ATTAGATACA TAGATCCTCG 420
TCGCGATATC GCATTTTCTA ACGTGATGGA TATATTAAAG TCGAATAAAG TGAACAATAA 480
TTAATTCTTT ATTGTCATCA TGGGTACCAA GGCGCGGATC CCCGGGTACC GAGCTCTTAC 540
CACAGGAATG GGGGCTCCTT CTGGTGCTTC TTGTCGGGGG TGGTCAGGCC CCACCTCAGC 600
AGGTGCTGCC TCAGCTCCTC GATCTTGGTC CTGTGCTGGC CGATCTCCAG GTCGCTGCCC 660
ACGTACAGGT CGTCCATGTA CTGATAGATC ACGATGTCGG GGTTCTGCTT CTTGAAGGGC 720
TCCAGGATCT TTGTCATGCT GCTCTGGAAG ATGGCGGGGC TGCCCTTCCA GCCCTGGGGC 780
AGCACGTTGT ACTGGTAGCG GATGCCGGGG GTCTCGTTGT TGATGCTGGG GATGGTGAAG 840
GCGCTGGCCA CGATCTCCTT AGCCACCACG GGAGGCAGGT TGAAGTCGCT AGCCATAGCC 900
CTCCAGTTGC TGTGGTACTT CTCGTGCTCG TCCTGGGCCT TGTCGATGCC GTCCAGGAAC 960
AGGATCTTCC TGATGCCGGC GCTCACCAGC TTGTCCACCT GCTCGTTGCC GCCGATGCCC 1020
TTGTGGGCGG GCACCCAGGC CAGGTACACC TTCTCCTTCT TGATCAGCTG CTCGATGATC 1080
TGGTTCACCA GCTCGCTCTC GCTCTTGTCG GGCTGGGCCT GGATGATGCC CAGGGCGTAC 1140
TGGCTGTCGG TCACGATGTT CACCTCCAGG CCTGAGTCCT GCAGGGCCAG GTAGATAGCC 1200
TGCAGCTCGG TCTTCTGGTT GGTGGTGTTG GTCAGGGGCA CCACCTTCTG GCGGCCCTTG 1260
TTGGTCACGT AGCCGGCCTT GCCCAGCTTG GTCTCCCTGT TGGCGGCGCC GTCCACGTAG 1320
AAGGTCTCGG CGCCCACGAT GGGCTCCTTC TCCAGCTGAT ACCACAGCTT CACCAGGGGA 1380
GGGGTGTTCA CGAACTCCCA CTCGGGAATC CAGGTGGCCT GCCAGTACTC GGTCCACCAG 1440
GTCTCCCAGG TCTCCTTCTG GATGGGCAGC TTGAACTTAG GAGTCTTGCC CCAGATCACG 1500
ATGCTCTCGG TGGTGATCTT CTGCACGGCC TCGGTCAGCT GCTTCACGTC GTTGGTGTGG 1560
GCGCCGCGCA TGCGGGCGTA CTTGCCGGTC TTCAGGTTCT TGAAGGGCTC CTGGTAGATC 1620
TGGTAGGTCC ACTGGCCCTG GCCCTGCTTC TGGATCTCGG CGATCAGGTC CTTGCTGGGG 1680
TCGTAGTACA CGCCGTGCAC GGGCTCCTTC AGGATCTCCC TGTTCTCGGC CAGCTCCAGC 1740
TCGGCCTCCT CGGTCAGGGG GATCACCTCG GTCAGAGCCT TTGTGCCCCT CAGCAGCTTG 1800
CACAGCTGCC TCACCTTGAT GCCGGGGTAG ATCTGGCTGG CCCAGTTCAG CTTGCCCACC 1860
AGCTTCTGAA TGTCGTTCAC GGTCCAGCTG TCCTTCTCGG GCAGCACGAT GGGCTGCACG 1920
GTCCACTTGT CGGGGTGCAG CTCGTAGCCC ATCCACAGGA ATGGTACTTG AGGTGTGACT 1980
GGAAAACCCA CCTCCTCCTC CTCTTGTGCT TCTAGCCAGG CACAATCAGC ATTGTTAGCT 2040
GCTGTGTTGC TACTTGTGAT TGCTCCATGT TTTTCTAGGT CTCGAGATGC TGCTCCCACC 2100
CCATCTGCTG CTGGCTCAGC TCGTCTCATT CTTTCCCTTA CAGCAGGCCA TCCAACCACA 2160
CTACTTTTTG ACCACTTGCC ACCCATCCTT GGATCAGGGA AGTAGCCTTG TGTGTGGTAG 2220
ATCCACAGAT CAAGGATATC TTGTCTTCGT TGGGAGTGAA TTAGCCCTTC CAGTCCCCCC 2280
TTTTCTTTTA AAAAGTGGCT AAGATCTACA GCTGCCTTGT AAGTCATTGG TCTTAAAGGG 2340
GTATACTTCC TGAAGTCCTC GTCCAGGGGC ACGCTGAAGT AGGCGTCGCC CACGTCCAGC 2400
ACGGTCACGC TCTTCTTCTT CTTCAGGCCG GCGGGGTGGG GGATGCCCAG CTGCACCTCC 2460
CAGAAGTCCT GGGTCCTCTT GTTCAGCTCC CTGAAGTCCA CCAGCTTCCT CCACTTGGTG 2520
CTGTCCTTCT TCTTGATGGC GAACACGGGG GTGTTGTAGG GGTTCTCGGG GCCGATCTTG 2580
CTGATCTTGC CCTCCTTCTC CATCTCGGTG CAGATCTCCA CCAGGGCCTT GATCTTCTCC 2640
TCGGTCAGGG GCCACTGCTT CACCTTAGGG CCGTCCATGC CGGGCTTCAG CTTCACGGGC 2700
A**CGGTCTCGA TGGGGCT**GAT GGGGAAGTTC AGGGTGCAGC CGATCTGGGT CAGCAGGTTC 2760
CTGCCGATGA TGTTCACAGG TGTAGGTCCC ACCAGCACGG TGCCGATGGC CTTGTGGCCG 2820
CAGATCTCGA TCAGGATCTG GTCGTACTGC CTCACCTTGA TGAAGCCGCC GATGCCGCCG 2880
ATCATCTTGG GCTTCCACCT GCCGGGCAGG CTCATCTCCT CCAGCACGGT GTCGTCGGCG 2940
CCGGTGGCCA GCAGGGCCTC CTTCAGCTGG CCACCGATCT TTATTGTGAC GAGGGGTCGT 3000
TGCCAAAGAG TGATCTGAGG GAAGTTAAAG GATACAGTTC CTTGTCTATC GGCTCCTGCT 3060
TCTGAGGGGG AGTTGTTGTC TCTACCCCAG ACCTGAAGCT CTCTTCTGGT GGGGCTGTTG 3120
GCTCTGGTCT GCTCTGAAGA AATGGTGGGG CTGTTGGCTC TGGTCTGCTC TGAAGAAAAT 3180
TCCCTGGCCT TCCCTTGTAG GAAGGCCAGA TCTTCCCTAA A**ATTAGCCTG CCTCTCGG**TG 3240
CAGTCCTTCA TCTGGTGGCC CTCCTTGCCG CACTTCCAGC AGCCCTTCTT CCTGGGGGCG 3300
CGGCAGTTCC TGGCGGTGTG GCCCTCCTTG CCGCAGTTGA AGCACTTCAC CATCTTCCTC 3360
TGGTTCCTGA AGTTGCCCCT CTGCATCATG ATGGTGGCGG TGTTGGTCAC CTGGCTCATG 3420
GCCTCGGCCA GCACCCTGGC CTTGTGGCCG GGGCCGCCCA CGCCCTGGCA GGCGGTCATC 3480
ATCTCCTCCA GGGTGGCGGC GGGTCCCAGG GCCTTCAGGA TGGTCTTGCA GTCGGGGTTG 3540
GCGTTCTGCA CCAGCAGGGT CTCGGTCATC CAGTTCTTCA CCTCCTGGCT GGCCTGCTCG 3600
GCGCGCAGGG TCTTGTAGAA CCTGTCCACG TAGTCCCTGA AGGGCTCTTT GGGGCCCTGC 3660
CTGATATCCA GGATGCTGGT GGGGCTGTAC ATCCTCACGA TCTTGTTCAG GCCCAGGATG 3720

```
ATCCACCTCT TGTAGATTTC GCCCACGGGG  ATGGGGGGGT TGTTGGTCAT CCAGCCGATC 3780
TGCTCCTGCA GGGTGCTGGT GGTGCCGGCG  ATGTCGCTGC CGCGGGGCTC CCTCATCTGG 3840
CCGGGGGCGA TGGGGCCGGC GTGCACGGGG  TGCACCCTGT CCCACTCGGC GGCCTCCTCG 3900
TTGATGGTCT CCTTCAGCAT CTGCATGGCG  GCCTGGTGGC CGCCCACGGT GTTCAGCATG 3960
GTGTTCAGGT CCTGGGGGGT GGCTCCCTCG  CTCAGGGCGC TGAACATGGG GATCACCTCG 4020
GGGCTGAAGG CCTTCTCCTC CACCACCTTC  ACCCAGGCGT TCAGGGTCCT GGGGCTGATG 4080
GCCTGGTGCA CCATCTGGCC CTGGATGTTC  TGCACGATGG GGTAGTTCTG GCTCACCTGG 4140
CTGCTGTGGC CGGTGTCGGC GGCGGCCTGC  TGGGCCTTCT TCTTGGACTT GTTCTGCTCC 4200
TCCTCGATCT TGTCCAGGGC CTCCTTGGTG  TCCTTGATCT CGATCCTCTG GTGCACGCAG 4260
TACAGGGTGG CCACGGTGTT GTACAGGCTC  CTCAGCTCCT CGCTGCCGGT CTGCAGGCTG 4320
GGCTGCAGCT GGCCCAGGAT CTGCCTGCAG  CCCTCGCTGG TCTCCAGCAG GCCGGGGTTC 4380
ACGGCGAACC TCTCCAGCTC CCTGCTGGCC  CACACGATGT GCTTCAGCTT ATACTTCTTC 4440
TTGCCGCCGG GCCTCAGCCT GATCTTCTCC  CACCTGTCCA GCTCGCCGCC GCTCAGCACG 4500
CTGGCCCTGG CGGCCATGCT CGAGTCTATT  TATATTCCAA AAAAAAAAAA TAAAATTTCA 4560
ATTTTTGTCG ACAAGCTTAA AAATTGAAAT  TTTATTTTTT TTTTTTGGAA TATAAATAAG 4620
CTCGAGCATG GACCGCGCCA AGCTGCTGCT  GCTGCTGCTG CTGCTGCTGC TGCCCCAGGC 4680
CCAGGCCGCT AGCGACCGCC TGTGGGTGAC  AGTGTACTAC GGCGTGCCCG TGTGGAAGGA 4740
CGCCACCACC ACCCTGTTCT GCGCCTCCGA  CGCCAAGGCC TACGACACCG AGGTGCACAA 4800
CGTGTGGGCC ACCCACGCCT GCGTGCCCAC  CGACCCCAAC CCCCAGGAGG TGGTGCTGGG 4860
CAACGTGACC GAGAACTTCA ACATGGGCAA  GAACAACATG GTGGAGCAGA TGCACGAGGA 4920
CATCATCAGC CTGTGGGACC AGTCCCTGAA  GCCCTGCGTG AAGCTGACCC CCCTGTGCGT 4980
GACCCTGAAC TGCACCAAGC TGAAGAACAG  CACCGACACC AACAACACCC GCTGGGGCAC 5040
CCAGGAGATG AAGAACTGCT CCTTCAACAT  CAGCACCTCC GTGCGGAACA AGATGAAGAG 5100
AGAGTACGCC CTGTTCTACT CCCTGGACAT  CGTGCCCATC GACAACGACA ACACCAGCTA 5160
CCGCCTGAGG TCCTGCAACA CCTCCATCAT  CACCCAGGCC TGCCCCAAGG TGAGCTTCGA 5220
GCCCATCCCC ATCCACTTCT GCGCCCCCGC  CGGCTTCGCC ATCCTGAAGT GCAACAACAA 5280
GACCTTCAAC GGCACCGGCC CCTGCACCAA  CGTGAGCACC GTGCAGTGCA CCCACGGCAT 5340
CCGCCCCGTG GTGTCCACCC AGCTGCTGCT  GAACGGCAGC CTGGCCGAGG AGGAGGTGGT 5400
GATCCGGTCC GAGAACTTCA CCAACAACGC  CAAGACCATC ATCGTGCAGC TGAACGAGAG 5460
CGTGGAGATC AACTGCACCA GACCCAACAA  CAACACCAGG AAGTCCATCC ACATCGGCCC 5520
CGGCCGCGCC TTCTACACCA CCGGCGACAT  CATCGGCGAC ATCCGGCAGG CCCACTGCAA 5580
CATCTCCAGA ACCAACTGGA CCAACACCCT  GAAGAGGGTG GCCGAGAAGC TGCGCGAGAA 5640
GTTCAACAAC ACCACCATCG TGTTCAACCA  GAGCAGCGGC GGCGACCCCG AGATCGTGAT 5700
GCACTCCTTC AACTGCGGCG GCGAGTTCTT  CTACTGCAAC ACCACCCAGC TGTTCAACTC 5760
CACCTGGAAC GAGACCAACA GCGAGGGCAA  CATCACCTCC GGCACCATCA CCCTGCCCTG 5820
CCGGATCAAG CAGATCATCA ACATGTGGCA  GGAGGTGGGC AAGGCCATGT ACGCCCCCCC 5880
CATCGGCGGC CAGATCAAGT GCCTGTCCAA  CATCACCGGC CTGCTGCTGA CCAGAGACGG 5940
CGGCTCCGAC AACAGCAGCA GCGGCAAGGA  GATCTTCCGC CCCGGCGGCG GCGACATGAG 6000
GGACAACTGG CGCTCCGAGC TGTACAAGTA  CAAGGTGGTG AAGATCGAGC CCCTGGGCAT 6060
CGCCCCCACC AAGGCCAAGA GGAGGGTGGT  GCAGCGCGAG AAGCGCTGAT AATAGGGATC 6120
CGCGCCAAAT TTAAATGATC CTGATCCTTT  TTCTGGGTAA GTAATACGTC AAGGAGAAAA 6180
CGAAACGATC TGTAGTTAGC GGCCGCCTAA  TTAACTAATA TTATATTTTT TATCTAAAAA 6240
ACTAAAAATA AACATTGATT AAATTTTAAT  ATAATACTTA AAAATGGATG TTGTGTCGTT 6300
AGATAAACCG TTTATGTATT TTGAGGAAAT  TGATAATGAG TTAGATTACG AACCAGAAAG 6360
TGCAAATGAG GTCGCAAAAA AACTGCCGTA  TCAAGGACAG TTAAAACTAT TACTAGGAGA 6420
ATTATTTTTT CTTAGTAAGT TACAGCGACA  CGGTATATTA GATGGTGCCA CCGTAGTGTA 6480
TATAGGATCG GCTCCTGGTA CACATATACG  TTATTTGAGA GATCATTTCT ATAATTTAGG 6540
AATGATTATC AAATGGATGC TAATTGACGG  ACGCCATCAT GATCCTATTC TAAATGGATT 6600
GCGTGATGTG ACTCTAGTGA CTCGGTTCGT  TGATGAGGAA TATCTACGAT CCATCAAAAA 6660
ACAACTGCAT CCTTCTAAGA TTATTTTAAT  TTCTGATGTA AGATCCAAAC GAGGAGGAAA 6720
TGAACCTAGT ACGGCGGATT TACTAAGTAA  TTACGCTCTA CAAAATGTCA TGATTAGTAT 6780
TTTAAACCCC GTGGCATCTA GTCTTAAATG  GAGATGCCCG TTTCCAGATC AATGGATCAA 6840
GGACTTTTAT ATCCCACACG GTAATAAAAT  GTTACAACCT TTTGCTCCTT CATATTCAGG 6900
GGAATTC                                                          6907
```

Left TK flanking sequence	1–502	Complementary
$_{IIIB}$Gag-Pol-Nef	ATG–TAA (537–4517)	Complementary
E/L promoter for $_{IIIB}$Gag-Pol-Nef	4527–4565	Complementary
E/L promoter for $_{BX08}$gp120	4580–4618	
$_{BX08}$gp120	ATG–TGA (4628–6109)	
Right TK flanking sequence	6216–6907	Complementary

References

[1] Stover J, Walker N, Garnett GP, Salomon JA, Stanecki KA, Ghys PD, et al. Can we reverse the HIV/AIDS pandemic with an expanded response? Lancet 2002;360(9326):73–7.

[2] Kwong PD, Wyatt R, Robinson J, Sweet RW, Sodroski J, Hendrickson WA. Structure of an HIV gp120 envelope glycoprotein in complex with the CD4 receptor and a neutralizing human antibody. Nature 1998;393(6686):648–59.

[3] Wyatt R, Sodroski J. The HIV-1 envelope glycoproteins: fusogens, antigens, and immunogens. Science 1998;280(5371):1884–8.

[4] Amara RR, Villinger F, Altman JD, Lydy SL, O'Neil SP, Staprans SI, et al. Control of a mucosal challenge and prevention of AIDS by a multiprotein DNA/MVA vaccine. Science 2001;292(5514):69–74.

[5] Barouch DH, Santra S, Schmitz JE, Kuroda MJ, Fu TM, Wagner W, et al. Control of viremia and prevention of clinical AIDS in rhesus monkeys by cytokine-augmented DNA vaccination. Science 2000;290(5491):486–92.

[6] Amara RR, Ibegbu C, Villinger F, Montefiori DC, Sharma S, Nigam P, et al. Studies using a viral challenge and CD8 T cell depletions on the roles of cellular and humoral immunity in the control of an SHIV-89.6P challenge in DNA/MVA-vaccinated macaques. Virology 2005;343(2):246–55.

[7] Zavala F, Rodrigues M, Rodriguez D, Rodriguez JR, Nussenzweig RS, Esteban M. A striking property of recombinant poxviruses: efficient inducers of *in vivo* expansion of primed CD8(+) T cells. Virology 2001;280(2):155–9.

[8] Bonnet MC, Tartaglia J, Verdier F, Kourilsky P, Lindberg A, Klein M, et al. Recombinant viruses as a tool for therapeutic vaccination against human cancers. Immunol Lett 2000;74(1):11–25.

[9] Didierlaurent A, Ramirez JC, Gherardi M, Zimmerli SC, Graf M, Orbea HA, et al. Attenuated poxviruses expressing a synthetic HIV protein stimulate HLA-A2-restricted cytotoxic T-cell responses. Vaccine 2004;22(25–26):3395–403.

[10] Gherardi MM, Najera JL, Perez-Jimenez E, Guerra S, Garcia-Sastre A, Esteban M. Prime-boost immunization schedules based on influenza virus and vaccinia virus vectors potentiate cellular immune responses against human immunodeficiency virus Env protein systemically and in the genitorectal draining lymph nodes. J Virol 2003;77(12):7048–57.

[11] Gomez CE, Abaitua F, Rodriguez D, Esteban M. Efficient CD8+ T cell response to the HIV-env V3 loop epitope from multiple virus isolates by a DNA prime/vaccinia virus boost (rWR and rMVA strains) immunization regime and enhancement by the cytokine IFN-gamma. Virus Res 2004;105(1):11–22.

[12] Webster DP, Dunachie S, Vuola JM, Berthoud T, Keating S, Laidlaw SM, et al. Enhanced T cell-mediated protection against malaria in human challenges by using the recombinant poxviruses [FP9] and modified vaccinia virus Ankara. Proc Natl Acad Sci USA 2005;102(13):4836–41.

[13] Cox WI, Tartaglia J, Paoletti E. Induction of cytotoxic T lymphocytes by recombinant canarypox (ALVAC) and attenuated vaccinia (NYVAC) viruses expressing the HIV-1 envelope glycoprotein. Virology 1993;195(2):845–50.

[14] Hel Z, Tsai WP, Thornton A, Nacsa J, Giuliani L, Tryniszewska E, et al. Potentiation of simian immunodeficiency virus (SIV)-specific CD4(+) and CD8(+) T cell responses by a DNA-SIV and NYVAC-SIV prime/boost regimen. J Immunol 2001;167(12):7180–91.

[15] Ramirez JC, Gherardi MM, Esteban M. Biology of attenuated modified vaccinia virus Ankara recombinant vector in mice: virus fate and activation of B- and T-cell immune responses in comparison with the Western Reserve strain and advantages as a vaccine. J Virol 2000;74(2):923–33.

[16] Chakrabarti S, Sisler JR, Moss B. Compact, synthetic, vaccinia virus early/late promoter for protein expression. Biotechniques 1997;23(6):1094–7.

[17] Pascolo S, Bervas N, Ure JM, Smith AG, Lemonnier FA, Perarnau B. HLA-A2.1-restricted education and cytolytic activity of CD8(+) T lymphocytes from beta2 microglobulin (beta2m) HLA-A2.1 monochain transgenic H-2Db beta2m double knockout mice. J Exp Med 1997;185(12):2043–51.

[18] Miyahira Y, Murata K, Rodriguez D, Rodriguez JR, Esteban M, Rodrigues MM, et al. Quantification of antigen specific CD8+ T cells using an ELISPOT assay. J Immunol Methods 1995;181(1):45–54.

[19] Guerra S, Lopez-Fernandez LA, Pascual-Montano A, Najera JL, Zaballos A, Esteban M. Host response to the attenuated poxvirus vector NYVAC: upregulation of apoptotic genes and NF-kappaB-responsive genes in infected HeLa cells. J Virol 2006;80(2):985–98.

[20] Amara RR, Villinger F, Staprans SI, Altman JD, Montefiori DC, Kozyr NL, et al. Different patterns of immune responses but similar control of a simian-human immunodeficiency virus 89.6P mucosal challenge by modified vaccinia virus Ankara (MVA) and DNA/MVA vaccines. J Virol 2002;76(15):7625–31.

[21] Hanke T, McMichael A. Pre-clinical development of a multi-CTL epitope-based DNA prime MVA boost vaccine for AIDS. Immunol Lett 1999;66(1–3):177–81.

[22] Cocchi F, DeVico AL, Garzino-Demo A, Arya SK, Gallo RC, Lusso P. Identification of RANTES, MIP-1 alpha, and MIP-1 beta as the major HIV-suppressive factors produced by CD8+ T cells. Science 1995;270(5243):1811–5.

[23] Alfano M, Poli G. Role of cytokines and chemokines in the regulation of innate immunity and HIV infection. Mol Immunol 2005;42(2):161–82.

[24] Berger EA, Murphy PM, Farber JM. Chemokine receptors as HIV-1 coreceptors: roles in viral entry, tropism, and disease. Annu Rev Immunol 1999;17:657–700.

[25] Najera JL, Gomez CE, Domingo-Gil E, Gherardi MM, Esteban M. Cellular and biochemical differences between two attenuated poxvirus vaccine candidates (MVA and NYVAC) and role of the C7L gene. J Virol 2006;80(12):6033–47.

[26] Blachere NE, Darnell RB, Albert ML. Apoptotic cells deliver processed antigen to dendritic cells for cross-presentation. PLoS Biol 2005;3(6):e185.

[27] Albert ML. Death-defying immunity: do apoptotic cells influence antigen processing and presentation? Nat Rev Immunol 2004;4(3):223–31.

[28] Rodriguez F, Harkins S, Slifka MK, Whitton JL. Immunodominance in virus-induced CD8(+) T-cell responses is dramatically modified by DNA immunization and is regulated by gamma interferon. J Virol 2002;76(9):4251–9.

[29] Palmowski MJ, Choi EM, Hermans IF, Gilbert SC, Chen JL, Gileadi U, et al. Competition between CTL narrows the immune response induced by prime-boost vaccination protocols. J Immunol 2002;168(9):4391–8.

[30] Liu F, Whitton JL, Slifka MK. The rapidity with which virus-specific CD8+ T cells initiate IFN-gamma synthesis increases markedly over the course of infection and correlates with immunodominance. J Immunol 2004;173(1):456–62.

[31] Draenert R, Brander C, Yu XG, Altfeld M, Verrill CL, Feeney ME, et al. Impact of intrapeptide epitope location on CD8 T cell recognition: implications for design of overlapping peptide panels. AIDS 2004;18(6):871–6.

[32] Barouch DH, Kunstman J, Kuroda MJ, Schmitz JE, Santra S, Peyerl FW, et al. Eventual AIDS vaccine failure in a rhesus monkey by viral escape from cytotoxic T lymphocytes. Nature 2002;415(6869):335–9.

[33] Pantaleo G, Menzo S, Vaccarezza M, Graziosi C, Cohen OJ, Demarest JF, et al. Studies in subjects with long-term nonprogressive human immunodeficiency virus infection. N Engl J Med 1995;332(4):209–16.

[34] Gea-Banacloche JC, Migueles SA, Martino L, Shupert WL, McNeil AC, Sabbaghian MS, et al. Maintenance of large numbers of virus-specific CD8+ T cells in HIV-infected progressors and long-term nonprogressors. J Immunol 2000;165(2):1082–92.

[35] Graham BS. Clinical trials of HIV vaccines. Annu Rev Med 2002;53:207–21.

[36] Iqbal SM, Ball TB, Kimani J, Kiama P, Thottingal P, Embree JE, et al. Elevated T cell counts and RANTES expression in the genital mucosa of HIV-1-resistant Kenyan commercial sex workers. J Infect Dis 2005;192(5):728–38.

[37] Antoine G, Scheiflinger F, Dorner F, Falkner FG. The complete genomic sequence of the modified vaccinia Ankara strain: comparison with other orthopoxviruses. Virology 1998;244(2):365–96.
[38] Tartaglia J, Perkus ME, Taylor J, Norton EK, Audonnet JC, Cox WI, et al. NYVAC: a highly attenuated strain of vaccinia virus. Virology 1992;188(1):217–32.
[39] Tscharke DC, Karupiah G, Zhou J, Palmore T, Irvine KR, Haeryfar SM, et al. Identification of poxvirus CD8+ T cell determinants to enable rational design and characterization of smallpox vaccines. J Exp Med 2005;201(1):95–104.
[40] Oseroff C, Kos F, Bui HH, Peters B, Pasquetto V, Glenn J, et al. HLA class I-restricted responses to vaccinia recognize a broad array of proteins mainly involved in virulence and viral gene regulation. Proc Natl Acad Sci USA 2005;102(39):13980–5.
[41] Anderson RJ, Hannan CM, Gilbert SC, Laidlaw SM, Sheu EG, Korten S, et al. Enhanced CD8+ T cell immune responses and protection elicited against Plasmodium berghei malaria by prime boost immunization regimens using a novel attenuated fowlpox virus. J Immunol 2004;172(5):3094–100.
[42] Bruna-Romero O, Gonzalez-Aseguinolaza G, Hafalla JC, Tsuji M, Nussenzweig RS. Complete, long-lasting protection against malaria of mice primed and boosted with two distinct viral vectors expressing the same plasmodial antigen. Proc Natl Acad Sci USA 2001;98(20):11491–6.
[43] Ramsburg E, Rose NF, Marx PA, Mefford M, Nixon DF, Moretto WJ, et al. Highly effective control of an AIDS virus challenge in macaques by using vesicular stomatitis virus and modified vaccinia virus Ankara vaccine vectors in a single-boost protocol. J Virol 2004;78(8):3930–40.
[44] Benson J, Chougnet C, Robert-Guroff M, Montefiori D, Markham P, Shearer G, et al. Recombinant vaccine-induced protection against the highly pathogenic simian immunodeficiency virus SIV(mac251): dependence on route of challenge exposure. J Virol 1998;72(5):4170–82.
[45] Nilsson C, Makitalo B, Berglund P, Bex F, Liljestrom P, Sutter G, et al. Enhanced simian immunodeficiency virus-specific immune responses in macaques induced by priming with recombinant Semliki Forest virus and boosting with modified vaccinia virus Ankara. Vaccine 2001;19(25–26):3526–36.
[46] Vuola JM, Keating S, Webster DP, Berthoud T, Dunachie S, Gilbert SC, et al. Differential immunogenicity of various heterologous prime-boost vaccine regimens using DNA and viral vectors in healthy volunteers. J Immunol 2005;174(1):449–55.

Available online at www.sciencedirect.com
ScienceDirect
Vaccine 25 (2007) 1969–1992
Vaccine
www.elsevier.com/locate/vaccine

Generation and immunogenicity of novel HIV/AIDS vaccine candidates targeting HIV-1 Env/Gag-Pol-Nef antigens of clade C

Carmen Elena Gómez [a], Jose Luis Nájera [a], Victoria Jiménez [a], Kurt Bieler [b], Jens Wild [b], Linda Kostic [c], Shirin Heidari [c], Margaret Chen [c], Marie-Joelle Frachette [d], Giuseppe Pantaleo [e], Hans Wolf [b], Peter Liljeström [c], Ralf Wagner [b], Mariano Esteban [a,*]

[a] *Department of Molecular and Cellular Biology, Centro Nacional de Biotecnología, CSIC, Ciudad Universitaria Cantoblanco, 28049 Madrid, Spain*
[b] *Institute of Medical Microbiology and Hygiene, University of Regensburg, Germany*
[c] *Department of Microbiology, Tumor and Cell Biology, Karolinska Institut, 17177 Stockholm, Sweden*
[d] *Sanofi Pasteur, 1541 Avenue Marcel Merieux, 69280 Marcy Létoile, France*
[e] *Laboratory of AIDS Immunopathogenesis, Department of Medicine, Centre Hospitalier Universitaire Vaudois, Av. De Beaumont 29-Hopital Beaumont, 1011 Lausanne, Switzerland*

Received 25 September 2006; received in revised form 6 November 2006; accepted 23 November 2006
Available online 6 December 2006

Abstract

Recombinants based on the attenuated vaccinia virus strains MVA and NYVAC are considered candidate vectors against different human diseases. In this study we have generated and characterized in BALB/c and in transgenic HHD mice the immunogenicity of two attenuated poxvirus vectors expressing in a single locus (TK) the codon optimized HIV-1 genes encoding gp120 and Gag-Pol-Nef (GPN) polyprotein of clade C (referred as MVA-C and NYVAC-C). In HHD mice primed with either MVA-C or NYVAC-C, or primed with DNA-C and boosted with the poxvirus vectors, the splenic T cell responses against clade C peptides spanning gp120/GPN was broad and mainly directed against Gag-1, Env-1 and Env-2 peptide pools. In BALB/c mice immunized with the homologous or the heterologous combination of poxvirus vectors or with Semliki forest virus (SFV) vectors expressing gp120/GPN, the immune response was also broad but the most immunogenic peptides were Env-1, GPN-1 and GPN-2. Differences in the magnitude of the cellular immune responses were observed between the poxvirus vectors depending on the protocol used. The specific cellular immune response triggered by the poxvirus vectors was Th1 type. The cellular response against the vectors was higher for NYVAC than for MVA in both HHD and BALB/c mice, but differences in viral antigen recognition between the vectors was observed in sera from the poxvirus-immunized animals. These results demonstrate the immunogenic potential of MVA-C and NYVAC-C as novel vaccine candidates against clade C of HIV-1.
© 2006 Elsevier Ltd. All rights reserved.

Keywords: HIV/AIDS; Clade C vaccine; Poxvirus vectors; MVA; NYVAC; DNA vectors; SFV vectors; Immune response; Mouse models

1. Introduction

Since the discovery of AIDS in 1981, the global spread of HIV has reached pandemic proportions. The number of individuals living with the human immunodeficiency virus (HIV) grew to unprecedented heights in 2005, with an estimated 40.3 million people infected worldwide, of which 4.9 million people contracted the disease in 2005. Sub-Saharan Africa continued to bear the major brunt of the epidemic with 25.8 million people living with the virus, accounting for about two-thirds (64%) of all reported HIV/AIDS cases (http://www.unaids.org). Within this current HIV pandemic, geographic distribution of HIV subtypes has shown that HIV-1 clade C (HIV-1C) is the most prevalent subtype causing more than half of all global infections and 94% of infections in

* Corresponding author. Tel.: +34 91 5854553; fax: +34 91 5854506.
E-mail address: mesteban@cnb.uam.es (M. Esteban).

0264-410X/$ – see front matter © 2006 Elsevier Ltd. All rights reserved.
doi:10.1016/j.vaccine.2006.11.051

southern Africa [1,2]. The high prevalence rates of HIV-1C in sub-Saharan Africa and the increasing incidence of this subtype and HIV-1C recombinants in rapidly growing epidemics in India and China, respectively, underscore the vital importance of developing efficacious vaccines that target HIV-1C.

Despite the present understanding of several aspects of HIV-1C, the development of effective vaccine targeting this clade has provided unprecedented scientific challenges mainly due to some unique features of the biology of HIV-1C infections. Some of these characteristics include: (i) high levels of intra-subtype viral diversity [3,4]; (ii) high viral loads [5]; (iii) preferential CCR5 co-receptor tropism [6,7]; (iv) a number of unique subtype signatures across the viral genome [4,8]. In spite of the difficulties that are concerned in generating an effective HIV-1C vaccine due to these and other more non-subtype specific attributes of HIV-1, several groups are committed to the development and evaluation of such vaccines.

It is generally accepted that for prophylactic HIV-1 vaccines to achieve protection, they will have to induce both humoral and cell-mediated immune responses. While efforts focused towards envelope-based humoral immunity inducing vaccines are still on-going [9], they have been hampered by the inaccessibility and instability of neutralizing epitopes on primary HIV isolates [10,11]. In view of that, recent vaccine approaches have focused on the induction of cellular immune responses [12–14]. Evidence for the role of CD8+ T cells in the control of virus replication includes temporal correlation between the appearance of HIV-specific CD8+T cells and the decline of primary viremia [15,16], the fact that several HLA class I alleles (HLA-B57, HLA-B27, HLA-B63, HLA-B*1503) are associated with slow disease progression [17,18], the early selection of CTL escape viral mutants during primary infection [19,20] and the rapid increase of viral loads in macaques infected with SIV after experimental depletion of CD8+T cells [21–23]. A variety of vaccines have been developed to induce cell-mediated immunity. Among them, naked DNA and live vectored recombinant vaccines have extensively proved their immunological properties [24–27]. The two strains of vaccinia virus, MVA and NYVAC are currently being examined as recombinant vaccines against HIV [28] (see www.eurovacc.org). With several exceptions, most pre-clinical HIV-1C vaccines have primarily used plamid DNA as vector platform, while clinically tested HIV-1C vaccines have used both DNA and recombinant viral vector system [29].

In view of the need for the development of an HIV-1 clade C vaccine, here we describe the construction and in vitro characterization of two novel attenuated poxvirus vectors MVA and NYVAC expressing four HIV-1 antigens (Env, Gag, Pol and Nef) from clade C in a single locus (the thymidine kinase region) of the viral genome. The viral vectors are referred as MVA-C and NYVAC-C, and have been designed to express gp120 as a cell released product and GPN as an intracellular polyprotein lacking regions involved in immunosupression. In addition, we have compared in transgenic HHD and in BALB/c mice how MVA-C and NYVAC-C activate specific cellular immune responses against peptide pools spanning the heterologous antigens when they were administered using different prime/boost vaccination approaches. Our findings showed that in cultured cells both recombinants efficiently express the four HIV-1 antigens in a stable manner, but in contrast to MVA-C, NYVAC-C induced potent apoptosis. In HHD mice primed with either MVA-C or NYVAC-C, or primed with DNA-C and boosted with the poxvirus vectors, the splenic T cell responses against clade C peptides spanning gp120/GPN was broad and mainly directed against Gag-1, Env-1 and Env-2 pools. However, in BALB/c mice immunized with homologous and heterologous combination of either the poxvirus vectors or Semliki forest virus (SFV) vectors expressing gp120/GPN, the Env-1, GPN-1 and GPN-2 clade C peptide pools were the most immunogenic. Differences in the magnitude of the specific cellular immune responses were induced by the two poxvirus vectors, particularly in the prime/boost immunization approaches. Our findings highlighted the immunological relevance of NYVAC-C and MVA-C as potential vaccine candidates against HIV/AIDS.

2. Materials and methods

2.1. Cells and poxviruses

Cells were maintained in a humidified air 5% CO_2 atmosphere at 37 °C. Primary chicken embryo fibroblast cells (CEF) and human cells (HeLa) were grown in Dulbecco's modified Eagle's medium (DMEM) supplemented with 10% fetal calf serum (FCS). The EL4gpnHHD cells expressing both the HIV-1 Gag-Pol-Nef polyprotein from clade B and the chimeric human (α-1, α-2 and mouse α-3) HLA-A2.1 heavy chain covalently linked to the human β2m light chain, denominated HHD molecule and the RMAS-HHD cells, were kindly provided by Arnaud Didierlaurent (Centre Hospitalier Universitaire Vaudois, Lausanne). They were grown in RPMI 1640 supplemented with 10% FCS. The poxvirus strains used in this work included: modified vaccinia virus Ankara (MVA) obtained after 586 passages in CEF cells (derived from clone F6 at passage 585, kindly provided by G. Sutter, Germany), the genetically attenuated vaccinia-based vector NYVAC (generated from the vaccinia virus Copenhagen strain by selected deletion of 18 viral genes [30]) and the recombinant NYVAC-C expressing the gp120 and Gag-Pol-Nef proteins from HIV-1_{CN54} (both parental NYVAC and recombinant NYVAC-C viruses provided by Sanofi-Pasteur). The parental and recombinant NYVAC and MVA viruses were grown in primary chicken embryo fibroblast (CEF) cells, similarly purified through two 45% (w/v) sucrose cushions, and titrated by immunostaining plaque assay as previously described [31]. The titration of the different viruses was performed in CEF at least three times.

2.2. DNA vectors and codon optimized genes

The RNA- and codon-optimized HIV-1_{CN54} gp120 and HIV-1_{CN54} Gag-Pol-Nef (GPN) gene constructs were designed and synthesized by GENEART GmbH (Regensburg, Germany). To generate the final DNA vaccine constructs, the $_{CN54}$gp120 and $_{CN54}$GPN genes were cloned into the pcDNA3.1 (Invitrogen, UK). Plasmids were purified using Maxi-Prep purification kits (Qiagen, Hilden, Germany) and diluted for injection in endotoxin-free phosphate buffered saline (PBS).

2.3. Construction of plasmid transfer vector

Plasmids pMA60gp120C/gagpolnefC-14,15 and pLZAW1 were provided by Sanofi-Pasteur. A 6.047 kbp DNA fragment containing the two synthetic early/late (E/L) promoters [32] in a back-to-back orientation individually driving a codon optimized gp120 and gagpolnef genes of HIV-1 clade C (CN54) was excised with EcoRV from plasmid pMA60gp120C/gagpolnefC-14,15, modified by incubation with Klenow DNA polymerase to generate blunt ends, and cloned into pLZAW1 vector (previously digested with restriction endonuclease AscI, modified by incubation with Klenow, and dephosphorylated by incubation with Alkaline Phosphatase, Calf Intestinal (CIP)) generating the plasmid transfer vector pLZAW1gp120C/gagpolnef-C-14 (Fig. 1). The resulting plasmid directs the insertion of the foreign genes into the TK locus of MVA genome and allows the generation of a recombinant virus without selectable marker.

2.4. Construction of the recombinant virus MVA-C

CEF from 11-day old SPF eggs were infected with MVA at a multiplicity of 0.05 PFU/cell and then transfected with 10 μg DNA of plasmid pLZAW1gp120C/gagpolnef-C-14 using lipofectamine reagent according to the manufacturer's protocol (Invitrogen, San Diego, CA). After 72 h post infection the cells were harvested, sonicated and used for recombinant virus screening. Recombinant MVA viruses containing the $_{CN54}$gp120 and $_{CN54}$Gag-Pol-Nef genes from clade C, and transiently co-expressing the β-gal marker gene (MVA-C (X-gal+)), were selected by consecutive rounds of plaque purification in CEF cells stained with 5-bromo-4-chloro-3-indolyl β-galactoside (X-Gal) (300 μg/mL). In the following plaque purification steps, recombinant MVA viruses containing the $_{CN54}$gp120 and $_{CN54}$Gag-Pol-Nef genes and having deleted the β-gal gene (by homologous recombination between the TK left arm and the short TK left arm repeat that are flanking the marker) were isolated by two additional consecutive rounds of plaque purification screening for non-staining viral foci in CEF cells in the presence of X-Gal (300 μg/mL). In each round of purification the isolated plaques were expanded in CEF cells for 3 days, and the crude virus obtained were used for the next plaque purification round. The resulting MVA-C virus was purified through two 45% (w/v) sucrose cushions and titrated by immunostaining in CEF cells. Purity of the recombinant virus was confirmed by PCR with primers spanning the junction and internal regions of the inserts and by DNA sequence analysis.

Table 1
DNA sequence of primers used in the PCR analysis of MVA-C recombinant virus

Oligos	Sequence	Position
TK-L	5′ TGATTAGTTTGATGCGATTC 3′	342–361
gp120-1213	5′ ATCATCACCATCCCCTGC 3′	929–946
gp120-1050	5′ GTCTTGTTCTGGAAGTGC 3′	1092–1109
gp120-10	5′ TCGAGCATGGACAGGGCC 3′	2132–2149
GPN-802	5′ TGGGTTTAAACAAGATCG 3′	3048–3064
GPN-2198	5′ TGGGTCCTCTTGTTCAGC 3′	4443–4460
GPN-2018	5′ CAAGGTGAAGCAGTGGCC 3′	4263–4280
GPN-3820	5′ CGGCCTTGCCGATCTTGG 3′	6065–6082
GPN-4000	5′ CCGACAAGAGCGAGAGCG 3′	6245–6262
TK-R	5′ TGTCCTTGATACGGCAG 3′	6823–6839

Their positions in the DNA sequence of MVA-C within the TK viral locus are represented.

2.5. PCR analysis of recombinant MVA-C

Viral DNA was extracted by the method of SDS-Proteinase K-Phenol from CEF cells infected at 5 PFU/cell with the recombinant MVA-C virus. Different set of primers annealing in the TK flanking sequences and in internal regions of the inserted genes were used for PCR analysis (see Table 1). The amplifications were performed with Platinum Taq DNA polymerase (Invitrogen, San Diego, CA), and the conditions were optimized for each set of primers. DNA extracted from CEF cells infected either with MVA-WT or with NYVAC-C viruses were used as negative and positive controls respectively.

2.6. Time-course expression of $_{CN54}$gp120 and $_{CN54}$GPN proteins from MVA-C and NYVAC-C

CEF cells grown in 12 well-plates were infected at 5 PFU/cell with the recombinants MVA-C and NYVAC-C. At 6, 18 and 24 h post infection (h pi), cells were collected and centrifuged at 1500 rpm for 10 min. The supernatant (S) was removed and concentrated by speed-vacuum. Cellular pellets (P) were lysed in cold buffer (50 mM Tris–HCl pH 8, 0.5 M NaCl, 10% NP-40, 1% SDS). The supernatant and pellet samples, both containing equal amounts of protein (12 μg), were run on 10% SDS-PAGE. The expression of $_{CN54}$gp120 and $_{CN54}$GPN proteins was visualized following Western blotting using polyclonal anti-gp120 antibodies and rabbit polyclonal anti-gag p24 serum (ARP 432, NIBSC, Centralised Facility for AIDS reagent, UK), respectively. Detection of cellular β-actin protein was used as an internal loading control.9

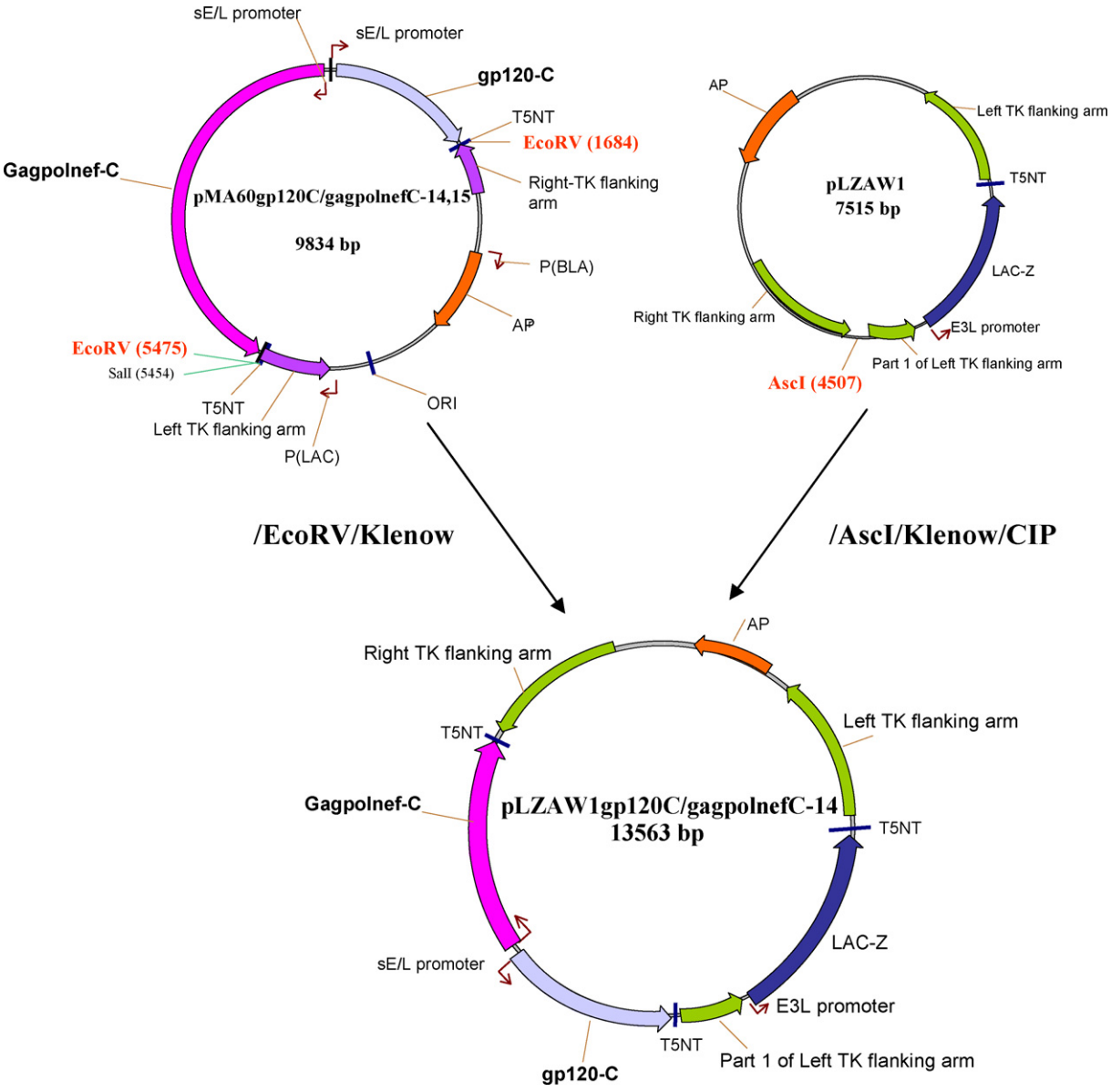

Fig. 1. Scheme for the construction of the transfer vector pLZAW1gp120C/gagpolnef-C-14. A 6.047 kbp DNA fragment containing the two synthetic early/late (E/L) promoters in a back-to-back orientation individually driving a codon optimized $_{CN54}$gp120 and $_{CN54}$GPN genes of HIV-1 clade C was excised with EcoRV from plasmid pMA60gp120C/gagpolnefC-14,15, modified by incubation with Klenow DNA polymerase to generate blunt ends, and cloned into pLZAW1 vector (previously digested with restriction endonuclease AscI, modified by incubation with Klenow, and dephosphorylated by incubation with Alkaline Phosphatase, Calf Intestinal (CIP)) generating the plasmid transfer vector pLZAW1gp120C/gagpolnef-C-14. The resulting plasmid directs the insertion of the foreign genes into the thymidine (TK) locus of MVA genome and allows the generation of a recombinant virus without the selectable marker.

2.7. Genetic stability of recombinant poxviruses

Monolayers of CEF cells were infected at 0.05 PFU/cells with MVA-C or NYVAC-C recombinants. At 72 h pi cells were collected by scrapping. After three freeze–thaw cycles and brief sonication, the cellular extract was centrifuged at 1500 rpm for 5 min and the supernatant was used for a new round of infection at 0.05 PFU/cell. The same procedure was repeated until passage 10. Expression of $_{CN54}$gp120 and $_{CN54}$GPN proteins at all passages was detected by Western blot and immunostaining assays using anti-gp120 and anti-gag p24 polyclonal antibodies, respectively.

2.8. Analysis of poxvirus growth

To determine virus-growth profiles, monolayers of CEF cells grown in 6 well tissue culture plates were infected at 0.01 PFU/cell with MVA-C or NYVAC-C recombinants. Following virus adsorption for 60 min at 37 °C, the inoculum was removed. The infected cells were washed twice with DMEM medium without serum, and incubated with

fresh DMEM containing 2% of FCS at 37 °C in a 5% CO_2 atmosphere. At 24, 48 and 72 h pi, cells were removed by scraping, centrifuged at 1500 rpm for 5 min and both pellet and supernatant were collected. The supernatants were stored at 4 °C for no more than 48 h before virus titration. The pellet was resuspended in serum-free medium at 20×10^6 cells/mL, freeze-thawed three times, sonicated, and centrifuged at 1500 rpm for 5 min. The supernatant was collected and referred as cell lysates. Virus titers in supernatants and cell lysates were determined by immunostaining assay in CEF cells using rabbit polyclonal antibodies against vaccinia virus (VV) strain WR.

2.9. Phase contrast microscopy and measurement of poxvirus induced apoptosis

To evaluate the cytopathic effects (CPE) under non-permissive conditions, HeLa cells were seeded into six-well tissue culture plates and grown to confluence. The cells (duplicate wells) were infected at 5 PFU/cell with MVA-C or NYVAC-C recombinants and cell morphology visualized by phase contrast microscopy at 24 h pi.

To evaluate apoptosis, the cleavage of poly ADP-ribose polymerase (PARP) was analyzed by Western blot at 4, 8 and 16 h post-infection in extracts from HeLa cells infected with MVA-C or NYVAC-C recombinants at 5 PFU/cell. Rabbit polyclonal anti-Human PARP was supplied by Cell Signaling and the monoclonal antiboby against β-actin was supplied by Sigma. In addition, apoptosis levels were measured using the cell death detection enzyme-linked immunosorbent assay (ELISA) kit (Roche) according to manufacturer's instructions. This assay is based on the quantitative sandwich enzyme immunoassay principle, and uses mouse monoclonal antibodies directed against DNA and histones to estimate the amount of cytoplasmic histone-associated DNA fragments.

2.10. Construction of the SFV expressing HIV-1 clade C Gag/Pol/Nef or Env

For construction of pSFV4.2-HIVC-Env/syngp120 (clade C, CN54), the sequence encoding the HIV-1 clade C syngp120 was isolated from pCR-Script-syngp120 as a NotI-ApaI fragment and ligated into the pSFV4.2 expression vector [33]. For production of pSFV4.2-HIVC-Gag-Pol-Nef, the sequence encoding Gag-Pol-Nef was isolated as a *Kpn*I–*Xho*I fragment from pScript-synGag-Pol-Nef. The fragment was first inserted into the pET43 transfer plasmid and thereafter excised as an *Xho*I–*Sma*I fragment for insertion into the pSFV4.2 vector. For generation of recombinant particles, RNAs from the two SFV recombinant plasmids were synthesized in vitro and packaged into SFV particles using the two-helper RNA system described elsewhere [33,34]. The recombinant SFV particles were harvested and purified by ultracentrifugation through a 20% sucrose cushion. Indirect immunofluorescence of infected BHK cells were performed to determine the titre of the recombinant virus stocks [33,34]. Antigen expression was verified in infected BHK-21 cells by metabolic labelling with [^{35}S]methionine and further confirmed by immunoprecipitation as described previously [35]. Immunoprecipitation and indirect immunofluorescence assays for analysis of Gag-Pol-Nef were performed with mAbs against p24 (EVA repository reagent Mab HIV-1 p55/p24 ARP313 (EH12E1)). For the analysis of expression of the syngp120, polyclonal antibodies against gp120 were used.

2.11. Peptides

The HIV-1 peptide pools Gag-1, Gag-2, Env-1, Env-2, GPN-1, GPN-2, GPN-3, NEF and CTRL, with each purified peptide at 25 μg per vial were provided by EuroVacc. They spanned the entire Env, Gag, Pol and Nef regions from clade C included in the immunogens as consecutive 15-mers overlapped by 11 amino acids. The $_{CN54}$gp120 protein (499 aa) was spanned by the Env-1 (aa: 1–239; 49 peptides) and Env-2 (aa: 229–499; 63 peptides) pools. The Gag-Pol-Nef fusion protein (1417 aa) was spanned by the following pools: Gag-1 (aa: 1–254; 60 peptides), Gag-2 (aa: 244–500; 61 peptides), GPN-1 (aa: 485–735; 60 peptides), GPN-2 (aa: 725–831 and aa: 1017–1175; 61 peptides), GPN-3 (aa: 1165–1417; 61 peptides) and NEF (aa: 838–1044; 49 peptides). The CTRL peptide pool was used as negative control. It contains 23 peptides mostly from CMV, EBV and influenza, each at 50 μg.

2.12. Mice immunization

BALB/c mice were purchased from Harlan. Transgenic HHD mice were kindly provided by Dr. Lemonnier (Pasteur Institute, France). They are double-knockout for H2-D^b and β2-microglobulin and transgenic for a chimeric HLA-A2 molecule [36]. HHD mice were immunized with 2×10^7 PFU of either MVA-C or NYVAC-C in 200 μL of PBS by intraperitoneal route (i.p.). When the heterologous DNA/rVV prime–boost approach was assayed, animals received 100 μg of DNA-C (50 μg of pcDNA-$_{CN54}$gp120 + 50 μg of pcDNA-$_{CN54}$GPN) by intramuscular route (i.m.) and two weeks later received an intraperitoneal inoculation of 2×10^7 PFU of the corresponding rVVs. When the homologous rVV/rVV prime–boost approach was used, animals received 2×10^7 PFU of the corresponding rVVs by i.p. route at day 0 and 15. In SFV-C prime/poxvirus-C boost approach age-and sex-matched BALB/c mice (7–12 wks of age) from Bomholtgard, Denmark were immunized with SFV-based HIV-clade C vaccine that contained the combination of SFV-HIV-C-GPN (0.5×10^7 IU) and SFV-HIV-C-gp120 (0.5×10^7 IU) resuspended in PBS. The SFV-LacZ virus (1×10^7 IU) was used as control. All viruses were produced with the Two-Helper RNA System [33,34] and purified by sucrose gradient ultracentrifugation. The booster was given on day 14 using different doses of MVA-C or NYVAC-C by i.m route. Ten days after the last immunization mice were sacrificed and spleens processed for ELISPOT

assay. At least two independent experiments have been performed for the different immunization protocols.

2.13. IFN-γ and IL-2 ELISPOT assay

Fresh IFN-γ ELISPOT assay was performed as previously described [37]. Briefly, 10^5–10^6 splenocytes (depleted of red blood cells) were plated in triplicate in 96-well nitrocellulose-bottomed plates previously coated with 6 μg/mL of anti-mouse IFN-γ mAb R4-6A2 (Pharmingen, San Diego, CA). HIV-1 peptide pools from clade C and negative control (CTRL) pool were resuspended in RPMI 1640 supplemented with 10% FCS and added to the cells at a final concentration of 5 μg/mL for each peptide. When the cellular response against the viral antigens was evaluated, RMAS-HHD cells were infected with MVA-WT or NYVAC-WT at 5 PFU/cell. At 4 h pi cells were washed and treated with mitomycin C (30 μg/mL; Sigma). The cross-reactive response against the clade B Gag-Pol-Nef antigen was evaluated using the EL4gpnHHD cells. As control, RMAS-HHD cells were used.

Plates were incubated at 37 °C, 5% CO_2 for 48 h (except for the experiments using SFV-C, in which they were incubated for 20 h), washed extensively with PBS containing 0.05% of Tween20 (PBS-T) and incubated 2 h at RT with a solution of 2 μg/mL of biotinylated anti-mouse IFN-γ mAb XMG1.2 (Pharmingen) in PBS-T. Afterwards, plates were washed with PBS-T and 100 μL of peroxidase-labeled avidin (Sigma, St. Louis, MO) at 1:800 dilution in PBS-T was added to each well. After 1 h of incubation at RT, wells were washed with PBS-T and PBS. The spots were developed by adding 1 μg/mL of the substrate 3,3′-diaminobenzidine tetrahydrochloride (Sigma) in 50 mM Tris–HCl, pH 7.5 containing 0.015% hydrogen peroxide. The spots were counted with the aid of a stereomicroscope (or in the case of experiments using SFV, using an automated Elispot reader (Axioplan 2 Imaging, Zeiss, Göttingen, Germany)). Fresh IL-2 ELISPOT assay was carried out identically as before but using the anti-mouse IL-2 mAb JES6-1A12 (Pharmingen) and biotinylated anti-mouse IL-2 mAb JES6-5H4 (Pharmingen) as capture and detection antibody respectively.

2.14. Evaluation of cytokine levels by ELISA

Splenocytes from immunized mice (5×10^5 cells) were stimulated with 2 μg/mL of each peptide pool at 37 °C, 5% CO_2 for 6 days. Culture supernatants were collected and stored at −70 °C until performing the assay. Levels of IFN-γ and IL-10 were evaluated using commercial ELISA kits (Pharmingen).

2.15. Antibody measurements by enzyme-linked immunosorbent assay (ELISA)

The humoral response against either the HIV-1 proteins from clade B $_{LAV}$gp160 and $_{SF2}$p55 Gag or against VV proteins were detected by ELISA. High binding polystyrene microtitre plates (Nunc) were coated with 100 μL of the specific protein diluted at 10 μg/mL in 0.05 M carbonate–bicarbonate buffer pH 9.6 overnight at 4 °C. The wells were washed twice with PBS plus 0.05% Tween 20 (PBS-T) and blocked with PBS containing 10% FCS (blocking solution) during 1 h at 37 °C. Serum samples diluted in blocking solution were added in a volume of 100 μL/well and incubated 2 h at 37 °C. Plates were washed five times with PBS-T before the detection antibody was added. Peroxidase-conjugated goat anti-mouse immunoglobulin G (IgG) antibody (Southern Biotechnology Associates, Birmingham, AL) was diluted 1:1000 in blocking solution and incubated for 1 h at 37 °C. The plates were washed again five times with PBS-T and the 3,3′,5,5′-tetramethylbenzidine (TMB) liquid substrate system for ELISA (Sigma) was used to reveal the reaction. After 10–15 min of incubation at RT, the reaction was stopped by adding 2N H_2SO_4, and absorbance was measured at 450 nm on a Multiskan Plus plate reader (Labsystem, Chicago, IL).

2.16. Statistical procedures

All the data were logarithmically transformed and the means compared using ANOVA and Duncan's multiple range test.

3. Results

3.1. Construction of MVA-C

MVA-C, a recombinant MVA expressing HIV-1 clade C Gag, Pol, Nef and Env antigens, was constructed by homologous recombination in CEF cells. Gag-Pol-Nef is a fusion protein composed of *gag*, *pol* and *nef* ORFs from HIV-1 clone CN54, that has been modified to enhance its immunogenicity and remove, for safety considerations, undesirable domains of the HIV antigens. Gp120 Env protein originates from the same HIV-1 isolate (CN54). In both cases, the codon usage was adapted to highly express human genes.

In this study we developed a new transfer vector which eliminated the marker gene from the final recombinant virus and allows the insertion of the *gag-pol-nef* and *env* ORFs in the same viral locus, both under the transcriptional control of the VV synthetic early/late viral promoter. The new vector contained a β-gal reporter gene sequence between two repetitions of the left TK flanking arm which allowed the reporter to be automatically deleted from the final recombinant virus by homologous recombination after two-three passages. The construction of the transfer vector pLZAW1gp120C/gagpolnef-C-14 is shown at Fig. 1.

Homologous recombination was achieved by infecting CEF cells with MVA and transfection with pLZAW1gp120C/gagpolnef-C-14. X-Gal staining plaques were picked twice to isolate recombinants free of the

parental MVA. Subsequently, non-staining plaques were picked repeatedly to isolate rMVA that had lost the reporter gene. Several independent clones of MVA-C were isolated, analyzed for expression of $_{CN54}$gp120 and $_{CN54}$GPN by Western blot and immunostaining of plaques, and propagated in CEF cells.

3.1.1. Screening of recombinant MVA-C virus by PCR analysis

The correct insertion of the HIV-1 genes in the recombinant MVA-C virus was confirmed by PCR and DNA sequence analysis. Viral DNA purified from CEF cells infected with MVA-C was amplified using different set of primers annealing in the TK flanking sequences and in internal regions of the inserted genes (see Table 1). The sizes of the expected PCR products are represented in Fig. 2A. For comparative purposes, DNA extracted from CEF cells infected with NYVAC-C or with the wild type strain of MVA (MVA-WT) were used. As shown in Fig. 2B, the amplifications performed with the different set of primers reveals that *gag-pol-nef* and *env* ORFs were inserted successfully into the MVA TK locus, and also that no wild-type contamination was present in the rMVA preparation. These results were confirmed by DNA sequence analysis of the MVA-C TK locus (see Appendix A).

3.2. Construction of NYVAC-C

The recombinant virus NYVAC-C containing, as for MVA-C, the same cassette of HIV-1 genes in the TK locus and under regulation of the synthetic early/late promoter, was generated by Sanofi-Pasteur. The approach was similar as for MVA-C but instead used a different transfer vector, plaque-lifting and ^{32}P-labeled of the inserts for the isolation of the recombinant virus. The correct inserts in the virus genome were confirmed by PCR and DNA sequence analyses (not shown).

3.3. Characterization of MVA-C and NYVAC-C recombinants

3.3.1. In vitro expression of $_{CN54}$gp120 and $_{CN54}$GPN proteins by MVA-C and NYVAC-C

In order to characterize the expression of $_{CN54}$gp120 and $_{CN54}$GPN proteins by MVA-C and NYVAC-C recombinants, a time course analysis was carried out. The kinetics of synthesis of Env protein was similar in MVA-C and NYVAC-C infected cells. $_{CN54}$gp120 was efficiently released from cells by 18 h pi. (Fig. 2C, left panel). As compared to NYVAC-C, the full length $_{CN54}$GPN fusion protein was produced in MVA-C infected cells but at different levels depending on the time point after infection (Fig. 2C, right panel). There is also breakdown of GPN in infected cells. With time (18 and 24 h pi) the $_{CN54}$GPN expression levels in cell extracts were apparently reduced in NYVAC-C versus MVA-C infected cells, probably due to the phosphorylation of the initiation factor eIF-2α, as previously described for NYVAC but not MVA [38].

3.3.2. Genetic stability of MVA-C and NYVAC-C

To verify that the MVA-C and NYVAC-C recombinants could be passage without lost of the transgene, a stability test was performed. The recombinants were continuously passaged from P2 stock to P10 in CEF cells. Expression of Env and Gag-Pol-Nef antigens at the different passages was determined by Western blot and immunostaining assay. As shown in Fig. 3A, MVA-C efficiently expresses $_{CN54}$gp120 and $_{CN54}$GPN proteins after 7, 8, 9 and 10 passages in CEF cells. Nearly 100% of plaques generated in cells infected with the P10 stock stained with antibody to both Gag and Env proteins (Fig. 3B). The genetic stability of the inserts for NYVAC-C was similarly confirmed after the tenth passage (not shown). These results revealed that MVA-C and NYVAC-C were genetically stable and express efficiently the foreign proteins after 10 consecutive passages.

3.3.3. Virus growth of MVA-C and NYVAC-C

To analyze the viral growth characteristics of MVA-C in comparison with NYVAC-C under permissive conditions, monolayers of CEF cells were infected at 0.01 PFU/cell with each virus for 0, 24, 48 and 72 h. Infectious viruses that remained cell-associated and released to the medium during the course of the infection were measured by immunostaining assay. As shown in Fig. 3C, left panel, the virus titers in the supernatant of cells infected with NYVAC-C were about 1 log lower than those obtained in the supernatant of cells infected with MVA-C at the three times assayed. However, the titers of cell-associated viruses in MVA-C and NYVAC-C infected cells were similar (Fig. 3C, right panel).

3.3.4. A hallmark of NYVAC-C infection is the induction of apoptosis, but not of MVA-C

We have recently described that during infection of cultured cells with parental NYVAC strain there is induction of apoptosis while parental MVA does not induce apoptosis [39]. To define if recombinant NYVAC-C also induces apoptosis and to compare it with MVA-C, we performed three different assays in human HeLa cells. As shown in Fig. 4, NYVAC-C infection triggers apoptosis in infected cells as measured by phase contrast microscopy (panel A), by PARP cleavage (panel B) and by ELISA test (panel C). These effects were minimally observed in cells infected with MVA-C. These differences may have an impact on immune responses. Thus, we next analyzed the immune responses elicited in mice by the two recombinant vectors.

3.4. Immunogenicity of MVA-C and NYVAC-C recombinants in HHD mice

To analyse whether $_{CN54}$gp120 and $_{CN54}$GPN proteins expressed by MVA-C and NYVAC-C were recognized by human MHC class I molecules, we immunized transgenic

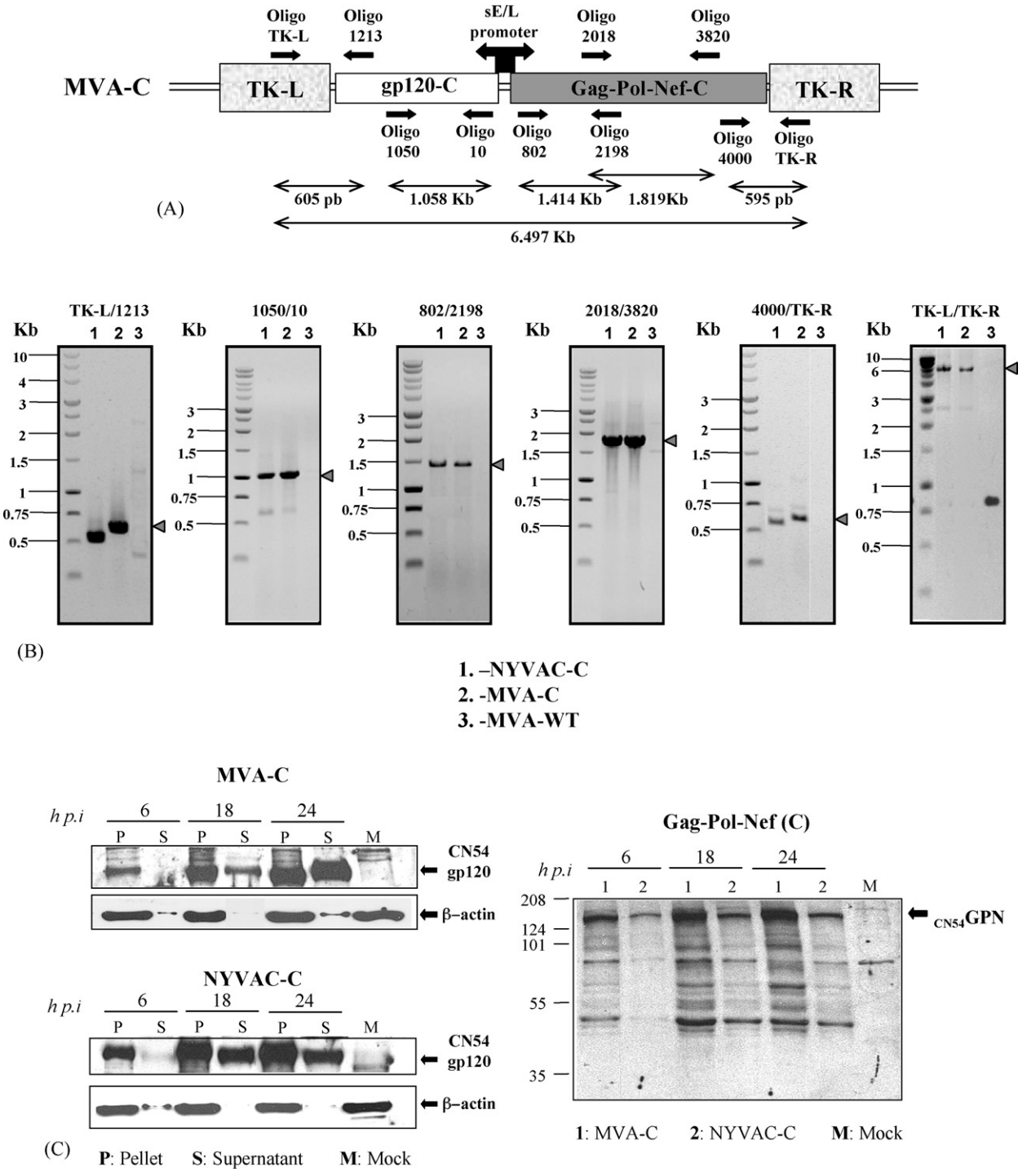

Fig. 2. Characterization of MVA-C and NYVAC-C recombinant viruses. (A) Scheme of the MVA-C insert within the TK viral locus. The positions of the different sets of primers used for PCR analysis and the expected sizes of PCR products are represented. (B) PCR analysis of the MVA-C insert in the TK viral locus. 100 ng of viral DNA extracted from CEF cells infected at 5 PFU/cell with NYVAC-C (lane 1), MVA-C (lane 2) or MVA-WT (lane 3) were used for PCR analysis. PCR conditions were optimized for each set of primers. (C) Time-course expression of $_{CN54}$gp120 and $_{CN54}$GPN proteins in cells infected with MVA-C and NYVAC-C recombinants. The expression of $_{CN54}$gp120 and $_{CN54}$GPN proteins at indicated times post-infection of CEF cells was visualized by western blot in supernatants (S) and pellet (P) samples of mock (M) or infected cells at 5 PFU/cell with MVA-C or NYVAC-C recombinant viruses. The cellular β-actin protein expression was used as internal loading control. Arrows at the right indicate the position of $_{CN54}$gp120, $_{CN54}$GPN and β-actin proteins.

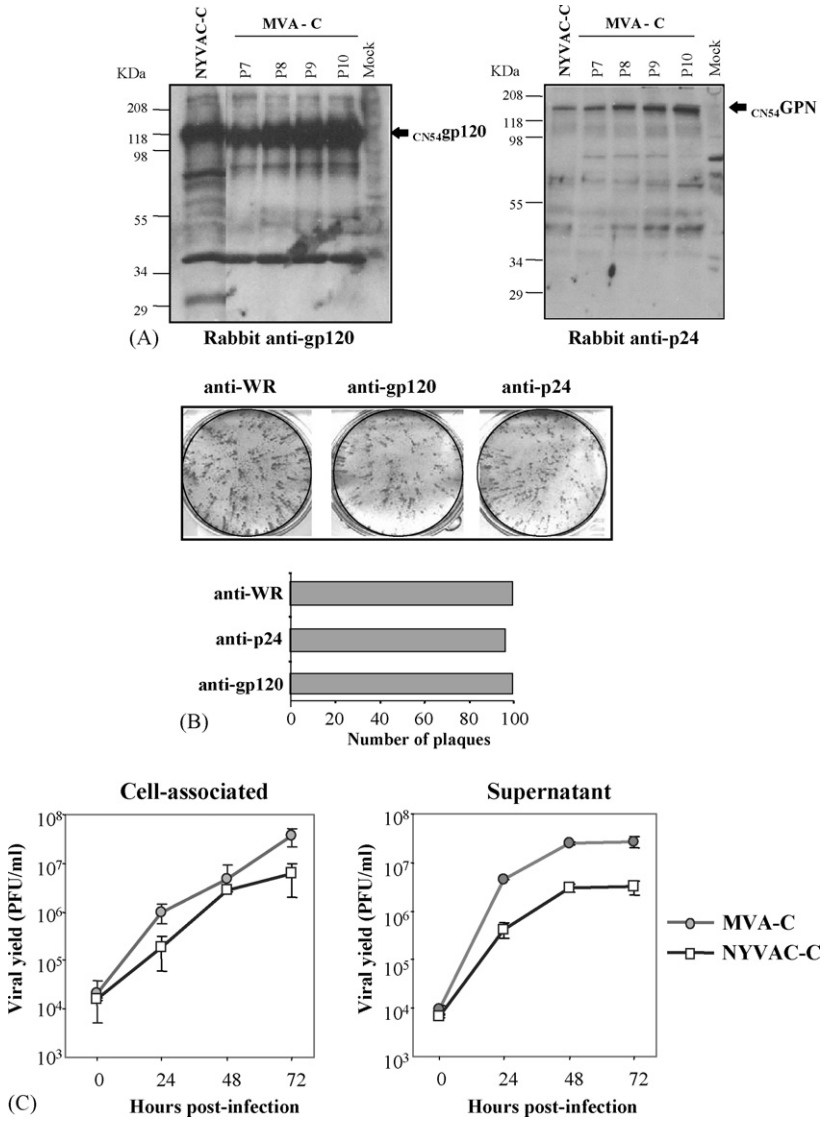

Fig. 3. (A) Analysis of MVA-C stability after several rounds of viral amplification in CEF cell culture. MVA-C stability after passages in CEF cells. The expression of $_{CN54}$gp120 and $_{CN54}$GPN proteins was visualized by western blot in samples of mock-infected CEF cells (Mock) and infected at 5 PFU/cell with either NYVAC-C (used as positive control) or the different passages of MVA-C (from P7 to P10). Arrows at the right indicate the position of $_{CN54}$gp120, $_{CN54}$GPN proteins. The immune reactive band of about 40 kDa appearing with anti-gp120 is of viral origin and not a breackdown product of gp120. (B) Immunostaining analysis of heterologous antigen expression by MVA-C after 10 passages in CEF cells. Plaques generated in CEF cells infected with a 10^{-5} dilution of P10 stock of MVA-C were analyzed by immunostaining using anti-gp120, anti-p24 and anti-WR polyclonal antibodies. The numbers of virus plaques that were positive for each antibody were represented in a graphic. (C) Virus growth of MVA-C and NYVAC-C in CEF cells. Monolayers of CEF cells were infected at 0.01 PFU/cell with MVA-C or NYVAC-C recombinants for 0, 24, 48 and 72 h. Cells were collected by centrifugation and infectious viruses associated to the cells (left panel) and released to the supernatant (right panel) during the course of the infection were quantified by immunostaining assay. Averages of three independent experiments are shown with standard error bars.

HHD mice that exclusively display a chimerical human HLA-A2.1 as MHC class I molecule [36]. Two groups of HHD mice ($n = 4$) were primed by the i.p route with 2×10^7 PFU of either MVA-C or NYVAC-C. Ten days after the immunization, the cellular immune responses induced in the spleen against VV antigens (WR strain) or against pools of overlapping peptides that span the HIV-1 $_{CN54}$gp120 and $_{CN54}$GPN proteins were evaluated by fresh IFN-γ ELISPOT assay. The cross-reactive response against Gag-Pol-Nef antigen from clade B was also assayed using the EL4gpnHHD cells. The numbers of spots obtained with the negative CTRL pool or with non-infected RMAS-HHD cells were subtracted in all cases.

As shown in Fig. 5A, MVA-C induced a significant enhancement of splenic T-cell response against the clade C peptide pools Gag-1, Env-1 and Env-2, in comparison with mice primed with NYVAC-C ($p < 0.05$). The GPN-1, GPN-3 and NEF pools were poorly recognized by this group, whereas no specific cellular response was detected against the

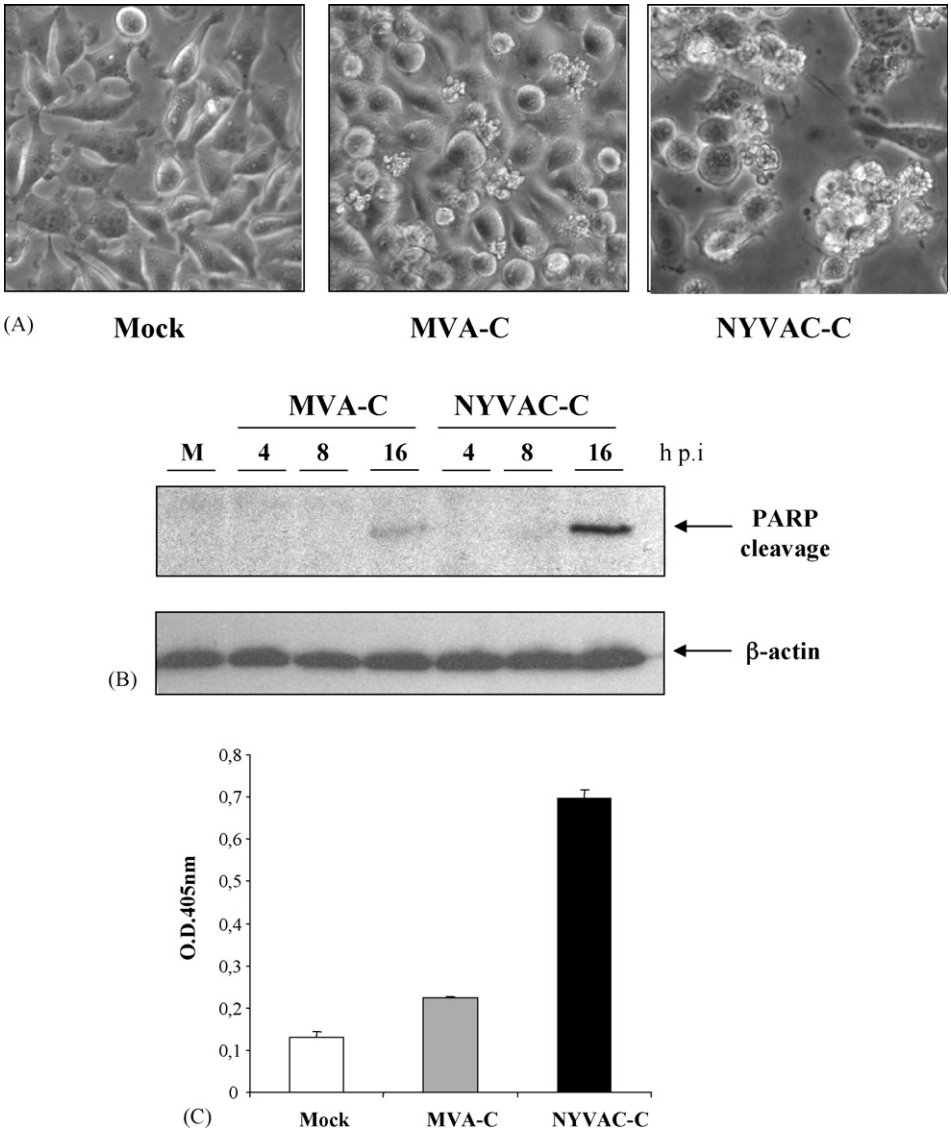

Fig. 4. Differences in apoptosis induction by MVA-C vs. NYVAC-C. (A) Cytopathic effects of MVA-C and NYVAC-C in human cells. Monolayers of HeLa cells were mock-infected or infected at 5 PFU/cell with recombinant MVA-C and NYVAC-C viruses. At 24 h pi the morphological changes characteristic of apoptosis in the cells were examined by phase-contrast microscopy. (B) Western blot analysis of PARP cleavage in HeLa cells infected with MVA-C and NYVAC-C. Monolayers of HeLa cells were mock-infected (M) or infected at 5 PFU/cell with recombinant MVA-C and NYVAC-C viruses. At different times post-infection the cell extracts were collected and analysed by western blot. The cellular β-actin protein expression was used as internal loading control. (C) Quantitation of apoptosis after infection with MVA-C or NYVAC-C. Monolayers of HeLa cells were mock-infected (Mock) or infected at 5 PFU/cell with recombinant MVA-C and NYVAC-C viruses and the extent of apoptosis was determined at 24 h pi by ELISA. Absorbance at 405 nm is represented.

Gag-2 and GPN-2 pools. Splenocytes from animals immunized with NYVAC-C only recognized the Env-1, Env-2, GPN-1 and GPN-2 pools, but the number of specific IFN-γ secreting cells against them were lower than 40. The magnitude of the total response for clade C pools, determined by the overall number of IFN-γ secreting cells, was more than 8 times higher in the group receiving MVA-C (Fig. 5B). In the same way, the breadth of the clade C-specific response per group, as measured by the number of positive pools, was also higher in animals primed with MVA-C.

The cross-reactive immune response against the GPN polyprotein from clade B was also assayed using the EL4gpnHHD cells as antigen presenting cells (APCs). As shown in Fig. 5C after priming, MVA-C induced higher cellular and humoral response than NYVAC-C against clade B antigens. When the anti-VV immune response was evaluated we observed that contrary to the anti-clade C or anti-clade B specific responses, NYVAC-C induced the highest cellular and humoral responses against VV-antigens (1.5 fold higher than that induced by MVA-C) (Fig. 5C).

Since a balance between a Th1 and Th2 type of immune responses may be critical for the control of HIV infection [40], our next approach was to determine the profile of cytokines triggered in immunized mice. Thus, we quanti-

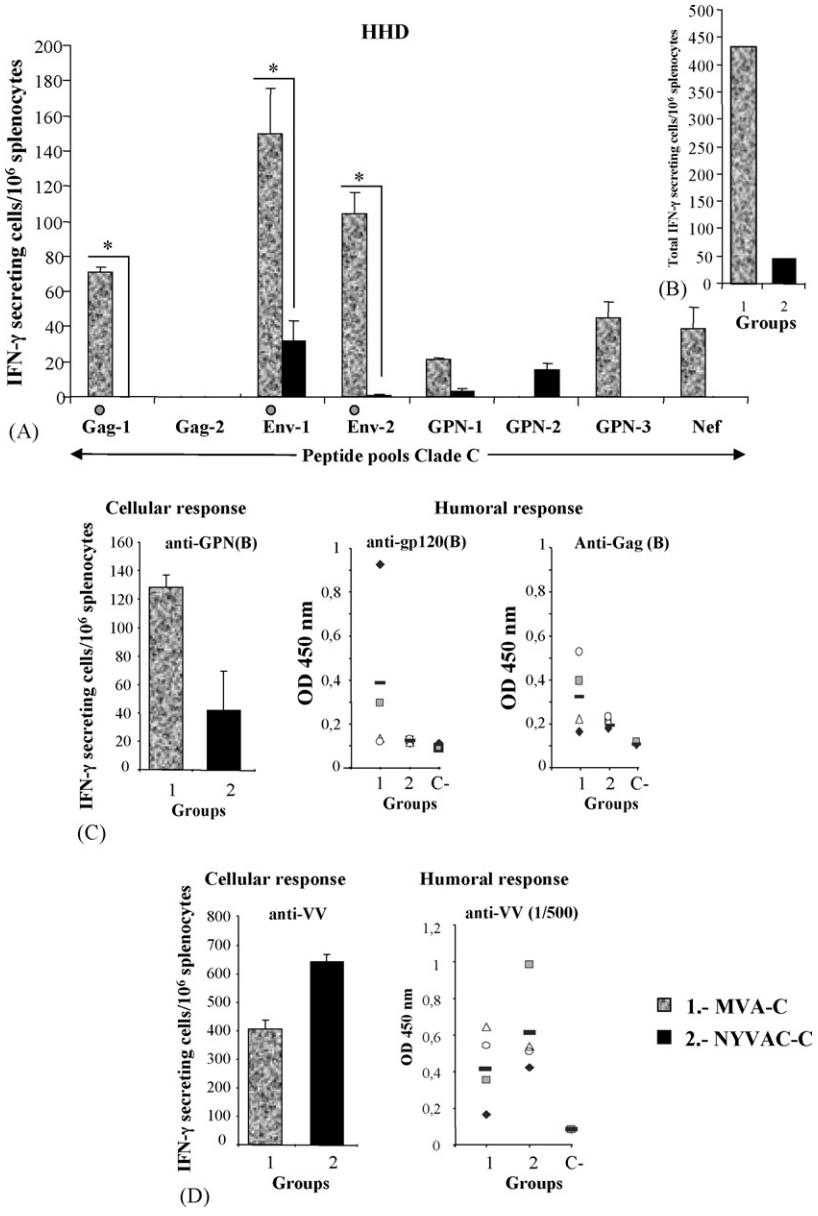

Fig. 5. Immunogenicity of MVA-C and NYVAC-C in HHD transgenic mice. (A) Cell-mediated immune response detected by fresh IFN-γ ELISPOT. Groups of 4 HHD transgenic mice were inoculated with 2×10^7 PFU of the corresponding rVV by i.p. route. Ten days later, the vaccine-elicited functional immune responses of splenocytes were measured in an IFN-γ ELISPOT assay following stimulation with 5 μg/mL of pools of overlapping peptides spanning the entire HIV-1 $_{CN54}$gp120 and $_{CN54}$GPN proteins. The number of spots obtained with the negative CTRL pool was subtracted in all cases. Peptide-specific IFN-γ secreting cells with standard deviation from triplicate cultures are shown. ○Statistically significant differences ($p < 0.05$) between each peptide pool and the CTRL pool. *Statistically significant differences ($p < 0.05$) between groups. (B) Magnitude of the total response for clade C pools. Bars represent the total number of antigen-specific IFN-γ secreting cells detected in each group against all the peptide pools spanning the Ags included in MVA-C and NYVAC-C recombinants. (C) Cross-reactive response against antigens from HIV-1 clade B. *Left panel*: Anti-GPN-B cellular response. Spleen cells from immunized animals were used as responder cells in the ELISPOT assay with EL4gpnHHD cells as targets. The number of spots obtained with control RMAS-HHD cells was subtracted in both groups. *Right panel*: Anti clade-B humoral response. Sera of mice were diluted at 1/50 and assayed in ELISA quantifying specific IgG Abs against $_{LAV}$gp160 and $_{SF2}$p55 Gag antigens from HIV-1 clade B. Sera from naïve mice were used as control group (C-). (D) Anti-VV immune response. Left panel: Anti-VV cellular response elicited against VV antigens. Spleen cells from immunized animals were used as responder cells in the ELISPOT assay with RMAS-HHD cells infected with either MVA-WT or NYVAC-WT as targets. The number of spots obtained with non-infected RMAS-HHD cells was subtracted. Right panel: Anti-VV humoral response. Sera of mice were diluted at 1/500 and assayed in ELISA quantifying specific IgG Abs against VV antigens. Sera from naïve mice were used as control group (C-).

Table 2
Cytokine production (pg/mL) by splenocytes from HHD mice immunized with MVA-C or NYVAC-C

A	MVA-C		NYVAC-C	
	IFN-γ	IL-10	IFN-γ	IL-10
Gag-1	2920	670	306	505
Gag-2	<20	590	166	292
Env-1	753	730	553	222
Env-2	1767	490	103	160
GPN-1	940	690	<20	132
GPN-2	883	395	<20	85
GPN-3	950	160	1256	97
NEF	<20	80	<20	57
Total	8213	3805	2384	1550
IFN-γ/IL-10	2.16		1.5	

HHD mice were immunized as described in Section 2. Ten days after the immunization the animals were sacrificed and their spleens were processed. The splenocytes from each group were stimulated in vitro with 2 μg/mL of different HIV-1 peptide pools from clade C and incubated for 6 days at 37 °C. Thereafter, cell supernatants were collected and stored at −70 °C. Cytokine levels were measured with specific commercial kits.

fied the levels of type 1 (IFN-γ) and type 2 (IL-10) cytokines in cell culture supernatants restimulated with specific HIV-1 peptide pools. As shown in Table 2, higher levels of IFN-γ were secreted against the different clade C pools by splenocytes from mice primed with MVA-C compared with NYVAC-C. The levels of IL-10 (as index of Th2) were also higher in MVA-C immunized mice, and the IFN-γ/IL-10 ratio obtained suggests induction of a Th1 type of immune response.

3.5. NYVAC-C efficiently boosts the response induced by priming with DNA-C in transgenic HHD mice

Since a DNA prime/rVV boost immunization regime has been shown to be an efficient vaccination approach in different animal models, specially in the ability to induce specific cellular immune responses to HIV antigens [41,42], we wished to evaluate the magnitude and breadth of the anti-clade C specific cellular response triggered in transgenic HHD mice using this strategy. For this purpose, groups of mice were first primed with two DNA vectors, one that expresses only HIV-1 Env ($_{CN54}$gp120), and the other expressing the Gag-Pol-Nef fusion protein from clade C (both vectors referred as DNA-C), and two weeks later the animals were boosted with the same dose of DNA-C (100 μg), or with 2×10^7 PFU of either MVA-C or NYVAC-C, both expressing the same antigens as DNA-C. Animals primed with sham DNA (DNA-ϕ) and boosted with NYVAC-WT were used as control. Vaccine-elicited functional immune responses of splenocytes were measured 10 days after the last immunization by fresh IFN-γ and IL-2 ELISPOT assays using pools of overlapping peptides specific to clade C of HIV-1. The number of spots obtained with the negative control (CTRL) pool was subtracted in all cases.

As shown in Fig. 6A, Env-1 and Env-2 peptide pools were efficiently recognized by splenocytes from mice immunized with DNA-C/MVA-C (group 1), DNA-C/NYVAC-C (group 2) or DNA-C/DNA-C (group 3) in contrast with the control group (DNA-ϕ/MVA-WT) where no specific response was detected ($p < 0.05$). The Gag-1 pool was immunogenic for animals boosted with MVA-C (group 1) or NYVAC-C (group 2), whereas GPN-2 and GPN-3 pools were only recognized by group 2 (DNA-C/NYVAC-C). The Gag-2, GPN-1 and NEF pools were poorly recognized. The magnitude of the total response for clade C pools, determined by the overall number of IFN-γ secreting cells was significantly higher in animals boosted with NYVAC-C ($p < 0.05$) (Fig. 6B).

To characterize in more detail the cellular immune response elicited in HHD mice using DNA/rVV approach, we performed a fresh IL-2 ELISPOT. As shown in Fig. 6C and A, the IL-2 and IFN-γ responses behaved similarly in the three groups. Env-1 and Env-2 pools were the most immunogenic epitopes, followed by Gag-1 and GPN-3. The total number of IL-2 secreting cells in the spleen of animals from group 2 (DNA-C/NYVAC-C) and group 3 (DNA-C/DNA-C) was higher than found in mice boosted with MVA-C (group 1), but not statistical differences were observed between the groups ($p > 0.05$) (Fig. 6D).

The Th type of immune response was also evaluated using all of the clade C peptide pools. As shown in Table 3, the total levels of IFN-γ found in the supernatants of stimulated splenocytes from groups 1 (DNA-C/MVA-C), 2 (DNA-C/NYVAC-C) and 3 (DNA-C/DNA-C) were higher than the levels of IL-10, demonstrating a clear polarization of the Th response towards a Th1-type. Similar to the ELISPOT results, animals boosted with NYVAC-C exhibited the highest magnitude and breath of the anti-clade C specific response.

3.6. Homologous and heterologous combinations of NYVAC-C and MVA-C recombinants efficiently improved the breadth of anti-clade C cellular immune response in BALB/c mice

Since competition or immunodominance between CTL epitopes would reduce the breadth of the total response induced by vaccination, next we determined if the breadth of HIV-1C specific response was increased by performing homologous and heterologous immunizations with a combination of MVA-C and NYVAC-C vectors. To this aim, we used BALB/c mice since in HHD mice there are a low proportion of total splenic CD8+T cells. Thus, BALB/c mice ($n = 5$) were inoculated intraperitoneally with 2×10^7 PFU of each recombinant virus at days 0 and 15, and 10 days after the last immunization the cellular immune response in splenocytes was evaluated by fresh IFN-γ ELISPOT.

As shown in Fig. 7A, heterologous (groups 1 and 2) and homologous (groups 3 and 4) combinations of MVA-C and NYVAC-C recombinants induced a significant enhancement of splenic T-cell response against the clade C peptide pools

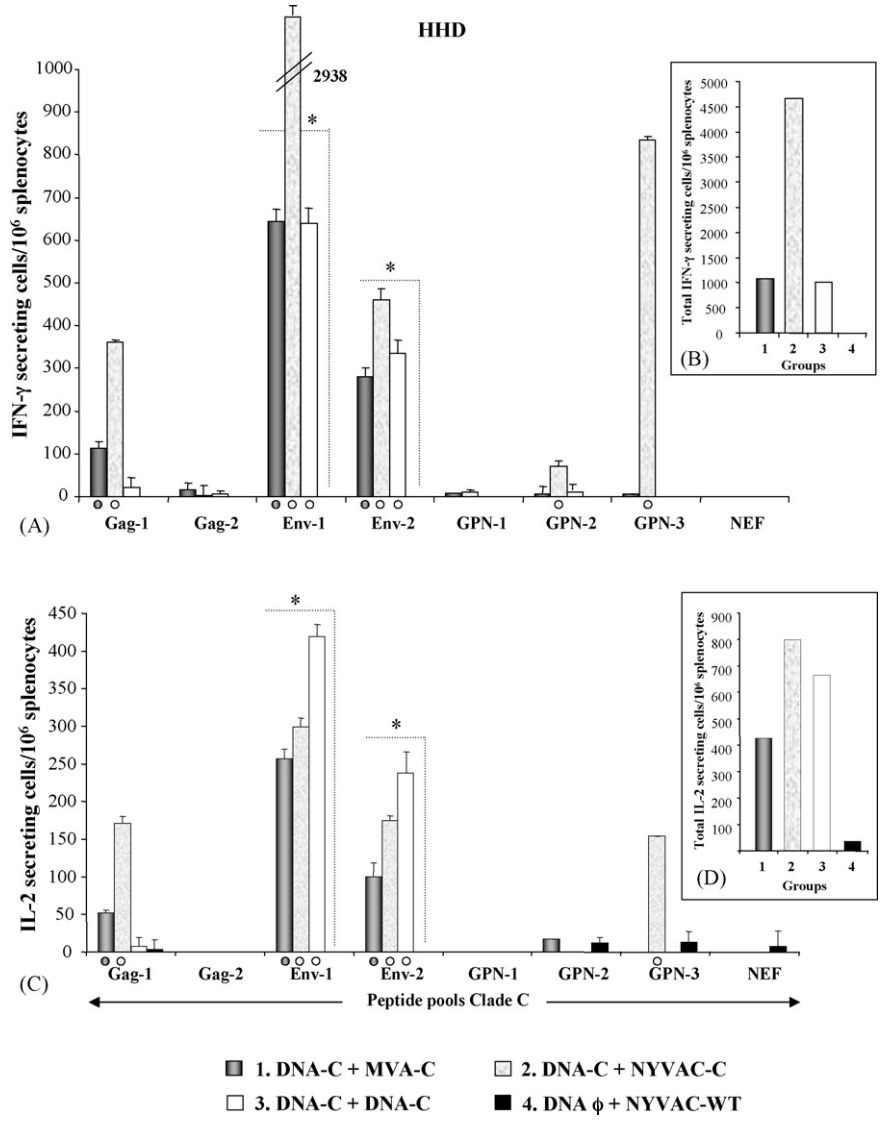

Fig. 6. Immunogenicity of MVA-C and NYVAC-C after DNA/rVV prime–boost protocol in HHD transgenic mice. (A) Cell-mediated immune response detected by fresh IFN-γ ELISPOT. Groups of 4 HHD transgenic mice were primed with 100 μg of either DNA-C or sham DNA (DNA-ϕ) by intramuscular route. Two weeks after priming, the mice received the same dose of DNA-C or an intraperitoneal inoculation of 2×10^7 PFU of the corresponding rVV. Vaccine-elicited functional immune responses of splenocytes were measured 10 days after the last immunization in an IFN-γ ELISPOT assay following stimulation with 5 μg/mL of pools of overlapping peptides spanning the HIV-1 $_{CN54}$gp120 and $_{CN54}$GPN proteins. The number of spots obtained with the negative CTRL pool was subtracted in all cases. Peptide-specific IFN-γ secreting cells with standard deviation from triplicate cultures are shown. ○Statistically significant differences ($p < 0.05$) between each peptide pool and the CTRL pool. *Statistically significant differences ($p < 0.05$) between groups. (B) Magnitude of the total response for clade C pools. Bars represent the total number of antigen-specific IFN-γ secreting cells detected in each group against all of the peptide pools spanning the Ags included in MVA-C and NYVAC-C recombinants. (C) Cell-mediated immune response detected by fresh IL-2 ELISPOT. The IL-2 response against clade C peptide pools in splenocytes from immunized animals was determined as previously described. The number of spots obtained with the negative CTRL pool was subtracted in all cases. Peptide-specific IL-2 secreting cells with standard deviation from triplicate cultures are shown. ○Statistically significant differences ($p < 0.05$) between each peptide pool and the CTRL pool. *Statistically significant differences ($p < 0.05$) between groups. (D) Magnitude of the total response for clade C pools. Bars represent the total number of antigen-specific IL-2 secreting cells detected in each group against all the peptide pools spanning the Ags included in MVA-C and NYVAC-C recombinants.

Env-1, GPN-1, GPN-2 and GPN-3, in comparison with mice immunized either with NYVAC-WT/MVA-WT (group 5) or with MVA-WT/NYVAC-WT (group 6) used as controls ($p < 0.05$). Animals from group 4 (NYVAC-C/NYVAC-C) failed to recognize the Gag-1 pool, which was efficiently identified by the rest of the groups. Interestingly, the combination of NYVAC-C/MVA-C (group 2) also recognized the Gag-2 peptide pool.

The magnitude of the total response, determined by the overall number of IFN-γ secreting cells (Fig. 7B), and the breadth of the clade C-specific response per group, as measured by the number of positive pools, were higher in mice

Table 3
Cytokine production (pg/mL) by splenocytes from HHD mice inoculated in DNA-C prime/rVV-C boost regime

A (pg/mL)	Gag-1	Gag-2	Env-1	Env-2	GPN-1	GPN-2	GPN-3	NEF	Total
DNA-C/MVA-C									
IFN-γ	2600	230	12700	11700	120	<20	<20	<20	27350
IL-10	180	30	340	250	70	60	600	<10	1530
DNA-C/NYVAC-C									
IFN-γ	14100	1670	39100	14100	<20	480	8040	<20	77490
IL-10	100	<10	<10	<10	<10	<10	<10	<10	100
DNA-C/DNA-C									
IFN-γ	1420	<20	33500	26500	1300	<20	<20	<20	62720
IL-10	50	30	630	640	<10	<10	<10	<10	1350
DNA-ϕ/NYVAC-WT									
IFN-γ	886	<20	<20	<20	<20	<20	<20	<20	886
IL-10	<10	<10	<10	<10	<10	<10	<10	<10	<10

HHD mice were immunized as described in Section 2. Ten days after the last immunization the animals were sacrificed and their spleens were processed. The splenocytes from each group were stimulated in vitro with 2 μg/mL of different HIV-1 peptide pools from clade B and incubated for 6 days at 37 °C. Thereafter, cell supernatants were collected and stored at −70 °C. Cytokine levels were measured with specific commercial kits.

primed with NYVAC-C and boosted with MVA-C recombinant (group 2). Animals receiving two doses of NYVAC-C (group 4) gave the lower number of total IFN-γ secreting cells.

We also examined the profile of cytokines produced by splenocytes from these mice after culturing with 2 μg/mL of each peptide pool. As shown in Table 4, all of the combinations assayed induced an evident Th1 type immune response characterized by elevated levels of IFN-γ and low or undetectable levels of IL-10. Interestingly, groups receiving heterologous NYVAC-C/MVA-C (group 2) or homologous MVA-C/MVA-C (group 3) combinations induced higher levels of INF-γ and broader reactive cellular responses in comparison with groups immunized with MVA-C/NYVAC-C (group 1) or NYVAC-C/NYVAC-C (group 4).

In addition, we examined by Western blot and ELISA the antibody responses elicited in BALB/c and HHD mice after vaccination with the combination of the poxvirus vectors. As shown in Fig. 8, panels A and B, in both animal models sera from MVA-C infected animals recognized similar VV (WR strain) proteins than sera from NYVAC-C infected mice, although differences in antibody recognition of the VV proteins were observed between the vectors. The extent of reactivity and pattern of VV proteins recognized by sera from infected HHD mice was distinct from the pattern seen in infected BALB/c mice. The anti-vector antibodies, as determined by ELISA, were markedly boosted by a second dose of the poxvirus vectors (Fig. 8, panel C). In BALB/c mice the anti-VV antibodies levels were reduced in NYVAC-C compared to MVA-C (Fig. 8, panel D) while in HHD mice the opposite was observed (panel C). The differences in VV antigen recognition by sera from mice vaccinated with MVA-C versus NYVAC-C is probably due to the inability of NYVAC to synthesize some of the late viral proteins, as previously described in cultured cells [38].

3.7. Heterologous combinations of SFV-C prime and MVA-C or NYVAC-C boost significantly enhanced T cell responses to clade C in BALB/c mice

In view of the enhanced breath of the immune response elicited by homologous poxvirus vectors and to reduce cross-reactive immune responses to the pox vector after boosting, next we analyzed the immunogenicity of prime/boost combination with alphavirus and poxvirus vectors. Since vaccination of humans by choice usually is given either intramuscularly (i.m.) or subcutaneously (s.c.), we chose the i.m. route of administration for the pox and the s.c. route for SFV. BALB/c mice ($n = 8$) mice were first inoculated on days 0 and 14 with 1×10^7 PFU of either MVA-C or NYVAC-C or 1×10^7 IU of SFV-C (5×10^6 each of SFV-GPN and SFV-env), with SFV-LacZ (1×10^7 IU) serving a negative control. Ten days after the boost cellular immune responses were measured by fresh IFN-γ ELISPOT. As shown in Fig. 9A, homologous combinations of the three vaccines, MVA-C/MVA-C, NYVAC-C/NYVAC-C and SFV-C/SFV-C, generated approximately the same responses, the GPN-1 and GPN-2 pools being the most recognized by all groups. The Env-1 pool was significantly immunogenic in both poxvirus vaccines.

Since dose sparing are of value considering potential future vaccination of the human population we repeated the heterologous prime–boost experiments keeping SFV-C prime at the original dose but lowering the booster doses of the poxvirus stepwise by a factor of 10. As shown in Fig. 9B and C, these combinations of SFV/pox significantly enhanced the T cell responses at all doses and in both groups, SFV-C/MVA-C and SFV-C/NYVAC-C, the responses against GPN-1, GPN-2 and Env-1 were again most prominent. Interestingly, lowering the booster dose with one or even two logs did not greatly reduce the final T cell responses and reducing the boost 3 logs still resulted in T cell responses that were

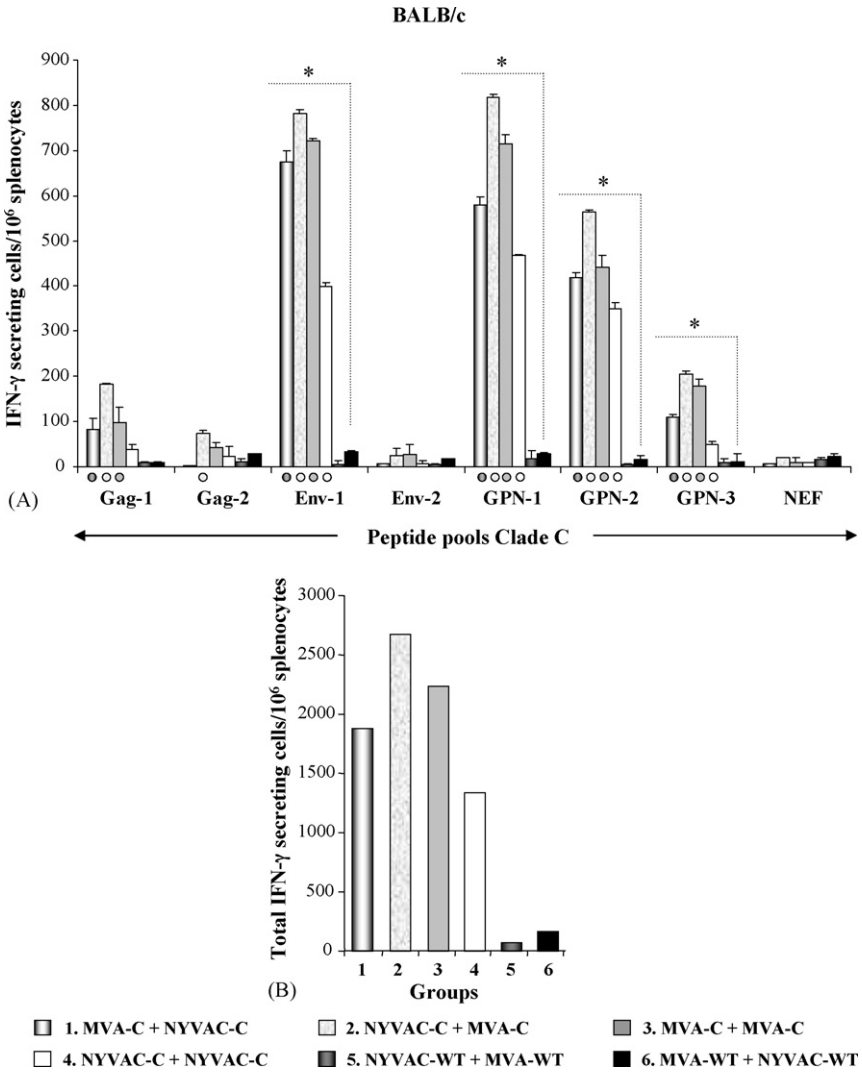

Fig. 7. Cellular immune response elicited in BALB/c mice after inoculation with homologous and heterologous combinations of MVA-C and NYVAC-C recombinants. (A) Cell-mediated immune response detected by fresh IFN-γ ELISPOT. Groups of 5 BALB/c mice were inoculated intraperitoneally with 2×10^7 PFU of each recombinant at day 0 and 15. Vaccine-elicited functional immune responses of splenocytes were measured 10 days after the last immunization in an IFN-γ ELISPOT assay following stimulation with 5 μg/mL of pools of overlapping peptides spanning the HIV-1 $_{CN54}$gp120 and $_{CN54}$GPN proteins. The number of spots obtained with the negative CTRL pool was subtracted in all cases. Peptide-specific IFN-γ secreting cells with standard deviation from triplicate cultures are shown. ○Statistically significant differences ($p < 0.05$) between each peptide pool and the CTRL pool. *Statistically significant differences ($p < 0.05$) between groups. (B) Magnitude of the total response for clade C pools. Bars represent the total number of antigen-specific IFN-γ secreting cells detected in each group against all the peptide pools spanning the Ags included in MVA-C and NYVAC-C recombinants.

significantly stronger than homologous prime–boost with two poxvirus vectors. Fig. 9D summarizes the T cell responses cumulatively for peptide pools used. Overall SFV-C plus MVA-C responses appeared to be lower in magnitude compared to SFV-C plus NYVAC-C responses, while the breadth was similar in prime/boost between SFV/pox and pox/pox vectors.

4. Discussion

In this study we have generated, characterized in vitro and defined the immunogenicity in mice of two novel attenuated poxvirus recombinants MVA-C and NYVAC-C, which are vaccine candidates against HIV/AIDS. Since the stimulation of an efficient and broad anti-HIV-1 T cell immune response has been widely demonstrated by multigenic vaccines including structural and regulatory HIV-1 proteins [29,43,44], we included the *env*, *gag*, *pol* and *nef* genes in our immunogens. MVA-C and NYVAC-C expressed in the same viral TK locus the Env (gp120) and Gag-Pol-Nef HIV-1 antigens from the Asian primary isolate CN54 (clade C). Both gene cassettes have been codon optimized and designed for optimal expression levels, combined with extensive safety mutations in relevant gene fragments (see Appendix A, DNA sequence of MVA-C). These antigens represent the major HIV-1C pro-

Table 4
Cytokine production (pg/mL) by splenocytes from BALB/c mice immunized with homologous and heterologous combination of MVA-C and NYVAC-C

(A (pg/mL)	Gag-1	Gag-2	Env-1	Env-2	GPN-1	GPN-2	GPN-3	NEF	Total
MVA-C/NYVAC-C									
IFN-γ	290	2050	43400	330	21800	2510	1510	<20	71890
IL-10	<10	<10	<10	340	500	<10	<10	<10	840
NYVAC-C/MVA-C									
IFN-γ	60	14700	89100	3250	113800	29900	80	<20	250890
IL-10	110	240	<10	<10	320	320	<10	230	1220
MVA-C/MVA-C									
IFN-γ	1170	15100	74500	3920	95100	15500	<20	350	205290
IL-10	230	80	<10	60	280	<10	50	<10	700
NYVAC-C/NYVAC-C									
IFN-γ	<20	<20	42200	<20	12800	<20	<20	<20	55000
IL-10	50	50	210	80	220	<10	<10	<10	610
NYVAC-WT/MVA-WT									
IFN-γ	1280	<20	8170	<20	3990	425	80	<20	13945
IL-10	<10	<10	60	190	25	<10	<10	<10	275
MVA-WT/NYVAC-WT									
IFN-γ	1308	720	2060	4000	<20	160	<20	<20	8248
IL-10	<10	<10	290	230	<10	<10	<10	<10	520

BALB/c mice were immunized as described in Section 2. Ten days after the last immunization the animals were sacrificed and their spleens were processed. The splenocytes from each group were stimulated in vitro with 2 μg/mL of different HIV-1 peptide pools from clade B and incubated for 6 days at 37 °C. Thereafter, cell supernatants were collected and stored at −70 °C. Cytokine levels were measured with specific commercial kits.

teins included in the vaccine candidates currently tested in clinical trials [29].

Some of the key features considered to be desirable in a poxvirus based vaccine included, replication to high yields in CEF, high levels of gene expression for the recombinant product, stability of the insert with prolonged passages of the vector and good immunogenicity of the foreign antigens. Here we demonstrated that MVA-C and NYVAC-C meet each of these criteria. The generated MVA-C and NYVAC-C efficiently express the heterologous $_{CN54}$gp120 and $_{CN54}$GPN proteins could be passage without the loss of the transgene and grew efficiently in CEF cells. However, in contrast to MVA-C, the NYVAC-C vector induces a potent apoptosis in human cells. Moreover, human gene profiling analysis of the parental strains NYVAC and MVA have revealed similarities but also clear differences in immunomodulatory genes such as IL-7, IL-1A, IL-8 and IL-15 (only increased in MVA-infected cells) while apoptotic pathways which may favour cross-presentation are increased only in NYVAC-infected cells [39]. By microarray analysis we have also observed clear differences in immunomodulatory genes induced by NYVAC versus MVA in virus-infected human dendritic cells (Guerra et al., manuscript in preparation). These and other biological differences exhibited in vitro by MVA and NYVAC strains [38], may have an impact on the immunogenicity and clinical application of these poxvirus vectors.

The majority of recent HIV-vaccine studies have aimed to develop T-cell-stimulating vaccines that induce HIV-specific CD8+ CTL responses, whose role in the control of virus load and evolution of disease has been well-documented [15,16,21–23]. Although vaccines that only stimulate the cellular arm of the immune response are not expected to provide protection against infection, they might control virus replication and reduce viral loads, thus resulting in lower probability of virus transmission to seronegative partners. In this report we have evaluated the cellular immune response induced in transgenic HHD and BALB/c mice by different novel (DNA, pox and SFV vectors) vaccine candidates expressing the Env, Gag, Pol and Nef HIV-1 antigens from clade C. We first analyzed the effect of a single inoculation of either MVA-C or NYVAC-C in transgenic HHD mice. We showed that in contrast to NYVAC-C, MVA-C stimulated an specific cellular immune response against the clade C peptide pools Env-1, Env-2 and Gag-1 as revealed in the fresh IFN-γ ELISPOT results. In addition, we showed that MVA-C also induces an efficient cross-reactive response against HIV-1 antigens from clade B. However, the cellular immune response against vaccine vector antigens was 1.6 fold higher in NYVAC-C immunized animals. The superiority of MVA-C in inducing a specific anti-HIV immune response after a single immunization might be related with the capacity of this virus to activate the host innate immune response. MVA induces cellular infiltration and induction of cytokines such as type I IFNs, TNF-α, and IL-6 [45], probably through TLR-mediated signalling which may lead to increased uptake and presentation of encoded and delivered antigen. Moreover, despite the ability of poxviruses to impair dendritic (DC) maturation in vitro, the important ability of MVA to boost CD8 T-cell response *in vivo* is mediated at the

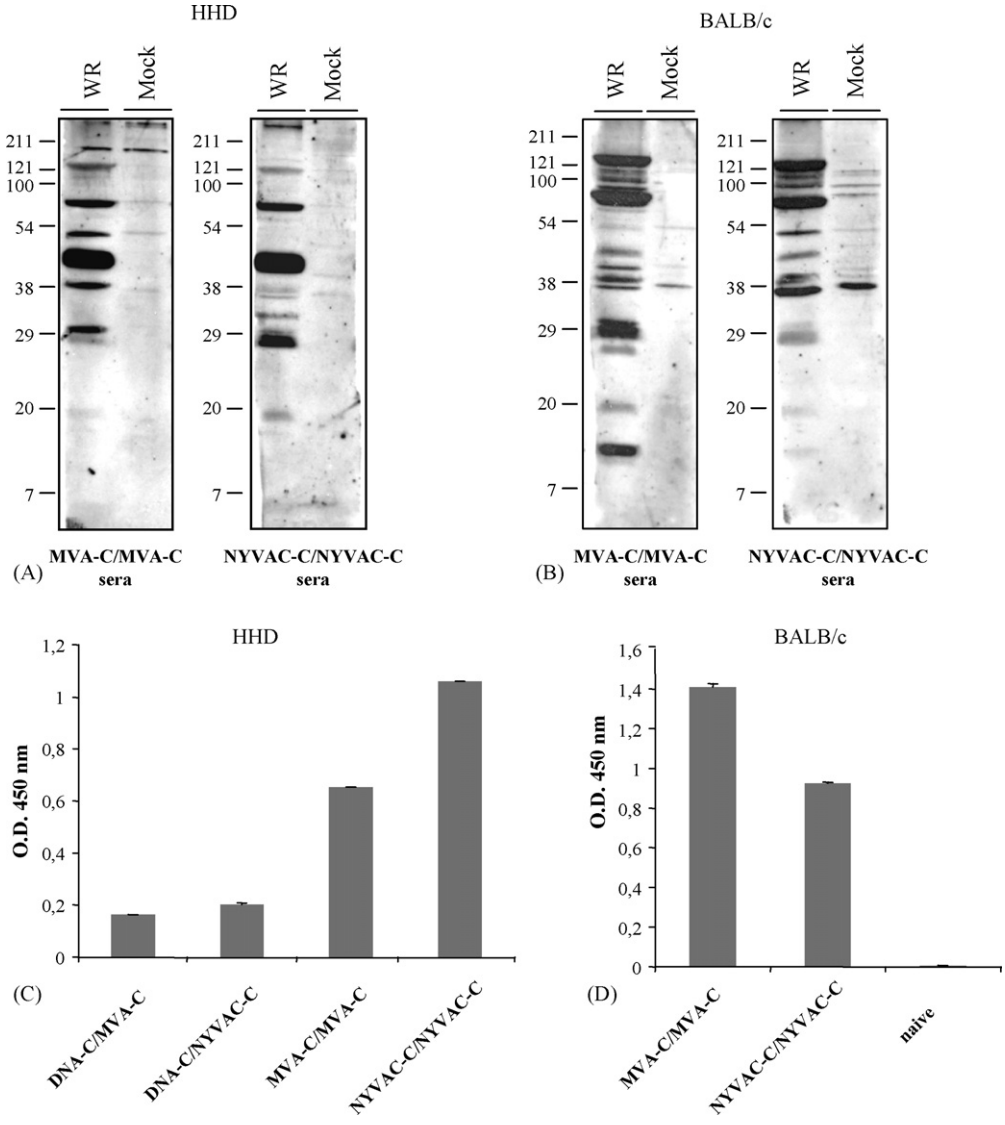

Fig. 8. Humoral immune response elicited in mice by the recombinant poxvirus vectors. Groups of BALB/c and HHD mice inoculated by the protocol DNA-C prime/pox boost (Fig. 6, groups 1 and 2) and by the pox/pox combination (Fig. 7, groups 3 and 4). Ten days after the last immunization, blood was collected and serum samples pooled from the animals. Evaluation of antibody reactivity by Western blot in HHD mice with sera at 1:100 dilution (A) and in BALB/c mice with sera at 1:200 dilution (B). Sera was used in Western blots with extracts obtained at 24 h from WR-infected and uninfected (Mock) BSC-40 cells. The molecular masses in kDa of marker proteins are indicated to the left of the gels. Evaluation of antibody levels by ELISA from sera of HHD (C) and BALB/c (D) mice immunized with the different protocols indicated at the bottom of the figure. The sera for all samples were used at 1:500 dilution.

level of the infected DC. MVA affect DCs *in vivo* by inducing their activation and maturation [46]. We do not discard the possibility that NYVAC-C might also activate the host innate immune response pathways, but this effect remains to be determined.

The experience gained so far with the first generation of HIV-1 vaccine candidates has been that many were modestly immunogenic and only induced short-lived immune responses [47]. One of the strategies used over the last decade to increase their immunogenicity was to combine these vaccines in prime–boost vaccination regimens. Vaccination strategies in which a DNA prime is boosted with a poxvirus vector are especially effective and have emerged as the predominant approach for eliciting protective CD8+ T cell immunity [24,41,42,48–50]. In this study we compared the immune response elicited in transgenic HHD mice primed with DNA vectors expressing the HIV-1 Env ($_{CN54}$gp120), and Gag-Pol-Nef antigens from clade C (referred as DNA-C) and boosted with either the poxvirus vectors (MVA-C and NYVAC-C) or with the same dose of DNA-C. We showed that prime–boost immunization scheme employing a naked DNA-C vector at priming and NYVAC-C at booster was an effective immunization protocol to induce specific cellular immune responses against HIV-1 peptide pools spanning Env and Gag HIV-1 antigens. When we analyzed the intrinsic cellular response directed against peptides represented in

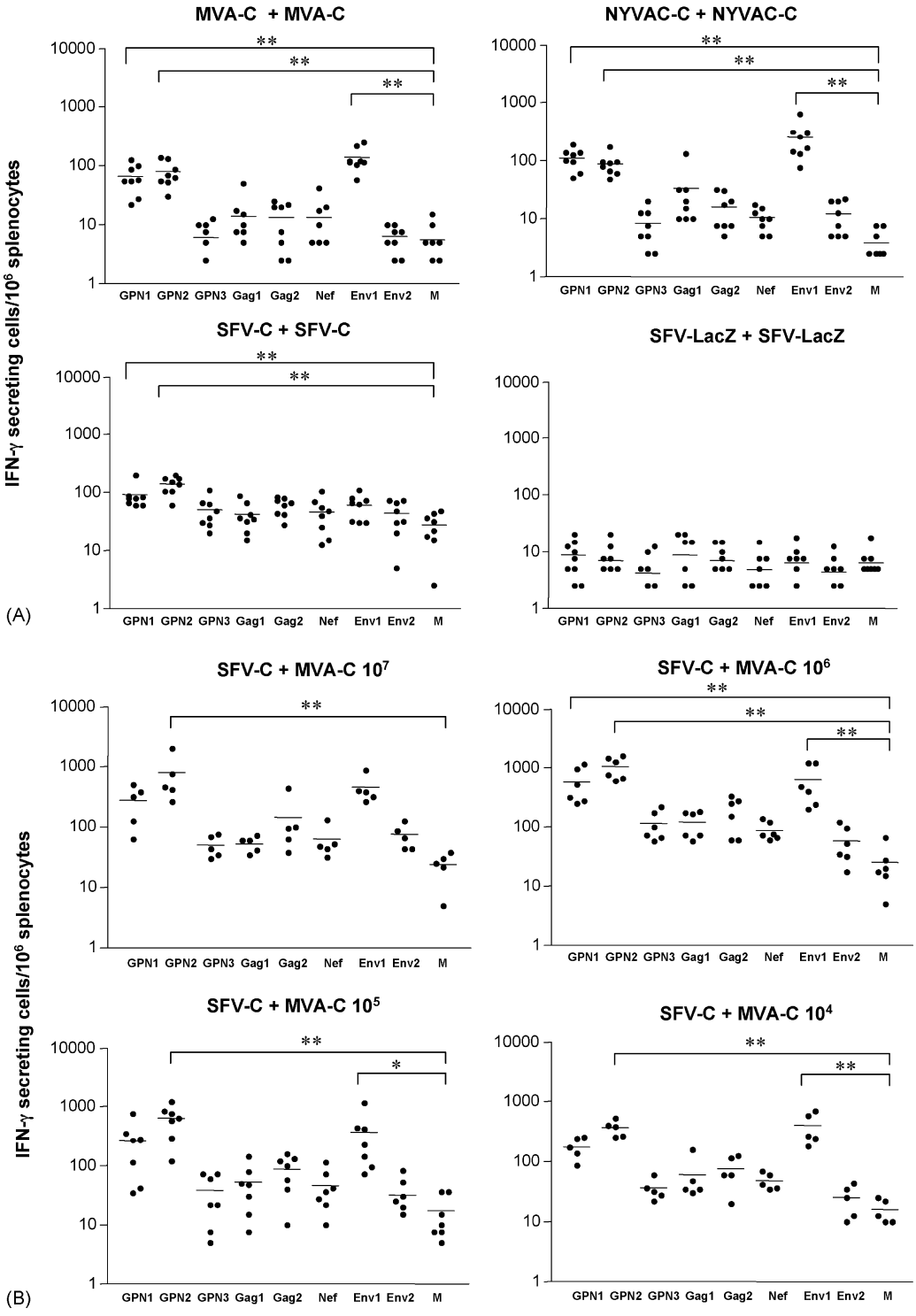

Fig. 9. Immune responses elicited in BALB/c mice after subcutaneous inoculation with homologous combinations of MVA-C or NYVAC-C or heterologous combination of SFV-C and MVA-C or NYVAC-C. (A) Statistical significance by one-way analysis of variance test: MVA-C/MVA-C: GPN1, GPN2 and Env1 vs. medium control, $p < 0.01$. NYVAC-C/NYVAC-C: GPN1, GPN2 and Env1 vs. medium, $p < 0.01$, $p < 0.05$ and $p < 0.01$, respectively. SFV-C/SFV-C: GPN1 and GPN2 vs. medium control, $p < 0.01$, respectively. (B) SFV-C/MVA-C (10^7): GPN2 vs. medium control, $p < 0.01$ SFV-C/MVA-C (10^6): GPN1, GPN2 and Env1 vs. medium, $p < 0.01$, $p < 0.01$ and $p < 0.01$, respectively. SFV-C/MVA-C (10^5): GPN2 and Env1 vs. medium control, $p < 0.01$ and $p < 0.05$, respectively. SFV-C/MVA-C (10^4): GPN2 and Env1 vs. medium control, $p < 0.01$. (C) SFV-C/NYVAC-C (10^7): GPN1, GPN2 and Env1 vs. medium control, $p < 0.01$. SFV-C/NYVAC-C (10^6): GPN1, GPN2 and Env1 vs. medium, $p < 0.01$. SFV-C/NYVAC-C (10^5): GPN1, GPN2 and Env1 vs. medium control, $p < 0.01$. SFV-C/NYVAC-C (10^4): GPN1, GPN2 and Env1 vs. medium control, $p < 0.01$. (D) Magnitude of total responses shown cumulatively. Homologous prime–boost results for SFV-C (S) MVA-C (M) and NYVAC-C (N) are shown and for the heterologous SFV-C prime poxvirus-C boost experiments the dilution factor are indicated below the bars. Numbers of top of bars indicate incremental factors over responses of corresponding poxvirus homologous prime–boost results.

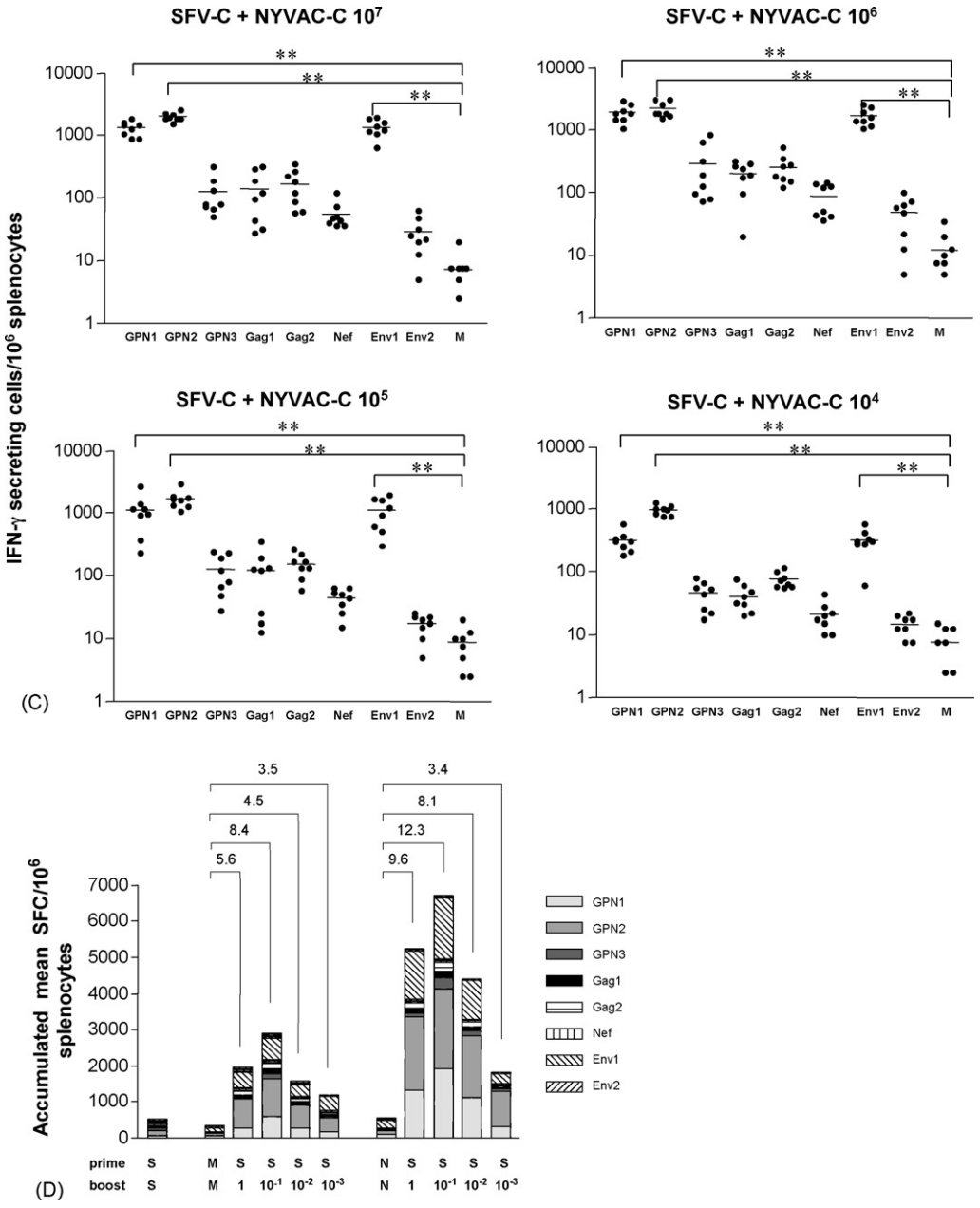

Fig. 9. (*Continued*).

each individual pool, we observed significant differences between them. Env-1 and Env-2 pools were the most immunogenic in the three groups of immunized mice. It has been reported that the immunological dominance between CTL epitopes would effectively reduce the breadth of the total response induced by vaccination [51,52]. In our case, the immunodominance exhibited by Env peptide pools might affect the recognition of the rest of peptide pools spanning the other HIV-1 antigens included in the candidate vaccines. When prime/boost was carried out with homologous and heterologous combinations of the poxvirus vectors in BALB/c mice, the heterologous NYVAC-C/MVA-C combination induced the highest and broadest cellular immune response. Interestingly, in this immunization approach the immunodominance of Env peptide pools was not observed. The GPN-1, GPN-2 and GPN-3 peptide pools were as efficiently recognized as the Env-1 peptide pools, whereas no specific response was detected against the Env-2 peptide pool. This result could be relevant in the design of an effective immunization protocol since it has been demonstrated that vaccines with very narrow CMI responses directed against one or a couple of epitopes can, over time, lose protective efficacy due to escape mutants of the infectious agent [19,53].

That the quality of the immune response obtained in prime/boost protocols using two different live recombinant vectors expressing the same HIV-1 antigens is better than homologous combination has been suggested by different groups. The use of strategies such as Ad5 vector followed by a poxvirus vector [54], or SFV vector followed by MVA [55], or VSV vector followed by MVA [56], or two successive adenovirus vectors, such as Ad11 and Ad35 [57], or two successive poxviruses, such as MVA and FPV (whose combination has been tested in Phase I trials in the USA and Brazil by Therion in collaboration with the NIAIDS), have extensively demonstrated the superiority of heterologous prime–boost regimens in inducing an efficient immune response. Our results indicate that combinations with MVA and NYVAC vectors, like NYVAC-C/MVA-C, that we have shown triggered a broad immune response to HIV-1C antigens, should be further explored in other animal models and humans. In this regard, the reduced antibody response to some late VV proteins raised in mice against NYVAC compared to MVA and the enhanced apoptosis induced by NYVAC might favour a NYVAC-C/MVA-C prime/boost combination.

The use of heterologous vectors to prime the immune response elicited by the two poxvirus vectors at boosting has also been examined with the alphavirus SFV. An enhanced cellular immune response over that elicited by the homologous poxvirus vectors was obtained in prime/boost with SFV-C/poxvirus. Under those conditions, both the breadth and magnitude of the HIV-1C response was enhanced over the homologous poxvirus vector combinations. In contrast with the DNA/poxvirus combinations, where Env-1, Env-2 and Gag-1 were the most antigenic peptides, for both homologous pox prime–boost and for heterologous SFV-pox prime–boost, the most antigenic peptides were GPN-1, GPN-2 and Env-1.

We have recently reported in mice a head-to-head comparison on the immunogenicity of MVA and NYVAC recombinants expressing the four HIV-1 antigens (gp120/Gag-Pol-Nef) from clade B [58]. A side-to-side comparison on the results presented in this study obtained with HIV-1 clade C antigens with respect to the analysis of the immune response to MVA and NYVAC expressing HIV-1 clade B antigens [58], revealed that the poxvirus recombinants behaved similarly in vitro and *in vivo* systems. In a DNA prime/poxvirus boost protocol, the Env peptide pools were immunodominant for both HIV-1 clades B and C, whereas in an homologous or heterologous combination of poxvirus vectors the breath of the immune response was, in addition to Env, expanded for the GPN pools. These observations could be interpreted in the way that when poxvirus vectors are used as booster, the priming vector DNA, SFV or pox influences the type of immune response. However, since these studies involved two different strains of mice (BALB/c and HHD) such conclusions must await further studies.

For HIV and most other viruses, induction of Th1 type response, characterized by the production of IL-12, IL-2 and IFN-γ is more likely to provide protection than induction of Th2 type response characterized by the production of IL-4, IL-5, IL-10, IL-13 [59]. In our case, the pattern of cytokine secretion after restimulation with the clade C peptide pools indicated that the different protocols assayed induced a Th1 type response.

Will the vectors generated in this study have utility as HIV/AIDS vaccines? There are several considerations in favour. First, similar MVA and NYVAC vectors as those described here but expressing HIV-1 89.6p *env* and SIVmac239GPN have been generated and shown in a DNA prime/pox boost protocol to elicit protection in macaques after a challenge with SHIV89.6p (Mooj, P et al., manuscript in preparation). Second, a phase I clinical trial conducted by EuroVacc using prime/boost with NYVAC-C indicated that the recombinant vector was safe and immunogenic (see www.EuroVacc.org). Third, another phase I clinical trial by EuroVacc in a DNA-C/NYVAC-C prime/boost protocol showed high immunogenicity of the vectors (manuscript in preparation). Thus, the results obtained in this investigation highlight the immunological relevance of the attenuated poxvirus vectors MVA-C and NYVAC-C as vaccine candidates against HIV/AIDS.

Acknowledgments

This investigation was supported by research grants from the EU (EuroVac QLRT-PL-1999-01321), the Spanish Ministry of Education and Science BIO2004-03954, the Spanish Foundation for AIDS Research (FIPSE 36344/02) and Fundación Marcelino Botín. J.L. Nájera was supported from FIPSE.

Appendix A. DNA sequence of MVA-C in the TK viral locus

```
|   10    |   20    |   30    |   40    |   50    |   60

AAGCTTTTGC GATCAATAAA TGGATCACAA  CCAGTATCTC TTAACGATGT TCTTCGCAGA 60
TGATGATTCA TTTTTTAAGT ATTTGGCTAG  TCAAGATGAT GAATCTTCAT TATCTGATAT 120
ATTGCAAATC ACTCAATATC TAGACTTTCT  GTTATTATTA TTATTGATCC AATCAAAAAA 180
TAAATTAGAA GCCGTGGGTC ATTGTTATGA  ATCTCTTTCA GAGGAATACA GACAATTGAC 240
AAAATTCACA GACTCTCAAG ATTTTAAAAA  ACTGTTTAAC AAGGTCCCTA TTGTTACAGA 300
TGGAAGGGTC AAACTTAATA AAGGATATTT  GTTCGACTTT GTGATTAGTT TGATGCGATT 360
CAAAAAAGAA TCCTCTCTAG CTACCACCGC  AATAGATCCT ATTAGATACA TAGATCCTCG 420
TCGCGATATC GCATTTTCTA ACGTGATGGA  TATATTAAAG TCGAATAAAG TGAACAATAA 480
TTAATTCTTT ATTGTCATCA TGGGTACCAA  GGCGCGATCG CATTTTCTAA CGTGATGGAT 540
ATATTAAAGT CGAATAAAGT GAACAATAAT  TAATTCTTTA TTGTCATCAT GTAATTAACT 600
AGCTACCCGG AATAAAAATT CCGGGAGATC  TCTCGAGAGA TCTTTATCAC CTCTTCTCCC 660
TCTCCACCAC CCTCCTCTTG GTGGTGGTGG  GGGCCACGCC CAGGGGCTTG ATCTCCACCA 720
CCTTGTACTT GTACAGCTCG CTCCTCCAGT  TGTTCCTCAT GTCGCCGCCG CCGGGCCTGA 780
AGGTCTCGGT GTCGTTGGGC TCGGTGCCGC  CGTCCCTCAC CAGCAGCAGG CCGGTGATGT 840
TGCTCTTGCA GGTGATGTTG CCCTTGATGG  GAGGGGCGTA CATGGCCCTG CCCACCTCCT 900
GCCACATGTT GATGATCTGC TTGATCCTGC  AGGGGATGGT GATGATGCTG CTGCTGTTGC 960
TCTTGGTGCC GTTGGGGGTG TAGGCGCCGT  TGAACAGGCC GCTGGTGTTG CAGTAGAAGA 1020
ACTCGCCCCT GCAGTTGAAG CTGTGGGTGG  TCACCTCCAG GTCGCCGCCG CTGCTGCTGG 1080
CGAACTTGAT GGTCTTGTTC TGGAAGTGCT  CGGCAAGCTT CTTGCTCACC CTCTGCAGGG 1140
TCTCGTTCCA CTTGTCCTCG CTGATGTTGC  AGTGGGCCTG CCTGATGTCG CCGATGATGT 1200
CGCCGGTGGC GTAGAAGGTC TGGCCGGGGC  CGATCCTGAT GCTCTTCCTG GTGTTGTTGC 1260
CGGGCCTGGT GCACACGATC TCCACGCTCT  GGTTCAGGTG CACGATGATG GTTTTCACGT 1320
TGTTGGTCAG GTTCTCGCTC CTGATGATGA  TCTCGCCCTC GGCCAGGCTG CCGTTCAGCA 1380
GCAGCTGGGT GCTCACCACG GGCTTGATGC  CGTGGGTGCA CTGCACGGTG CTCACGTTGT 1440
GGCAGGGGCC GGTGCCGTTG AAGATCTTGT  CGTTGCACTT CAGGATGGCG TAGCCGGCGG 1500
GGGTGCAGTA GTGGATGGGG ATGGGGTCGA  AGGTCACCTT GGGGCAGGCC TGGGTGATGG 1560
CGCTGGTGTT GCAGTTGATC AGCCTGTAGT  ACTCGCTGCT GTTCTCGCTG TAGTTCTTCT 1620
TGGTCAGGGG CACGATGTCC AGCCTGTAGA  ACAGGGCGTA CACGGTCTGC TTCCTGTCCC 1680
TCACCACGGT GGTGGCGTTG AAGCTGCAGT  TCTTCATCTC CTTCATGCTC TCGTGGTAGG 1740
TCTCGTGGTA GGTGTCGTTG CTGTTGCTGC  TCACGTTCCT GCACTCCAGG GTCACGCACA 1800
GGGGGGTCAG CTTCACGCAG GGCTTCAGGC  TCTGGTCCCA CAGGCTGATG ACGTCCTCCT 1860
GCATCTGGTT CACCATCTCG TTCTTCCACA  TGTTGAAGTT CTCGGTCACG TTCTCCAGCA 1920
CCATCTCCTG GGGGTTGGGG TCGGCGGGCA  CGCAGGCGTG GGTGGCCCAC ACGTTGTGCA 1980
CCTCGGTGTC GTAGGCCTTG GCGTCGCTGG  CGCAGAACAG GGTGGTGGTG GCGCCCTTCC 2040
ACACGGGCAC GCCGTAGTAC ACGGTCACCC  ACAGGTTGCC CACGGCCTGG GCCTGGGGCA 2100
GCAGCAGCAG CAGCAGCAGC AGCAGCAGCT  TGGGCCTGTC CATGCTCGAG CTTATTTATA 2160
TTCCAAAAAA AAAAAATAAA ATTTCAATTT  TTAAGCTTGT CGACAAAAAT TGAAATTTTA 2220
TTTTTTTTTT TTGGAATATA AATAGACTCG  AGCATGGCCG CCAGGGCCAG CATCCTGAGG 2280
GGCGGCAAGC TGGACAAGTG GGAGAAGATC  AGGCTGAGGC CCGGCGGCAA GAAGCACTAC 2340
ATGCTGAAGC ACCTGGTGTG GGCCAGCAGG  GAGCTGGAGA GGTTCGCCCT GAACCCCGGC 2400
CTGCTGGAGA CCAGCGAGGG CTGCAAGCAG  ATCATGAAGC AGCTGCAGAG CGCCCTGCAG 2460
ACCGGCACCG AGGAGCTGAG GAGCCTGTTC  AACACCGTGG CCACCCCCTA CTGCGTGCAC 2520
ACCGAGATCG ACGTGAGGGA CACCAGGGAG  GCCCTGGACA AGATCGAGGA GGAGCAGAAC 2580
AAGATCCAGC AGAAGACCCA GCAGGCCAAG  GAGGCCGACG GCAAGGTGAG CCAGAACTAC 2640
CCCATCGTGC AGAACCTGCA GGGCCAGATG  GTGCACCAGC CCATCAGCCC CAGGACCCTG 2700
AATGCATGGG TGAAGGTGGT GGAGGAGAAG  GCCTTCAGCC CCGAGGTGAT CCCCATGTTC 2760
AGCGCCCTGA GCGAGGGCGC CACCCCTCAG  GACCTGAACA CCATGCTGAA CACCGTGGGC 2820
GGCCACCAGG CCGCCATGCA GATCCTGAAG  GACACCATCA ACGAGGAGGC CGCCGAGTGG 2880
GACAGGCTGC ACCCCGTGCA CGCCGGCCCC  ATCGCCCCCG GCCAGATGAG GGAGCCCAGG 2940
GGCAGCGACA TCGCCGGCAC CACCAGCAAC  CTGCAGGAGC AGATCGCCTG GATGACCAGC 3000
AACCCACCCG TGCCCGTGGG CGACATCTAC  AAGAGGTGGA TCATCCTGGG TTTAAACAAG 3060
ATCGTGAGGA TGTACAGCCC CACCAGCATC  CTGGACATCA AGCAGGGCCC CAAGGAGCCC 3120
TTCAGGGACT ACGTGGACAG GTTCTTCAAG  ACCCTGAGGG CCGAGCAGGC CACCCAGGGC 3180
GTGAAGAACT GGATGACCGA CACCCTGCTG  GTGCAGAACG CCAACCCCGA CTGCAAGACC 3240
ATCCTGAGGG CCCTGGGCCC CGGCGCCAGC  ATCGAGGAGA TGATGACCGC CTGCCAGGGC 3300
GTGGGCGGCC CCAGCCACAA GGCCAAGGTG  CTGGCCGAGG CCATGAGCCA GACCAACAGC 3360
GCCATCCTGA TGCAGAGGAG CAACTTCAAG  GGCAGCAAGA GGATCGTGAA GTGCTTCAAC 3420
TGCGGCAAGG AGGGCCACAT CGCCAGGAAC  TGCAGGGCCC CCAGGAAGAA GGGCTGCTGG 3480
AAGTGCGGCA AGGAGGGCCA CCAGATGAAG  GACTGCACCG AGAGGCAGGC CAACTTCCTG 3540
GGCAAGATCT GGCCCAGCCA CAAGGGCGGC  CCCGGCAACT TCCTGCAGAA CAGGCCCGAG 3600
CCCACCGCCC CCCCCGAGGA GAGCTTCAGG  TTCGAGGAGG AGACCACCAC CCCCAGCCAG 3660
AAGCAGGAGC CCATCGACAA GGAGCTGTAC  CCCCTGACCA GCCTGAAGAG CCTGTTCGGC 3720
AACGACCCCA GCAGCCAGGA ATTCTTCAGG  GAGAACCTGG CCCTGCCCCA GGGCAGGGCC 3780
AGGGAGTTCA GCAGCGAGCA GACCAGGGCC  AACAGCCCCA CCAGGGGCGA GCTGCAGGTG 3840
TGGGGCAGGG ACAACAACAG CATCAGCGAG  GCCGGCGCCA ACAGGCAGGG CACCATCAGC 3900
```

Appendix A (*Continued*)

```
TTCAACTTCC CCCAGATCAC CCTGTGGCAG  AGGCCCCTGG TGACCATCAA GATCGGCGGC 3960
CAGCTGAAGG AGGCCCTGCT GAACACCGGC  GCCGGCGACA CCGTGCTGGA GGACCTGAAC 4020
CTGCCCGGCA AGTGGAAGCC CAAGATGATC  GGCGGCATCG GCGGCTTCAT CAAGGTGAGG 4080
CAGTACGAGC AGATCCCCAT CGAGATCTGC  GGCCACAAGG CCATCGGCAC CGTGCTGGTG 4140
GGCCCCACCC CCGTGAACAT CATCGGCAGG  AACCTGCTGA CCCAGCTGGG CTGCACCCTG 4200
AACTTCCCCA TCAGCCCCAT CGAGACCGTG  CCCGTGAAGC TGAAGCCCGG CATGGACGGC 4260
CCCAAGGTGA AGCAGTGGCC CCTGACCGAG  GAGAAGATCA AGGCCCTGAC CGCCATCTGC 4320
GACGAGATGG AGAAGGAGGG CAAGATCACC  AAGATCGGCC CCGAGAACCC CTACAACACC 4380
CCCATCTTCG CCATCAAGAA GAAGGACAGC  ACCAAGTGGA GGAAGCTGGT GGACTTCAGG 4440
GAGCTGAACA AGAGGACCCA GGACTTCTGG  GAGGTGCAGC TGGGCATCCC CCACCCCGCC 4500
GGCCTGAAGA AGAAGAAGAG CGTGACCGTG  CTGGACGTGG GCGACGCCTA CTTCAGCATC 4560
CCCCTGTACG AGGACTTCAG GAAGTACACC  GCCTTCACCA TCCCCAGCAG GAACAACGAG 4620
ACCCCCGGCA TCAGCTACCA GTACAACGTG  CTGCCCCAGG GCTGGAAGGG CAGCCTCGCC 4680
ATCTTCCAGA GCAGCATGAC CATCGAGGAG  CTGATCTACA GCAAGAAGAG GCAGGAGATC 4740
CTGGACCTGT GGGTGTACCA CACCCAGGGC  TACTTCCCCG ACTGGCACAA CTACACCCCC 4800
GGCCCCGGCG TGAGGTTCCC CCTGACCTTC  GGCTGGTGCT TCAAGCTGGT GCCCGTGGAC 4860
CCCAGGGAGG TGGAGGAGGC CAACGAGGGC  GAGGACAACT GCCTGCTGCA CCCCGTGTGC 4920
CAGCACGGCA TGGAGGACGA CCACAGGGAG  GTGCTGAAGT GGAAGTTCGA CAGCCAGCTG 4980
GCCCACAGGC ACAGGGCCAG GGAGCTGCAC  CCCGAGTTCT ACAAGGACTG CATGGGCGGC 5040
AAGTGGAGCA AGAGCAGCAT CGTGGGCTGG  CCCGCCATCA GGGAGAGGAT GAGGAGGACC 5100
GAGCCCGCCG CCGACGGCGT GGGCGCCGTG  AGCAGGGACC TGGAGAAGCA CGGCGCCATC 5160
ACCAGCAGCA ACACCGCCGC CACCAACGAG  GACTGCGCCT GGCTGGAGGC CCAGGAGGAG 5220
GGCGAGGTGG GCTTCCCCGT GAGGCCCCAG  GTGCCCCTGA GGCCCATGAC CTACAAGGGC 5280
GCCGTGGACC TGAGCTTCTT CCTGAAGGAG  AAGGGCGGCC TGGAGGGCCT GAGGCAGCAC 5340
CTGCTGAGGT GGGGCTTCAC CACCCCCGAC  AAGAAGCACC AGAAGGAGCC CCCCTTCCTG 5400
TGGATGGGCT ACGAGCTGCA CCCCGACAAG  TGGACCGTGC AGCCCACCCA GCTGCCCGAG 5460
AAGGATAGCT GGACCGTGAA CGACATCCAG  AAGCTGGTGG GCAAGCTGAA CTGGGCCAGC 5520
CAGATCTACC CCGGCATCAA GGTGAGGCAG  CTGTGCAAGC TGCTGAGGGG CGCCAAGGCC 5580
CTGACCGACA TCGTGCCCCT GACCGAGGAG  GCCGAGCTGG AGCTGGCCGA GAACAGGGAG 5640
ATCCTGAAGG AGCCCGTGCA CGGCGTGTAC  TACGACCCCA GCAAGGACCT GATCGCCGAG 5700
ATCCAGAAGC AGGGCCAGGA GCAGTGGACC  TACCAGATCT ACCAGGAGCC CTTCAAGAAC 5760
CTGAAGACCG GCAAGTACGC CAAGATGAGG  ACCGCCCACA CCAACGACGT GAAGCAGCTG 5820
ACCGAGGCCG TGCAGAAGAT CGCCATGGAG  GGCATCGTGA TCTGGGGCAA GACCCCCAAG 5880
TTCAGGCTGC CCATCCAGAA GGAGACCTGG  GAGACCTGGT GGACCGACTA CTGGCAGGCC 5940
ACCTGGATCC CCGAGTGGGA GTTCGTGAAC  ACCCCTCCCC TGGTGAAGCT GTGGTATCAG 6000
CTGGAGAAGG ACCCCATCGT GGGCGTGGAG  ACCTTCTACG TGGACGGCGC CGCCAACAGG 6060
GAGACCAAGA TCGGCAAGGC CGGCTACGTG  ACCGACAGGG GCAGGAAGAA GATCGTGAGC 6120
CTGACCGAGA CCACCAACCA GAAGACCGAG  CTGCAGGCCA TCTGCATCGC CCTGCAGGAC 6180
AGCGGCAGCG AGGTGAACAT CGTGACCGAC  AGCCAGTACG CCCTGGGCAT CATCCAGGCC 6240
CAGCCCGACA AGAGCGAGAG CGAGCTGGTG  AACCAGATCA TCGAGCAGCT GATGAAGAAG 6300
GAGAGGGTGT ACCTGAGCTG GGTGCCCGCC  CACAAGGGCA TCGGCGGCAA CGAGCAGGTG 6360
GACAAGCTGG TGAGCAGCGG CATCAGGAAG  GTGCTGAAGA CCCTGGAGCC CTTCAGGAAG 6420
CAGAACCCCG GCATCGTGAT CTACCAGTAC  ATGGACGACC TGTACGTGGG CAGCGACCTG 6480
GAGATCGGCC AGCACAGGAC CAAGTAAAGA  TCTCTCGAGG AGCTCAAGCG GGCGGATCCC 6540
CCGGGCTGCA GGAATTCGAT CGCGCCAAAT  TTAAATGATC CTGATCCTTT TTCTGGGTAA 6600
GTAATACGTC AAGGAGAAAA CGAAACGATC  TGTAGTTAGC GGCCGCCTAA TTAACTAATA 6660
TTATATTTTT TATCTAAAAA ACTAAAAATA  AACATTGATT AAATTTTAAT ATAATACTTA 6720
AAAATGGATG TTGTGTCGTT AGATAAACCG  TTTATGTATT TTGAGGAAAT TGATAATGAG 6780
TTAGATTACG AACCAGAAAG TGCAAATGAG  GTCGCAAAAA AACTGCCGTA TCAAGGACAG 6840
TTAAAACTAT TACTAGGAGA ATTATTTTTT  CTTAGTAAGT TACAGCGACA CGGTATATTA 6900
GATGGTGCCA CCGTAGTGTA TATAGGATCG  GCTCCTGGTA CACATATACG TTATTTGAGA 6960
GATCATTTCT ATAATTTAGG AATGATTATC  AAATGGATGC TAATTGACGG ACGCCATCAT 7020
GATCCTATTC TAAATGGATT GCGTGATGTG  ACTCTAGTGA CTCGGTTCGT TGATGAGGAA 7080
TATCTACGAT CCATCAAAAA ACAACTGCAT  CCTTCTAAGA TTATTTTAAT TTCTGATGTA 7140
AGATCCAAAC GAGGAGGAAA TGAACCTAGT  ACGGCGGATT TACTAAGTAA TTACGCTCTA 7200
CAAAATGTCA TGATTAGTAT TTTAAACCCC  GTGGCATCTA GTCTTAAATG GAGATGCCCG 7260
TTTCCAGATC AATGGATCAA GGACTTTTAT  ATCCCACACG GTAATAAAAT GTTACAACCT 7320
TTTGCTCCTT CATATTCAGG GGAATTC                                      7347
```

Left TK flanking sequence	1–502	Complementary
$_{CN54}$gp120	ATG-TGA (647–2143)	Complementary
E/L promoter for $_{CN54}$gp120	2153–2191	Complementary
E/L promoter for $_{CN54}$Gag-Pol-Nef	2206–2244	
$_{CN54}$Gag-Pol-Nef	ATG-TAA (2254–6507)	
Right TK flanking sequence	6656–7347	Complementary

Primers used to characterize the viral recombinants are in bold and underlined.

References

[1] Esparza J, Bhamarapravati N. Accelerating the development and future availability of HIV-1 vaccines: why, when, where, and how? Lancet 2000;355(9220):2061–6.

[2] Osmanov S, Pattou C, Walker N, Schwardlander B, Esparza J. Estimated global distribution and regional spread of HIV-1 genetic subtypes in the year 2000. J Acquir Immune Defic Syndr 2002;29(2):184–90.

[3] van Harmelen J, Williamson C, Kim B, Morris L, Carr J, Karim SS, et al. Characterization of full-length HIV type 1 subtype C sequences from South Africa. AIDS Res Hum Retroviruses 2001;17(16):1527–31.

[4] Novitsky VA, Montano MA, McLane MF, Renjifo B, Vannberg F, Foley BT, et al. Molecular cloning and phylogenetic analysis of human immunodeficiency virus type 1 subtype C: a set of 23 full-length clones from Botswana. J Virol 1999;73(5):4427–32.

[5] Neilson JR, John GC, Carr JK, Lewis P, Kreiss JK, Jackson S, et al. Subtypes of human immunodeficiency virus type 1 and disease stage among women in Nairobi, Kenya. J Virol 1999;73(5):4393–403.

[6] Peeters M, Vincent R, Perret JL, Lasky M, Patrel D, Liegeois F, et al. Evidence for differences in MT2 cell tropism according to genetic subtypes of HIV-1: syncytium-inducing variants seem rare among subtype C HIV-1 viruses. J Acquir Immune Defic Syndr Hum Retrovirol 1999;20(2):115–21.

[7] Abebe A, Demissie D, Goudsmit J, Brouwer M, Kuiken CL, Pollakis G, et al. HIV-1 subtype C syncytium- and non-syncytium-inducing phenotypes and coreceptor usage among Ethiopian patients with AIDS. AIDS 1999;13(11):1305–11.

[8] Rodenburg CM, Li Y, Trask SA, Chen Y, Decker J, Robertson DL, et al. Near full-length clones and reference sequences for subtype C isolates of HIV type 1 from three different continents. AIDS Res Hum Retroviruses 2001;17(2):161–8.

[9] Burton DR, Desrosiers RC, Doms RW, Koff WC, Kwong PD, Moore JP, et al. HIV vaccine design and the neutralizing antibody problem. Nat Immunol 2004;5(3):233–6.

[10] Richman DD, Wrin T, Little SJ, Petropoulos CJ. Rapid evolution of the neutralizing antibody response to HIV type 1 infection. Proc Natl Acad Sci USA 2003;100(7):4144–9.

[11] Wei X, Decker JM, Wang S, Hui H, Kappes JC, Wu X, et al. Antibody neutralization and escape by HIV-1. Nature 2003;422(6929):307–12.

[12] Emini EA, Koff WC. AIDS/HIV. Developing an AIDS vaccine: need, uncertainty, hope. Science 2004;304(5679):1913–4.

[13] Garber DA, Silvestri G, Feinberg MB. Prospects for an AIDS vaccine: three big questions, no easy answers. Lancet Infect Dis 2004;4(7):397–413.

[14] Letvin NL. Strategies for an HIV vaccine. J Clin Invest 2002;110(1):15–20.

[15] Koup RA, Safrit JT, Cao Y, Andrews CA, McLeod G, Borkowsky W, et al. Temporal association of cellular immune responses with the initial control of viremia in primary human immunodeficiency virus type 1 syndrome. J Virol 1994;68(7):4650–5.

[16] Kuroda MJ, Schmitz JE, Charini WA, Nickerson CE, Lifton MA, Lord CI, et al. Emergence of CTL coincides with clearance of virus during primary simian immunodeficiency virus infection in rhesus monkeys. J Immunol 1999;162(9):5127–33.

[17] Frahm N, Adams S, Kiepiela P, Linde CH, Hewitt HS, Lichterfeld M, et al. HLA-B63 presents HLA-B57/B58-restricted cytotoxic T-lymphocyte epitopes and is associated with low human immunodeficiency virus load. J Virol 2005;79(16):10218–25.

[18] Frahm N, Kiepiela P, Adams S, Linde CH, Hewitt HS, Sango K, et al. Control of human immunodeficiency virus replication by cytotoxic T lymphocytes targeting subdominant epitopes. Nat Immunol 2006;7(2):173–8.

[19] Barouch DH, Kunstman J, Kuroda MJ, Schmitz JE, Santra S, Peyerl FW, et al. Eventual AIDS vaccine failure in a rhesus monkey by viral escape from cytotoxic T lymphocytes. Nature 2002;415(6869):335–9.

[20] Allen TM, O'Connor DH, Jing P, Dzuris JL, Mothe BR, Vogel TU, et al. Tat-specific cytotoxic T lymphocytes select for SIV escape variants during resolution of primary viraemia. Nature 2000;407(6802):386–90.

[21] Schmitz JE, Kuroda MJ, Santra S, Sasseville VG, Simon MA, Lifton MA, et al. Control of viremia in simian immunodeficiency virus infection by CD8+ lymphocytes. Science 1999;283(5403):857–60.

[22] Lifson JD, Rossio JL, Piatak Jr M, Parks T, Li L, Kiser R, et al. Role of CD8(+) lymphocytes in control of simian immunodeficiency virus infection and resistance to rechallenge after transient early antiretroviral treatment. J Virol 2001;75(21):10187–99.

[23] Amara RR, Ibegbu C, Villinger F, Montefiori DC, Sharma S, Nigam P, et al. Studies using a viral challenge and CD8 T cell depletions on the roles of cellular and humoral immunity in the control of an SHIV-89.6P challenge in DNA/MVA-vaccinated macaques. Virology 2005;343(2):246–55.

[24] Hel Z, Tsai WP, Thornton A, Nacsa J, Giuliani L, Tryniszewska E, et al. Potentiation of simian immunodeficiency virus (SIV)-specific CD4(+) and CD8(+) T cell responses by a DNA-SIV and NYVAC-SIV prime/boost regimen. J Immunol 2001;167(12):7180–91.

[25] Excler JL. AIDS vaccine development: perspectives, challenges & hopes. Indian J Med Res 2005;121(4):568–81.

[26] Sutter G, Staib C. Vaccinia vectors as candidate vaccines: the development of modified vaccinia virus Ankara for antigen delivery. Curr Drug Targets Infect Disord 2003;3(3):263–71.

[27] Benson J, Chougnet C, Robert-Guroff M, Montefiori D, Markham P, Shearer G, et al. Recombinant vaccine-induced protection against the highly pathogenic simian immunodeficiency virus SIV(mac251): dependence on route of challenge exposure. J Virol 1998;72(5):4170–82.

[28] Sauter SL, Rahman A, Muralidhar G. Non-replicating viral vector-based AIDS vaccines: interplay between viral vectors and the immune system. Curr HIV Res 2005;3(2):157–81.

[29] Nkolola JP, Essex M. Progress towards an HIV-1 subtype C vaccine. Vaccine 2006;24(4):391–401.

[30] Tartaglia J, Perkus ME, Taylor J, Norton EK, Audonnet JC, Cox WI, et al. NYVAC: a highly attenuated strain of vaccinia virus. Virology 1992;188(1):217–32.

[31] Ramirez JC, Gherardi MM, Esteban M. Biology of attenuated modified vaccinia virus Ankara recombinant vector in mice: virus fate and activation of B- and T-cell immune responses in comparison with the Western Reserve strain and advantages as a vaccine. J Virol 2000;74(2):923–33.

[32] Chakrabarti S, Sisler JR, Moss B. Compact, synthetic, vaccinia virus early/late promoter for protein expression. Biotechniques 1997;23(6):1094–7.

[33] Karlsson GB, Liljestrom P. Delivery and expression of heterologous genes in mammalian cells using self-replicating alphavirus vectors. Methods Mol Biol 2004;246:543–57.

[34] Smerdou C, Liljestrom P. Two-helper RNA system for production of recombinant Semliki forest virus particles. J Virol 1999;73(2):1092–8.

[35] Skoging U, Vihinen M, Nilsson L, Liljestrom P. Aromatic interactions define the binding of the alphavirus spike to its nucleocapsid. Structure 1996;4(5):519–29.

[36] Pascolo S, Bervas N, Ure JM, Smith AG, Lemonnier FA, Perarnau B. HLA-A2.1-restricted education and cytolytic activity of CD8(+) T lymphocytes from beta2 microglobulin (beta2m) HLA-A2.1 monochain transgenic H-2Db beta2m double knockout mice. J Exp Med 1997;185(12):2043–51.

[37] Miyahira Y, Murata K, Rodriguez D, Rodriguez JR, Esteban M, Rodrigues MM, et al. Quantification of antigen specific CD8+ T cells using an ELISPOT assay. J Immunol Methods 1995;181(1):45–54.

[38] Najera JL, Gomez CE, Domingo-Gil E, Gherardi MM, Esteban M. Cellular and biochemical differences between two attenuated poxvirus vaccine candidates (MVA and NYVAC) and role of the C7L gene. J Virol 2006;80(12):6033–47.

[39] Guerra S, Lopez-Fernandez LA, Pascual-Montano A, Najera JL, Zaballos A, Esteban M. Host response to the attenuated poxvirus vector NYVAC: upregulation of apoptotic genes and NF-kappaB-responsive genes in infected HeLa cells. J Virol 2006;80(2):985–98.

[40] Hanke T, McMichael A. Pre-clinical development of a multi-CTL epitope-based DNA prime MVA boost vaccine for AIDS. Immunol Lett 1999;66(1–3):177–81.
[41] Amara RR, Villinger F, Staprans SI, Altman JD, Montefiori DC, Kozyr NL, et al. Different patterns of immune responses but similar control of a simian-human immunodeficiency virus 89.6P mucosal challenge by modified vaccinia virus Ankara (MVA) and DNA/MVA vaccines. J Virol 2002;76(15):7625–31.
[42] Gomez CE, Abaitua F, Rodriguez D, Esteban M. Efficient CD8+ T cell response to the HIV-env V3 loop epitope from multiple virus isolates by a DNA prime/vaccinia virus boost (rWR and rMVA strains) immunization regime and enhancement by the cytokine IFN-gamma. Virus Res 2004;105(1):11–22.
[43] Sundback M, Douagi I, Dayaraj C, Forsell MN, Nordstrom EK, McInerney GM, et al. Efficient expansion of HIV-1-specific T cell responses by homologous immunization with recombinant Semliki Forest virus particles. Virology 2005;341(2):190–202.
[44] Liu J, Wyatt LS, Amara RR, Moss B, Robinson HL. Studies on in vitro expression and in vivo immunogenicity of a recombinant MVA HIV vaccine. Vaccine 2006;24(16):3332–9.
[45] Guerra S, Lopez-Fernandez LA, Conde R, Pascual-Montano A, Harshman K, Esteban M. Microarray analysis reveals characteristic changes of host cell gene expression in response to attenuated modified vaccinia virus Ankara infection of human HeLa cells. J Virol 2004;78(11):5820–34.
[46] Behboudi S, Moore A, Gilbert SC, Nicoll CL, Hill AV. Dendritic cells infected by recombinant modified vaccinia virus Ankara retain immunogenicity in vivo despite in vitro dysfunction. Vaccine 2004;22(31–32):4326–31.
[47] Girard MP, Steele D, Chaignat CL, Kieny MP. A review of vaccine research and development: human enteric infections. Vaccine 2006;24(15):2732–50.
[48] Wyatt LS, Earl PL, Liu JY, Smith JM, Montefiori DC, Robinson HL, et al. Multiprotein HIV type 1 clade B DNA and MVA vaccines: construction, expression, and immunogenicity in rodents of the MVA component. AIDS Res Hum Retroviruses 2004;20(6):645–53.
[49] Vuola JM, Keating S, Webster DP, Berthoud T, Dunachie S, Gilbert SC, et al. Differential immunogenicity of various heterologous prime–boost vaccine regimens using DNA and viral vectors in healthy volunteers. J Immunol 2005;174(1):449–55.
[50] Zavala F, Rodrigues M, Rodriguez D, Rodriguez JR, Nussenzweig RS, Esteban M. A striking property of recombinant poxviruses: efficient inducers of in vivo expansion of primed CD8(+) T cells. Virology 2001;280(2):155–9.
[51] Rodriguez F, Harkins S, Slifka MK, Whitton JL. Immunodominance in virus-induced CD8(+) T-cell responses is dramatically modified by DNA immunization and is regulated by gamma interferon. J Virol 2002;76(9):4251–9.
[52] Palmowski MJ, Choi EM, Hermans IF, Gilbert SC, Chen JL, Gileadi U, et al. Competition between CTL narrows the immune response induced by prime–boost vaccination protocols. J Immunol 2002;168(9):4391–8.
[53] Pantaleo G, Menzo S, Vaccarezza M, Graziosi C, Cohen OJ, Demarest JF, et al. Studies in subjects with long-term nonprogressive human immunodeficiency virus infection. N Engl J Med 1995;332(4):209–16.
[54] Casimiro DR, Bett AJ, Fu TM, Davies ME, Tang A, Wilson KA, et al. Heterologous human immunodeficiency virus type 1 priming-boosting immunization strategies involving replication-defective adenovirus and poxvirus vaccine vectors. J Virol 2004;78(20):11434–8.
[55] Nilsson C, Makitalo B, Berglund P, Bex F, Liljestrom P, Sutter G, et al. Enhanced simian immunodeficiency virus-specific immune responses in macaques induced by priming with recombinant Semliki Forest virus and boosting with modified vaccinia virus Ankara. Vaccine 2001;19(25–26):3526–36.
[56] Ramsburg E, Rose NF, Marx PA, Mefford M, Nixon DF, Moretto WJ, et al. Highly effective control of an AIDS virus challenge in macaques by using vesicular stomatitis virus and modified vaccinia virus Ankara vaccine vectors in a single-boost protocol. J Virol 2004;78(8):3930–40.
[57] Lemckert AA, Sumida SM, Holterman L, Vogels R, Truitt DM, Lynch DM, et al. Immunogenicity of heterologous prime–boost regimens involving recombinant adenovirus serotype 11 (Ad11) and Ad35 vaccine vectors in the presence of anti-ad5 immunity. J Virol 2005;79(15):9694–701.
[58] Gómez CE, Nájera JL, Pérez Jiménez E, Jiménez V, Wagner R, Graf M, et al. Head-to-head comparison on the immunogenicity of two HIV/AIDS vaccine candidates based on the attenuated poxvirus strains MVA and NYVAC co-expressing in a single locus the HIV-1BX08 gp120 and HIV-1IIIB Gag-Pol-Nef proteins of clade B. Vaccine, in press. doi:10.1016/j.vaccine.2006.09.090.
[59] Graham BS. Clinical trials of HIV vaccines. Annu Rev Med 2002;53:207–21.

JOURNAL OF VIROLOGY, Aug. 2007, p. 8707–8721 Vol. 81, No. 16
0022-538X/07/$08.00+0 doi:10.1128/JVI.00444-07
Copyright © 2007, American Society for Microbiology. All Rights Reserved.

Distinct Gene Expression Profiling after Infection of Immature Human Monocyte-Derived Dendritic Cells by the Attenuated Poxvirus Vectors MVA and NYVAC▽†

Susana Guerra,[1] José Luis Nájera,[1] José Manuel González,[1] Luis A. López-Fernández,[2] Nuria Climent,[3,5] José M. Gatell,[3,5] Teresa Gallart,[4,5] and Mariano Esteban[1]*

Department of Molecular and Cellular Biology,[1] and Department of Immunology and Oncology,[2] Centro Nacional de Biotecnología, Consejo Superior de Investigaciones Científicas (CSIC), Campus Universidad Autónoma, E-28049 Madrid, Spain, and Servicios de Enfermedades Infecciosas[3] and de Inmunología,[4] Hospital Clínic de Barcelona, and AIDS Research Group, Instituto de Investigaciones Biomedicas August Pi i Sunyer (IDIBAPS),[5] Universidad de Barcelona, Villaroel 170, 08036 Barcelona, Spain

Received 1 March 2007/Accepted 17 May 2007

Although recombinants based on the attenuated poxvirus vectors MVA and NYVAC are currently in clinical trials, the nature of the genes triggered by these vectors in antigen-presenting cells is poorly characterized. Using microarray technology and various analysis conditions, we compared specific changes in gene expression profiling following MVA and NYVAC infection of immature human monocyte-derived dendritic cells (MDDC). Microarray analysis was performed at 6 h postinfection, since these viruses induced extensive cytopathic effects, rRNA breakdown, and apoptosis at late times postinfection. MVA- and NYVAC-infected MDDC shared upregulation of 195 genes compared to uninfected cells: MVA specifically upregulated 359 genes, and NYVAC upregulated 165 genes. Microarray comparison of NYVAC and MVA infection revealed 544 genes with distinct expression patterns after poxvirus infection and 283 genes specifically upregulated after MVA infection. Both vectors upregulated genes for cytokines, cytokine receptors, chemokines, chemokine receptors, and molecules involved in antigen uptake and processing, including major histocompatibility complex genes. mRNA levels for interleukin 12β (IL-12β), beta interferon, and tumor necrosis factor alpha were higher after MVA infection than after NYVAC infection. The expression profiles of transcription factors such as NF-κB/Rel and STAT were regulated similarly by both viruses; in contrast, OASL, MDA5, and IRIG-I expression increased only during MVA infection. Type I interferon, IL-6, and Toll-like receptor pathways were specifically induced after MVA infection. Following MVA or NYVAC infection in MDDC, we found similarities as well as differences between these virus strains in the expression of cellular genes with immunological function, which should have an impact when these vectors are used as recombinant vaccines.

Attenuated strains of vaccinia virus (VACV), MVA and NYVAC, are currently being tested as vaccine vectors (8, 35, 49, 77). NYVAC is a derivative of VACV strain Copenhagen, from which 18 open reading frames were specifically deleted from the parental viral genome; genes involved in host range, virulence, and pathogenesis were thus lost (75). NYVAC-derived vectors are able to express antigens from a broad range of species (75). A number of examples using NYVAC as a delivery system for recombinant vaccines to pathogens and tumors have been reported (22, 39, 52, 71). Phase I/II clinical trials using NYVAC against human immunodeficiency virus (HIV) type 1 and pathogens are currently under way and showed immunogenicity and a good safety profile (55). MVA was generated after more than 500 passages in chicken embryo fibroblasts and has lost approximately 15% of the parental viral genome (5, 48); the structural genes remained unaltered, but genes involved in immune evasion factors and host range (5, 48, 78) have been deleted or fragmented. In mammals, MVA recombinants induce protective immunity against a wide spectrum of pathogens (49, 66). Differences in the degree and magnitude of the immune response to HIV proteins have been observed between MVA and NYVAC vectors (24). Phase I/II clinical trials with MVA-based recombinants have been performed or are under way for HIV type 1, malaria, and tumors (13, 18, 23, 33). MVA is also a potentially safe candidate for a vaccine against smallpox should this virus reemerge as a bioterrorism weapon (10).

While there is major interest in the use of MVA and NYVAC as vectors for antigen delivery and as vaccines for pathogens and tumors, little is known of the impact of these vectors on host genome expression by antigen-presenting cells (APC). Whereas other viruses productively infect dendritic cells (DC), including cytomegalovirus, varicella zoster virus, and measles virus (1, 26, 59), several studies indicate that poxviruses do not produce an infectious cycle in DC (20, 21, 38, 40), while Langerhans cells allow VACV replication (19). Recent findings show that MVA infection of human DC interrupts cell maturation and leads to apoptosis associated with a decrease in Bcl-2 and Bcl-X_L levels late in infection in a virus multiplicity-dependent manner (15). Both MVA and NYVAC are potent in vivo activators of T-cell-specific immune re-

* Corresponding author. Mailing address: Centro Nacional de Biotecnología, CSIC, Campus Universidad Autónoma, 28049 Madrid, Spain. Phone: (34) 91/585-4553. Fax: (34) 91/585-4506. E-mail: mesteban@cnb.uam.es.

† Supplemental material for this article may be found at http://jvi.asm.org/.

▽ Published ahead of print on 30 May 2007.

Downloaded from jvi.asm.org at Centro Nacional de Biotecnología - Biblioteca on October 15, 2007

sponses to recombinant antigens, indicating efficient antigen delivery in APC and the activation of immune T cells, possibly due to virus infection of activated DC (80).

DC, the best-known group of APC, are bone marrow-derived leukocytes. They act as sentinels of the immune system and are present in an immature state in almost all peripheral tissues, where they can induce specific T-cell-mediated immune responses (6). Maturation is induced by the contact of immature DC with various products of infectious agents (4, 14). During maturation, DC lose their ability to take up antigens and migrate from the sites of antigen accumulation to the areas of antigen presentation, primarily the T-cell zones of secondary lymphoid organs (6, 58). Due to the essential role of DC in immune response development, we characterized the impact of two vaccine poxvirus vectors, MVA and NYVAC, on the gene expression profile of human monocyte-derived dendritic cells (MDDC) infected for a relatively brief period (6 h postinfection [hpi]). This infection time was chosen to identify upregulated genes, since rRNA breakdown effects at this time are minimal compared to those at late times postinfection, when rRNA breakdown and apoptosis are found in infected MDDC (15). DNA microarray technology allows monitoring of the expression of several thousand individual genes (32) and has been used to identify the genomic expression profiles of human HeLa cells in response to infection by both virulent VACV (WR strain) as well as attenuated MVA and NYVAC (28–30) and other VACV strains (43, 46).

In this investigation, we have defined the characteristics of MVA and NYVAC infection of MDDC in culture and show that MVA infection upregulates a larger number of genes encoding immunomodulatory molecules than NYVAC, with higher expression levels. We demonstrated a distinct regulation of host genes by the poxvirus vectors in infected MDDC under three microarray conditions, comparing MVA- or NYVAC-infected with uninfected cells, MVA-infected with NYVAC-infected cells, and MVA/NYVAC-infected HeLa cells with MVA/NYVAC-infected MDDC. Levels of alpha interferon (IFN-α), tumor necrosis factor alpha (TNF-α), and proinflammatory cytokines such as interleukin 6 (IL-6) were higher in MVA-infected MDDC than in NYVAC-infected MDDC. Genes involved in the antiviral response such as retinoic acid-inducible protein I (RIG-I), melanoma differentiation-associated gene 5 (MDA5), and 2′-5′-oligoadenylate (5-OA) synthetase-like (OASL) were upregulated exclusively in MVA-infected MDDC. Our findings show similarities and differences in the genes induced by MVA and NYVAC in human MDDC. These genes are important for the innate immune response and could influence the extent of the host response and protective efficacy when these two poxvirus vectors are used as vaccines.

MATERIALS AND METHODS

Cells, viruses, and infection conditions. HeLa cells (ATCC) were cultured in Dulbecco's modified Eagle's medium supplemented with 10% newborn bovine serum and antibiotics. Human MDDC were generated as previously reported, with minor modifications (51, 56). Peripheral blood mononuclear cells were obtained by using a standard Ficoll gradient for heparinized blood extracted from healthy individuals. To obtain human monocytes, peripheral blood mononuclear cells (3×10^6 to 4×10^6 cells/ml) were incubated (2 h at 37°C) in a humidified atmosphere with 5% CO_2 in MDDC medium (serum-free XVIVO-15 medium; BioWhittaker, Walkersville, MD) with 1% human blood group AB serum, 50 μg/ml gentamicin (Braun, Melsungen, Germany), and 2.5 μg/ml amphotericin B (Bristol-Myers Squibb, Rueil-Malmaison, France). Adherent cells were washed four times with prewarmed serum-free XVIVO-10 medium and cultured in MDDC medium as described above. To obtain immature MDDC, cells were stimulated for 5 days by the addition of 1,000 U/ml each of IL-4 and granulocyte-macrophage colony-stimulating factor (both from Prospec-Tany Technogene, Rehovot, Israel) at days 0 and 2. MDDC immunophenotyping was confirmed by flow cytometry using the following monoclonal antibodies to cell surface markers: fluorescein isothiocyanate (FITC)-conjugated anti-HLA-DR, anti-CD14, and anti-CD19 and an immunoglobulin Gγ1 (IgGγ1) isotype-matched control; phycoerythrin (PE)-conjugated anti-HLA-DR, anti-CD11c, anti-CD14, anti-CD40, anti-CD45, and anti-CD56 and an IgG-γ1 control; and peridinin-chlorophyll-protein complex-anti-CD3 and -anti-CD14 and an IgG-γ1 control (all from BD Biosciences, San Diego, CA). PE-anti-CD80, -CD83, and -CD86 were from Coulter, and PE-anti-CD209 was from eBioscience (San Diego, CA). Cells were washed with phosphate-buffered saline (PBS), resuspended at 2×10^6 cells/ml (50 μl/tube), and incubated with FITC-, PE-, and/or PerCP-conjugated monoclonal antibody (30 min at 4°C). Cells were washed with PBS, fixed with 1% formaldehyde in PBS, and analyzed by flow cytometry in an EPICS Profile cytometer (Coulter, Hialeah, FL). Cell populations were selected by forward- and side-light-scatter parameters. This analysis showed that the purity of MDDC was ≥95%, and the phenotype observed was characteristic of immature MDDC: $CD3^-$ $CD8^-$ $CD14^-$ $CD19^-$ $CD56^-$ $HLA\text{-}DR^+$ $CD80^-$ $CD83^-$ $CD86^+$ $CD11c^+$ $CD40^+$ $CD45^+$ $CD209^+$.

These immature MDDC were used for virus infection. NYVAC (28a, 75) and MVA (24, 29) strains were cultured in chicken embryo fibroblast cells, purified by two sucrose cushions, and titrated on BHK-21 cells by immunostaining of fixed infected cultures with a polyclonal anti-VACV antibody (62). MDDC were infected at 5 PFU/cell, virus inoculum was removed after 1 h, fresh medium was added, and infection continued for another 5 h. Cells were collected and centrifuged, supernatants were saved for an enzyme-linked immunosorbent assay (ELISA), and cells were washed twice with PBS and processed for RNA extraction or Western blot analyses.

Metabolic labeling of proteins. MDDC were infected with 5 PFU/cell, and at the indicated times (10^6 cells/time postinfection), cells were washed with methionine-free medium and incubated in methionine-free medium containing [^{35}S]methionine (50 μCi/well for 30 min at 37°C). Proteins from cell extracts prepared in lysis buffer were fractionated by 12% sodium dodecyl sulfate (SDS)-polyacrylamide gel electrophoresis (PAGE) and developed by autoradiography.

Microarray labeling. Ultraspect_II RNA (Biotecx, Houston, TX) was used to isolate total RNA from purified human MDDC infected with NYVAC or MVA (3×10^6 cells/time postinfection; 5 PFU/cell), or mock infected. RNA was then purified with Megaclear (Ambion, Foster City, CA), and the integrity was confirmed by using an Agilent (Santa Clara, CA) 2100 Bioanalyzer. Total RNA (1.5 μg) was amplified with an Amino Allyl MessageAmp aRNA kit (Ambion); 54 to 88 μg of amplified RNA (aRNA) was obtained. The mean RNA size was 1,500 nucleotides, as observed using the Agilent 2100 Bioanalyzer. For each sample, 6 μg aRNA was labeled with one aliquot of Cy3 or Cy5 Mono NHS Ester (CyDye postlabeling reactive dye pack; GE Healthcare) and purified using Megaclear. Incorporation of Cy5 and Cy3 was measured using 1 μl of probe in a Nanodrop spectrophotometer (Nanodrop Technologies). For each hybridization, Cy5 and Cy3 probes (150 mol each) were mixed and dried by speed vacuum and resuspended in 9 μl RNase-free water. Labeled aRNA was fragmented by adding 1 μl 10× fragmentation buffer (Ambion), followed by incubation (70°C for 15 min). The reaction was terminated with the addition of 1 μl stop solution (Ambion) to the mixture. Two dye-swapped hybridizations were performed for each comparison; in one, the mock-infected sample was Cy3 labeled, and the MVA-infected sample was Cy5 labeled; in the second, labeling was reversed. Double labeling was used to abolish dye-specific labeling and hybridization differences.

Slide treatment and hybridization. Slides containing 22,264 spots (19,256 different oligonucleotides) corresponding to Human Genome Oligo set version 2.2 (QIAGEN, Hilden, Germany) were obtained from the Genomic and Microarrays Laboratory (Cincinnati University, Cincinnati, OH). Information about printing and the oligonucleotide set can be found on their website (http://microarray.uc.edu). Slides were prehybridized and hybridized as described previously (28–30). Images from Cy3 and Cy5 channels were equilibrated and captured with an Axon 4000B scanner, and spots were quantified using GenePix 5.1 software. Data for replicates were analyzed using Almazen software (Bioalma, Spain). Basically, Lowess normalization was applied to each replicate, and the log ratios were merged with the corresponding standard deviations and *z* scores.

Gene expression analysis. The original data set contained 19,256 oligonucleotides per slide. In each analysis, genes with an interreplicate mean signal of

Downloaded from jvi.asm.org at Centro Nacional de Biotecnología - Biblioteca on October 15, 2007

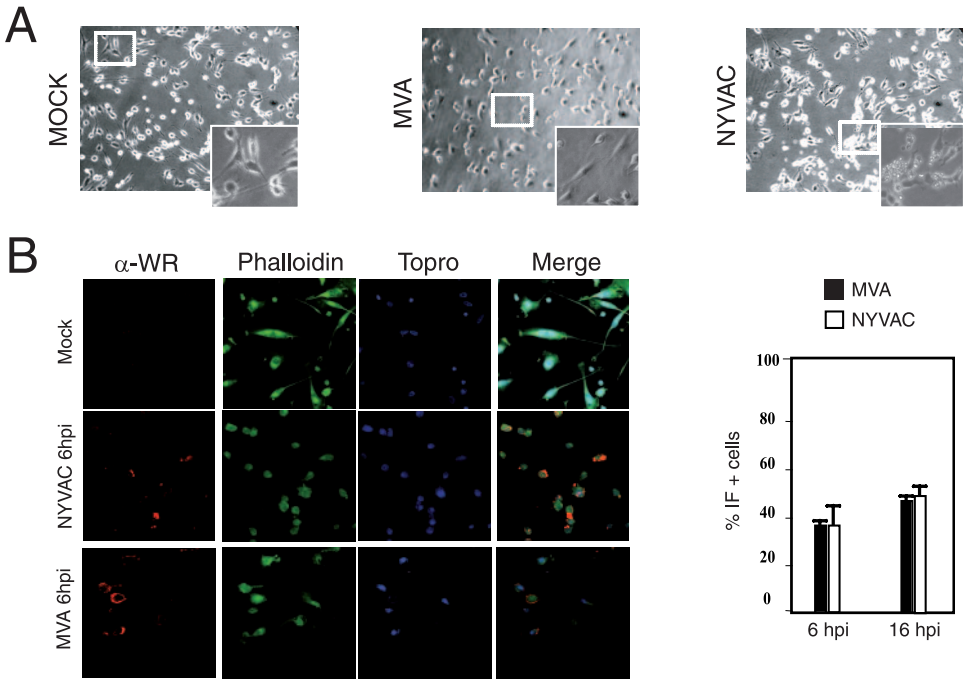

FIG. 1. Cellular and biochemical changes in human immature MDDC following infection with MVA or NYVAC poxvirus vectors. (A) Morphological changes in immature MDDC mock infected or infected with MVA or NYVAC (5 PFU/cell) in six-well plates; changes were examined by phase-contrast microscopy at 6 hpi. The upper panels show representative fields (magnification, ×4); the lower panels show the indicated areas at a higher magnification. (B) IF analysis. MDDC cultured on coverslips were infected with MVA or NYVAC (5 PFU/cell), and cells were fixed at 6 hpi and treated with a rabbit polyclonal antibody to VACV proteins (α-WR), followed by a Texas Red-labeled secondary antibody, phalloidin-FITC (for actin staining), and ToPro (for DNA staining) (left panels). Cells expressing viral antigens were quantified by IF in four independent experiments (right panel).

<100 or an interreplicate standard deviation of >1 were filtered out. Genes were considered to be differently expressed if the expression change (*n*-fold) was <−2 (downregulated) or >2 (upregulated). Functional analyses of regulated genes were generated by Ingenuity Pathways Analysis (Ingenuity Systems [www.ingenuity.com]). Hierarchical clustering was carried out using SpotFire Decision Site for Functional Genomics software. Ward's method with an average value-ordering function and a half-square Euclidean distance function was used.

Quantitative real-time RT-PCR. RNA (1 μg) was reverse transcribed using the superscript first-strand synthesis system for reverse transcription (RT)-PCR (Invitrogen, Carlsbad, CA). A 1:40 dilution of the RT reaction mixture was used for quantitative PCR. The primers and probe set used to amplify TNF, IFN-β, IFN-stimulated gene 15 (ISG15), NF-κB-2, IL-12, IL-7, IL-6, IFN-γ, OASL, ATF-3, ADORA, and H2AFY were purchased from Applied Biosystems. RT-PCRs were performed according to Assay-on-Demand, optimized for TaqMan Universal PCR MasterMix, No AmpErase UNG (28–30). All samples were assayed in duplicate. Threshold cycle values were used to plot a standard curve in which the threshold cycle decreased in linear proportion to the log of the template copy number. Correlation values of standard curves were always >99%.

Immunofluorescence. MDDC cultured on coverslips were infected with MVA or NYVAC (5×10^5 cells/time postinfection; 5 PFU/cell). At 6 and 16 hpi, cells were washed with PBS, fixed with 4% paraformaldehyde, and permeabilized with 0.1% Triton X-100 in PBS (room temperature for 10 min). Cells were incubated with primary anti-WR (anti-VV), anti-A36R or anti-B5R (both obtained from R. Blasco, INIA, Spain), or anti-E3L (obtained from B. L. Jacobs, University of Arizona) antibodies, followed by fluorescein- or Texas red-conjugated isotype-specific secondary antibodies. F-actin was stained with fluorescein-conjugated phalloidin (Molecular Probes, Carlsbad, CA); DNA was stained with ToPro (Molecular Probes). Images were obtained using a Bio-Rad Radiance 2100 confocal laser microscope.

Western blot. HeLa and MDDC were infected (10^6 cells/time postinfection; 5 PFU/cell) with MVA or NYVAC and collected, and cell extracts were prepared at 2, 6, and 16 hpi by lysis in buffer (50 mM Tris-HCl [pH 8.0], 0.5 M NaCl, 10% NP-40, 1% SDS) for 5 min on ice. Protein lysates (100 μg) were fractionated by 14% or 8% SDS-PAGE, transferred onto nitrocellulose membranes, and incubated with anti-poly(ADP-ribose) polymerase (PARP) (Cell Signaling, Boston, MA), anti-actin (Santa Cruz, Santa Cruz, CA), anti-E3L, anti-A14L (64), anti-A4L (60), anti-A27L (63), anti-Al7L (61), anti-phosphorylated interferon-responsive factor 3 (IRF-3) (Upstate, Chicago, IL), anti-IRF-3 (Cell Signaling), anti-IRF-7 (Santa Cruz), anti-B5R, anti-phosphorylated IF-2α (Biosource, Camarillo, CA), or anti-alpha subunit of eukaryotic initiation factor 2 (eIF-2α) (Santa Cruz) antibodies, followed by secondary antibodies (mouse and rabbit peroxidase conjugates). Protein expression was detected using ECL reagents (Amersham, Uppsala, Sweden).

Cytokine determination. IL-2, IL-4, IL-6, IL-10, TNF-α, IFN-γ, IL-1β, IL-8, and IL-12 levels in 30 μl of supernatants were determined using Cytometric Bead Array, human Th1/Th2 cytokine, and Cytometric Bead Array human inflammation kits (BD Bioscience) according to the manufacturer's protocol.

RESULTS

Infection with attenuated poxvirus vectors MVA and NYVAC causes extensive cell damage in human MDDC. To characterize the impact of MVA and NYVAC infection on immature human MDDC, we first defined the induced cytopathic effects by phase-contrast and immunofluorescence (IF) microscopy. At 6 hpi, MVA or NYVAC infection at 5 PFU/cell resulted in alterations in cell morphology characterized by cell rounding and cytoplasmic contraction; the cytopathic effect was more pronounced in NYVAC than after MVA infection (Fig. 1A). The effects on cell morphology were severe by 16 hpi in MDDC infected with either virus strain (not shown). The number of MVA- or NYVAC-infected MDDC was monitored by IF after staining with a polyclonal antibody to VACV proteins. At 6 hpi, approximately 35% of MVA- or NYVAC-infected MDDC stained for viral proteins, which increased to 45% by 16 hpi (Fig. 1B). Since the use of higher virus multi-

Downloaded from jvi.asm.org at Centro Nacional de Biotecnología - Biblioteca on October 15, 2007

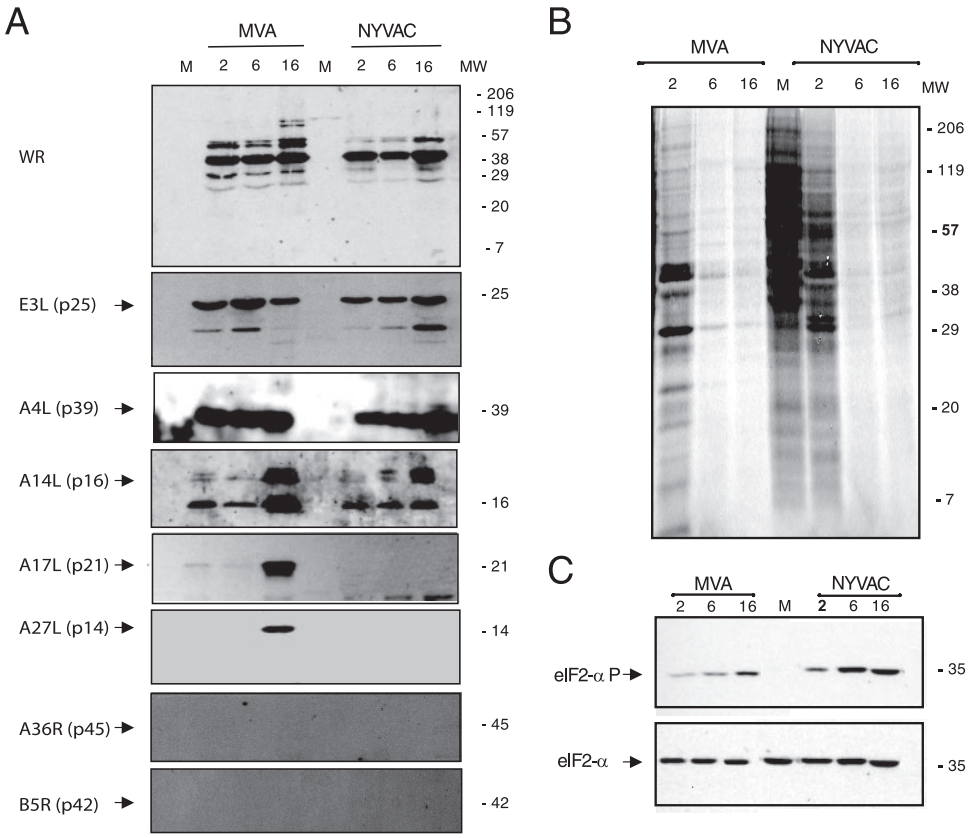

FIG. 2. Protein synthesis evaluation in MDDC after MVA or NYVAC infection. (A) Viral protein expression during NYVAC and MVA infection. MDDC were mock infected (M) or infected with MVA or NYVAC (5 PFU/cell). At the indicated times postinfection, equal amounts of proteins from cell extracts were fractionated by SDS-PAGE, transferred onto nitrocellulose, and treated with antibodies to VACV proteins (WR) or specific virus early (p25) and late proteins (p21, p14, p39, p16, and p42). Molecular weight (MW) (in thousands) is indicated based on protein standards. (B) Metabolic labeling of proteins during NYVAC and MVA infection. MDDC were mock infected (M) or infected with MVA or NYVAC (5 PFU/cell). At the times indicated, cells were labeled (30 min) with [^{35}S]Met-Cys Promix (50 μCi/ml), and equal amounts of proteins were analyzed by SDS-PAGE (10%) and autoradiography. (C) The gel in B was transferred onto nitrocellulose and incubated with antibodies to total eIF-2α or eIF-2α phosphorylated (P) at Ser51. Molecular weight (MW) (in thousands) is indicated based on protein standards.

plicities caused extensive MDDC damage, we used 5 PFU/cell in these studies.

To examine viral protein synthesis in MDDC during MVA or NYVAC infection, we performed Western blotting using antibodies specific for early p25 (E3L) and late viral proteins p14 (A27L), p21 (A17L), p16 (A14L), p39 (A4L), and p42 (B5R). Proteins encoded by the E3L, A4L, and A14L genes were detected efficiently in lysates of cells infected with both viruses (Fig. 2A). The late proteins encoded by the A17L and A27L genes were detected only in lysates of MVA-infected cells, concurring with previous reports for HeLa cells (53). The protein encoded by the B5R gene was not detected in lysates of cells infected with either virus, as determined by Western blot (Fig. 2A) and IF (not shown) analyses. MVA-infected MDDC gave a similar result for A36R gene expression, as previously described (15).

To document the overall protein expression pattern and the shutoff effect, MDDC were metabolically labeled with [^{35}S]methionine at 2, 6, and 16 h after MVA or NYVAC infection and analyzed by SDS-PAGE and autoradiography. We observed a severe translational block in protein synthesis by 6 hpi in cells infected with either virus (Fig. 2B). This blockade coincided with an increase in phosphorylation of the small subunit of the initiation factor eIF-2α (Fig. 2C), as described previously for NYVAC in HeLa cells (28, 53). These findings show that MVA or NYVAC infection of MDDC caused shutoff by 6 hpi, whereas the synthesis of early and some late viral proteins continued, indicating functional cell translational machinery. It has been previously reported that the viral C7L gene is able to prevent eIF-2α phosphorylation in NYVAC-infected HeLa cells (53). The presence of this gene in the MVA genome might explain the different levels in eIF-2α phosphorylation between MVA- and NYVAC-infected MDDC, although we cannot rule out the possibility of other mechanisms.

Since NYVAC infection of HeLa cells induces apoptosis (28a, 53), we used an antibody that recognizes both full-length and cleaved PARP-1 (73) to analyze whether apoptosis occurs in infected MDDC. In both MVA and NYVAC infection, cleavage of 89-kDa PARP-1 was evident by 16 hpi, with no apoptosis at 6 hpi (Fig. 3A). After IF staining with the E3 antibody for an early viral protein and ToPro for the appearance of apoptotic bodies, we found similar numbers of apoptotic cells for both viruses at 16 hpi (nearly 40% of total infected cells) (Fig. 3B). This result contrasts with the low

Downloaded from jvi.asm.org at Centro Nacional de Biotecnología - Biblioteca on October 15, 2007

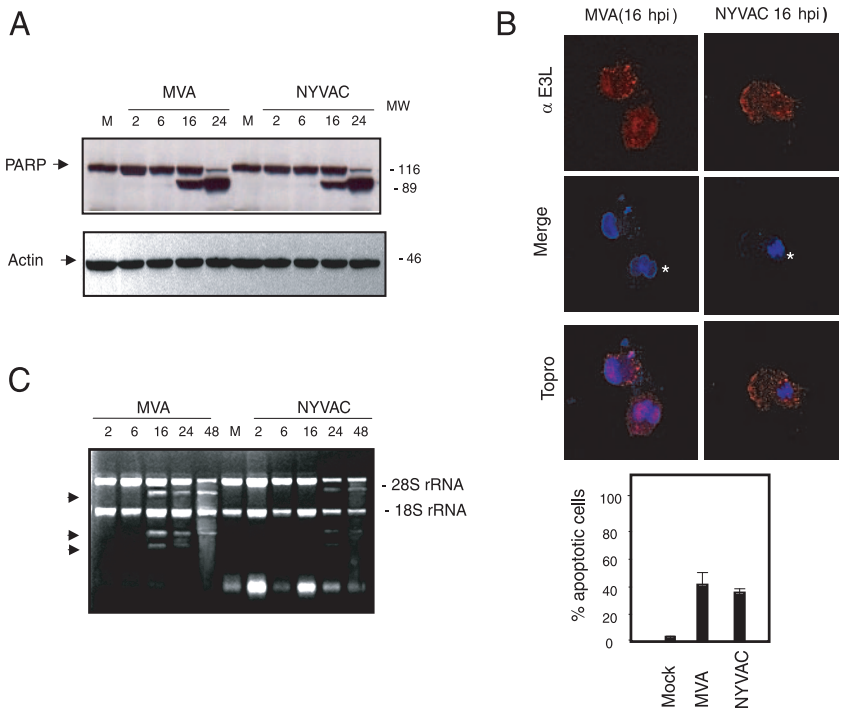

FIG. 3. Apoptosis induction and rRNA breakdown during MVA or NYVAC infection of MDDC. (A) Time course of PARP-1 cleavage during MVA and NYVAC infection. MDDC were mock infected (M) or infected with MVA or NYVAC (5 PFU/cell); at the times indicated, total proteins (100 μg) were fractionated by SDS-PAGE, transferred onto nitrocellulose, and immunoblotted with anti-PARP-1. An 89-kDa PARP-1 cleavage product was observed at 16 hpi. Molecular weight standards (MW) (in thousands) are indicated (right). Equivalence of protein loading was confirmed using anti-actin controls. (B) Quantification of cells in apoptosis after MVA or NYVAC infection. MDDC were mock infected (M) or infected with MVA or NYVAC (5 PFU/cell); at 16 hpi, cells were fixed and processed to visualize apoptosis by IF using antibodies to the viral E3 protein (red) and ToPro for DNA staining (blue). The percentage of cells in apoptosis was determined by counting ~2,000 cells in two independent experiments (bottom). (C) MVA or NYVAC infection of MDDC causes rRNA breakdown. Total rRNA was isolated from uninfected MDDC (M) or MDDC infected with MVA or NYVAC at the indicated times postinfection; 2 μg of each sample was applied for electrophoresis, and the gel was stained with ethidium bromide. Arrows indicate bands corresponding to characteristic rRNA degradation products.

apoptotic effect induced by MVA in human HeLa cells (28a, 53).

We previously showed that NYVAC but not MVA infection of HeLa cells triggers rRNA degradation late in infection, with the same cleavage pattern observed during activation of the interferon-induced 2-5A oligonucleotide synthetase/RNase L system (53). We therefore examined rRNA integrity in MVA- and NYVAC-infected MDDC. Total RNA was isolated from infected and mock-infected cells and fractionated by formaldehyde-agarose gel electrophoresis. There was no rRNA degradation in uninfected cells or in infected cells at 6 hpi; in contrast, we observed a breakdown of 28S and 18S rRNA at later times in cells infected with both viruses (Fig. 3C). These results revealed that MVA and NYVAC infection of MDDC does not induce apoptosis or rRNA degradation at 6 hpi, but these effects appeared later in infection.

Differential gene regulation following MVA or NYVAC infection of human MDDC compared to mock-infected cells. Since MDDC are the most potent APC and the only cells able to activate naive T cells (47), we studied the impact of both viruses on MDDC gene expression at a time when host rRNA had not been degraded by virus infection. We used chips carrying oligonucleotides from 19,256 human genes to profile MDDC gene expression and hybridized cDNA samples from infected and uninfected (mock-infected) cells at 6 hpi. The gene expression data were selected as described in Materials and Methods. Compared to uninfected cells, we identified 1,215 genes differentially expressed in MDDC after MVA infection (21.6% of the genes selected), 554 of which were upregulated and 661 of which were downregulated (see examples in Table S1 in the supplemental material). A similar experiment comparing NYVAC-infected with uninfected MDDC showed variance in the regulation of 728 genes after NYVAC infection (13.5% of the genes selected), 360 of which were upregulated and 368 of which were downregulated (see examples in Table S2 in the supplemental material).

Host genes with altered expression in MVA- or NYVAC-infected MDDC belong to a number of functional categories (Fig. 4A). Both poxvirus vectors regulated similar numbers of genes involved in cell death, cancer, gene expression, cell development, and organism survival. NYVAC nonetheless selectively regulated more genes involved in cell growth, proliferation, and morphology than MVA. In contrast, MVA regulated a larger number of genes involved in the immune response and immune system development than NYVAC (Fig. 4A). Examples of the differentially regulated genes are presented in Table 1. Genes differentially expressed after poxvirus infection were represented using Venn diagrams to display differently and similarly regulated genes for MVA and NYVAC (Fig. 4B). MVA and NYVAC shared 195 genes that were upregulated

Downloaded from jvi.asm.org at Centro Nacional de Biotecnología - Biblioteca on October 15, 2007

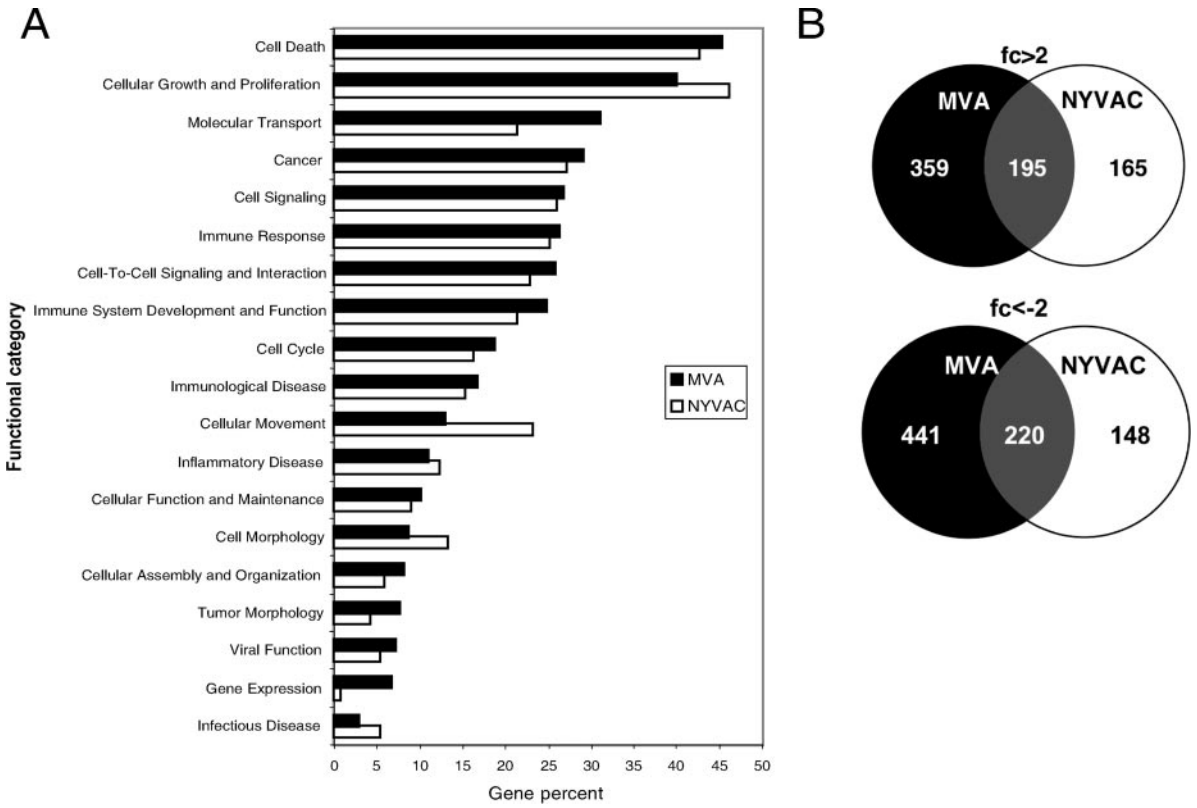

FIG. 4. Functional classification of genes with altered expression in MVA- or NYVAC-infected MDDC versus uninfected cells after microarray analysis. Genes with altered expression in MVA- or NYVAC-infected MDDC were compared with uninfected cells. (A) The *y* axis shows the most representative high-level functions associated with genes regulated in MVA- or NYVAC-infected MDDC, according to ingenuity pathway analysis. The *x* axis represents the percentage of the total number of regulated genes associated with a given function. (B) Venn diagrams represent common or specific genes upregulated (>2-fold) or downregulated (<−2-fold) in MVA- or NYVAC-infected MDDC compared to mock-infected cells.

and 220 that were downregulated, whereas 359 genes were upregulated only by MVA and 165 genes were upregulated only by NYVAC. In infected MDDC, MVA specifically downregulated more genes than NYVAC (441 versus 148 genes). Both viruses produced an increase in specific immune molecules such as CXCL2, TNF-α, and several interferon-induced proteins (IFIT1, IFIT4, ISG15, and ISG20), with higher expression levels in MVA-infected MDDC than in NYVAC-infected MDDC. An alternative visualization using hierarchical cluster analysis was also developed (not shown).

Comparison of MVA and NYVAC infection of human MDDC shows specific differences in host gene expression levels. To further document specific differences between the two vectors, we performed microarrays with cDNAs prepared from MDDC infected with MVA and NYVAC for 6 h, but we now compared NYVAC-infected samples with MVA-infected samples. We evaluated specific transcriptional differences between the two vectors by removing those genes regulated equally by both viruses from the processed data. We identified 11,800 genes with similar expression levels for both viruses; 544 genes showed expression pattern differences after poxvirus infection (4.4% of the genes selected), 283 of which had at least twofold-higher transcriptional levels after MVA than after NYVAC infection. Human genes differentially expressed in MVA versus NYVAC infection of MDDC are shown in Table 2 and in Table S3 in the supplemental material. Genes including TNF-α, IFN-β, and IL-12β were increased by fivefold or higher after MVA infection compared to NYVAC infection. MVA and NYVAC infections produced 12- and 4-fold upregulation, respectively, of a recently described member of the NF-κB family, such as MAIL (molecule possessing ankyrin repeats induced by lipopolysaccharide) (Tables 1 and 2).

The microarray findings indicate that both poxvirus vectors triggered similar but also distinct regulatory pathways in MDDC, with MVA upregulating more host genes than NYVAC.

Validation of microarray data by quantitative real-time RT-PCR. To confirm the microarray results, we validated the changes in transcript levels using real-time RT-PCR to verify the transcriptional changes in 12 selected genes (*TNF*, *IFN*-β, *ISG15*, *NF-κB-2*, *IL12*, *IL7*, *IL6*, *IFN*-γ, *OASL*, *ATF-3*, *ADORA*, and *H2AFY*); *HPRT* was used as an internal control. The assay was performed with the same RNAs as those used in the microarray experiment (Table 2). The expression pattern and relative mRNA abundance of the selected genes concurred with microarray data in all cases, with only slight variations, validating the microarray findings (see Table S4 in the supplemental material). Indeed, clear differences were observed in the expression levels of selected genes for both viruses.

Downloaded from jvi.asm.org at Centro Nacional de Biotecnología - Biblioteca on October 15, 2007

TABLE 1. Representative genes regulated by MVA or NYVAC in infected MDDC according to predicted biological function

Description	GenBank accession no.	Gene	Fold change in transcription	
			MVA	NYVAC
IFN and IFN-induced genes				
IFN-induced protein with tetratricopeptide repeats 4	NM_001549	*IFIT4*	52.45	3.37
IFN-induced protein with tetratricopeptide repeats 1	NM_001548	*IFIT1*	47.8	4.65
IFN-induced, hepatitis C virus-associated microtubular aggregate protein (44 kDa)	NM_006417	*MTAP44*	20.95	2.63
IRF-2	NM_002199	*IRF2*	6.54	3.48
IRF-7	NM_004031	*IRF7*	2.52	1.3
IFN-α1	NM_024013	*IFNA1*	2.51	1.92
Myxovirus (influenza virus) resistance 1, IFN-inducible protein p78 (mouse)	NM_002462	*MX1*	2.26	1.44
IRF-5	NM_002200	*IRF5*	−2.31	1.06
IFN-α-inducible protein 27	NM_005532	*IFI27*	−2.46	−1.62
IFN-γ-inducible protein 30	NM_006332	*IFI30*	−2.79	−2.79
Interleukins				
IL-6 (IFN, beta 2)	NM_000600	*IL6*	4.05	1
IL-1α	NM_000575	*IL1A*	−1.43	2.01
IL-8	NM_000584	*IL8*	−2.9	−1.39
IL-1β	NM_000576	*IL1B*	−2.25	1.39
TNF (TNF superfamily, member 2)	NM_000594	*TNF*	52.21	6.79
Other cytokines				
GRO2 oncogene (SCYB2), CXCL2	NM_002089	*GRO2*	6.58	2.22
Small inducible cytokine A3	NM_002983	*SCYA3*	4.22	1.12
Small inducible cytokine A5 (RANTES)	NM_002985	*SCYA5*	4.17	−1.17
Small inducible cytokine A4	NM_002984	*SCYA4*	3.74	−1.14
Colony-stimulating factor 2 (granulocyte-macrophage)	NM_000758	*CSF2*	3.13	−1.08
Apoptosis				
Nuclear factor of kappa light polypeptide gene enhancer in B cells inhibitor α	NM_020529	*NFKBIA*	9.59	6.02
MAIL, NFKBIZ	NM_031419	*MAIL*	12.99	4.91
BCL2-associated athanogene 3	NM_004281	*BAG3*	8.42	1.28
Calpain 1, (mu/I) large subunit	NM_005186	*CAPN1*	4.1	1.78
Antiviral immune response				
Melanoma differentiation-associated protein 5	NM_022168	*MDA5*	7.77	1.67

To further validate these results (see Table S4 in the supplemental material), we used cDNAs from MDDC obtained from two other healthy volunteers. MDDC were infected with MVA or NYVAC for 6 h, cDNA was prepared, and RT-PCR was performed as described above (Table 3). The results for three donors revealed a similar pattern of cytokine gene expression induced by the two poxvirus vectors (Table 3), validating the microarray data.

Differences in host gene expression levels in MVA- and NYVAC-infected MDDC compared to infected HeLa cells. To provide further evidence for distinct gene regulation by NYVAC and MVA, we compared gene expression levels between HeLa cells infected with MVA or NYVAC with MDDC infected with the same poxvirus vectors. Genes expressed in 6-h NYVAC- or MVA-infected HeLa cells were subtracted from the genes regulated by both viruses in infected MDDC. Thus, we selected those genes showing at least twofold-higher expression levels in one cell type than in the other. We identified 1,245 genes that were differentially expressed after MVA infection of MDDC compared to HeLa cells (34.5% of the genes selected); of these genes, 463 were upregulated and 782 were downregulated in infected MDDC compared to infected HeLa cells. In the case of NYVAC infection, 1,970 genes were differentially expressed in MDDC versus HeLa cells (51.1% of the selected genes); of these genes, 1,009 were upregulated and 961 were downregulated in infected MDDC compared to HeLa cells. MVA- and NYVAC-infected MDDC shared 268 upregulated and 380 downregulated genes (data not shown). Functional analysis of genes with at least twofold-higher expression levels in MVA- or NYVAC-infected MDDC showed similar percentages for the main functional categories including immune response, cell death, or cell signaling (data not shown). Examples of these genes are shown in Table 4 and in Tables S4 and S5 in the supplemental material.

Several genes that were upregulated in MVA-infected MDDC also showed higher expression levels than their counterparts in MVA-infected HeLa cells or in NYVAC-infected MDDC. These include TNF-α, IFN-β, interferon-induced IFIT1 and IFIT4 genes, cytokines such as GRO2 (CXCL2), and genes involved in the antiviral immune response (RIG-I, MDA5, and GBP5).

Downloaded from jvi.asm.org at Centro Nacional de Biotecnología - Biblioteca on October 15, 2007

TABLE 2. Differential gene expression profiling of MVA-infected versus NYVAC-infected human DC[a]

Description	GenBank accession no.	Gene	Fold change of MVA/NYVAC
IFNs and IFN-induced genes			
IFN-induced protein with tetratricopeptide repeats 4	NM_001549	*IFIT4*	11.45
IFN-induced protein with tetratricopeptide repeats 1	NM_001548	*IFIT1*	7.38
IFN-induced, hepatitis C virus-associated microtubular aggregate protein (44 kDa)	NM_006417	*MTAP44*	5.52
Guanylate binding protein 5	NM_052942	*GBP5*	5.37
IFN-β1, fibroblast	NM_002176	*IFNB1*	5.06
IFN-stimulated protein, 15 kDa	NM_005101	*ISG15*	2.56
IFN-stimulated gene (20 kDa)	BC016341	*ISG20*	2.51
IRF-7	NM_004031	*IRF7*	2.31
IFN-α1	NM_024013	*IFNA1*	1.18
Interleukins			
IL-12β (NK cell-stimulatory factor 2)	NM_002187	*IL12B*	5.44
IL-6 (IFN-β2)	NM_000600	*IL6*	4.05
IL-1α	NM_000575	*IL1A*	−2.42
IL-1β	NM_000576	*IL1B*	−3.14
TNF and related genes			
TNF (TNF superfamily, member 2)	NM_000594	*TNF*	10.38
TNF receptor-associated factor 6	NM_004620	*TRAF6*	1.7
Tumor necrosis factor receptor superfamily, member 10b	AF016266	*TNFRSF10B*	−1.07
Other cytokines			
Small inducible cytokine A4	NM_002984	*SCYA4*	5.61
Small inducible cytokine A5 (RANTES)	NM_002985	*SCYA5*	3.06
GRO2 oncogene (SCYB2), CXCL2	NM_002089	*GRO2*	2.78
Small inducible cytokine subfamily B member 10, CXCL10, IP-10	NM_001565	*SCYB10*	2.35
Colony-stimulating factor 2 (granulocyte-macrophage)	NM_000758	*CSF2*	1.94
Apoptosis			
BCL2-associated athanogene 3	NM_004281	*BAG3*	4.55
MAIL, NFKBIZ	NM_031419	*MAIL*	2.85
Calpain 1 (mu/I) large subunit	NM_005186	*CAPN1*	1.72
Antiviral immune response			
RNA helicase	NM_014314	*RIG-I*	5.72
Melanoma differentiation-associated protein 5	NM_022168	*MDA5*	5.05
OASL	NM_003733	*OASL*	4.53

[a] Shown is a comparison of gene expression profiling between MVA- and NYVAC-infected MDDC. Representative human genes specifically regulated by each vector according to predicted biological function are shown.

TABLE 3. Expression levels of selected genes by real-time RT-PCR[a]

Gene product	Fold change by real-time RT-PCR					
	MVA vs mock			NYVAC vs mock		
	DC 1	DC 2	DC 3	DC 1	DC 2	DC 3
TNF	36.63	25.45	44.32	2.23	4.95	4.48
IFN-β	43.86	28.87	27.76	2.15	4.98	1.85
ISG15	3.82	4.62	3.81	2.15	2.27	2.26
IL-12	7.91	5.89	7.98	2.08	1.98	1.79
IL-7	1.78	0.90	2.07	1.27	1.55	0.81
IL-6	2.01	2.36	3.03	1.16	1.41	2.54
IFN-γ	1.45	1.82	1.4	1.19	0.98	1
NFκ2	2.02	3.05	3.64	1.68	2.06	2
OASL	27.66	37.66	26.63	2.13	1.43	0.519
ATF-3	1.96	2.19	1.98	3.51	3.75	3.91
H2AFY	1.44	1.89	1.98	3.73	0.75	0.91
ADORAA2	0.714	1.18	3.6	1.28	1.18	0.63

[a] MDDC from three donors (DC1, DC2, and DC3) were mock, MVA, or NYVAC infected and processed for RT-PCR.

The comparative profiling of infected MDDC versus HeLa cells provides additional evidence that both poxvirus vectors affect host gene expression differently.

Induction of immunomodulatory molecules and activation of IFN pathways in MVA- and NYVAC-infected MDDC. While the above-described experiments indicate that both MVA and NYVAC produced an increase in gene expression of certain cytokines (see Tables S1 and S2 in the supplemental material), MVA elicited higher expression levels of specific immunomodulatory molecules such as TNF-α, IFN-β, CCL5, and IL-12. IL-1α and IL-1β expression levels were nonetheless slightly enhanced after NYVAC infection. Genes involved in the antiviral response, such as OASL, RIG-I, and MDA5, were upregulated after MVA infection. We therefore analyzed the correlation between transcription and translational levels of specific immunomodulatory molecules after poxvirus infection of MDDC. Since we observed high transcriptional levels of TNF-α after MVA infection of MDDC in the microarrays, we used ELISA to evaluate TNF-α levels in supernatants of infected MDDC from three healthy volunteers. High TNF-α

Downloaded from jvi.asm.org at Centro Nacional de Biotecnología - Biblioteca on October 15, 2007

TABLE 4. Differential gene expression in MVA/NYVAC-infected DC compared to that in MVA/NYVAC-infected HeLa cells[a]

Description	GenBank accession	Gene	Fold change	
			MVA	NYVAC
Immune response, inflammatory response				
Small inducible cytokine A3	NM_002983	*SCYA3*	66.81	10.63
IFN-induced protein with tetratricopeptide repeats 4	NM_001549	*IFIT4*	32.52	10.87
TNF (TNF superfamily, member 2)	NM_000594	*TNF*	31.40	5.60
IL-8	NM_000584	*IL8*	20.53	31.45
V-fos FBJ murine osteosarcoma viral oncogene homolog	NM_005252	*FOS*	20.49	1.75
Guanylate binding protein 5	NM_052942	*GBP5*	15.21	
CD83 antigen (activated B lymphocytes, immunoglobulin superfamily)	NM_004233	*CD83*	14.53	12.41
IFN-β1, fibroblast	NM_002176	*IFNB1*	13.70	4.52
GRO2 oncogene	NM_002089	*GRO2*	13.21	1.64
Pre-B-cell colony-enhancing factor	NM_005746	*PBEF*	8.01	13.38
MDA5	NM_022168	*MDA5*	6.66	
Nuclear factor of kappa light polypeptide gene enhancer in B cells 1 (p105)	NM_003998	*NFKB1*	5.70	12.59
RNA helicase	NM_014314	*RIG-I*	5.42	
IFN-α-inducible protein (clone IFI-6–16)	NM_022873	*G1P3*	4.69	2.77
IRF-7	NM_004031	*IRF7*	4.24	3.37
IFN-induced protein with tetratricopeptide repeats 1	NM_001548	*IFIT1*	3.88	8.63
IFN-γ-inducible protein 30	NM_006332	*IFI30*	3.51	5.85
Myxovirus (influenza virus) resistance 1, IFN-inducible protein p78 (mouse)	NM_002462	*MX1*	3.45	
Small inducible cytokine A4	NM_002984	*SCYA4*		14.94
Apoptosis				
TNF-α-induced protein 3	NM_006290	*TNFAIP3*	18.24	20.04
Apolipoprotein E	NM_000041	*APOE*	15.45	4.58
TNF receptor-associated factor 1	NM_005658	*TRAF1*	2.43	4.92
Death-associated protein 6	NM_001350	*DAXX*	−1.22	6.17
IL-1β	NM_000576	*IL1B*		5.49
Cathepsin B	NM_001908	*CTSB*		11.43
Cell cycle, signaling				
Carcinoembryonic antigen-related cell adhesion molecule 6	M18216	*CEACAM6*	78.47	10.14
Endothelial PAS domain protein 1	NM_001430	*EPAS1*	11.21	7.29
Leupaxin	NM_004811	*LPXN*	9.59	7.45
Fibrinogen, gamma polypeptide	NM_021870	*FGG*	7.79	13.30
Prostaglandin E receptor 1 (subtype EP1), 42kD	NM_000955	*PTGER1*	5.76	10.54
Mitogen-activated protein kinase 6	NM_002748	*MAPK6*	5.33	8.48
Wingless-type MMTV integration site family, member 10B	NM_003394	*WNT10B*	4.25	6.44
Pleckstrin	NM_002664	*PLEK*		11.08
CD53 antigen	NM_000560	*CD53*		9.48
RAP1B, member of RAS oncogene family	NM_015646	*RAP1B*		15.26

[a] Both cell types were infected with MVA or NYVAC (5 PFU/cell), and total RNA was extracted at 6 hpi and processed for microarray and data analysis (see Materials and Methods and Results). FBJ, Finkel-Biskis-Junkins; PAS, Per-Arnt-Sim.

levels were induced in MDDC from all volunteers after MVA infection compared to NYVAC infection, with higher levels at 6 than at 16 hpi (Fig. 5A).

Since high levels of type I *IFN* gene expression (Table 2) were produced after poxvirus infection of MDDC, and IFN expression is regulated by IRFs (IRF-3 and IRF-7), we analyzed the levels of these two factors involved in the IFN-responsive pathway. Western blot analysis showed increased IRF-7 levels after MVA and NYVAC infection of MDDC but not after infection of HeLa cells (Fig. 5B). To induce *IFN* gene expression, IRF phosphorylation is needed (72). We thus used Western blotting to determine levels of IRF-3, both unphosphorylated and phosphorylated, in MVA- or NYVAC-infected MDDC. The results showed an increase in IRF-3 phosphorylation in MVA- and NYVAC-infected compared to uninfected cells (Fig. 5B). Phosphorylation levels were higher in NYVAC- than in MVA-infected MDDC, although this increase was not observed in HeLa cells. Levels of the VACV protein E3, an inhibitor of IRF-3 phosphorylation (72), were considerably higher after MVA infection than after NYVAC infection.

These findings indicate that the enhanced transcriptional levels of genes encoding immunomodulatory molecules observed in microarray after MVA or NYVAC infection correlate with protein levels, at least for TNF, and that the induction of type I *IFN* gene expression may be mediated by poxvirus-induced expression of RIG-I/MDA5. This in turn would trigger the phosphorylation of IRF-3, translocation to the nucleus, and the activation of *IFN* gene expression.

DISCUSSION

Efficient antiviral immunity involves both innate and adaptive immune responses. Adaptive immunity leads to viral clearance and generates long-term immunological memory through the generation of specific T and B cells. DC found in an immature state in all tissues orchestrate the development of

Downloaded from jvi.asm.org at Centro Nacional de Biotecnología - Biblioteca on October 15, 2007

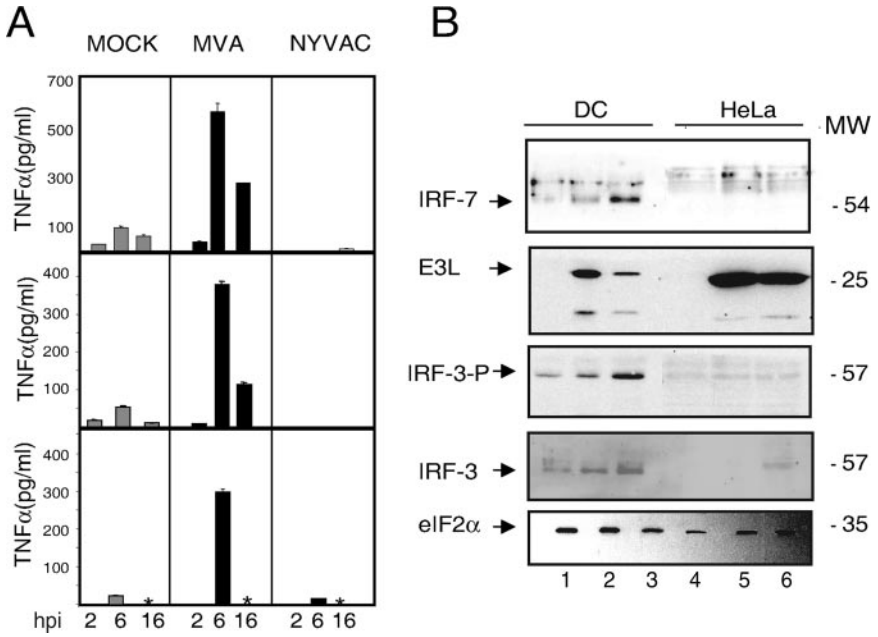

FIG. 5. Validation of microarray data at the protein level. (A) TNF-α levels in cell supernatants after MVA or NYVAC infection. MDDC from three different donors were mock infected or infected with MVA or NYVAC (5 PFU/cell) for 2, 6, and 16 h, and TNF levels in supernatants were measured by ELISA. Values indicate duplicate samples in two independent experiments. An asterisk indicates a lack of data. (B) IRF-3 and IRF-7 levels in virus-infected MDDC. Mock (lanes 1 and 4)-, MVA (lanes 2 and 5)-, or NYVAC (lanes 3 and 6)-infected (5 PFU/cell) MDDC or HeLa cell extracts were fractionated by SDS-PAGE, transferred onto nitrocellulose, and incubated with antibodies to IRF-7, IRF-3, phosphorylated IRF-3 (IRF-3-P), eIF-2α (as a protein loading control), and the viral protein E3L (as a virus infection control). The molecular weight of protein standards (MW) (in thousands) is indicated (right).

adaptive immunity (6). Following pathogen recognition, there are changes in the expression of DC proinflammatory genes, including those coding for cytokines, chemokines, and costimulatory molecules, in a process known as DC maturation (6, 58). These functional changes are necessary for initiating adaptive immunity. Immediately after viral infection, host innate immune defenses are induced. These immune responses are critical for the activation of adaptive immunity. There is nonetheless a 4- to 7-day delay before the adaptive immune response is initiated, during which time the innate immune response has an important role in early viral clearance (37). VACV attempts to subvert the innate response by secreting proteins that inactivate complement (41), inhibit the IFN response (9, 74), protect it from inflammatory responses, and prevent natural killer (NK) cell activation (2).

Poxvirus vectors are efficient activators of host immune responses to virally expressed antigens of distinct origin and are being used as potential vaccines for several pathogens and tumors (49, 50, 55). It is therefore important to define the transcriptional changes in human APC, particularly in MDDC, after VACV vector infection. Here, we showed that MDDC infected with MVA or NYVAC at 5 PFU/cell caused extensive morphological damage to the cells at late times postinfection. This is characterized by the severe inhibition of protein synthesis by 6 hpi and apoptosis induction together with rRNA cleavage at 16 hpi. In spite of a general translational block induced by the two vectors, some of the early (E3) and late (A4, A14, and A27) viral proteins examined were produced in the infected cells, although differences were observed between these vectors. In contrast to MVA infection, NYVAC-infected MDDC do not produce A17 or A27 proteins, and both viruses do not synthesize A36R or B5R proteins. The difference in viral gene expression between the two vectors might be related to the extent of eIF-2α phosphorylation and RNA degradation induced during infection as well as the presence or absence of certain viral genes in the poxvirus vectors. In agreement with other investigators, MVA induced apoptosis late in the infection and inhibition of some of the late proteins. In view of the severity of the effect triggered by the two poxvirus vectors in MDDC late in the infection, we used 6 hpi and a multiplicity of 5 PFU/cell for gene expression profiling. We applied genomic studies using microarrays and various data analysis conditions to define the impact of infection of immature human MDDC with the two attenuated VACV strains MVA and NYVAC. We identified genes regulated by MVA and NYVAC infection of MDDC at a postinfection time before rRNA breakdown and defined that these two vectors trigger some similar and some distinct host gene expression profiles. For this study, we used three approaches. First, we identified genes that were selectively expressed in MVA- or NYVAC-infected MDDC compared to mock-infected cells. We subsequently defined genes that were specifically regulated by MVA in comparison with NYVAC infection, and finally, we described genes regulated in MVA- or NYVAC-infected HeLa cells compared to MDDC infected by these viruses. Our analysis showed that in infected human MDDC, MVA upregulates more genes than NYVAC. Since the expression of genes involved in host defense is markedly enhanced after MVA infection, we discuss the contribution of some of these genes to MDDC responses, taking the viral genes that counteract host immune responses

Downloaded from jvi.asm.org at Centro Nacional de Biotecnología - Biblioteca on October 15, 2007

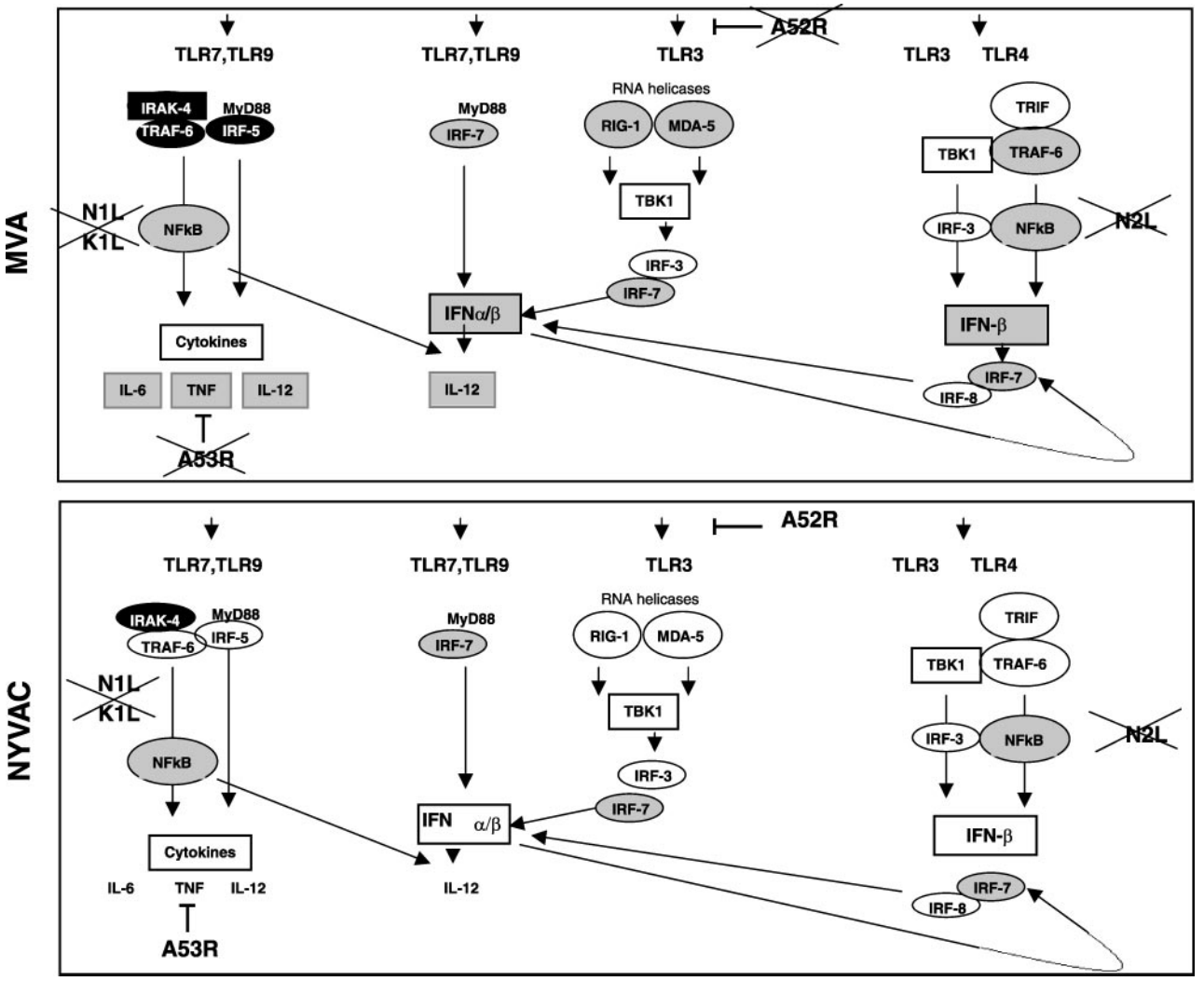

FIG. 6. Signaling pathways regulated by MVA or NYVAC infection in MDDC. Genes whose expression levels are enhanced in MDDC by the poxvirus vector infection are shown in gray, and downregulated genes are shown in black. Viral genes known to interfere with selected pathways are indicated. MVA lacks genes that interfere TLR signaling (A52R and A53R), which are present in NYVAC.

into consideration. It should be noted that the effect of the poxvirus vectors on host genome profiling is due to the contribution of the infected and noninfected cells (Fig. 1) together with the immunomodulators released during infection acting in an autocrine and paracrine manner.

TLR. An efficient innate immune response is a prerequisite for the activation of adaptive immune responses. Toll-like receptors (TLR) are expressed predominantly in APC such as macrophages and MDDC. TLR3 is a double-stranded RNA receptor with a key role in antiviral and inflammatory responses through cross-priming of several physiological pathways including the activation of IFN responses, NF-κB, mitogen-activated protein kinase pathways, and the caspase cascade (54). We found that TLR3 expression was clearly upregulated after MVA infection of MDDC, implying a possible role for TLR3 in double-stranded RNA-initiated antiviral and inflammatory responses. Altered TLR expression has been linked to enhanced responsiveness to viral infection, as reported previously for viruses such as respiratory syncytial virus (27), VACV (34), and hepatitis C virus (45). In VACV, two viral genes have been implicated in TLR-dependent signaling, the A46R and A52R genes. While the A46R gene is present in both MVA and NYVAC genomes, the A52R gene is found only in NYVAC. Since this viral gene is involved in the blockade of NF-κB by several TLR, including TLR3, we propose that the upregulation of the TLR3 pathway after MVA infection (Fig. 6) could be due to the absence of the A52R gene in its genome. This activation was not observed after NYVAC infection. The A52R gene has been described to associate with both IL-1 receptor-associated kinase 2 (IRAK2) and TNF receptor-associated factor 6 (TRAF6), two key proteins in TLR signal transduction (34). We observed the upregulation of TRAF6 and the downregulation of IL-1α and IL-1β only in MVA-infected MDDC.

Comparison of a TLR signaling pathway in MVA- and NYVAC-infected MDDC showed similar transcription levels in genes encoding receptor/adaptors, with some genes slightly repressed (phosphatidylinositol 3-kinase and IRAK1) and

Downloaded from jvi.asm.org at Centro Nacional de Biotecnología - Biblioteca on October 15, 2007

some genes slightly enhanced (TRAF6 and TBK1). Transcription levels were similar in genes encoding transcription factors and inflammatory cytokines, with some enhanced genes in MVA-infected (IFN-α, IFN-β, TNF-α, IL-12β, CCL3, CCL4, CCL5, and CXCL10) and in NYVAC-infected (IFN-β and TNF-α) cells. Neither MVA nor NYVAC had any effect on costimulatory molecule expression (CD40, CD80, and CD86). Transcription of genes involved in the antiviral immune response and cytokine production was clearly more enhanced in MVA-infected MDDC than in NYVAC-infected MDDC.

Type I IFN production and antiviral response. The most consistent changes in MDDC infection by the attenuated poxvirus vectors involved genes implicated in the type I IFN-α/β response (Tables 1 to 3). By generating an intracellular environment that restricts viral replication, type I IFN represent a first line of defense against virus infection (25). The IFN signaling system produces a broadly effective innate response by creating an antiviral state in both an autocrine and a paracrine manner (81). IFN gene expression is regulated by IRF-3 phosphorylation, homodimerization, and nuclear translocation (67). Once in the nucleus, IRF-3 interacts with IRF-3-responsive promoters and the transcriptional coactivator histone acetyltransferase CBP/p300, leading to the transcription of IRF-responsive genes; together with NF-κB and AP-1, IRF-3 also promotes IFN-β transcription. The microarray experiments showed a clear upregulation of RIG-I and MDA5 levels only after MVA infection (Tables 1 to 3). As RIG-I and MDA-5 mRNA expression levels are strongly enhanced by type I IFN (70), we propose that the elevated IFN levels produced after MVA infection might be involved in the upregulation of RIG-I and MDA5, which can also activate the expression of type I IFN in a feedback mechanism (Fig. 6). This is supported by the enhanced IRF-3 phosphorylation observed in MVA-infected MDDC cells (Fig. 5B).

RIG-I and MDA5 upregulation was not observed in previous studies using mRNA microarrays from MVA-infected HeLa cells (29). The specificity of RIG-I and MDA5 expression in MVA-infected MDDC was also confirmed in a microarray experiment comparing the expression profiles of MVA-infected HeLa cells and MDDC at 6 hpi (Table 4; also see Table S4 in the supplemental material). These observations indicate a cell type-specific involvement of RIG-I in the antiviral response to poxvirus infection. This concurs with the observations made previously by Ichikawa et al., where type I IFN induction in fibroblasts and myeloid DC was RIG-I dependent, while type I IFN induction in periferical DC was independent of RIG-I (36). RNA virus recognition by RIG-I and MDA5 is reported to involve distinct mechanisms (36), but little is known of the mechanisms used by their helicases in infection with DNA viruses.

Type I IFN levels were notably higher during MVA infection than during NYVAC infection. There was no apparent RIG-I or MDA-5 upregulation during NYVAC infection, possibly due to low IFN levels or to specific differences between MVA and NYVAC genomes. VACV genes involved in inhibiting the IFN response include the E3L (16), B18R (17), K3L (12), and N1L (31) genes. Although MVA and NYVAC share common deleted genes, including serpins (the B13R and B14R genes), the M2L and N1L genes, which are involved in signaling, and host range genes (the K1L gene), most other deleted genes differ between the two strains. The differences in deleted genes between MVA and NYVAC must play a role in the host genome expression pattern induced after MDDC infection with these vectors (Fig. 6).

Proinflammatory cytokine production (TNF-α, IL-12, and IL-6). Another important difference between MVA and NYVAC infection was the activation of TNF-α, IL-12, and IL-6, which were upregulated more than 10-, 5-, and 4-fold, respectively, in MVA versus NYVAC infection. Since NF-κB plays an important role in the expression of inflammatory cytokines, including TNF-α and IL-12, our results suggest an activation of this pathways by MVA, as previously described for HeLa cells (28, 29). Upregulation of these immunomodulators is likely to have an important role in MDDC function. TNF-α would be released by MDDC while in peripheral tissues to further recruit MDDC precursors and sustain antigen capture and presentation. On the contrary, IL-12 would be released by MDDC in lymph nodes to polarize Th cells toward a Th1 phenotype (42). The fact that viruses encode proteins that act to subvert nearly all aspects of TNF-α signaling (11) emphasizes the importance of the TNF-α/TNF receptor axis in antiviral immunity and virus-host interactions. Poxviruses have evolved various strategies to prevent apoptosis, including the ability to inhibit secreted TNF-α (57). In microarrays and Western blots, we found an increase in TNF-α mRNA (Tables 1 to 4) and protein levels (Fig. 5A) in MVA-infected but not in NYVAC-infected MDDC. As the A53R gene is deleted in MVA and is intact in NYVAC, we propose that by its high-affinity binding to human TNF (3), the A53R gene product may be responsible for the decreased TNF levels observed in NYVAC-infected MDDC supernatants.

Apoptosis signaling. During our transcriptional profiling analysis of MVA- and NYVAC-infected MDDC, we observed a clear rRNA breakdown associated with infection by MVA and NYVAC (Fig. 3). MVA infection produced high levels of the 5-OA synthetase-like messenger (Table 2) at 6 hpi, and this is probably the reason for the apparent increase in RNA degradation by MVA compared to NYVAC infection. Activation of this enzyme mediates an antiviral and antitumor function by cleaving cellular and viral RNAs, promoting a general inhibition of protein synthesis and apoptosis (53, 69). The rRNA breakdown products are identical to those produced in cells infected with a VACV recombinant expressing RNase L (not shown), suggesting that MVA or NYVAC infection in MDDC triggers the activation of the 5-OA synthetase/RNase L pathway at late times postinfection (Fig. 3C). Both MVA and NYVAC induced apoptosis in infected MDDC, indicating that a poxvirus-infected MDDC will eventually die. Taking into consideration that the viral E3 protein, a PKR inhibitor (7, 9, 44, 65, 68, 79), is produced at high levels after infection of MDDC with both viruses (Fig. 2), which should block PKR activation, in view of the levels eIF-2α phosphorylation triggered by the poxvirus vectors, we cannot rule out the possibility of another kinase being responsible for eIF-2α phosphorylation and apoptosis induction after MDDC infection. The role of apoptosis in the immune response is still unclear, but antigens produced by apoptotic cells have been reported to increase antigen immunogenicity, which is likely to be more effective in cross-priming (76).

In summary, we have identified important differences in host

Downloaded from jvi.asm.org at Centro Nacional de Biotecnología - Biblioteca on October 15, 2007

genome expression profiling of human immature MDDC after infection with the attenuated poxvirus vectors MVA and NYVAC. This has been achieved using microarray technology and direct comparison of cDNAs from three different systems: MVA- or NYVAC-infected versus mock-infected MDDC, MVA- versus NYVAC-infected MDDC, and MVA- or NYVAC- infected MDDC versus infected HeLa cells. We identified a number of genes that were expressed similarly as well as others that showed differential expression profiling by these viral vectors. In general, MVA infection upregulated more genes than NYVAC infection. Of note are the differences in TNF-α and IFN-β levels, which were higher after MVA infection of MDDC than after NYVAC infection. These differences in vector behavior might be related to the number of genes in the genome of each vector, with MVA lacking more immunomodulatory genes than NYVAC. These poxvirus vectors induced apoptosis in MDDC, suggesting that a cell infected in vivo will not survive. Furthermore, the differences in host gene expression and levels of immunomodulatory molecules produced in MDDC might affect the quality of the immune response induced by each of these vectors when used as vaccines against pathogens and tumors.

ACKNOWLEDGMENTS

We are indebted to R. Bablanian for critically reviewing the manuscript, V. Jiménez for expert technical assistance, and C. Mark for excellent editorial help. We thank Alberto Pascual-Montano and Integromics, SL, for help in clustering. We thank J. Tartaglia (Sanofi-Pasteur) for the generous gift of NYVAC, G. Sutter for MVA, and B. L. Jacobs for anti-E3 antibody.

This work was supported by grants from the Spanish Ministry of Education and Science (BIO2004-03954 and SAF2005-05566), the Spanish Ministry of Health (FIS2006-1259), the Spanish Foundation for AIDS Research (FIPSE 36344/02 and FIPSE 36536-05), Fundación Botín, and the European Union (EuroVac QLRT-PL-1999-01321 and QLK2-CT-2002-01867). The Department of Immunology and Oncology was founded and is supported by the Spanish National Research Council (CSIC) and by Pfizer.

REFERENCES

1. **Abendroth, A., G. Morrow, A. L. Cunningham, and B. Slobedman.** 2001. Varicella-zoster virus infection of human dendritic cells and transmission to T cells: implications for virus dissemination in the host. J. Virol. **75:**6183–6192.
2. **Alcami, A.** 2003. Viral mimicry of cytokines, chemokines and their receptors. Nat. Rev. Immunol. **3:**36–50.
3. **Alcami, A., A. Khanna, N. L. Paul, and G. L. Smith.** 1999. Vaccinia virus strains Lister, USSR and Evans express soluble and cell-surface tumour necrosis factor receptors. J. Gen. Virol. **80:**949–959.
4. **Aliprantis, A. O., R. B. Yang, M. R. Mark, S. Suggett, B. Devaux, J. D. Radolf, G. R. Klimpel, P. Godowski, and A. Zychlinsky.** 1999. Cell activation and apoptosis by bacterial lipoproteins through Toll-like receptor-2. Science **285:**736–739.
5. **Antoine, G., F. Scheiflinger, F. Dorner, and F. G. Falkner.** 1998. The complete genomic sequence of the modified vaccinia Ankara strain: comparison with other orthopoxviruses. Virology **244:**365–396.
6. **Banchereau, J., and R. M. Steinman.** 1998. Dendritic cells and the control of immunity. Nature **392:**245–252.
7. **Beattie, E., K. L. Denzler, J. Tartaglia, M. E. Perkus, E. Paoletti, and B. L. Jacobs.** 1995. Reversal of the interferon-sensitive phenotype of a vaccinia virus lacking E3L by expression of the reovirus S4 gene. J. Virol. **69:**499–505.
8. **Beattie, E., E. B. Kauffman, H. Martinez, M. E. Perkus, B. L. Jacobs, E. Paoletti, and J. Tartaglia.** 1996. Host-range restriction of vaccinia virus E3L-specific deletion mutants. Virus Genes **12:**89–94.
9. **Beattie, E., E. Paoletti, and J. Tartaglia.** 1995. Distinct patterns of IFN sensitivity observed in cells infected with vaccinia K3L− and E3L− mutant viruses. Virology **210:**254–263.
10. **Belyakov, I. M., P. Earl, A. Dzutsev, V. A. Kuznetsov, M. Lemon, L. S. Wyatt, J. T. Snyder, J. D. Ahlers, G. Franchini, B. Moss, and J. A. Berzofsky.** 2003. Shared modes of protection against poxvirus infection by attenuated and conventional smallpox vaccine viruses. Proc. Natl. Acad. Sci. USA **100:**9458–9463.
11. **Benedict, C. A., P. S. Norris, and C. F. Ware.** 2002. To kill or be killed: viral evasion of apoptosis. Nat. Immunol. **3:**1013–1018.
12. **Carroll, K., O. Elroy-Stein, B. Moss, and R. Jagus.** 1993. Recombinant vaccinia virus K3L gene product prevents activation of double-stranded RNA-dependent, initiation factor 2 alpha-specific protein kinase. J. Biol. Chem. **268:**12837–12842.
13. **Cebere, I., L. Dorrell, H. McShane, A. Simmons, S. McCormack, C. Schmidt, C. Smith, M. Brooks, J. E. Roberts, S. C. Darwin, P. E. Fast, C. Conlon, S. Rowland-Jones, A. J. McMichael, and T. Hanke.** 2006. Phase I clinical trial safety of DNA- and modified virus Ankara-vectored human immunodeficiency virus type 1 (HIV-1) vaccines administered alone and in a prime-boost regime to healthy HIV-1-uninfected volunteers. Vaccine **24:**417–425.
14. **Cella, M., M. Salio, Y. Sakakibara, H. Langen, I. Julkunen, and A. Lanzavecchia.** 1999. Maturation, activation, and protection of dendritic cells induced by double-stranded RNA. J. Exp. Med. **189:**821–829.
15. **Chahroudi, A., D. A. Garber, P. Reeves, L. Liu, D. Kalman, and M. B. Feinberg.** 2006. Differences and similarities in viral life cycle progression and host cell physiology after infection of human dendritic cells with modified vaccinia virus Ankara and vaccinia virus. J. Virol. **80:**8469–8481.
16. **Chang, H. W., J. C. Watson, and B. L. Jacobs.** 1992. The E3L gene of vaccinia virus encodes an inhibitor of the interferon-induced, double-stranded RNA-dependent protein kinase. Proc. Natl. Acad. Sci. USA **89:**4825–4829.
17. **Colamonici, O. R., B. Porterfield, P. Domanski, R. K. Handa, S. Flex, C. E. Samuel, R. Pine, and M. O. Diaz.** 1994. Ligand-independent anti-oncogenic activity of the alpha subunit of the type I interferon receptor. J. Biol. Chem. **269:**27275–27279.
18. **Corona Gutierrez, C. M., A. Tinoco, T. Navarro, M. L. Contreras, R. R. Cortes, P. Calzado, L. Reyes, R. Posternak, G. Morosoli, M. L. Verde, and R. Rosales.** 2004. Therapeutic vaccination with MVA E2 can eliminate precancerous lesions (CIN 1, CIN 2, and CIN 3) associated with infection by oncogenic human papillomavirus. Hum. Gene Ther. **15:**421–431.
19. **Deng, L., P. Dai, W. Ding, R. D. Granstein, and S. Shuman.** 2006. Vaccinia virus infection attenuates innate immune responses and antigen presentation by epidermal dendritic cells. J. Virol. **80:**9977–9987.
20. **Drillien, R., D. Spehner, A. Bohbot, and D. Hanau.** 2000. Vaccinia virus-related events and phenotypic changes after infection of dendritic cells derived from human monocytes. Virology **268:**471–481.
21. **Engelmayer, J., M. Larsson, M. Subklewe, A. Chahroudi, W. I. Cox, R. M. Steinman, and N. Bhardwaj.** 1999. Vaccinia virus inhibits the maturation of human dendritic cells: a novel mechanism of immune evasion. J. Immunol. **163:**6762–6768.
22. **Franchini, G., S. Gurunathan, L. Baglyos, S. Plotkin, and J. Tartaglia.** 2004. Poxvirus-based vaccine candidates for HIV: two decades of experience with special emphasis on canarypox vectors. Expert Rev. Vaccines **3:**S75–S88.
23. **Gilbert, S. C., V. S. Moorthy, L. Andrews, A. A. Pathan, S. J. McConkey, J. M. Vuola, S. M. Keating, T. Berthoud, D. Webster, H. McShane, and A. V. Hill.** 2006. Synergistic DNA-MVA prime-boost vaccination regimes for malaria and tuberculosis. Vaccine **24:**4554–4561.
24. **Gomez, C. E., J. L. Najera, V. Jimenez, K. Bieler, J. Wild, L. Kostic, S. Heidari, M. Chen, M. J. Frachette, G. Pantaleo, H. Wolf, P. Liljestrom, R. Wagner, and M. Esteban.** 2007. Generation and immunogenicity of novel HIV/AIDS vaccine candidates targeting HIV-1 Env/Gag-Pol-Nef antigens of clade C. Vaccine **25:**1969–1992.
25. **Grandvaux, N., B. R. tenOever, M. J. Servant, and J. Hiscott.** 2002. The interferon antiviral response: from viral invasion to evasion. Curr. Opin. Infect. Dis. **15:**259–267.
26. **Grosjean, I., C. Caux, C. Bella, I. Berger, F. Wild, J. Banchereau, and D. Kaiserlian.** 1997. Measles virus infects human dendritic cells and blocks their allostimulatory properties for CD4+ T cells. J. Exp. Med. **186:**801–812.
27. **Groskreutz, D. J., M. M. Monick, L. S. Powers, T. O. Yarovinsky, D. C. Look, and G. W. Hunninghake.** 2006. Respiratory syncytial virus induces TLR3 protein and protein kinase R, leading to increased double-stranded RNA responsiveness in airway epithelial cells. J. Immunol. **176:**1733–1740.
28. **Guerra, S., L. A. Lopez-Fernandez, M. Angel Garcia, A. Zaballos, and M. Esteban.** 2006. Human gene profiling in response to the active protein kinase, interferon-induced serine/threonine protein kinase (PKR), in infected cells. Involvement of the transcription factor ATF-3 in PKR-induced apoptosis. J. Biol. Chem. **281:**18734–18745.

28a. **Guerra, S., L. A. López-Fernández, A. Pascual-Montano, J. L. Nájera, A. Zaballos, and M. Estaban.** 2006. Host response to the attenuated poxvirus vector NYVAC: upregulation of apoptotic genes and NF-κB-responsive genes in infected HeLa cells. J. Virol. **80:**985–998.

29. **Guerra, S., L. A. Lopez-Fernandez, R. Conde, A. Pascual-Montano, K. Harshman, and M. Esteban.** 2004. Microarray analysis reveals characteristic changes of host cell gene expression in response to attenuated modified vaccinia virus Ankara infection of human HeLa cells. J. Virol. **78:**5820–5834.
30. **Guerra, S., L. A. Lopez-Fernandez, A. Pascual-Montano, M. Munoz, K. Harshman, and M. Esteban.** 2003. Cellular gene expression survey of vaccinia virus infection of human HeLa cells. J. Virol. **77:**6493–6506.

Downloaded from jvi.asm.org at Centro Nacional de Biotecnología - Biblioteca on October 15, 2007

31. **Haga, I. R., and A. G. Bowie.** 2005. Evasion of innate immunity by vaccinia virus. Parasitology **130:**S11–S25.
32. **Harper, N., M. A. Hughes, S. N. Farrow, G. M. Cohen, and M. MacFarlane.** 2003. Protein kinase C modulates tumor necrosis factor-related apoptosis-inducing ligand-induced apoptosis by targeting the apical events of death receptor signaling. J. Biol. Chem. **278:**44338–44347.
33. **Harrop, R., N. Connolly, I. Redchenko, J. Valle, M. Saunders, M. G. Ryan, K. A. Myers, N. Drury, S. M. Kingsman, R. E. Hawkins, and M. W. Carroll.** 2006. Vaccination of colorectal cancer patients with modified vaccinia Ankara delivering the tumor antigen 5T4 (TroVax) induces immune responses which correlate with disease control: a phase I/II trial. Clin. Cancer Res. **12:**3416–3424.
34. **Harte, M. T., I. R. Haga, G. Maloney, P. Gray, P. C. Reading, N. W. Bartlett, G. L. Smith, A. Bowie, and L. A. O'Neill.** 2003. The poxvirus protein A52R targets Toll-like receptor signaling complexes to suppress host defense. J. Exp. Med. **197:**343–351.
35. **Hornemann, S., O. Harlin, C. Staib, S. Kisling, V. Erfle, B. Kaspers, G. Hacker, and G. Sutter.** 2003. Replication of modified vaccinia virus Ankara in primary chicken embryo fibroblasts requires expression of the interferon resistance gene E3L. J. Virol. **77:**8394–8407.
36. **Ichikawa, T., K. Nakao, K. Nakata, K. Hamasaki, Y. Takeda, Y. Kajiya, S. Higashi, K. Ohkubo, Y. Kato, N. Ishii, and K. Eguchi.** 2001. Geranylgeranylacetone induces antiviral gene expression in human hepatoma cells. Biochem. Biophys. Res. Commun. **280:**933–939.
37. **Janeway, C., Jr., and R. Medzhitov.** 2000. Viral interference with IL-1 and Toll signaling. Proc. Natl. Acad. Sci. USA **97:**10682–10683.
38. **Jenne, L., C. Hauser, J. F. Arrighi, J. H. Saurat, and A. W. Hugin.** 2000. Poxvirus as a vector to transduce human dendritic cells for immunotherapy: abortive infection but reduced APC function. Gene Ther. **7:**1575–1583.
39. **Kanesa-thasan, N., J. J. Smucny, C. H. Hoke, D. H. Marks, E. Konishi, I. Kurane, D. B. Tang, D. W. Vaughn, P. W. Mason, and R. E. Shope.** 2000. Safety and immunogenicity of NYVAC-JEV and ALVAC-JEV attenuated recombinant Japanese encephalitis virus-poxvirus vaccines in vaccinia-non-immune and vaccinia-immune humans. Vaccine **19:**483–491.
40. **Kastenmuller, W., I. Drexler, H. Ludwig, V. Erfle, C. Peschel, H. Bernhard, and G. Sutter.** 2006. Infection of human dendritic cells with recombinant vaccinia virus MVA reveals general persistence of viral early transcription but distinct maturation-dependent cytopathogenicity. Virology **350:**276–288.
41. **Kotwal, G. J., S. N. Isaacs, R. McKenzie, M. M. Frank, and B. Moss.** 1990. Inhibition of the complement cascade by the major secretory protein of vaccinia virus. Science **250:**827–830.
42. **Langenkamp, A., M. Messi, A. Lanzavecchia, and F. Sallusto.** 2000. Kinetics of dendritic cell activation: impact on priming of TH1, TH2 and non-polarized T cells. Nat. Immunol. **1:**311–316.
43. **Langland, J. O., J. C. Kash, V. Carter, M. J. Thomas, M. G. Katze, and B. L. Jacobs.** 2006. Suppression of proinflammatory signal transduction and gene expression by the dual nucleic acid binding domains of the vaccinia virus E3L proteins. J. Virol. **80:**10083–10095.
44. **Lee, S. B., and M. Esteban.** 1994. The interferon-induced double-stranded RNA-activated protein kinase induces apoptosis. Virology **199:**491–496.
45. **Li, K., E. Foy, J. C. Ferreon, M. Nakamura, A. C. Ferreon, M. Ikeda, S. C. Ray, M. Gale, Jr., and S. M. Lemon.** 2005. Immune evasion by hepatitis C virus NS3/4A protease-mediated cleavage of the Toll-like receptor 3 adaptor protein TRIF. Proc. Natl. Acad. Sci. USA **102:**2992–2997.
46. **Ludwig, H., J. Mages, C. Staib, M. H. Lehmann, R. Lang, and G. Sutter.** 2005. Role of viral factor E3L in modified vaccinia virus Ankara infection of human HeLa Cells: regulation of the virus life cycle and identification of differentially expressed host genes. J. Virol. **79:**2584–2596.
47. **Mellman, I., and R. M. Steinman.** 2001. Dendritic cells: specialized and regulated antigen processing machines. Cell **106:**255–258.
48. **Meyer, H., G. Sutter, and A. Mayr.** 1991. Mapping of deletions in the genome of the highly attenuated vaccinia virus MVA and their influence on virulence. J Gen. Virol. **72:**1031–1038.
49. **Moss, B.** 1996. Genetically engineered poxviruses for recombinant gene expression, vaccination, and safety. Proc. Natl. Acad. Sci. USA **93:**11341–11348.
50. **Moss, B., M. W. Carroll, L. S. Wyatt, J. R. Bennink, V. M. Hirsch, S. Goldstein, W. R. Elkins, T. R. Fuerst, J. D. Lifson, M. Piatak, N. P. Restifo, W. Overwijk, R. Chamberlain, S. A. Rosenberg, and G. Sutter.** 1996. Host range restricted, non-replicating vaccinia virus vectors as vaccine candidates. Adv. Exp. Med. Biol. **397:**7–13.
51. **Munoz-Fontela, C., M. Collado, E. Rodriguez, M. A. Garcia, A. Alvarez-Barrientos, J. Arroyo, C. Nombela, and C. Rivas.** 2005. Identification of a nuclear export signal in the KSHV latent protein LANA2 mediating its export from the nucleus. Exp. Cell Res. **311:**96–105.
52. **Myagkikh, M., S. Alipanah, P. D. Markham, J. Tartaglia, E. Paoletti, R. C. Gallo, G. Franchini, and M. Robert-Guroff.** 1996. Multiple immunizations with attenuated poxvirus HIV type 2 recombinants and subunit boosts required for protection of rhesus macaques. AIDS Res. Hum. Retrovir. **12:**985–992.
53. **Najera, J. L., C. E. Gomez, E. Domingo-Gil, M. M. Gherardi, and M. Esteban.** 2006. Cellular and biochemical differences between two attenuated poxvirus vaccine candidates (MVA and NYVAC) and role of the C7L gene. J. Virol. **80:**6033–6047.
54. **Nishiya, T., E. Kajita, S. Miwa, and A. L. Defranco.** 2005. TLR3 and TLR7 are targeted to the same intracellular compartments by distinct regulatory elements. J. Biol. Chem. **280:**37107–37117.
55. **Ockenhouse, C. F., P. F. Sun, D. E. Lanar, B. T. Wellde, B. T. Hall, K. Kester, J. A. Stoute, A. Magill, U. Krzych, L. Farley, R. A. Wirtz, J. C. Sadoff, D. C. Kaslow, S. Kumar, L. W. Church, J. M. Crutcher, B. Wizel, S. Hoffman, A. Lalvani, A. V. Hill, J. A. Tine, K. P. Guito, C. de Taisne, R. Anders, W. R. Ballou, et al.** 1998. Phase I/IIa safety, immunogenicity, and efficacy trial of NYVAC-Pf7, a pox-vectored, multiantigen, multistage vaccine candidate for Plasmodium falciparum malaria. J. Infect. Dis. **177:**1664–1673.
56. **Pacheco, R., J. M. Martinez-Navio, M. Lejeune, N. Climent, H. Oliva, J. M. Gatell, T. Gallart, J. Mallol, C. Lluis, and R. Franco.** 2005. CD26, adenosine deaminase, and adenosine receptors mediate costimulatory signals in the immunological synapse. Proc. Natl. Acad. Sci. USA **102:**9583–9588.
57. **Pomerantz, J., N. Schreiber-Agus, N. J. Liegeois, A. Silverman, L. Alland, L. Chin, J. Potes, K. Chen, I. Orlow, H. W. Lee, C. Cordon-Cardo, and R. A. DePinho.** 1998. The Ink4a tumor suppressor gene product, p19Arf, interacts with MDM2 and neutralizes MDM2's inhibition of p53. Cell **92:**713–723.
58. **Ridge, J. P., F. Di Rosa, and P. Matzinger.** 1998. A conditioned dendritic cell can be a temporal bridge between a CD4+ T-helper and a T-killer cell. Nature **393:**474–478.
59. **Riegler, S., H. Hebart, H. Einsele, P. Brossart, G. Jahn, and C. Sinzger.** 2000. Monocyte-derived dendritic cells are permissive to the complete replicative cycle of human cytomegalovirus. J. Gen. Virol. **81:**393–399.
60. **Risco, C., J. R. Rodriguez, W. Demkowicz, R. Heljasvaara, J. L. Carrascosa, M. Esteban, and D. Rodriguez.** 1999. The vaccinia virus 39-kDa protein forms a stable complex with the p4a/4a major core protein early in morphogenesis. Virology **265:**375–386.
61. **Rodriguez, D., M. Esteban, and J. R. Rodriguez.** 1995. Vaccinia virus A17L gene product is essential for an early step in virion morphogenesis. J. Virol. **69:**4640–4648.
62. **Rodriguez, D., J. R. Rodriguez, J. F. Rodriguez, D. Trauber, and M. Esteban.** 1989. Highly attenuated vaccinia virus mutants for the generation of safe recombinant viruses. Proc. Natl. Acad. Sci. USA **86:**1287–1291.
63. **Rodriguez, J. F., R. Janeczko, and M. Esteban.** 1985. Isolation and characterization of neutralizing monoclonal antibodies to vaccinia virus. J. Virol. **56:**482–488.
64. **Rodriguez, J. R., C. Risco, J. L. Carrascosa, M. Esteban, and D. Rodriguez.** 1998. Vaccinia virus 15-kilodalton (A14L) protein is essential for assembly and attachment of viral crescents to virosomes. J. Virol. **72:**1287–1296.
65. **Romano, P. R., F. Zhang, S.-L. Tan, M. T. Garcia-Barrio, M. G. Katze, T. E. Dever, and A. G. Hinnebusch.** 1998. Inhibition of double-stranded RNA-dependent protein kinase PKR by vaccinia virus E3: role of complex formation and the E3 N-terminal domain. Mol. Cell. Biol. **18:**7304–7316.
66. **Schneider, J., S. C. Gilbert, T. J. Blanchard, T. Hanke, K. J. Robson, C. M. Hannan, M. Becker, R. Sinden, G. L. Smith, and A. V. Hill.** 1998. Enhanced immunogenicity for CD8+ T cell induction and complete protective efficacy of malaria DNA vaccination by boosting with modified vaccinia virus Ankara. Nat. Med. **4:**397–402.
67. **Servant, M. J., B. ten Oever, C. LePage, L. Conti, S. Gessani, I. Julkunen, R. Lin, and J. Hiscott.** 2001. Identification of distinct signaling pathways leading to the phosphorylation of interferon regulatory factor 3. J. Biol. Chem. **276:**355–363.
68. **Sharp, T. V., F. Moonan, A. Romashko, B. Joshi, G. N. Barber, and R. Jagus.** 1998. The vaccinia virus E3L gene product interacts with both the regulatory and the substrate binding regions of PKR: implications for PKR autoregulation. Virology **250:**302–315.
69. **Silverman, R. H.** 2003. Implications for RNase L in prostate cancer biology. Biochemistry **42:**1805–1812.
70. **Siren, J., T. Imaizumi, D. Sarkar, T. Pietila, D. L. Noah, R. Lin, J. Hiscott, R. M. Krug, P. B. Fisher, I. Julkunen, and S. Matikainen.** 2006. Retinoic acid inducible gene-I and mda-5 are involved in influenza A virus-induced expression of antiviral cytokines. Microbes Infect. **8:**2013–2020.
71. **Sivanandham, M., P. Shaw, S. F. Bernik, E. Paoletti, and M. K. Wallack.** 1998. Colon cancer cell vaccine prepared with replication-deficient vaccinia viruses encoding B7.1 and interleukin-2 induce antitumor response in syngeneic mice. Cancer Immunol. Immunother. **46:**261–267.
72. **Smith, E. J., I. Marie, A. Prakash, A. Garcia-Sastre, and D. E. Levy.** 2001. IRF3 and IRF7 phosphorylation in virus-infected cells does not require double-stranded RNA-dependent protein kinase R or Ikappa B kinase but is blocked by vaccinia virus E3L protein. J. Biol. Chem. **276:**8951–8957.
73. **Soldani, C., and A. I. Scovassi.** 2002. Poly(ADP-ribose) polymerase-1 cleavage during apoptosis: an update. Apoptosis **7:**321–328.
74. **Symons, J. A., A. Alcami, and G. L. Smith.** 1995. Vaccinia virus encodes a soluble type I interferon receptor of novel structure and broad species specificity. Cell **81:**551–560.
75. **Tartaglia, J., M. E. Perkus, J. Taylor, E. K. Norton, J. C. Audonnet, W. I. Cox, S. W. Davis, J. van der Hoeven, B. Meignier, M. Riviere, et al.** 1992. NYVAC: a highly attenuated strain of vaccinia virus. Virology **188:**217–232.
76. **Terenzi, F., M. J. deVeer, H. Ying, N. P. Restifo, B. R. Williams, and R. H.**

Downloaded from jvi.asm.org at Centro Nacional de Biotecnología - Biblioteca on October 15, 2007

Silverman. 1999. The antiviral enzymes PKR and RNase L suppress gene expression from viral and non-viral based vectors. Nucleic Acids Res. **27:** 4369–4375.

77. **Vanderplasschen, A., and P. P. Pastoret.** 2003. The uses of poxviruses as vectors. Curr. Gene Ther. **3:**583–595.
78. **Wyatt, L. S., M. W. Carroll, C. P. Czerny, M. Merchlinsky, J. R. Sisler, and B. Moss.** 1998. Marker rescue of the host range restriction defects of modified vaccinia virus Ankara. Virology **251:**334–342.
79. **Xiang, Y., R. C. Condit, S. Vijaysri, B. Jacobs, B. R. Williams, and R. H. Silverman.** 2002. Blockade of interferon induction and action by the E3L double-stranded RNA binding proteins of vaccinia virus. J. Virol. **76:** 5251–5259.
80. **Yates, N. L., and M. A. Alexander-Miller.** 2006. Vaccinia virus infection of mature dendritic cells results in activation of virus-specific naïve $CD8^+$ T cells: a potential mechanism for direct presentation. Virology **359:**349–361.
81. **Yoneyama, M., M. Kikuchi, T. Natsukawa, N. Shinobu, T. Imaizumi, M. Miyagishi, K. Taira, S. Akira, and T. Fujita.** 2004. The RNA helicase RIG-I has an essential function in double-stranded RNA-induced innate antiviral responses. Nat. Immunol. **5:**730–737.

Downloaded from jvi.asm.org at Centro Nacional de Biotecnología - Biblioteca on October 15, 2007

Journal of General Virology (2007), **88**, 2473–2478 DOI 10.1099/vir.0.83018-0

Short Communication

Virus distribution of the attenuated MVA and NYVAC poxvirus strains in mice

Carmen Elena Gómez,[1]† José Luis Nájera,[1]† Elena Domingo-Gil,[1] Laura Ochoa-Callejero,[2] Gloria González-Aseguinolaza[2] and Mariano Esteban[1]

Correspondence
Mariano Esteban
mesteban@cnb.uam.es

[1]Department of Molecular and Cellular Biology, Centro Nacional de Biotecnología, CSIC, Ciudad Universitaria Cantoblanco, 28049 Madrid, Spain

[2]Division of Hepatology and Gene Therapy, Center for Investigation in Applied Medicine (CIMA), University of Navarra, 31080 Pamplona, Spain

Received 21 March 2007
Accepted 9 May 2007

Recombinant vaccinia viruses based on the attenuated NYVAC and MVA strains are promising vaccine candidates against a broad spectrum of diseases. Whilst these vectors are safe and immunogenic in animals and humans, little is known about their comparative behaviour *in vivo*. In this investigation, a head-to-head analysis was carried out of virus dissemination in mice inoculated by the mucosal or systemic route with replication-competent (WRluc) and attenuated recombinant (MVAluc and NYVACluc) viruses expressing the luciferase gene. Bioluminescence imaging showed that, in contrast to WRluc, the attenuated recombinants expressed the reporter gene transiently, with MVAluc expression limited to the first 24 h and NYVACluc giving a longer signal, up to 72 h post-infection, for most of the routes assayed. Moreover, luciferase levels in MVAluc-infected tissues peaked earlier than those in tissues infected by NYVACluc. These findings may be of immunological relevance when these vectors are used as recombinant vaccines.

Some of the most promising vaccine candidates being evaluated in clinical trials against AIDS, malaria and cancer are based on poxvirus recombinants. They are valuable tools for the expression of foreign antigens directly inside the cells of the host organism, as would happen in natural infection, and induce potent cellular immune responses against the heterologous product (Bonnet *et al.*, 2000; Zavala *et al.*, 2001). Among poxviruses, highly attenuated strains, such as modified vaccinia virus Ankara (MVA) or NYVAC, are considered the strains of choice for preclinical and clinical vaccine development. MVA was derived from the Ankara strain of vaccinia virus (VACV) by approximately 570 serial passages in primary chick embryo fibroblasts and has genome deletions (30 kbp) that include VACV genes involved in host immune regulation and host range (Mayr *et al.*, 1978; Antoine *et al.*, 1998). NYVAC was derived from the Copenhagen strain of VACV. It was attenuated genetically by the deletion of 18 non-essential genes implicated in host range or virulence (Tartaglia *et al.*, 1992a, b). The major advantage of MVA and NYVAC is the safety record and, despite their limited replication in human and most mammalian cell types, both viral strains provide a high level of gene expression and are immunogenic when delivering foreign antigens in animals and humans (Cox *et al.*, 1993; Amara *et al.*, 2001; Hel *et al.*, 2001; Gherardi *et al.*, 2003; Didierlaurent *et al.*, 2004; Gomez *et al.*, 2004, 2007a, b; Webster *et al.*, 2005). Although the capacity of these attenuated vectors to produce levels of recombinant antigens similar to those produced by replication-competent viruses has been demonstrated widely, to date an *in vivo* comparative analysis of virus dissemination of MVA and NYVAC strains when administered by different routes has not been done.

Molecular imaging offers many unique opportunities to study biological processes in intact organisms. Bioluminescence imaging (BLI) is based on the sensitive detection of visible light produced during enzyme (luciferase)-mediated oxidation of a molecular substrate when the enzyme is expressed *in vivo* as a molecular reporter (Sadikot & Blackwell, 2005). This technology has been applied in studies to monitor transgene expression, progression of infection, tumour growth and metastasis, transplantation, viral infections and gene therapy (Edinger *et al.*, 1999; Doyle *et al.*, 2004; Ray *et al.*, 2004). This non-invasive technique allows quantification in the same animal of the spatial and temporal progression of the infection, identifying animal-to-animal variations in viral replication and dissemination. In this study, we have followed, by BLI and biochemical analyses, the distribution in mice of MVA and NYVAC vectors, in comparison with the

†These authors contributed equally to this work.

replication-competent VACV strain Western Reserve (WR), when administered by different routes.

The poxvirus recombinants used in this study expressed the luciferase reporter gene and were derived from MVA (kindly provided by G. Sutter, Paul-Ehrlich-Institut, Langen, Germany), NYVAC (kindly provided by Sanofi-Pasteur) and WR strains. MVAluc and WRluc recombinants were described previously (Rodriguez *et al.*, 1988; Ramirez *et al.*, 2000). NYVACluc was generated in this work according to standard methods by using the same plasmid-transfer vector, pSCLUC, as was used for the generation of WRluc and MVAluc, which placed the gene under control of the virus p7.5 early/late promoter and the insertion site in the thymidine kinase (TK) locus of the viral genome (Rodriguez *et al.*, 1988).

To visualize dissemination of the different viruses *in vivo*, female BALB/c mice, 6–8 weeks old (Harlan OLAC), were inoculated by the following routes: intraperitoneal (i.p., 200 μl), intramuscular (i.m., 50 μl), intranasal (i.n., 50 μl), intrarectal (i.r., 50 μl) or intragastric (i.g., 50 μl), with 1×10^7 p.f.u. of either MVAluc or NYVACluc per animal or with 1×10^6 p.f.u. of WRluc diluted in PBS per mouse. In the case of the tail-scarification (t.s.) route, 1×10^6 p.f.u. virus per mouse was administered in a total volume of 10 μl. Animals were anaesthetized with 100 μl per 20 g weight of a 1 : 9 mixture of ketamine-500 (Merial) and 2 % xylazine (Bayer) before t.s. and i.m. inoculation, and 100 μl D-luciferin (Xenogen) at a concentration of 30 mg ml^{-1} diluted in 150 mM NaCl solution was injected by the i.p. route. The animals were placed in the imaging chamber of the Xenogen IVIS system, which includes a cooled CCD camera. A greyscale photograph of the animals was acquired, followed by a bioluminescent acquisition starting at 10 min after the luciferin injection. Images were collected for 3 min each in the ventral and dorsal positions. Regions of interest (ROIs) were drawn over the positions of greatest signal intensity on the animal, as well as over regions of 'no' signal, which were used as background readings. Light intensity was quantified by using photons s^{-1} cm^{-2} sr^{-1}. The greyscale photograph and data images from all studies were superimposed by using LivingImage (Xenogen). Luciferase activity is depicted with a pseudocolour scale, using red as the highest and blue as the lowest photon flux. Measurements of BLI were performed daily and the progression of infection was monitored until disappearance of the signal. Serial images were obtained from animals and the mean photon flux was quantified. There was no bioluminescence above background level in mock-infected mice, which were used as a negative control.

First, we determined how the systemic routes, i.p., i.m. and t.s., impacted on luciferase expression, as an index of virus dissemination in the whole animal. In mice inoculated i.p. with either MVAluc or NYVACluc, light emission was detected in the abdominal region, demonstrating the dissemination of the virus beyond the site of peritoneal infection. This is observed clearly in WRluc-infected animals, with extensive virus spreading and luciferase expression lasting for longer than 4 days (Fig. 1a). The highest levels of luciferase in animals receiving the attenuated viruses were detected at day 1 post-inoculation (p.i.); however, whereas in MVAluc-infected mice, the signal decreased markedly at day 2 p.i. and no luciferase activity was detected at later times, in NYVACluc-infected mice, the signal remained detectable until day 3 p.i. This was confirmed by photon-flux quantification performed at the site of inoculation (Fig. 1b). The levels of luciferase increased by about 4 logs above background for WRluc at the different times assayed, whilst for NYVACluc and MVAluc, the increments were 74- and 16-fold, respectively, at day 1 p.i., and 15- and 2.5-fold, respectively, at day 2 p.i.

The i.m. route is generally the way used to administer poxvirus and DNA vaccine candidates in clinical trials. This route has been preferred to s.c. or i.d. delivery to minimize the severity of reactions associated with the injection. When we inoculated animals by the i.m. route with the different viruses, we observed that the luciferase signal was mainly restricted to the inoculation site (Fig. 1c). Photon-flux quantification showed that, in contrast to WRluc-infected mice, the luciferase levels at the site of virus inoculation decreased in a time-dependent manner for MVAluc and NYVACluc vectors (Fig. 1d). Whilst by day 1 p.i., the two attenuated viruses induced similar levels of luciferase, at day 2 p.i., differences were observed between the vectors. NYVACluc-induced values were 100-fold higher than background, whereas MVAluc levels were only 4-fold higher. By the t.s. route, the expression of luciferase in animals inoculated with MVAluc or NYVACluc was very low and was restricted to the site of inoculation, in contrast to mice receiving WRluc, in which the signal increased gradually after infection, a sign of WR virus spreading in the animal. This was confirmed by photon-flux quantification (Fig. 1e). Next, we examined the expression pattern of MVAluc and NYVACluc following i.n., i.r. and i.g. inoculations. By i.n. inoculation, luciferase expression in MVAluc- and NYVACluc-infected mice was transient and restricted to the lungs. In contrast, bioluminescence was detected in the nose and the chest of mice receiving WRluc and increased with time, an indication of virus spreading within the respiratory tract, affecting trachea, lungs and brain (data not shown). Systemic dissemination of the viruses to abdominal organs was not observed at any time point. Photon-flux quantification revealed that the luciferase-expression levels for the two attenuated vectors were low, and remained longer in NYVACluc-infected animals (Fig. 1f). Following i.r. inoculation, very low levels of luciferase were observed in animals receiving MVAluc and NYVACluc vectors at any time p.i. (Fig. 1 g). After i.g. inoculation of MVAluc and NYVACluc, luciferase expression was transient, with the highest values observed at day 2 p.i. In NYVACluc-infected mice, the levels of the reporter gene were higher than for MVAluc-infected mice and were more sustained (data not shown).

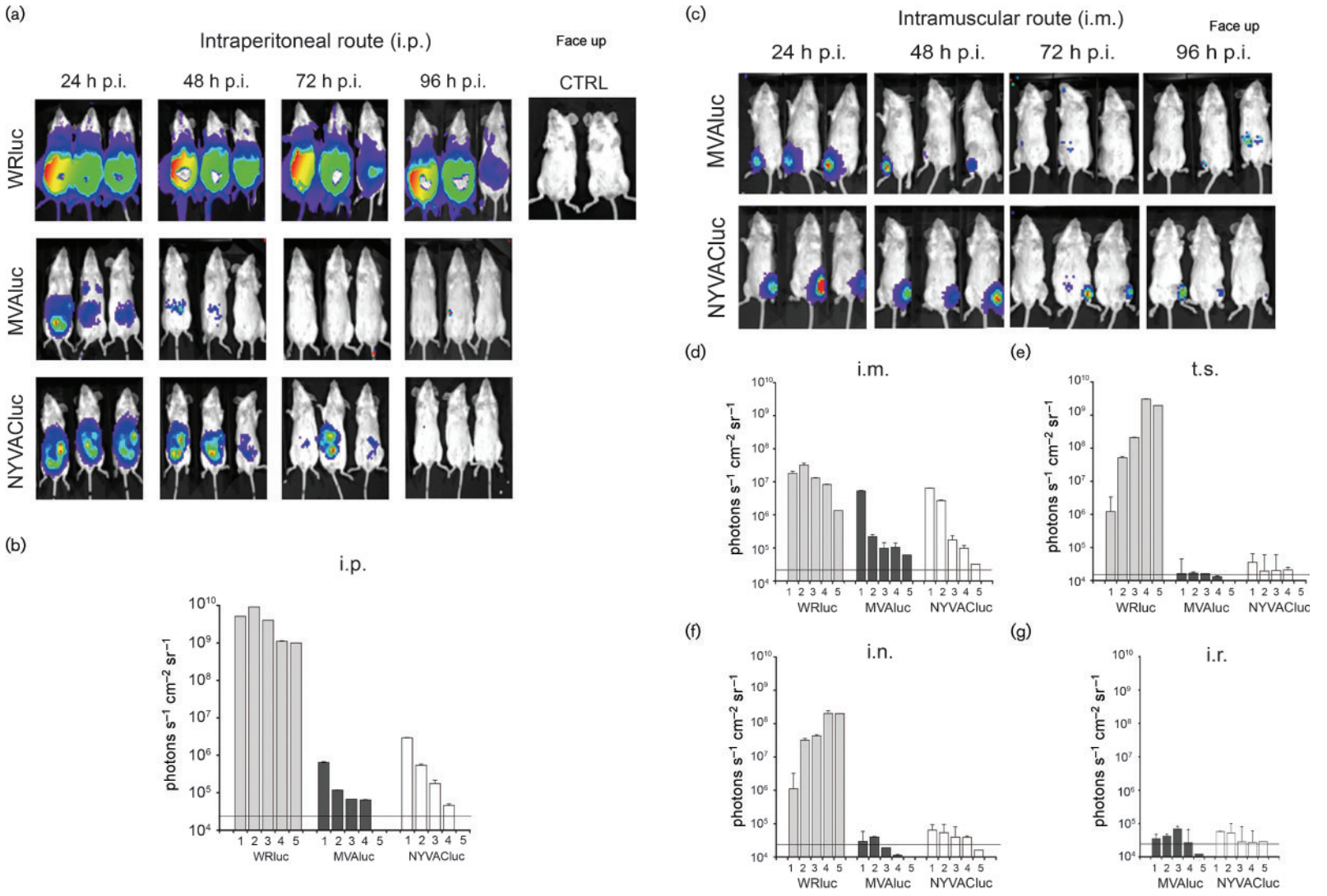

Fig. 1. (a, c) BLI distribution of WRluc, MVAluc and NYVACluc in mice inoculated by the i.p. (a) or i.m. (c) route. In the right-hand panel of (a), mock-infected mice (CTRL) are shown. (b, d–g) Quantification of the luciferase signal in the ROI during i.p. (b), i.m. (d), t.s. (e), i.n. (f) and i.r. (g) infections. Mean ± SD values for photon fluxes over time are represented. The solid line represents the background level of bioluminescence.

As revealed by BLI analysis with the luciferase reporter, and by comparison of different virus-inoculation routes in mice, the i.p. and i.m. routes are the most efficient to obtain high levels of heterologous gene expression. In contrast to WRluc, the attenuated MVAluc and NYVACluc viruses expressed the luciferase gene transiently, demonstrating their restricted replication capacity *in vivo*, as documented previously for MVAluc (Ramirez *et al.*, 2000). Interestingly, in NYVACluc-infected mice, the luciferase signal from 24 h p.i. onward was more sustained in the whole animal than that for MVAluc, indicating that the NYVACluc reporter remains longer within the infected cells.

Whilst the above results revealed differences in levels of bioluminescence from 24 h onward for both MVA and NYVAC vectors when inoculated by systemic routes, it was important to define the kinetics of vector expression shortly after virus infection. To this aim, we quantified the enzyme activity in tissue extracts of mice inoculated i.p., as this is the most effective route for virus dissemination. Gene expression of recombinant viruses in different mouse tissues was monitored by a highly sensitive luciferase assay, described previously (Rodriguez *et al.*, 1988). Different groups of mice received an i.p. inoculation (1×10^7 p.f.u. per animal) of MVAluc, NYVACluc or WRluc. Peritoneal cells were harvested by mouse peritoneal-cavity lavage with 10 ml sterile PBS, centrifuged at room temperature for 5 min at 1200 r.p.m. and stored at −70 °C. At various times p.i., animals were sacrificed and spleens, draining lymph nodes and ovaries were dissected under sterile conditions and stored at −70 °C. Tissues from individual mice were homogenized in Promega luciferase extraction buffer (300 µl per spleen and 200 µl per ovary, lymph node or peritoneal extract) by using an Ultraturrax T8 mechanical homogenizer (Janke & Kunkel). Luciferase activity was measured in the presence of luciferin and ATP by using a Lumat LB 9501 luminometer (Berthold Technologies)

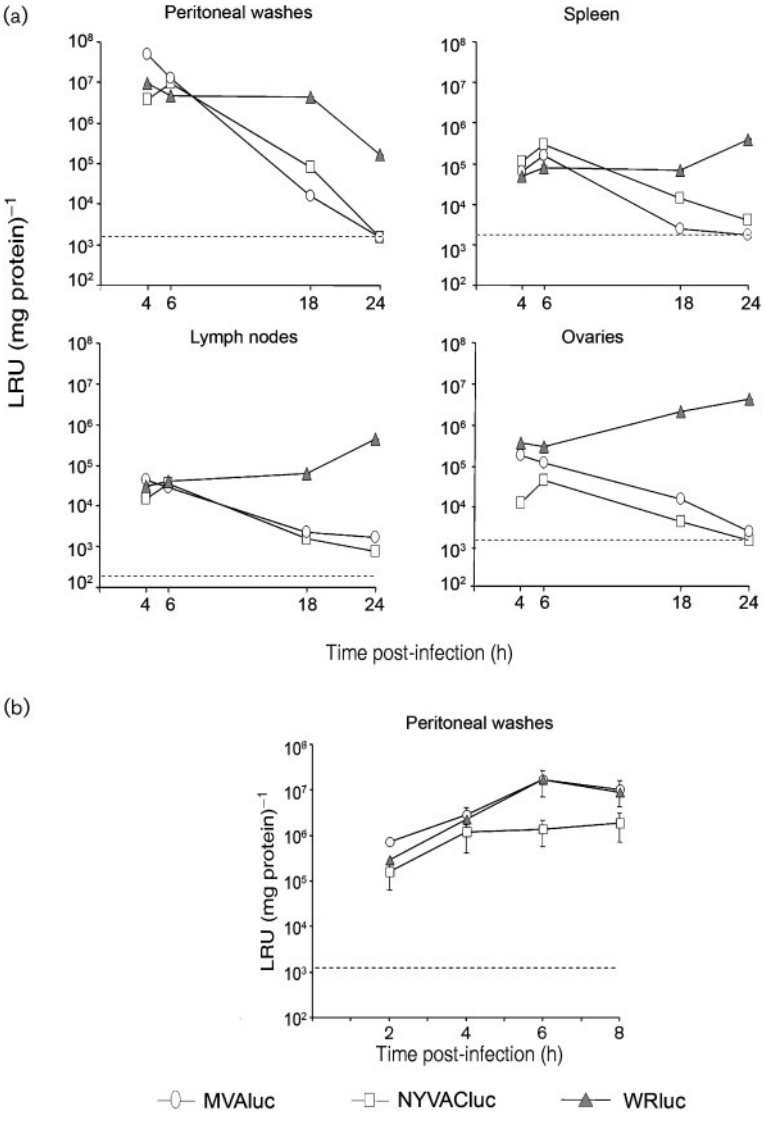

Fig. 2. Kinetics of luciferase expression by WRluc, MVAluc and NYVACluc in different mouse target tissues. (a) BALB/c mice were inoculated i.p. with the different viruses and, at indicated times, the extent of virus gene expression in different tissue extracts was evaluated by luciferase assay. Background levels in control uninfected tissues are shown as dashed lines. Results represent mean values from samples of three animals per time and group with standard deviations covered by each symbol. (b) Virus gene expression in cells from the peritoneal cavity of naïve mice, isolated and infected with 3 p.f.u. of WRluc, MVAluc or NYVACluc per cell. At the indicated times p.i., the extent of virus gene expression was evaluated by luciferase assay. Results represent mean values of three independent experiments with SD.

according to the manufacturer's instructions, and was expressed as luciferase reference units (LRU) (mg protein)$^{-1}$. Protein content in tissue extracts was measured with a BCA Protein Assay kit (Pierce Biotechnology). As shown in Fig. 2, luciferase levels at 4 h p.i. in peritoneal washes, ovaries and lymph nodes from MVAluc-infected mice were 5- to 10-fold higher than those found in tissues from NYVACluc-infected mice, except for the spleen, where the levels were similar between the two viruses. By 6 h p.i., these levels were comparable and decreased with time, falling to background values by 48 h p.i. By this time, the values in WRluc were 2–4 log units higher than for either MVAluc or NYVACluc. We also quantified the virus titres in peritoneal washes, ovaries, lymph nodes and spleen of infected mice. In contrast to tissues from WRluc-infected mice, where infectious virus was observed, there was no infectious virus at 24–48 h p.i. in samples from NYVACluc- and MVAluc-infected mice (data not shown). These results are in agreement with previous findings for MVAluc (Ramirez *et al.*, 2000) and indicate higher efficiency of virus gene expression for MVA versus NYVAC shortly after infection.

To verify the differences observed *in vivo* between both attenuated recombinants at early times p.i., we isolated cells from the peritoneal cavity of naïve animals and infected them with the different viruses. As shown in Fig. 2(b), expression of luciferase at the different times assayed was about 1 log unit higher in MVAluc- than in NYVACluc-infected cells. This was not due to differences in virus uptake by the cells, but rather to a post-entry event, as similar levels of luciferase were observed between 2 and 4 h p.i. in HeLa cells infected with MVAluc or NYVACluc (3 p.f.u. per cell; data not shown). As MVA and replication-competent VACV exhibited different tropisms for primary human cells (Chahroudi *et al.*, 2005), the differences that we observed between the two attenuated recombinants might be related to the susceptibility of such cells to infection with MVA or NYVAC. Whilst the peritoneal exudates had the highest level of luciferase activity after infection, it remains to be defined whether the same cells present in the peritoneal washout of an uninfected mouse are infected *in vivo*. As similar levels of binding and infection have been observed in murine splenic B cells exposed to replication-competent VACV or MVA (Chahroudi *et al.*, 2005), our results may also reflect a biological mechanism that distinguishes the post-binding infectious process or the timing of early gene expression of MVA and NYVAC in certain cell types. Further studies should be directed to the identification of the cell types infected by the two attenuated viruses in animals and humans.

The results described here and those described previously on the biology of these two virus strains in cultured cells (Najera *et al.*, 2006), their impact on host genome profiling in HeLa cells (Guerra *et al.*, 2004, 2006) and head-to-head comparisons of the immunogenicity of both vectors expressing human immunodeficiency virus type 1 antigens in mice (Gomez *et al.*, 2007a, b) all suggest that MVA and NYVAC have different behaviours in their ability to replicate and impact on host immune responses. Hence, they should be explored as poxvirus vector vaccines with differential *in vitro* and *in vivo* characteristics.

Acknowledgements

This investigation was supported by research grants from the EU (EuroVac QLRT-PL-1999-01321 and Vaccinia Vectors QLK2-CT-2002-01867), the Spanish Ministry of Education and Science BIO2004-03954, the Spanish Foundation for AIDS Research (FIPSE 36344/02) and Fundación Marcelino Botín to M. E. J. L. N. was supported by FIPSE. We thank Maria Victoria Jiménez for expert technical assistance.

References

Amara, R. R., Villinger, F., Altman, J. D., Lydy, S. L., O'Neil, S. P., Staprans, S. I., Montefiori, D. C., Xu, Y., Herndon, J. G. & other authors (2001). Control of a mucosal challenge and prevention of AIDS by a multiprotein DNA/MVA vaccine. *Science* **292**, 69–74.

Antoine, G., Scheiflinger, F., Dorner, F. & Falkner, F. G. (1998). The complete genomic sequence of the modified vaccinia Ankara strain: comparison with other orthopoxviruses. *Virology* **244**, 365–396.

Bonnet, M. C., Tartaglia, J., Verdier, F., Kourilsky, P., Lindberg, A., Klein, M. & Moingeon, P. (2000). Recombinant viruses as a tool for therapeutic vaccination against human cancers. *Immunol Lett* **74**, 11–25.

Chahroudi, A., Chavan, R., Kozyr, N., Waller, E. K., Silvestri, G. & Feinberg, M. B. (2005). Vaccinia virus tropism for primary hematolymphoid cells is determined by restricted expression of a unique virus receptor. *J Virol* **79**, 10397–10407.

Cox, W. I., Tartaglia, J. & Paoletti, E. (1993). Induction of cytotoxic T lymphocytes by recombinant canarypox (ALVAC) and attenuated vaccinia (NYVAC) viruses expressing the HIV-1 envelope glycoprotein. *Virology* **195**, 845–850.

Didierlaurent, A., Ramirez, J. C., Gherardi, M., Zimmerli, S. C., Graf, M., Orbea, H. A., Pantaleo, G., Wagner, R., Esteban, M. & other authors (2004). Attenuated poxviruses expressing a synthetic HIV protein stimulate HLA-A2-restricted cytotoxic T-cell responses. *Vaccine* **22**, 3395–3403.

Doyle, T. C., Burns, S. M. & Contag, C. H. (2004). In vivo bioluminescence imaging for integrated studies of infection. *Cell Microbiol* **6**, 303–317.

Edinger, M., Sweeney, T. J., Tucker, A. A., Olomu, A. B., Negrin, R. S. & Contag, C. H. (1999). Noninvasive assessment of tumor cell proliferation in animal models. *Neoplasia* **1**, 303–310.

Gherardi, M. M., Najera, J. L., Perez-Jimenez, E., Guerra, S., Garcia-Sastre, A. & Esteban, M. (2003). Prime-boost immunization schedules based on influenza virus and vaccinia virus vectors potentiate cellular immune responses against human immunodeficiency virus Env protein systemically and in the genitorectal draining lymph nodes. *J Virol* **77**, 7048–7057.

Gomez, C. E., Abaitua, F., Rodriguez, D. & Esteban, M. (2004). Efficient $CD8^+$ T cell response to the HIV-env V3 loop epitope from multiple virus isolates by a DNA prime/vaccinia virus boost (rWR and rMVA strains) immunization regime and enhancement by the cytokine IFN-γ. *Virus Res* **105**, 11–22.

Gomez, C. E., Najera, J. L., Jimenez, E. P., Jimenez, V., Wagner, R., Graf, M., Frachette, M. J., Liljestrom, P., Pantaleo, G. & Esteban, M. (2007a). Head-to-head comparison on the immunogenicity of two

HIV/AIDS vaccine candidates based on the attenuated poxvirus strains MVA and NYVAC co-expressing in a single locus the HIV-1BX08 gp120 and HIV-1(IIIB) Gag-Pol-Nef proteins of clade B. *Vaccine* **25**, 2863–2885.

Gomez, C. E., Najera, J. L., Jimenez, V., Bieler, K., Wild, J., Kostic, L., Heidari, S., Chen, M., Frachette, M. J. & other authors (2007b). Generation and immunogenicity of novel HIV/AIDS vaccine candidates targeting HIV-1 Env/Gag-Pol-Nef antigens of clade C. *Vaccine* **25**, 1969–1992.

Guerra, S., Lopez-Fernandez, L. A., Conde, R., Pascual-Montano, A., Harshman, K. & Esteban, M. (2004). Microarray analysis reveals characteristic changes of host cell gene expression in response to attenuated modified vaccinia virus Ankara infection of human HeLa cells. *J Virol* **78**, 5820–5834.

Guerra, S., Lopez-Fernandez, L. A., Pascual-Montano, A., Najera, J. L., Zaballos, A. & Esteban, M. (2006). Host response to the attenuated poxvirus vector NYVAC: upregulation of apoptotic genes and NF-κB-responsive genes in infected HeLa cells. *J Virol* **80**, 985–998.

Hel, Z., Tsai, W. P., Thornton, A., Nacsa, J., Giuliani, L., Tryniszewska, E., Poudyal, M., Venzon, D., Wang, X. & other authors (2001). Potentiation of simian immunodeficiency virus (SIV)-specific $CD4^+$ and $CD8^+$ T cell responses by a DNA-SIV and NYVAC-SIV prime/boost regimen. *J Immunol* **167**, 7180–7191.

Mayr, A., Stickl, H., Muller, H. K., Danner, K. & Singer, H. (1978). The smallpox vaccination strain MVA: marker, genetic structure, experience gained with the parenteral vaccination and behavior in organisms with a debilitated defence mechanism. *Zentralbl Bakteriol* [*B*] **167**, 375–390 (in German).

Najera, J. L., Gomez, C. E., Domingo-Gil, E., Gherardi, M. M. & Esteban, M. (2006). Cellular and biochemical differences between two attenuated poxvirus vaccine candidates (MVA and NYVAC) and role of the C7L gene. *J Virol* **80**, 6033–6047.

Ramirez, J. C., Gherardi, M. M. & Esteban, M. (2000). Biology of attenuated modified vaccinia virus Ankara recombinant vector in mice: virus fate and activation of B- and T-cell immune responses in comparison with the Western Reserve strain and advantages as a vaccine. *J Virol* **74**, 923–933.

Ray, P., De, A., Min, J. J., Tsien, R. Y. & Gambhir, S. S. (2004). Imaging tri-fusion multimodality reporter gene expression in living subjects. *Cancer Res* **64**, 1323–1330.

Rodriguez, J. F., Rodriguez, D., Rodriguez, J. R., McGowan, E. B. & Esteban, M. (1988). Expression of the firefly luciferase gene in vaccinia virus: a highly sensitive gene marker to follow virus dissemination in tissues of infected animals. *Proc Natl Acad Sci U S A* **85**, 1667–1671.

Sadikot, R. T. & Blackwell, T. S. (2005). Bioluminescence imaging. *Proc Am Thorac Soc* **2**, 537–540.

Tartaglia, J., Cox, W. I., Taylor, J., Perkus, M., Riviere, M., Meignier, B. & Paoletti, E. (1992a). Highly attenuated poxvirus vectors. *AIDS Res Hum Retroviruses* **8**, 1445–1447.

Tartaglia, J., Perkus, M. E., Taylor, J., Norton, E. K., Audonnet, J. C., Cox, W. I., Davis, S. W., van der Hoeven, J., Meignier, B. & other authors (1992b). NYVAC: a highly attenuated strain of vaccinia virus. *Virology* **188**, 217–232.

Webster, D. P., Dunachie, S., Vuola, J. M., Berthoud, T., Keating, S., Laidlaw, S. M., McConkey, S. J., Poulton, I., Andrews, L. & other authors (2005). Enhanced T cell-mediated protection against malaria in human challenges by using the recombinant poxviruses FP9 and modified vaccinia virus Ankara. *Proc Natl Acad Sci U S A* **102**, 4836–4841.

Zavala, F., Rodrigues, M., Rodriguez, D., Rodriguez, J. R., Nussenzweig, R. S. & Esteban, M. (2001). A striking property of recombinant poxviruses: efficient inducers of in vivo expansion of primed $CD8^+$ T cells. *Virology* **280**, 155–159.

Differential CD4$^+$ versus CD8$^+$ T-cell responses elicited by different Pox-based HIV-1 vaccine candidates provide comparable efficacy in primates

Petra Mooij[1*], Sunita S Balla-Jhagjhoorsingh[1], Gerrit Koopman[1], Niels Beenhakker[1], Patricia van Haaften[1], Ilona Baak[1], Ivonne Nieuwenhuis[1], Ivanela Kondova[1], Ralf Wagner[2] , Hans Wolf[2], Carmen E Gómez[3] , José L Nájera[3], Victoria Jiménez[3], Mariano Esteban[3], and Jonathan L Heeney[1,4].

[1]Department of Virology, Biomedical Primate Research Center, 2288 GJ Rijswijk, The Netherlands, [2]Institut für Medizinische Mikrobiologie und Hygiene der Universität Regensburg, 39053, Germany, [3]Department of Cell and Molecular Biology, Centro Nacional de Biotecnologia, CSIC, Madrid, 28049, Spain, and the [4]University of Cambridge, Department of Veterinary Medicine, Cambridge, CB3 0ES, UK.

* Corresponding author:

Petra Mooij. Department of Virology, Biomedical Primate Research Centre (BPRC), P.O. Box 3306, 2280 GH Rijswijk, The Netherlands. Tel. +31 152842615. Fax. +31 152842601. E-mail: mooij@bprc.nl

Condensed title: Poxvirus vector immunity to HIV/AIDS

Word count abstract: 207

Character count text: 38,343

Key words: poxvirus vectors, MVA, NYVAC, CD4, CD8, T-cell immunity, AIDS, polyfunctional, HIV-1, vaccination

Abbreviations used in this paper:

SEB	Staphylococcal enterotoxin-B
APC	Allophycocyanin
PERCP	Peridinin-chlorophyll-protein complex
PE	Phycoerythrine
CY7	Cyanin 7
ECD	Energy Coupled Dye
CFSE	Carboxy-fluorescein diacetate succinimidyl ester
Tcm	T-central memory
Tem	T-effector memory
CEF	Chicken embryo fibroblasts

Abstract

Poxvirus vectors have proven to be highly effective for boosting immune responses in diverse vaccine settings. Recent reports reveal marked differences in gene expression of human dendritic cells infected with two leading Poxvirus-based Human Immunodeficiency Virus (HIV) vaccine candidates, New York Vaccinia virus (NYVAC) and modified vaccinia virus Ankara (MVA). To understand how complex genomic changes in these two vaccine vectors translate into antigen specific systemic immune responses we undertook a head to head vaccine immunogenicity and efficacy study in the pathogenic HIV-1 model of AIDS in Indian Rhesus macaques. Differences in the immune responses in outbred animals were not distinguished by ELISpot, but by multiparameter FACS analysis, revealing a difference in the number of animals responding with predominant $CD8^+$ T-cell responses to vaccine inserts (MVA), to those which elicit a dominant $CD4^+$ T-cell response (NYVAC). Remarkably, vector induced differences in $CD4^+/CD8^+$ T-cell immune responses persisted for more than a year post-challenge, and even accompanied antigenic modulation throughout control of chronic infection. Importantly, strong pre-exposure HIV-1/Simian Immunodeficiency Virus (SIV)-specific $CD4^+$ T-cell responses did not prove deleterious with respect to accelerated disease progression. In contrast, in this setting strong vaccine induced polyfunctional $CD4^+$ T-cell responses were capable of eliciting similar efficacy as those generating stronger $CD8^+$ T-cell responses.

Introduction

The global spread of HIV has reached pandemic proportions (http://www.unaids.org). Despite more than two decades of research since the discovery of HIV as the etiology of AIDS, the development of an effective HIV-1 vaccine remains an unfulfilled priority. While it is generally accepted that ultimately a prophylactic HIV-1 vaccine should induce both humoral and cell-mediated immune responses to a number of different HIV antigens (1, 2), envelope-based immunogens capable of inducing broad neutralizing responses are currently not available (3-5). Recent vaccine approaches have focused on vaccines capable of inducing potent $CD8^+$ T-cell responses to control virus load, to reduce transmission and to slow disease development (6, 7). Evidence for the role of T-cell responses in the control of HIV includes the correlation between HIV-specific $CD8^+$ T-cells and the control of plasma viremia (8, 9), the association of certain restricting MHC class I alleles, conserved T-cell epitopes and slow disease progression (10-16), and the rapid increase in viral load after experimental $CD8^+$ lymphocyte depletion in SIV or SHIV infected rhesus macaques (17-19). Others have shown correlation with certain MHC alleles and control of SIV (20-23) or specific cellular immune correlates with prolonged survival in rhesus macaques (24). It has been demonstrated that vaccine induced $CD8^+$ T-cell responses are capable of controlling SIVmac replication even in the absence of neutralizing antibodies (25), providing a strong rationale for the development of T-cell based vaccines. Recently the quality of the HIV-specific $CD8^+$ T-cells associated with the control of HIV-1 virus load in human long term nonprogessors has been described, revealing characteristics of a polyfunctional profile simultaneously producing IFN-γ, IL-2, TNF-α, MIP1-β and capable of degranulation (26). In contrast, while anti-HIV $CD8^+$ and $CD4^+$ T-cell responses have been demonstrated to have a

positive effect on controlling virus load, HIV-1 specific $CD4^+$ T-cell responses have also been implicated as possibly being deleterious. Indeed, the finding that HIV-1 preferentially infects HIV-specific $CD4^+$ T-cells has suggested a possible contra-indication for the prophylactic induction of strong HIV-1 specific $CD4^+$ T-cell responses (27, 28).

Two of the leading Poxvirus-based vaccine vector candidates for the delivery of HIV antigens for induction of T-cell mediated immune responses include modified vaccinia virus Ankara (MVA), and New York vaccinia virus (NYVAC) vectors. Following the successful global eradication of smallpox in the 1970s attenuated vaccinia vectors have the advantage of the relative absence of pre-existing immunity to poxvirus in the large young human population at risk for HIV-1 infection. Historical development and use of MVA as vaccine against smallpox established an extraordinary safety profile. MVA is a highly attenuated virus through more than 500 *in vitro* passages in chicken embryo fibroblasts. During the course of attenuation, 15% of the parental viral genome was lost, having an impact on the function of genes involved in immune evasion and host range restrictions (29-33). Despite the limited replication in human and most mammalian cells, MVA has shown to efficiently express foreign recombinant genes (34). In animal models, MVA as a vaccine vector has been found to induce very immunogenic responses to its inserts when administered by systemic and mucosal routes as well as providing protection against various infectious agents including immunodeficiency viruses (for review see ref. (35-37)). The NYVAC vector is derived from the vaccinia virus strain Copenhagen (COP), from which 18 genes, encoding proteins involved in host range and virulence were deleted (38). NYVAC-derived vectors are able to express multiple antigens from a wide range of species (39) and have been used in several pre-clinical and clinical trials

(40-44). The complement of genes that have been altered, modified or lost are very different between these two vectors as has recently been revealed by gene profiling (45). Such dramatic differences in their ability to modulate host immune responses have been revealed in studies on human monocyte derived dendritic cells (mDC) infected with either MVA or NYVAC vectors (46). Compared to normal mDC these vaccine vectors had a profound impact, upregulating 195 of the same genes, while differing in the 359 genes that were specifically upregulated by MVA, and the 165 by NYVAC. At the mRNA level although IL-12β, IFN-β and TNF-α were upregulated by both vectors, they were increased to higher levels by MVA. Interestingly Type 1 IFN, IL-6 and TLR pathways were distinctly induced in mDC by MVA (46). In mice comparison of the immune responses revealed a greater magnitude of Ag responses to HIV-1 inserts expressed by MVA vs NYVAC (47). However distinct differences in polyfunctional T-cell subsets have not been explored in either human or nonhuman primates.

Despite the fact that both MVA and NYVAC have been evaluated in phase-I clinical trials, a direct head to head comparison in immunogenicity between these vectors is lacking. Indeed, possible comparisons have been hampered by the use of different vaccine antigen inserts, construct differences, differences in immunological readouts and the lack of quality controlled vaccine lots such as required by GMP. Here we have undertaken a detailed head to head comparison between MVA and NYVAC vectors expressing identical SIV/HIV-1 gene inserts. The study design utilized the DNA prime/pox-virus boost strategy (48-60). The immunization protocol was based on the same EuroVacc clinical trial design as recently completed in human volunteers. Vaccine constructs contained identical SIV/HIV-1 antigen inserts to allow a proper immunologic comparison of MVA and NYVAC based vectors. As HIV-1 Env was one of the

immunogenic components, efficacy was subsequently evaluated in the SHIV model of AIDS in Rhesus macaques (*Macaca mulatta* of Indian origin).

Here we reveal distinct differences in individual HIV-SIV-specific vaccine induced $CD4^+$ and $CD8^+$ T-cell responses in outbred primates. Similar to our findings in human volunteers (61), primates developed a dominant $CD4^+$ T-cell response to NYVAC encoded antigens, while the exact same insert in MVA induced more CD8 T-cell oriented responses to the same HIV antigens. To determine the differences in vaccine efficacy and to explore the potentially deleterious impact on enhancement of antigen-specific $CD4^+$ T-cell infection on disease progression, all animals were exposed to pathogenic SHIV and followed for evidence of protection from disease development.

Results

Similarities in the magnitude of antigen specific IFN-γ, IL-2 and IL-4 ELISpot responses.

DNA priming of viral vectors expressing common antigen inserts is currently the leading vaccine strategy for T-cell based vaccines in clinical trials, while the IFN-γ ELISpot is the most frequently used immunological endpoint. To investigate possible differences in modulation of antigen specific cytokine responses by the genetically distinct MVA and NYVAC vectors, we included IL-2 and IL-4 ELISpot assays to detect peptide specific responses to each of the four vaccine encoded antigens, Gag, Pol, Nef and Env. Priming with DNA induced low level Env specific, IFN-γ and IL-2 responses, (Fig. 1 top left panels, and data not shown). Env specific IFN-γ and IL-2 responses were relatively stable and did not decline prior to pox-vector boost immunizations. Certain animals also developed an Env specific IL-4 response upon DNA immunization, but overall these responses were lower as compared to IFN-γ and IL-2 responses (Fig. 1 right panels, $p<0.0001$). As anticipated, antigen specific responses were further increased after boosting with either type of pox vector, increasing IFN-γ, IL-2 (not shown) and IL-4 responses to all vaccine antigens (Fig. 1). The second poxvirus immunization resulted in an additional increase of the antigen specific Env responses (from 560 to 1171 mean SFC/10^6 PBMC, $p<0.035$ for MVA and from 446 to 1074 mean SFC/10^6 PBMC, $p<0.004$ for NYVAC) and Gag specific IFN-γ responses (from 101 to 331 mean SFC/10^6 PBMC, $p<0.045$ for MVA, wk 22 vs wk 26, Wilcoxon's). Also here the greatest magnitude of responses were observed to SHIV Env which scored consistently positive in ELISpot assays during follow-up. This observation was entirely consistent with our findings in the human clinical trial (61).

While MVA and NYVAC pox vectors gave highly comparable ELISpot responses based on the magnitude and antigen specificity of responses, there were occasional exceptions. These included higher IFN-γ responses induced by MVA to Env at week 30 (826 vs 329 mean SFC/10^6 PBMC, $p<0.027$) and to Gag at week 26 (331 vs 61 mean SFC/10^6 PBMC, $p<0.011$) as compared to the NYVAC group. Statistically significant differences were not observed between the MVA and NYVAC induced antigen specific IL-2 and IL-4 responses.

Qualitative differences between pox-vector vaccine candidates reveal preferential $CD8^+$ versus $CD4^+$ T-cell responses

Multiparameter intracellular FACS analysis was employed to determine the phenotypic characteristics of the cytokine producing T-cell populations (Fig. 2 A). Following Poxvirus vector immunizations and prior to exposure to virus, Env specific cytokine producing T-cells were dominant in animals of both MVA and NYVAC groups (Fig. 2 A and B), confirming the ELISpot data. Most frequent cytokine producing cells were $CD4^+$ T-cells (Fig. 2 A and 2 B) (of effector memory, EM, $CD45RA^-/CCR7^-$ and central memory, CM, $CD45RA^-/CCR7^+$ phenotype, Fig. S1) in both groups. However, in addition to $CD4^+$ T-cell mediated responses, five out of seven MVA boosted animals also developed Env specific cytokine responses mediated by $CD8^+$ T-cells (Fig. 2 B, right panel) which were significantly higher than in NYVAC boosted animals ($p = 0.035$, Fig. 2 B). From those animals that showed a strong Env-specific $CD8^+$ T-cell response, memory phenotyping was performed, revealing an effector phenotype ($CD8^+/CD45RA^+/CCR7^-$, Fig. S1). Further analysis of the antigen specific T-cells revealed that the $CD4^+$ and $CD8^+$ T-cells of the majority of the immunized animals

produced either IFN-γ or IFN-γ and IL-2 simultaneously (Fig. 2 A and C). The frequency of IFN-γ producing $CD8^+$ T-cells was higher in MVA boosted animals than in NYVAC boosted animals ($p = 0.0187$, Fig. 2 C).

To further corroborate polyfunctionality based on FACS based assays, the proliferative capacity of both $CD4^+$ and $CD8^+$ T-cell populations was studied in all animals of both immunization groups (Fig. 3 A and B). As revealed in figure 3B, proliferation was mainly Env specific, consistent with ELISpot and ICS data. In MVA boosted animals, the Env specific proliferation was mediated by both $CD4^+$ as well as $CD8^+$ T-cells (Fig. 3 A and B), while in NYVAC boosted animals the Env-specific proliferation was preferentially mediated by $CD4^+$ T-cells ($p = 0.0054$ CD4 vs CD8 Env proliferation). Furthermore, Gag-specific proliferating $CD4^+$ T-cells were detected in NYVAC immunized animals but not in MVA animals ($p = 0.0074$, Fig. 3 B). In MVA boosted animals, the Gag specific proliferating T-cell were $CD8^+$ (Fig. 3 B, right panel). Notably, the frequency of the antigen-specific $CD8^+$ T-cells in MVA boosted animals tended to be higher than in the NYVAC boosted animals, but did not reach statistical significance.

To investigate possible differences of preferential induction of T-cells by the different poxvirus vaccine vectors, the relative contribution of $CD4^+$ and $CD8^+$ T-cells to the total response was determined in those animals that showed an antigen specific cytokine and/or proliferative response. Antigen specific cytokine responses were predominantly mediated by $CD4^+$ T-cells in both groups (Fig. 4 A). Importantly, while NYVAC immunization resulted in antigen specific cytokine responses that were mediated almost exclusively by $CD4^+$ T-cells (mean +/- SD: 92.7% +/- 12.7, $p = 0.0003$ CD4 vs CD8), the cytokine responses induced by MVA immunization were mediated by only 75% by $CD4^+$ T-cells (75% +/- 16.3) and 25% by CD8+ T-cells, ($p = 0.042$ MVA vs NYVAC, Fig. 4

A). In five out of seven NYVAC boosted animals the response was mediated for 100% by $CD4^+$ T-cells, while this was only observed in one out of six MVA boosted responders. In this respect the proliferative responses corroborated the antigen specific cytokine responses. A higher proportion of the antigen specific proliferation was mediated by $CD4^+$ T-cells following NYVAC immunization (68.6% +/- 22.2) than after MVA boost (40.2% +/- 22.7, $p = 0.0227$, Fig. 4 B). Overall NYVAC boost induced a predominantly $CD4^+$ T-cell mediated proliferative response (CD4 68.6% vs CD8 31.4%, $p = 0.0048$), while MVA induced both $CD4^+$ T-cell antigen specific proliferation as well as $CD8^+$ T-cell mediated proliferative responses (CD4 40.2% vs CD8 59.8%, $p = 0.0821$, Fig. 4 B).

Gene array analysis supports differential pox-vaccine induced $CD4^+$/$CD8^+$ T-cell responses.

Differential modulation of host gene expression likely explains the differences between MVA and NYVAC strains *in vitro* and *in vivo* systems (46, 62, 63). Considerable evidence has accumulated to indicate that $CD8^+$ T-cells, in addition to antigen and costimulation, require 'third signal' cytokines, which support strong clonal expansion, development of effector functions, or establishment of a long-lived responsive memory population (64, 65). Such 'third signals' can be provided by either IL-12 and/or type I IFN (IFNα/β) produced by mature DC. Their activation is mediated through activation of a signalling pathway(s) distinct from those activated by the TCR and CD28. Re-analysis of gene profiling data from human dendritic cells activated by MVA or NYVAC infection (table 1) revealed a highly marked upregulation in MVA infected cells at the mRNA level of IL-12, IFN-α and IFN-β, as well as interferon regulatory factor (IRF-7)

and protein implicated in the Type I IFN production (MDA5, RIG). Consequently, many interferon stimulated genes (ISGs) were also differentially upregulated in MVA infected DC (IFIT1 (ISG56), IFIT4 (ISDG60), SCYB10 (CXCR3 ligand chemokine chiefly active on effector Th1 cells). Moreover, the differentiation programme initiated in common by IL-12 and IFNα/β regulate numerous genes involved in several functions. Among them, genes relevant for effector cell regulation of gene expression such as GADD45B (66) and the transcription factor NFAT5 (67), genes involved in signal transduction (MAP2K5) and cell cycle regulation (Cyclin B1) (65), and members of the TNF family (68), are consistently upregulated in MVA. Interestingly, genes encoding for pro-inflammatory cytokines as TNF and IL-6, and for CC-chemokines as SCYA3, SCYA4 or SCYA5 (RANTES), which are involved in the modulation of the immune response, are differentially expressed between MVA and NYVAC. These profiling data support the preferential stimulation of CD8 T-cells by MVA. In the case of NYVAC, it is significant that all of the above $CD8^+$ T-cell stimulatory genes are markedly reduced after virus infection of DCs, further supporting differential CD8 versus CD4 behaviour between two vaccine vector strains *in vivo*. Moreover, in a recent study evaluating in mice the biodistribution of MVA and NYVAC recombinant viruses expressing the luciferase gene, it was observed that the reporter signal was more sustained in animals infected with NYVAC than with MVA (62). The longer viral gene expression may possibly influence the T-cell response. In contrast to CD8 T-cells in which relatively short antigen pulse seems sufficient for APC to drive clonal expansion and differentiation, for $CD4^+$ T-cells antigen persistence is required throughout their expansion phase (69).

$CD4^+$ dominant versus $CD8^+$ predominant responses and vaccine efficacy against pathogenic challenge

Given the differences on the impact of these two Poxvirus vaccine vectors on gene expression profiles in mDC, and their differences in $CD4^+$ dominant (NYVAC) and a more $CD8^+$ predominant T-cell response (MVA induced both $CD8^+$ and $CD4^+$ T-cell responses) we set out to determine if these characteristic differences impacted on immunity when exposed to pathogenic $SHIV_{89.6p}$ infection. This challenge was selected because of the HIV-1 Envelope antigen to which both vaccine strategies had marked T-cell responses. Furthermore, the dominant HIV vaccine antigen specific $CD4^+$ T-cell responses to this antigen induced by one of the vaccine candidates allowed us to determine if there may be a detrimental effect in terms for greater propensity for accelerated disease progression due to preferential infection and loss of HIV Ag specific $CD4^+$ T-cells (28).

Prior to challenge, neutralization assays to pseudotyped or wild type challenge virus as well as to parental HIV-1 strains revealed that these T-cell-based vaccine strategies had not induced sufficient neutralizing antibody responses (Fig. S2) to protect these animals from infection. Peak virus loads at two weeks post challenge ranged from $4.1x10^3$ – $2.5x10^6$ RNA copies/ml and were similar in all groups (Fig. 5, top). Virus load in 5 control animals remained high and persisted in four of these five animals above 10^5 RNA copies/ml followed by ensuing AIDS like disease. Upon necropsy, histology confirmed the diagnosis of AIDS, hallmarked by lymphoid depletion in the peripheral and mesenteric lymph nodes, spleen (animals R99013 and R99041), GALT (R99041) and tonsils (R00001 and R99013). Interestingly, one out of six control animals (R00045) was a "natural" controller (similar to certain human long term non progressors), and was able

to reduce virus load below detectable levels by 10 weeks post challenge (Fig. 5, upper right).

In the $CD8^+$ MVA immunized group, five out of seven animals were able to reduce virus load below 10^3 RNA copies/ml (Fig. 5, top left). One animal (97027) controlled virus load below 10^4 RNA copies/ml, while only one animal (98051) in this group failed to control virus load (evidence for vaccine escape in this animal is being sought). Histological examination of lymphoid tissues upon necropsy (at the end of the study period, 66 weeks post challenge) of this animal revealed mild lymphoid depletion of GALT, indicative for immunodeficiency and consistent with its high virus load and corresponding low peripheral $CD4^+$ T-cell counts. All other study animals remained healthy during the study period.

In the $CD4^+$ dominant NYVAC immunized group, six out of seven animals reduced virus load below 10^3 RNA copies/ml (Fig. 5 top middle). Only one animal (94062) was unable to reduce virus load, but remained healthy during the study. Histological examination of lymphoid tissue after necropsy of all DNA/NYVAC immunized animals revealed no lesions attributable to AIDS defining illness. Absolute $CD4^+$ T-cell loss inversely correlated with virus load after challenge (Fig. 5 middle row). In four of five control animals with high virus load a progressive loss of $CD4^+$ T-cells occurred.

In both immunized groups (n=14), only 2 animals which were unable to control virus load below 10^4 RNA copies/ml, and developed evidence of $CD4^+$ T-cell loss (98051 in the DNA/MVA group and 94062 in the DNA/NYVAC group, Fig. 5). In all other immunized animals, $CD4^+$ T-cells did not decline and remained within the normal range.

A more sensitive indicator of subtle changes within the CD4 T-cell population is the loss of $CD4^+$ central memory T-cell subset (Tcm $CD4^+/CCR7^+/CD45RA^-$) (70). A gradual

decline of $CD4^+$ Tcm was observed in the two control animals that did not develop a progressive loss of absolute $CD4^+$ T-cell numbers and survived throughout the study period. The most dramatic decline was observed in the animal with high virus load (9068, Fig. 5 right bottom), while animal R00045 that was able to reduce virus load to undetectable levels, maintained its $CD4^+$ Tcm population at a level above 25%. Because of the very low frequency of $CD4^+$ T-cells that developed in the other control animals, an accurate loss of $CD4^+$ Tcm cells could not be determined. In the immunized animals from both groups, the $CD4^+$ Tcm population remained relatively stable up until 30 weeks after infection (Fig. 5). Thereafter a subtle but gradual decline of the $CD4^+$ Tcm population was observed. In the majority of immunized animals the $CD4^+$ Tcm population remained above 25% of total $CD4^+$ T-cells. In the one immunized animal that developed a CD4 decline over time (98051, DNA/MVA group), a dramatic drop in % $CD4^+$ Tcm was observed.

In summary, both immunization strategies resulted in the preservation of absolute $CD4^+$ T-cell levels, reduced virus load, and prolonged survival (Fig. 6).

Changes in antigen specific responses following infection

To further elucidate immune responses associated with protection from disease in the immunized groups, antigen specific cellular immune responses were further studied post-challenge. Surprisingly, anamnestic T-cell responses were not observed directly after challenge. This may have been due to an initial decline of antigen-specific IFN-γ, IL-2 and IL-4 responses in both vaccine groups (data not shown). During the acute phase of plasma viremia IL-2 and IL-4 responses became briefly undetectable in the majority of animals after challenge. In contrast to the control animals, in vaccinated animals HIV-1

Env, SIV Gag and SIV Nef specific IFN-γ responses reappeared as detected 22 weeks after challenge (Fig. 7, left) and subsequently persisted. In contrast, by week 41 post challenge antigen-specific IFN-γ responses were lost in all but one of the control animals while in the majority of the immunized animals these responses were maintained (Fig. 7, right).

At the time of euthanasia (66 weeks post challenge for immunized animals and earlier for symptomatic control animals) antigen-specific cytokine induction was monitored intracellularly by polychromatic FACS analysis (ICS).

Vaccine induced preservation of T-cell responses

In the majority of control animals, cytokine production was not detected upon antigen stimulation in either $CD4^+$ nor in $CD8^+$ T-cell subsets (Fig. 8 A). However in the immunized animals, HIV-1 Env- and SIV Gag-specific cytokine responses were observed. In contrast to the pre-challenge ICS data, post-infection responses were primarily directed against SIV Gag and to a lesser extent against HIV-1 Env. The Gag specific $CD4^+$ T-cells were of the effector memory ($CD45RA^-/CCR7^-$) and central memory phenotype ($CD45RA^-/CCR7^+$), while the $CD8^+$ T-cells were of the effector phenotype ($CD45RA^+/CCR7^-$, Fig. S1). Similar to the situation prior to challenge, CD8 responses were higher in the MVA boosted animals ($p = 0.0148$ for SIV Gag). In the NYVAC boosted animals, the frequency of Env specific $CD4^+$ T-cells was in general higher than in MVA boosted animals (Fig. 8 A), but did not reach statistical significance ($p = 0.062$). The most predominant cytokine produced was IFN-γ, with a small contribution of IFN-γ and IL-2 double positive cells (Fig. 8 B).

At the time of euthanasia, Env and Gag-specific proliferating $CD4^+$ T-cells could not be found in the control animals, except one LTNP animal that reduced virus load below detectable levels (R00045, Fig. 8 C). In contrast to controls, detectable levels of Env and Gag-specific proliferating $CD4^+$ T-cells were observed in immunized animals. Although low, the frequency of Gag-specific $CD4^+$ proliferating T-cells was significantly higher in NYVAC boosted animals than in MVA boosted animals ($p = 0.0416$). In addition modest Env and Gag-specific proliferation mediated by $CD8^+$ T-cells was observed (Fig. 8 C right panel). The frequency of antigen specific proliferating $CD8^+$ T-cells was higher in immunized animals as compared to controls (only animals controlling virus load R00045 and 9068 showed antigen specific proliferating $CD8^+$ T-cells), and were comparable in both vaccine groups.

We set out to investigate whether differences of preferential induction of T-cells by the two poxvirus vaccine vectors induced before challenge, would change after infection. The relative contribution of $CD4^+$ and $CD8^+$ T-cells to the total response was determined in those animals that showed an antigen specific cytokine and/or proliferative responses. In the DNA/MVA immunized animals the antigen specific cytokine responses were mediated by (74% of the total response) $CD8^+$ T-cells ($p = 0.0356$ CD4 vs CD8). This remained much higher as compared to the NYVAC boosted animals ($p = 0.0072$ MVA vs NYVAC, Fig. 9 A), which elicited a predominant $CD4^+$ T-cell response ($p<0.0001$, CD4 vs CD8), of which 80% of the total response was contributed by $CD4^+$ T-cells (Fig. 9 A). This preferential induction of $CD8^+$ T-cells by MVA and of $CD4^+$ T-cells by NYVAC is similar to the data obtained before challenge, although the response switched from an Env predominant response before to a Gag predominant response following challenge. The relative contribution of $CD4^+$ T-cells to the total proliferative response was low in

both groups (Fig. 9 B), possibly as a reflection of a degree of functional loss following SHIV infection of the $CD4^+$ T-cell population.

Discussion

This study evaluated head to head the immunogenicity and efficacy of two DNA prime-poxvirus boost HIV-1 vaccine candidates in the Indian rhesus macaque model of AIDS. The two novel attenuated poxvirus vectors MVA and NYVAC were engineered to express the identical inserts consisting of HIV-1 and SIV genes, codon optimized for increased antigen expression and designed to express the gp120 of $SHIV_{89.6p}$ as a cell release product, while the Gag/Pol/Nef of SIV_{mac239} remained as an intracellular polyprotein. The Gag/Pol/Nef polygene was constructed by the removal of regions involved in immunosuppression (such as MHC-I downregulation motifs of Nef) and assembly (to prevent VLP formation) (47, 71). Our results demonstrated that both Pox-vector boosts were highly immunogenic, significantly boosting cellular immune responses to the HIV-1 and SIV inserts. The magnitude of the responses increased, and broadened as IFN-γ, IL-2 and IL-4 responses to all antigens were detected. This observation was consistent with earlier findings where a broadening of the DNA primed immune response to other (subdominant) epitopes by poxvirus boosting was reported (53, 72). The Env-specific vaccine responses prior to challenge were relatively immunodominant and mediated mainly by $CD4^+$ T-cells. This is attributable to the vaccine construct, designed such that the Env protein would be secreted, likely favoring $CD4^+$ T-cell responses (73). The cause of the relative immunodominance of Env remains speculative and is most probably not related to the level of antigen expression at the cellular level. Western blot analysis of MVA and NYVAC infected CFE cells showed similar levels of expression of both Env protein and of the polyprotein Gag/Pol/Nef (see supplemental data online). However, when the immunogenicity of these vaccine vectors was evaluated in HLA-A2 class I transgenic mice a similar Env immunodominant

response was observed (47). Factors such as MHC binding affinity, efficiency of epitope processing and competition between T-cells for access to APCs could possibly contribute to the observed immunodominant response (71, 74, 75).

Antigen-specific cytokine production by total PBMC as measured by ELISpot assay was similar in both vaccine groups. However, phenotypic analysis by ICS and in CFSE proliferation assays revealed clear differences between the two poxvirus vaccine vectors. The Env-specific CD8-mediated cytokine production (IFN-γ and/or IL-2) was higher in MVA boosted animals, while Gag-specific CD4-mediated proliferation was greater in NYVAC boosted animals. The MVA vaccine vector thus tended to induce $CD8^+$ T-cell responses in addition to CD4, while the NYVAC vector boosted $CD4^+$ T-cell mediated responses to a greater level than MVA. These differences were likely influenced by the different immune modulatory effects that these poxvirus vectors have on their host cells. Human gene profiling analysis of MVA infected Hela cells has revealed an upregulation of immunomodulatory genes such as IL-1a, IL-6, IL-7, IL-8 and IL-15 (76), which could create a pro-inflammatory microenvironment allowing expansion of $CD8^+$ T-cell populations. Maintenance of specific $CD8^+$ memory T-cells could contribute to MVA-induced expression of cytokines such as IL-15 (77). While it has been described that NYVAC induces much more cell apoptosis (45, 63). Uptake of apoptotic cells by antigen presenting cells may result in vaccine antigens being processed through the endocytosis pathway facilitating presentation by MHC class-II molecules, thus favoring $CD4^+$ T-cell mediated immune responses (78). Alternatively, cross-presentation and stimulation of $CD8^+$ T-cell responses cannot be ruled out (79, 80), and both phenomena likely contribute to the cumulative antigen specific T-cell response. In addition to the relatively dominant $CD4^+$ T-cell mediated immune responses, low but consistent $CD8^+$ T-cell responses

(proliferation) were observed. The preferential induction of HIV-specific $CD4^+$ T-cells by the NYVAC vector did not result in a greater propensity for accelerated disease progression due to preferential infection and loss of HIV Ag specific $CD4^+$ T-cells (28), since both poxvirus vaccines induced similar protection from disease progression.

Importantly, antigen-specific T-cells induced by both NYVAC and MVA vectors were polyfunctional in that they were able to express both IFN-γ and IL-2 simultaneously, showed proliferative capacity and were of effector memory ($CD45RA^-/CCR7^-$) and central memory ($CD45RA^-/CCR7^+$) phenotype before challenge; and of effector ($CD8^+/CD45RA^+/CCR7^-$) and memory ($CD4^+/CD45RA^-/CCR7^{+/-}$) phenotype after challenge. The induction of polyfunctional T-cells by vaccinia virus immunization confirms earlier findings by others (81), but we have not investigated whether these were of the unusual phenotype ($CD45RO^-CD27^{intermediate}$). The presence of "polyfunctional phenotypes" have been shown to correlate with a "long term non-progressor" status in rhesus macaques (82) and HIV infected individuals (26, 83, 84) and to correlate with a beneficial control of virus load (19, 85, 86). An effective AIDS vaccine should induce such T-cells in order to effectively eradicate HIV infected cells. Besides the induction of polyfunctional T-cells, both vaccine vectors induced low levels of neutralizing antibodies to the challenge virus, but higher titres to relevant pseudoviruses. This is likely due to the increased inherent neutralization sensitivity of single sequence, replication incompetent pseudoviruses (87). Vaccine induced T-cell and humoral immune responses were not sufficient to protect animals from $SHIV_{89.6p}$ infection. However, immunized animals which became infected, were protected from disease progression for more than a year (66 weeks), while four out of six control animals developed histological evidence of AIDS like disease before the end of the study period. As memory $CD4^+$ T-cells are critical for

maintaining immune competence while serving as the primary target of HIV infection, it is of the utmost importance to prevent infection and destruction of these cells. The majority of immunized animals controlled virus load and $CD4^+$ T-cells at pre-infection levels, as well as the $CD4^+$ Tcm population.

The Env dominant response observed prior to infection gradually shifted towards a Gag dominant response following infection. The vaccine induced Env-specific responses were mediated mainly by $CD4^+$ T-cells, which are the targets for SHIV infection. Since all vaccinated animals became infected, the function and the number of these Env-specific $CD4^+$ T-cells might have been transiently affected by the virus infection (88, 89), even though no clear $CD4^+$ T-cell decline was observed. The post challenge induction of Gag- as well as Nef responses represent an anamnestic response preferentially observed in immunized animals. This underscores that, despite the relative immunodominance of Env, the immunization against the other vaccine antigens has been beneficial.

The preferential induction of antigen-specific $CD8^+$ responses by MVA and $CD4^+$ T-cell responses by NYVAC, reiterates post-immunization pre-challenge observations, but surprisingly directed against different antigens. It is therefore likely that this is not due to imprinting per se, but possibly due to the induction of a particular cytokine environment by the respective vaccine vectors (45, 63, 76) such that they favored preferential induction of either $CD8^+$ or $CD4^+$ T-cell responses.

Although immunization did not protect against SHIV infection, it did reduce viral load, prolonged survival and maintenance of $CD4^+$ T (cm) cells. However, the relative loss of Env-specific responses, the reduced CD4 responses, reduced IL-2 production (ELISpot as well as ICS) and reduced proliferative capacity after challenge would indicate an insidious loss of T-cell function, which may eventually have an effect on long term

survival. While both vaccine candidates induced similar efficacy, it was apparently exerted through different mechanisms themselves, which may have implications for the long term management of the infection and future refinements in HIV vaccine design.

Materials and Methods

Vaccines

DNA immunogens HIV-1 Env and SIV Gag/Pol/Nef

SIV_{mac239} pcDNA-GagPolNef and $SHIV_{89.6P}$ pcDNA- Env (KB9 molecular clone (90)) constructs were made and provided by Dr. R. Wagner (Regensburg, Germany). Similar techniques were used for construction of synthetic polygenes as have been used for preparing the pcDNA-GagPolNef of $HIV\text{-}1_{IIIB}$ (91) and pcDNA-Env of a Chinese clade C HIV-1 strain CN54 (92) described elsewhere (47). For detailed description see supplemental data online. Upscaling was performed by Cobra Biomanufacturing Plc, Keele, Staffordshire, UK.

Generation of vaccine vectors

The NYVAC (38) and MVA vectors expressing SIV_{mac239} *gagpolnef* and $SHIV_{89.6p}$ *env* were constructed similarly as described elsewhere (47, 71). For detailed description and DNA sequence of the inserted genes see supplemental data online.

Study design

The study comprised of 3 groups of 7 animals each and 2 naïve infection control animals (outbred rhesus macaques (*Macaca mulatta*) of Indian origin). At weeks 0 and 4, two groups of 7 animals each were immunized (‘primed”) with DNA. Prior to administration, the DNA constructs pcDNA-GagPolNef SIV_{mac239} pcDNA-$Env_{89.6P}$ were mixed together. Two mg of each construct (4 mg total) was administered intramuscularly (i.m.) in the upper leg. One group of 7 control animals received “empty” DNA vectors. At weeks 20

and 24, one group of seven animals was immunized ('boosted') with NYVAC containing SIV_{mac239}-*gagpolnef* and $SHIV_{89.6p}$ *env* genes ($5x10^8$ pfu/500μl i.m. in the right upper arm), while another group of 7 animals was boosted with MVA containing the same genes ($5x10^8$ pfu/500μl i.m). Seven control animals were "boosted" with empty NYVAC vectors ($5x10^8$ pfu/500μl i.m. in the right upper arm).

Eight weeks after the final immunization all animals were challenged with 50-100 MID_{50} of the pathogenic virus strain $SHIV_{89.6p}$ (90, 93-95) generously provided by N. Letvin (Beth Israel Hospital, Boston, USA), through the intravenous route (1ml of a 1:1000 dilution of the virus stock, containing $3.2x10^4$ $TCID_{50}$/ml ($1x10^8$ RNA eq/ml) and approximately $5x10^4$ MID_{50}/ml). The study protocol and experimental procedures were approved by the institute's animal ethical care and use committee and were performed in accordance with Dutch law and International ethical and scientific standards and guidelines.

Enumeration of peptide specific T-cell responses by IFN-γ, IL-2 or IL-4 ELISpot assays

Quantification of antigen specific cytokine secreting cells was performed on freshly isolated PBMC by IFN-γ, IL-2 and IL-4 enzyme-linked immunospot (ELISpot) assays, according to the manufacturer's instructions (U-Cytech, Utrecht, The Netherlands). Positive control was SEB 1μg/ml, negative control was medium alone. Antigen specific responses were measured against 5 μg/ml peptide pools: 15-mers with 11 aa overlap spanning the entire Gagpolnef polyprotein (Synpep Corporation, Dublin, CA, USA, provided by EuroVacc consortium), and 20-mers overlapping by 10 aa spanning the Env gp120 of $SHIV_{89.6p}$ (NIH AIDS Research & Reference Reagent Program, Rockville,

USA). Peptide pools were made as follows: Gag1 54 peptides (SIVg1-SIVg213), Gag2 54 peptides (SIVg217-SIVgp429), Pol1 60 peptides (SIVgp433-SIVp669), Pol2 60 peptides (SIVp673-SIVpn689, SIVnp941-SIVp1157), Pol3 59 peptides (SIVp1161-SIVp1393), Nef 62 peptides (SIVpn693-SIVnp937), Env 49 peptides (4702-4749). Results are expressed as the mean number of spot forming cells (SFC) per 10^6 PBMC from triplicate assays minus background values (mean number of SFC plus 2xSD of triplicate assays with medium alone). Mean spots of each animal (dots) are expressed per antigen (responses to 2 Gag pools and 3 Pol pools were combined).

Phenotyping of T-cell responses by intracellular cytokine analysis

The phenotype of responding T-cells was analyzed by ICS assay and FACS analysis as described elsewhere (96) with minor modifications. PBMC were O/N incubated, in the presence of the costimulatory molecules CD28 and CD49d (2μg/ml each), with medium alone (negative control), 1μg/ml SEB (positive control) or stimulated with 1μg/ml of the same peptide pools as used in the ELISpot assay as described above. Cells were stained with directly conjugated antibodies (Becton Dickinson (BD), Biosciences, CA, USA) to CD3 (PerCP-labeled), CD4 (PE-CY7 labeled), CD8 (APC-CY7 labeled), and to CD14 and CD20 (ECD labeled, Beckman Coulter, Marseille, France) for exclusion of monocytes and B-cells. Memory phenotyping was possible by staining with antibodies to CCR7 (FITC labeled, R&D systems, Minneapolis, MN, USA) and CD45RA (custom biotin labeled by BD, followed by streptavidin Pacific Orange, Molecular Probes, Leiden, The Netherlands). The cells were fixed and permeabilised with Cytofix/Cytoperm buffer (BD) and stained intracellularly with IFN-γ (APC-labeled) and IL-2 (PE-labeled) in

Perm/wash solution (BD). 100,000 – 200,000 events were acquired on the FACS Aria (Becton Dickinson, CA, USA) and FACS Diva Software was used for analysis.

Antigen specific proliferation

Proliferative capacity upon antigen stimulation of PBMC was investigated using the CFSE proliferation assay as described elsewhere (97, 98). Cells were stimulated with either medium alone, gag peptide pool, env peptide pool (both at 4μg/peptide/ml), or ConA (5 μg/ml). Cells were incubated for 6 days at 37ºC and 5% CO_2. Cells were stained for viability with the 'Live/Dead fixable violet dead cell' dye (Mol. Probes, L34955). After Live/Dead staining cells were stained with the following antibodies: $CD3^{APC}$, $CD4^{PerCPCy5.5}$, $CD8^{APCCy7}$, $CD45RA^{biotin}$ (all BD Biosciences), $CD14^{ECD}$ and $CD20^{ECD}$ (Beckman Coulter). Cells were fixed overnight in 2% paraformaldehyde at 4ºC and cells were acquired on a FACSAria (BD).

Gene array analysis

Human monocyte derived dendritic cells (MDDC) were infected with MVA or NYVAC and incubated for 6 hours. Cells were collected and processed for RNA extraction. Detailed description of gene array analysis has been described elsewhere (46).

Virus neutralization assay

The neutralizing activity of the sera from immunized and infected rhesus macaques was tested on the challenge virus strain $SHIV_{89.6P}$ and the HIV-$1_{89.6}$ virus (NIH AIDS Research and Reference Reagent Program, cat no 1966, gen bank U39362) (93), or the

pseudoviruses $SHIV_{89.6}$ Sodroski and $SHIV_{89.6P}$ KB9 using the envelope of $SHIV_{89.6}$ (NIH AIDS Research and Reference Reagent Program, cat no 4131) or $SHIV_{KB9}$ (NIH AIDS Research and Reference Reagent Program, cat no 4129) (90). Virus stocks were prepared on human PBMCs and pseudovirus stocks were prepared on 293 T cells. For the neutralization assay 50 $TCID_{50}$ of the virus stock were incubated with serum samples (final dilution 1/15) from the animals in duplicate for 1 h at 37 °C in a total volume of 150 µl Dulbecco medium with 10% FCS in 96 well flat bottom culture plates. Freshly trypsinized TZM-bl cells (10,000 cells in 100 µl medium containing 37.5 µg/ml DEAE-dextran) were added to each well. Control wells received cells plus virus (virus control), or cells only (background control) (99). After 48 h culture, supernatant was removed and 150 µl lysis buffer (PBS 1% Triton 1mM $CaCl_2$ and 1mM $MgCL_2$) was added and incubated for 45 minutes at 4 °C. 100 µl of cell lysate was transferred to 96 well black/white solid plates for measurement of luminescence using a Victor 3 light luminometer. 100 µl of Britelite reagent (Perkin Elmer) was added. The amount of luminescence measured before immunization (groups 1 and 2) or before challenge (group 3) was set as 100% infected cells, which means 0% neutralization.

Determination of plasma virus load and detection of proviral DNA

Plasma virus load was determined with quantitative competitive RNA RT-PCR using plasma from EDTA treated blood samples (100). The lower detection limit was 40 RNA equivalents/ml.

T lymphocyte subset analysis

Quantitative changes in PBMC subsets after challenge were monitored by FACS analysis as previously described (101). The following mAbs combinations were used: a) $CD20^{FITC}$, $CD16^{PE}$, $HLA\text{-}DR^{PerCP}$, $CD3^{APC}$, $CD4^{PE\text{-}CY7}$, $CD8^{APC\text{-}CY7}$, b) $CCR7^{FITC}$, $CD62L^{PE}$, $CD45RA^{Biotin}$, $CD3^{APC}$, $CD4^{PE\text{-}CY7}$, $CD8^{APC\text{-}CY7}$. MAb were obtained from Becton & Dickinson/Pharmingen ($CD20^{FITC}$ clone L27, $CD16^{PE}$ clone B7.3.1, $HLA\text{-}DR^{PerCP}$ clone L243, $CD3^{APC}$ clone SP34, $CD4^{PE\text{-}CY7}$ clone SK3, $CD8^{APC\text{-}CY7}$ clone SK1, $CD45RA^{Biotin}$ clone 5H9,), or R & D Systems (Minneapolis, USA) $CCR7^{FITC}$ clone FAB197F and AbD Serotec (Dusseldorf, Germany) $CD62L^{PE}$ clone FMC46. Polystyrene Fluorspheres (Beckman & Coulter) were used to calculate absolute lymphocyte count. Flow cytometry was performed on a FACSAria (Becton Dickinson (BD). 20,000 events in the lymphocyte-gate were analyzed per monoclonal antibody mix.

Statistical analysis

Statistical analysis was performed by the Wilcoxon's rank sum test or unpaired *t-test* (with Welch correction) depending on the normal distribution of the data. $p<0.05$ was considered to be significant.

Online Supplemental Material

Fig. S1 shows flow cytometry profiles of antigen-specific IFN-γ producing $CD4^+$ and $CD8^+$ memory T-cells of two representative animals (one from each vaccine group) before challenge and at time of euthanasia. Fig. S2 shows the relatively low neutralizing antibody titres to the replicating challenge virus and to several pseudotype viruses.

A detailed description of the construction of the immunogens is given in the online supplemental material section. Fig. S3 shows the schematic representation of the

GagPolNef and Env polyprotein expressed by the MVA and NYVAC vaccine vectors. The generation of the MVA-89.6P-SIVgagpolnef and NYVAC-89.6P-SIVgagpolnef vaccine constructs is described in detail. Fig. S4 A and B shows the schematic representation of the generation of the plasmid transfer vector pLZAW1-89.6P-SIVgpn-18. Fig. S5 A represents a schematic drawing of the vaccine vectors MVA and NYVAC and shows PCR analysis of the MVA-89.6P-SIVgpn and NYVAC-89.6P-SIVgpn vaccine stocks. Fig. S5 B shows Env and GagPolNef expression of the MVA-89.6P-SIVgpn and NYVAC-89.6P-SIVgpn vaccines by Western blot analysis.

The DNA sequence of the EnvGagPolNef insert of the vaccine is given.

Online supplemental material is available at…..

Acknowledgements

We are indebted to T. de Koning and H. van Westbroek for documentation. This study was supported by funding of the EuroVacc (European Vaccine Effort Against HIV/AIDS) project QLK2-CT-1999-01321. We are grateful to Jose Manuel Gonzalez for bioinformatic assistance in gene array analysis.

References

1. Heeney, J.L., and S.A. Plotkin. 2006. Immunological correlates of protection from HIV infection and disease. *Nat Immunol* 7:1281-1284.
2. Mooij, P., and J.L. Heeney. 2001. Rational development of prophylactic HIV vaccines based on structural and regulatory proteins. *Vaccine* 20:304-321.
3. Burton, D.R., R.C. Desrosiers, R.W. Doms, W.C. Koff, P.D. Kwong, J.P. Moore, G.J. Nabel, J. Sodroski, I.A. Wilson, and R.T. Wyatt. 2004. HIV vaccine design and the neutralizing antibody problem. *Nat Immunol* 5:233-236.
4. Richman, D.D., T. Wrin, S.J. Little, and C.J. Petropoulos. 2003. Rapid evolution of the neutralizing antibody response to HIV type 1 infection. *Proc Natl Acad Sci U S A* 100:4144-4149.
5. Wei, X., J.M. Decker, S. Wang, H. Hui, J.C. Kappes, X. Wu, J.F. Salazar-Gonzalez, M.G. Salazar, J.M. Kilby, M.S. Saag, N.L. Komarova, M.A. Nowak, B.H. Hahn, P.D. Kwong, and G.M. Shaw. 2003. Antibody neutralization and escape by HIV-1. *Nature* 422:307-312.
6. Letvin, N.L. 2006. Progress and obstacles in the development of an AIDS vaccine. *Nat Rev Immunol* 6:930-939.
7. Fischer, W., S. Perkins, J. Theiler, T. Bhattacharya, K. Yusim, R. Funkhouser, C. Kuiken, B. Haynes, N.L. Letvin, B.D. Walker, B.H. Hahn, and B.T. Korber. 2007. Polyvalent vaccines for optimal coverage of potential T-cell epitopes in global HIV-1 variants. *Nat Med* 13:100-106.
8. Koup, R.A., J.T. Safrit, Y. Cao, C.A. Andrews, G. McLeod, W. Borkowsky, C. Farthing, and D.D. Ho. 1994. Temporal association of cellular immune responses

with the initial control of viremia in primary human immunodeficiency virus type 1 syndrome. *J Virol* 68:4650-4655.

9. Kuroda, M.J., J.E. Schmitz, W.A. Charini, C.E. Nickerson, M.A. Lifton, C.I. Lord, M.A. Forman, and N.L. Letvin. 1999. Emergence of CTL coincides with clearance of virus during primary simian immunodeficiency virus infection in rhesus monkeys. *J Immunol* 162:5127-5133.

10. O'Connor, D.H., B.R. Mothe, J.T. Weinfurter, S. Fuenger, W.M. Rehrauer, P. Jing, R.R. Rudersdorf, M.E. Liebl, K. Krebs, J. Vasquez, E. Dodds, J. Loffredo, S. Martin, A.B. McDermott, T.M. Allen, C. Wang, G.G. Doxiadis, D.C. Montefiori, A. Hughes, D.R. Burton, D.B. Allison, S.M. Wolinsky, R. Bontrop, L.J. Picker, and D.I. Watkins. 2003. Major histocompatibility complex class I alleles associated with slow simian immunodeficiency virus disease progression bind epitopes recognized by dominant acute-phase cytotoxic-T-lymphocyte responses. *J Virol* 77:9029-9040.

11. Carrington, M., and S.J. O'Brien. 2003. The influence of HLA genotype on AIDS. *Annu Rev Med* 54:535-551.

12. Kaslow, R.A., M. Carrington, R. Apple, L. Park, A. Munoz, A.J. Saah, J.J. Goedert, C. Winkler, S.J. O'Brien, C. Rinaldo, R. Detels, W. Blattner, J. Phair, H. Erlich, and D.L. Mann. 1996. Influence of combinations of human major histocompatibility complex genes on the course of HIV-1 infection. *Nat Med* 2:405-411.

13. McNeil, A.J., P.L. Yap, S.M. Gore, R.P. Brettle, M. McColl, R. Wyld, S. Davidson, R. Weightman, A.M. Richardson, and J.R. Robertson. 1996.

Association of HLA types A1-B8-DR3 and B27 with rapid and slow progression of HIV disease. *Qjm* 89:177-185.

14. Migueles, S.A., M.S. Sabbaghian, W.L. Shupert, M.P. Bettinotti, F.M. Marincola, L. Martino, C.W. Hallahan, S.M. Selig, D. Schwartz, J. Sullivan, and M. Connors. 2000. HLA B*5701 is highly associated with restriction of virus replication in a subgroup of HIV-infected long term nonprogressors. *Proc Natl Acad Sci U S A* 97:2709-2714.

15. Frahm, N., S. Adams, P. Kiepiela, C.H. Linde, H.S. Hewitt, M. Lichterfeld, K. Sango, N.V. Brown, E. Pae, A.G. Wurcel, M. Altfeld, M.E. Feeney, T.M. Allen, T. Roach, M.A. St John, E.S. Daar, E. Rosenberg, B. Korber, F. Marincola, B.D. Walker, P.J. Goulder, and C. Brander. 2005. HLA-B63 presents HLA-B57/B58-restricted cytotoxic T-lymphocyte epitopes and is associated with low human immunodeficiency virus load. *J Virol* 79:10218-10225.

16. Frahm, N., P. Kiepiela, S. Adams, C.H. Linde, H.S. Hewitt, K. Sango, M.E. Feeney, M.M. Addo, M. Lichterfeld, M.P. Lahaie, E. Pae, A.G. Wurcel, T. Roach, M.A. St John, M. Altfeld, F.M. Marincola, C. Moore, S. Mallal, M. Carrington, D. Heckerman, T.M. Allen, J.I. Mullins, B.T. Korber, P.J. Goulder, B.D. Walker, and C. Brander. 2006. Control of human immunodeficiency virus replication by cytotoxic T lymphocytes targeting subdominant epitopes. *Nat Immunol* 7:173-178.

17. Schmitz, J.E., M.J. Kuroda, S. Santra, V.G. Sasseville, M.A. Simon, M.A. Lifton, P. Racz, K. Tenner-Racz, M. Dalesandro, B.J. Scallon, J. Ghrayeb, M.A. Forman, D.C. Montefiori, E.P. Rieber, N.L. Letvin, and K.A. Reimann. 1999. Control of

viremia in simian immunodeficiency virus infection by CD8+ lymphocytes. *Science* 283:857-860.

18. Lifson, J.D., J.L. Rossio, M. Piatak, Jr., T. Parks, L. Li, R. Kiser, V. Coalter, B. Fisher, B.M. Flynn, S. Czajak, V.M. Hirsch, K.A. Reimann, J.E. Schmitz, J. Ghrayeb, N. Bischofberger, M.A. Nowak, R.C. Desrosiers, and D. Wodarz. 2001. Role of CD8(+) lymphocytes in control of simian immunodeficiency virus infection and resistance to rechallenge after transient early antiretroviral treatment. *J Virol* 75:10187-10199.

19. Amara, R.R., C. Ibegbu, F. Villinger, D.C. Montefiori, S. Sharma, P. Nigam, Y. Xu, H.M. McClure, and H.L. Robinson. 2005. Studies using a viral challenge and CD8 T cell depletions on the roles of cellular and humoral immunity in the control of an SHIV-89.6P challenge in DNA/MVA-vaccinated macaques. *Virology* 343:246-255.

20. Loffredo, J.T., J. Maxwell, Y. Qi, C.E. Glidden, G.J. Borchardt, T. Soma, A.T. Bean, D.R. Beal, N.A. Wilson, W.M. Rehrauer, J.D. Lifson, M. Carrington, and D.I. Watkins. 2007. Mamu-B*08-Positive Macaques Control Simian Immunodeficiency Virus Replication. *J. Virol* 81:8793-8808.

21. Mothe, B.R., J. Weinfurter, C. Wang, W. Rehrauer, N. Wilson, T.M. Allen, D.B. Allison, and D.I. Watkins. 2003. Expression of the major histocompatibility complex class I molecule Mamu-A*01 is associated with control of simian immunodeficiency virus SIVmac239 replication. *J Virol* 77:2736-2740.

22. Pal, R., D. Venzon, N.L. Letvin, S. Santra, D.C. Montefiori, N.R. Miller, E. Tryniszewska, M.G. Lewis, T.C. VanCott, V. Hirsch, R. Woodward, A. Gibson, M. Grace, E. Dobratz, P.D. Markham, Z. Hel, J. Nacsa, M. Klein, J. Tartaglia, and

G. Franchini. 2002. ALVAC-SIV-gag-pol-env-based vaccination and macaque major histocompatibility complex class I (A*01) delay simian immunodeficiency virus SIVmac-induced immunodeficiency. *J Virol* 76:292-302.

23. Yant, L.J., T.C. Friedrich, R.C. Johnson, G.E. May, N.J. Maness, A.M. Enz, J.D. Lifson, D.H. O'Connor, M. Carrington, and D.I. Watkins. 2006. The high-frequency major histocompatibility complex class I allele Mamu-B*17 is associated with control of simian immunodeficiency virus SIVmac239 replication. *J Virol* 80:5074-5077.

24. Sun, Y., J.E. Schmitz, A.P. Buzby, B.R. Barker, S.S. Rao, L. Xu, Z.Y. Yang, J.R. Mascola, G.J. Nabel, and N.L. Letvin. 2006. Virus-specific cellular immune correlates of survival in vaccinated monkeys after simian immunodeficiency virus challenge. *J Virol*

25. Wilson, N.A., J. Reed, G.S. Napoe, S. Piaskowski, A. Szymanski, J. Furlott, E.J. Gonzalez, L.J. Yant, N.J. Maness, G.E. May, T. Soma, M.R. Reynolds, E. Rakasz, R. Rudersdorf, A.B. McDermott, D.H. O'Connor, T.C. Friedrich, D.B. Allison, A. Patki, L.J. Picker, D.R. Burton, J. Lin, L. Huang, D. Patel, G. Heindecker, J. Fan, M. Citron, M. Horton, F. Wang, X. Liang, J.W. Shiver, D.R. Casimiro, and D.I. Watkins. 2006. Vaccine-induced cellular immune responses reduce plasma viral concentrations after repeated low-dose challenge with pathogenic simian immunodeficiency virus SIVmac239. *J Virol* 80:5875-5885.

26. Betts, M.R., M.C. Nason, S.M. West, S.C. De Rosa, S.A. Migueles, J. Abraham, M.M. Lederman, J.M. Benito, P.A. Goepfert, M. Connors, M. Roederer, and R.A. Koup. 2006. HIV nonprogressors preferentially maintain highly functional HIV-specific CD8+ T-cells. *Blood*

27. Brenchley, J.M., L.E. Ruff, J.P. Casazza, R.A. Koup, D.A. Price, and D.C. Douek. 2006. Preferential infection shortens the life span of human immunodeficiency virus-specific CD4+ T cells in vivo. *J Virol* 80:6801-6809.

28. Douek, D.C., J.M. Brenchley, M.R. Betts, D.R. Ambrozak, B.J. Hill, Y. Okamoto, J.P. Casazza, J. Kuruppu, K. Kunstman, S. Wolinsky, Z. Grossman, M. Dybul, A. Oxenius, D.A. Price, M. Connors, and R.A. Koup. 2002. HIV preferentially infects HIV-specific CD4+ T cells. *Nature* 417:95-98.

29. Altenburger, W., C.P. Suter, and J. Altenburger. 1989. Partial deletion of the human host range gene in the attenuated vaccinia virus MVA. *Arch Virol* 105:15-27.

30. Antoine, G., F. Scheiflinger, F. Dorner, and F.G. Falkner. 1998. The complete genomic sequence of the modified vaccinia Ankara strain: comparison with other orthopoxviruses. *Virology* 244:365-396.

31. Blanchard, T.J., A. Alcami, P. Andrea, and G.L. Smith. 1998. Modified vaccinia virus Ankara undergoes limited replication in human cells and lacks several immunomodulatory proteins: implications for use as a human vaccine. *J Gen Virol* 79 (Pt 5):1159-1167.

32. Meyer, H., G. Sutter, and A. Mayr. 1991. Mapping of deletions in the genome of the highly attenuated vaccinia virus MVA and their influence on virulence. *J Gen Virol* 72 (Pt 5):1031-1038.

33. Wyatt, L.S., M.W. Carroll, C.P. Czerny, M. Merchlinsky, J.R. Sisler, and B. Moss. 1998. Marker rescue of the host range restriction defects of modified vaccinia virus Ankara. *Virology* 251:334-342.

34. Sutter, G., and B. Moss. 1992. Nonreplicating vaccinia vector efficiently expresses recombinant genes. *Proc Natl Acad Sci U S A* 89:10847-10851.

35. Sutter, G., and C. Staib. 2003. Vaccinia vectors as candidate vaccines: the development of modified vaccinia virus Ankara for antigen delivery. *Curr Drug Targets Infect Disord* 3:263-271.

36. Gherardi, M.M., and M. Esteban. 2005. Recombinant poxviruses as mucosal vaccine vectors. *J Gen Virol* 86:2925-2936.

37. Corbett, M., W.M. Bogers, J.L. Heeney, S. Gerber, C. Genin, A. Didierlaurent, H. Oostermeijer, R. Dubbes, G. Braskamp, S. Lerondel, C.E. Gomez, M. Esteban, I. Kondova, P. Mooij, S.S. Balla-Jhagjhoorsingh, N. Beenhakker, G. Koopman, S. Van der Burg, J.P. Kraehenbuhl, and A. Le Pape. 2007 in press. Aerosol Immunization with NYVAC and MVA Vectored Vaccines: Simple, Safe and Immunogenic. *Proc Natl Acad Sci U S A*.

38. Tartaglia, J., M.E. Perkus, J. Taylor, E.K. Norton, J.C. Audonnet, W.I. Cox, S.W. Davis, J. van der Hoeven, B. Meignier, M. Riviere, and et al. 1992. NYVAC: a highly attenuated strain of vaccinia virus. *Virology* 188:217-232.

39. Tartaglia, J., W.I. Cox, S. Pincus, and E. Paoletti. 1994. Safety and immunogenicity of recombinants based on the genetically-engineered vaccinia strain, NYVAC. *Dev Biol Stand* 82:125-129.

40. Myagkikh, M., S. Alipanah, P.D. Markham, J. Tartaglia, E. Paoletti, R.C. Gallo, G. Franchini, and M. Robert-Guroff. 1996. Multiple immunizations with attenuated poxvirus HIV type 2 recombinants and subunit boosts required for protection of rhesus macaques. *AIDS Res Hum Retroviruses* 12:985-992.

41. Benson, J., C. Chougnet, M. Robert-Guroff, D. Montefiori, P. Markham, G. Shearer, R.C. Gallo, M. Cranage, E. Paoletti, K. Limbach, D. Venzon, J. Tartaglia, and G. Franchini. 1998. Recombinant vaccine-induced protection against the highly pathogenic simian immunodeficiency virus SIV(mac251): dependence on route of challenge exposure. *J Virol* 72:4170-4182.

42. Kanesa-thasan, N., J.J. Smucny, C.H. Hoke, D.H. Marks, E. Konishi, I. Kurane, D.B. Tang, D.W. Vaughn, P.W. Mason, and R.E. Shope. 2000. Safety and immunogenicity of NYVAC-JEV and ALVAC-JEV attenuated recombinant Japanese encephalitis virus--poxvirus vaccines in vaccinia-nonimmune and vaccinia-immune humans. *Vaccine* 19:483-491.

43. Siemens, D.R., S. Crist, J.C. Austin, J. Tartaglia, and T.L. Ratliff. 2003. Comparison of viral vectors: gene transfer efficiency and tissue specificity in a bladder cancer model. *J Urol* 170:979-984.

44. Franchini, G., S. Gurunathan, L. Baglyos, S. Plotkin, and J. Tartaglia. 2004. Poxvirus-based vaccine candidates for HIV: two decades of experience with special emphasis on canarypox vectors. *Expert Rev Vaccines* 3:S75-88.

45. Guerra, S., L.A. Lopez-Fernandez, A. Pascual-Montano, J.L. Najera, A. Zaballos, and M. Esteban. 2006. Host response to the attenuated poxvirus vector NYVAC: upregulation of apoptotic genes and NF-kappaB-responsive genes in infected HeLa cells. *J Virol* 80:985-998.

46. Guerra, S., J.L. Najera, J.M. Gonzalez, L. Lopez, N. Climent, J.M. Gatell, T. Gallart, and M. Esteban. 2007. Distinct gene expression profiling after infection of immature human monocyte-derived dendritic cells by the attenuated poxvirus vectors MVA and NYVAC. *J Virol*

47. Gomez, C.E., J.L. Najera, V. Jimenez, K. Bieler, J. Wild, L. Kostic, S. Heidari, M. Chen, M.J. Frachette, G. Pantaleo, H. Wolf, P. Liljestrom, R. Wagner, and M. Esteban. 2007. Generation and immunogenicity of novel HIV/AIDS vaccine candidates targeting HIV-1 Env/Gag-Pol-Nef antigens of clade C. *Vaccine* 25:1969-1992.

48. Hanke, T., R.V. Samuel, T.J. Blanchard, V.C. Neumann, T.M. Allen, J.E. Boyson, S.A. Sharpe, N. Cook, G.L. Smith, D.I. Watkins, M.P. Cranage, and A.J. McMichael. 1999. Effective induction of simian immunodeficiency virus-specific cytotoxic T lymphocytes in macaques by using a multiepitope gene and DNA prime-modified vaccinia virus Ankara boost vaccination regimen. *J Virol* 73:7524-7532.

49. Amara, R.R., F. Villinger, J.D. Altman, S.L. Lydy, S.P. O'Neil, S.I. Staprans, D.C. Montefiori, Y. Xu, J.G. Herndon, L.S. Wyatt, M.A. Candido, N.L. Kozyr, P.L. Earl, J.M. Smith, H.L. Ma, B.D. Grimm, M.L. Hulsey, J. Miller, H.M. McClure, J.M. McNicholl, B. Moss, and H.L. Robinson. 2001. Control of a mucosal challenge and prevention of AIDS by a multiprotein DNA/MVA vaccine. *Science* 292:69-74.

50. Kent, S.J., A. Zhao, S.J. Best, J.D. Chandler, D.B. Boyle, and I.A. Ramshaw. 1998. Enhanced T-cell immunogenicity and protective efficacy of a human immunodeficiency virus type 1 vaccine regimen consisting of consecutive priming with DNA and boosting with recombinant fowlpox virus. *J Virol* 72:10180-10188.

51. Robinson, H.L., D.C. Montefiori, R.P. Johnson, K.H. Manson, M.L. Kalish, J.D. Lifson, T.A. Rizvi, S. Lu, S.L. Hu, G.P. Mazzara, D.L. Panicali, J.G. Herndon, R.

Glickman, M.A. Candido, S.L. Lydy, M.S. Wyand, and H.M. McClure. 1999. Neutralizing antibody-independent containment of immunodeficiency virus challenges by DNA priming and recombinant pox virus booster immunizations [see comments]. *Nat Med* 5:526-534.

52. Makitalo, B., P. Lundholm, J. Hinkula, C. Nilsson, K. Karlen, A. Morner, G. Sutter, V. Erfle, J.L. Heeney, B. Wahren, G. Biberfeld, and R. Thorstensson. 2004. Enhanced cellular immunity and systemic control of SHIV infection by combined parenteral and mucosal administration of a DNA prime MVA boost vaccine regimen. *J Gen Virol* 85:2407-2419.

53. Hel, Z., W.P. Tsai, A. Thornton, J. Nacsa, L. Giuliani, E. Tryniszewska, M. Poudyal, D. Venzon, X. Wang, J. Altman, D.I. Watkins, W. Lu, A. von Gegerfelt, B.K. Felber, J. Tartaglia, G.N. Pavlakis, and G. Franchini. 2001. Potentiation of simian immunodeficiency virus (SIV)-specific CD4(+) and CD8(+) T cell responses by a DNA-SIV and NYVAC-SIV prime/boost regimen. *J Immunol* 167:7180-7191.

54. Hel, Z., J. Nacsa, E. Tryniszewska, W.P. Tsai, R.W. Parks, D.C. Montefiori, B.K. Felber, J. Tartaglia, G.N. Pavlakis, and G. Franchini. 2002. Containment of simian immunodeficiency virus infection in vaccinated macaques: correlation with the magnitude of virus-specific pre- and postchallenge CD4+ and CD8+ T cell responses. *J Immunol* 169:4778-4787.

55. Nkolola, J.P., E.G. Wee, E.J. Im, C.P. Jewell, N. Chen, X.N. Xu, A.J. McMichael, and T. Hanke. 2004. Engineering RENTA, a DNA prime-MVA boost HIV vaccine tailored for Eastern and Central Africa. *Gene Ther* 11:1068-1080.

56. Im, E.J., J.P. Nkolola, K. di Gleria, A.J. McMichael, and T. Hanke. 2006. Induction of long-lasting multi-specific CD8+ T cells by a four-component DNA-MVA/HIVA-RENTA candidate HIV-1 vaccine in rhesus macaques. *Eur J Immunol* 36:2574-2584.

57. Mwau, M., I. Cebere, J. Sutton, P. Chikoti, N. Winstone, E.G. Wee, T. Beattie, Y.H. Chen, L. Dorrell, H. McShane, C. Schmidt, M. Brooks, S. Patel, J. Roberts, C. Conlon, S.L. Rowland-Jones, J.J. Bwayo, A.J. McMichael, and T. Hanke. 2004. A human immunodeficiency virus 1 (HIV-1) clade A vaccine in clinical trials: stimulation of HIV-specific T-cell responses by DNA and recombinant modified vaccinia virus Ankara (MVA) vaccines in humans. *J Gen Virol* 85:911-919.

58. Goonetilleke, N., S. Moore, L. Dally, N. Winstone, I. Cebere, A. Mahmoud, S. Pinheiro, G. Gillespie, D. Brown, V. Loach, J. Roberts, A. Guimaraes-Walker, P. Hayes, K. Loughran, C. Smith, J. De Bont, C. Verlinde, D. Vooijs, C. Schmidt, M. Boaz, J. Gilmour, P. Fast, L. Dorrell, T. Hanke, and A.J. McMichael. 2006. Induction of multifunctional human immunodeficiency virus type 1 (HIV-1)-specific T cells capable of proliferation in healthy subjects by using a prime-boost regimen of DNA- and modified vaccinia virus Ankara-vectored vaccines expressing HIV-1 Gag coupled to CD8+ T-cell epitopes. *J Virol* 80:4717-4728.

59. Dorrell, L., H. Yang, B. Ondondo, T. Dong, K. di Gleria, A. Suttill, C. Conlon, D. Brown, P. Williams, P. Bowness, N. Goonetilleke, T. Rostron, S. Rowland-Jones, T. Hanke, and A. McMichael. 2006. Expansion and diversification of virus-specific T cells following immunization of human immunodeficiency virus type 1

(HIV-1)-infected individuals with a recombinant modified vaccinia virus Ankara/HIV-1 Gag vaccine. *J Virol* 80:4705-4716.

60. Cebere, I., L. Dorrell, H. McShane, A. Simmons, S. McCormack, C. Schmidt, C. Smith, M. Brooks, J.E. Roberts, S.C. Darwin, P.E. Fast, C. Conlon, S. Rowland-Jones, A.J. McMichael, and T. Hanke. 2006. Phase I clinical trial safety of DNA- and modified virus Ankara-vectored human immunodeficiency virus type 1 (HIV-1) vaccines administered alone and in a prime-boost regime to healthy HIV-1-uninfected volunteers. *Vaccine* 24:417-425.

61. Harari, A., P.A. Bart, W. Stöhr, G. Tapia, M. Garcia, E. Medjitna-Rais, S. Burnet, O. Erlwein, T. Barber, C. Moog, P. Liljestrom, R. Wagner, H. Wolf, J.P. Kraehenbuhl, M. Esteban, J.L. Heeney, M.J. Frachette, J. Tartaglia, S. McCormack, A. Babiker, J. Weber, and G. Pantaleo. 2007 in press. An HIV-1 Clade C DNA Prime, NYVAC Boost Vaccine Regimen Induces Vigorous, Broad, Polyfunctional and Long-Lasting T-Cell Responses. *Journal of Experimental Medicine*

62. Gomez, C.E., J.L. Najera, E. Domingo-Gil, L. Ochoa-Callejero, G. Gonzalez-Aseguinolaza, and M. Esteban. 2007. Virus distribution of the attenuated MVA and NYVAC poxvirus strains in mice. *Journal of General Virology* 88:2473-2478.

63. Najera, J.L., C.E. Gomez, E. Domingo-Gil, M.M. Gherardi, and M. Esteban. 2006. Cellular and biochemical differences between two attenuated poxvirus vaccine candidates (MVA and NYVAC) and role of the C7L gene. *J Virol* 80:6033-6047.

64. Mescher, M.F., P. Agarwal, K.A. Casey, C.D. Hammerbeck, Z. Xiao, and J.M. Curtsinger. 2007. Molecular basis for checkpoints in the CD8 T cell response: tolerance versus activation. *Semin Immunol* 19:153-161.

65. Mescher, M.F., J.M. Curtsinger, P. Agarwal, K.A. Casey, M. Gerner, C.D. Hammerbeck, F. Popescu, and Z. Xiao. 2006. Signals required for programming effector and memory development by CD8+ T cells. *Immunol Rev* 211:81-92.

66. Lu, B. 2006. The molecular mechanisms that control function and death of effector CD4+ T cells. *Immunol Res* 36:275-282.

67. Sundrud, M.S., and A. Rao. 2007. New twists of T cell fate: control of T cell activation and tolerance by TGF-beta and NFAT. *Curr Opin Immunol* 19:287-293.

68. Anel, A., A. Bosque, J. Naval, A. Pineiro, L. Larrad, M.A. Alava, and M.J. Martinez-Lorenzo. 2007. Apo2L/TRAIL and immune regulation. *Front Biosci* 12:2074-2084.

69. Obst, R., H.M. van Santen, D. Mathis, and C. Benoist. 2005. Antigen persistence is required throughout the expansion phase of a CD4(+) T cell response. *J Exp Med* 201:1555-1565.

70. Okoye, A., M. Meier-Schellersheim, J.M. Brenchley, S.I. Hagen, J.M. Walker, M. Rohankhedkar, R. Lum, J.B. Edgar, S.L. Planer, A. Legasse, A.W. Sylwester, M. Piatak, Jr., J.D. Lifson, V.C. Maino, D.L. Sodora, D.C. Douek, M.K. Axthelm, Z. Grossman, and L.J. Picker. 2007. Progressive CD4+ central memory T cell decline results in CD4+ effector memory insufficiency and overt disease in chronic SIV infection. *J Exp Med* 204:2171-2185.

71. Gomez, C.E., J.L. Najera, E.P. Jimenez, V. Jimenez, R. Wagner, M. Graf, M.J. Frachette, P. Liljestrom, G. Pantaleo, and M. Esteban. 2007. Head-to-head comparison on the immunogenicity of two HIV/AIDS vaccine candidates based on the attenuated poxvirus strains MVA and NYVAC co-expressing in a single locus the HIV-1(BX08) gp120 and HIV-1(IIIB) Gag-Pol-Nef proteins of clade B. *Vaccine* 25:2863-2885.

72. Santra, S., D.H. Barouch, B. Korioth-Schmitz, C.I. Lord, G.R. Krivulka, F. Yu, M.H. Beddall, D.A. Gorgone, M.A. Lifton, A. Miura, V. Philippon, K. Manson, P.D. Markham, J. Parrish, M.J. Kuroda, J.E. Schmitz, R.S. Gelman, J.W. Shiver, D.C. Montefiori, D. Panicali, and N.L. Letvin. 2004. Recombinant poxvirus boosting of DNA-primed rhesus monkeys augments peak but not memory T lymphocyte responses. *Proc Natl Acad Sci U S A* 101:11088-11093.

73. Santra, S., Y. Sun, J.G. Parvani, V. Philippon, M.S. Wyand, K. Manson, A. Gomez-Yafal, G. Mazzara, D. Panicali, P.D. Markham, D.C. Montefiori, and N.L. Letvin. 2007. Heterologous prime/boost immunization of rhesus monkeys by using diverse poxvirus vectors. *J Virol* 81:8563-8570.

74. Palmowski, M.J., E.M. Choi, I.F. Hermans, S.C. Gilbert, J.L. Chen, U. Gileadi, M. Salio, A. Van Pel, S. Man, E. Bonin, P. Liljestrom, P.R. Dunbar, and V. Cerundolo. 2002. Competition between CTL narrows the immune response induced by prime-boost vaccination protocols. *J Immunol* 168:4391-4398.

75. Rodriguez, F., S. Harkins, M.K. Slifka, and J.L. Whitton. 2002. Immunodominance in virus-induced CD8(+) T-cell responses is dramatically modified by DNA immunization and is regulated by gamma interferon. *J Virol* 76:4251-4259.

76. Guerra, S., L.A. Lopez-Fernandez, R. Conde, A. Pascual-Montano, K. Harshman, and M. Esteban. 2004. Microarray analysis reveals characteristic changes of host cell gene expression in response to attenuated modified vaccinia virus Ankara infection of human HeLa cells. *J Virol* 78:5820-5834.

77. Schluns, K.S., K. Williams, A. Ma, X.X. Zheng, and L. Lefrancois. 2002. Cutting edge: requirement for IL-15 in the generation of primary and memory antigen-specific CD8 T cells. *J Immunol* 168:4827-4831.

78. Inaba, K., S. Turley, F. Yamaide, T. Iyoda, K. Mahnke, M. Inaba, M. Pack, M. Subklewe, B. Sauter, D. Sheff, M. Albert, N. Bhardwaj, I. Mellman, and R.M. Steinman. 1998. Efficient presentation of phagocytosed cellular fragments on the major histocompatibility complex class II products of dendritic cells. *J Exp Med* 188:2163-2173.

79. Blachere, N.E., R.B. Darnell, and M.L. Albert. 2005. Apoptotic cells deliver processed antigen to dendritic cells for cross-presentation. *PLoS Biol* 3:e185.

80. Albert, M.L. 2004. Death-defying immunity: do apoptotic cells influence antigen processing and presentation? *Nat Rev Immunol* 4:223-231.

81. Precopio, M.L., M.R. Betts, J. Parrino, D.A. Price, E. Gostick, D.R. Ambrozak, T.E. Asher, D.C. Douek, A. Harari, G. Pantaleo, R. Bailer, B.S. Graham, M. Roederer, and R.A. Koup. 2007. Immunization with vaccinia virus induces polyfunctional and phenotypically distinctive CD8+ T cell responses. *J Exp Med* 204:1405-1416.

82. Sadagopal, S., R.R. Amara, D.C. Montefiori, L.S. Wyatt, S.I. Staprans, N.L. Kozyr, H.M. McClure, B. Moss, and H.L. Robinson. 2005. Signature for long-term vaccine-mediated control of a Simian and human immunodeficiency virus

89.6P challenge: stable low-breadth and low-frequency T-cell response capable of coproducing gamma interferon and interleukin-2. *J Virol* 79:3243-3253.

83. Boaz, M.J., A. Waters, S. Murad, P.J. Easterbrook, and A. Vyakarnam. 2002. Presence of HIV-1 Gag-specific IFN-gamma+IL-2+ and CD28+IL-2+ CD4 T cell responses is associated with nonprogression in HIV-1 infection. *J Immunol* 169:6376-6385.

84. Pantaleo, G., and A. Harari. 2006. Functional signatures in antiviral T-cell immunity for monitoring virus-associated diseases. *Nat Rev Immunol* 6:417-423.

85. Zimmerli, S.C., A. Harari, C. Cellerai, F. Vallelian, P.A. Bart, and G. Pantaleo. 2005. HIV-1-specific IFN-gamma/IL-2-secreting CD8 T cells support CD4-independent proliferation of HIV-1-specific CD8 T cells. *Proc Natl Acad Sci U S A* 102:7239-7244.

86. Kannanganat, S., B.G. Kapogiannis, C. Ibegbu, L. Chennareddi, P. Goepfert, H.L. Robinson, J. Lennox, and R.R. Amara. 2007. HIV-1 Controllers but not Non-Controllers Maintain Triple Cytokine Co-expressing CD4 T Cells. *J Virol*

87. Li, M., F. Gao, J.R. Mascola, L. Stamatatos, V.R. Polonis, M. Koutsoukos, G. Voss, P. Goepfert, P. Gilbert, K.M. Greene, M. Bilska, D.L. Kothe, J.F. Salazar-Gonzalez, X. Wei, J.M. Decker, B.H. Hahn, and D.C. Montefiori. 2005. Human immunodeficiency virus type 1 env clones from acute and early subtype B infections for standardized assessments of vaccine-elicited neutralizing antibodies. *J Virol* 79:10108-10125.

88. Koopman, G., H. Niphuis, W. Newman, T.K. Kishimoto, V.C. Maino, and J.L. Heeney. 2001. Decreased expression of IL-2 in central and effector CD4 memory cells during progression to AIDS in rhesus macaques. *Aids* 15:2359-2369.

89. Sun, Y., S.R. Permar, A.P. Buzby, and N.L. Letvin. 2007. Memory CD4+ T-lymphocyte loss and dysfunction during primary simian immunodeficiency virus infection. *J Virol* 81:8009-8015.

90. Karlsson, G.B., M. Halloran, J. Li, I.W. Park, R. Gomila, K.A. Reimann, M.K. Axthelm, S.A. Iliff, N.L. Letvin, and J. Sodroski. 1997. Characterization of molecularly cloned simian-human immunodeficiency viruses causing rapid CD4+ lymphocyte depletion in rhesus monkeys. *J Virol* 71:4218-4225.

91. Didierlaurent, A., J.C. Ramirez, M. Gherardi, S.C. Zimmerli, M. Graf, H.A. Orbea, G. Pantaleo, R. Wagner, M. Esteban, J.P. Kraehenbuhl, and J.C. Sirard. 2004. Attenuated poxviruses expressing a synthetic HIV protein stimulate HLA-A2-restricted cytotoxic T-cell responses. *Vaccine* 22:3395-3403.

92. Su, L., M. Graf, Y. Zhang, H. von Briesen, H. Xing, J. Kostler, H. Melzl, H. Wolf, Y. Shao, and R. Wagner. 2000. Characterization of a virtually full-length human immunodeficiency virus type 1 genome of a prevalent intersubtype (C/B') recombinant strain in China. *J Virol* 74:11367-11376.

93. Collman, R., J.W. Balliet, S.A. Gregory, H. Friedman, D.L. Kolson, N. Nathanson, and A. Srinivasan. 1992. An infectious molecular clone of an unusual macrophage-tropic and highly cytopathic strain of human immunodeficiency virus type 1. *J Virol* 66:7517-7521.

94. Reimann, K.A., J.T. Li, G. Voss, C. Lekutis, K. Tenner-Racz, P. Racz, W. Lin, D.C. Montefiori, D.E. Lee-Parritz, Y. Lu, R.G. Collman, J. Sodroski, and N.L. Letvin. 1996. An env gene derived from a primary human immunodeficiency virus type 1 isolate confers high in vivo replicative capacity to a chimeric simian/human immunodeficiency virus in rhesus monkeys. *J Virol* 70:3198-3206.

95. Reimann, K.A., J.T. Li, R. Veazey, M. Halloran, I.W. Park, G.B. Karlsson, J. Sodroski, and N.L. Letvin. 1996. A chimeric simian/human immunodeficiency virus expressing a primary patient human immunodeficiency virus type 1 isolate env causes an AIDS-like disease after in vivo passage in rhesus monkeys. *J Virol* 70:6922-6928.

96. Balla-Jhagjhoorsingh, S.S., G. Koopman, P. Mooij, W. Koornstra, S. McCormack, J. Weber, G. Pantaleo, and J.L. Heeney. 2004. Long-term persistence of HIV-1 vaccine-induced CD4+CD45RA-CD62L-CCR7- memory T-helper cells. *Aids* 18:837-848.

97. Lyons, A.B., and C.R. Parish. 1994. Determination of lymphocyte division by flow cytometry. *J Immunol Methods* 171:131-137.

98. Parish, C.R. 1999. Fluorescent dyes for lymphocyte migration and proliferation studies. *Immunol Cell Biol* 77:499-508.

99. Wei, X., J.M. Decker, H. Liu, Z. Zhang, R.B. Arani, J.M. Kilby, M.S. Saag, X. Wu, G.M. Shaw, and J.C. Kappes. 2002. Emergence of resistant human immunodeficiency virus type 1 in patients receiving fusion inhibitor (T-20) monotherapy. *Antimicrob Agents Chemother* 46:1896-1905.

100. Ten Haaft, P., B. Verstrepen, K. Uberla, B. Rosenwirth, and J. Heeney. 1998. A pathogenic threshold of virus load defined in simian immunodeficiency virus- or simian-human immunodeficiency virus-infected macaques. *J Virol* 72:10281-10285.

101. Mooij, P., W.M. Bogers, H. Oostermeijer, W. Koornstra, P.J. Ten Haaft, B.E. Verstrepen, G. Van Der Auwera, and J.L. Heeney. 2000. Evidence for viral

virulence as a predominant factor limiting human immunodeficiency virus vaccine efficacy. *J Virol* 74:4017-4027.

Figure legends

Figure 1. T-cell responses in time

IFN-γ (left panels) and IL-4 (right panels) production by PBMC of individual animals immunized with DNA/MVA or DNA/NYVAC to HIV-$1_{89.6p}$ Env, and SIV_{mac239} Gag, Pol and Nef peptides as measured by ELISpot assay in time. Background responses (mean number of SFC plus 2xSD of triplicate assays with medium alone) were subtracted. Responses are presented as number of spot forming cells (SFC) per 10^6 PBMC. Arrows indicate immunization time points at weeks 0, 4 (DNA), 20 and 24 (pox virus).

Figure 2. Vaccine induced antigen-specific $CD4^+$ and $CD8^+$ T-cell responses 2 weeks before challenge.

(A) Representative flow cytometry profiles of vaccine-induced $CD4^+$ (left) and $CD8^+$ (right) T-cell responses directed against Env in monkeys R99005 immunized with DNA/MVA and R00033 immunized with DNA/NYVAC. CD4 and CD8 T-cell responses were defined using polychromatic flow cytometry. Blood mononuclear cells were stimulated with the relevant peptide pools and stained with CD4, CD8, IFN-γ and IL-2 antibodies.

(B) Cytokine production by $CD4^+$ (left) and $CD8^+$ (right) T-cells of all individual animals immunized with DNA/MVA (black squares) or DNA/NYVAC (black dots) to HIV-$1_{89.6p}$ Env (grey boxes) and SIV_{mac239} Gag peptides (clear boxes) as measured by ICS assay two weeks before challenge. Box-whisker plots indicate the interquartile range and the median (horizontal line) of the groups. Responses are presented as number of cytokine producing $CD3^+$ T-cells per 10^6 lymphocytes. Statistical significant differences between immunization groups are given by showing the p values (Mann-Whitney test).

(C) Cumulative intracellular cytokine responses to HIV-$1_{89.6p}$ Env and SIV_{mac239} Gag peptide pools by $CD4^+$ (left) and $CD8^+$ (right) T-cells of individual animals (dots) immunized with DNA/MVA (black squares) or DNA/NYVAC (black circles) as measured by FACS analysis, two weeks before challenge. $CD4^+$ and $CD8^+$ T-cells producing either one cytokine (IFN-γ or IL-2) or IFN-γ and IL-2 simultaneously upon antigen stimulation are presented. Pies represents the average response across animals of each group of the $CD4^+$ and $CD8^+$ HIV-$1_{89.6p}$ Env and SIV_{mac239} Gag-specific T-cell responses grouped by function (expressing either one cytokine IFN-γ or IL-2 or two simultaneously), relative to the total antigen-specific response. Statistical significant differences between immunization groups are given by showing the p values (Mann-Whitney test).

Figure 3. Vaccine induced antigen specific $CD4^+$ and $CD8^+$ T-cell mediated proliferation 2 weeks before challenge.

(A) Representative flow cytometry profiles of CFSE labeled PBMC of monkey R99005 immunized with DNA/MVA and R00033 immunized with DNA/NYVAC, stimulated with Env peptides, cultured for 6 days and stained with CD3, CD4 (and CD8) antibodies. Monkey R99005 showed Env-specific $CD4^+$ and $CD4^-$ (mainly $CD8^+$) proliferating (CFSE low) T-cells, while monkey R00033 showed predominantly Env-specific $CD4^+$ proliferating T-cells.

(B) Percentage of antigen-specific proliferating $CD4^+$ and (C) $CD8^+$ T-cells of all individual animals (dots) immunized with DNA/MVA (black squares) or DNA/NYVAC (black dots) to HIV-$1_{89.6p}$ Env (grey boxes) and SIV_{mac239} Gag peptides (clear boxes) two

weeks before challenge. Responses are presented as percentage of CFSE low $CD3^+/CD4^+$ and $CD3^+/CD8^+$ T-cells. Background responses (medium alone) were subtracted.

Figure 4. Relative contribution of $CD4^+$ and $CD8^+$ T-cells to the total antigen specific response before challenge.

The relative contribution of $CD4^+$ and $CD8^+$ T-cells to the total Gag (dark grey) and Env (light grey) specific cytokine (A) and proliferative (B) responses of each animal immunized with DNA/MVA and DNA/NYVAC was determined. The mean percentage and standard deviation (SD) of each group is presented. Statistical differences between groups (MVA vs NYVAC) or between relative contribution of $CD4^+$ and $CD8^+$ T-cells to the response within groups (MVA CD4 vs CD8 and NYVAC CD4 vs CD8) was measured by student's t-test . P values are shown at the right of the figure.

Figure 5. Efficacy

Viral RNA load (top), absolute number of circulating $CD4^+$ T-cells (middle) and percentage of $CD4^+$ T central memory (CM) cells (bottom) after challenge of each individual animal is presented. Left column represents results of DNA/MVA immunized animals, middle column shows results of DNA/NYVAC immunized animals, while the right column presents results of control animals.

Figure 6. Survival

Percentage of animals that remained disease free after $SHIV_{89.6p}$ challenge of DNA/MVA (black squares) or DNA/NYVAC (black dots) immunized and control (black diamonds) animals.

Figure 7. T-cell responses after challenge

IFN-γ production by peripheral blood mononuclear cells (PBMC) of individual animals immunized with DNA/MVA (black squares) or DNA/NYVAC (black dots) or control animals (black diamonds) to HIV-$1_{89.6p}$ Env, and SIV_{mac239} Gag, Pol and Nef peptides as measured by ELISpot assay at 22 weeks post challenge (left panels) and at 41 weeks post challenge (right panels). Box-whisker plots indicate the interquartile range and the median (horizontal line) of the groups. Background responses (mean number of SFC plus 2xSD of triplicate assays with medium alone) were subtracted. Responses are presented as number of spot forming cells (SFC) per 10^6 PBMC.

Figure 8. Antigen-specific $CD4^+$ and $CD8^+$ T-cell responses at time of euthanasia.

(A) Cytokine production by $CD4^+$ (left) and $CD8^+$ (right) T-cells of individual animals (dots) immunized with DNA/MVA (black squares) or DNA/NYVAC (black dots) or control animals (black diamonds) to HIV-$1_{89.6p}$ Env (grey boxes) and SIV_{mac239} Gag peptides (clear boxes) as measured by ICS assay at time of euthanasia. Box-whisker plots indicate the interquartile range and the median (horizontal line) of the groups. Responses are presented as number of cytokine producing $CD3^+$ T-cells per 10^6 lymphocytes. Statistical significant differences between immunization groups are given by showing the p values (Mann-Whitney test).

(B) Cumulative intracellular cytokine responses by $CD4^+$ (left) and $CD8^+$ (right) T-cells of individual animals (dots) immunized with DNA/MVA (black squares) or DNA/NYVAC (black circles) or control animals (black diamonds) to HIV-$1_{89.6p}$ Env and SIV_{mac239} Gag peptide pools as measured by FACS analysis. $CD4^+$ and $CD8^+$ T-cells producing either one cytokine (IFN-γ or IL-2) or two simultaneously upon antigen stimulation are presented. Pies represents the average response across animals of each group of the $CD4^+$ and $CD8^+$ HIV-$1_{89.6p}$ Env and SIV_{mac239} Gag -specific T-cell responses grouped by function (expressing either one cytokine IFN-γ or IL-2 or two simultaneously), relative to the total antigen-specific response.

(C) Percentage of antigen-specific proliferating $CD4^+$ (left) and $CD8^+$ (right) T-cells of individual animals (dots) immunized with DNA/MVA (black squares) or DNA/NYVAC (black dots) or control animals (black diamonds) to HIV-$1_{89.6p}$ Env (grey boxes) and SIV_{mac239} Gag peptides (clear boxes). Responses are presented as percentage of CFSE low $CD3^+/CD4^+$ and $CD3^+/CD8^+$ T-cells. Background responses (medium alone) were subtracted. Statistical significant differences between immunization groups are given by showing the p values (Mann-Whitney test).

Figure 9. Relative contribution of $CD4^+$ and $CD8^+$ T-cells to the total antigen specific response at time of euthanasia.

The relative contribution of $CD4^+$ and $CD8^+$ T-cells to the total Gag (dark grey) and Env (light grey) specific cytokine (A) and proliferative (B) responses of each animal immunized with DNA/MVA and DNA/NYVAC was determined. The mean percentage and standard deviation (SD) of each group is presented. Statistical differences between groups (MVA vs NYVAC) or between relative contribution of $CD4^+$ and $CD8^+$ T-cells to

the response within groups (MVA CD4 vs CD8 and NYVAC CD4 vs CD8) was measured by student's t-test . P values are shown at the right of the figure.

Table 1. Differences in mRNA levels of immunomodulators after MVA and NYVAC infection of human DCs that might be involved in CD4+ and CD8+ T-cell activation

Description	GenBank accession	Gene symbol	MVA vs Mock	NYVAC vs Mock	MVA vs NYVAC
Interferon-induced protein with tetratricopeptide repeats 4	NM_001549	IFIT4	52.45	3.37	11.44
Tumor necrosis factor (TNF superfamily, member 2)	NM_000594	TNF	52.21	6.79	10.38
Interferon-induced protein with tetratricopeptide repeats 1	NM_001548	IFIT1	47.8	4.65	7.38
Mitogen-activated protein kinase kinase 5	NM_002757	MAP2K5	15.59	2.07	6.54
RNA helicase	NM_014314	RIG-I	21.81	-	5.72
Small inducible cytokine A4	NM_002984	SCYA4	3.74	-1.14	5.61
Interferon-induced, hepatitis C-associated microtubular aggregate protein (44kD)	NM_006417	MTAP44	20.95	2.63	5.52
Interleukin 12B (natural killer cell stimulatory factor 2, cytotoxic lymphocyte maturation factor 2,	NM_002187	IL12B	9.76	-	5.44
Interferon, beta 1, fibroblast	NM_002176	IFNB1	137.82	-	5.06
Melanoma differentiation associated protein-5	NM_022168	MDA5	7.77	1.67	5.05
Cyclin B1	NM_031966	CCNB1	7.87	-1.06	3.64
Small inducible cytokine A5 (RANTES)	NM_002985	SCYA5	4.17	-1.17	3.06
Interleukin 6 signal transducer (gp130, oncostatin M receptor)	NM_002184	IL6ST	2.15	-1.19	2.91
V-fos FBJ murine osteosarcoma viral oncogene homolog	NM_005252	FOS	3.38	1.00	2.86
GRO2 oncogene (SCYB2)	NM_002089	GRO2	6.58	2.22	2.78
Tumor necrosis factor (ligand) superfamily, member 13b	NM_006573	TNFSF13B	1.84	-1.21	2.67
Small inducible cytokine subfamily B (Cys-X-Cys), member 10	NM_001565	SCYB10	8.33	-	2.35
Interferon regulatory factor 7	NM_004031	IRF7	2.52	1.3	2.31
Menage a trois 1 (CAK assembly factor)	NM_002431	MNAT1	5.85	1.72	2.27
Small inducible cytokine A3	NM_002983	SCYA3	4.22	1.12	-
Colony stimulating factor 2 (granulocyte-macrophage)	NM_000758	CSF2	3.13	-1.08	1.94
Growth arrest and DNA-damage-inducible, beta	NM_015675	GADD45B	2.22	1.56	1.31
Nuclear factor of activated T-cells 5, tonicity-responsive	AF346509	NFAT5	2.81	-	1.24
Interleukin 10 receptor, alpha	NM_001558	IL10RA	-1.39	-2.12	1.21
Major histocompatibility complex, class II, DQ beta 1	NM_002123	HLA-DQB1	2.18	2.49	1.02
Proteasome (prosome, macropain) subunit, beta type, 10	NM_002801	PSMB10	-3.04	-1.20	-1.03
Interferon consensus sequence binding protein 1, IRF8	NM_002163	ICSBP1	-1.19	3.32	-1.07
Tumor necrosis factor (ligand) superfamily, member 9 (4-1BB-L)	NM_003811	TNFSF9	-1.59	-2.10	-1.07
Inhibitor of DNA binding 2B, dominant negative helix-loop-helix protein	M96843	ID2B	-2.16	-1.78	-1.07
CD86 antigen (CD28 antigen ligand 2, B7-2 antigen)	NM_006889	CD86	1.44	1.12	-1.13
Transforming growth factor, beta 1	NM_000660	TGFB1	-2.43	-2.09	-1.16
CD80 antigen (CD28 antigen ligand 1, B7-1 antigen)	NM_005191	CD80	-1.53	-1.14	-1.20
V-jun sarcoma virus 17 oncogene homolog (avian)	NM_002228	JUN	1.91	2.93	-1.34
Interleukin 10 receptor, beta	Z17227	IL10RB	-2.59	-1.21	-1.38
Major histocompatibility complex, class II, DR beta 5	NM_002125	HLA-DRB5	-2.92	-5.59	-1.65
Interleukin 8	NM_000584	IL8	-2.90	-1.39	-1.89
Ras homolog gene family, member B	NM_004040	ARHB	-1.50	2.08	-1.97
Interferon gamma receptor 2 (interferon gamma transducer 1)	NM_005534	IFNGR2	-2.52	-1.18	-2.05
Secreted phosphoprotein 1 (osteopontin, bone sialoprotein I, early T-lymphocyte activation 1)	NM_000582	SPP1	-1.60	-2.64	-2.13
Jun D proto-oncogene	NM_005354	JUND	1.41	2.78	-2.42
Interleukin 1, alpha	NM_000575	IL1A	-1.43	2.01	-2.42
Mal, T-cell differentiation protein 2	NM_052886	MAL2	-2.49	-1.09	-2.54
Interferon regulatory factor 5	NM_002200	IRF5	-2.31	1.06	-2.65
Interleukin 1, beta	NM_000576	IL1B	-2.25	1.39	-3.14
Prostate differentiation factor	NM_004864	PLAB	-1.77	3.32	-3.94
FOS-like antigen 2	AK055579	FOSL2	1.36	4.13	-4.09
Deoxythymidylate kinase (thymidylate kinase)	NM_012145	DTYMK	1.54	12.02	-8.18
Cyclin-dependent kinase inhibitor 2C (p18, inhibits CDK4)	NM_001262	CDKN2C	-3.10	1.18	-

Fold change in transcription level is indicated in red when genes are upregulated, or in green when down regulated compared to non-infected MDDC (mock) or comparing MVA infected MDDC with NYVAC infected MDDC. Up or downregulation <2 is considered as not significant.

Figure 1

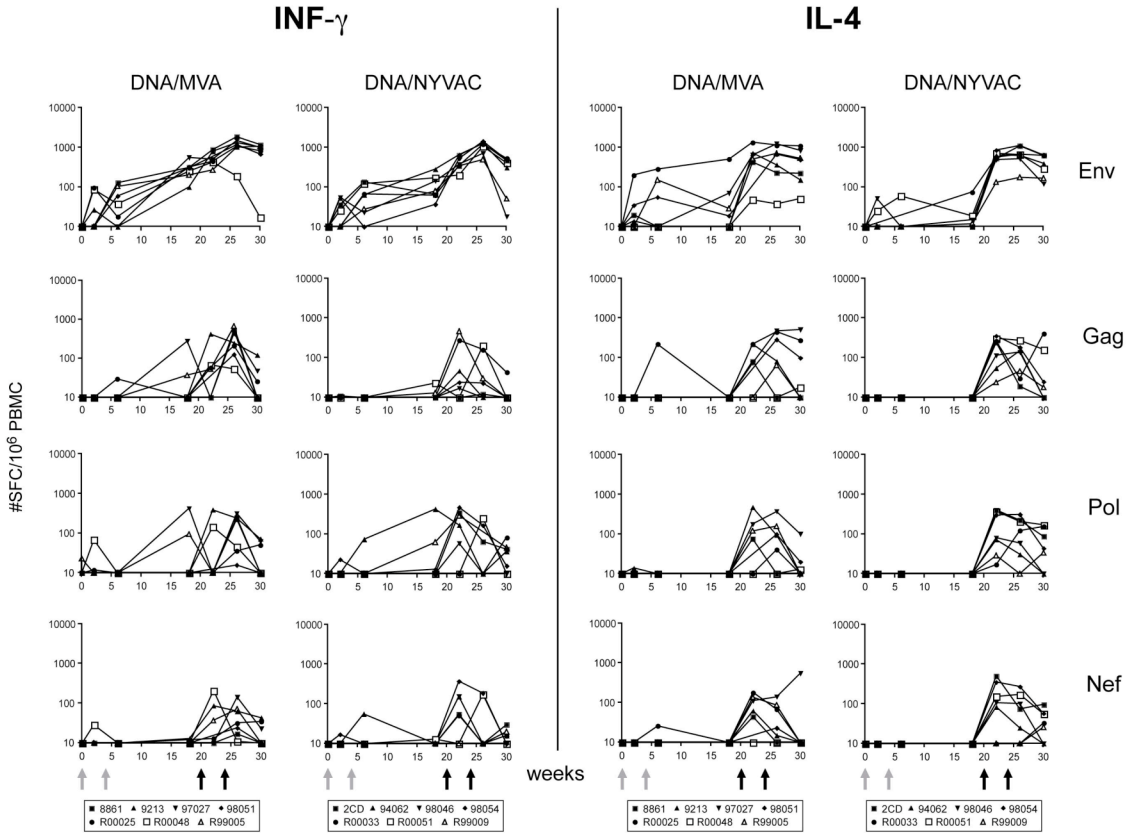
INF-γ
IL-4
DNA/MVA
DNA/NYVAC
DNA/MVA
DNA/NYVAC
Env
Gag
Pol
Nef
#SFC/10^6 PBMC
weeks
8861 9213 97027 98051
R00025 R00048 R99005
2CD 94062 98046 98054
R00033 R00051 R99009
8861 9213 97027 98051
R00025 R00048 R99005
2CD 94062 98046 98054
R00033 R00051 R99009

Figure 2

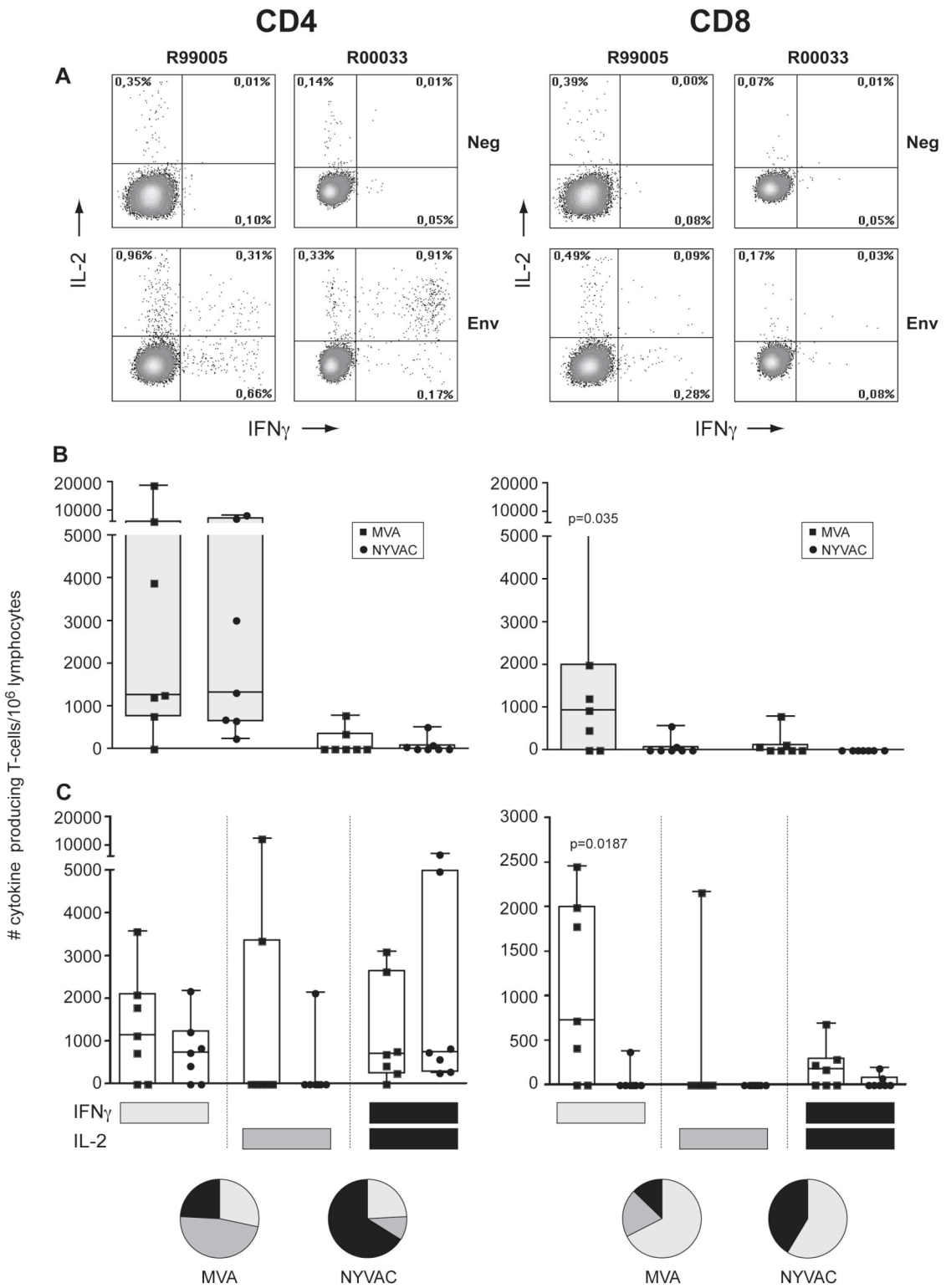
CD4
CD8
R99005
R00033
A
Neg
Env
IL-2
IFNγ
0,35%
0,01%
0,10%
0,14%
0,01%
0,05%
0,96%
0,31%
0,66%
0,33%
0,91%
0,17%
0,39%
0,00%
0,08%
0,07%
0,01%
0,05%
0,49%
0,09%
0,28%
0,17%
0,03%
0,08%
B
C
cytokine producing T-cells/10^6 lymphocytes
MVA
NYVAC
p=0.035
p=0.0187
IFNγ
IL-2

Figure 3

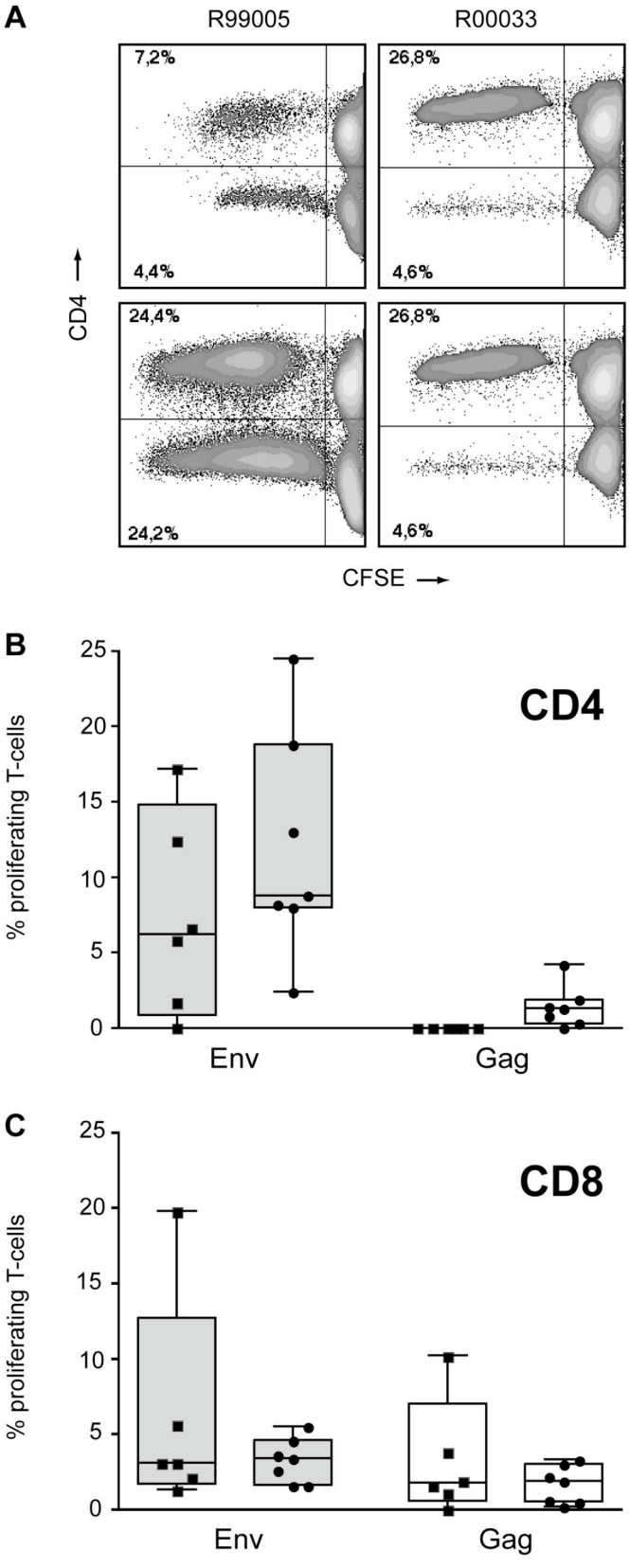
A
R99005
R00033
7,2%
26,8%
4,4%
4,6%
24,4%
26,8%
24,2%
4,6%
CD4
CFSE
B
CD4
% proliferating T-cells
25
20
15
10
5
0
Env
Gag
C
CD8
% proliferating T-cells
25
20
15
10
5
0
Env
Gag

Figure 4

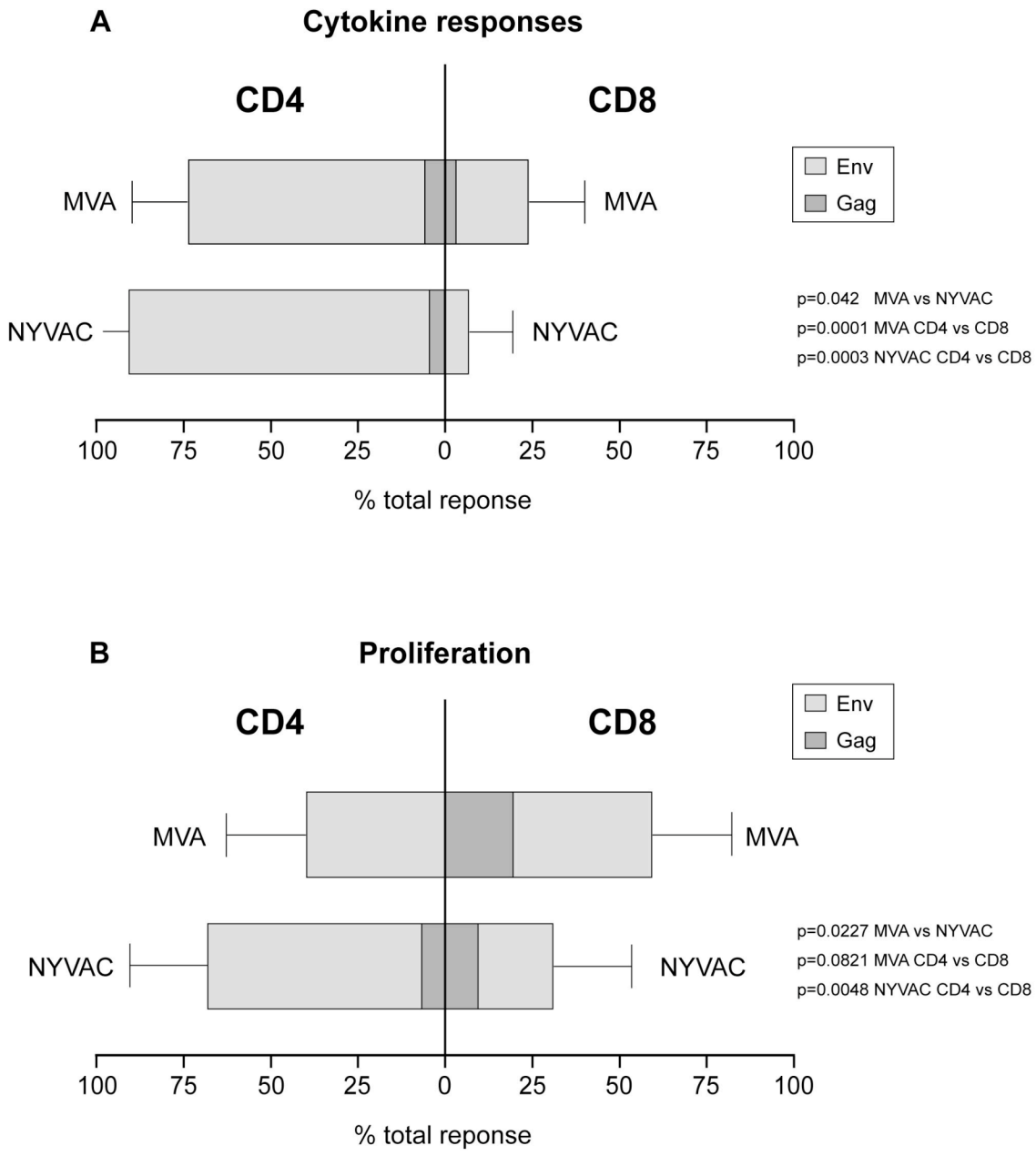
A
Cytokine responses
CD4
CD8
MVA
MVA
NYVAC
NYVAC
Env
Gag
p=0.042 MVA vs NYVAC
p=0.0001 MVA CD4 vs CD8
p=0.0003 NYVAC CD4 vs CD8
100 75 50 25 0 25 50 75 100
% total reponse
B
Proliferation
CD4
CD8
MVA
MVA
NYVAC
NYVAC
Env
Gag
p=0.0227 MVA vs NYVAC
p=0.0821 MVA CD4 vs CD8
p=0.0048 NYVAC CD4 vs CD8
100 75 50 25 0 25 50 75 100
% total reponse

Figure 5

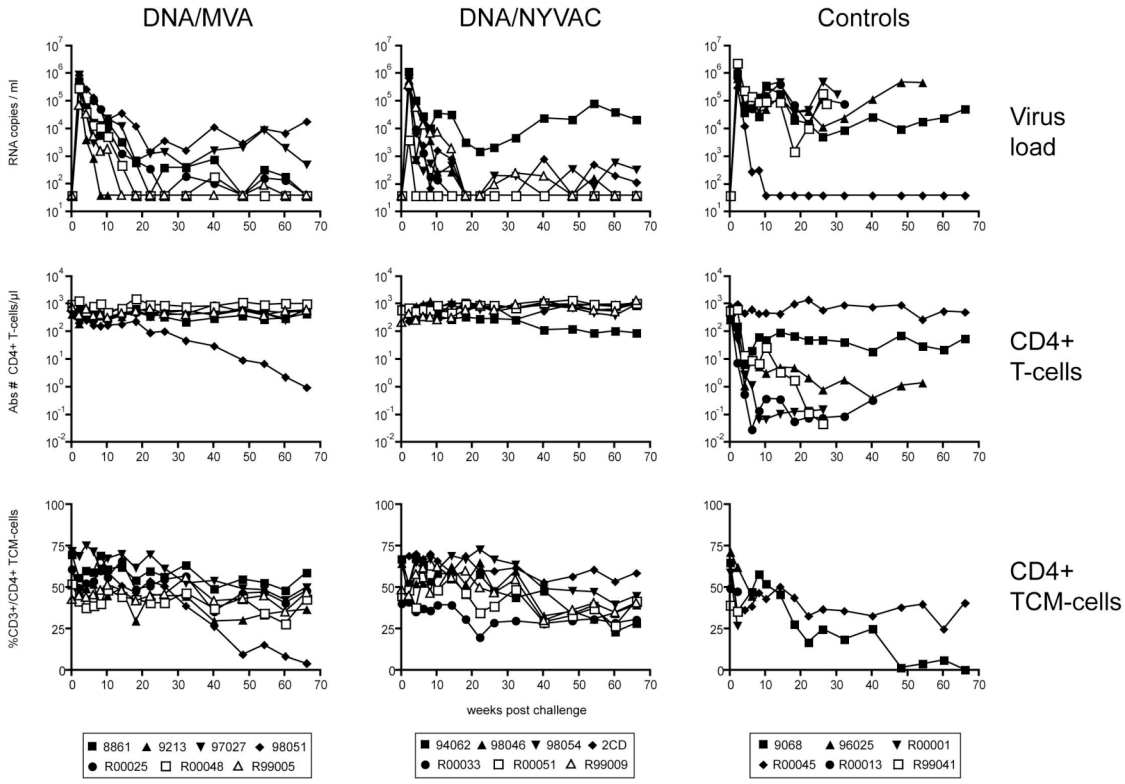
DNA/MVA
DNA/NYVAC
Controls
RNA copies / ml
Virus load
Abs # CD4+ T-cells/µl
CD4+ T-cells
%CD3+/CD4+ TCM-cells
CD4+ TCM-cells
weeks post challenge
8861 9213 97027 98051 R00025 R00048 R99005
94062 98046 98054 2CD R00033 R00051 R99009
9068 96025 R00001 R00045 R00013 R99041

Figure 6

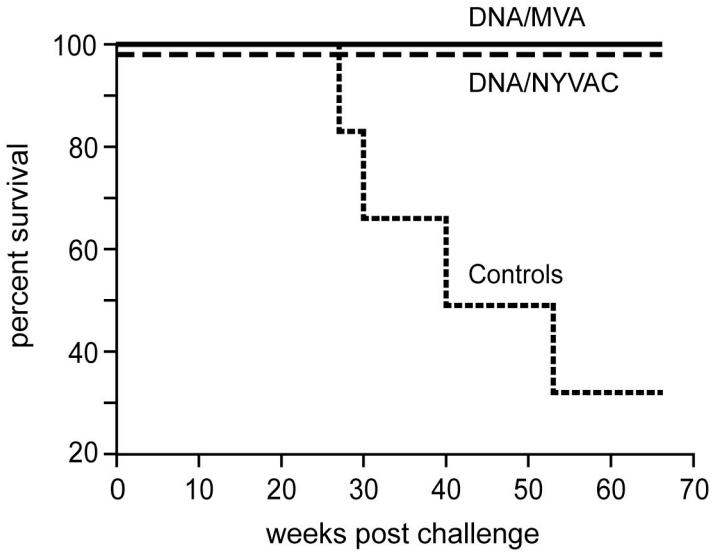
DNA/MVA
DNA/NYVAC
Controls
percent survival
100
80
60
40
20
0
10
20
30
40
50
60
70
weeks post challenge

Figure 7

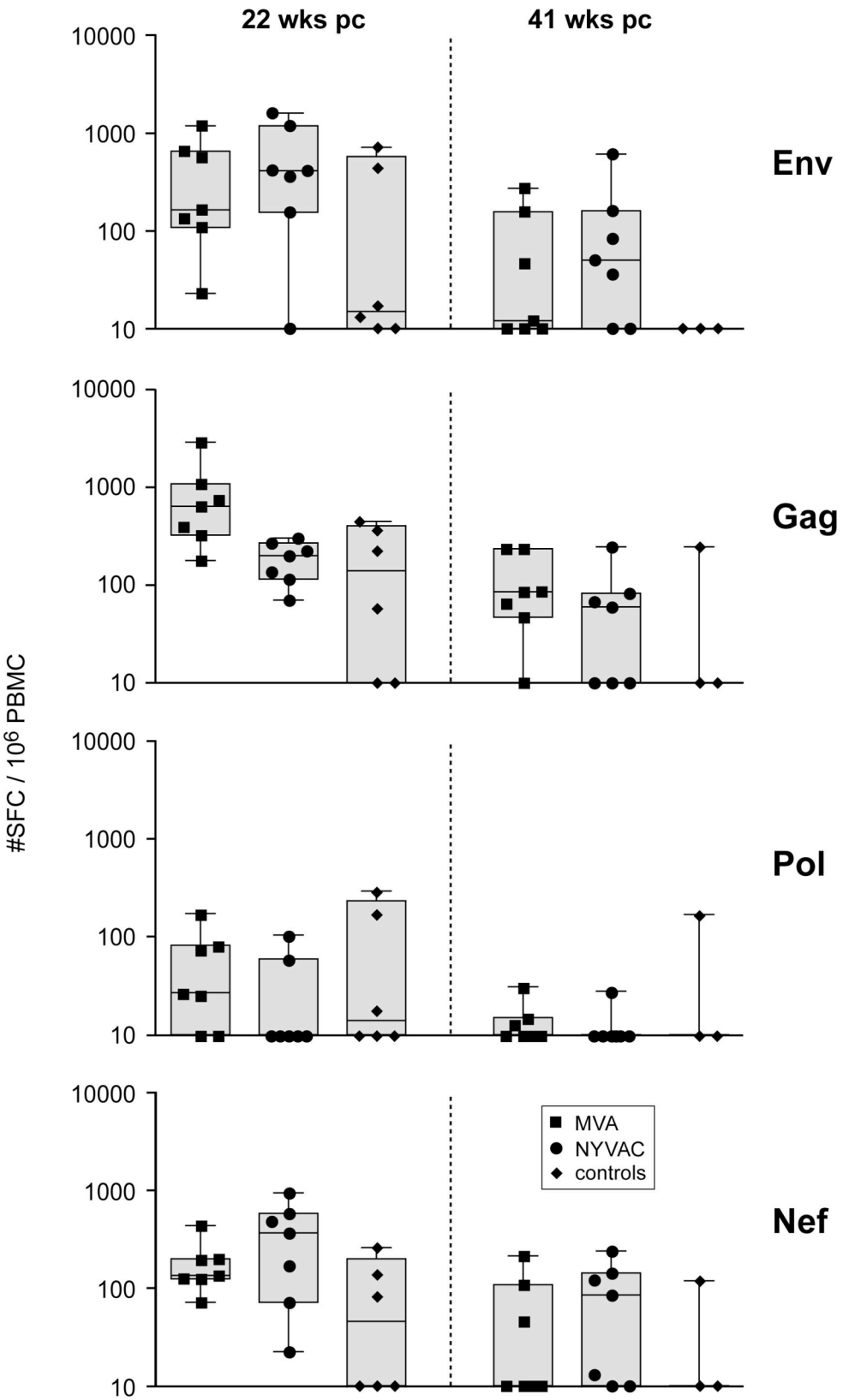
22 wks pc
41 wks pc
10000
1000
100
10
#SFC / 10^6 PBMC
Env
Gag
Pol
Nef
MVA
NYVAC
controls

Figure 8

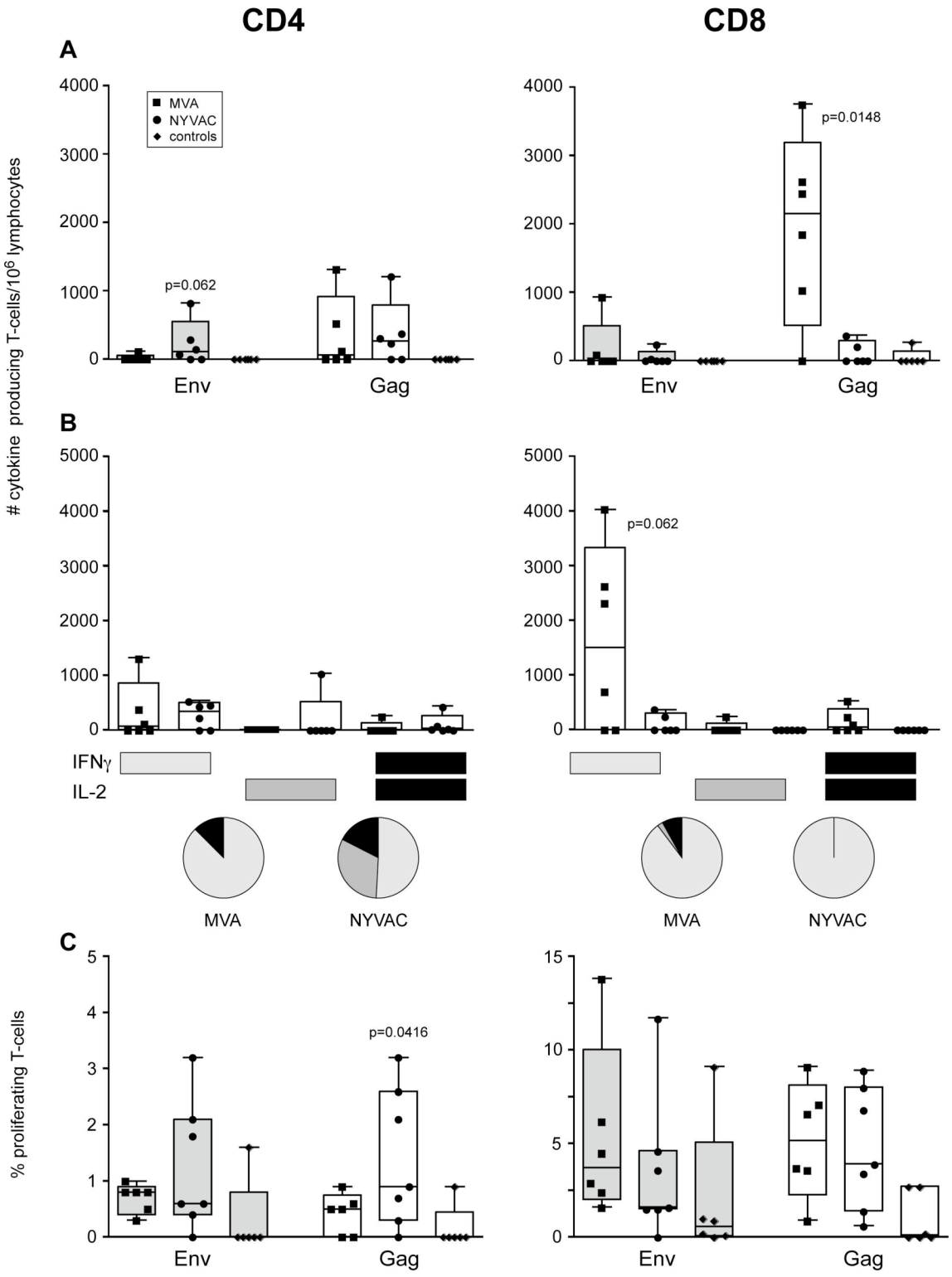
CD4
CD8
A
B
C
MVA
NYVAC
controls
p=0.062
p=0.0148
p=0.062
p=0.0416
Env
Gag
IFNγ
IL-2
MVA
NYVAC
cytokine producing T-cells/10^6 lymphocytes
% proliferating T-cells

figure 9

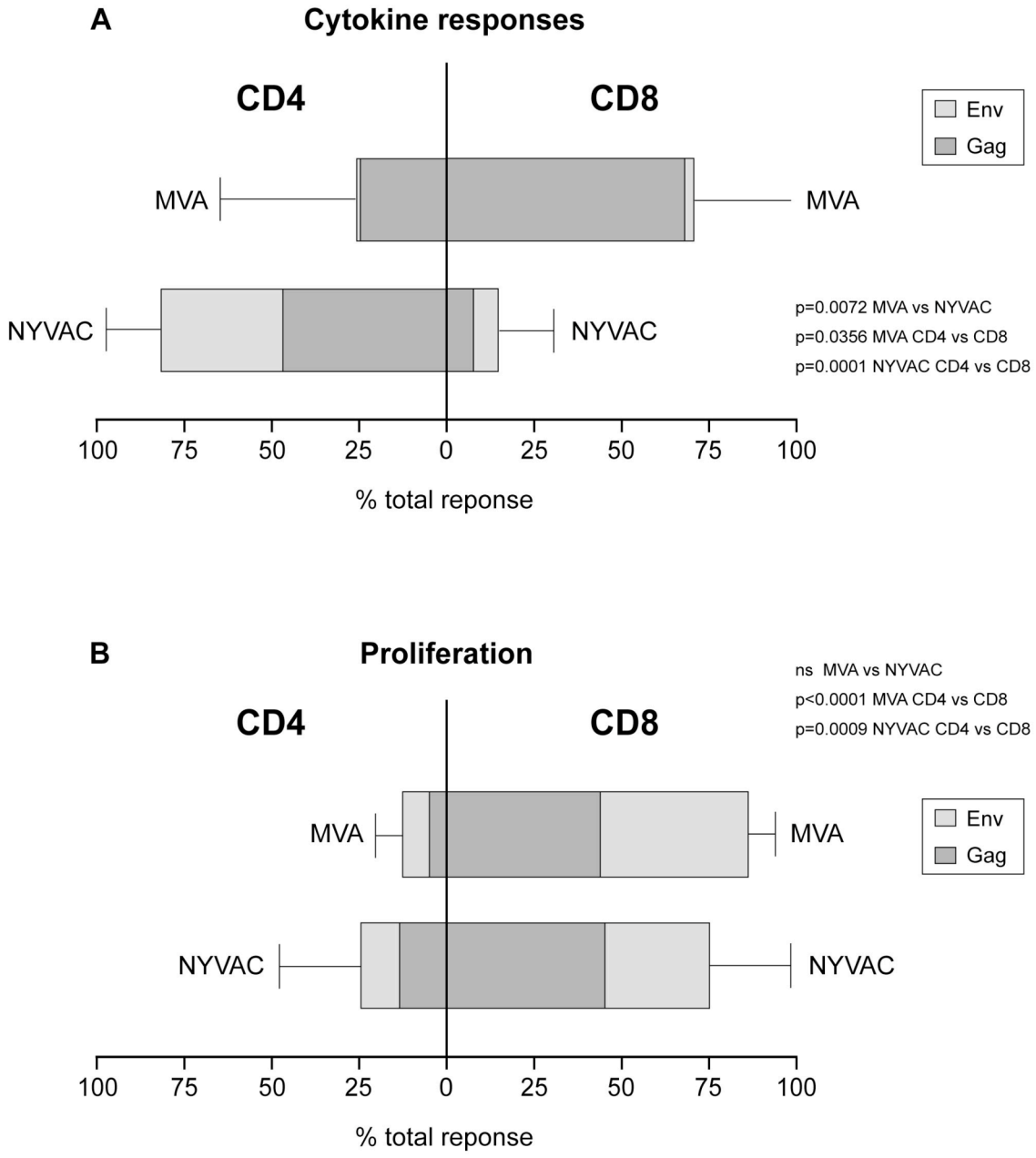
A
Cytokine responses
CD4
CD8
Env
Gag
MVA
MVA
NYVAC
NYVAC
p=0.0072 MVA vs NYVAC
p=0.0356 MVA CD4 vs CD8
p=0.0001 NYVAC CD4 vs CD8
100 75 50 25 0 25 50 75 100
% total reponse
B
Proliferation
ns MVA vs NYVAC
p<0.0001 MVA CD4 vs CD8
p=0.0009 NYVAC CD4 vs CD8
CD4
CD8
Env
Gag
MVA
MVA
NYVAC
NYVAC
100 75 50 25 0 25 50 75 100
% total reponse